frontiers | Research Topics

Human-environmental interactions in prehistoric periods, volume II

Edited by
Guanghui Dong, Harry F. Lee and Ren Lele

Published in
Frontiers in Earth Science
Frontiers in Ecology and Evolution

FRONTIERS EBOOK COPYRIGHT STATEMENT

The copyright in the text of individual articles in this ebook is the property of their respective authors or their respective institutions or funders. The copyright in graphics and images within each article may be subject to copyright of other parties. In both cases this is subject to a license granted to Frontiers.

The compilation of articles constituting this ebook is the property of Frontiers.

Each article within this ebook, and the ebook itself, are published under the most recent version of the Creative Commons CC-BY licence. The version current at the date of publication of this ebook is CC-BY 4.0. If the CC-BY licence is updated, the licence granted by Frontiers is automatically updated to the new version.

When exercising any right under the CC-BY licence, Frontiers must be attributed as the original publisher of the article or ebook, as applicable.

Authors have the responsibility of ensuring that any graphics or other materials which are the property of others may be included in the CC-BY licence, but this should be checked before relying on the CC-BY licence to reproduce those materials. Any copyright notices relating to those materials must be complied with.

Copyright and source acknowledgement notices may not be removed and must be displayed in any copy, derivative work or partial copy which includes the elements in question.

All copyright, and all rights therein, are protected by national and international copyright laws. The above represents a summary only. For further information please read Frontiers' Conditions for Website Use and Copyright Statement, and the applicable CC-BY licence.

ISSN 1664-8714
ISBN 978-2-8325-3597-4
DOI 10.3389/978-2-8325-3597-4

About Frontiers

Frontiers is more than just an open access publisher of scholarly articles: it is a pioneering approach to the world of academia, radically improving the way scholarly research is managed. The grand vision of Frontiers is a world where all people have an equal opportunity to seek, share and generate knowledge. Frontiers provides immediate and permanent online open access to all its publications, but this alone is not enough to realize our grand goals.

Frontiers journal series

The Frontiers journal series is a multi-tier and interdisciplinary set of open-access, online journals, promising a paradigm shift from the current review, selection and dissemination processes in academic publishing. All Frontiers journals are driven by researchers for researchers; therefore, they constitute a service to the scholarly community. At the same time, the *Frontiers journal series* operates on a revolutionary invention, the tiered publishing system, initially addressing specific communities of scholars, and gradually climbing up to broader public understanding, thus serving the interests of the lay society, too.

Dedication to quality

Each Frontiers article is a landmark of the highest quality, thanks to genuinely collaborative interactions between authors and review editors, who include some of the world's best academicians. Research must be certified by peers before entering a stream of knowledge that may eventually reach the public - and shape society; therefore, Frontiers only applies the most rigorous and unbiased reviews. Frontiers revolutionizes research publishing by freely delivering the most outstanding research, evaluated with no bias from both the academic and social point of view. By applying the most advanced information technologies, Frontiers is catapulting scholarly publishing into a new generation.

What are Frontiers Research Topics?

Frontiers Research Topics are very popular trademarks of the *Frontiers journals series*: they are collections of at least ten articles, all centered on a particular subject. With their unique mix of varied contributions from Original Research to Review Articles, Frontiers Research Topics unify the most influential researchers, the latest key findings and historical advances in a hot research area.

Find out more on how to host your own Frontiers Research Topic or contribute to one as an author by contacting the Frontiers editorial office: frontiersin.org/about/contact

Human-environmental interactions in prehistoric periods, volume II

Topic editors

Guanghui Dong — Lanzhou University, China

Harry F. Lee — The Chinese University of Hong Kong, China

Ren Lele — Lanzhou University, China

Citation

Dong, G., Lee, H. F., Lele, R., eds. (2023). *Human-environmental interactions in prehistoric periods, volume II*. Lausanne: Frontiers Media SA.

doi: 10.3389/978-2-8325-3597-4

Table of contents

frontiers | Frontiers in Earth Science

TYPE Editorial
PUBLISHED 15 September 2023
DOI 10.3389/feart.2023.1260161

Check for updates

OPEN ACCESS

EDITED AND REVIEWED BY
Steven L. Forman,
Baylor University, United States

*CORRESPONDENCE
Guanghui Dong,
ghdong@lzu.edu.cn

RECEIVED 17 July 2023
ACCEPTED 09 August 2023
PUBLISHED 15 September 2023

CITATION
Dong G, Lee HF and Ren L (2023), Editorial: Human-Environmental Interactions in Prehistoric Periods – Volume II.
Front. Earth Sci. 11:1260161.
doi: 10.3389/feart.2023.1260161

COPYRIGHT
© 2023 Dong, Lee and Ren. This is an open-access article distributed under the terms of the Creative Commons Attribution License (CC BY). The use, distribution or reproduction in other forums is permitted, provided the original author(s) and the copyright owner(s) are credited and that the original publication in this journal is cited, in accordance with accepted academic practice. No use, distribution or reproduction is permitted which does not comply with these terms.

Editorial: Human-Environmental Interactions in Prehistoric Periods – Volume II

Guanghui Dong[1,2]*, Harry F. Lee[3] and Lele Ren[4]

[1]Ministry of Education Key Laboratory of Western China's Environmental System, College of Earth and Environmental Sciences, Lanzhou University, Lanzhou, China, [2]Academician and Expert Workstation of Yunnan Province, Zhaotong University, Zhaotong, China, [3]Department of Geography and Resource Management, The Chinese University of Hong Kong, New Territories, China, [4]School of History and Culture, Lanzhou University, Lanzhou, China

KEYWORDS

human-land relation, subsistence strategy, vegetation and landscape dynamics, late Paleolithic, Neolithic and Bronze age, East Asia

Editorial on the Research Topic
Human-Environmental Interactions in Prehistoric Periods – Volume II

The interaction between human evolution and living environment change has been increasingly concerned and discussed in recent decades, with the rapid accumulation of archaeological and paleo-environmental data and the promotion of inter-disciplinary research (Dearing et al., 2006; Dong et al., 2020). Environments provide necessary habitats and resources of living and production for the survival and development of humans and their societies. Meanwhile, humans have gradually adapted to diverse living environments since the migration waves of archaic humans that were driven by climate change (Timmermann and Friedrich, 2016; Timmermann et al., 2022), and humans have begun to influence the natural environment in regional and even global scales at least since the late Neolithic and Bronze Age (Ruddiman et al., 2016; Huang et al., 2017). Overall, the patterns of human-environment interaction varied notably in the prehistoric era, especially during the late Paleolithic, Neolithic, and Bronze periods.

The impact of human activities on the natural environment was variable during the Paleolithic era, while significant climate events generally resulted in ecosystem change which influenced the living space of hunting-gathering groups (Magill et al., 2013; Robinson et al., 2017). Human habitats extensively expanded to high altitude and latitude areas during the late Paleolithic period (Pitulko et al., 2016; Zhang et al., 2018). Foragers improved their adaptability by adjusting their subsistence strategies, such as the so-called "Broad Spectrum Revolution" (Stiner et al., 2000). During the Neolithic and Bronze Ages, substantial climatic and environmental changes were considered essential triggers for the rise and fall of ancient civilizations and cultures (Weiss and Bradley, 2001; Dong et al., 2017). However, the scope and intensity of human colonization in Eurasia during this period far exceeded those in the Paleolithic Age, which was facilitated by the "Agriculture and Neolithic Revolution" and the extensive dispersal of new technologies and ideologies across the Old World (Chen et al., 2015; Frachetti et al., 2017). Farming and herding groups settled in many ecosystems of mid-latitude Eurasia since the late Neolithic period (Liu et al., 2019; Dong et al., 2022) and might have significantly influenced ecosystem and soil dynamics in local and regional scales during the Bronze Age (Zhang et al., 2017; Cheng et al., 2018).

Though significant progress has been achieved focusing on prehistoric human-environment interaction evolution, some important Research Topic remain unclear or debated. For example, how have humans adapted to harsh environments in different geographical conditions and cultural landscapes? Could prehistoric groups respond to the same climate events in other ways? Was the general decline of forest vegetation in the East Asian Monsoon region since the late mid-Holocene primarily triggered by human activities or natural climate change? Have prehistoric groups migrated to build trans-regional exchange or mitigate survival pressure? The twelve case studies in this Research Topic provide valuable new data and perspectives to promote the research on the above mentioned Research Topic.

Recent archaeological studies indicated that northern Xinjiang of northwest China acted as key passageways for the dispersal of modern humans during the late Paleolithic (Li et al., 2020) and trans-Eurasian exchange during the late Neolithic and Bronze Age (Zhou et al., 2020; Qiu et al., 2023). Liu et al. explore the environmental background for prehistoric human occupations in the area based on the application of optically stimulated luminescence dating and analysis of pollen and multiple paleoclimate proxies from a loess-paleosol sequence in the Ili Valley of northwest Xinjiang. The results suggest that the environment was cold and dry with frequent dust storms during ~36–22 ka B.P. Meanwhile, vegetation recovered, and the climate warmed and precipitation increased since ~22 ka B.P. in the area. Yin et al. examine the relationship between geomorphic features and economic strategies of the 127 archaeological sites and cemeteries dated between 3,000–200 BCE in Xinjiang. They propose that humans adopted to different livelihoods to inhabit diverse landscapes in Xinjiang during the Bronze and early Iron Ages. For instance, sites near mountains were more likely to develop a mixed pastoral-hunting economy, and oasis communities of a specific size were more likely to build a mixed agricultural-pastoral economy.

Pollen analysis has also been applied to detect the effects of prehistoric human activities on natural environments. In South China, the influence of human activities on vegetation succession was traced back to ~6,000 BP (Cheng et al., 2018). To investigate the anthropogenic impact on the vegetation cover in the Lower Yangtze region, Deng et al. drill a sediment core from a rice field outside the Luotuodun Neolithic site and conduct radiocarbon dating and palynological and paleoclimatic indexes analysis. Their work suggests that human activities influenced regional marshland landscapes since ~7,500 BP, much earlier than deforestation around 6,500 BP. Based on the simulation of forest vegetation change in the northeastern Qinghai-Tibet Plateau, Wende et al. suggest that forest vegetation roughly expanded from the early Holocene to 6,000 BP and was scarcely disturbed by human activities, while the shrinking trend of forest vegetation during 5,300–2,600 BP was affected by human activities. The significant disturbance of prehistoric humans on vegetation cover in the northeastern Qinghai-Tibet Plateau occurred between 4,000 and 2,600 BP, which was induced by forest resource exploitation related to agricultural development and pastoralism expansion.

The transport networks for massive human migrations and trans-regional exchange in Eurasia during the prehistoric era have been intensively discussed recently (Li et al., 2020; Ma et al., 2022). The Qinghai-Tibet Plateau (QTP) is generally identified as a barrier for human migrations during prehistoric times. Lancuo et al. reconstruct the communication routes for human societies on the QTP from the Neolithic to Bronze Age through high-precision route simulation. They propose that river valleys on the QTP were often chosen as routes to facilitate ancient humans' adaptation to the cold, hypoxia, and gradually increasing altitude promoted by the interaction between agricultural and pastoral groups during the Neolithic and Bronze periods. In the lower reach of the Yangtze River, it is unclear the pathway for ancestors of the Liangzhu culture (5,300–4,200 BP) migrated northward from the Taihu Lake Plain to the Jianghuai region. Xiao et al. suggest the area between Changzhou-Jiangyin-Zhangjiagang should be the best place for Liangzhu groups to cross the Yangtze River. This work also discusses the potential routes based on the comprehensive analysis of archaeological, paleogeographic, and dating datasets in the areas where the Liangzhu sites are scattered.

The studies of prehistoric human strategies in response to significant global climate deterioration events are compelling questions in the research of human-environment interaction. How Paleolithic groups adapted to the harsh environment in arid areas of northwestern China during the cold-dry Younger Dryas event (~12,900–11,700 BP) remains enigmatic due to the absence of archaeobotanical and zooarchaeological data in sites dated to that period. Zheng et al. explore the research topic based on the archaeobotanical analysis in the Pigeon Mountain site location 10. Macro-plant remains from culture layers were dated to ~12,400–12,100 BP. They propose that humans might have utilized wild plant resources, including *Agriophyllum squarrosum* and *Artemisia sieversiana*, in addition to hunting prey in Pigeon Mountain ca. 12,000 to 13,000 years ago. This interesting case study suggests the exploitation of wild plant resources potentially enhanced foragers' adaptability to arid and cold habitats before the dawn of the Neolithic era.

How Neolithic groups responded to the well-known 4.2 ka event at transitional periods between the middle and late Holocene is an intensively debated Research Topic. Zhang and Zhang analyze thousands of document-based data on archaeological sites and compared two pairs of successive cultural types, i.e., the Majiayao (5,300–4,000 BP)-Qijia (4,200–3,600 BP) cultures and the Longshan (4,600–3,900 BP)-Yueshi (3,900–3,500 BP) cultures in both ends of northern China, using the one-way analysis of variance (one-way ANOVA) and standard deviational ellipse (SDE) with its parameters and frequency histogram. They find that the locations of prehistoric settlements for the "inherited" (i.e., the Qijia and Yueshi) cultures became more decentralized on the regional scale. Such a pattern is explained by human resilience (including adaptation and even migration) for pursuing better living conditions in response to the 4.2 ka climate event. Focusing on the same Research Topic, Wei et al. analyze the assemblage of plant remains, grain size, and carbon isotope of millet macro-fossils from two excavated sites that were dated between ~4,800 and 4,400 BP and ~4,200–3,900 BP in the mid-lower Hulu River Valley, western Loess Plateau. They conclude that local Neolithic farmers might have adopted a strategy of expanding cultivated lands to promote social development under a relatively cold-dry climate during ~4,200–3,900 BP rather than improving cultivation management or altering cropping patterns that occurred around 5,500 BP in the same area (Yang et al., 2022; Ma et al., 2023). These studies suggest that Neolithic groups may adopt different strategies to adapt to the same climate deterioration events on

local to regional scales, implying human-environment interaction became complicated during the late prehistoric period, which was affected by both natural and social factors, such as spatial differences in geographical environment, and human subsistence strategies.

The spatial-temporal variation of human subsistence strategies during late prehistoric times is a research focus. Zooarchaeological and isotopic analysis serve as essential approaches to reconstruct ancient human livelihoods. Most zooarchaeological studies focused on the variations in the proportions of terrestrial mammal (especially livestock) remains from the Neolithic to Bronze Age. However, how prehistoric humans utilized fish resources has not been well understood. Yu and Cui investigate the relation between the body size and age of modern Chinese sea bass in different regions of coastal China. They provide a empirical analysis to explore the body size and age of Chinese sea bass remains identified from the Guyue Neolithic site in the Pearl River Delta region. Understanding human strategies for using fishery resources in coastal areas of south China during the late Neolithic period is valuable. The spatial patterns of human livelihoods in East Asia changed remarkably compared to the Neolithic era, after the introduction of wheat, barley, sheep/goats, and cattle that were first domesticated in West Asia. Lu et al. obtain and analyze new isotopic data from Bronze sites in the Hengduan Mountain Region of southwestern China, and inferred that humans adopted diverse subsistence strategies in the context of the trans-Eurasia exchange, to adapt the spatial heterogeneity of local environments in the Hengduan Mountian Region during ~2,750 BP–2,450 BP.

Most studies of human subsistence strategy in East Asia are often focused on Neolithic-Bronze Age. Whereas, the variation in livihood for the early historical period is not fully understood. Wang et al. report new zooarchaeological data from the excavation at the Nantou Locale of Xitou site in the Guanzhong region. The results show that pigs were the dominant animal subsistence in the site during ~5,000–2,000 BCE, the importance of cattle and caprines in animal subsistence increased between ~11th and 8th centuries BCE, while pigs became the most important livestock again during the Han-Tang periods (~2nd century BCE -10th century C.E.). The variation of animal resource exploitation strategies in the Guanzhong region from the Neolithic to historical periods was affected by both social and natural factors, which is valuable in understanding the significance of changing animal utilization strategies in human-environment interaction evolution throughout prehistoric and historical periods.

In summary, the 12 case studies in the Research Topic "Human-Environmental Interactions in Prehistoric Periods II" discussed different aspects of prehistoric human-environment interaction in East Asia, spanning from the late Paleolithic, Neolithic, Bronze Age, early Iron Age to historical periods. These works contribute to a better understanding of the trajectories, patterns, and influencing factors of the evolution of human-environment interaction from a long-term perspective. However, the interaction between human activities and their living environment in human history is very complex and varies significantly in both time and space. More interdisciplinary research, especially between archaeology and earth sciences, and the application of new methods (e.g., sedimentary ancient DNA) are crucial to promoting the advancement in this research field in the near future.

Author contributions

GD: Writing–original draft, Writing–review and editing. HL: Writing–original draft, Writing–review and editing. RL: Writing–original draft, Writing–review and editing.

Funding

This work was supported by the NSFC-INSF Joint Research Project (Grant No. 42261144670) and Academician and Expert Workstation of Yunnan Province (No. 202305AF150183).

Conflict of interest

The authors declare that the research was conducted in the absence of any commercial or financial relationships that could be construed as a potential conflict of interest.

Publisher's note

All claims expressed in this article are solely those of the authors and do not necessarily represent those of their affiliated organizations, or those of the publisher, the editors and the reviewers. Any product that may be evaluated in this article, or claim that may be made by its manufacturer, is not guaranteed or endorsed by the publisher.

References

Chen, F. H., Dong, G. H., Zhang, D. J., Liu, X. Y., Jia, X., An, C. B., et al. (2015). Agriculture facilitated permanent human occupation of the Tibetan Plateau after 3600 BP. *Science* 347, 248–250. doi:10.1126/science.1259172

Cheng, Z. J., Weng, C. Y., Steinke, S., and Mohtadi, M. (2018). Anthropogenic modification of vegetated landscapes in southern China from 6, 000 years ago. *Nat. Geosci.* 11 (12), 939–943. doi:10.1038/s41561-018-0250-1

Dearing, J. A., Battarbee, R. W., Dikau, R., Larocque, R., and Oldfield, F. (2006). Human–environment interactions: learning from the past. *Reg. Environ. Change* 6, 1–16. doi:10.1007/s10113-005-0011-8

Dong, G. H., Du, L. Y., Yang, L., Lu, M. X., Qiu, M. H., Li, H. M., et al. (2022). Dispersal of crop-livestock and geographical-temporal variation of subsistence along the Steppe and Silk Roads across Eurasia in prehistory. *Sci. China Earth Sci.* 65, 1187–1210. doi:10.1007/s11430-021-9929-x

Dong, G. H., Li, R., Lu, M. X., Zhang, D. J., and James, N. (2020). Evolution of human-environmental interactions in China from the late paleolithic to the bronze age. *Prog. Phys. Geog.* 44 (2), 233–250. doi:10.1177/0309133319876802

Dong, G. H., Liu, F. W., and Chen, F. H. (2017). Environmental and technological effects on ancient social evolution at different spatial scales. *Sci. China Earth Sci.* 60, 2067–2077. doi:10.1007/s11430-017-9118-3

Frachetti, M. D., Smith, C. E., Traub, C. M., and Williams, T. (2017). Nomadic ecology shaped the highland geography of Asia's Silk Roads. *Nature* 543, 193–198. doi:10.1038/nature21696

Huang, X. Z., Liu, S. S., Dong, G. H., Qiang, M. R., Bai, Z. J., Zhao, Y., et al. (2017). Early human impacts on vegetation on the northeastern Qinghai-Tibetan Plateau during the middle to late Holocene. *Prog. Phys. Geog.* 41 (3), 286–301. doi:10.1177/0309133317703035

Li, F., Petraglia, M., Roberts, P., and Gao, X. (2020). The northern dispersal of early modern humans in eastern Eurasia. *Sci. Bull.* 65, 1699–1701. doi:10.1016/j.scib.2020.06.026

Liu, X. Y., Jones, P. J., Matuzeviciute, G. M., Hunt, H., Lister, D. L., An, T., et al. (2019). From ecological opportunism to multi-cropping: mapping food globalisation in prehistory. *Quat. Sci. Rev.* 206, 21–28. doi:10.1016/j.quascirev.2018.12.017

Ma, M. M., Dong, J. J., Yang, Y. S., Martin, K. J., Wang, J., Chen, G. K., et al. (2023). Isotopic evidence reveals the gradual intensification of millet agriculture in Neolithic western Loess Plateau. *Fundam. Res.* doi:10.1016/j.fmre.2023.06.007

Ma, M. M., Lu, Y. X., Dong, G. H., Ren, L. L., Min, R., Kang, L. H., et al. (2022). Understanding the transport networks complex between south Asia, southeast Asia and China during the late neolithic and bronze age. *Holocene* 33 (2), 147–158. doi:10.1177/09596836221131698

Magill, C. R., Ashley, G. M., and Freeman, K. H. (2013). Ecosystem variability and early human habitats in eastern Africa. *Proc. Natl. Acad. Sci. U. S. A.* 110 (4), 1167–1174. doi:10.1073/pnas.1206276110

Pitulko, V. V., Tikhonov, A. N., Pavlova, E. Y., Nikolskiy, P., Kuper, K., and Polozov, R. N. (2016). Early human presence in the Arctic: evidence from 45000-year-old mammoth remains. *Science* 351 (6270), 260–263. doi:10.1126/science.aad0554

Qiu, M. H., Liu, R. L., Li, X. Y., Du, L. Y., Ruan, Q. R., Pollard, A. M., et al. (2023). Earliest systematic coal exploitation for fuel extended to ~3600 B.P. *Sci. Adv.* 9, eadh0549. doi:10.1126/sciadv.adh0549

Robinson, J. R., Rowan, J., Campisano, C. J., Wynn, J. G., and Reed, K. E. (2017). Late Pliocene environmental change during the transition from Australopithecus to Homo. *Nat. Ecol. Evol.* 1 (6), 0159. doi:10.1038/s41559-017-0159

Ruddiman, W. F., Fuller, D. Q., Kutzbach, J. E., Tzedakis, P. C., Kaplan, J. O., Ellis, E. C., et al. (2016). Late Holocene climate: natural or anthropogenic? *Rev. Geophys.* 54 (1), 93–118. doi:10.1002/2015rg000503

Stiner, M. C., Munro, N. D., and Surovell, T. A. (2000). The tortoise and the hare: small-game use, the broad-spectrum revolution, and paleolithic demography. *Curr. Anthropol.* 41, 39–79. doi:10.1086/300102

Timmermann, A., and Friedrich, T. (2016). Late Pleistocene climate drivers of early human migration. *Nature* 538 (7623), 92–95. doi:10.1038/nature19365

Timmermann, A., Yun, K. S., Raia, P., Ruan, J. Y., Mondanaroet, A., Zeller, E., et al. (2022). Climate effects on archaic human habitats and species successions. *Nature* 604, 495–501. doi:10.1038/s41586-022-04600-9

Weiss, H., and Bradley, R. S. (2001). What drives societal collapse? *Science* 291, 609–610. doi:10.1126/science.1058775

Wende, Z. M., Hou, G. L., Gao, J. Y., Chen, X. M., Jin, S. M., and Lancuo, Z. M. (2021). Reconstruction of cultivated land in the northeast margin of Qinghai–Tibetan plateau and anthropogenic impacts on palaeo-environment during the mid-holocene. *Front. Earth Sci.* 9, 681995. doi:10.3389/feart.2021.681995

Yang, Y. S., Wang, J., Li, G., Dong, J. J., Cao, H. H., Ma, M. M., et al. (2022). Shift in subsistence crop dominance from broomcorn millet to foxtail millet around 5500 BP in the western Loess Plateau. *Front. Plant Sci.* 13, 939340. doi:10.3389/fpls.2022.939340

Zhang, S. J., Yang, Y. S., Storozum, M. J., Li, H. M., Cui, Y. F., and Dong, G. H. (2017). Copper smelting and sediment pollution in bronze age China: A case study in the hexi corridor, northwest China. *Catena* 156, 92–101. doi:10.1016/j.catena.2017.04.001

Zhang, X. L., Ha, B. B., Wang, S. J., Chen, Z. J., Ge, J. Y., Long, H., et al. (2018). The earliest human occupation of the high-altitude Tibetan Plateau 40 thousand to 30 thousand years ago. *Science* 362 (6418), 1049–1051. doi:10.1126/science.aat8824

Zhou, X. Y., Yu, J. J., Spengler, R. N., Shen, H., Zhao, K. L., Ge, J. Y., et al. (2020). 5,200-year-old cereal grains from the eastern Altai Mountains redate the trans-Eurasian crop exchange. *Nat. Plants* 6, 78–87. doi:10.1038/s41477-019-0581-y

frontiers | Frontiers in Ecology and Evolution

TYPE Original Research
PUBLISHED 08 November 2022
DOI 10.3389/fevo.2022.1018615

Check for updates

OPEN ACCESS

EDITED BY
Ren Lele,
Lanzhou University, China

REVIEWED BY
Lisa Yeomans,
University of Copenhagen, Denmark
Masashi Maruyama,
Tokai University, Japan

*CORRESPONDENCE
Chong Yu
yuchong3@mail.sysu.edu.cn

SPECIALTY SECTION
This article was submitted to Paleoecology, a section of the journal Frontiers in Ecology and Evolution

RECEIVED 13 August 2022
ACCEPTED 10 October 2022
PUBLISHED 08 November 2022

CITATION
Yu C and Cui Y (2022) Body size and age estimation of Chinese sea bass (*Lateolabrax maculatus*) and evidence of Late Neolithic fishing strategies, a case study from the Guye site. *Front. Ecol. Evol.* 10:1018615. doi: 10.3389/fevo.2022.1018615

COPYRIGHT
© 2022 Yu and Cui. This is an open-access article distributed under the terms of the Creative Commons Attribution License (CC BY). The use, distribution or reproduction in other forums is permitted, provided the original author(s) and the copyright owner(s) are credited and that the original publication in this journal is cited, in accordance with accepted academic practice. No use, distribution or reproduction is permitted which does not comply with these terms.

Body size and age estimation of Chinese sea bass (*Lateolabrax maculatus*) and evidence of Late Neolithic fishing strategies, a case study from the Guye site

Chong Yu[1]* and Yong Cui[2]

[1]School of Sociology and Anthropology, Sun Yat-sen University, Guangzhou, China, [2]Guangdong Provincial Institute of Archaeology and Cultural Relics, Guangzhou, China

Fishing was an important form of subsistence economy among ancient societies. However, details of past fishing activities have been rarely studied in China. This paper uses data extracted from a modern fish collection to estimate the body size and age of Chinese sea bass from the Guye site, a common species that is frequently discovered in archaeological sites of coastal South China. The distribution of body size and age were reconstructed and combined with fish biology and ecology; the current dataset revealed that the main fishing grounds of the Late Neolithic Guye people were close to the shoreline, and the main fishing season was from spring to early autumn.

KEYWORDS

body size estimation, age estimation, Chinese sea bass, Guye site, ichthyoarchaeology

Introduction

The reconstruction of fish body size is an important indicator that not only provides crucial information about the size range and distribution of fish size in an ichthyoarchaeological assemblage, but allows further interpretation of past fishing methods, grounds, gears, and seasons (Wheeler and Jones, 1989). Previous ichthyofaunal studies in China focused on the freshwater taxa from the Tianluoshan and Jiahu sites in the Lower Yangtze River region (Nakajima et al., 2011, 2012, 2015, 2019; Matsui et al., 2016; Zhang, 2018; Maruyama et al., 2021). The regression formulas for common carp (*Cyprinus carpio*) and snake head (*Channa argus*) were calculated aiming to look for early aquaculture and rice paddy field management (Zhang, 2018; Nakajima et al., 2019).

However, given that the varied fish species from the Pearl River Delta region of South China are very different from those of the Lower Yangtze River region, it is necessary to select some species of fish to initially develop the use of osteometric measurements as a means of estimating fish body size. This study provides regression formulas for size estimation of Chinese sea bass (*Lateolabrax maculatus*), the most abundant marine species in the Guye site and is also commonly recovered from archaeological sites bordering coastal South China (Yu and Cui, 2021). The present study reveals the

patterns of the body size and age of Chinese sea bass that are linked with fishing strategies in coastal South China during the Late Neolithic age, which helps to elucidate the mechanisms of the sustainability and complexity of fishing-hunting-gathering communities in antiquity.

Ichthyological biology and ecology

There has been disagreement on the ichthyological taxonomy of Lateolabrax (Teleostei: Perciformes: Lateolabracidae: Lateolabrax). FishBase (Froese and Pauly, 2022) and the latest version of *Fishes of the World* (Nelson et al., 2016) suggest there are only two species in genus Lateolabrax, namely *L. japonicus* (Japanese sea bass) and *L. latus* (black fin sea bass). However, local ichthyologists argued that *L. maculatus* (Chinese sea bass) and *L. japonicus* are different species based on modern morphology, genetics, ecological habits, and natural distributions (Yokogawa, 1993, 2004, 2019; Yokogawa and Seki, 1995). The Chinese sea bass is characterized by its lifelong black spots on body and dorsal fins although some might gradually downsize with growth, generally they are still larger than the scales (Figure 1). It is broadly distributed along the entire Chinese coast's offshore waters including the Bohai Sea, Yellow Sea, East China Sea, South China Sea, and west coast of the Korean Peninsula (Figure 2) (Feng and Jiang, 1998). Black spots on Japanese sea bass are usually scattered above lateral line on the juvenile individuals and then vanish at 21–25 cm standard length, the spots are about the size of, or smaller than, the scales. This fish is commonly found in the east coast of the Korean Peninsula and Sea of Japan (Yokogawa and Seki, 1995; Yokogawa, 2004). Black fin sea bass have no black spots and are distributed along the entire Japanese coast's offshore waters including the west coast of the Sea of Japan, and the west shores of the Honshu, Shikoku, and Kyushu islands (Katayama, 1957; Overseas fishery cooperation foundation of Japan, 2009; Wu and Zhong, 2021). Although we are unable to distinguish the bone characteristics among them due to the lack of comparative material, the main fisheries in prehistoric coastal South China can be identified as *L. maculatus* according to their modern distribution.

Chinese sea bass is a euryhaline teleost which can live in salinities ranging from freshwater to seawater environments. Some juveniles can survive in freshwater where they grow into adults before migrating back into the ocean to spawn. Chinese sea bass are frequently found in the moving water of rocky reefs when they are inshore. They migrate seasonally, leaving the coast during winter to stay in wintering grounds and spawn, usually in an offshore area; and enter shallow waters near the coast or inside the bay in spring and summer for feeding. The older the fish is, the further they migrate (Feng and Jiang, 1998).

Materials and methods

Modern fish collection

A total of 20 Chinese sea bass were collected at fish markets of coastal China, including Dalian (Liaoning province), Ningbo (Zhejiang province), Guangzhou, and Zhanjiang (Guangdong province) (Figure 2). Body measurements were conducted, including standard length (SL) in millimeters, and the total fresh weight (W) in grams (Figure 1). The Chinese sea bass involved in this study ranged from 116 to 740 mm and from 23 to 5675 g (Table 1). According to Feng and Jiang (1998), this species can reach 817 mm in standard length, which indicates that our collection covered almost the full range of size that this species can attain, although the number of individuals is not

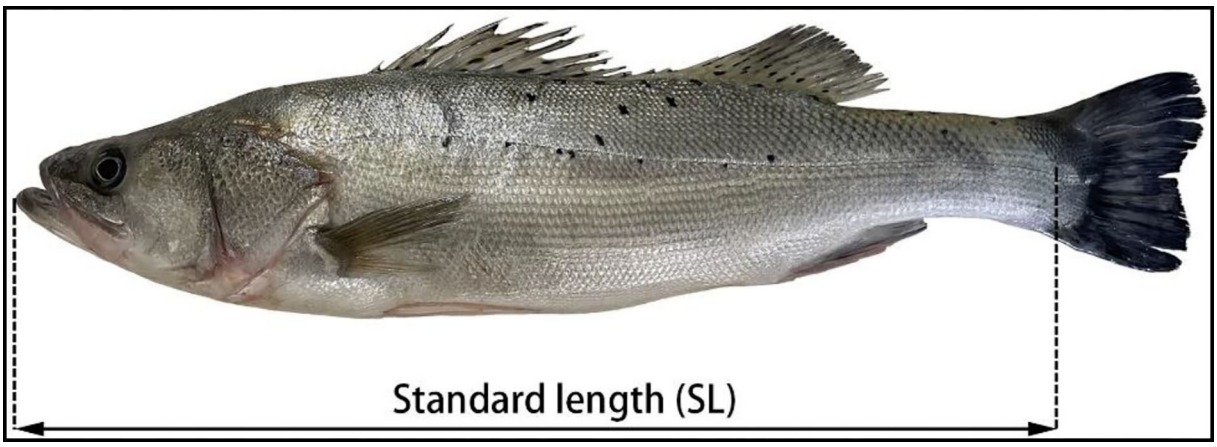

FIGURE 1
Chinese sea bass and measurement illustration of standard length (SL).

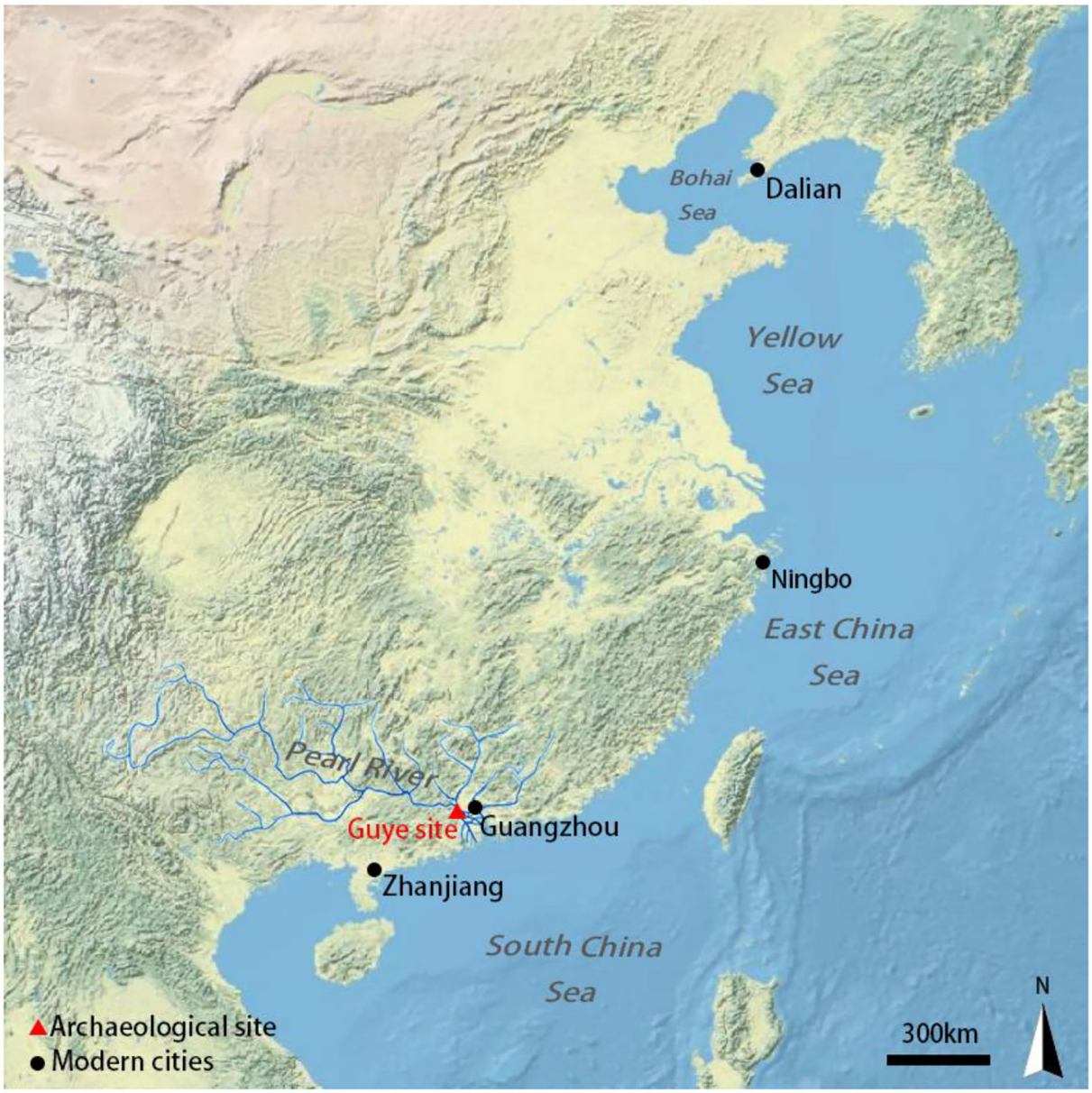

FIGURE 2
Location of the Guye site and the comparative collections.

as great as many similar studies (Yeomans, 2016; Lidour et al., 2018; Martínez-Polanco and Béarez, 2020; Rurua et al., 2020; Martínez-Polanco et al., 2022).

Osteological nomenclature of bones mainly follows Lepiksaar (1994) and Dye and Longenecker (2004). Bone measurements are described in Table 2 and illustrated in Figure 3. All biometric data were taken using a Mitutoyo caliper (precision: tenths of a millimeter) with a precision of two decimal points. The same dimensions of the right and left sides are averaged.

Archaeological samples

The site of Guye (Late Neolithic period, 5,900–5,400 cal. BP) is situated on the west bank of the Pearl River Delta, and was proved to be the earliest shell midden site of the region (Cui, 2007). All the excavated sediments were systematically wet sieved using different sizes of meshes (1.5 and 4 mm). This sampling method provided enormous amounts of faunal remains. Preliminary zooarchaeological investigations have revealed that the subsistence economy of Guye heavily

TABLE 1 Standard length, weight, and location of collection of Chinese sea bass (*Lateolabrax maculatus*) used in this study.

No.	SL (mm)	W (g)	Location of collection
006	330	650	Guangzhou
029	320	594	Guangzhou
035	340	718	Guangzhou
054	310	700	Guangzhou
167	430	1,043	Dalian
202	620	3,605	Ningbo
203	200	162	Ningbo
204	185	128	Ningbo
205	116	23	Ningbo
211	480	165	Zhanjiang
212	490	2,139	Zhanjiang
217	740	5,675	Ningbo
419	592	2,620	Ningbo
420	625	4,270	Ningbo
456	620	3,400	Ningbo
457	535	2,200	Ningbo
458	710	4,250	Ningbo
470	620	2,910	Ningbo
475	437	1,250	Ningbo
476	655	3,910	Ningbo

relied on fishing. Among the whole assemblage, 11,407 fish bones were sorted with a total of 2,452 remains identified to family level or below (i.e., genus, species), making it the first ichthyofaunal dataset from prehistoric populations in coastal South China. Chinese sea bass was the most common marine species, it comprised about 22% of the total NISP and MNI (Yu and Cui, 2021).

The calculation of regression formulas

The calculation of regression formulas for Chinese sea bass was based on a set of modern fish collected with known length and weight (Table 1). Clear dimensions shown on Figure 3 were used to generate length-length and length-weight equations represented by $Y = aX^b$ whereas Y is the standard length and weight of the fish, respectively, X is the measurement of the representative dimension from the modern collection. The quality of the relationship is given by the coefficient of determination (R^2) which ranges from 0 to 1. The value of R^2 shows whether the model would be a good fit for the given data set. Generally, a higher coefficient indicates a better fit for the model. With good coefficient of determination, the functions can be used to estimate the length and the weight of the fish from its isolated bones.

Result

Length-weight equation

A standard length-weight model was obtained in the form $W = aSL^b$, with the W in grams and the SL in millimeters. The standard length-weight relationships reflected a slight allometric growth ($b = 2.815$), with a high coefficient of determination ($R^2 = 0.9879$) (Figure 4).

Bones measurements and regression analysis

Equations are given in the form $SL_{fish} = aM^b_{bone}$, where all the measurements are taken and calculated in millimeters. The a and b parameters and R^2 are provided in Table 3. All of the equations show a good coefficient of determination; the maximal R^2 is 0.9925, the minimal R^2 is 0.9591, with an average of 0.9803. The correlations of the preopercle measurements ($R^2_{M1} = 0.9909$; $R^2_{M2} = 0.9887$; $R^2_{AVG} = 0.9898$) are very good. Followed by hyomandibular ($R^2_{M1} = 0.9888$; $R^2_{M2} = 0.9904$; $R^2_{AVG} = 0.9896$). The measurements of maxilla provide the lowest coefficients, still superior to 0.967, however.

Ichthyoarchaeological application

The ichthyoarchaeological application of regression formulas needs a set of measurements from frequent and well-preserved bones in the archaeological assemblages. According to the distribution of fish skeletal parts from the Guye site, the most frequently recovered element of Chinese sea bass is the opercle (Table 4), which is diagnostic with its thickness and pointedness at the posterior end. However, the opercle is very porous as seen from the cross section, which might be the cause of high fragmentation of this element, and therefore it lacks measurable dimension. The anterior of the dentary is very robust and the three oval openings on the outer surface make it easy to identify (Yu, 2022). Thus, the anterior height of the dentary (Den M1) was selected for the reconstruction of body length, due to its high correlation coefficient and frequency ($R^2 = 0.9729$) of corresponding bones in the archaeological contexts (Figure 5).

In total, 70 measurements of Den M1 were collected from the Guye assemblage, the minimal reconstructed length was 148.47 mm (SL) and the maximum was 728.7 mm (SL), which gave a mean of 417.79 mm (SL) and a median of 433.18 mm (SL). The main size class represented was 250–550 mm ($N = 51$; 72.86% of the total population) (Figure 6).

TABLE 2 Descriptions of the bone measurements taken from Chinese sea bass (*Lateolabrax maculatus*) skeletons.

Measurements	Abbreviation	Description
Vomer M1	Vom M1	Maximal mediolateral width of the vomer
Basioccipital M1	Boc M1	Maximal width of the articular surface of the basioccipital
Basioccipital M2	Boc M2	Maximal height of the articular surface of the basioccipital
Premaxilla M1	Pmx M1	Maximal length of the ascending process of the premaxilla
Premaxilla M2	Pmx M2	Maximal length of the premaxilla, from the rostral tip to the tip of the caudal process
Premaxilla M3	Pmx M3	Thickness of the tooth plate
Maxilla M1	Mx M1	Distance between the dorsal condyle and the ventral tips of the external and internal processes
Maxilla M2	Mx M2	Maximal width of the dorsal condyle
Maxilla M3	Mx M3	Maximal length of the maxilla, from the rostral tip of the external process to the tip of the caudal processes
Dentary M1	Den M1	Anterior height of the dentary
Dentary M2	Den M2	Maximal height, between the coronoid and the ventral processes
Dentary M3	Den M3	Maximal length, from the rostral tip of the dentary to the caudal tips of the coronoid and ventral processes
Articular M1	Art M1	Maximal length, between posterior ventralis angulus and the anterior process
Articular M2	Art M2	Maximal height, between the coronoid processes and anterior ventralis angulus
Articular M3	Art M3	Maximal width of the quadrate facet
Quadrate M1	Qd M1	Distance between the external tip of the lateral condyle and the internal tip of the mesial condyle
Quadrate M2	Qd M2	Distance between the ventral tip of the mesial condyle and the dorsal tip of the ectopterygoid margin
Quadrate M3	Qd M3	Distance between the tip of the mesial condyle and the tip of the preopercular process
Palatine M1	Pal M1	Maximal length of the palatine
Hyomandibular M1	Hm M1	Distance between the sphenotic facet and the opercular process
Hyomandibular M2	Hm M2	Distance between the symplectic facet and the line joining the tips of the sphenotic and pterotic facets
Opercle M1	Op M1	Maximal height of opercle
Opercle M2	Op M2	Maximal width, from the articular fossa to the tip of the posterior angulus
Preopercle M1	Pop M1	Maximal length of the preopercle
Preopercle M2	Pop M2	Maximal height of the preopercle
Post-temporal M1	Ptp M1	Distance between the tips of the two processes
Post-temporal M2	Ptp M2	Distance between ventral process tip and posterior tip
Post-temporal M3	Ptp M3	Distance between dorsal process tip and posterior tip
First vertebra M1	FV M1	Maximal width of the exoccipital articular surface
First vertebra M2	FV M2	Maximal height of the vertebra
First vertebra M3	FV M3	Maximal height of the centrum (cranial side)
First vertebra M4	FV M4	Maximal width of the centrum (cranial side)
First vertebra M5	FV M5	Maximal width between the lateral processes (cranial side)
Sagitta M1	Sag M1	Maximal length (rostro-caudal axis)
Sagitta M2	Sag M2	Maximal height (dorso-ventral axis)
Cleithrum M1	Cl M1	Maximal length of the cleithrum
Cleithrum M2	Cl M2	Distance between the tip of the anterodorsal process and the scapula joint

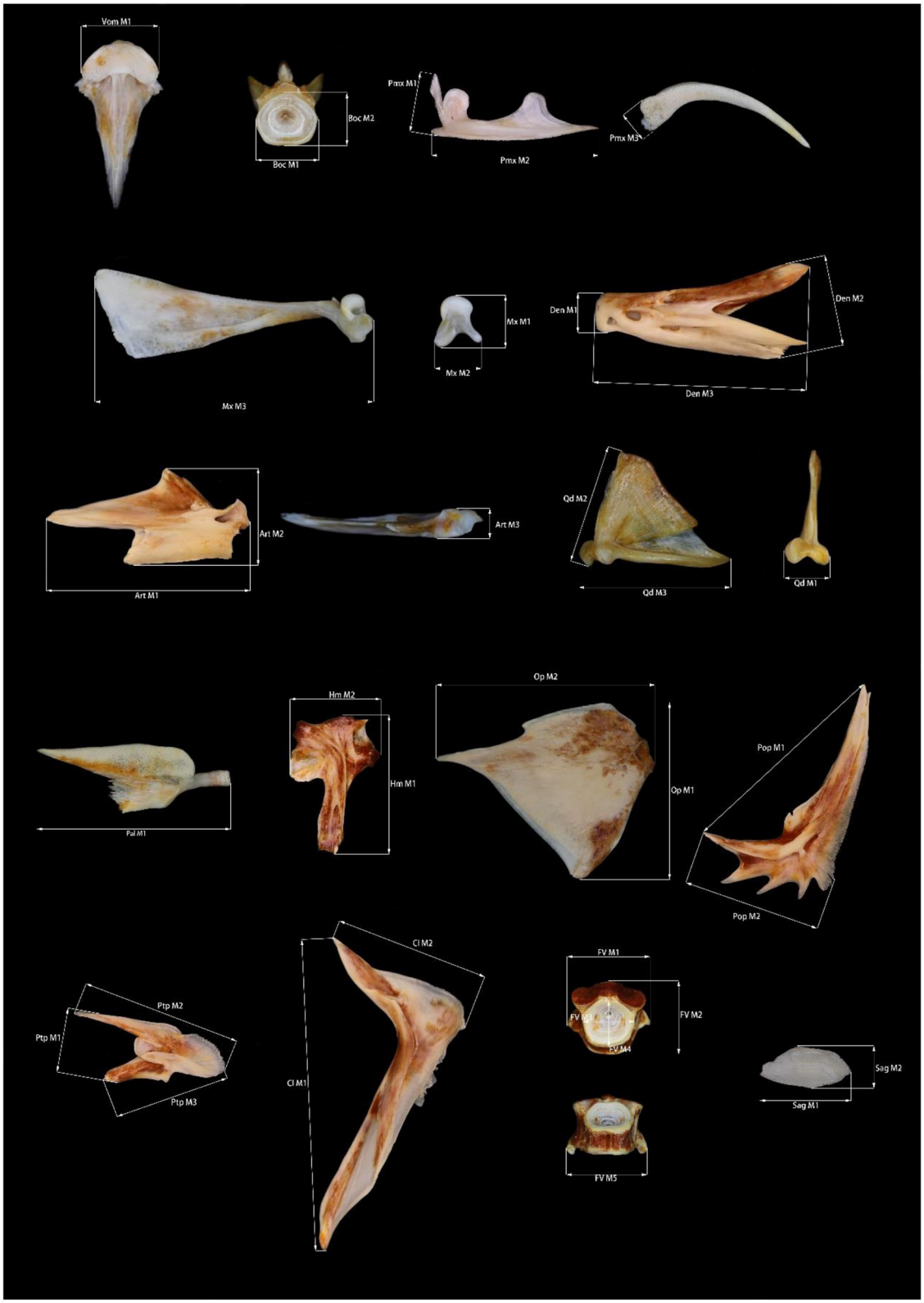

FIGURE 3
Position of the osteological measurements taken from Chinese sea bass.

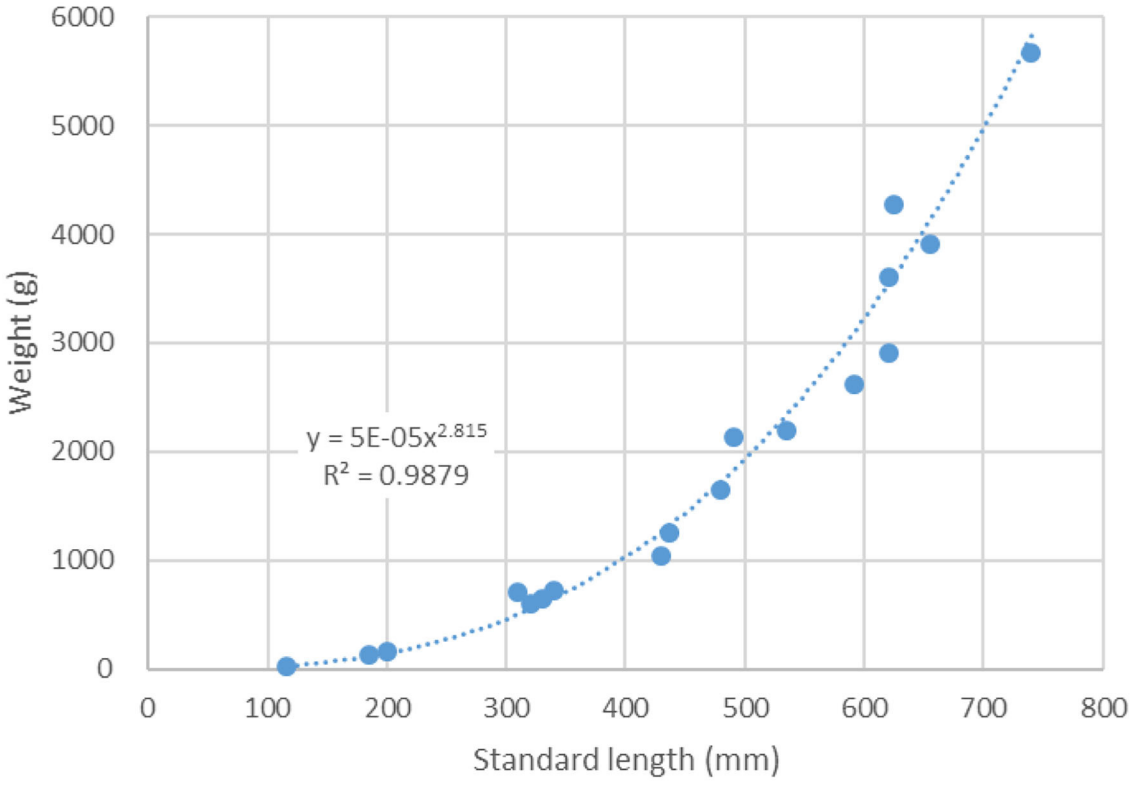

FIGURE 4
Standard length (SL) to weight (W) relationship of the modern sample of *Lateolabrax maculatus*.

Discussion and interpretation

Length–age relation

Growth in fish is indeterminate, which means growth continues throughout the life span of an individual, although at a constantly decelerating rate. Hence older animals are generally larger (Helfman et al., 2009). To estimate the age of Chinese sea bass, we used data collected from 528 individuals from the north Yellow Sea and Bohai Sea by Feng and Jiang (1998) to generate an age-length equation (Figure 7). We then applied estimated body length by dentary anterior height to calculate age for each individual.

It is obvious that the proportion of individuals caught at an age <1 year-old is quite small (4.48%), while 65.67 % of the sea bass were caught between 1 and 3 years of age, 14.93% of the corpus were consumed around 3–4 years-old and same proportion for individuals older than 4 years of age (Figure 8). As Chinese sea bass were sexually mature around 3 years old (Feng and Jiang, 1998), this means that <30% of the catches were mature individuals.

Seasonality evidence and fishing strategies

In the fish assemblages of the Guye site, Chinese sea bass and mullet were the most common marine species. About 17% of the total NISP and MNI belong to Mugilidae, represented by opercle, dentary, lachrymal, and vertebrae. However, it is difficult to differentiate them to the genus level due to similar morphological appearances, especially in archaeological contexts. Based on their body size in modern fishery records, we assumed that mullets in the corpus probably belong to *Liza haematocheilus* (redlip mullet) or *Mugil cephalus* (striped mullet) (Yu and Cui, 2021).

Redlip mullet inhabit shallow coastal waters; they can also enter freshwater regions of rivers. They migrate offshore in the winter and move back inshore in spring for feeding and spawning. Striped mullet are frequently found coastally in estuaries and freshwater environments and inhabit sandy or muddy bottoms. Adults form huge schools and migrate offshore in large aggregations during fall and spawn during winter. Parent fish and larvae migrate back inshore to the feeding

TABLE 3 Regression formula parameters for estimating the total length of Chinese sea bass (*Lateolabrax maculatus*) from bone measurements (in mm).

Measurements	a	b	R^2	N
Vomer M1	32.363	1.0347	0.9795	17
Basioccipital M1	52.558	0.9497	0.9834	18
Basioccipital M2	57.968	0.992	0.9773	18
Premaxilla M1	25.109	1.134	0.9648	20
Premaxilla M2	7.5645	1.1416	0.9828	20
Premaxilla M3	61.087	1.066	0.9722	20
Maxilla M1	53.062	1.0568	0.9606	20
Maxilla M2	36.416	1.2029	0.9607	20
Maxilla M3	7.0716	1.0722	0.9796	20
Dentary M1	58.369	0.954	0.9729	18
Dentary M2	20.826	1.0152	0.9744	20
Dentary M3	6.9928	1.0843	0.9806	20
Articular M1	6.2663	1.11	0.9837	20
Articular M2	19.631	1.0169	0.9791	20
Articular M3	83.009	0.92	0.9591	20
Quadrate M1	67.341	0.9926	0.9749	20
Quadrate M2	18.46	1.0646	0.9849	20
Quadrate M3	13.263	1.0909	0.9908	20
Palatine M1	8.082	1.1539	0.9832	20
Hyomandibular M1	9.5926	1.1009	0.9888	20
Hyomandibular M2	19.569	1.0205	0.9904	20
Opercle M1	7.1141	1.0784	0.9883	20
Opercle M2	13.713	0.8861	0.9754	20
Preopercle M1	6.1935	1.0859	0.9909	20
Preopercle M2	9.6735	1.1153	0.9887	20
Post-temporal M1	21.256	1.1385	0.9832	20
Post-temporal M2	12.914	1.026	0.9925	20
Post-temporal M3	20.333	0.9728	0.9883	20
First vertebra M1	31.457	1.0049	0.9828	19
First vertebra M2	42.394	0.9708	0.9891	19
First vertebra M3	49.368	1.0331	0.9799	19
First vertebra M4	50.137	0.9613	0.9866	19
First vertebra M5	35.055	0.9443	0.9852	19
Cleithrum M1	3.9189	1.091	0.9904	20
Cleithrum M2	11.544	1.0182	0.9782	20
Sagitta M1	10.427	1.3363	0.9799	18
Sagitta M2	19.457	1.5234	0.9679	18

ground in spring and summer times. Striped mullet move into deeper waters as they grow (Zhao et al., 2016). Because we are unable to identify those mullets to genus or species, it is not possible to reconstruct their body size. However, their migratory patterns are almost the same as Chinese sea bass, that is, offshore during winter and inshore during spring and summer.

TABLE 4 Distribution of Chinese sea bass skeletal parts at the Guye site (in descending order of NISP).

Skeletal parts	NISP	NISP %
Opercle	167	37.70
Dentary	89	20.09
Articular	55	12.42
Premaxilla	52	11.74
Preopercle	30	6.77
Cleithrum	27	6.09
Hyomandibular	7	1.58
Palatine	5	1.13
Ceratohyal	4	0.90
Post-temporal	3	0.68
Pharyngeal bone	2	0.45
Urohyal	2	0.45
Total	443	100.00

Fishing methods in nearshore and offshore water areas are different in the modern marine fishery. Mid-water or bottom trawl and purse net are commonly used in offshore water together with advanced fishing boats, particularly during winter (Yang, 2007). In the Guye site, Chinese sea bass and mullet comprised about two-thirds of the total marine species (both NISP and MNI) (Yu and Cui, 2021). If we assume that large-scale fishing activities in offshore water during winter in the Late Neolithic period is rare, then most of the marine fish were caught when winter migration ended, during spring, summer, and early autumn in nearshore and bay areas.

Conclusion

This study, for the first time, provides regression formulas for size estimation of fish species from the coastal South China area. Measurements taken on bones of modern Chinese sea bass enable us to reconstruct the body size of fish discovered in archaeological sites. Based on the length-age equation, the majority of Chinese sea bass collected from the Guye site ranged from 250 to 550 mm and aged from 1 to 3 years old. Based on fish biology and ecology, the cluster of these individuals indicates a fishing ground close to the shoreline. In conjunction with evidence on the characteristics of migration patterns from mullet, the main fishing seasons could be ranged from spring to early autumn.

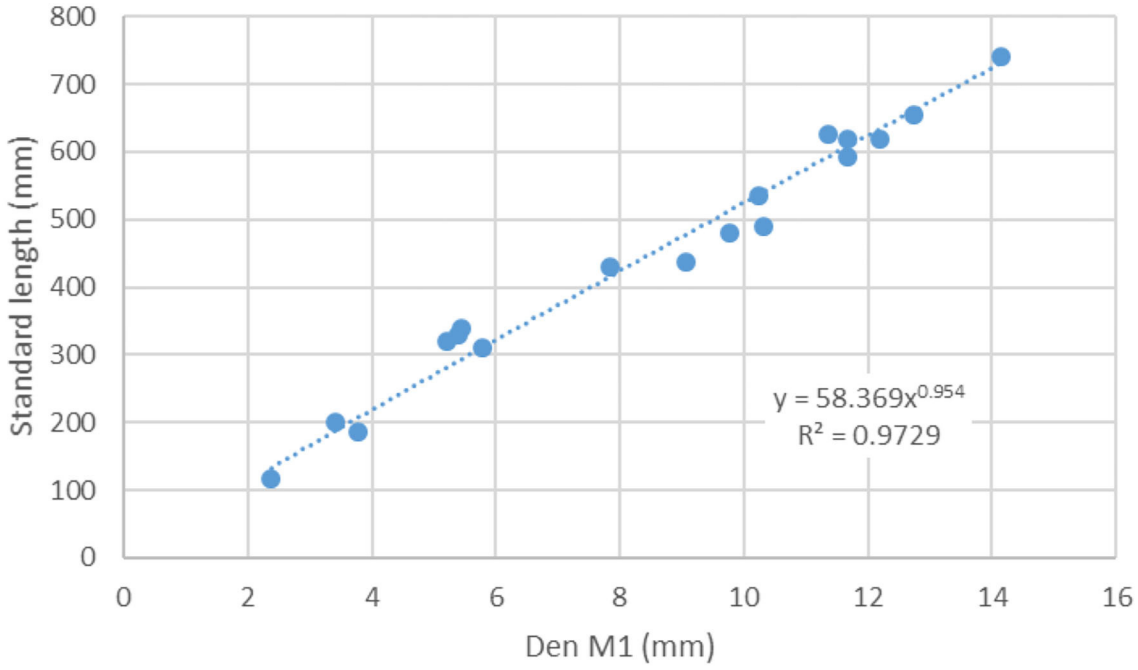

FIGURE 5
Lateolabrax maculatus graph modeling the regression formulas of Den M1 vs. SL.

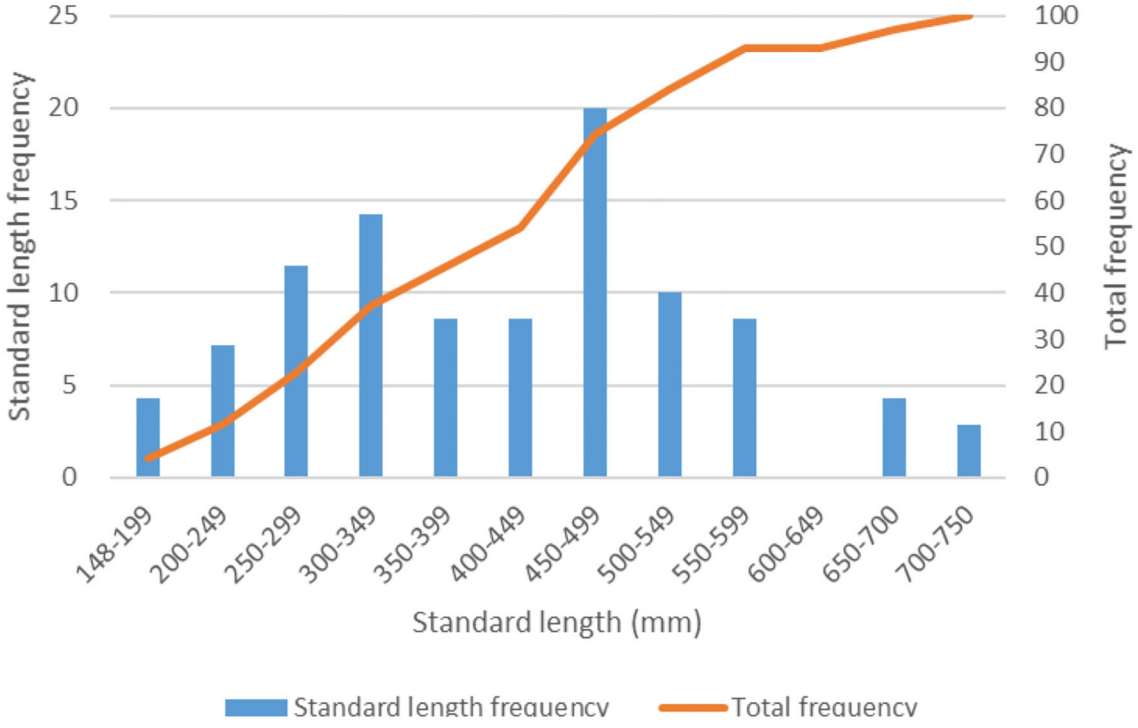

FIGURE 6
Estimated standard lengths of Chinese sea bass of Guye site, $N = 70$.

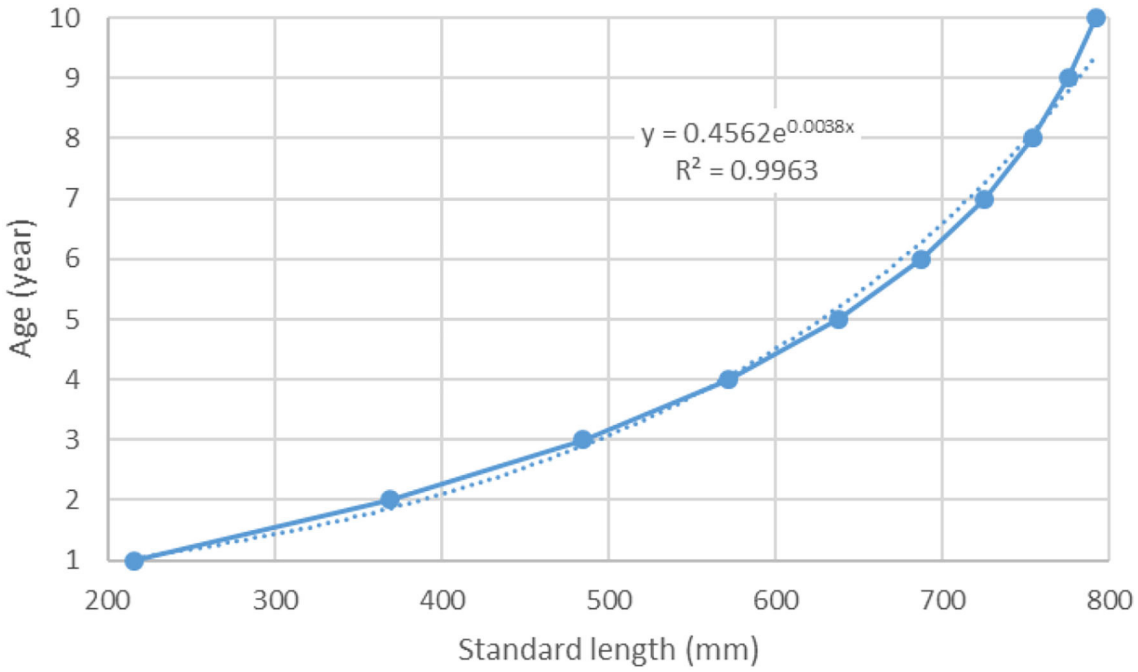

FIGURE 7
Age-length relationship of Chinese sea bass.

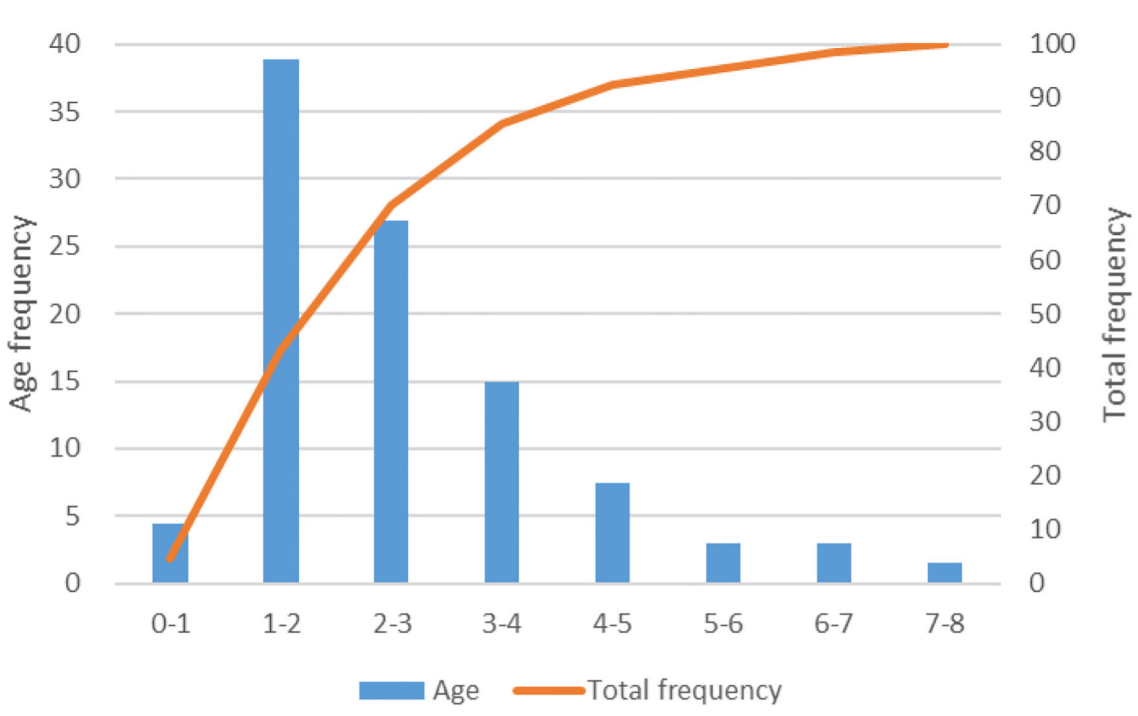

FIGURE 8
Frequency of estimated age classes of archeological Chinese sea bass.

Data availability statement

The original contributions presented in the study are included in the article/supplementary material, further inquiries can be directed to the corresponding author.

Ethics statement

Ethical review and approval were not required for the study of animals in accordance with the local legislation and institutional requirements.

Author contributions

CY: conceptualization, methodology, formal analysis, data curation, funding acquisition, writing—original draft, writing—review, and editing. YC: resources and fieldwork administration. All authors contributed to the article and approved the submitted version.

Funding

This study was supported by the National Social Science Fund of China (Grant No. 18CKG005).

Acknowledgments

We would like to thank Zixian Jiang for her contribution to photo editing. We are also grateful to the reviewers who helped us improve the final version of this paper.

Conflict of interest

The authors declare that the research was conducted in the absence of any commercial or financial relationships that could be construed as a potential conflict of interest.

Publisher's note

All claims expressed in this article are solely those of the authors and do not necessarily represent those of their affiliated organizations, or those of the publisher, the editors and the reviewers. Any product that may be evaluated in this article, or claim that may be made by its manufacturer, is not guaranteed or endorsed by the publisher.

References

Cui, Y. (2007). *Discoveries of Guye Shell Midden Site in Guangdong Province, Gaoming County*. Weekly of China's Cultural Relics Jan 12th

Dye, T. S., and Longenecker, K. R. (2004). *Manual of Hawaiian fish remains identification based on the skeletal reference collection of Alan C. Ziegler and Including Otoliths*. Honolulu: Society for Hawaiian Archaeology.

Feng, Z., and Jiang, Z. (1998). *Research on Sea Bass*. Beijing: China Ocean Press.

Froese, R., and Pauly, D. (2022). *FishBase*. World Wide Web electronic publication. Available online at: www.fishbase.org (accessed October 8, 2022).

Helfman, G., Collette, B., Facey, D., and Bowen, B. (2009). *The Diversity of Fishes*. Chichester: Wiley-Blackwell.

Katayama, M. (1957). Four new species of serranid fishes from Japan. *Jpn. J. Ichthyol.* 6, 153–159.

Lepiksaar, J. (1994). *Introduction to Osteology of Fishes for Paleozoologists*. Göteborg.

Lidour, K., Vorenger, J., and Béarez, P. (2018). Size and weight estimations of the spangled emperor (Teleostei: Lethrinidae: *Lethrinus nebulosus*) from bone measurements elucidate the fishing grounds exploited and ancient seasonality at Akab (United Arab Emirates). *Int J. Osteoarchaeol.* 28, 681–694. doi: 10.1002/oa.2683

Martínez-Polanco, M. F., and Béarez, P. (2020). An osteometric approach to reconstruct the length and weight of *Lutjanus argentiventris* (Perciformes: Lujtanidae) for archaeological and ecological purposes. *Neotropical Ichthyol.* 18, 1–16. doi: 10.1590/1982-0224-2019-0106

Martínez-Polanco, M. F., Béarez, P., Jiménez-Acosta, M., and Cooke, R. G. (2022). Allometry of Mexican hogfish (*Bodianus diplotaenia*) for predicting the body length of individuals from two pre-Columbian sites in the Pearl Island archipelago (Panama). *Int J. Osteoarchaeol.* 32, 669–681. doi: 10.1002/oa.3094

Maruyama, M., Kikuchi, H., Sun, G., Yu, C., and Zhang, Y. (2021). Fish utilization during the Neolithic in the lower Yangtze river, China: a case study of Tianluoshan site. *Zooarchaeology* 38, 1–9.

Matsui, A., Shinkai, R., Maruyama, M., and Sun, G. (2016). "Fish remains from the Tianluoshan site," in: *The Origin and Diffusion of Livestock and Poultry in Neolithic East Asia: New Zooarchaeological Evidence from China*, eds A. Matsui and H. Kikuchi (Nara: Meishinsha). p. 7–14.

Nakajima, T., Hudson, M. J., Uchiyama, J., Makibayashi, K., and Zhang, J. (2019). Common carp aquaculture in Neolithic China dates back 8,000 years. *Nat Ecol Evol* 3, 1415–1418. doi: 10.1038/s41559-019-0974-3

Nakajima, T., Lv, P., Zhang, J., Nakajima, M., Makibayashi, K., and Yuan, J. (2015). Cyprinid pharyngeal bone and tooth remains from the Neolithic Jiahu site, Wuyang County, Henan Province, China. *Quaternary Sci.* 35, 192–198.

Nakajima, T., Nakajima, M., Mizuno, T., Sun, G., He, S., and Liu, H. (2012). On the pharyngeal tooth remains of crucian and common carp from the Neolithic Tianluoshan site, Zhejiang Province, China, with remarks on the relationship between freshwater fishing and rice cultivation in the Neolithic Age. *Int. J. Osteoarchaeol.* 22, 294–304. doi: 10.1002/oa.1206

Nakajima, T., Nakajima, M., Sun, G., and Nakamura, S. (2011). "Pharyngeal tooth remains from the fish bone pit (K3) at Tianluoshan," in *Integrated Studies on the Natural Remains from Tianluoshan*. Centre for the Study of Chinese Archaeology in Peking University, and Zhejiang Province Institute of Archaeology and Cultural Heritage (Beijing: Cultural Relics Press). p. 206–236.

Nelson, J. S., Grande, T. C., and Wilson, M. V. H. (2016). *Fishes of the World*. Hoboken: John Wiley and Sons, Inc. doi: 10.1002/9781119174844

Overseas fishery cooperation foundation of Japan (2009). *Names and Illustrations of Fishes from the East China Sea and the Yellow Sea*. Nagasaki: Nihon Shiko Printing Co., LTD.

Rurua, V. A., Béarez, P., Hermann, A., and Conte, E. (2020). Length and weight reconstruction of *Chlorurus microrhinos* (Scaridae) from isolated cranial bones and vertebrae. *Cybium* 44, 61–68. doi: 10.26028/cybium/2020-441-008

Wheeler, A., and Jones, A. K. G. (1989). *Fishes*. Cambridge: Cambridge University Press.

Wu, H., and Zhong, J. (2021). *Key to Marine and Estuarial Fishes of China*. Beijing: China Agriculture Press.

Yang, L. (2007). *Fishing Gears and Fishing Methods in South China Sea*. Guangzhou: Guangdong Science and Technology Press.

Yeomans, L. (2016). Size estimation of kingsoldier bream (*Argyrops spinifer*) and evidence of fishing strategies. *Int. J. Osteoarchaeol.* 26, 799–807. doi: 10.1002/oa.2481

Yokogawa, K. (1993). Nomenclatural reassessment of the sea bass *Lateolabrax maculatus* (McClelland, 1844) (Percichthyidae) and a redescription of the species. *Biogeography* 15, 21–32.

Yokogawa, K. (2004). *Biological characteristics and specific divergence of fishes in genus Lateolabrax (Perciformes: Percichthyidae)* (Dissertation). Ehime University.

Yokogawa, K. (2019). Morphological differences between species of the sea bass genus *Lateolabrax* (Teleostei, Perciformes), with particular emphasis on growth-related changes. *ZooKeys* 859, 69–115. doi: 10.3897/zookeys.859.32624

Yokogawa, K., and Seki, S. (1995). Morphological and genetic differences between Japanese and Chinese sea bass of the genus Lateolabrax. *Jpn. J. Ichthyol.* 41, 437–445.

Yu, C. (2022). Identification of skeletons of *Lateolabrax maculatus* and *Lates calcarifer* from archaeological sites. *Cult. Relicsin Southern China* 2, 155–161.

Yu, C., and Cui, Y. (2021). Fishing-reliant subsistence system among prehistoric coastal communities in South China: an ichthyoarchaeological case study on the Guye site. *Archaeol. Anthropol. Sci.* 13, 129. doi: 10.1007/s12520-021-01381-6

Zhang, Y. (2018). "Exploring the wetland: Integrating the fish and plant remains into a case study from Tianluoshan, a Middle Neolithic site in China," in *Environmental Archaeology*, eds E. Pişkin, A. Marciniak, and M. Bartkowiak (Cham: Springer). p. 199–227. doi: 10.1007/978-3-319-75082-8_10

Zhao, S., Xu, H., Zhong, J., and Chen, J. (2016). *Marine Fishes of Zhejiang Province*. Hangzhou: Zhejiang Science and Technology Publishing House.

frontiers | Frontiers in Earth Science

TYPE Original Research
PUBLISHED 10 January 2023
DOI 10.3389/feart.2022.1079055

Check for updates

OPEN ACCESS

EDITED BY
Ren Lele,
Lanzhou University, China

REVIEWED BY
Xiaolin Ren,
Institute for the History of Natural Sciences (CAS), China
Li Wu,
Anhui Normal University, China

*CORRESPONDENCE
Zhuoma Lancuo,
lczm1980@163.com
Guangliang Hou,
hgl20@163.com

SPECIALTY SECTION
This article was submitted to Quaternary Science, Geomorphology and Paleoenvironment, a section of the journal Frontiers in Earth Science

RECEIVED 25 October 2022
ACCEPTED 21 December 2022
PUBLISHED 10 January 2023

CITATION
Lancuo Z, Hou G, Xu C, Jiang Y, Wang W, Gao J and Wende Z (2023), Simulation of exchange routes on the Qinghai-Tibetan Plateau shows succession from the neolithic to the bronze age and strong control of the physical environment and production mode.
Front. Earth Sci. 10:1079055.
doi: 10.3389/feart.2022.1079055

COPYRIGHT
© 2023 Lancuo, Hou, Xu, Jiang, Wang, Gao and Wende. This is an open-access article distributed under the terms of the Creative Commons Attribution License (CC BY). The use, distribution or reproduction in other forums is permitted, provided the original author(s) and the copyright owner(s) are credited and that the original publication in this journal is cited, in accordance with accepted academic practice. No use, distribution or reproduction is permitted which does not comply with these terms.

Simulation of exchange routes on the Qinghai-Tibetan Plateau shows succession from the neolithic to the bronze age and strong control of the physical environment and production mode

Zhuoma Lancuo[1]*, Guangliang Hou[2,3,4]*, Changjun Xu[5], Yuan Jiang[1], Wen Wang[6], Jingyi Gao[2,3] and Zhuoma Wende[2,3]

[1]School of Finance and Economics, Qinghai University, Xining, China, [2]Key Laboratory of Tibetan Plateau Land Surface Processes and Ecological Conservation (Ministry of Education), College of Geographical Science, Qinghai Normal University, Xining, China, [3]Qinghai Province Key Laboratory of Physical Geography and Environmental Process, College of Geographical Science, Qinghai Normal University, Xining, China, [4]Academy of Plateau Science and Sustainability, People's Government of Qinghai Province and Beijing Normal University, Xining, China, [5]Key Laboratory of Geomatics Technology and Application of Qinghai Province, Provincial Geomatics Center of Qinghai, Xining, Qinghai, China, [6]State Key Laboratories of Plateau Ecology and Agriculture, Qinghai University, Xining, Qinghai, China

The Qinghai-Tibetan Plateau (QTP) is essential for converging eastern, western, and northern prehistoric cultural spheres of Asia and Europe and for human adaptation to extreme environments. Reconstruction of the location and development of prehistoric exchange routes on the Qinghai-Tibetan Plateau underpins understanding human response to harsh environments and interaction and exchange between the three cultural spheres. This study simulates exchange routes for the Neolithic and Bronze Ages, using elevation, slope, vegetation, and rivers as cost data and site points as node data. A weighted network consisting of nodes and lines is constructed within the Qinghai-Tibetan Plateau using a weighted cumulative cyclic connectivity model among nodes-the simulation abstracts exchange routes as a path search problem on this weighted network. The final simulated route is the road with the lowest incremental cost. The results give a total length of Neolithic routes of about 16,900 km, with 15 main roads, and a total length of Bronze Age routes of approximately 16,300 km, with 18 main roads. Pathway development from the Neolithic to the Bronze Age shows an apparent successional relationship, with a spatial evolution from the marginal corridor to the marginal hinterland. The simulated routes overlap highly with archaeological evidence for transmission routes of corn and millet agriculture and wheat agriculture-domesticated animals-bronze metallurgy technology, indicating the reliability of the simulation results. Further analysis showed that the unique physical geography of the QTP constrained the formation and evolution of routes. River valleys were commonly chosen as routes to acclimatize people to the high, cold, and low oxygen levels of the Qinghai-Tibetan Plateau. Scattered small agricultural bases, established in areas of the QTP suitable for agricultural planting, are the basis for intersecting exchange routes. Road formation also reflects the clear differentiation in the agro-pastoral industry between high and low altitudes related to climate, ecological environment, and elevation. Interaction between agricultural and nomadic

populations is the crucial motivation for forming and developing the exchange routes.

KEYWORDS

Qinghai-Tibet Plateau, route simulation, development and evolution, Neolithic, bronze

1 Introduction

Long-distance migration laid the basic pattern for the distribution of modern humans and their cultures (Árnason, 2017) and was accompanied by cultural and technological exchanges that promoted the development of human civilization (Zeder, 2008; Anthony, 2010). The Qinghai-Tibetan Plateau (QTP) is an important area where the three major cultural spheres of the East, West, and North met in the early period of Asia and Europe (Han, 2021) and played an essential role in the intersection of Asian and European civilizations (Huo, 2017). The extreme and harsh natural environment of the QTP has a significant impact on human social organization (Chen et al., 2022), and mechanisms of human adaptation to harsh environments, especially plateau hypoxia, are currently a focus for academic research (Huerta-Sánchez et al., 2014). A complete picture of human occupation of the QTP should include the processes of adaptation by human physiology, production technology, habitat patterns, social organization, and cultural communication ability (Chen et al., 2022), which are critical to a more profound understanding of human adaptation mechanisms (Ding et al., 2020).

The first human presence on the QTP has been documented using archaeological materials, with hominin handprints and footprints found at Qusang, on the high plateau, dating to around 200ka.BP (Zhang D. et al., 2021), and Denisovan human bones at Xiahe, Gansu (160ka.BP) (Zhang et al., 2020). In the Late Pleistocene (40–30ka.BP), humans were present in the hinterland of the QTP, where the natural environment was very harsh (Zhang et al., 2018), and on the edge of the Qaidam Basin (Liu, 1995). Human expansion from the edge to the main body of the plateau is presumed to have occurred in stages from the Late Paleolithic to the Mesolithic (20–6ka.BP) (Hou et al., 2019). There is also evidence of exchange between populations from the hinterland of the QTP and those from the Qinghai Lake Basin during this period (Zhang et al., 2016) and of technological influences of "trans-Himalayan" dispersal in the southwestern QTP (Lv, 2014). In the Neolithic period, there was cultural expansion and penetration from east to west, represented by the Majiayao culture type and termed the "path of painted pottery" (Han, 2013). Wheat crops and bronze metallurgy were introduced in the Bronze Age through the Eurasian steppe–Xinjiang–Hexi Corridor route (Dong et al., 2022a). In the historical period, there is documentary evidence for migration and exchange routes on and around the QTP, including the Qiang people, ancient roads of the Tang Dynasty to the Tubo Dynasty, and trade routes of tea and horses. Isotope evidence has been used to trace ancient human migration activities at the Heishui ancient city site in Gansu Province and the Lajia site in Qinghai Province (Zhao et al., 2016). DNA analysis has provided insights into the timing of Sino-Tibetan divergence (Qin et al., 2010) and the origin of ethnic groups (Kang et al., 2010), from which routes of human migration can be estimated (Zhang et al., 2019). Overall, the current understanding of exchange routes on the QTP is mainly approximated from archaeological information, historical documents, genetics, and isotopes.

An alternative approach uses GIS combined with modelling to simulate and concretize communication routes. Applications have included the reconstruction of trade exchange routes for prehistoric and historical periods, for example, the simulation of Silk Roads in the Asian mountains (Frachetti et al., 2017) and the reconstruction of the overland Silk Road and the Central Asia-Xinjiang "Silk Road" (Ma et al., 2017). On the QTP, recent studies include GIS-based simulation of prehistoric exchange routes (Zhu et al., 2018), simulation of the "Tangfan Ancient Road" connection to the interior (LanCuo et al., 2019), and reconstruction of exchange routes within and between prehistoric cultural areas (Hou et al., 2021).

Archaeological and modelling studies suggest a diverse network of migration and exchange routes existed on the QTP over different periods and populations. However, quantitative and systematic analysis of exchange routes for the crucial Neolithic to the Bronze Age period is still lacking, which limits understanding of the evolution of early human interaction and exchange on the QTP. This study addresses this gap by simulating exchange routes on the QTP from the Neolithic to the Bronze period and analyzes factors controlling their formation to reveal the inner dynamics of their development. The results allow systematic and quantitative analysis of exchange route locations over time that provides insight into the unique cultural landscape of the QTP, mechanisms of human activities and environmental adaptation, and cultural exchange from a longer time scale.

2 Study area

2.1 Natural environment

The QTP has an average altitude of 4,400 m (above sea level), and it covers an estimated area of $2{,}580.9\times10^3$ km^2 (area within China) (Figure 1). Topographically, the QTP is bordered to the north by the Altun Mountains and Qilian Mountains extending in a west-east direction; to the south by the Himalayan Mountains extending from northwest to southeast; to the west by the Karakoram Mountains and the Kunlun Mountains extending in an east-west direction; and in the southeast are the stands the north-south trending Hengduan Mountains. Geographically, the QTP is in southwest China and bounded by India, Nepal, and Bhutan to the south, Kashmir, Pakistan, and Tajikistan to the west. In the north, the plateau connects with the Tarim Basin and the Hexi Corridor; to the southeast, it connects with Yunnan-Guizhou and Sichuan; to the northeast, it is bounded by the Loess Plateau (Zhang Y.L et al., 2021).

The QTP is the source region of several major rivers, including the Yangtze River, Yellow River, and Lantsang. Outflowing river systems are mainly concentrated in the east and south of Tibet, with inland river systems in the northwest and the Qiangtang Plateau in the hinterland of the QTP (Zheng and Zhao, 2017). Lakes cover a large

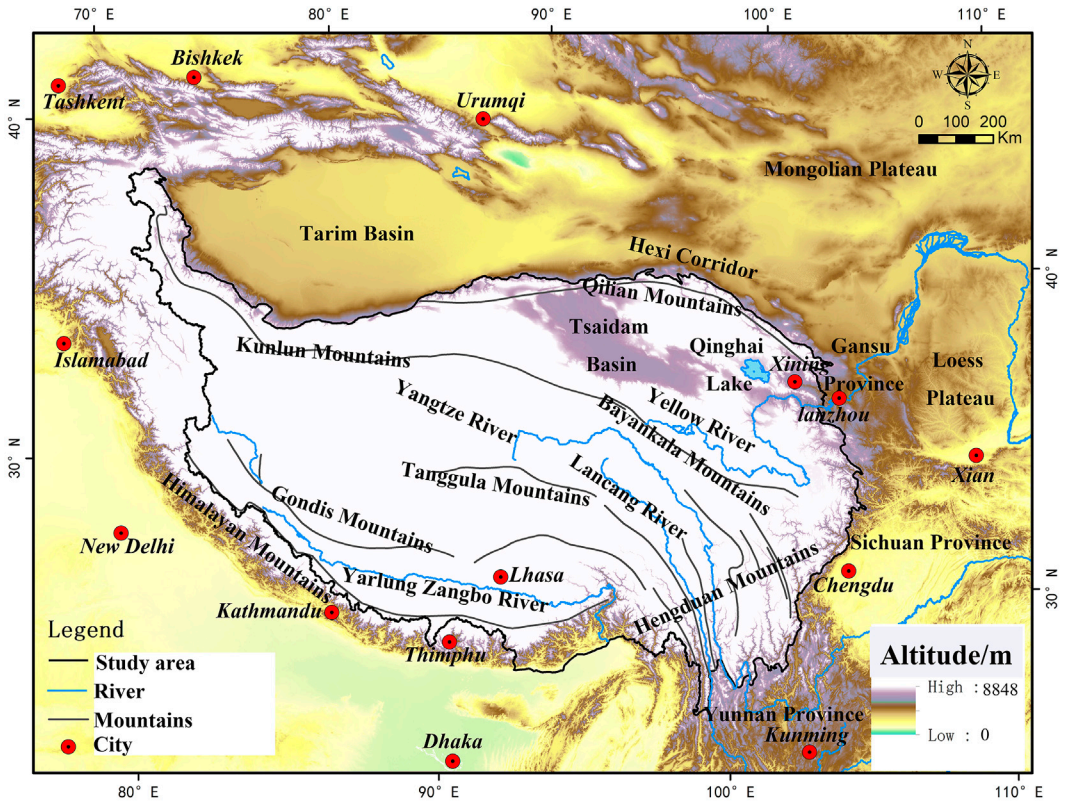

FIGURE 1
Location of the study area.

area of the QTP, with the Great Lakes of northern Tibet accounting for 48% of the total (Ma et al., 2011). The vegetation of the QTP generally shows a zonal turnover of montane forest–alpine meadow–mountain/alpine grassland–mountain/alpine desert, with apparent horizontal zone differentiation (Zheng et al., 1979). The altitude of the plateau decreases from west to east (Sun, 1996); the high-altitude results in relatively low temperatures and extreme coldness (Zheng and Zhao, 2017). Since the QTP is located at a low latitude with thin air, solar radiation is extreme (Wu and Ma, 2010). In summary, the most significant characteristic of the QTP study area is the exceptional and harsh environment for human survival.

2.2 Stage classification

The early cultures on the QTP mainly cover the Neolithic period (NP) and the Bronze -Age (BA). The Layihai site (6.745 ± 85ka.BP), in the upper reaches of the Yellow River on the QTP, is transitional from Late Paleolithic to the Neolithic (Gai and Wang, 1983). The Qijia culture (4–3.6ka.BP) represents the transition from the Neolithic to Bronze Age. Hence, this study takes the NP as 6–4ka.BP. The start of the BA coincides with the Qijia culture (4–3.6ka.BP) (Zhang and Dong, 2017), and it endured until the establishment of the Qin Dynasty, the first centralized state in the historical period. Therefore, the BA is defined in the study as 4–2ka.BP.

3 Materials and methods

3.1 Calculation procedures

Human movement and nodes are the essential elements that make up an exchange road network. Moreover, in practice, the cost of walking needs to be considered. This study assumes communication routes form a network structure composed of people accumulating along multiple nodes. The flow of people on the route chooses the relatively low-cost path between two points, so the network must be weighted. Human flow and nodes constitute the communication network elements, and edge lines connecting the nodes are the communication routes. Eq. 1 is used to build a weighted exchange network G within the QTP:

$$G = \langle V, E, W \rangle \tag{1}$$

Where, V is the node set, E is the network connection, and W is the cost.

Archaeological site points are used as the node set (V). The cost (W) is used to calculate the cost distance, an edge line (E) connects nodes based on cost distance, and a weighted network (G) is constructed based on node-edge lines. Finally, the optimal simulated route (S) is determined based on the route with the lowest cumulative cost in the weighted network.

The complete computational process incorporates (Step 1) Collection of archaeological site locations (Step 2) Cost calculation

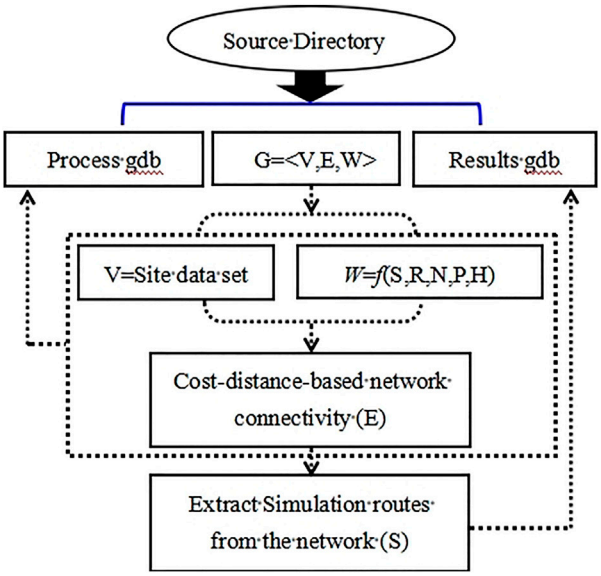

FIGURE 2
Flowchart showing workflow for calculation of elements in the exchange route simulation. G is a weighted network, E is a network connection, W is the cost, S is the optimal path between nodes V. S is the slope, R is the river, N is NDVI, P is NPP, and H is altitude. The calculation was designed using the Geographic Information Systems software ArcGIS (ESRI Corporation, Red lands, CA, United States) and executed in Python using the native Python geoprocessing tools in ArcGIS.

using geographic data (Step 3) Calculation of linkage routes between nodes based on costs; and (Step 4) Calculation of the minimum cost route in the network. The algorithm flow diagram is shown in (Figure 2), and full calculation instructions are in (Supplementary Material S3).

3.2 Data and materials

3.2.1 Archaeological site data set

Archaeological data comprised 4,431 sites, including 1,040 Neolithic period and 3,391 Bronze Age sites. Survey data were obtained from the State Administration of Cultural Heritage's Atlas of Chinese Cultural Relics (State Administration of Cultural Heritage, 1996; 2001; 2009; 2010; 2011). The point coordinate information from the literature was collated and vectorized.

3.2.2 Geographic data set

1) QTP range and boundary (Zhang et al., 2021). 2) DEM with a resolution of 90 m (Chinese Academy of Sciences, 2000). 3) China 1: 250,000 River Classification dataset (Chinese Academy of Sciences, 2001). 4) China 1:1,000,000 spatial distribution of vegetation types (Chinese Academy of Sciences, 2001). 5) Data sets of accumulated temperature ≥0°C and ≥10°C (Chinese Academy of Agriculture Sciences, 1995). 6) Annual mean precipitation in China on a 1-km grid (1971–2000) (Chinese Academy of Sciences, 1971–2000). 7) Monthly synthetic product data of 500 M NDVI for the Chinese region. Coordinate system: EPSG:4326 (WGS84). Calculated by MODND1D, NDVI is derived by taking the maximum daily value within a month; to eliminate the influence of the growing and withering seasons on overall values, the multi-year average for 2010–2016 was used as the NDVI data set in this study (Chinese Academy of Sciences, 2010–2016). 8) 1 km surface temperature data. Coordinate system: EPSG:4326 (WGS84). Temperature is obtained by synthetic calculation using MYDLT1D product, taking monthly averages with a temporal resolution of 1 day. This study used multi-year averages from 2010–2016 and monthly averages for the whole year (2010–2016) as the surface temperature data set (Chinese Academy of Sciences, 2010–2016).

4 Results

4.1 Neolithic period route simulation

The total length of simulated routes for the NP is 16,933 km, divided into four areas, northeast, east, southeast, and southwest, with 15 main routes (Figure 3A). The northeast route area has a total length of 1,438 km (Figure 3B), with four route segments, NP-MPX, NP-MHL, NP-HBJ, and NP-LGZ, forming a comparatively dense network. Route NP-MPX follows the Yellow River from the northeast of the QTP into the Xining Basin. Route segments NP-MXH and NP-GXG connect the northeastern margin of the QTP to the Gonghe Basin. The eastern route area has a total length of 1,880 km (Figure 3C), comprising three main routes that run along the eastern edge of the QTP connecting the present-day provinces of eastern Qinghai province, southern Gansu province, and western Sichuan Province. Route NP-TLD connects the Yangtze River's main tributary and the Yellow River Tributary from north to south, while routes NP-MXD and NP-XDK follow the tributaries of the Yangtze River from east to west. The total length of the southeastern route area is 1,032 km (Figure 3D), comprising two single branches. Route NP-LMD follows a north-south direction along the deep mountain valley of the Lancang River basin, and route NP-KDD runs east-west across the Hengduan Mountains. Finally, the southwest route area has 12,584 km (Figure 3E), comprising four main routes. Route NP-SSA is located in the hinterland of northern Tibet, route NP-LRR connects the Lhasa Valley and western Tibet along the Yarlung Zangbo River basin, route NP-CMD is positioned in the Lhasa Valley, and route NP-DAQ connects the Lhasa Valley with northern Tibet province.

4.2 Bronze age route simulation

The total length of simulated routes for the BA is 16,933 km, comprising 15 main routes across four areas: northeast, east, southeast, and southwest (Figure 4A). The northeast route area covers 5,371 km and is divided into six segments (Figure 4B). Segment BA-MHH runs east-west from the northeastern QTP to the vicinity of Gonghe Basin. Segment BA-HMG forms a dense

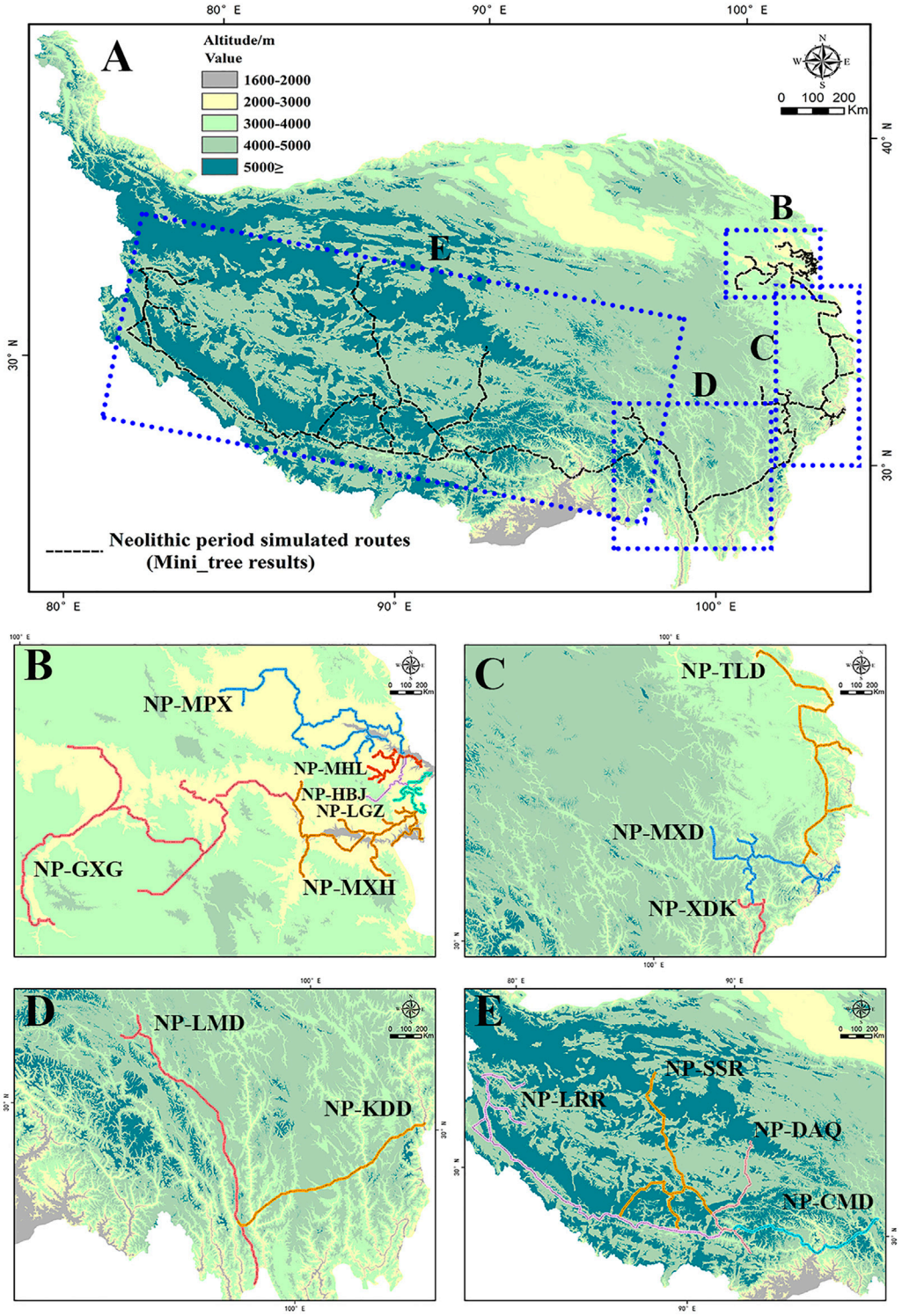

FIGURE 3
Simulated exchange routes for the neolithic period (NP). **(A)** overview of simulated routes and location of sub-areas; **(B)** northeast route area; **(C)** east route area; **(D)** southeast route area; **(E)** southwest route area. Individual route segments are labelled NP-XXX, with XXX referring to location codes.

network in northern Qinghai province. A branch of the BA-XGG route extends southward as far as the southern part of Qinghai province, while the BA-GGQ trunk route follows the northern edge of the Qinghai Lake Basin as far as the southern foothills of the Qilian Mountains. The main branch of segment BA-GDG extends westward to the north and south edges of the Qaidam Basin, connecting the Qinghai Lake Basin to the Qaidam Basin.

The eastern route area has a total length of 1,047 km and comprises two north-south oriented main routes (Figure 4C),

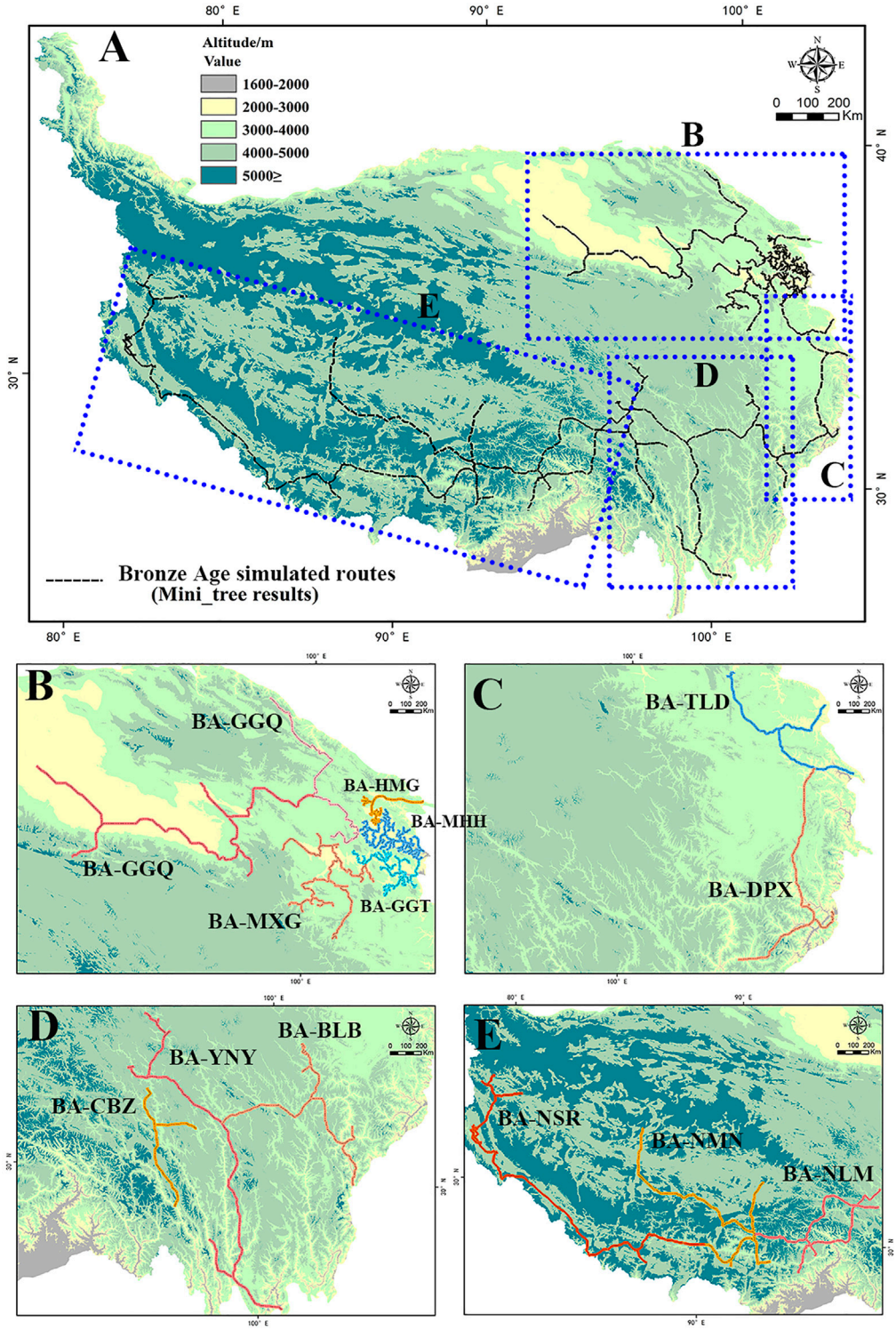

FIGURE 4
Simulated exchange routes for the Bronze age (BA). **(A)** overview of simulated routes and location of sub-areas; **(B)** northeast route area; **(C)** east route area; **(D)** southeast route area; **(E)** southwest route area. Individual route segments are labelled BA-XXX, with XXX referring to location codes.

BA-TLD and BA-DPX. The trunk routes run from the present-day southeastern Qinghai province, through southern Gansu province, to the western Sichuan Province. The southeast route area has a total length of 2,570 km, comprising three main north-south segments (Figure 4D). Route BA-BLB travels along the deep mountain valleys of the Dadu and Minjiang River basins from the southern Qinghai province to the western Sichuan Province. Route BA-YNY extends along the source of the Yangtze River to the Upper Yangtze River, from southern Qinghai province to northwestern Yunnan Province. Route BA-CBZ route runs

through the Changdu region of Tibet province. The southwest route area has a total length of 7,397 km, comprising three main routes (Figure 4E). Trunk line BA-NLM enters the Lhasa River Valley and South Tibet Valley from Qinghai province in an east-west direction. Trunk line BA-NMN forms a complex north-south to the east-west road network around the Lhasa River Valley and connects it to northern Tibet. Trunk line BA-NSR forms a direct route to western Tibet along the north and south banks of the Yarlung Zangbo River, connecting the Lhasa Valley, South Tibet Valley, West Tibet, and southwest Tibet. In the southwest route area, route BA-NSR emerges through the Pulan and Jilong basins as a connector to the southern Himalayan gorges.

4.3 Evolutionary process

The simulation results for the NP show that the routes in the northeast area follow the important tributaries of the upper reaches of the Yellow River. The route enters the QTP from the northeast, goes into the Xining Basin along the Yellow River, and extends from the Xining Basin to the Gonghe Basin. The eastern route area is a hub that connects the northeast and southeast route areas; it cuts across current administrative boundaries, connecting northeastern Qinghai Province, southern Gansu Province, and western Sichuan Province. Although there are only two routes in the southeast area, they make it possible for people to cross the Hengduan Mountains to connect with the southwest QTP. Southwest area routes follow the Yarlung Zangbo River, with the main trunk line extending to the hinterland of the QTP in the north and northeast of Tibet province.

For the BA, the simulation results indicate a core complex route network in the northeast comprising multiple trunks and branch lines, with extensions from the core area to the southern foothills of the Qilian Mountains and the Qaidam Basin. The eastern area remains a hub connecting northeastern and southeastern routes. In the southeast area, the route through the Hengduan Mountains allows unimpeded traffic with the southwest route area. It connects through Pulan Basin and Jilong Basin to the southern gorge of the Himalayas by a new route that was not present in the NP.

The northeast area shows the greatest change from NP to BA, with an increase in the total route length from 1,438 to 5,371 km. Extension of routes BA-GGQ and BA-GDG to the southern foothills of the Qilian Mountains and the Qaidam Basin accounts for most of the increase (adding about 3,900 km). Total route distance in the southeast area increased from 1,032 km in the NP to 2,570 km in the BA, with an increase from two to three main routes, including route BA-BLB, which was directly derived from NP-KDD. The total route length in the eastern area decreased from 1,880 to 1,047 km, with routes NP-MXD and NP-XDK merging and simplifying to form route BA-DPX. The total route distance in the southwest area decreased from 12,584 to 7,397 km due to routes extending less far into the northern Tibetan Plateau.

In summary, route development on the QTP from the NP to the BA shows characteristics of inheritance and evolution. Specifically, the BA route in the northeast area appears to have directly evolved and extended from the NP route, while routes in the eastern area shifted westwards from the NP to BA, and the southeast areas shifted from south to north. In the southwest area, the single route of the NP extended and increased in complexity to form a dense network between the Lhasa Valley and the Southern Tibetan Valley in the BA. Overall, the simulation results show the spatial evolution of routes from the NP to BA from the edge corridor to the hinterland.

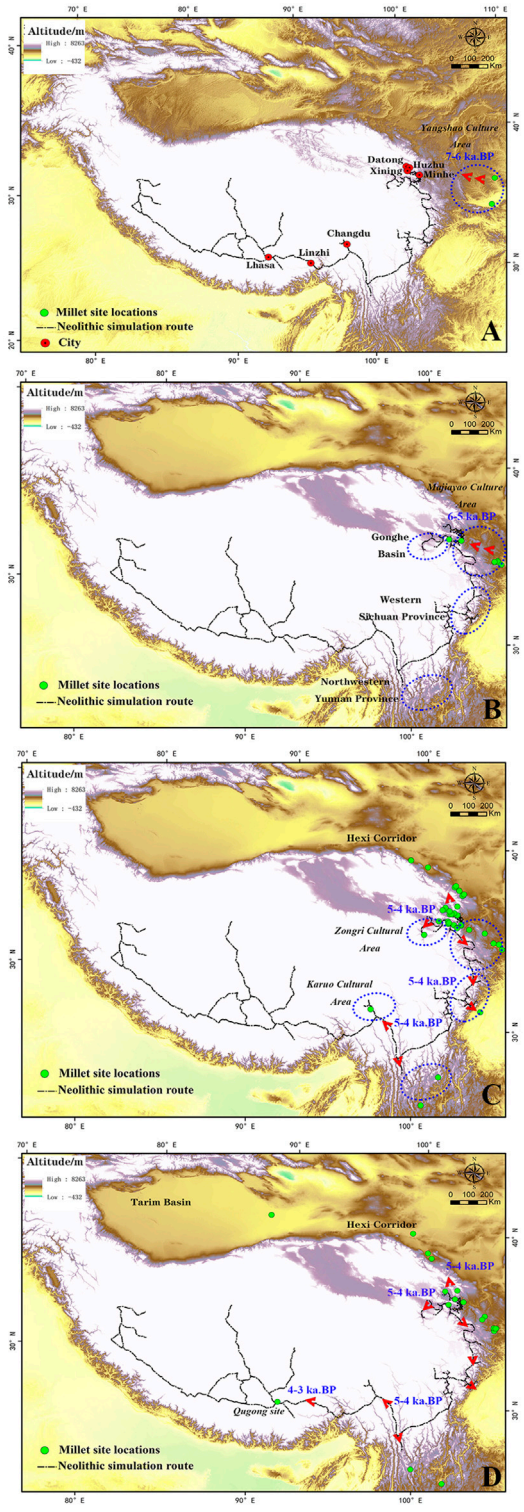

FIGURE 5
Simulated exchange routes compared with archaeological evidence for the spread of millet agriculture in the Neolithic period. **(A)** 7–6ka.BP; **(B)** 6–5ka.BP; **(C)** 5–4ka.BP; **(D)** 4–3ka.BP. Point data of site locations are from Dong et al. (2022a), Dong et al. (2022b). Blue dotted ovals mark the extent of cultural areas. Red arrows mark the assumed direction of movement.

4.4 Validation against archaeological evidence

4.4.1 Neolithic archaeological evidence

The Majiayao culture developed in the middle and late Holocene in the upper reaches of the Yellow River, in the present-day Gansu and Qinghai provinces, under the influence of the Yangshao culture (7–6ka.BP) that was present in the middle reaches of the Yellow River, between the present day Gansu and Henan provinces (Figure 5A). The distinctive features of the Majiayao culture are the cultivation of millet and the production of painted pottery. Based on the distribution of excavation sites with evidence for millet crop, it has been shown that millet agriculture spread to the Yellow River valley around 5.2ka.BP and continued to spread westward to the Hexi Corridor between 5–4.5ka.BP (Dong et al., 2017). Based on the spread of millet agriculture, several transmission routes of Majiayao culture on the QTP have been speculated. One potential route is through Minhe County–Xining–Huzhu County–Datong County to the Hexi Corridor in the northeastern QTP; another route is through northern Sichuan and Yunnan provinces along the eastern edge of the QTP (Hong et al., 2011).

To verify our simulated NP routes, we extracted and mapped archaeological sites on the QTP with millet agricultural elements for the period 6–2.5ka.BP and compared routes with site locations (Figure 5). The results show that in the period 6–5ka.BP, the millet-dominated Majiayao culture had already spread through the NP-MPX route in northeastern QTP (Figure 5B). Between 5–3.5ka.BP, millet agriculture spread westward in northeastern QTP through the NP-MPX route to Minhe County–Huzhu County–Datong County. However, it was not until the BA that millet sites spread to the Hexi Corridor, along routes BA-HMG and BA-GGQ. During this period, millet crops spread westward, with the NP-TLD route linking with NP-MXD and NP-XDK to reach western Sichuan Province (Figure 5C and Figure 5D). Dissemination to northwestern Yunnan Province was made possible by route NP-KDD, which is consistent with the Majiayao cultural dissemination route proposed by archaeologists in the region (Han, 2013; Xiang, 2018). The simulation results show that a cultural exchange between the Zongri and Majiayao cultures was realized through the NP-MXH connection to NP-GXG. The Zongri culture of the Gonghe Basin (5.2–4.1ka.BP) is a Neolithic culture that developed locally on the QTP but was strongly influenced by the Majiayao culture (Chen et al., 1998). Human bone isotope evidence also supports the Majiayao culture's influence on the Zongri (Cui et al., 2006).

The earliest site with evidence of sarcophagus burial culture is Zongri, which appears to have spread to influence the western part of Sichuan Province and the northern part of Yunnan Province, as well as the Changdu and Linzhi regions of Tibet province (Li, 2011). In the western region of Sichuan Province, the Karuo culture is thought to have been influenced by both the Zongri and Majiayao cultures (Han, 2013). Moreover, Karuo culture or similar sites are also present in the southern Tibetan valley of Tibet province (Huo, 2013; Lv, 2014). The route simulation results show that an exchange between the Zongri and Karuo cultures would have been along NP-GXG and NP-MXH. The connection between the Majiayao and Karuo cultures in western Sichuan Province is provided by NP-TLD and NP-MXD, connecting to NP-KDD and NP-LMD. The spread of Karuo culture in the southern Tibetan valley and of the sarcophagus burial culture to sites such as Changdu and Linzhi in Tibet was realized along routes NP-CMD and NP-LMD.

Similarities between the Burzahom culture of Kashmir and the Karuo culture demonstrate connections between QTP cultures and those of Central Asia (Gao et al., 2021), and potential exchange routes have been speculated. The millet and barley dating at the Qugong Karuo culture site in Lhasa, which dated 3.4ka.BP, supports cross-cultural exchange between the Karuo culture and Middle Asia. Some suggested that the Karuo culture expanded westward along the Yarlung Tsangpo River, crossed the Himalayan Pass to reach the southern edge of the range, then expanded westward along the foothills of Kashmir (Han, 2013; Lv, 2014). Our simulation results confirm a bidirectional propagation route through NP-CMD and NP-LRR along the Yarlung Tsangpo River.

4.4.2 Bronze age archaeological evidence

Archaeological evidence from the BA suggests that barley and wheat from Central Asia were introduced to eastern Qinghai *via* the gateway of the Oasis Road in the Hexi Corridor on the northeastern QTP (Jia, 2012; Dong et al., 2022a). This is supported by isotope evidence from human bones that demonstrates a food source dominated by C3 crops (mainly barley) and studies that show wheat agriculture as the chosen survival strategy of people that settled on the northeastern QTP; these strategies contributed to the permanent settlement of the people on the high altitudes areas (Ma, 2013; Chen et al., 2015).

There is ample evidence for wheat and barley agriculture at archaeological sites on the high-altitude plateau in Tibet that was introduced along pathways from northeast India (Stevens et al., 2016). Plant remains of wheat crops are found at the Changguogou site in Tibet (Fu, 2001) and are believed to be associated with the spread of barley crops from Kashmir (Han, 2013). Stone grinding wheels and stone grinding sticks used to process grains at the Qugong site in Tibet indicate that agricultural production was an indispensable economic production category for the inhabitants (Tang, 2014). House remains at the Bangga, and Xiaoenda sites in Tibet indicate settlements formed by sedentary agriculture on a large scale (Huo, 2013). Genomic data show barley was introduced to southern Tibet around 4.5–3.5ka.BP through North Pakistan, India, and Nepal (Zeng et al., 2018), and carbonized plant remains identified as barley found at the Dingdong site, Tibet, dated to 2.4–1.9ka.BP (Lv, 2007).

To verify our simulated BA routes, we extracted and mapped archaeological sites on the QTP with barley agricultural elements for the period 4.5–2ka.BP and compared routes with site locations (Figure 6). Simulated routes BA-GGQ and BA-HMG border the Hexi Corridor and fit with archaeological evidence for the introduction of barley crops into the northeastern QTP, with route BA-GDG allowing northward expansion to the edge of the Qaidam Basin and route BA-MXG northwestward to the Gonghe Basin. The simulated route BA-NSR is in a suitable location to facilitate the spread of barley crops from South Asia to the southern part of the plateau. There may also be a branch route to spread into southern Tibet through the Jilong and Pulan valleys.

Archaeological findings suggest that the Bronze culture (arsenic copper) of the Qijia culture in the Gansu and Qinghai regions influenced the Siba culture, which then spread to Xinjiang (Zhang, 2016). Aside from barley/wheat agriculture, the influence of BA cultures can also be documented through the spread of Bronze metallurgy. The transmission route would likely be through the

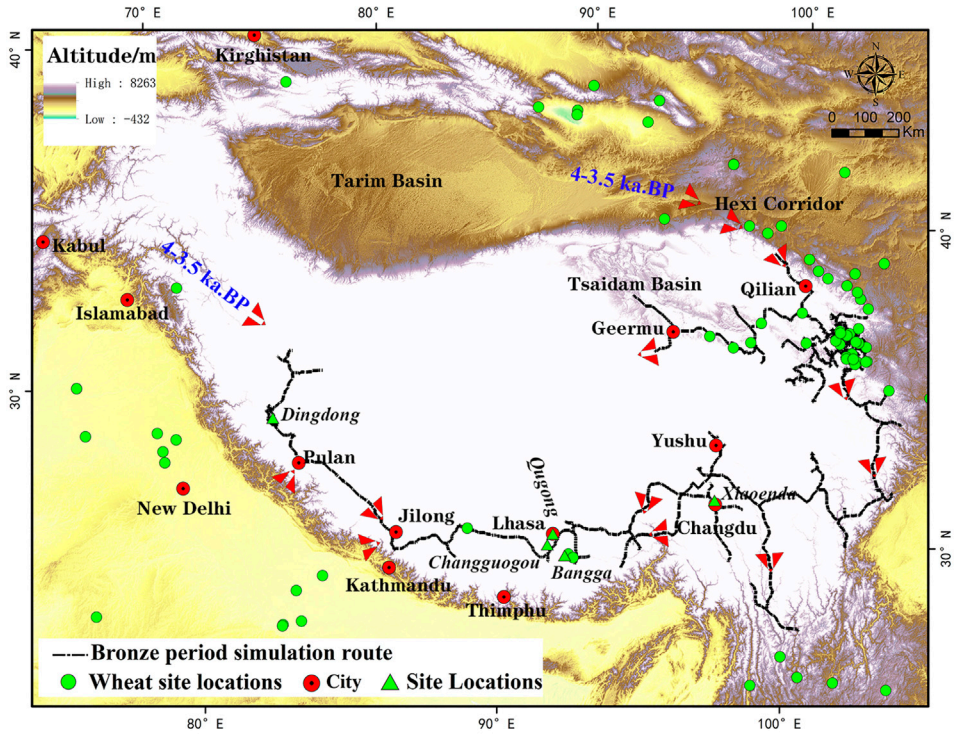

FIGURE 6
Simulated exchange routes compared with archaeological evidence for the spread of wheat agriculture in the Bronze Age, 4–3.5ka.BP. Red arrows mark the direction of movement. Point data of site locations are from Dong et al. (2022a), Dong et al. (2022b).

TABLE 1 Comparison of route distance and cost in the Neolithic to Bronze Age, from our exchange route simulation.

Period	Area	Total distance\km	Total cost	Cost/Per km	Number of road nodes	Distance/km/Per node
Neolithic	Northeast route	1,438	5,432	4	448	3
	Eastern route	1880	6,761	4	164	11
	Southeast route	1,032	3,349	3	10	103
	Southwest route	12,584	13,544	1	112	112
Bronze	Northeast route	5,371	18,963	4	1,618	3
	Eastern route	1,047	3,339	3	43	24
	Southeast route	2,570	8,999	4	102	25
	Southwest route	7,397	29,550	4	105	70

Yellow River and Qilian Mountains into the Hexi Corridor and up to the Xinjiang region (Cui, 2015).

Based on typological similarities of iron-handled bronze mirrors found at the Qugong site, Tibet (Tang, 2014), there are two possible routeways for their spread. One suggestion is that iron-handled bronze mirrors spread from Central Asia to Xinjiang province to Tibet province and continued eastward into the Hengduan Mountains region (Huo, 2000). Others argue that bronze mirrors from the Qugong site are more similar to those from northern South Asia (Zhao, 1994), with technique influence such as mounting style and the decorations at the back of the mirror from southern Central Asia or northern India (Lv, 2009). Some also argue that the bronze decoration style is influenced by bronzes technique from sites in Yunnan Province (Tong, 2010). Comparing the archaeological evidence with the simulated routes shows that Bronze culture transmission routes in the northeastern Tibetan Plateau are consistent with routes BA-GGQ and BA-HMG. Bronze metallurgy in Tibet may have been transmitted in both directions by connecting routes BA-BLB and BA-YNY through BA-NMN and BA-NLM.

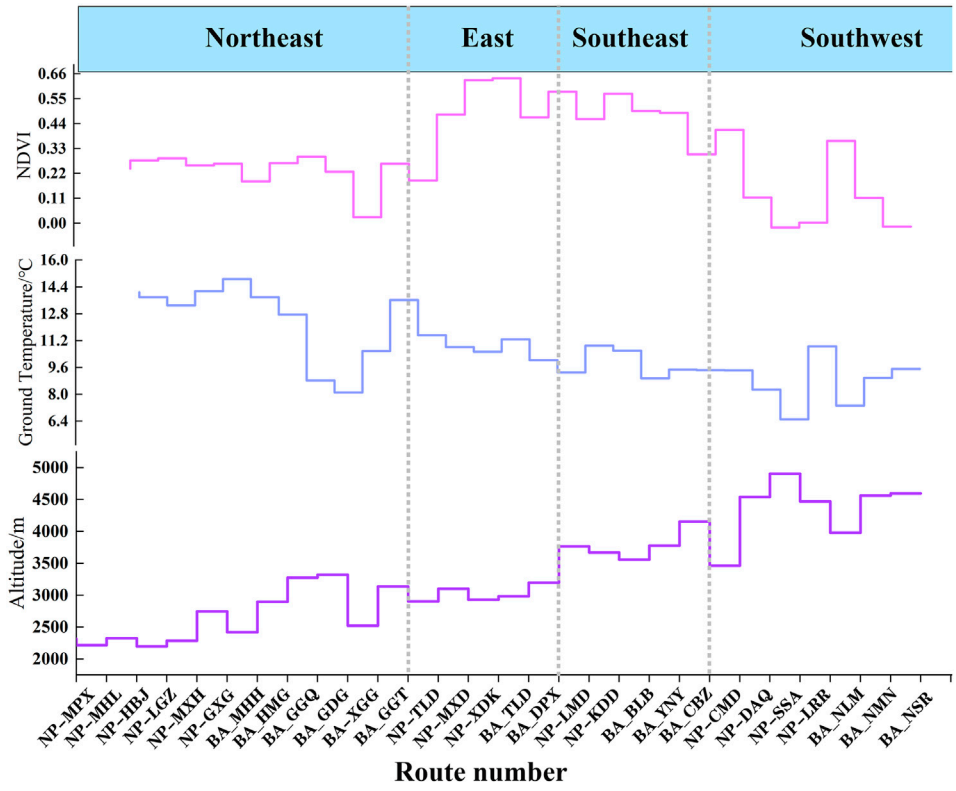

FIGURE 7
Altitude, ground temperature and NDVI with simulated Neolithic–Bronze Age exchange routes. See Figures 3, 4 for route locations.

5 Discussion

5.1 Relationship between route formation and cost

Table 1 compares the NP and BA route distance and cost properties (Table 1). Both the northeast and southeast route areas show increases in the total distance of the routes and total cost from the Neolithic to the Bronze Age, but the cost/km did not change in the former and increased in the latter. The eastern and southwestern route areas saw a decrease in the total distance, but the total cost and cost/km decreased in the former and increased in the latter.

The average distance between nodes was significantly higher in the NP than the BA, largely due to a smaller number of nodes, with 743 on Neolithic routes compared with 1,863 on Bronze age routes. Specifically, route NP-KDD in the southeastern area utilized a smaller number of nodes in the NP, which ensures lower costs for long-distance communication. In contrast, increased nodes and shorter distance between nodes on the BA route BA-BLB achieves cost control. In the southwest route area, the distance between nodes of route NP-LRR is 232 km, and the cost per km is less than 1 (Supplementary Figure S1). By the BA, the average distance between nodes in the southwest route area is below 100 km for all routes, which was achieved by reducing the distance between nodes and thus balancing the relationship between distance and cost. In summary, a relatively low-cost route is created by increasing or decreasing the number of nodes and reducing the average distance between nodes.

We used the unordered multiple choice model estimate method to determine if elevation, slope, surface temperature, and vegetation influenced route selection. The results show that elevation, slope, surface temperature, and vegetation of the simulated routes are all essential factors influencing route selection (Supplementary Tabel S2). The cold temperatures of the QTP are a hazard to human health. Studies show that constant low temperatures can cause damage to body functions (Sun et al., 1998). Currently, the incidence of cardiovascular and cerebrovascular diseases in China is higher in the colder autumn and winter seasons (Yang and Ye, 2003). Therefore, the mortality rate of cardiovascular and cerebrovascular diseases is closely related to climate change (Tan and Qu, 2003). The effect of cold air on patient lethality is even more prominent (Wang et al., 2002). It has been shown that the relative oxygen concentration (ROC) in near-earth air in terms of atmospheric pressure and oxygen partial pressure decreases significantly with increasing altitude (Zha et al., 2016). Further studies have found that surface vegetation cover and temperature may also affect ROC; with constant altitude, ROC changes with vegetation cover and temperature (Shi et al., 2019).

The above analysis shows that although high mountain ranges block the QTP, the broad intermountain valleys and river canyons between high mountain ranges are natural routeways for ancient human passage. River valley passage was chosen because of the relatively low elevation, high surface temperature, and good vegetation cover (Figure 7). The most important vegetation types on the simulated route are concentrated in the relatively low-elevation river valleys of the QTP (Figure 8). This combination of factors leads to the relatively high oxygen content in the valleys. Ancient humans

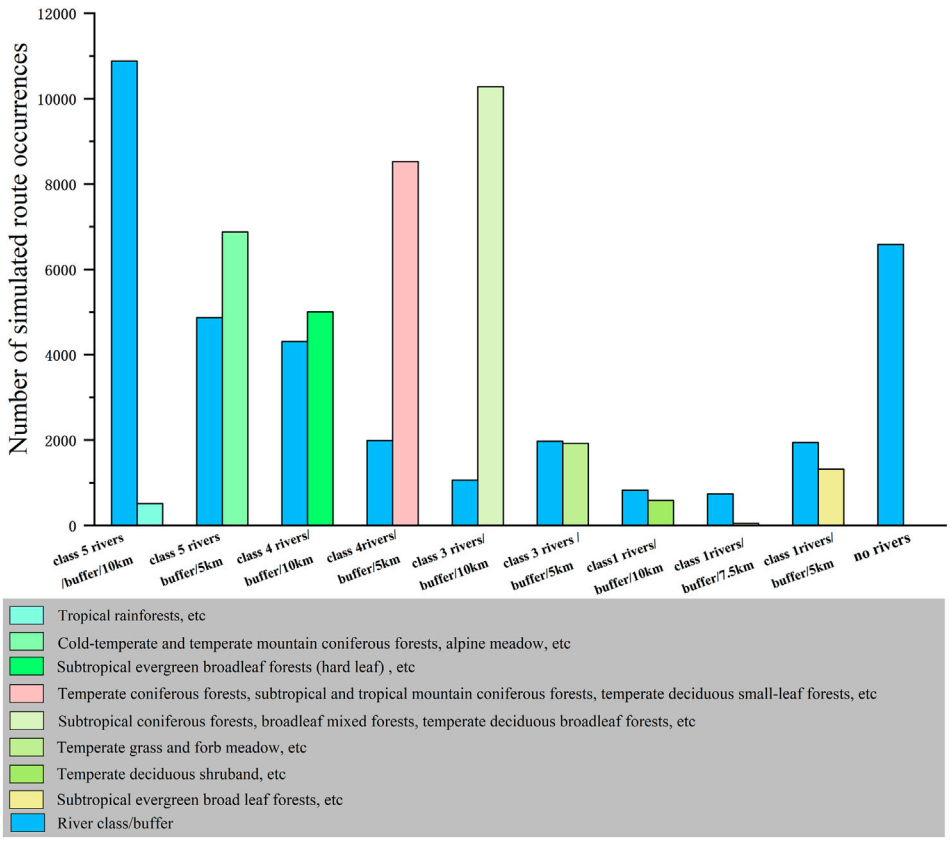

FIGURE 8
River and vegetation types associated with simulated Neolithic–Bronze Age exchange routes.

adapted their behaviour to deal with the low temperature, lack of oxygen, and gradually increasing plateau altitude.

5.2 Formation of routes about agricultural cultivation

Millet is a typical temperature-loving and drought-tolerant crop, with a growth period requiring a cumulative temperature ≥10°C of 1,600–3,000°C. The most suitable temperature for the growing environment is 15°C–25°C, and the average annual temperature needs to reach 5°C–10°C. Millet has a higher yield and is suitable for environments with 450–550 mm of precipitation; it is more drought tolerant and can survive in environments with 350–450 mm of precipitation, so it has a broader distribution in the highlands (Li, 1987). The sensitive response of millet agriculture to water, heat, and frost prevents it from surviving in areas above 2,500 m in altitude (Chai, 1999). Wheat agriculture requires a temperature in the range of 10°C–15°C. Barley is a cool-loving crop and requires an effective cumulative temperature ≥0°C of 1,200°C–1,500°C (Chen, 2013), so it is the most important grain crop in the QTP. The climate of the QTP has significant altitudinal differentiation, with the warmest monthly mean temperature in river valleys at 2,500–4,000 m above sea level (12°C–18°C), while the plateau surface and high mountains at 4,000–4,500 m elevation have lower temperatures (6°C–10°C) (Zheng et al., 1979). In summary, the typical agroecology of the plateau is valley agriculture.

The Neolithic millet-cultivating agricultural population occupied the low-altitude valleys of the plateau, influenced by water, heat, and frost conditions. Archaeological sites associated with millet agriculture are concentrated at altitudes below 2,600 m (Figure 9J). Wheat crops replaced millet during the Bronze Age as the most critical crop resource utilized by prehistoric humans on the QTP (Chen et al., 2015). The cultivation of wheat crops expanded the space for agricultural production, raising the elevation of cultivation in plateau valleys upward by at least 1,000 m, as evidenced by the altitudinal distribution of wheat crop archaeological sites (Figure 9J).

The simulated Neolithic routes correspond to an area suitable for agricultural corn production, with ≥10°C accumulation temperatures of 1,600–3,000°C and within the 400–600 mm isopleth (Figure 10E). The simulated Bronze Age routes are located in an area with ≥0°C accumulation temperature of 1,000–1,500°C and 300–400 mm isopleth (Figure 10E), which is suitable for wheat crop cultivation. These dispersed small-scale agricultural locations are the basis for the tandem simulation routes.

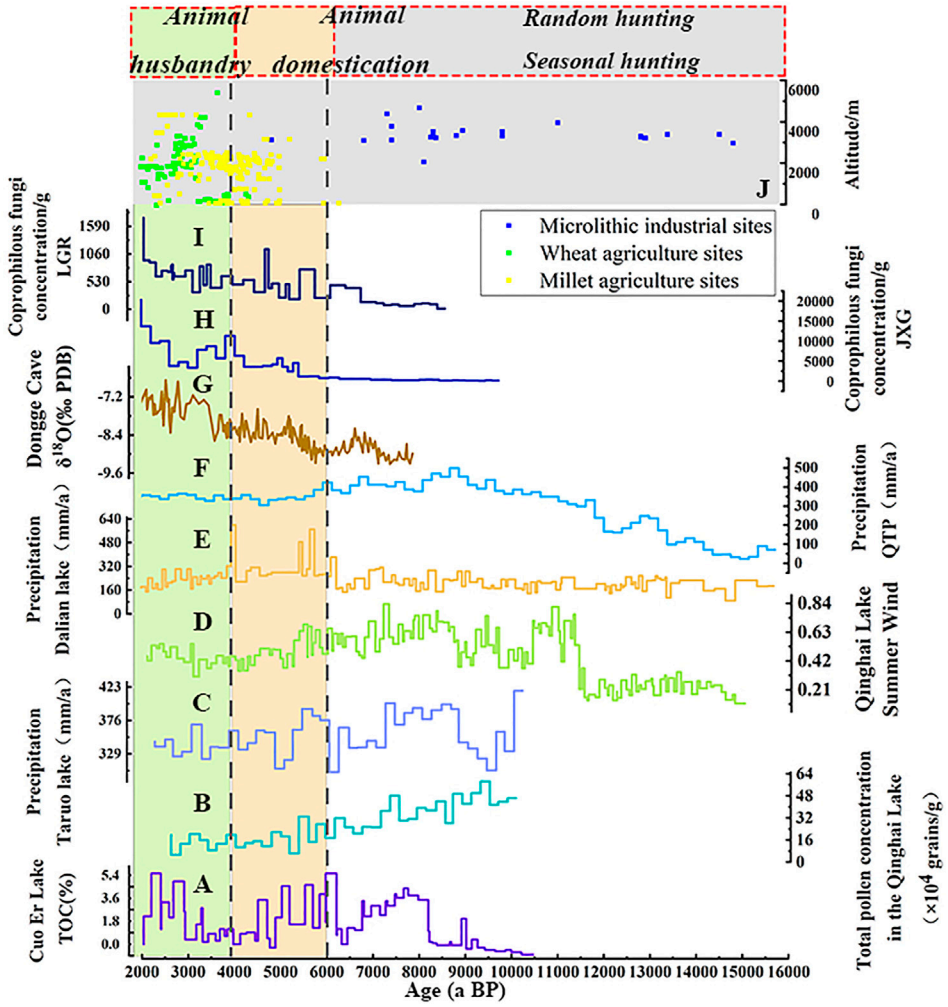

FIGURE 9
Comparison of Paleolithic–Bronze Age activities and various indicators of environmental change on the Qinghai-Tibetan Plateau (QTP) **(A)** Total organic carbon (TOC) (%) in the sedimentary record at Cuo Er Lake, central QTP (Wu et al., 2006); **(B)** Total pollen concentration in Qinghai Lake, northeastern QTP (×104 grains/g) (Shen et al., 2005); **(C)** Integrated precipitation curve in Taruo lake, southwest QTP (Ma et al., 2014); **(D)** Qinghai Lake summer monsoon index, northeastern QTP (An et al., 2012); **(E)** Quantified reconstruction of rainfall in Dalian Lake (Cheng et al., 2010); **(F)** Synthetic reconstruction of rainfall trend for the QTP (Hou et al., 2012); **(G)** Record of monsoon intensity from Dongge cave (Dykoski et al., 2005); **(H)** Total coprophilous fungi concentration curve at Jiangxi Gou 2 (JXG) site, Qinghai Lake Basin, northeastern QTP (Wei et al., 2020a); **(I)** Total coprophilous fungi concentration curve at Langgeri (LGR), Qinghai Lake Basin, northeastern QTP (Wei et al., 2020b). **(J)** Site altitude: corn site (yellow squares), wheat site (green squares), and hunter-gatherer site (blue squares).

5.3 Relationship between route formation and regional segmentation of the production model

Climatic fluctuations from the Last Ice Age to the early Holocene drove hunter-gatherer populations to migrate frequently between high and low elevations (Zhang et al., 2016). The hunter-gatherer population exhibited a combination of random and seasonal fixed travel (Madsen et al., 2006). Faunal remains within Qinghai Lake Basin suggest that hunter-gatherer populations hunted randomly for high-return ungulates (Brantingham et al., 2013) to meet the needs of small-scale populations for short-term subsistence (Wang et al., 2020). The Jiangxigou and Layihai sites in the lake basin are central camps that were used repeatedly (Yi et al., 2011). In addition, travellers' use of fire pits has also been recorded in the Kunlun Mountains region at Yeniugou (Tang et al., 2013) and Dongjicuona sites (Gao et al., 2020). Specific case studies show that early Holocene hunter-gatherers already developed a hunting pattern incorporating travelling between high and low altitudes in different seasons. In this model, the low-elevation Shalongka site (8.4–6.2ka.BP) is representative of a winter camp, and the high-elevation Canxionggasu site (8.3–7.5ka.BP) is representative of a summer camp (Hou et al., 2020) (Figure 10A).

Frequent wandering migration and short-term, small-scale survival strategies in different seasons result from adaptation to the plateau environment, with its uneven seasonal distribution of resources and significant diurnal temperature range. Seasonal resources on the QTP are easy to predict and imply a high success rate for hunters (Wang et al., 2020). Plants begin to grow in April-May, reach maturity in July-September, enter their terminal phase in mid-late September, the decline in mid-late October and enter dormancy from mid-November to April (Kong et al., 2017).

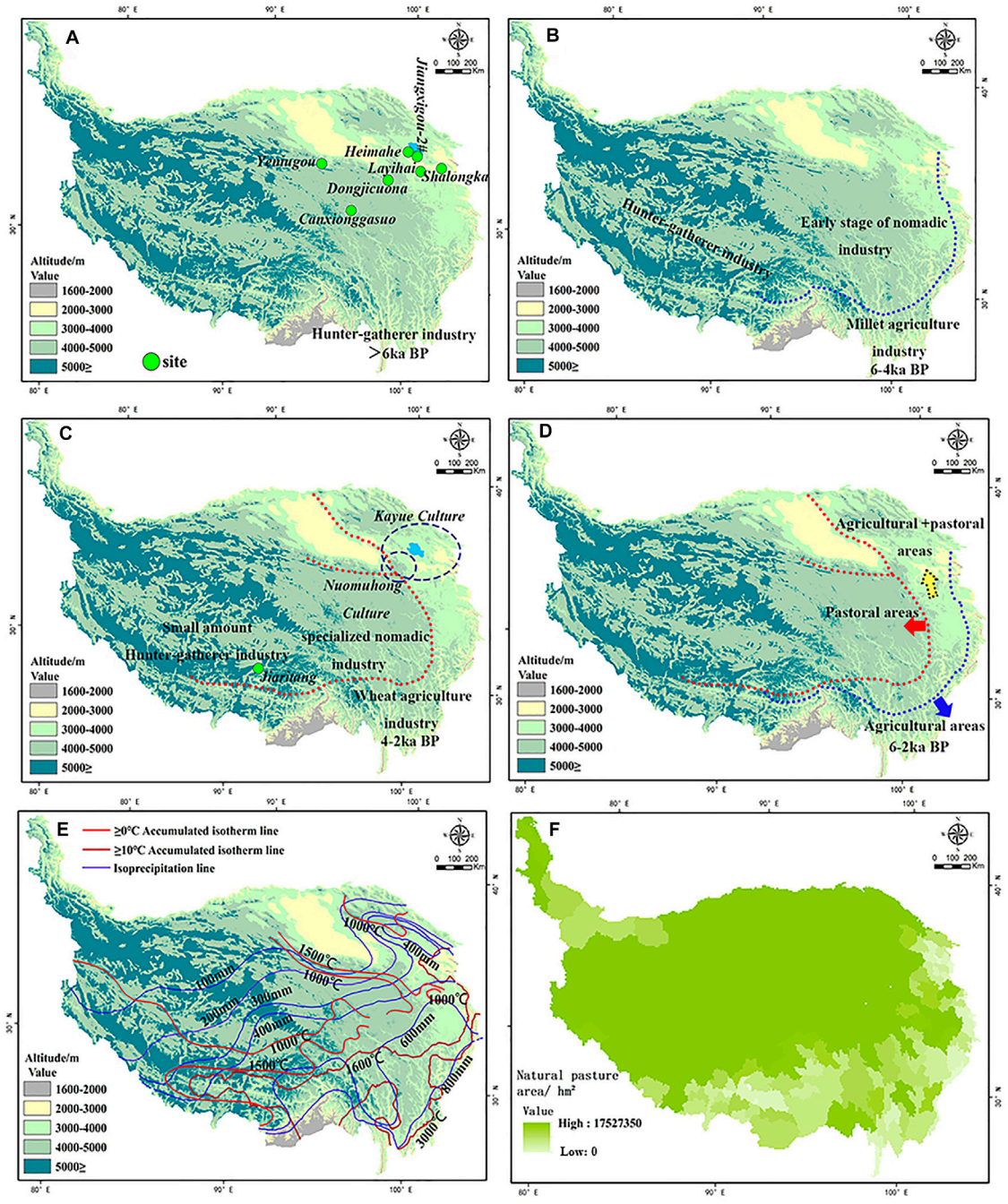

FIGURE 10
Evolution of agricultural and pastoral activity on the Qinghai-Tibetan Plateau 6–2ka.BP. **(A)** Hunter-gatherer industry, >6ka.BP; **(B)** Early stage of nomadic industry and emergence of millet agriculture, 6–4ka.BP; **(C)** Emergence of the wheat agriculture industry, 4–2ka.BP; **(D)** Trends in the location of agriculture and nomadic herding areas, 6–2ka.BP; **(E)** Temperature and precipitation trends; **(F)** Natural pasture area.

Vegetation reconstructions show that the QTP was dominated by desert vegetation during the LGM and evolved to meadow and grassland after 14ka.BP (Hou et al., 2017). An increase in temperature and precipitation after the LGM in the Qinghai Lake Basin led to a transition in vegetation type from desert grassland to alpine meadow/subalpine scrub (Shen et al., 2005). Stalagmite oxygen isotope records from Dongge cave show that the Asian monsoon began to weaken after 6ka.BP (Dykoski et al., 2005) (Figure 9G), resulting in a relatively dry cold environment and degraded vegetation. The summer winds index in the Qinghai Lake Basin also gradually weakened at this time, and regional precipitation decreased, resulting in a decrease in forest area and an increase in grassland area (An et al., 2012) (Figure 9D). After 4ka.BP, the spore pollen record of Qinghai Lake indicates a dry and cold climate, with forests in the area evolving to forested grasslands and dry grasslands (Shen et al., 2005) (Figure 9B). Various other paleoenvironmental indicators support the shift to a dry, cold climate and reduction in forest and the development of grassland vegetation at this time. These include a

reduction in mean annual precipitation at Dalian Lake in the Gonghe Basin (Cheng et al., 2010) (Figure 9E), a decrease in total organic content at Cuo Er lake on the central plateau (Wu et al., 2006) (Figure 9A), decrease in precipitation at Taruo Lake on the southwest plateau (Ma et al., 2014) (Figure 9C), and decrease in average annual precipitation of the QTP (Hou et al., 2012) (Figure 9F). The harsh natural environment after 4ka.BP significantly reduced the potential for agricultural cultivation (Zhang and Dong, 2017).

At the present-day, alpine grassland and alpine meadow-based grassland ecosystems account for over 80% of the total area of the QTP, with only 10% of available land suitable for arable farming (Department of Animal Husbandry and Veterinary Medicine, Ministry of Agriculture of the People's Republic of China, 1994). Alpine grassland dominated by *Stipapupurea* and alpine meadows dominated by *Stipacapillacea* provides suitable grazing for yak and sheep (Zheng and Zhao, 2017). The largest areas of pasture on the QTP are concentrated at altitudes of >3,000 m (Figure 10F) (Department of Animal Husbandry and Veterinary Medicine, 1994, Ministry of Agriculture of the People's Republic of China, 1994). Whole genome sequencing shows that the domestication of yaks on the QTP occurred around 7.3ka.BP (Qiu et al., 2015). Yak domestication probably resulted from humans following the migratory route of wild yaks onto the northern QTP during the Paleolithic; humans migrated to the QTP alpine grassland region for grazing in the early to middle Holocene (Rhode et al., 2007). Early grazing in the Qinghai Lake Basin occurred between 6–5.5ka.BP, intensifying from 5.5–4.2ka.BP (Wei et al., 2020a; Wei et al., 2020b) (Figures 9H, I). Domesticated cattle, goats, and sheep spread from west Asia to the northeastern edge of the QTP through the Hexi Corridor around 4.5–4ka.BP; horses were domesticated around 4–3.6ka.BP and spread into the Gansu-Qinghai region *via* the Hexi Corridor (Ren and Dong, 2016). Specialized nomadic economies emerged in the Kayue (3.6–2.6ka.BP) and Nuomuhong (3.4–2.7ka.BP) cultures (Zhang and Dong, 2017). The large number of fine stone tools excavated from the Jiaritang site (3ka.BP–circa 7th century AD) suggests that the nomadic livelihoods continued on the QTP until the Late Bronze Age (Tang, 2012; Huo, 2013) (Figure 10C).

The above evidence highlights the long history of the hunter-gatherer industry, since before 6ka.BP, on the QTP due to the unique climate and ecosystem (Figure 10A). After the emergence of millet agriculture, the earliest industrial divide in the agricultural and nomadic economy of the plateau developed (Figure 10B). The beginnings of a scattered nomadic herding economy from 6–4ka.BP likely developed from the conversion of hunter-gatherer populations directly. Two factors facilitate the conversion: 1) the abundant pasture resource provides the basis for the domestication of animals by the highland hunting population; 2) the survival strategy of frequent moving between high and low altitudes adopted by hunting people has similarities in the typical nomadic practice of winter and summer pasture transitions at different altitudes. A specialised nomadic pastoral economy emerged with the spreading of domesticated animals from the Central Asia-Hexi Corridor around 4–2ka.BP. Wheat-based agriculture developed a new industrial division on the eastern plateau (Figure 10C).

A range of evidence indicates the existence of trade and exchange between hunter-gatherers and agricultural cultivators on the QTP around 5ka.BP (Hou et al., 2016). Studies of nomadic societies in Central Asia have found that in addition to economic products such as butter, cheese, yoghurt, and meat, nomadic populations exchanged grains from farmers from which they obtained their caloric intake (Frachetti, 2009). In addition to meat, yaks also provide secondary products, such as fuel (dung), milk, cheese, and hides, that may be traded. Seashells excavated from Majiayao and Zongri culture sites were probably circulated as currency (Chen et al., 1998). The complementary nature of the agricultural and nomadic economies led to forming of a mixed agro-pastoralist zone with solid altitudinal differentiation of activity. Agricultural cultivation is mainly in valley areas at 2,000–3,000 m elevation, with mixed agriculture and nomadic activity between 3,000–4,000 m, with hunter-gatherer and nomadic economies dominating areas >3,000 m. Thus, in addition to climatic and environmental factors, altitude is an important controlling factor in the location of agriculture and animal husbandry on the QTP (Figure 10D).

Analysis of the simulated routes in this study shows that agricultural cultivation areas and semi-agricultural zones are also essential requirements for forming stable routes; we argue that cultural and economic exchanges of agricultural and nomadic populations were essential in forming stable routes. The exchange between agricultural and nomadic populations began in the NP and intensified in the Bronze Age with the enhanced cross-continental exchange.

6 Conclusion

The unique physical geography has constrained the formation, development, and evolution of routes on the QTP. Exchange routes on the QTP show inheritance and development relationships from the Neolithic to the Bronze Age. Spatially, there is an evolution from marginal corridors to marginal hinterlands. The river valleys of the plateau were commonly chosen as route ways to allow people to adapt to the cold, lack of oxygen, and gradually increasing altitude of the QTP. Scattered small agricultural bases that developed in areas of the QTP suitable for agricultural planting were essential bases for string exchange routes. Route formation is also associated with the apparent differentiation of the agro-pastoral industry between high and low elevations. Climate, ecological environment, and altitude are critical factors leading to differentiation. Interaction between agricultural and nomadic populations is the key motivation for forming and developing exchange routes. The simulated routes present an integrated picture of the complex human interaction and exchange process in the Neolithic to Bronze Age on the QTP. Early plateau routes reflect a gradual process of adaptation in production mode by people to the QTP. Our analysis also shows that the QTP was not a barrier to transcontinental cultural exchange between Asia and Europe but played an excellent intermediary role, which is crucial to the formation of the unique human landscape of the QTP.

Data availability statement

The datasets presented in this study can be found in online repositories. The names of the repository/repositories and accession number(s) can be found in the article/Supplementary Material.

Author contributions

ZL and GH conceived and designed the study. ZL, GH, CX, YJ, WW, JG, and ZW conducted fieldwork. ZL, GH, and CX analyzed

data. ZL wrote the first draft of the manuscript. ZL, GH, CX, and ZW revised the manuscript.

Funding

This study was supported by the Natural Science Foundation of China (Grant Nos 42261030 and 42171165), The Qinghai Provincial Project for Thousand Top Innovative Talents (Grant No. 2019006), and the Qinghai province "Kunlun Talent - High-end Innovation and Entrepreneurship Talent" Program.

Acknowledgments

We are grateful for the manuscript reviews by the Editor and two reviewers. We thank Xiao Han Su, Xin Yao Tang, Xin Yue Feng, and Xin Long from Qinghai University for their help with collating data. We also thank Dr Pei Yang for the helpful discussion.

Conflict of interest

The authors declare that the research was conducted in the absence of any commercial or financial relationships that could be construed as a potential conflict of interest.

Publisher's note

All claims expressed in this article are solely those of the authors and do not necessarily represent those of their affiliated organizations, or those of the publisher, the editors and the reviewers. Any product that may be evaluated in this article, or claim that may be made by its manufacturer, is not guaranteed or endorsed by the publisher.

Supplementary material

The Supplementary Material for this article can be found online at: https://www.frontiersin.org/articles/10.3389/feart.2022.1079055/full#supplementary-material

References

An, Z. S., Colman, S. M., Zhou, W. J., Li, X. Q., Brown, E. T., Jull, A. J., et al. (2012). Interplay between the westerlies and asian monsoon recorded in lake Qinghai sediments since 32 ka. *Sci. Rep.* 2 (1), 619–627. doi:10.1038/srep00619

Anthony, D. W. (2010). *The horse, the wheel, and language: How bronze Age riders from the eurasian steppes shaped the modern world*. Princeton: Princeton University Press.

Árnason, Ú. (2017). A phylogenetic view of the out of Asia/Eurasia and out of Africa hypotheses in the light of recent molecular and palaeontological finds. *Gene* 627, 473–476. doi:10.1016/j.gene.2017.07.006

Brantingham, P. J., Gao, X., Madsen, D. B., Rhode, D., Perreault, C., Woerd, J., et al. (2013). Late occupation of the high-elevation northern Tibetan Plateau based on cosmogenic, luminescence, and radiocarbon ages. *Geoarchaeology* 28 (5), 413–431. doi:10.1002/gea.21448

Chai, Y. (1999). *Broomcorn millet*. Beijing: China Agriculture Press.

Chen, F. H., Dong, G. H., Zhang, D. J., Liu, X. Y., Jia, X., An, C. B., et al. (2015). Agriculture facilitated permanent human occupation of the Tibetan Plateau after 3600 B.P. *Science* 347 (6219), 248–250. doi:10.1126/science.1259172

Chen, F. H., Xia, H., Gao, Y., Zhang, D. J., Yang, X. Y., and Dong, G. H. (2022). The processes of prehistoric human activities in the Tibetan plateau: Occupation, adaptation and permanent settlement. *Geogr. Sci.* 42 (01), 1–14. [In Chinese]. doi:10.13249/j.cnki.sgs.2022.01.001

Chen, H. H., Wang, G. S., Mei, D. Z., and Suo, N. (1998). Excavation on Zongri site, tongde, Qinghai. Archaeology. 000 (005), 1-14, 35+97–101. CNKI:SUN:KAGU.0.1998-05-000[In Chinese].

Chen, Y. H. (2013). Technical application and measures of barley production in Gannan Prefecture. *Gansu Agric.* 000 (007), 6–11. [In Chinese]. doi:10.15979/j.cnki.cn62-1104/f.2013.07.029

Cheng, B., Chen, F. H., and Zhang, J. W. (2010). Palaeovegetational and palaeoenvironmental changes in Gonghe Basin since last deglaciation. *Acta Geogr. Sin.* 65 (11), 1336–1344. doi:10.11821/xb201011003

Chinese Academy of Agriculture Sciences (1995). Data from: Institute of Agricultural Natural Resources and Regional Planning, Chinese Academy of Agricultural Sciences. Establishment of National basic resources and dynamic information service system of environment remote sensing(96-B02-01): Construction data at the temperature and humidity data level at the background level of the ecological environment(96-B02-01-02). Available at: http://www.caas.cn/.

Chinese Academy of Sciences (2010–2016). Data from: Geospatial data Cloud Platform, computer network information center, Chinese Academy of Sciences. China 1km Surface Temperature Monthly Synthesis Product. Available at: http://www.gscloud.cn.

Chinese Academy of Sciences (2000). *Data from: International scientific &technical data mirror site*. China: Computer Network Information Center, Chinese Academy of Sciences. China 90mDEM data.

Chinese Academy of Sciences (2010–2016). Data from: National earth systems science data center, Chinese Academy of Sciences. 500m NDVI monthly synthetic product data in China's land area. Available at: http://www.gscloud.cn.

Chinese Academy of Sciences (1971–2000). Data from: Resource discipline innovation Platform. Average annual precipitation data of a 1km raster in China. Available at: http://www.data.ac.cn.

Chinese Academy of Sciences (2001). Data from: Resources and environment science and data center, Chinese Academy of Sciences. Spatial distribution data of vegetation types in China 1:1,000,000. Available at: http://www.resdc.cn.

Chinese Academy of Sciences (2001). Data from: Resources and environment science and data center, Chinese Academy of Sciences. China 1:250,000 river grading data. Available at: http://www.resdc.cn.

Cui, Y. H. (2015). Research on the Silk road in Qinghai: Jade road Qiang tathagate. *J. Qinghai Natl. Inst. Soc. Sci.* 41 (03), 38–42. doi:10.3969/j.issn.1674-9227.2015.03.006

Cui, Y. P., Hu, Y. W., Chen, H. H., Dong, Y., Guan, L., Weng, G. Y., et al. (2006). Stable isotopic analysis on human bones form ZongRi site. *Quat. Sci.* 26 (4), 604–611. doi:10.3321/j.issn:1001-7410.2006.04.016

Department of Animal Husbandry and Veterinary Medicine (1994), Ministry of agriculture of the People's republic of China. Data form: China agricultural science and technology press. Grassland Resource Data in China. Available at: http://www.castp.cn/.

Ding, M., Wang, T., Ko, A. M. S., Chen, H., Wang, H., Dong, G., et al. (2020). Ancient mitogenomes show plateau populations from last 5200 years partially contributed to present-day Tibetans. *Proc. R. Soc. B* 287, 20192968. doi:10.1098/rspb.2019.2968

Dong, G. H., Du, L. Y., Yang, L., Lu, M. X., Qiu, M. H., Li, H. M., et al. (2022a). Dispersal of crop-livestock and geographical-temporal variation of subsistence along the Steppe and Silk Roads across Eurasia in prehistory. *Sci. China Earth Sci.* 65 (7), 1187–1210. doi:10.1007/s11430-021-9929-x

Dong, G. H., Lu, Y. X., Liu, P. L., and Li, G. (2022b). Spatio-temporal patterns of human activities and their influencing factors along the ancient Silk road in northwest China from 6000 a B.P. To 2000 a B.P. *Quat. Sci.* 42 (01), 1–16+332. doi:10.11928/j.issn.1001-7410.2022.01.01

Dong, G. H., Yang, Y. S., Han, J. Y., Wang, H., and Chen, F. H. (2017). Exploring the history of cultural exchange in prehistoric Eurasia from the perspectives of crop diffusion and consumption. *Sci. China Earth Sci.* 047 (005), 1110–1123. doi:10.1007/s11430-016-9037-x

Dykoski, C. A., Edwards, R. L., Cheng, H., Yuan, D. X., Cai, Y. J., Zhang, M. L., et al. (2005). A high-resolution, absolute-dated Holocene and deglacial Asian monsoon record from Dongge Cave, China. *Earth Planet. Sci. Lett.* 233 (1-2), 71–86. doi:10.1016/j.epsl.2005.01.036

Frachetti, M. D. (2009). *Pastoralist landscapes and social interaction in bronze Age eurasia*. California: University of California Press.

Frachetti, M. D., Smith, C. E., Traub, C. M., and Williams, T. (2017). Nomadic ecology shaped the highland geography of Asia's Silk Roads. *Nature* 543 (7644), 193–198. doi:10.1038/nature21696

Fu, D. X. (2001). Discovery, identification and study of neolithic crop remains in Changguogou site, xizang province. *Archaeology* 000 (003), 66–74. CNKI:SUN:KAGU.0.2001-03-007 [In Chinese].

Gai, P., and Wang, G. D. (1983). Excavation report on a mesolithic site at Layihai, upper yellow river. *Acta Anthropol. Sin.* 2 (01), 49–116. CNKI:SUN:RLXB.0.1983-01-005.

Gao, J. Y., Hou, G. L., Wei, H. C., Chen, Y. C., E, C. Y., Chen, X. L., et al. (2020). Prehistoric human activity and its environmental background in Lake Donggi Cona basin, northeastern Tibetan Plateau. *Holocene* 30 (5), 657–671. doi:10.1177/0959683619895583

Gao, Y., Yang, J., Ma, Z., Tong, Y., and Yang, X. (2021). New evidence from the Qugong site in the central Tibetan plateau for the prehistoric highland Silk road. *Holocene* 31 (2), 230–239. doi:10.1177/0959683620941144

Han, J. Y. (2013). The polychrome ceramic roads and early sino-western cultural communications. *Archaeol. Cult. Relics* 000 (001), 28–37. doi:10.3969/j.issn.1000-7830.2013.01.003

Han, J. Y. (2021). Three grand cultural spheres on the Holocene eurasian continent. *Archaeology* 000 (011), 64–75+2. CNKI:SUN:KAGU.0.2021-11-006[In Chinese].

Hong, L. Y., Cui, J. F., Wang, H., and Chen, J. (2011). Analysis and discussion on the source of faience pottery of the Majiayao type in Western Sichuan. *South Ethnology Archaeol.* 7 (00), 1–58. CNKI:SUN:NFMZ.0.2011-00-003[In Chinese].

Hou, G. L., E, C. Y., and Xiao, J. Y. (2012). Synthetical reconstruction of the precipitation series of the Qinghai-Tibet Plateau during the Holocene. *Prog. Geogr.* 31 (09), 1117–1123. doi:10.11820/dlkxjz.2012.09.001

Hou, G. L., E, C. Y., Yang, Y., and Wang, Q. B. (2016). Codependent and exchange: The source analysis of prehistoric pottery in the northeast Tibetan plateau. *J. Earth Environ.* 7 (06), 556–569. doi:10.7515/JEE201606003

Hou, G. L., Gao, J. Y., Chen, Y. C., Xu, C. J., Lancuo, Z. M., Xiao, Y. M., et al. (2020). Winter-to-summer seasonal migration of microlithic human activities on the Qinghai-Tibet Plateau. *Sci. Rep.* 10 (1), 1–13. doi:10.1038/s41598-020-68518-w

Hou, G. L., Lancuo, Z. M., Zhu, Y., and Pang, L. H. (2021). Communication route and its evolution on the Qinghai-Tibet Plateau during prehistoric time. *J. Geogr.* 76 (05), 1294–1313. doi:10.11821/dlxb202105018

Hou, G. L., Xu, C. J., Lv, C. Q., Chen, Q., and Lancuo, Z. M. (2019). The environmental background of Yangshao culture expansion in the mid-holocene. *Geogr. Res.* 38 (02), 437–444. doi:10.11821/dlyj020171214

Hou, G. L., Yang, P., Cao, G. C., Chong, Y. E., and Wang, Q. B. (2017). Vegetation evolution and human expansion on the Qinghai-Tibet Plateau since the last deglaciation. *Quatern. Int.* 430, 82–93. doi:10.1016/j.quaint.2015.03.035

Huerta-Sánchez, E., Jin, X., Bianba, Z., Peter, B. M., Vinckenbosch, N., Liang, Y., et al. (2014). Altitude adaptation in Tibetans caused by introgression of Denisovan-like DNA. *Nature* 512 (7513), 194–197. doi:10.1038/nature13408

Huo, W. (2000). From the new archaeological materials on the problem of copper mirror with handle in southwest China. *Sichuan Cult. relics* 000 (002), 3–8. CNKI:SUN:SCWW.0.2000-02-000[In Chinese].

Huo, W. (2013). Prehistoric transportation and trade in Tibet from archaeological findings. *China Tibetol.* 000 (002), 5–24. CNKI:SUN:CTRC.0.2013-02-003[In Chinese].

Huo, W. (2017). The formation, development and historical significance of the "Plateau Silk Road. *Soc. Sci.* 000 (011), 19–24. doi:10.3969/j.issn.1002-3240.2017.11.004

Jia, X. (2012). "Study on the cultural evolution and plant remains of Neolithic-Bronze Age in the northeast region of Qinghai Province,"PhD Thesis (Lanzhou: Lanzhou University).

Kang, L., Li, S., Gupta, S., Zhang, Y., Liu, K., Zhao, J., et al. (2010). Genetic structures of the Tibetans and the Deng people in the Himalayas viewed from autosomal STRs. *J. Hum. Genet.* 55 (5), 270–277. doi:10.1038/jhg.2010.21

Kong, D. D., Zhang, Q., Huang, W. L., and Gu, X. H. (2017). Vegetation phenology change in Tibetan Plateau from 1982 to 2013 and its related meteorological factors. *Acta Geogr. Sin.* 72 (1), 39–52. doi:10.11821/dlxb201701004

Lancuo, Z. M., Hou, G. L., Xu, C. J., Liu, Y. Y., Zhu, Y., Wang, W., et al. (2019). Simulating the route of the tang-tibet ancient road for one branch of the Silk road across the Qinghai-Tibet Plateau. *PLoS One* 14 (12), e0226970. doi:10.1371/journal.pone.0226970

Li, S. C. (2011). The origin and proliferation of sarcophagus burial -- the case of China. *Sichuan Cult. Relics* 000 (006), 64–69. CNKI:SUN:SCWW.0.2011-06-007[In Chinese].

Li, S. K. (1987). Agroclimatic regionalization of China. *J. Nat. Resour.* 000 (001), 71–83. doi:10.11849/zrzyxb.1987.01.008

Liu, J. Z. (1995). Tibetan plateau small Qaidam lake and the observation of each hear stone products. *World Antiq.* 000 (003), 6–20. CNKI:SUN:WWJK.0.1995-03-001[In Chinese].

Lv, H. L. (2009). Addition discussion of bronze handle-mirror of Tibet. *J. Tibetol.* 00 (00), 33–45+291. CNKI:SUN:ZAXK.0.2009-00-004[In Chinese].

Lv, H. L. (2007). Excavation on the dwelling site at Dingdong in ari prefecture, Tibet. *Archaeology* 000 (011), 36–46+102. CNKI:SUN:KAGU.0.2007-11-004[In Chinese].

Lv, H. L. (2014). Neolithic age of Western Tibet: A trans-himalayan perspective. *Archaeology* 000 (012), 77–89. CNKI:SUN:KAGU.0.2014-12-007[In Chinese].

Ma, J., Li, F. Y., Pang, G. W., Li, C. R., and Liu, W. (2017). The restoration of the ancient Silk road on land and analysis of geographical features along the route. *Geogr. Geo-Information Sci.* 33 (4), 123–128. doi:10.3969/j.issn.1672-0504.2017.04.021

Ma, M. M. (2013). "Dietary changes and agricultural development in Hehuang and its adjacent areas during the 2000 BC -- stable isotope evidence," [PhD Thesis]. (Lanzhou: Lanzhou University).

Ma, Q. F., Zhu, L. P., Lv, X. M., Guo, Y., Ju, J. T., Wang, J. P., et al. (2014). Pollen-inferred Holocene vegetation and climate histories in Taro Co, southwestern Tibetan Plateau. *Chin. Sci. Bull.* 59 (26), 2630–2642. doi:10.1360/csb2014-59-26-2630

Ma, R. H., Yang, G. S., Duan, H. T., Jiang, J. H., Wang, S. M., Feng, X. Z., et al. (2011). China's lakes at present: Number, area and spatial distribution. *Sci. China Earth Sci.* 41 (3), 283–289. doi:10.1007/s11430-010-4052-6

Madsen, D. B., Ma, H. Z., Brantingham, P. J., Gao, X., Rhode, D., Zhang, H. Y., et al. (2006). The late upper paleolithic occupation of the northern Tibetan plateau margin. *J. Archaeol. Sci.* 33 (10), 1433–1444. doi:10.1016/j.jas.2006.01.017

Qin, Z. D., Yang, Y. J., Kang, L. L., Yan, S., Cho, K., Cai, X. Y., et al. (2010). A mitochondrial revelation of early human migrations to the Tibetan Plateau before and after the last glacial maximum. *Am. J. Phys. Anthropol.* 143 (4), 555–569. doi:10.1002/ajpa.21350

Qiu, Q., Wang, L. Z., Wang, K., Yang, Y. Z., Ma, T., Wang, Z. F., et al. (2015). Yak whole-genome resequencing reveals domestication signatures and prehistoric population expansions. *Nat. Commun.* 6 (1), 10283–10287. doi:10.1038/ncomms10283

Ren, L. L., and Dong, G. H. (2016). The history for origin and diffusion of "Six livestock". *Chin. J. Nat.* 38 (04), 257–262. doi:10.3969/j.issn.0253-9608.2016.04.005

Rhode, D., Madsen, D. B., Brantingham, P. J., and Dargye, T. (2007). Yaks, yak dung, and prehistoric human habitation of the Tibetan Plateau. *Dev. Quat. Sci.* 9, 205–224. doi:10.1016/S1571-0866(07)09013-6

Shen, J. B., Liu, X. Q., Wang, S. M., and Matsumoto, R. (2005). Palaeoclimatic changes in the Qinghai Lake area during the last 18, 000 years. *Quatern. Int.* 136 (1), 131–140. doi:10.1016/j.quaint.2004.11.014

Shi, P. J., Chen, Y. Q., Zhang, A. Y., He, Y., Gao, M. N., Yang, J., et al. (2019). Factors contribution to oxygen concentration in Qinghai-Tibetan Plateau. *Chin. Sci. Bull.* 64 (07), 715–724. doi:10.1360/N972018-00655

State Administration of Cultural Heritage (2011). *Atlas of Chinese cultural Relics: Gansu fascicule*. Beijing: Surveying and Mapping Publishing House.

State Administration of Cultural Heritage (1996). *Atlas of Chinese cultural Relics: Qinghai fascicule*. Beijing: China Map Press.

State Administration of Cultural Heritage (2009). *Atlas of Chinese cultural Relics: Sichuan fascicule*. Beijing: Cultural Relics Publishing House.

State Administration of Cultural Heritage (2010). *Atlas of Chinese cultural Relics: Tibet autonomous region fascicule*. Beijing: Cultural Relics Publishing House.

State Administration of Cultural Heritage (2001). *Atlas of Chinese cultural Relics: Yunnan fascicule*. Kunming: Yunnan Science and Technology Press.

Stevens, C. J., Murphy, C., Roberts, R., Lucas, L., Silva, F., and Fuller, D. Q. (2016). Between China and South Asia: A middle asian corridor of crop dispersal and agricultural innovation in the bronze age. *Holocene* 26 (10), 1541–1555. doi:10.1177/0959683616650268

Sun, H. L. (1996). New advances in the study of the Qinghai Tibetan plateau. *Adv. Earth Sci.* 11 (06), 18–24. doi:10.11867/j.issn.1001-8166.1996.06.0536

Sun, Y. D., Pei, X. H., and Lin, Z. (1998). Effects of low temperatures on human health. *J. Med. Res.* 27 (8), 26–28. CNKI:SUN:YXYZ.0.1998-08-014[In Chinese].

Tan, J. G., and Qu, H. C. (2003). The relationship between prehospital sudden death and meteorological variation. *Meteorological Sci. Technol.* 31 (01), 58–61. doi:10.3969/j.issn.1009-5918.2001.03.003

Tang, H. S. (2014). Revisiting issues related to prehistoric sites in Tibet including Karo and Qugong sites. *Tibetan Acad. J.* 000 (001), 11–31+236. CNKI:SUN:ZAXK.0.2014-01-002[In Chinese].

Tang, H. S. (2012). The economic types and related issues of the bronze age in Tibetan plateau. *J. Tsinghua Univ. Philosophy Soc. Sci. Ed.* 27 (01), 148–158+161. doi:10.13613/j.cnki.qhdz.002052

Tang, H. S., Zhou, C. L., Li, Y. Q., and Liang, Z. (2013). A new discovery of microlithic information at the entrance to the northern qingzang plateau of the Kunlun mountains of Qinghai. *Chin. Sci. Bull.* 58 (03), 247–253. doi:10.1360/972012-550

Tong, T. (2010). The source of the decorative style of the three Tibetan bronze mirrors with handles. *J. Tibetan Stud.* 00 (01), 137–148+294. CNKI:SUN:ZAXK.0.2010-00-009[In Chinese].

Wang, J., Xia, H., Yao, J. T., Sheng, X. K., Cheng, T., Wang, Q. Q., et al. (2020). Subsistence strategies of prehistoric hunter-gatherers on the Tibetan plateau during the last deglaciation. *Sci. China Earth Sci.* 50 (03), 395–404. doi:10.1007/s11430-019-9519-8

Wang, X. M., Xie, J. F., Wang, B. S., and Qin, Y. M. (2002). Analysis of the relationship between Brain-Heart Vascular Syndrome and meteorological elements and medical meteorological grade prediction. *Jilin Meteorol.* 000 (003), 32–35. CNKI:SUN:JLQX.0.2002-03-010[In Chinese].

Wei, H. C., Chongyi, E., Zhang, J., Sun, Y. J., Li, Q. K., Hou, G. L., et al. (2020a). Climate change and anthropogenic activities in Qinghai Lake basin over the last 8500 years derived from pollen and charcoal records in an aeolian section. *Catena* 193, 104616. doi:10.1016/j.catena.2020.104616

Wei, H. C., Hou, G. L., Fan, Q. S., Madsen, D. B., Qin, Z. J., Du, Y. S., et al. (2020b). Using coprophilous fungi to reconstruct the history of pastoralism in the Qinghai Lake Basin, northeastern Qinghai-Tibetan plateau. *Prog. Phys. Geogr. Earth Environ.* 44 (1), 70–93. doi:10.1177/0309133319869596

Wu, R. S., and Ma, Y. M. (2010). Comparative analysis of the radiation characteristics of the Qinghai-Tibet Plateau different from that of the Earth and trees. *Plateau meteorol.* 29 (02), 251–259. Available at: http://iritpcas.ac.cn:8080/handle/131C11/1546.

Wu, Y. H., Lücke, A., Jin, Z. D., Wang, S. M., Schleser, G. H., Battarbee, R. W., et al. (2006). Holocene climate development on the central Tibetan plateau: A sedimentary record from cuoe lake. *Palaeogeogr. Palaeoclimatol. Palaeoecol.* 234 (2-4), 328–340. doi:10.1016/j.palaeo.2005.09.017

Xiang, J. H. (2018). Re-examination of the sources of faience pottery in Majiayao culture in Western Sichuan Province, focusing on the analysis of the chemical composition of pottery. *Sichuan Cult. Relics* 000 (004), 81–90. CNKI:SUN:SCWW.0.2018-04-010[In Chinese].

Yang, X. W., and Ye, D. X. (2003). Medical meteorological research on brain-heart vascular syndrome in China. *Meteorological Sci. Technol.* 31 (6), 376–380. doi:10.3969/j.issn.1671-6345.2003.06.012

Yi, M. J., Gao, X., Zhang, X. L., Sun, Y. J., Brantingham, P. J., Madsen, D. B., et al. (2011). A preliminary report on investigations in 2009 of some prehistoric sites in the Tibetan plateau marginal region. *Acta Anthropol. Sin.* 30 (002), 124–136. doi:10.16359/j.cnki.cn11-1963/q.2011.02.002

Zeder, M. A. (2008). Domestication and early agriculture in the Mediterranean Basin: Origins, diffusion, and impact. *Proc. Natl. Acad. Sci.* 105 (33), 11597–11604. doi:10.1073/pnas.0801317105

Zeng, X. Q., Guo, Y., Xu, Q. J., Mascher, M., Guo, G. G., Li, S. C., et al. (2018). Origin and evolution of qingke barley in Tibet. *Nat. Commun.* 9 (1), 5433–5511. doi:10.1038/s41467-018-07920-5

Zha, R. B., Sun, G. N., Dong, Z. B., and Yu, Z. K. (2016). Assessment of atmospheric oxygen practical pressure and plateau reaction of tourists in the Qinghai-Tibet Plateau. *Ecol. Environ. Sci.* 25 (01), 92–98. doi:10.16258/j.cnki.1674-5906.2016.01.013

Zhang, D. J., Dong, G. H., Wang, H., Ha, B. B., and Qiang, M. R. (2016). Historical processes and possible driving mechanisms of prehistoric human dispersal to the Qinghai-Tibetan Plateau. *Sci. China Earth Sci.* 46 (08), 1007–1023. doi:10.1007/s11430-015-5482-x

Zhang, D. J., Xia, H., Cheng, T., and Chen, F. H. (2020). New portraits of the denisovans. *Sci. Bull.* 65 (01), 1–3. doi:10.1016/j.scib.2019.10.013

Zhang, D., Matthew, R. B., Chen, H., Wang, L. B., Zhang, H. W., Sally, C. R., et al. (2021). Earliest parietal art: Hominin hand and foot traces from the middle Pleistocene of Tibet. *Sci. Bull.* 66 (24), 2506–2515. doi:10.1016/j.scib.2021.09.001

Zhang, M. H., Yan, S., Pan, W. Y., and Jin, L. (2019). Phylogenetic evidence for Sino-Tibetan origin in northern China in the late neolithic. *Nature* 569 (7754), 112–115. doi:10.1038/s41586-019-1153-z

Zhang, S. J., and Dong, G. H. (2017). Human adaptation strategies to different altitude environment during mid-late bronze age in northeast Tibetan plateau. *Quat. Sci.* 37 (4), 696–708. doi:10.11928/j.issn.1001-7410.2017.04.03

Zhang, X. L., Ha, B. B., Wang, S. J., Chen, Z. J., Ge, J. Y., Long, H., et al. (2018). The earliest human occupation of the high-altitude Tibetan Plateau 40 thousand to 30 thousand years ago. *Science* 362 (6418), 1049–1051. doi:10.1126/science.aat8824

Zhang, Y. L., Li, B. Y., Liu, L. S., and Zheng, D. (2021). Redetermine the region and boundaries of the Qinghai Tibetan plateau. *Geogr. Res.* 40 (6), 1543–1553. doi:10.11821/dlyj020210138

Zhang, Y. (2016). The discovery and dissemination of arsenic and copper in ancient China. *World Antiq.* 00 (02), 20–23. doi:10.3969/j.issn.1009-1092.2016.02.007

Zhao, C. Y., Wang, M. H., and Ye, M. L. (2016). Strontium isotope analysis of human teeth and bones from the Lajia site in Qinghai province. *Acta Anthropol. Sin.* 35 (02), 212–222. doi:10.16359/j.cnki.cn11-1963/q.2016.0019

Zhao, H. M. (1994). Problems related to the iron handle bronze mirror unearthed in Qugong, Tibet. *Archaeology* 000 (007), 642–649. CNKI:SUN:KAGU.0.1994-07-008[In Chinese].

Zheng, D., Zhang, R. Z., and Yang, Q. Y. (1979). Discussion on the natural zone of the Qinghai-Tibet Plateau. *Acta Geogr. Sin.* 34 (1), 1–11. CNKI:SUN:DLXB.0.1979-01-000[In Chinese].

Zheng, D., and Zhao, D. S. (2017). Characteristics of the natural environment of the Tibetan Plateau. *Sci. Technol. Rev.* 35 (06), 13–22. doi:10.3981/j.issn.1000-7857.2017.06.001

Zhu, Y., Hou, G. L., Lancuo, Z. M., Pang, L. H., and Gao, J. Y. (2018). GIS-based analysis of traffic routes and regional division of the Qinghai-Tibetan Plateau in prehistoric period. *Prog. Geogr.* 37 (03), 438–449. doi:10.18306/dlkxjz.2018.03.014

frontiers | Frontiers in Earth Science

TYPE Original Research
PUBLISHED 17 January 2023
DOI 10.3389/feart.2022.1041374

Check for updates

OPEN ACCESS

EDITED BY
Harry F. Lee,
The Chinese University of Hong Kong, China

REVIEWED BY
Fang Tian,
Capital Normal University, China
Xin Zhou,
University of Science and Technology of China, China

*CORRESPONDENCE
Yunfa Miao,
yunfine2000@sina.com
Zhiyong Ling,
lingzhiyong@foxmail.com

SPECIALTY SECTION
This article was submitted to Quaternary Science, Geomorphology and Paleoenvironment, a section of the journal Frontiers in Earth Science

RECEIVED 10 September 2022
ACCEPTED 27 October 2022
PUBLISHED 17 January 2023

CITATION
Liu P, Zhang S, Qiu M, Ruan Q, Luo J, Miao Y and Ling Z (2023), Vegetation history and its links to climate change during the last 36 ka in arid Central Asia: Evidence from a loess-paleosol sequence in the Eastern Ili Valley. *Front. Earth Sci.* 10:1041374. doi: 10.3389/feart.2022.1041374

COPYRIGHT
© 2023 Liu, Zhang, Qiu, Ruan, Luo, Miao and Ling. This is an open-access article distributed under the terms of the Creative Commons Attribution License (CC BY). The use, distribution or reproduction in other forums is permitted, provided the original author(s) and the copyright owner(s) are credited and that the original publication in this journal is cited, in accordance with accepted academic practice. No use, distribution or reproduction is permitted which does not comply with these terms.

Vegetation history and its links to climate change during the last 36 ka in arid Central Asia: Evidence from a loess-paleosol sequence in the Eastern Ili Valley

Peilun Liu[1,2,3], Shanjia Zhang[1], Menghan Qiu[1], Qiurong Ruan[4], Jiaming Luo[4], Yunfa Miao[2]* and Zhiyong Ling[5]*

[1]Key Laboratory of Western China's Environmental Systems, Lanzhou University, Lanzhou, China, [2]Key Laboratory of Desert and Desertification, Northwest Institute of Eco-Environment and Resources, Chinese Academy of Sciences, Lanzhou, China, [3]College of Resources and Environment, University of Chinese Academy of Sciences, Beijing, China, [4]Institute of Cultural Relics and Archaeology in Xinjiang, Urumqi, China, [5]Key Laboratory of Comprehensive and Highly Efficient Utilization of Salt Lake Resources, Qinghai Provincial Key Laboratory of Geology and Environment of Salt Lakes, Qinghai Institute of Salt Lakes, Xining, China

Detailed vegetation history response to complex influencing factors of arid Central Asia (ACA) is crucial to understanding ecological sustainability. Here, we present the first pollen record in the Ili Valley during the Last Glacial Maximum (LGM) using the Jirentai (JRT) loess-paleosol sequence. Combining the results of multi-climate proxies and optically stimulated luminescence (OSL) dating, we aim to reconstruct the vegetative response to climate change during the last 36 ka. Our results show that rapid loess accumulation in the JRT section began in the Late MIS3 (Marine isotope stage 3), and a thin paleosol layer developed in the Late LGM and Post Glacial. The pollen concentrations in the loess are significantly lower than in the paleosol, but the pollen assemblages are richer. *Artemisia* and *Asteraceae* are the dominant non-arboreal types in the loess, and abundant arboreal species are present (e.g., *Pinus*, *Picea, Quercus,* Betulaceae). The percentage of *Artemisia* remains high in the paleosol, and typical drought-tolerant plants are an important component (e.g., Orthomorphic, *Ephedra*). We suggest that the rich variety of pollen in loess is transported by frequent and intense dust activities, and these pollen may come from regional vegetation. Less diverse pollen assemblages in paleosol respond to the vegetation surrounding the JRT section. The vegetation history obtained from the JRT section shows that the lowlands of the Ili Valley were typical desert or desert-steppe vegetation for the past 36 ka. The surrounding mountains are dominated by *Pinus* and *Picea* forests. During the Early LGM, vegetation conditions deteriorated in both of mountainous and lowland. The above phenomena coincide with the pollen records from lakes in the ACA. Our results further suggest that mountain forests reappear and the lowland environment improves in response to increased insolation in the Northern Hemisphere at high latitudes in the Late LGM. This point in time is earlier by about 5–10 ka compared to previous records. We attribute it to the fact that pollen assemblages from the loess-paleosol sequence are more sensitive to vegetation and climate change

during the transition from the glacial to interglacial and propose a simple model to characterize them.

KEYWORDS

vegetation, Central Asia, ili valley, last glacial maximum, loess-paleosol sequence, pollen

1 Introduction

Vegetation history and its response to complex influencing factors (e.g., climate change, human activities) are beneficial to addressing the frequent extreme events that are expected in a future global warming scenario (Li et al., 2018; Lu et al., 2019; Fordham et al., 2020; Mottl et al., 2021; Zhang et al., 2022). The ACA is one of the driest regions in the world. The mean annual precipitation (MAP) in most areas is less than 300 mm, while evaporation is several times higher than precipitation. Thus, this region is dominated by temperate desert, Gobi, and sandy land (Narisma et al., 2007; Chen et al., 2008). At the same time, the ACA is known as an important source of global dust activities (Prospero et al., 2002; Uno et al., 2009; Marx et al., 2018). In addition, the ecology of the ACA has become increasingly fragile over the past half-century. Increased water scarcity and significant expansion of desert areas are prominent due to global warming and population growth (Chen et al., 2011; Siegfried et al., 2012; Hu and Han., 2022). Therefore, it is crucial to proceed with the reconstruction of vegetation history at different spatial and temporal scales in the ACA.

Abundant Late Quaternary paleoclimatic researches have been carried out in the ACA to investigate the relationships between climate change and environmental conditions, as well as to predict and respond to possible ecological crises (Yao et al., 1997; Chen et al., 2008; Wang and Feng, 2013). In the present Holocene Interglacial, the precipitation pattern of the ACA is dominated by the westerlies. In contrast to the East Asian monsoon region, relatively wet conditions occurred in the middle to late Holocene (Chen et al., 2016; Chen et al., 2019). At the glacial-interglacial scale, climate change in the ACA is synchronized with the East Asian monsoon region. Both regions are controlled by global ice volume and display a cold-dry climatic pattern in the glacial period (Ding et al., 2002; Li et al., 2016; Yang et al., 2020).

Pollen is an excellent indicator of vegetation history (Miao et al., 2017; Chevaliera et al., 2020; Zhao et al., 2021; Li et al., 2022). At present, only a small number of pollen records have been used to reconstruct the vegetation history in the ACA during the Last Glacial, such as lakes Manas, Balikun, Ebi, and Ailike (Rhodes et al., 1996; Tao et al., 2010; An et al., 2013; Zhao et al., 2015; Jia et al., 2020; Chen and Liu., 2022). These records reflect the severe deterioration of vegetation condition in the ACA during the LGM. However, due to lower sedimentation rates, low-resolution sediments from glacial periods provide noticeably less information than during the interglacial. Since the Late Quaternary, aeolian deposits have been widely distributed in the ACA and thicker sediments formed under cold and windy conditions (Li et al., 2016; Song et al., 2021; Li et al., 2022). They provide ideal materials for targeted reconstruction of the vegetation history within the glacial.

The Ili Valley is situated in the northeastern part of the ACA (Figure 1). Within the Holocene stage, it belongs to the core area of the "westerlies-dominated climate regime" (Chen et al., 2019). The prevailing westerly winds bring abundant precipitation to the river valley and surrounding mountains (Ye et al., 2000). A lacustrine section from the Ili Valley had been used to reconstruct the vegetation history since the Late MIS3. However, it is lacking the sediment during the LGM (Li et al., 2011; Zhao et al., 2013; Zhao et al., 2019). The dust dynamics of aeolian deposits in the Ili Valley have been well studied during the Last Glacial, and the accumulation rate is mainly influenced by the Siberian High-pressure system (Li et al., 2019; Yang et al., 2020; Kang et al., 2022). Here, using a loess-paleosol sequence collected near the Jirentai site on the second terrace of the Kashi River as material, we provide the first pollen record from the Ili Valley during the LGM with luminescence dating and the results of multi-climate proxies (e.g., grain size, magnetic susceptibility, total organic carbon (TOC), and elemental content). Furthermore, we reconstructed the vegetation history for the past ~36 ka and explored its links to climate change. Finally, we compared the changing characteristics of pollen records from lake sediments and the loess-paleosol sequence in the ACA during this period and point out the advantages of using aeolian deposits to reconstruct arid zone vegetation in the glacial period.

2 Study area

The Ili Valley is located in Central Asia and is surrounded by the Tian Shan orogenic belt. The topography of the valley has a trumpet shape that narrows from west to east and gradually increases in elevation. Despite being part of the same westerlies-dominated climatic regime as the vast adjacent desert, such as the Saryesik-Atyrau Desert and the Taklamakan Desert (Figure 1). The special topography hinders the mid-latitude westerlies and brings more abundant precipitation to the Ili Valley, especially in the late spring and summer (Shi et al., 2007). The MAP of the region is between 200 and 500 mm, with accumulations of up to 1000 mm in the high mountains. The

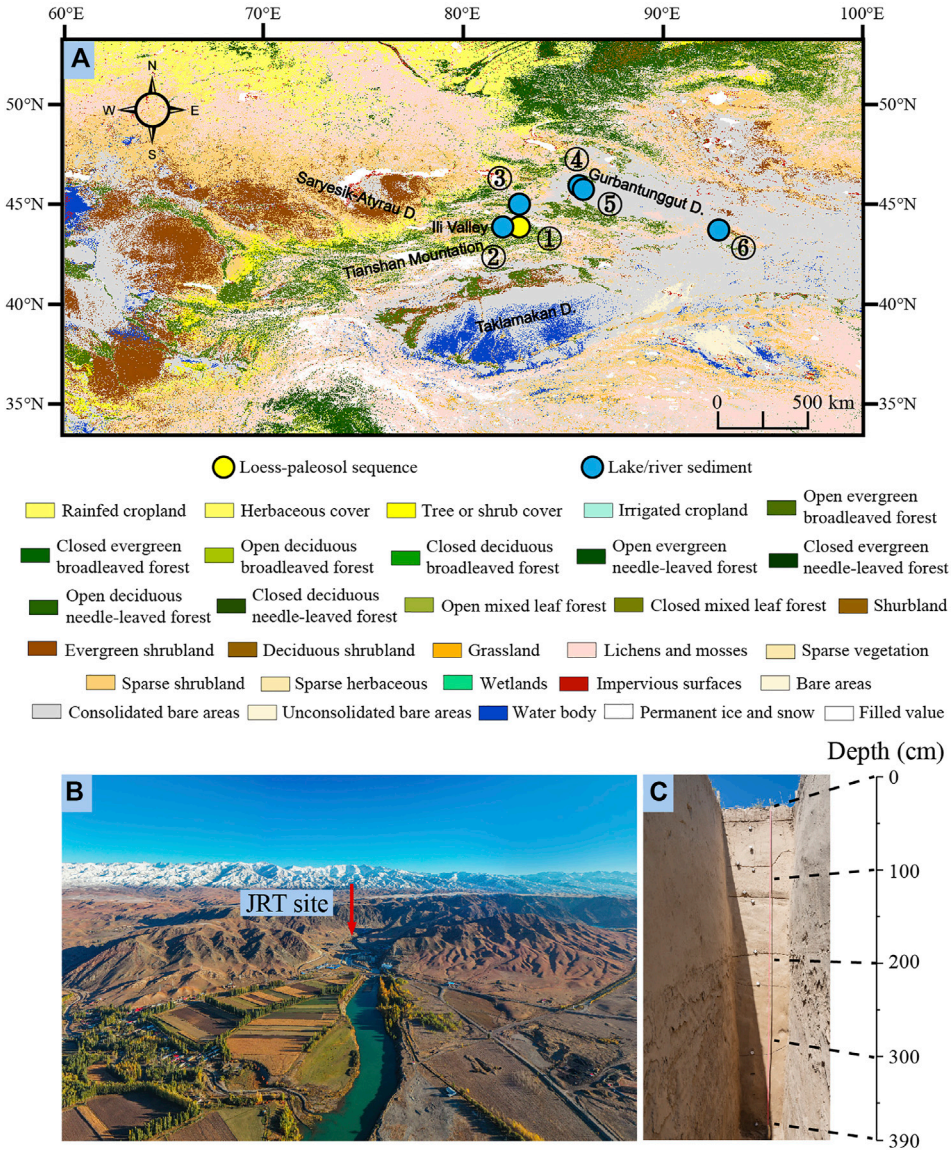

FIGURE 1
Land cover and geomorphology around the Ili Valley in ACA (The land cover data in panel **(A)** are derived from Liu and Zhang (2021)). **(A)** Location of the JRT section and other pollen records mentioned in this paper (1. JRT section, this study; 2. Yili section (Li et al., 2011); 3. Lake Abi; 4. Lake Ailike; 5. Lake Manas; 6. Lake Bilikun); **(B)** Environmental conditions surrounding the JRT section; **(C)** JRT section and OSL sampling depths.

rainfall in the mountains forms runoff that further shapes the environment of the lowlands, such as the Kashi River and Turks River (Xia et al., 2018). The mean annual temperature (MAT) ranges from 3 to 10°C. The natural environment of the Ili Valley is sensitive to climate change. Over the past half-century, the Ili Valley has been characterized by warming and humidification. The frequency of both extreme climate hazards and secondary hazards has also increased significantly (Li, 1991; Li et al., 2012; Wu et al., 2018).

The modern vegetation distribution has been used as a basis for reconstructing past vegetation-climate relationships. Greater evaporation at the bottom of Ili valley leads to drought in the lowlands. Consequently, the vegetation types below 1500 m above sea level (a.s.l.) are mainly montane steppe and desert (The main plant type are Poaceae, *Artemisia*, Asteraceae, Amaranthaceae). With the increasing altitude, the vegetation zones show a significant vertical zonality. Montane forest-meadow (e.g., Betulaceae, Lamiaceae, Poaceae, Rosaceae), subalpine meadow (e.g., Rosaceae, Geraniaceae, *Artemisia*), alpine meadow (e.g., *Artemisia*, Polygonaceae), and alpine cushion-like vegetation (e.g., Rosaceae, Caryophyllaceae) occur sequentially. Alpine coniferous forest zones (The main

establishment species is *Picea*) develop at altitudes up to 2800 m a.s.l. and represent the best vegetation condition (Xinjiang Expedition Team Chinese Academy of Sciences, 1978; Xu et al., 2010; Tian et al., 2012; Zhao and Li., 2013; Niu et al., 2022).

Aeolian deposits with significant differences in thickness are widely distributed on the piedmont and river terraces in the Ili Valley. Frequent dust activities in winter and spring triggered by Siberian High-pressure leads to an eastward transport of unsorted sediments on piedmont slopes and alluvial-riverine plains. Dune sediments from distant sources are also one of the material sources of aeolian deposition (Orlovsky et al., 2005; Youn et al., 2014; Li et al., 2020). Sediment thickness becomes thicker and then thinner with increasing elevation (Ye, 2001; Fang et al., 2002). Despite the differences in deposition rates due to topographic features, the aeolian accumulation rate in the Ili Valley is relatively high during the glacial period. These deposits thus provide an ideal terrestrial archive for reconstructing the vegetation history and climatic changes during this period (Youn et al., 2014; Li et al., 2016; Li et al., 2019).

3 Materials and methods

3.1 Jirentai section and field work

The Jirentai (JRT) section (82.78°E, 43.85°N, 1226 m a.s.l.) is located in eastern Ili Valley and overlays on the third terrace of the north bank of the Kashi River (Figure 1). The loess at this terrace has formed around 60 ka, and is piled on top of gravels (Zhang et al., 2021). It consists of undisturbed 3.9 m long wind-formed deposits with sparse weed growth on the surface. Based on field observations, a remarkable paleosol layer about 25 cm thick develops on a deep loess layer. We collected five samples at ~5 cm intervals at the top of the profile. In addition, 120 samples were collected at 1 cm intervals between 25 and 150 cm and 125 samples at 2 cm intervals between 150 and 390 cm. All 250 samples were measured for grain size, magnetic susceptibility, total organic carbon (TOC), and elemental content. In addition, to establish the age of the section, ten optically stimulated luminescence (OSL) dating samples were obtained from the sections at depths of 30, 60, 80, 90, 110, 130, 190, 230, 320, and 390 cm, respectively.

3.2 Climate proxy analyses

All soil samples were dry in their natural state. We weighed appropriate mass of samples for each of the four process-independent experiments. Extracting branches and leaves from the soil before performing the necessary pre-treatment process. The grain size was measured using a laser particle size analyzer, with a measurement range of 0.02–2000 μm and a systematic error of less than 2%. A Magix PW2403 X-ray fluorescence Xinjiang Expedition Team Chinese Academy of Sciences, 1978 analyzer was used to determine the elemental content of sediments with an analytical precision of better than 1–2%. The magnetic susceptibility was measured using a Bartington MS2B magnetic susceptibility meter at both low frequency (470 Hz) (χ_{lf}) and high frequency (4700 Hz) (χ_{hf}), and the mass-specific frequency-dependent magnetic susceptibility (χ_{fd}) was calculated by: $\chi_{fd} = \chi_{lf} - \chi_{hf}$, following. The TOC was measured using an elemental analyzer (Jena HT 1300 total carbon analyzer, Germany).

All experiments were conducted at the MOE Key Laboratory of Western China's Environmental System, Lanzhou University.

3.3 Optically stimulated luminescence dating sample measurement

Ten samples were used to extract minerals for equivalent dose (De) determination in a darkroom with a red light. After eliminating carbonates and organic matter, medium-grained (38–63 μm) quartz particles were extracted from samples and were selected as the material to construct a single-piece regeneration dose-standard curve (SAR-SGC) for dating (Murray and Wintle, 2000). Quartz grains were treated with 40% HF solution for 2 h to remove feldspar grains. Afterward, fluoride was removed from the obtained quartz particles with 10% HCl. The key to this process is to ensure that feldspar contamination is effectively removed to avoid underestimation of age. Luminescence measurements were collected using an automated Risø TL/OSL-DA-20 reader equipped with blue diodes (470 ± 20 nm) and IR laser diodes (830 nm). Irradiation was conducted using a 90Sr/90Y beta source built into the Risø reader. For the quartz samples used in this experiment, the natural and regenerative dose samples were treated with blue-emitting diodes. The Preheat temperatures was kept at 260°C for 10 s and the cut heat was 220°C for 10 s. The luminescence stimulation used blue LEDs at 130°C for 40 s, and the OSL signal was detected by a 9235QA photomultiplier tube through a 7.5-mm-thick Hoya U-340 filters. Signals over the first 1.6 s of stimulation were integrated for growth curve construction after background subtraction (final 8 s) to estimate the equivalent dose De value. The concentrations of U, Th, and K were determined using neutron activation analysis. Finally, the standard growth curve of Lx/Tx-Rx was established, and the natural light release signal intensity value LN/TN was inserted into the standard growth curve to find the equivalent dose value De (Murray and Wintle, 2000; Lai and Ou, 2003).

This experiment was conducted in the Light Release Laboratory, Qinghai Institute of Salt Lake, Chinese Academy of Sciences.

TABLE 1 OSL dating results of samples from the JRT section.

Sample Id	K (%)	Th (ppm)	U (ppm)	Water content (%)	Depth(m)	Dose rate (Gy/Ka)	De (Gy)	OSL age (ka)
JRTGKP-1	1.96 ± 0.04	12.56 ± 0.70	2.55 ± 0.40	6 ± 5	0.3	3.77 ± 0.28	23.8 ± 2.2	6.3 ± 0.7
JRTGKP-2	1.97 ± 0.04	12.05 ± 0.70	2.70 ± 0.40	6 ± 5	0.6	3.76 ± 0.28	84.9 ± 2.3	22.6 ± 1.8
JRTGKP-3	1.79 ± 0.04	10.89 ± 0.70	2.45 ± 0.30	6 ± 5	0.8	3.42 ± 0.25	73.7 ± 2.4	21.5 ± 1.7
JRTGKP-4	1.79 ± 0.04	12.13 ± 0.70	2.59 ± 0.40	6 ± 5	0.9	3.56 ± 0.27	79.1 ± 5.5	22.2 ± 2.3
JRTGKP-5	1.97 ± 0.04	11.71 ± 0.70	2.91 ± 0.40	6 ± 5	1.1	3.77 ± 0.28	89.8 ± 3.3	23.8 ± 2.0
JRTGKP-6	2.02 ± 0.04	11.93 ± 0.70	3.10 ± 0.40	6 ± 5	1.3	3.89 ± 0.29	90.9 ± 5.8	23.4 ± 2.3
JRTGKP-7	2.04 ± 0.04	12.81 ± 0.70	3.42 ± 0.40	8 ± 5	1.9	3.94 ± 0.29	117.7 ± 6.6	29.8 ± 2.8
JRTGKP-8	2.12 ± 0.04	12.52 ± 0.70	3.13 ± 0.40	8 ± 5	2.3	3.90 ± 0.29	117.3 ± 4.4	30.1 ± 2.5
JRTGKP-9	2.00 ± 0.04	12.60 ± 0.70	3.03 ± 0.40	8 ± 5	3.2	3.75 ± 0.28	125.7 ± 3.8	33.5 ± 2.7
JRTGKP-10	2.09 ± 0.04	13.92 ± 0.80	3.31 ± 0.40	8 ± 5	3.9	3.99 ± 0.30	125.9 ± 6.3	31.5 ± 2.8

3.4 Pollen analysis

In total, 46 samples were selected from the section for pollen analysis. After weighing 20 g of soil per sample for pre-treatment. A known number of *Lycopodium* spores (27637/slice) was added prior to the chemical treatment to calculate pollen concentrations. Solutions of 10% HCl and 10% HF were used to remove impurities, such as carbonate, nitrate and organic fractions. An ultrasonic shaker and a sieve cloth were used to further remove impurities smaller than 10 μm. The remaining material was preserved and made into samples. At least 300 grains of terrestrial plant pollen from each sample were identified under a microscope, or the entire sample was counted when the pollen count was insufficient. Pollen identification followed pollen atlases specific to the arid and semi-arid areas of China (Wang et al., 1995; Tang et al., 2016). Pollen diagrams were generated using Tilia v2.6.1 (Grimm, 1987; 2004).

This experiment was conducted in the Key Laboratory of Desert and Desertification, Northwest Institute of Eco-environment and Resources, Chinese Academy of Sciences.

4 Results

4.1 Optically stimulated luminescence dating results

The quartz OSL ages range from 6.3 ± 0.7 to 33.5 ± 2.7 ka. All the OSL ages are in stratigraphic order (within acceptable error) in the JRT section (Table 1). Based on direct dating results showing the top 30 cm of sediments formed in the middle to late Holocene, and aeolian sediments accumulated at depths between 130 and 60 cm in the LGM and 390–190 cm in the Late MIS3. The dating results are densely distributed in the LGM and Late MIS3, reflecting the rapid dust accumulation during this phase and also explaining part of the age reversal (e.g., JRTGKP-3)

Due to significant depositional hiatuses and differences in sedimentary facies, an age-depth one-to-one model was deemed unsuitable for the application. Rather a chronological framework was constructed by dividing the section into four depositional phases by combining the results of multi-climate proxies.

4.2 Grain size and multi-climate proxies result

Grain sizes within the aeolian deposition are likely influenced by multiple independent materialization processes (Újvári et al., 2016). Here, sand is defined as particle sizes >63 μm, while the particle sizes of clay do not exceed 2 μm. Sand fraction content fluctuates between 6.01% and 16.5% throughout the whole section. At depths of 390–140 cm, the fluctuation in sand fraction is intense, as evidenced by a variance of 5.12. It also has demonstrated a similar shifting trend as the mean grain size (MGZ) at the same depths (Figure 2). There are five distinct peaks with a rapid decrease followed by a slow increase in the sand fraction between two adjacent peaks. At this stage, changes in the clay fraction content were not significant. At depths of 140–90 cm, both the sand fraction content and MGZ showed a rapidly decreasing trend with a corresponding increase in the content of the clay component. At depths of 90–0 cm, the continuous decrease in MGZ shows an inverse trend relative to the change in clay fraction content. However, the sand fraction content is relatively stable (a variance of 3.28) and even increased slightly compared to the previous period. The above phenomenon suggests that the dominant factor controlling the grain size composition of the JRT section shifted at a cut-off of approximately 90 cm and played a

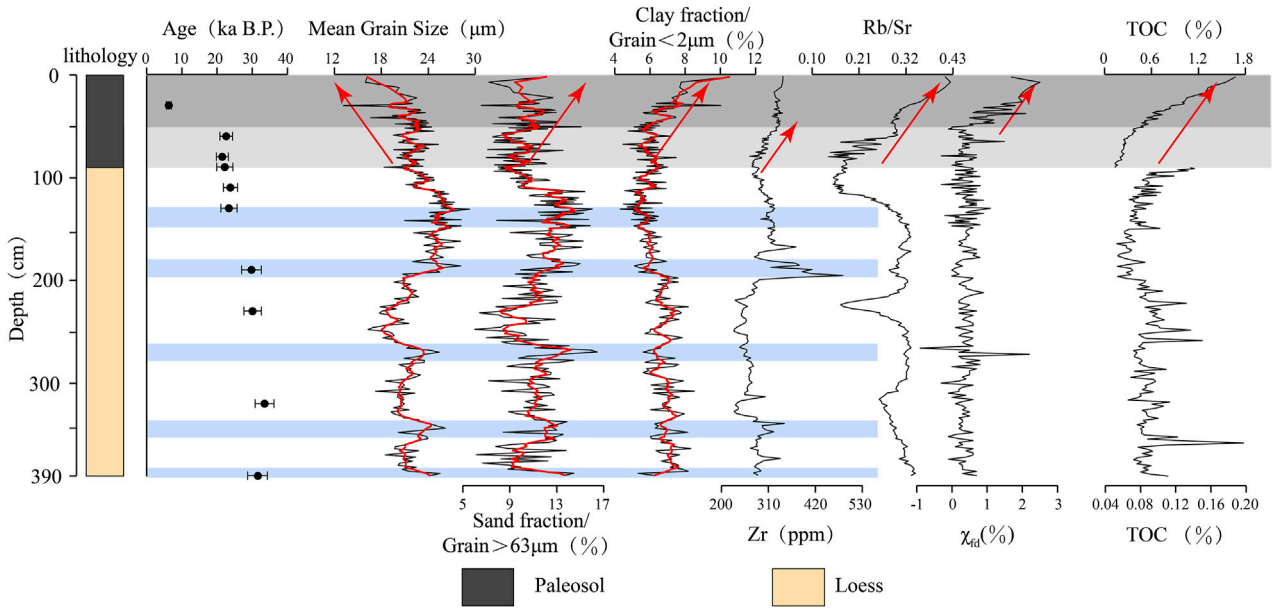

FIGURE 2
Grain size and multi-climate proxies result of the JRT section. The loess-paleosol sequence is determined by a combination of field observation and climate proxies; The two gray boxes indicate the sediments with soil-forming action and vegetation development; the red arrow marks the trend of each indicator in the paleosol; the red line is the smoothed curve obtained by the adjacency averaging method; the blue box contains the five high relatively high values of MGZ and sand fraction.

more important role above 50 cm (Figure 2). Their influence in the sediment size fraction characteristics of JRT section is that the coarse fraction contributes more to the MGZ in the depth of 390–90 cm, while the fine fraction dominates the MGZ in the 90–0 cm.

Because of their different chemical properties, the Rubidium/Strontium ratio (Rb/Sr) is always used to indicate the degree of chemical weathering (Gallet et al., 1996; Chen et al., 2001). Zirconium (Zr) is extremely stable during chemical weathering. Therefore, it is often used to indicate changes in sediment sources (Taylor and McLennan, 1985; Li et al., 2020). In the top ~50 cm of the JRT section, the content of Zr is stable, and the Rb/Sr is significantly higher than for sediments below 50 cm and is continuously increasing. This suggests that the formation of the upper sediment was accompanied by strong weathering and soil formation processes (Figure 2).

Soil TOC is closely related to input, burial time, and decomposition level (Meyers, 1997; Chen et al., 2005; Zhang and Liu, 2008). The parameter χ_{fd} responds to the content of superparamagnetic particles. Thereby indirectly reflecting the environmental characteristics and vegetative conditions (Liu et al., 1990). The significant change in TOC occurred at a depth of about 90 cm and followed by a rapid increase above that layer. Its corresponding change in χ_{fd} occurred at a depth of 50 cm. There phenomenon suggests the soil in the lower and central parts of JRT section is typical loess and not conducive to vegetation development. A top 50/90 cm paleosol layer developed in a warmer and wetter context and was accompanied by a significantly improved vegetation condition (Figure 2).

4.3 Chronological framework

Based on grain size and multi climate proxies results, we have divided the JRT section into four stages: Stage 1 at a depth (Sun and Wu, 1987) of 390–140 cm, stage 2 at 140–90cm, stage 3 at 90–50 cm, and stage 4 at 50 cm. Combined with OSL dating results, they belong to the Late MIS3, Early LGM, Late LGM, and Post Glacial, respectively (Figure 3).

4.4 Pollen data

We had identified 35 terrestrial pollen taxa from the JRT section. Arboreal pollen is dominated by *Pinus* and *Picea*, while *Artemisia* and Orthomorphic commonly account for more than 80% of non-arboreal pollen. Owing to the rarity of some pollen taxa, we have clearly marked only 14 species in the pollen diagrams (Figure 3).

Since less than 300 pollen grains can be identified in sediments below 90 cm. The following detailed description

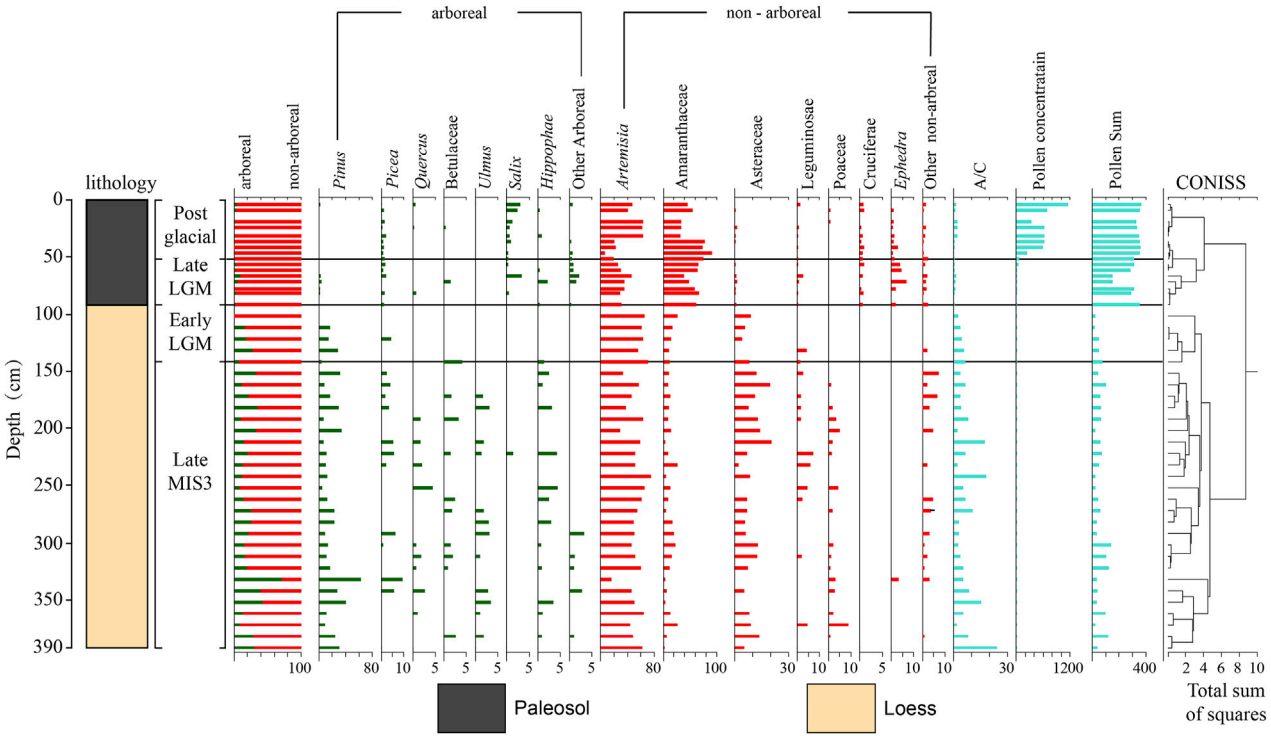

FIGURE 3
Percentage pollen diagram of selected taxa of JRT section. The four stages divided by the black line are based on OSL, grain size, and the results of multi-climate proxies, as described in Section 4.3.

and discussion of pollen are mainly based on the chronological framework established in Section 4.3. Pollen records from all strata within a stage are assumed to reflect the overall vegetation condition. We only compare the differences between the different stages to compensate for the lack of pollen number in individual strata.

4.4.1 Stage 1 (390–140 cm, late marine isotope stage 3)

At this stage, an average of 60.192 pollen per sample were identified. The pollen concentration is extremely low and the average concentration is only 7.722 grains/g. But there are relatively rich types of pollen. *Pinus*, *Artemisia*, and Asteraceae are the dominant pollen components. At the same time, pollen of *Picea*, *Quercus* and Betulaceae occasionally occurs in the sediment. In addition, the A/C (*Artemisia*/Chenopodiaceae) at this stage (7.528) is the highest in the entire record (Figure 3).

4.4.2 Stage 2 (140–90 cm, early last glacial maximum)

At this stage, an average of 34.5 pollen per sample were identified. The most important feature of this stage is an extremely monotonous pollen species. The dominant pollen component is *Artemisia* (55.102–70.270%). Amaranthaceae pollen tended to increase, while the percentage of *Pinus* pollen rapidly decrease (Figure 3).

4.4.3 Stage 3 (90–50 cm, late last glacial maximum)

Pollen of *Picea* and *Pinus* occurs simultaneously at this stage. The dominant component of pollen shifts to *Amaranthaceae* (56.898%). Cruciferae and *Ephedra* establish themselves as important components of non-arboreal pollen. Most notable is the significant overall increase in pollen concentration compared to the previous two stages (Figure 3).

4.4.4 Stage 4 (50–0 cm, Post glacial)

From 517.084 to 11447.727 grains/g, pollen concentration increased rapidly. Another notable change is that *Picea* has completely replaced *Pinus* as the most important arboreal pollen, but at a relatively low percentage (0.303–1.286%). *Artemisia* and Amaranthaceae are still the dominant pollen component. The sum of the percentages of these two pollen types is as high as 94.484%. In addition, *Ephedra* and *Salix* pollen are repeatedly present. The A/C shows an overall increasing trend, but the average value is only 0.947 (Figure 3).

5 Discussion

5.1 Pollen sources in the loess-paleosol sequence of the jirentai section

Judging and distinguishing the material source and sedimentary facies is one of the bases for applying fossil pollen characteristics to reconstruct vegetation history (Xu et al., 2015; Chevaliera et al., 2020). Factors such as the properties of the sediment and its geographical location influence the pollen source it receives (Luo et al., 2009; Huang et al., 2010; Zhang et al., 2022; Zhao et al., 2022). Based on field observation and multi-climate proxy results, we point out that the sediment in the JRT section can be distinguished in at least two distinct phases: A deep aeolian loess and a thin paleosol layer. The boundary between these two layers is at a depth of approximately 50 cm, and 90–50 cm represents the transition phase (Figure 3).

In the JRT section, the pollen assemblage of the loess layer is significantly different from that of in the paleosol. *Pinus*, *Artemisia*, Asteraceae and an abundance of other pollen species (e.g., *Picea*, Betulaceae, Poaceae) occur in the loess layer. *Artemisia* and *Amaranthaceae* are the absolute dominant components of fossil pollen in the paleosol layer. *Ephedra* and *Sliax* pollen attain higher proportions. In overall terms, species are more abundant but pollen concentration is lower in the loess layer in the JRT section, while the opposite is true in the paleosol (Figure 3).

Studies of pollen assemblages in modern surface soil and their relationships to vegetation carried out in the Ili Valley and surrounding areas have shown that *Pinus*, *Picea*, *Ephedra*, *Artemisia,* and Orthomorphic are reported to be over-represented. These types of pollen have high pollen production or can be spread over longer distances by wind (Yang et al., 2004; Luo et al., 2009; Zhao and Li, 2013; Niu et al., 2022). Therefore, the ecological significance of these pollen needs to be considered to the nature of the sediments and their geographical location.

As described in Section 3.1, the JRT section is a typical aeolian deposition close to the Kashi River's modern channel. The main transporting force for pollen sources of the JRT section were either wind-powered or hydrodynamic. Furthermore, changes in the local hydrological environment may also have led to vegetation conditions at micro-landscapes that exhibit different characteristics from those of the surrounding area.

In terms of aeolian dust dynamics alone, the rate of accumulation of Ili loess over the past 36 ka has been influenced mainly by the intensity of the Siberian High-pressure system. A strong Siberian high-pressure will drive cold air over the ACA and lead to frequent and intense dust activities in winter and spring (Ye et al., 2000; Orlovsky et al., 2005; Li et al., 2019; Kang et al., 2022; Li et al., 2022). In addition, the typical aeolian deposits of the Ili Valley are extremely poor for forming soil with poor vegetation cover (Li et al., 2020; Yang et al., 2020). During the Last Glacical, local and poorly developed vegetation provided only a very limited amount of pollen for the JRT section. Frequent dust activity facilitated pollen dispersal over longer distances (Figure 4C,F,G). *Pinus* is the most typical representative. Modern it do not grow in the Ili Valley and surrounding mountains. In the JRT section, a relatively high sand fraction content, the percentage of *Pinus* pollen, pollen concentration, and low A/C and TOC occur simultaneously at depths of 390–140 cm (Figure 4A–E). Therefore, we suggest the existence of a spatially extensive pollen source of fossil pollen within the loess layer of the JRT section and that the pollen assemblages exhibit regional vegetation characteristics.

During the Late LGM and Post Glacial, relatively high rates of soil deposition occurred in the middle to late Holocene in the Ili Valley (Kang et al., 2022). Because of weaker dust activity, this phenomenon is most likely attributed to an increase in effective moisture and the development of vegetation, thus enhancing the ability of the ground to trap dust (Figure 4G,H) (Chen et al., 2016; Cheng et al., 2017; Gao et al., 2019; Kang et al., 2020; Wang et al., 2020). The results of multi-climate proxies from the JRT section show a strong soil-forming tendency in the paleosol layer and a significantly higher TOC, which also responds to the development of local vegetation (Figure 2). Correspondingly, *Pinus* pollen in the paleosol layer has largely disappeared. The A/C ratio follows a similar trend to TOC and pollen concentration, with an overall increase (Figure 4A,B,D). Based on these evidences, we suggest that vegetation surrounding the JRT section was the main pollen source for the paleosol.

Based on the above discussion and the modern distribution of vegetation in the Ili Valley, we point out that frequent dust activities bring abundant pollen to the JRT section during the loess layer. *Picea* and *Pinus* are typical representatives. They grow in modern only in high altitude mountainous areas and far from the JRT section, but have high percentage of pollen in the loess layer. *Artemisia* is also the dominant pollen type at this stage and has been shown to be super-representative due to its high productivity and the ability to be dispersed over long distances (Xu et al., 2013; Xu and Zhang., 2013). However, a targeted study suggest that *Artemisia's* wind-dependent dispersal ability is much weaker than that of *Picea* and *Pinus*, and its over-representation can be attributed to its high productivity (Wang and Wang., 1983; Cai et al., 2014). The proportion of *Artemisia* and Amaranthaceae is stable in this phase and the A/C corresponds well to TOC. We hypothesize that it comes from a relatively small area. During the Late LGM and Post Glacial, the high percentage of pollen from Artemisia, Amaranthaceae and Ephedra, which may be dependent on the development of paleosols and grow near the JRT section. *Sailx* perhaps depends on wet areas in the Ili Valley such as along the Kash River. The almost disappearance of *Pinus* and the very low percentage of Picea reflect to the presence of spruce forests in mountainous areas.

Based on the above discussion, we also suggest that A/C can reflect the vegetation condition of the lowlands of the Ili Valley, although it differs in source areas at different stages.

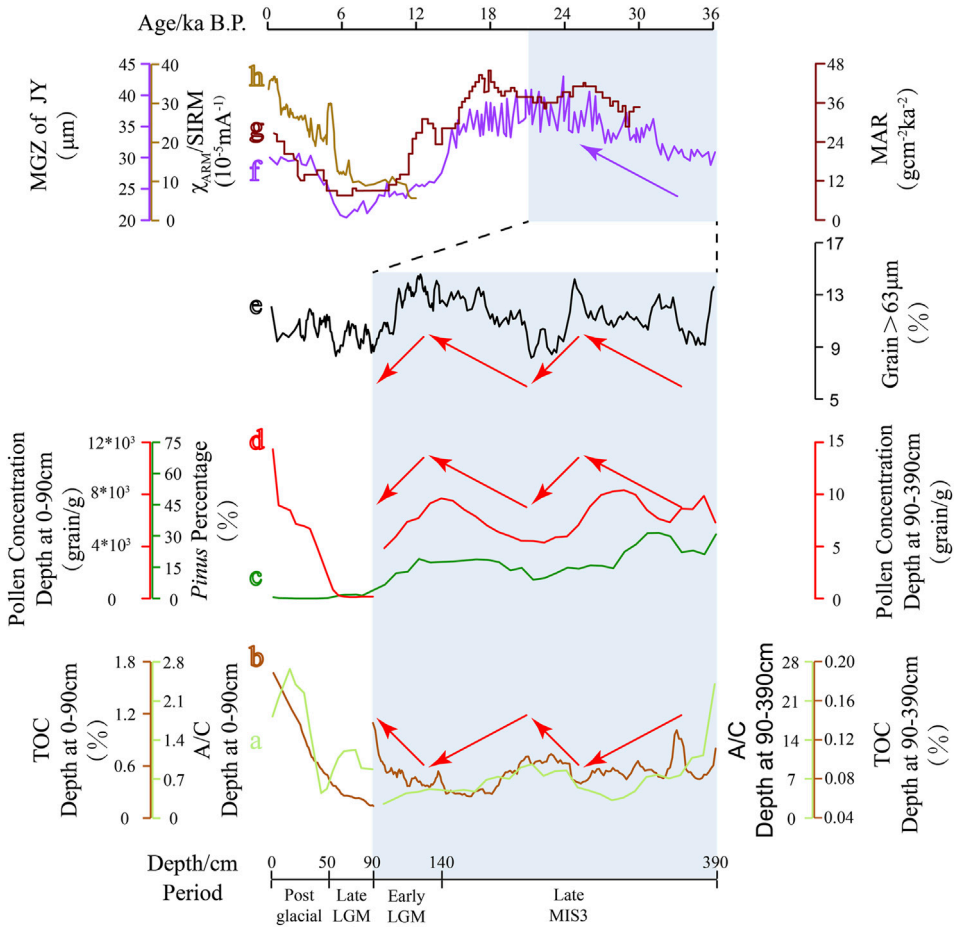

FIGURE 4
Comparison records of pollen assemblages, dust activity, and climate between JRT and ACA during the last 36 ka. **(A–E):** The smoothed curve obtained by the adjacency averaging method of TOC, A/C, pollen concentration (Bounded by a depth of 90 cm, these three proxies have significantly different values in the sediment. Thus, they were separated in the graph and set separately on the y-axis), the percentage of *Pinus* and sand fraction content of the JRT (this study). **(F):** Mean grain sizes of the Jingyuan loess section located in the northwestern China Loess Plateau (Sun et al., 2010); **(G)**: stacked mass accumulation rate (MAR) record in the Ili valley (Kang et al., 2022); **(H)**: the χ_{ARM}/SIRM ratio of the LJW10 Holocene paleosol section (Chen et al., 2016); The red arrows mark the trend of the climate proxies in the JRT section; The purple arrow marks the enhancing trend of Siberian High-pressure from Late MIS3 to LGM; The two blue bars represent the same time period, which is defined by the intensity of the stronger Siberian High-pressure.

5.2 Vegetation history in the Ili Valley during the last 36 ka

The pollen record from the JRT section provides a clear and brief history of vegetation in the eastern Ili Valley during the last 36 ka. We continue to base our analysis on the four stages described above and discuss its change process (Figure 3).

During the Late MIS3, the relatively stable and high percentage (mean of 51.296%) of *Artemisia* reflect the general desert-steppe status within the lowland areas of the Ili Valley. Moisture-loving *Asteraceae, Poaceae* and some arboreal plants (e.g., *Quercus, Betulaceae,* and *Ulmus*) may grow in localized areas with humid condition. The highest percentage of *Pinus* that occurs in this stage and has a very large variation (4.3%–62.5%), suggesting that *Pinus* forests were present in the surrounding mountains of the Ili Valley. Based on its relationship with TOC and sand fraction, we further suggest that the forest line may have declined when the environment deteriorated. The situation regarding *Picea* is similar to it. So stronger dust activities can carry more abundant pollen into the lowland areas.

Compared with the previous stage, the change of pollen concentration in the Early LGM is not obvious. However, the sustained increase in the percentage of *Amaranthaceae* suggests the deterioration of vegetation. The extremely monotonous pollen spectra (*Artemisia*, *Pinus*, *Asteraceae*) assemblage further confirms the phenomenon. The entirety of the lowland areas of the Ili Valley is dominated by typical desert vegetation. Sand fraction is still high in JRT section. Changes in

Pinus concentrations responded to the trend of diminishing dust activity, and *Picea* almost disappeared. These results may foreshadow the degradation of forests in the mountains.

The increase in pollen concentration reveals the initial development of vegetation surrounding the JRT section in the Late LGM. Amaranthaceae is the dominant local vegetation species. In addition, the typical drought-tolerant vegetation *Ephedra* occurred in the pollen spectra. This observation, when combined with the disappearance of Asteraceae and Poaceae, allows us to infer that the vegetation was a typical desert type at the early stage of soil formation surrounding the JRT section. Despite the further weakening of dust activity, the frequent occurrence of *Picea* pollen in the JRT section indicates the expansion of montane forests at this stage.

Changes in fossil pollen assemblage and concentration suggest that the vegetation condition surrounding the JRT section has improved remarkably during the Post Glacial. However, the worst vegetation condition surrounding the JRT section persisted into the Holocene, which differs markedly from the situation of the mountain forests. Counter-trending the changes in the content of *Artemisia* and *Amaranthaceae*, the percentage of *Ephedra* decrease slightly but is still present. *Salix* may grow along the Kashi River or be supported by groundwater, but it only represents the vegetation status of a micro-landscape. Among arboreal plants, only *Picea* and *Salix* play important roles. Although the weak dust activity is a cause, the average concentration of *Picea* pollen of less than 1% indicates that the *Picea* forests are far from the JRT section (Luo et al., 2009; Zhao and Li, 2013). In summary, the vegetation condition near the JRT section has improved significantly. It provides a large source of pollen for the JRT section. But it is a typical desert steppe or riverine meadow vegetation type.

5.3 Relationship between vegetation and climate change in the arid Central Asia during the last glacial maximum

An abundant and detailed vegetation history in the modern Interglacial can be obtained from the various sediments of the ACA. Along with the increased effective moisture during the middle and late Holocene, these records show some commonalities, such as a rich variety of pollen species, a reduction in the percentage of *Ephedra*, and an increase in both pollen concentration and the percentage of *Artemisia* pollen (Tarasov et al., 1997; Chen et al., 2008; Huang et al., 2009; Ran et al., 2015; Zhang and Feng, 2018; Wang and Zhang, 2019; Chen et al., 2019; Zhao et al., 2022).

However, with the decrease in solar radiation at high latitudes and the southward shift and weakening of westerly belt during the LGM (Berger and Loutre, 1991; Clark et al., 2009; Lei et al., 2021), precipitation and river runoff significantly decreased in the ACA. These factors limit the development of ideal fossil pollen carrier sediments such as lake and peat (Yang and Liu., 2003; Li et al., 2016; Zhang et al., 2016; Duan et al., 2018; Zhao et al., 2021). Studies from different regions have shown that small lake basins with short shorelines receive more endemic pollen than larger lake basins, and the mixing effect on pollen is weaker, which may lead to a poorer response of lake pollen assemblages to regional vegetation and climate change (Davis and Brubaker, 1973; Jacobson and Bradshaw, 1987; Sun and Wu, 1987; Jackson, 1990; Tian et al., 2009). Significant increases in sediment sand fraction indicate Lakes Ailike, Ebi, Manas, and Balikun have shrunk rapidly since the LGM. This phase generally lasted for nearly 10,000 years or even longer (Rhodes et al., 1996; Zhao et al., 2015; Jia et al., 2020; Chen and Liu., 2022). Some similar changes are also observed in the pollen records, such as the monotony of pollen types and the decrease in the proportion of *Pinus* and *Picea* (Figure 5). The above phenomena point to the vegetation near the lake basin become the main fossil pollen source because of the shrinking of the lake. This could also be attributed to the degradation of regional woodland vegetation features experienced during this time or a combination thereof. However, more detailed information can not be obtained from these lakes.

Our results effectively complement the vegetation history and its links to the climate of this period. Compared to the Late MIS3, significant vegetation degradation occurred in both the montane forest and the lowland desert steppe during the Early LGM. In the Late LGM, paleosols gradually developed around the JRT section. The presence of *Picea* in the pollen spectra also indicates the recovery of montane vegetation (Figure 4). These changes occurred significantly earlier than in the lake sediment records, but coincided with the increased insolation in the mid-to-high-latitude Northern Hemisphere (Berger and Loutre, 1991). Modern observations show that vegetation development at high latitudes in the Northern Hemisphere responds to increases in temperature and CO_2 concentration (Lucht et al., 2002; Piao et al., 2006). Therefore, we speculate that increased insolation in the Northern Hemisphere was a direct factor in the development of the montane forest zone in the ACA during the Late LGM. The corresponding increase in precipitation from glacial meltwater and westerly rapids has also effectively improved the vegetation conditions in the lowland areas of ACA.

However, the present information from the lake records indicates that the vegetation condition in the ACA began to degrade in the Early LGM. The phenomenon lasted for nearly 10,000 years or even longer (Figure 5). The process of global lake response to climate change in recent decades explains this phenomenon (Woolway et al., 2020). When the climate turns warm, the increased evaporation and the mean of precipitation or river recharge will exert a combined influence on the lake area. Higher evaporation rates will cause a decrease in lake level and reduction in surface water extent. Several of the lakes mentioned above are dependent on runoff and meltwater recharge. The changing conditions of these lakes of rapid warming in the Late LGM

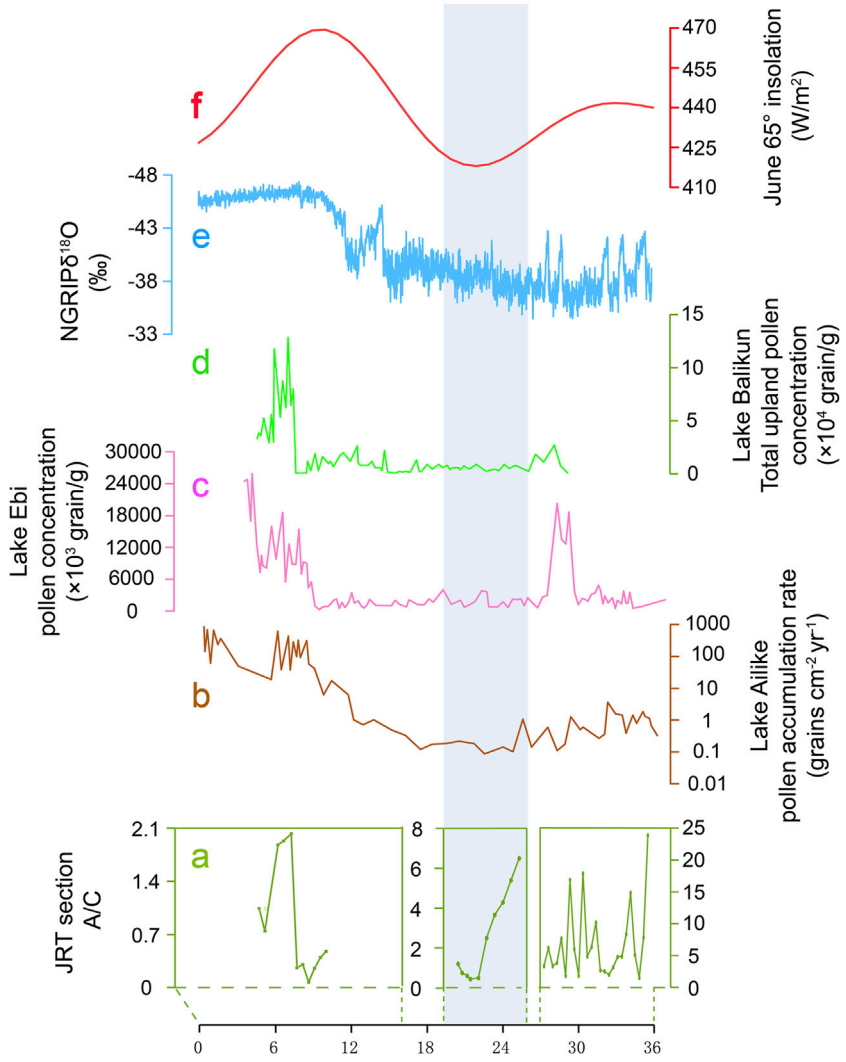

FIGURE 5
Comparison of the vegetation condition obtained from sediment fossil pollen reconstruction with climate records in the ACA. **(A)** A/C of the JRT section; **(B)** Pollen accumulation rate of Lake Ailike (Chen and Liu, 2022); **(C)** Pollen concentration of Lake Ebi (Jia et al., 2020); **(D)** Total upload pollen concentration of Lake Balikun (Tao et al., 2010; Zhao et al., 2015); **(E)** Greenland NGRIP $\delta^{18}O$ record on GICC053 1.0063 chronology (WAIS Divide Project Members, 2015); **(F)** Solar insolation at 65°N for July (Berger and Loutre, 1991). The blue bar represents the time of the LGM (Clark et al., 2009); The X-axis of the data from the JRT section uses a dashed line, which only represents that the corresponding data exists in an approximate time period.

and Post Glacial can be inferred from the patterns of change in lake states under global warming. More recharge and higher evaporation work together to affect the water balance of the lake, and a smaller lake area may have lasted longer and lagged behind the temperature rise during the Late LGM and Post Glacial (Figure 5). Endemic pollen is always the main pollen source in such lakes. When the regional vegetation was restored, the pollen record in these lakes could not respond effectively to this change.

To simplify, we designed a model diagram to express the differences in pollen response to vegetation and climate in loess-paleosol sequences and lake sediments in the ACA. Both the vegetation surrounding the depositional area and the region provide pollen sources for sediments mainly through the action of wind or water. Pollen assemblages from lakes during the interglacial and from the loess during the glacial are more likely to come from an enlarged area and tending to reflect the relationship between the regional vegetation and climatic conditions. When the climate changes, at least for a shift from cold-dry to warm-wet, the response of the lake state and its pollen assemblage is a lag (Figure 6).

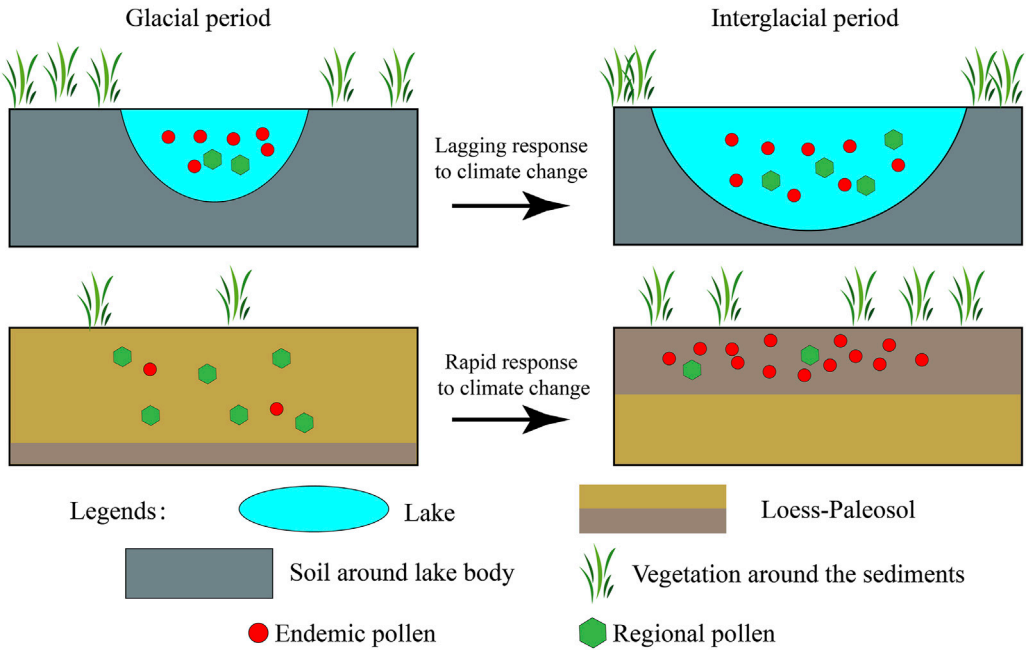

FIGURE 6
A model for expressing variation in pollen assemblages and responses to climate change in the lake and loess-paleosol sequence under ideal conditions.

6 Conclusions

A local/regional vegetation history was revealed by a loess-paleosol sequence in the eastern Ili Valley since the Late MIS3. In brief, the environment of lowland areas is always drought and harsh. Typical desert/desert steppe is dependent on rivers and groundwater. Mountainous forests can develop in suitable environments, such as the Late MIS3 and Post Glacial. In the Early LGM, significant vegetation deterioration occurred in both the lowland area of the valley and the mountains. Our results further show that vegetation restoration and environmental improvement occurred in the Late LGM and were attributed to increased Northern Hemisphere high-latitude insolation. This point in time is much earlier than previously known from lake sediments. A simple model diagram was designed to explain this phenomenon. We suggest that change in the loess-paleosol sequence and its pollen assemblage is more sensitive to vegetation and climate change during the transition from the glacial to interglacial.

Data availability statement

The raw data supporting the conclusions of this article will be made available by the authors, without undue reservation.

Author contributions

YM and ZL designed the study. MQ, QR, JL participated in the fieldwork. PL conducted the experiment and data analysis. PL, YM, ZL, SZ, and MQ wrote and revised the manuscript. All authors contributed to the article and approved the submitted version.

Funding

This research is supported by the Pan-Third Pole Environment Study for a Green Silk Road (Pan-TPE) (XDA2004010101), and the National Natural Science Foundation of China (NSFC, Grants No. 42030505, 42161144012).

Conflict of interest

The authors declare that the research was conducted in the absence of any commercial or financial relationships that could be construed as a potential conflict of interest.

Publisher's note

All claims expressed in this article are solely those of the authors and do not necessarily represent those of their affiliated organizations, or those of the publisher, the editors and the reviewers. Any product that may be evaluated in this article, or claim that may be made by its manufacturer, is not guaranteed or endorsed by the publisher.

References

An, C. B., Tao, S. C., Zhao, J. J., Chen, F. H., Lv, Y. B., Dong, W. M., et al. (2013). Late Quaternary (30.7-9.0 cal ka BP) vegetation history in Central Asia inferred from pollen records of Lake Balikun, northwest China. *J. Paleolimnol.* 49 (2), 145–154. doi:10.1007/s10933-012-9649-7

Berger, A., and Loutre, M. F. (1991). Insolation values for the climate of the last 10 million years. *Quat. Sci. Rev.* 10 (4), 297–317. doi:10.1016/0277-3791(91)90033-Q

Cai, P., Wan, T., Han, X. L., Ge, Y. H., and Xu, Z. P. (2014). Research on pollen of Artemisia frigida spread. *Grassl. Prataculture* 26 (04), 26–29. doi:10.3969/j.issn.2095-5952.2014.04.007

Chen, F. H., Chen, J. H., Wang, W., Chen, S. Q., Huang, X. Z., Jin, L. Y., et al. (2019). Westerlies Asia and monsoonal Asia: Spatiotemporal differences in climate change and possible mechanisms on decadal to sub-orbital timescales. *Earth. Sci. Rev.* 192, 337–354. doi:10.1016/j.earscirev.2019.03.005

Chen, F. H., Huang, W., Jin, L. Y., Chen, J. H., and Wang, J. S. (2011). Spatiotemporal precipitation variations in the arid Central Asia in the context of global warming. *Sci. China Earth Sci.* 41 (11), 1812–1821. doi:10.1007/s11430-011-4333-8

Chen, F. H., J, J., Chen, J. H., Li, G. Q., Zhang, X. J., Xie, H. C., et al. (2016). A persistent Holocene wetting trend in arid central Asia, with wettest conditions in the late Holocene, revealed by multi-proxy analyses of loess-paleosol sequences in Xinjiang, China. *Quat. Sci. Rev.* 146, 134–146. doi:10.1016/j.quascirev.2016.06.002

Chen, F. H., Yu, Z. C., Yang, M. L., Ito, E., Wang, S. M., Madsan, D. B., et al. (2008). Holocene moisture evolution in arid central Asia and its out-of-phaserelationship with Asian monsoon history. *Quat. Sci. Rev.* 27 (3-4), 351–364. doi:10.1016/j.quascirev.2007.10.017

Chen, J., Wang, Y. J., Chen, Y., Liu, L. W., Ji, J. F., and Lu, H. Y. (2001). Rb and Sr geochemical characterization of the Chinese loess and its implications for palaeomonsoon climate. *Acta Geol. Sin.* 75 (02), 259–266. doi:10.1111/j.1755-6724.2000-02-025

Chen, Q. Q., Shen, C. D., Sun, Y. M., Peng, S. L., Yi, W. X., Li, Z. A., et al. (2005). Meahanism of distribution of soil organic matter with deoth due to evolution of soil profiles at the dinghushan biosphere reserve. *Acta. Pedol. Sin.* 42 (1), 1–8.

Chen, Y. R., and Liu, X. Q. (2022). Vegetation and climate changes since the middle MIS 3 inferred from a Lake Ailike pollen record, xinjiang, arid central Asia. *Quat. Sci. Rev.* 290, 107636. doi:10.1016/j.quascirev.2022.107636

Cheng, L. Q., Song, Y. G., Sun, H. Y., and Orzbaev, R. (2017). Spatio-temporal distribution of dust sedimentation rate of Tianshan loess since MIS3 and its implications. *Mar. Geol. Quat. Geol.* 39 (1), 143–153. doi:10.16562/j.cnki.0256-1492.2017032001

Chevaliera, M., Davisa, B. A. S., Heirib, O., Seppäc, H., Chase, B. M., Gajewski, K., et al. (2020). Pollen-based climate reconstruction techniques for late Quaternary studies. *Earth. Sci. Rev.* 210, 103384. doi:10.1016/j.earscirev.2020.103384

Clark, P. U., Dyke, A. S., Shakun, J. D., Carlson, A. E., Clark, J., Wohlfarth, B., et al. (2009). The last glacial Maximum. *Science* 325 (5941), 710–714. doi:10.1126/science.1172873

Davis, B. M., and Bruaker, L. B. (1973). Differential stedimentation of pollen grains in lakes. *Limnol. Oceanogr.* 18 (4), 635–646. doi:10.4319/lo.1973.18.4.0635

Ding, Z. L., Ranov, V., Yang, S. L., Finaev, J. M., Han, J. M., and Wang, G. A. (2002). The loess record in southern Tajikistan and correlation with Chinese loess. *Earth Planet. Sci. Lett.* 200 (3-4), 387–400. doi:10.1016/S0012-821X(02)00637-4

Duan, F. T., An, C. B., Zhao, Y. T., Zhang, X. N., Zhou, A. F., and Huang, X. Z. (2018). A preliminaey study on the climate change since the last interglaciation based on lake sediments from Xinjiang, Northwest China. *Quat. Sci.* 35 (5), 1156–1165. doi:10.11928/j.issn.1001-7410.2018.05.10

Fang, X. M., Shi, Z. T., Yan, M. D., Li, J. J., and Jiang, P. A. (2002). Loess in the tian Shan and its implications for the develop-ment of the Gurbantunggut Desert and drying of northern xinjiang. *Chin. Sci. Bull.* 47 (16), 1381–1387. doi:10.1360/02tb9305

Fordham, D. A., Jackson, S. T., Brown, S. C., Huntley, B., Brook, B. W., Dahl-Jensen, D., et al. (2020). Using paleo-archives to safeguard biodiversity under climate change. *Science* 363 (1072), eabc5654. doi:10.1126/science.abc5654

Gallet, S., John, B. M., and Toril, M. (1996). Geochemical characterization of the Luochuan loess-paleosol sequence, China, and paleoclimatic implications. *Chem. Geol.* 133 (1-4), 67–88. doi:10.1016/S0009-2541(96)00070-8

Gao, F. Y., Jia, J., Xia, D. S., and Wang, Y. J. (2019). Assessment of the dominant climatic factor affecting pedogenic development in eolian sequences during the Holocene in arid central Asia. *Quat. Int.* 502, 78–84. doi:10.1016/j.quaint.2018.04.039

Grimm, E. C. (1987). CONISS: A FORTRAN 77 program for stratigraphically constrained cluster analysis by the method of incremental sum of squares. *Comput. Geosci.* 13 (1), 13–35. doi:10.1016/0098-3004(87)90022-7

Grimm, E. C. (2004). *TILIA and TILIA.GRAPH v.2.0.2*. USA: Illinois State Museum, Spring-field.

Hu, Q., and Han, Z. H. (2022). Northward expansion of desert climate in central Asia in recent decades. *Geophys. Res. Lett.* 49 (11). doi:10.1029/2022GL098895

Huang, X. Z., Chen, F. H., Fan, Y. X., and Yang, M. L. (2009). Dry late-glacial and early Holocene climate in arid central Asia indicated by lithological and palynological evidence from Bosten Lake, China. *Quat. Int.* 194, 19–27. doi:10.1016/j.quaint.2007.10.002

Huang, X. Z., Zhou, G., Ma, Y. L., Xu, Q. H., and Chen, F. H. (2010). Pollen distribution in large freshwater lake of arid region: A case study on the surface sediments from Bosten lake, xinjiang, China. *Front. Earth Sci. China* 4 (2), 174–180. doi:10.1007/s11707-009-0060-2

Jackson, S. T. (1990). Pollen sourcearea and representation in small lakes of the Northeastern United States. *Rev. Palaeobot. Palynol.* 63, 53–76. doi:10.1016/0034-6667(90)90006-5

Jacobson, G. L., and Bradshaw, R. H. W. (1987). The selection of sites for paleovegetational studies. *Quat. Res.* 16 (1), 80–96. doi:10.1016/0033-5894(81)90129-0

Jia, H., Wu, J. L., Zhang, H., and Yi, S. (2020). Pollen-based climate reconstruction from Ebi Lake in northwestern China, Central Asia, over the past 37, 000 years. *Quat. Int.* 544, 96–103. doi:10.1016/j.quaint.2020.02.033

Kang, S. G., Wang, X. L., Roberts, H. M., Duller, G. A. T., Song, Y. G., Liu, W. G., et al. (2020). Increasing effective moisture during the Holocene in the semiarid regions of the Yili basin, central asia: Evidence from loess sections. *Quat. Sci. Rev.* 246, 106553. doi:10.1016/j.quascirev.2020.106553

Kang, S. G., Wang, X. L., Wang, N., Song, Y. G., Liu, W. G., Wang, D., et al. (2022). Siberian High modulated suborbitalscale dust accumulation changes over the past 30 ka in the eastern Yili Basin, Central Asia. *Paleoceanogr. Paleoclimatol.* 37, e2021PA004360. doi:10.1029/2021PA004360

Lai, Z. P., and Ou, X. J. (2003). Basic procedures of optically stimulated luminescence (OSL) dating. *Prog. Geogr.* 32, 683–693. doi:10.11820/dlkxjz.2013.05.001

Lei, J., Shi, Z. G., Xie, X. N., Shi, Y. Y., Li, X. Z., Liu, X. D., et al. (2021). Seasonal variation of the westerly Jet over asia in the last glacial Maximum: Role of the Tibetan plateau heating. *J. Clim.* 37 (7), 2723–2740. doi:10.1175/JCLI-D-20-0438.1

Li, C., Cao, Z. Z., Ding, L., Shi, Y., and Yang, Z. H. (2012). Climate change Characters in recent 50 Years in Yili valley xinjiang. *J. Shanxi Agric. Sci.* 40 (5), 508–514. doi:10.3969/j.issn.1002-2481.2012.05.23

Li, G. Q., Rao, Z. G., Duan, Y. W., Xia, D. S., Wang, L. B., Madsen, D. B., et al. (2016). Paleoenvironmental changes recorded in a luminescence dated loess/paleosol sequence from the Tianshan Mountains, arid central Asia, since the Penultimate Glaciation. *Earth Planet. Sci. Lett.* 448, 1–12. doi:10.1016/j.epsl.2016.05.008

Li, J. F. (1991). *Climate in Xinjiang*. Beijing: China Meteorological Press.

Li, L. Q., Kürschner, K. M., Lu, N., Chen, H. Y., An, P. C., and Wang, Y. D. (2022). Palynological record of the Carnian Pluvial Episode from the northwestern Sichuan basin, SW China. *Rev. Palaeobot. Palynol.* 304, 104704. doi:10.1016/j.revpalbo.2022.104704

Li, X. Q., Zhao, K. L., Dodson, J., and Zhou, X. Y. (2011). Moisture dynamics in central asia for the last 15 kyr: New evidence from Yili valley, xinjiang, NW China. *Quat. Sci. Rev.* 30 (23-24), 3457–3466. doi:10.1016/j.quascirev.2011.09.010

Li, Y., Piao, S. L., Li, L. Z. X., Chen, A. P., Wang, X. H., Ciais, P., et al. (2018). Divergent hydrological response to large-scale afforestation and vegetation greening in China. *Sci. Adv.* 4 (5), eaar4182. doi:10.1126/sciadv.aar4182

Li, Y., Song, Y. G., Fitzsimmons, K. E., Chen, X. L., Prud'homme, C., and Zong, X. L. (2020). Origin of loess deposits in the north tian Shan piedmont, central asia. *Palaeogeogr. Palaeoclimatol. Palaeoecol.* 559, 109972. doi:10.1016/j.palaeo.2020.109972

Li, Y., Song, Y. G., Kaskaoutis, D. G., Zhang, X. X., Chen, X. L., Shukurov, N., et al. (2022). Atmospheric dust dynamics over central asia: A perspective view from loess deposits. *Gondwana Res.* 109, 150–165. doi:10.1016/j.gr.2022.04.019

Li, Y., Song, Y. G., Qiang, M. R., Miao, Y. F., and Zeng, M. X. (2019). Atmospheric dust variations in the Ili basin, northwest China, during the last glacial period as revealed by a high mountain loess-paleosol sequence. *J. Geophys. Res. Atmos.* 124 (15), 8449–8466. doi:10.1029/2019JD030470

Liu, L. Y., and Zhang, X. (2021). *Global land-cover product with fine classification system at 30 M using time-Series Landsat Imagery V1.0*. Aerospace Information Research Institute, Chinese Academy of Sciences. doi:10.12237/casearth.6123651428a58f70c2a51e49

Liu, X. M., Liu, D. S., Heller, F., and Xu, T. C. (1990). Frequency-dependent susceptibility of loess and quaternary paleoclimate. *Quatern. Sci.* 10 (01), 42–50. doi:10.1007/s00376-999-0032-1

Lu, H. X., Liu, W. G., Yang, H., Wang, H. Y., Liu, Z. H., Leng, Q., et al. (2019). 800-kyr land temperature variations modulated by vegetation changes on Chinese Loess Plateau. *Nat. Commun.* 10, 1958. doi:10.1038/s41467-019-09978-1

Lucht, W., Prentice, I. C., Myneni, R. B., Stich, S., Friedlingsten, p., Cramer, W., et al. (2002). Climatic Control of the high-latitude vegetation greening trend and Pinatubo effect. *Science* 296 (5573), 1687–1689. doi:10.1126/science.1071828

Luo, C. X., Zheng, Z., Tarasov, P., Pan, A. D., Huang, K. Y., Beaudouin, C., et al. (2009). Characteristics of the modern pollen distribution and their relationship to vegetation in the Xinjiang region, northwestern China. *Rev. Palaeobot. Palynol.* 153, 282–295. doi:10.1016/j.revpalbo.2008.08.007

Marx, S. K., Kamber, B. S., Mcgowan, H. A., Petherick, L. M., Mctainsh, G. H., Stromsoe, N., et al. (2018). Palaeo-dust records: A window to understanding past environments. *Glob. Planet. Change* 165, 13–43. doi:10.1016/j.gloplacha.2018.03.001

Meyers, P. A. (1997). Organic geochemical proxies of paleoceanographic, paleolimnologic, and paleoclimatic processes. *Org. Geochem.* 27 (5-6), 213–250. doi:10.1016/S0146-6380(97)00049-1

Miao, Y. F., Warny, S., Clift, P. D., Liu, C., and Gregory, M. (2017). Evidence of continuous Asian summer monsoon weakening as a response to global cooling over the last 8 Ma. *Gondwana Res.* 52, 48–58. doi:10.1016/j.gr.2017.09.003

Mottl, O., Flantua, S., Bhatta, K. P., Felde, V. A., Giesecke, T., Goring, S., et al. (2021). Global acceleration in rates of vegetation change over the past 18, 000 years. *Science* 372 (6544), 860–864. doi:10.1126/science.abg1685

Murray, A. S., and Wintle, A. G. (2000). Luminescence dating of quartz using an improved single-aliquot regenerative-dose protocol. *Radiat. Meas.* 32 (1), 57–73. doi:10.1016/S1350-4487(99)00253-X

Narisma, G. T., Foley, J. A., Licker, R., and Ramankutty, N. (2007). Abrupt changes in rainfall during the twentieth century. *Geophys. Res. Lett.* 34, 067100–L7316. doi:10.1029/2006GL028628

Niu, D. Y., Li, J. Y., Wang, N. L., Du, J. F., and Chen, X. J. (2022). Relationship between pollen assemblages in surface soil and modern vegetation and climate in the Western Tianshan Mountains, Xinjiang. *J. Glaciol. Geocryol.* 44 (3), 1–13. doi:10.7522/j.issn.1000-0240.2022.0088

Orlovsky, L., Orlovsky, N., and Durdyev, A. (2005). Dust storms in Turkmenistan. *J. Arid. Environ.* 60, 83–97. doi:10.1016/j.jaridenv.2004.02.008

Piao, S. L., Friedlingstein, P., Ciais, P., Zhou, L. M., and Chen, A. P. (2006). Effect of climate and CO2 changes on the greening of the Northern Hemisphere over the past two decades. *Geophys. Res. Lett.* 33, L23402. doi:10.1029/2006GL028205

Prospero, J. M., Ginoux, P., Torres, O., Nicholson, S. E., and Gill, T. M. (2002). Environmental characterization of global sources of atmospheric soil dust identified with the NIMBUS 7 Total Ozone Mapping Spectrometer (TOMS) absorbing aerosol product. *Rev. Geophys.* 40 (1), 1–31. doi:10.1029/2000rg000095

Ran, M., Zhang, C. J., and Feng, Z. D. (2015). Climatic and hydrological variations during the past 8000 years in northern Xinjiang of China and the associated mechanisms. *Quat. Int.* 358, 21–34. doi:10.1016/j.quaint.2014.07.056

Rhodes, T. E., Gasse, F., Lin, R. F., Fonts, J. C., Wei, K. Q., Bertrand, P., et al. (1996). A late Pleistocene-Holocene lacustrine record from lake Manas, Zunggar (northern xinjiang, Western China). *Palaeogeogr. Palaeoclimatol. Palaeoecol.* 120, 105–121. doi:10.1016/0031-0182(95)00037-2

Shi, Y. F., Shen, Y. P., Kang, E., Li, D. L., Ding, Y. J., Zhang, G. W., et al. (2007). Recent and future climate change in northwest China. *Clim. Change* 80, 379–393. doi:10.1007/s10584-006-9121-7

Siegfried, T., Bernauer, T., Guiennet, R., Sellars, S., Robertson, A. W., Mankin, J., et al. (2012). Will climate Change exacerbate or mitigate water stress in central Asia? *Clim. Change* 112, 881–899. doi:10.1007/s10584-011-0253-z

Song, Y. G., Li, Y., Cheng, L. Q., Zong, X. L., Kang, S. G., Ghafarpour, A., et al. (2021). Spatio-temporal distribution of quaternary loess across central asia. *Palaeogeogr. Palaeoclimatol. Palaeoecol.* 567 (110279), 110279. doi:10.1016/j.palaeo.2021.110279

Sun, X. J., and Wu, Y. S. (1987). Distribution and quantity of sporopollen and algae in surface sediments of the Dianchi lake, Yunnan Preovince. *Mar. Geo. Quat. Geo.* 7 (04), 83–94.

Sun, Y. B., Wang, X. L., Liu, Q. S., and Clemens, S. C. (2010). Impacts of post-depositional processes on rapid monsoon signals recorded by the last glacial loess deposits of northern China. *Earth Planet. Sci. Lett.* 289 (1–2), 171–179. doi:10.1016/j.epsl.2009.10.038

Tang, L. Y., Mao, L. M., Shu, J. W., Li, C. H., Shen, C. M., and Zhou, Z. Z. (2016). *An Illustrated Handbook of Quaternary pollen and spores in China*. Beijing: Science Press.

Tao, S. C., An, C. B., Chen, F. H., Tang, L. Y., Wang, Z. L., Lü, Y. B., et al. (2010). Pollen-inferred vegetation and environmental changes since 16.7 ka BP at Balikun Lake, Xinjiang. *Chin. Sci. Bull.* 55 (22), 2449–2457. doi:10.1007/s11434-010-3174-8

Tarasov, P. E., Jolly, D., and Kaplan, J. O. (1997). A continuous Late Glacial and Holocene record of vegetation changes in Kazakhstan. *Palaeogeogr. Palaeoclimatol. Palaeoecol.* 136, 281–292. doi:10.1016/S0031-0182(97)00072-2

Taylor, S. R., and McLennan, S. M. (1985). *The continental crust: Its composition and Evolution*. Oxford: Blackwell.

Tian, F., Xu, Q. H., Li, Y. C., Cao, X. Y., Wang, X. L., and Zhang, L. Y. (2009). Pollen assemblage characteristics of lakes in the monsoon fringe area of China. *Sci. Bull. (Beijing).* 54 (4), 3354–3363. doi:10.1007/s11434-008-0408-0

Tian, Z. P., Zhuang, L., and Li, J. G. (2012). The vertical distribution of vegetation patterns and its relationship with environment factors at the northern slope of Ili river valley: A bimodal distribution pattern. *Acta eco. Sin.* 32 (4), 1151–1162. doi:10.5846/stxb201012271856

Újvári, G., Kok, J. F., Varga, G., and Kovács, J. (2016). The physics of wind-blown loess: Implications for grain size proxy interpretations in Quaternary paleoclimate studies. *Earth. Sci. Rev.* 154, 247–278. doi:10.1016/j.earscirev.2016.01.006

Uno, I., Eguchi, K., Yumimoto, K. E., Takemura, T., Shimizu, A., Uematsu, M., et al. (2009). Asian dust transported one full circuit around the globe. *Nat. Geosci.* 2 (8), 557–560. doi:10.1038/ngeo583

WAIS Divide Project Members (2015). Precise interpolar phasing of abrupt climate change during the last ice age. *Nature* 520, 661–665. doi:10.1038/nature14401

Wang, F. X., Qian, N. F., Zhang, Y. L., and Yang, H. Q. (1995). *Pollen Flora of China*. Beijing: Science Press.

Wang, K. F., and Wang, X. Z. (1983). *Introduction to sporology*. Beijing: Peking University Press.

Wang, Q., Wei, H. T., Khormali, F., Wang, L. B., Yan, H. Y., Xie, H. C., et al. (2020). Holocene moisture variations in Western arid central Asia inferred from loess records from NE Iran. *Geochem. Geophys. Geosyst.* 21 (3). doi:10.1029/2019GC008616

Wang, W., and Feng, Z. D. (2013). Holocene moisture evolution across the Mongolian plateau and its surrounding areas: A synthesis of climatic records. *Earth. Sci. Rev.* 122, 38–57. doi:10.1016/j.earscirev.2013.03.005

Wang, W., and Zhang, D. L. (2019). Holocene vegetation evolution and climatic dynamics inferred from an ombrotrophic peat sequence in the southern Altai Mountains within China. *Glob. Planet. Change* 179, 10–22. doi:10.1016/j.gloplacha.2019.05.003

Woolway, R. I., Kraemer, B. M., Merchant, C. J., O'Reilly, C. M., and Sharma, S. (2020). Global lake responses to climate change. *Nat. Rev. Earth Environ.* 1, 388–403. doi:10.1038/s43017-020-0067-5

Wu, L. P., Yang, Y. H., Yang, J. Y., Feng, X. C., and Zeng, K. K. (2018). Analysis of precipitation variation characteristics in Kashi River basin in Ili Valley. *J. AnHui Agric. Sci.* 50 (10), 190–194. doi:10.3969/j.issn.0517-6611.2022.10.043

Xia, H. F., Xie, H. B., Liu, H., Wen, G. C., and Li, W. (2018). Relations of vegetation with topography and groundwater in Yili river valley of xinjiang. *J. Yangtze River Sci. Res. Inst.* 35 (9), 54–57. doi:10.11988/ckyyb.20170133

Xinjiang Expedition Team Chinese Academy of Sciences (1978). *Vegetation and its Utilization in Xinjiang*. Beijing: Sciences Press.

Xu, Q. H., Cao, X. Y., Tian, F., Zhang, S. R., Li, Y. C., Li, M. Y., et al. (2013). Relative pollen productivities of typical steppe species in northern China and their potential in past vegetation reconstruction. *Sci. China Earth Sci.* 43 (12), 1254–1266. doi:10.1007/s11430-013-4738-7

Xu, Q. H., Li, M. Y., Zhang, S. R., Zhang, Y. H., Zhang, P. P., and Lu, J. Y. (2015). Modern pollen processes of China: Progress and problems. *Sci. Sin. -Terrae.* 45 (11), 1661–1682. doi:10.1360/zd2015-45-11-1661

Xu, Q. H., and Zhang, S. R. (2013). A clear advance in Soft Actuators Advances in Earth Science. *Science* 28 (9), 968–969. doi:10.1126/science.1243314

Xu, Y. J., Chen, Y. N., Li, W. H., Fu, A. L., Mao, X. D., and Gui, D. W. (2010). Distribution pattern and environmental interpretation of plant species diversity in the mountainous region of Ili River Valley, Xinjiang, China. *Chin. J. Plant Ecol.* 34 (10), 1142–1154. doi:10.3773/j.issn.1005-264x.2010.10.003

Yang, H., Li, G. Q., Huang, X., Wang, X. Y., Zhang, Y. N., Jonell, T. N., et al. (2020). Loess depositional dynamics and paleoclimatic changes in the Yili Basin, Central Asia, over the past 250 ka. *Catena* 195, 104881. doi:10.1016/j.catena.2020.104881

Yang, X. P., and Liu, D. S. (2003). Palaeoenvironments in desert regions of northwest China around 30 ka B.P. *Quat. Sci.* 23 (1), 6. doi:10.3321/j.issn:1001-7410.2003.01.003

Yang, Z. J., Kong, Z. C., Yan, S., Ni, J., Ma, K. P., and Xu, Q. H. (2004). Pollen distribution in Topsoil along the Daxigou Valley in the Headwaters of the Urumqi river the central Tianshan mountains. *Arid. Land Geogr.* 27 (4), 543–547. doi:10.3321/j.issn:1000-6060.2004.04.017

Yao, T. D., Thom, L. G., Shi, Y. F., Qin, D. H., Jiao, K. Q., Yang, Z. H., et al. (1997). A study of climate change records since the last interglacial in the Guria ice core[J]. *Sci. Sin. (Terrae)* (05), 447–452.

Ye, W., Dong, G. R., Yuan, Y. J., and Ma, Y. J. (2000). Climate instability in the Yili region, Xinjiang during the last glaciation. *Chin. Sci. Bull.* 45 (6), 1604–1609. doi:10.1007/bf02886222

Ye, W. (2001). *The characteristics and Paleaoclimate of loess deposits in westerly are*. Beijing: Ocean Press.

Youn, J. H., Seong, Y. B., Choi, J. H., Abdrakhmatov, K., and Ormukov, C. (2014). Loess deposits in the northern Kyrgyz tien Shan: Implications for the paleoclimate reconstruction during the late quaternary. *Catena* 117, 81–93. doi:10.1016/j.catena.2013.09.007

Zhang, D. L., and Feng, Z. D. (2018). Holocene climate variations in the Altai mountains and the surrounding areas: A synthesis of pollen records. *Earth. Sci. Rev.* 185, 847–869. doi:10.1016/j.earscirev.2018.08.007

Zhang, L., Yang, Lin., Zohner, C. M., Crowther, T. W., Li, M. C., Shen, F. X., et al. (2022). Direct and indirect impacts of urbanization on vegetation growth across the world's cities. *Sci. Adv.* 8, eabo0095. doi:10.1126/sciadv.abo0095

Zhang, P., and Liu, W. G. (2008). Loess sedimentary organic matter records from the central chines loess plateau and the implication of C/N ratio. *Mar. Geol. Quat. Geol.* 28 (06), 119–124. doi:10.3724/SP.J.1140.2008.06119

Zhang, S. R., Sun, Y. H., Li, M. Y., Wang, N., and Xu, Q. H. (2022). Paleovegetation and paleotemperature in North China during the mid-Holocene based on sedimentological and palynological evidence from Lake Baiyangdian. *Palaeogeogr. Palaeoclimatol. Palaeoecol.* 595, 110982. doi:10.1016/j.palaeo.2022.110982

Zhang, X. N., Zhou, A. F., Zhang, C., Hao, S. T., Zhao, Y. T., and An, C. B. (2016). High-resolution records of climate change in arideastern central Asia during MIS 3 (51 600-25 300 cal a BP) from Wulungu Lake, north-Western China. *J. Quat. Sci.* 31 (6), 577–586. doi:10.1002/jqs.2881

Zhang, Y. P., Zhang, J. F., Ruan, Q. R., Wang, Y. Q., Han, J. Y., Zhang, J. N., et al. (2021). Geomorphological background and formation process of the Goukou site in Jirentai, Xinjiang[J]. *Quateanary. Sci.* 41 (5), 1376–1393. doi:10.11928/j.issn.1001-7410.2021.05.13

Zhao, K. L., Li, X. Q., Dodson, J., Zhou, X. Y., and Atahan, P. (2013). Climate instability during the last deglaciation in central Asia, reconstructed by pollen data from Yili Valley, NW China. *Rev. Palaeobot. Palynol.* 189, 8–17. doi:10.1016/j.revpalbo.2012.10.005

Zhao, K. L., and Li, X. Q. (2013). Modern pollen and vegetation relationships in the Yili basin, xinjiang, NW China. *Chin. Sci. Bull.* 58, 4133–4142. doi:10.1007/s11434-013-5896-x

Zhao, K. L., Li, X. Q., Xu, H., Zhou, X. Y., Dodson, J., and Liu, J. C. (2019). Increased winter-spring precipitation from the last glaciation to the Holocene inferred from a δ13Corg record from Yili Basin (Xinjiang, NW China). *Sci. China Earth Sci.* 62, 1125–1137. doi:10.1007/s11430-018-9333-x

Zhao, Y. T., An, C. B., Mao, L. M., Zhao, J. J., Tang, L. Y., Zhou, A. F., et al. (2015). Vegetation and climate history in arid Western China during MIS2: New insights from pollen and grain-size data of the Balikun Lake, eastern Tien Shan. *Quat. Sci. Rev.* 126, 112–125. doi:10.1016/j.quascirev.2015.08.027

Zhao, Y. T., An, C. B., Zhou, A. F., Zhang, X. N., Zhao, J. J., Dong, W. M., et al. (2021). Late Pleistocene hydroclimatic variabilities in arid north-west China: Geochemical evidence from Balikun lake, eastern Tienshan, China. *J. Quat. Sci.* 36 (3), 415–425. doi:10.1002/jqs.3288

Zhao, Y. T., Miao, Y. F., Lei, Y., Cao, X. Y., and Xiang, M. X. (2021). Progress, problems and prospects of palynology in reconstructing environmental change in inland arid areas of Asia. *Sci. Cold Arid Regions* 13 (4), 271–291. doi:10.3724/SP.J.1226.2021.20049

Zhao, Y. T., Miao, Y. F., Li, Y., Fang, Y. M., Zhao, J. J., Wang, X. L., et al. (2022). Non-linear response of mid-latitude Asian dryland vegetation to Holocene climate fluctuations. *Catena* 213 (106212), 106212. doi:10.1016/j.catena.2022.106212

frontiers | Frontiers in Earth Science

TYPE Original Research
PUBLISHED 20 January 2023
DOI 10.3389/feart.2023.1121469

Check for updates

OPEN ACCESS

EDITED BY
Harry F. Lee,
The Chinese University of Hong Kong, China

REVIEWED BY
Yan Liu,
East China Normal University, China
Junwu Shu,
Nanjing Institute of Geology and Paleontology (CAS), China

*CORRESPONDENCE
Zhiyuan Shang,
shangzy@njnu.edu.cn

SPECIALTY SECTION
This article was submitted to Quaternary Science, Geomorphology and Paleoenvironment, a section of the journal Frontiers in Earth Science

RECEIVED 11 December 2022
ACCEPTED 10 January 2023
PUBLISHED 20 January 2023

CITATION
Xiao J, Shang Z, Zhang Z, Xiao S and Jia X (2023), A preliminary study on the mechanism of the Liangzhu culture's migration across the Yangtze river. *Front. Earth Sci.* 11:1121469. doi: 10.3389/feart.2023.1121469

COPYRIGHT
© 2023 Xiao, Shang, Zhang, Xiao and Jia. This is an open-access article distributed under the terms of the Creative Commons Attribution License (CC BY). The use, distribution or reproduction in other forums is permitted, provided the original author(s) and the copyright owner(s) are credited and that the original publication in this journal is cited, in accordance with accepted academic practice. No use, distribution or reproduction is permitted which does not comply with these terms.

A preliminary study on the mechanism of the Liangzhu culture's migration across the Yangtze river

Jiayi Xiao[1,2], Zhiyuan Shang[1]*, Zixin Zhang[1,2], Shengjun Xiao[1,3] and Xin Jia[1,2]

[1]School of Geography, Nanjing Normal University, Nanjing, China, [2]Institute of Environmental Archaeology, Nanjing Normal University, Nanjing, China, [3]Nanjing Center, China Geological Survey, Nanjing, China

The Liangzhu culture (5300–4200 cal BP) was the most famous Neolithic culture of who settled near the lower reaches of the Yangtze River in China. The core and initial distribution area of Liangzhu originated around Taihu Lake, located on the south bank of the Yangtze River delta. Recently, archaeological studies believe that the Jianghuai area and Huanghuai area north of the Yangtze River are also important distribution areas of Liangzhu culture. The route for Liangzhu culture migrating across the Yangtze River is inferred as follows: One would have crossed the Yangtze River from Nanjing-Zhenjiang belt and continued to migrate northward; while the other would have crossed the River near the estuary before moving north along the ancient coastline to the Jianghuai during the late period of Liangzhu, or crossed the Yangtze River from the east of the present Beijing-Hangzhou Grand Canal to Jianghuai and Huanghuai. According to the formation of the Yangtze River delta during the Holocene and the evolution of the estuarine sand bar, it is believed that there were large shoals in the Yangtze River channel in the middle-Holocene. The Liangzhu ancestors around 5000 cal BP had the ability of making canoes over 8 m. Based on the archaeological research of the Neolithic period, the evolution of the Yangtze River channel in the Holocene, the history of ancient Chinese shipbuilding, and the modern examples of crossing the Yangtze River with boat, it can be concluded that the present Changzhou–Jiangyin–Zhangjiagang line should be the main and reasonable route for the Liangzhu culture migrating across the Yangtze River.

KEYWORDS

Liangzhu culture, Liangzhu ancestors migrating across Yangtze River, Yangtze River delta, early-middle Holocene, river-mouth sandbar, ancient canoe

Introduction

Regarded as one of the most important birthplaces of Chinese prehistoric cultural development, the Jiangsu-Zhejiang-Shanghai region, located at the mouth of the Yangtze River, has played host to Neolithic cultures including the Majiabang, Songze Liangzhu, Qianshanyang, and the Guangfulin since 7000 cal BP. Centered on the Taihu Lake basin and on the Hangzhou-Jiaxing-Huzhou plain, which is located on the south bank of the Yangtze River Delta, the Liangzhu culture were considered the zenith of the Neolithic cultures, with hundreds of sites and relics having been discovered (Zhao, 2018). Since the turn of the century, however, several large Liangzhu sites have been excavated in the Jianghuai and Huanghuai regions north of the Yangtze. Numerous works on the Neolithic culture and the evolution of

paleoclimate and paleogeography during the Holocene have been undertaken (Wang et al., 2004; Sun et al., 2006; Chen et al., 2008; Wang et al., 2010; Chen et al., 2017; Zheng et al., 2018) and fruitful results have been achieved in the Jiangsu–Zhejiang–Shanghai region. The Liangzhu were known to have originated to the south of the Yangtze, so the question of how the Liangzhu migrated across the river is a scientific problem that needs to be addressed by archaeological research, also is an important researching content of Liangzhu culture in the north of the Yangtze River. According to the distribution range, and the remains and artifacts unearthed at the Liangzhu cultural sites, some archaeologists have proposed several possible migration routes of Liangzhu across the Yangtze River. One was centered on the Zhenjiang area, while another took them from Zhangjiagang near the estuary of the Yangtze up the north coast to the eastern Jianghuai region in late period of Liangzhu. The riverway was narrower and no too much obstruction for Liangzhu ancestors' across the Yangtze (Institute of Archaeology, Nanjing Museum, et al., 1996; Luan, 1996; Cui, 2011).

However, the Liangzhu culture was concentrated in the eastern Taihu plain, and crossing of the Yangtze River were made throughout the entire Liangzhu period. In crossing the river from Zhenjiang, the ancestors of the Liangzhu to the south of the Yangtze would have had to have made a detour to the west before crossing the Yangtze to the north.

The origin, distribution, and diffusion of prehistoric cultures cannot be separated from the changes in the paleogeographic conditions in the distribution area. When considering changes in sea level, the development of the Yangtze River delta, and the evolution of the Yangtze river channel during the Holocene period, the ancestors could have crossed the river from the northern end of the Taihu plain.

This study aims to discuss the most credible routes and paleogeography mechanisms of how the Liangzhu crossed the Yangtze based on the formation of the Yangtze River delta and the paleoenvironmental factors present during the Holocene period.

The distribution of the liangzhu around the Yangtze River delta and the jianghuai region

A rise in sea level accompanied a period of global warming after the last ice age. Since deglaciation, the mud and sand of the Yangtze River, the Qiantang River, the Huai River, and the Yellow River, which all flowed into the sea, increasingly deposited and formed a sand-mouth delta, before gradually extending eastward to the modern-day Yangtze River delta and the Jianghuai plain. The southern boundary of the accumulated plains area of the Yangtze River delta follows the line of Zhenjiang, Jiangyin, Zhangjiagang, Taicang Changshu, Waigang, Xujing, Wuqiao, and Caojing. The south bank of the delta is situated at the south of the boundary and includes the Taihu and Hangjiahu plains. The northern boundary is located on the line of Yizheng, Yangzhou, Taizhou, and Hai'an near the new Tongyang Canal. The north side, located to the north of the boundary, includes the Lixia River plain and the eastern Jianghuai plain (Li et al., 1999). The entire region lies between 119°22′, 121°10′E and 32°16′, 33°58′N. The average annual temperature of the region is 14.6°C, with a minimum of 1.1°C in January and a maximum of 27.3°C in July. The average annual precipitation is 1022 mm.

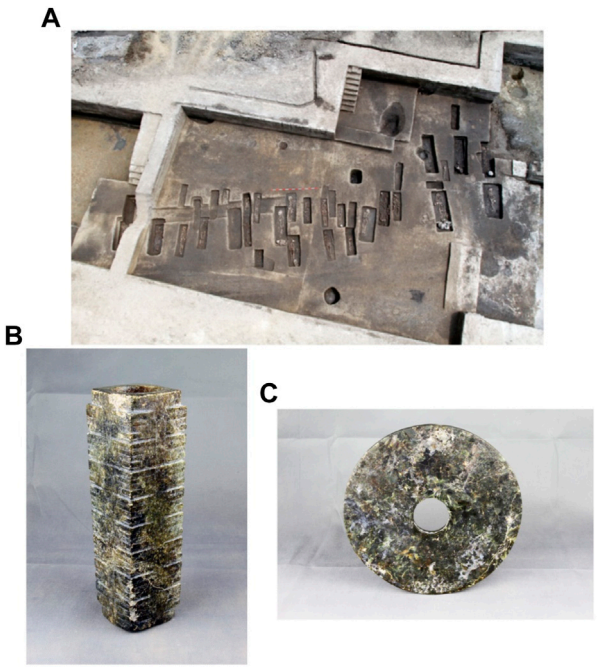

FIGURE 1
Liangzhu cultural relics at the Jiangzhuang site in Xinghua and Dongtai cities, Jiangsu Province: **(A)** the excavation site; **(B)** Excavated Cong (upper radial diameter: 6.8 cm, lower radial diameter: 6.4 cm, bore diameter: 4.6 cm, height: 23.5 cm) and **(C)** Bi (diameter: 24 cm, bore diameter: 5.1–5.2 cm, thickness: 1.3–1.4 cm) (A: Nanjing Museum, 2016; B and C are provided by Nanjing Museum).

The Yangtze River delta and its north-south banks consist of low-lying, flat terrain containing many lakes, ponds, and rivers. This favorable natural environment was ideal for prehistoric cultures migrating into the area. The Liangzhu were considered the peak Neolithic culture on the Jiangsu, Zhejiang, Shanghai, and Taihu plains, and existed from 5300 to 4200 cal BP. In the 1930s, the Liangzhu site was investigated and excavated on the outskirts of Hangzhou in Zhejiang Province (Zhao, 2018). Over more than 80 years, spectacular archaeological findings have been unearthed due to the tireless and intensive research by the archaeologists, which revealed that the Liangzhu culture is combined with different branches such as "Liangzhu ancient country," "Liangzhu ruins group," "dam construction," "earthen building engineering," "rice culture," and "jade culture" etc and all these branches were closely bound up with each other (Wang, 2015; Zhao, 2018; Zheng, 2018; Yi, 2019). The ancient city of Liangzhu was also placed on the World Heritage List in July 2019. At present, it is universally acknowledged that the Liangzhu culture originated and flourished in the Hangzhou Bay and Taihu Lake areas south of the Yangtze River.

During the past 2 decades, archaeologists have excavated sites in the Jianghuai region north of the Yangtze River that are culturally connected to the Liangzhu. The main sites are the Jiangzhuang site (Nanjing Museum, 2016), the Luzhuang site (Nanjing Museum et al., 1996), the Kaizhuang site (Yancheng Museum, 2005), the Dongyuan site (Nanjing Museum et al., 2004), and the third stage of the Longqiuzhuang site (The Archaeological Team of Longqiuzhuang, 1999; Cui et al., 2011).

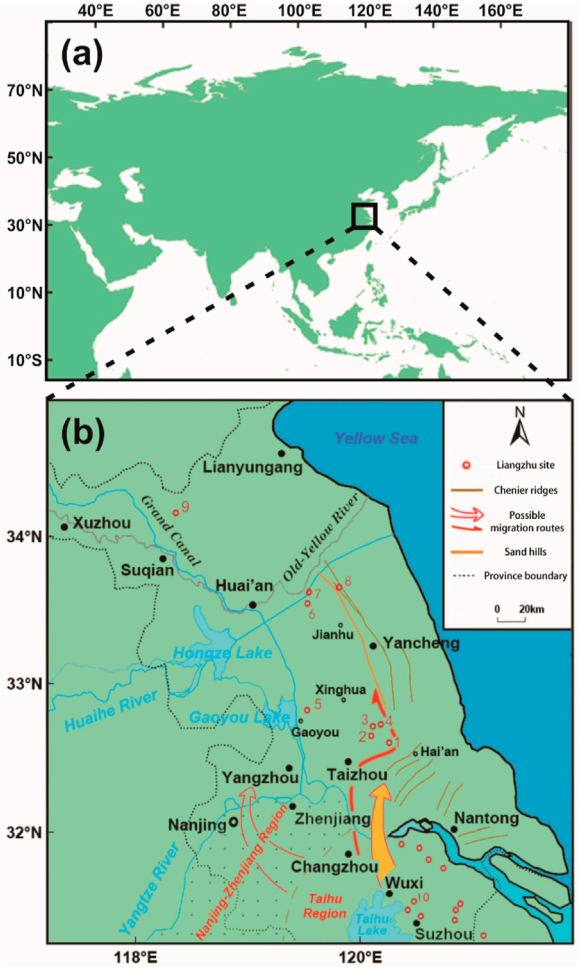

FIGURE 2
Figure showing the study area **(A)** and the possible route map of Liangzhu culture migrating across the Yangtze River **(B)** (The red circles represent: 1. Qingdun site, 2. Kaizhuang site, 3. Taozhuang site, 4. Jiangzhuang site, 5. Longqiuzhuang site, third stage, 6. Liyuan site, 7. Luzhuang site, 8. Dongyuan site, 9. Huating site, and 10. Qiuchengdun site; the three possible routes are drawn based on Cui (red hollow arrow in the west), Luan (red solid arrow in the middle) and this study (red arrow with yellow filling in the east)).

Of these sites, the Jiangzhuang site contains a large-scale settlement that has only recently been excavated. A high-ranking Liangzhu cemetery with a simple cultural appearance as well as *Cong* (rectangular jade with a round hole), *Bi* (round flat jade with a hole), and other jade ritual vessels were unearthed in a Liangzhu cemetery north of the Yangtze River for the first time and were found to date from the early-middle Liangzhu period (Nanjing Museum, 2016; Figure 1). This discovery was ranked in the "Top Ten New Archaeological Discoveries of 2015" list in China, owing to the rich remains and the cultural connotations of the site (http://www.kaogu.cn/zixun/2016nianquanguoshidakaoguxinfaxian/2016/0517/53925.html). In addition, more than ten Liangzhu sites were also discovered in the vicinity, such as Tingchi Port, Hu Zhuang, and Dacao Zhuang. Archaeological research has provided evidence that the Liangzhu culture flourished in the eastern Jianghuai region, and the area has become an important part of the research surrounding this world-renowned culture.

With the discovery of Liangzhu cultural sites such as Jiangzhuang and Luzhuang, the opinion that "Distribution of Liangzhu culture did not cross the Yangtze River" has been gradually eroded (Wu, 1988; Li et al., 1999). It is now clear that the Liangzhu migrated north across the Yangtze River (Cui, 2011). According to the spatial distribution and cultural connotations of the sites, the unearthed artifacts, and the features of the remains, the archaeologists deduced several routes that the Liangzhu may have taken north to the Yangtze River (Figure 2). Firstly, the Zhenjiang area. There are many known Liangzhu cultural sites and remains in the Zhenjiang area, and it is believed that the ancestors of the Liangzhu may have crossed the Yangtze River north from the narrower riverway between Zhenjiang and Nanjing (Cui, 2011).Secondly, approximately 4,200 years ago, ancestors living during the late period of Liangzhu culture crossed the river from near Zhangjiagang, which was located in the north of Taihu Lake, and moved northward along the coastline at that time to settle near the Sheyang rivermouth or to migrate further north (Institute of Archaeology et al., 1996). Thirdly, the ancestors crossed the Yangtze River from the narrower riverway east of present Beijing-Hangzhou Grand Canal and migrated northward through the Jianghuai area (Luan, 1996).

The liangzhu culture and the environment of the Yangtze River delta

During the Holocene period, the Yangtze River delta was formed by the combined flow of the Yangtze River, the Huai River and the Qiantang River, etc. flowing into the sea. The development of the delta along its north and south wings has been extensively studied, with a large number of papers being published on the subject (Wang et al., 1981; Shan et al., 1986; Yan and Xu, 1987; Liu et al., 1992; Tang et al., 1993; Chen and Stanley, 1998; Guo et al., 2013; Ding et al., 2019). It is generally accepted that the mud and silt carried by the Yangtze River were deposited in the estuary forming the Yangtze River delta. Additionally, the mud and sand brought by the Qiantang River, the Huai River, and the ancient Yellow River contributed to the formation of the south and north wings of the delta. Taihu Lake may have also been connected with the sea 7,000 years ago (Wang et al., 1981). The eastward movement of the Yangtze River estuary and the development of the south wing of the delta formed the Taihu Lake plain, with a flat terrain and a crisscrossed water network.

This favorable environment meant that the Neolithic culture series of Majiabang–Songze–Liangzhu–Qianshanyang–Guangfulin in the Taihu Basin and Hangjiahu plain was the peak period for Neolithic cultures, with abundant natural resources, thriving populations and settlements, and increased spatial distribution (Chen et al., 1997). The interactions between sea-level fluctuation and silt accumulation in the Holocene resulted in the formation of several silt dams in the north of the Yangtze approximately 7,000 years ago (Yan and Xu, 1987; Figure 3). Shallow, lagoon-like lakes gradually began to form between the silt dam to the west and Gaoyou and Hongze lakes to the east. In particular, the Lixia River area is the lowest elevation in the north of the Yangtze River in Jiangsu, with a developed water system and abundant plants and animals. These shallow lakes could have been silted up a bit and become flat land adjacent to the water where the ancient inhabitants could have settled. The geomorphologic conditions of the transition zone between land and sea provided a

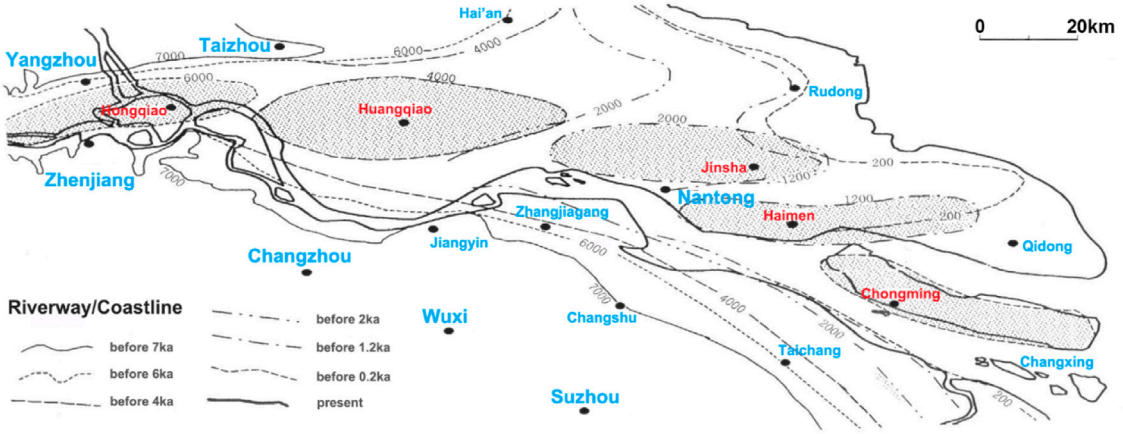

FIGURE 3
Schematic diagram of the evolution of the estuary and silt body of the Yangtze during the Holocene period. Redraw based on Cao et al., 2006.

suitable geographical environment for external Neolithic cultures to migrate to, including the Liangzhu, who extended their range into this area north of the Yangtze. Geoscientists and environmental archaeologists have carried out in-depth studies on the early and middle Holocene anthropogenic environment in the Yangtze River delta region and have demonstrated and confirmed the formation process and the mechanism of the Neolithic cultures in the east of Jianghuai and Huanghuai and of the delta (Stanley and Chen, 1996; Chen et al., 1997; Zhu et al., 2003; Zong et al., 2007; Wang et al., 2010; Zheng et al., 2018). The area provides a scientific historical reference for the potential for people to live in harmony with the natural environment of the Yangtze River delta region in the future. However, no archaeological research has currently been conducted regarding exactly where the Liangzhu crossed the river and the migration routes.

Discussion

The Liangzhu's migration route across the Yangtze River

The archaeological sites and remains of the Liangzhu culture to the north and south of the Yangtze have led to speculation that the Liangzhu culture initially crossed the river in the Nanjing-Zhenjiang region, and in their later period crossed near present-day Zhangjiagang before moving north along the coast, and crossed the river from the east of present-day Grand Canal. These routes and time across the river is logical from an archaeological viewpoint. The Liangzhu ruins to the south of the Yangtze are mostly distributed throughout the eastern Taihu plain (Chen, 2017). If the Yangtze River delta and the formation process of the Yangtze River channel during the Holocene are considered, the Nanjing-Zhenjiang region would not have been the ideal point for crossing the river. Near the estuary, the mud and sand were sedimented and formed the estuary bar, which contributed to the weakened river flow when the water flows into the sea.

Previous studies suggest that the development of the Yangtze River delta during the Holocene was characterized by distinct phases (Wang et al., 1981; Hori et al., 2001; Song et al., 2013). The estuary was near the Zhenjiang-Yangzhou line during the maximum sea transgression of Holocene before moving eastwards with the sediment of mud and silt carried by the river and the fluctuations of sea level. Thereafter, six river mouth bars of substages were formed around the estuary while the sedimentary center of the delta advanced toward the sea. These phases of bar formation were known as the Hongqiao phase (6500–5000 cal BP), the Huangqiao phase (6500–4000 cal BP), the Jinsha phase (4500–2000 cal BP), the Haimen phase (2500–1200 cal BP), the Chongming phase (1700–200 cal BP), and the Changxing phase (700 cal BP to the present day) (Ling, 2001). The six substage silt bars were dynamically superimposed from northwest to southeast and overlapped or linked between the adjacent two substage silt bodies. The broad seacoast channel was divided by sand bar bodies into two or more narrower branches (northern and southern). When the Yangtze River delta moved gradually eastward, the river water shifted to the south due to the Coriolis effect, and the sand in the river gradually merged into the land on the north bank. Nowadays, Hongqiao in Yangzhou, Huangqiao in Taizhou, Tongzhou (Jinsha), and Haimen in Nantong and other areas are much more likely to have been sand bars in the river during the past. At present, Chongming Island and Changxing Island, which formed over a period of 1,000 years, are still present at the mouth of the Yangtze. The northern branch of Chongming Island is gradually silting up, and the island will eventually be incorporated into the north wing and will become a spit of land.

A further simulation study found that there were two sand bodies in the wide estuary of the Yangtze River around 5250 cal BP. In around 4250 cal BP, the two sand bodies were almost connected with the land in the west, while a new channel into the sea appeared in the east. Due to the accumulation of sand bodies, most of the channels to the sea in the Yangtze River were located approximately 3 m below the water surface. The evolution of the sand bodies and channels greatly assisted the Liangzhu in crossing the river (Xie and Yuan, 2012; Figure 4).

The Liangzhu culture were mainly found between the Ningzhen Mountains in the west and Shanghai in the east, between the Qiantang River basin in the south, and the Huanghuai plain in the north. This region is a transitional zone between land and ocean located in the middle-low latitudes of the northern hemisphere. Because of the moderate temperature, abundant precipitation, low-lying terrain,

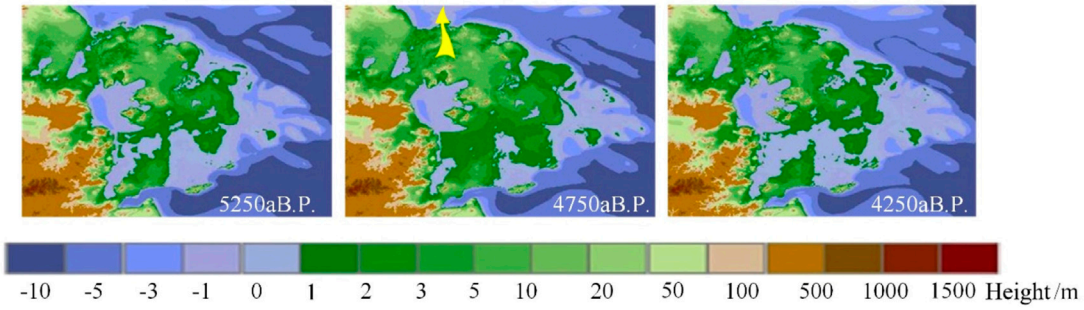

FIGURE 4
Simulation results of the evolution of the land and sea environment in the Yangtze River delta (the yellow arrow on 4750 cal BP indicates the rough migration route. Redraw based on Xie and Yuan, 2012).

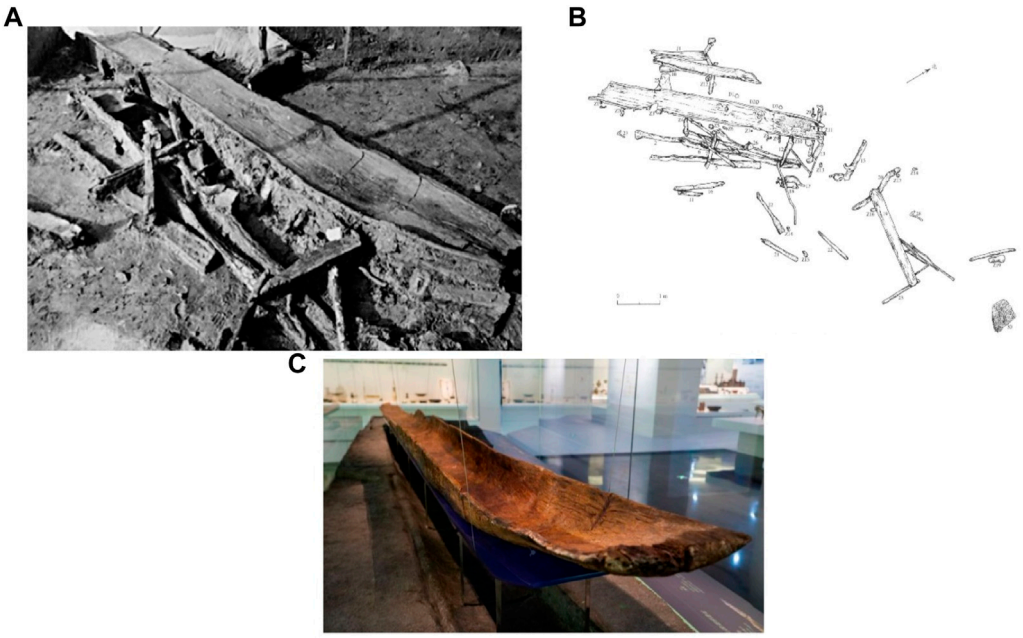

FIGURE 5
Photograph of unearthed canoe remnant **(A)** Zhejiang Provincial Institute of Cultural Relics and Archaeology, Xiaoshan Museum, 2004) and its planned distribution **(B)** Wu, 2012); the longest and most complete canoe **(C)** https://www.163.com/dy/article/H8D7FJ6R05149IKJ.html).

and numerous branching streams, shallow lakes, and ponds, the area was ideal for human habitation and multiplication. Additionally, implements and tools suitable for using underwater have also been found in the area. The ancient city of Liangzhu, which was the heart of Liangzhu culture, contained a developed waterway transportation network to Taihu Lake and other areas (Wang, 2016; Zhao, 2018). Additionally, a large number of ancient dams and a relatively intact hydrological "system" have also been discovered (Zhao, 2018). An excavated canoe also proved that watercraft were used in Jiangsu and Zhejiang as early as the pre-Liangzhu culture period, probably for shipping purposes and for fishing and gathering aquatic plants.

The Xiaoshan Kuahuqiao (cross-lake bridge) site, not far from Liangzhu City, is an early-middle Neolithic site dating from 8200 to 7000 cal BP in the Qiantang River basin, Zhejiang Province (Archaeology of Zhejiang province, 2004). One of the highlights found at this site was a relatively well-preserved canoe with wooden oars, which is thought to be the earliest known Chinese canoe (Archaeology of Zhejiang province, 2004; Gong, 2012). The canoe remnant is 5.60 m long, 0.52 m wide, and 0.15 m deep (Figure 5A; 5B). It was manufactured by using an entire Masson pine, which had been burned and then chipped with an adze. It was thought to have been manufactured around 8000–7500 cal BP and the site where it was excavated was probably a "shipyard". This discovery proves that 5 m long canoes were being made in the Qiantang River basin more than 3,000 years before the arrival of the Liangzhu. Canoes may also have been produced and used during the early Neolithic period in Jiangsu and Zhejiang. More importantly, a canoe of 7.35 m long and 0.45 m wide and 0.23 m deep, dating to about 5,000 cal aBP,

was also unearthed in 2010 from the cultural layer at the Maoshan Site in Yuhang district, near Liangzhu, is by far the longest and most complete prehistoric canoe unearthed in China (Figure 5C).

This canoe was undoubtedly made during the Liangzhu period. In addition, dock facilities were excavated in Bianjiashan and Mojiaoshan near Liangzhu City. Several wooden oars were also found. Along with those found at the Kuahuqiao and the Hemudu sites (Gong, 2012), which predated the Liangzhu, wooden oars have been unearthed at Liangzhu sites including Bianjiashan, Mojiaoshan, Shuitianpan in Hangzhou, Qianshanyang in Wuxing, and Shahe in Liyang, implying that "the inhabitants of the Liangzhu culture were good at using boats" (Institute of Archaeology et al., 1996; Wang, 2016).

Whether it was very difficult to cross the Yangtze River in a canoe and need to using paddles or oars? During the crossing-Yangtze River-campaign between the army of the Kuomintang (KMT) and the Communist Party (CPC) in 1949, three companies (300–400 men) of the People's Liberation Army (PLA, the army led by the CPC) crossed the river on the night of 21 April 1949, from the north bank of Yangtze River to Shuangshan island with wooden boats of 10–30 tons, with sails and manual oars, and loaded with soldiers, weapons and ammunition. The distance between north bank to Shuangshan island is about 3 km (Party's History and Local History Office of Zhangjiagang Municipal Committee, CPC. 2005). About 30 min later, the first troops reached Shuangshan island, then the wooden ships returned and continued to transport troops and weapons to Shuangshan Island. At dawn on April 22, the PLA captured the Shuangshan island, then crossed the river from Shuangshan island and took over Shazhou (now administrated by Zhangjiagang City) in the daytime of April 22. In addition, before the civil war between KMT and CPC armies in 1949, the CPC had established a secret communication line in the south and north of Zhangjiagang, relying on small fishing boats to transfer military information and secret workers across the Yangtze River, relying on the "one leaf boat". Judging from the photos taken at that time, the boat was no more than 10 m long and 1.8 m wide, and the power was only one or two paddles or oars. Several PLA military leaders were transported from the north of the Yangtze River to the south even with such small boats. These evidences are now stored in Jiangsu Zhangjiagang City Shuangshan Island River Crossing Campaign exhibition Hall, Suzhou Revolutionary Museum and other places. Similarly, in the Anhui section of the Crossing-Yangtze-River Campaign between KMT and CPC in April 1949, the boats carrying the PLA across the Yangtze River was more than 8 m long, carrying 18 soldiers and two boatmen (Zhang, 2020). From the course of the PLA's crossing campaign in April 1949, it can be proved that the Liangzhu ancestors could travel back and forth between the Yangtze River by canoes in a relatively short period of time (within 5–6 h) in calm and tranquil weather.

According to the building history of the ancient canoes in the Jiangsu-Zhejiang area and the Taihu plain, and the wooden oars found at several Liangzhu sites, the Liangzhu first crossed the south branch of the Yangtze River ancient riverway *via* the Changzhou - Jiangyin - Zhangjiagang line north of Taihu Lake by using canoes and arrived at estuarine sandbars during the Huangqiao period (or early Jinsha period), then crossed the Yangtze River north branch and arrived in the north side of the Yangtze River. Regarding the several river routes determined by archaeological research, there is a suspicion of go far afield that the Liangzhu favored the Nanjing-Zhenjiang route to cross the Yangtze River. It has also been shown that the Liangzhu crossed the Yangtze from Zhangjiagang throughout the entire cultural period, not only occurred in the late period. Additionally, they can reach the north bank directly and then migrate northward.

Combined with historical documents, archaeological research also holds that it is feasible for Liangzhu ancestors to cross the river near the rivermouth by rowing north along the seawall (Luan, 1996). Theoretically, it is possible to sail north along the seawall with small boats, taking into account factors such as the coastline, coastal landforms, coastal currents and tidal currents around 5,000 years ago. But if a large estuary had a surge similar to the current Qiantang River estuary, it would be more difficult to travel north by using small boats.

We has studied the period of land-forming in the east area of Jianghuai north of the Yangtze River (Xiao et al., 2023). At about 5800cal aBP, the area south of the ancient Huai River, east of the Beijing-Hangzhou Canal, north of the Yangtze River, east to Xigang (Figure 2B) was already continental. Due to the formation of the Gangxi sand hills, it becomes the boundary between sea and land. The west side of Gangxi is a shallow lake swamp environment with lagoon and dense water network and provided a new living space for Liangzhu culture to move north and north Neolithic culture to move south.

The ancient fauna founded in Longqiuzhuang site are mainly represented by animals that like warm and wet environment, such as elk, swertia and freshwater fishes, mussels, etc., which implied the developed fishing and hunting economy. Fishing and hunting, livestock and rice cultivation were the means for the ancestors of Longqiuzhuang to survive (The Archaeological Team of Longqiuzhuang, 1999). Among the plants unearthed from Jiangzhuang site, the remains were rice, *Euryale Salisb*, water chestnut, *Nymphoides*, Potamogetonaceae, etc. and the bones unearthed were aquatic animals such as fish, turtles and terrestral animals such as the most common Cervidae, followed by pigs, dogs, water buffalo, etc. (Nanjing Museum. 2016).

The archaeological researches have confirmed that the water network of shallow freshwater lakes and swamps in the eastern Jianghuai could provide rich food resources for the ancestors of Liangzhu. Based on the study of palaeogeography and archaeology, it can be concluded that Liangzhu ancestors crossed the Yangtze River in Changzhou–Jiangyin - Zhangjiagang, then directly crossed the dike of the Yangtze River and sailed north or east and west along the water network with small boats. The shallow marsh provided abundant food, which was convenient for Liangzhu ancestors to settle down and develop in a suitable place after crossing the river. In addition, according to common sense, an ordinary being who grew up on land must have 10–20 years of sea training to get used to the physical effects of seasickness, and has little physical capacity during seasickness. But there is no risk of seasickness on land. Since the Liangzhu ancestors could sail on land and water in the east Jianghuai, there was no need to sail north outside the sea in the stormy environment.

Conclusion

The more in-depth archaeological studies are conducted, the more the consensus confirms that the Liangzhu culture of the Yangtze River delta originated to the south of the Taihu plain. However, in the late 1980s, the prevailing viewpoint (Song et al., 2013) that the Liangzhu culture remained south of the Yangtze was disproved by subsequent archaeological studies, as the discovery of

many relics of the Liangzhu culture, with large-scale, rich cultural connotations, were found to the north of the river, particularly around its eastern reaches and around the Huaihe River. After considering the development of the Yangtze River delta during the Holocene period, and the ancient canoes, wooden oars, and docks, which have been unearthed by archaeological digs, it is entirely feasible that the Liangzhu arrived at the sand bar in the center of the Yangtze River after crossing its south branch along the Changzhou–Jiangyin–Zhangjiagang line, before migrating to the northern bank after moving across its northern branch. The Nanjing-Zhenjiang line was the likely route for Liangzhu ancestors west of Taihu Lake to cross the Yangtze River, but it should not be the main route for Liangzhu culture to cross the Yangtze River. Sailing north across the Yangtze River along the dike is much more difficult at sea than at the land-based water network. But it should be a feasible route for Liangzhu ancestors migrating northward along the west side of the sand hills (see details in Figure 2B). According to the dating results of unearthed canoe and wooden oars, as well as the evolution of the Yangtze riverways and deltas throughout the Holocene period, and other supporting studies of archaeology and paleogeography, the formation and evolution of the sand bar at the estuary during the Huangqiao period (before 4000 cal BP) met the geographical conditions for ancient ancestors to cross the river in the early Liangzhu period. During the whole Liangzhu period, the area between Changzhou - Jiangyin - Zhangjiagang should be the best place to cross the river. Further archaeological studies need to be conducted to determine whether earlier cultures before Liangzhu to cross the Yangtze River (Cao et al., 2006).

Data availability statement

The original contributions presented in the study are included in the article/supplementary material, further inquiries can be directed to the corresponding author.

Author contributions

JX: Conceptualization, Funding acquisition, Investigation, Methodology, Resources, Validation. ZS (corresponding author): Project administration, Visualization, Writing–original draft and review & editing. ZZ: Visualization, Writing–review & editing. SX: Site Investigation, Revision. XJ: Funding acquisition, Supervision. All authors have read and agreed to the published version of the manuscript.

Funding

This work was jointly supported by the National Natural Science Foundation of China (Grant No. 41472141, 42271163) and was funded by the Priority Academic Program Development of Jiangsu Higher Education Institutions (PAPD) and the Innovation Team at Nanjing Normal University.

Conflict of interest

The authors declare that the research was conducted in the absence of any commercial or financial relationships that could be construed as a potential conflict of interest.

The handling editor HFL declared a past co-authorship with the author XJ.

Publisher's note

All claims expressed in this article are solely those of the authors and do not necessarily represent those of their affiliated organizations, or those of the publisher, the editors and the reviewers. Any product that may be evaluated in this article, or claim that may be made by its manufacturer, is not guaranteed or endorsed by the publisher.

References

Cao, G. J., Wang, J., and Qu, G. X. (2006). Channel evolution of the Yangtze River estuary section since Holocene. *Yangtze River* 37 (2), 25–27, 36. doi:10.16232/j.cnki.1001-4179.2006.02.010

Chen, T. (2017). "Mid-to late Holocene hydrology changes in the south Taihu area of the Yangtze delta plain, China, and its relationship to the development of Neolithic culture," (Shanghai, China: East China Normal University), 16–19. Doctoral Dissertation.

Chen, Z., and Stanley, D. J. (1998). Sea-level rise on eastern China's Yangtze Delta. *J. Coast. Res.* 14 (1), 360–366.

Chen, Z. Y., Hong, X. Q., Li, S., Wang, L., and Shi, X. M. (1997). Study of archaeology-related environment evolution of Taihu lake in southern Changjiang Delta plain. *Acta Geogr. Sin.* 52 (2), 131–137. doi:10.11821/xb199702005

Chen, Z. Y., Zong, Y. Q., Wang, Z. H., Wang, H., and Chen, J. (2008). Migration patterns of neolithic settlements on the abandoned yellow and Yangtze River deltas of China. *Quat. Res.* 70, 301–314. doi:10.1016/j.yqres.2008.03.011

Cui, Y. J. (2011). The research on culture and society in the prehistoric eastern jiang-huai region. *Shandong Univ. Dr. Diss.* 29 (45), 63–65.

Ding, D. L., Zhang, X. H., Yu, J. J., Wang, L. Y., Wang, F., and Shang, S. W. (2019). Sediment grain size distribution patterns of the late Quaternary on the back side of the northern Yangtze River Delta and their environmental implications. *Mar. Geol. Quat. Geol.* 39 (4), 34–45. doi:10.16562/j.cnki.0256-1492.2019022801

Gong, C. Q. (2012). "Canoe in pictures[A]. Kuahuqiao site Museum of xiaoshan, Hangzhou," in Proceedings of the International Symposium on Kuahuqiao Culture (Beijing: Cultural Relics Publishing House), 158–168.

Guo, S. Q., Ma, Q. B., Zhang, X. Y., Ge, Y., and Gong, X. L. (2013). Holocene environmental changes in the Lixiahe area. *Geol. China* 40 (1), 341–351.

Hori, K., Saito, Y., Zhao, Q., Cheng, X., Wang, P., Sato, Y., et al. (2001). Sedimentary facies and Holocene progradation rates of the Changjiang (Yangtze) delta, China. *Geomorphology* 41 (2-3), 233–248. doi:10.1016/S0169-555X(01)00119-2

Institute of ArchaeologyNanjing MuseumYancheng Antiquity Preservation committeeYancheng Museum (1996). *The discovery of Lu Zhuang relics, the light of oriental civilization-collected essays in commemoration of 60th anniversary of the discovery of the Liangzhu culture*. Yancheng, China: Yancheng Museum.

Li, C. X., Chen, Q. Q., Fan, D. D., Zhang, J. Q., and Yang, S. Y. (1999). Palaeogeography and palaeoenvironment in changjiang delta since last glaciation. *J. Palaeogeogr.* 1 (4), 12–25. doi:10.3969/j.issn.1671-1505.1999.04.002

Ling, S. (2001). Shoal's merging into land and evolution of north coastline of Changjiang estuary. *J. Oceanogr. Taiwan Strait* 20 (4), 484–489.

Liu, K. B., Sun, S. C., and Jiang, X. H. (1992). Environmental change in the Yangtze River delta since 12000 years B.P. *Quat. Res.* 38 (1), 32–45. doi:10.1016/0033-5894(92)90028-H

Luan, F. S. (1996). The northward migration of Liangzhu culture. *Cult. Relics Central China* 3, 51–58.

Museum, Nanjing (2016). The relics of Liangzhu culture at Jiangzhuang site in Xinghua and Dongtai cities, Jiangsu province. *Archaeology* 7, 19–31.

Nanjing Museum, Yancheng MuseumFuning Bureau of Culture (2004). Neolithic dongyuan site in funing county, Jiangsu province. *Archaeology* 6, 7–21.

Party's History and Local History Office of Zhangjiagang Municipal Committee, CPC (2005). Local history of Zhangjiagang (sandbar). *CPC* 1. 111.

Shan, S. M., Wang, W. P., and Wang, T. K. (1986). *Jiangsu geographical*. Jiangsu, China: Jiangsu People Press.

Song, B., Li, Z., Saito, Y., Okuno, J., Li, Z., Lu, A., et al. (2013). Initiation of the Changjiang (Yangtze) delta and its response to the mid-Holocene sea-level change. *Palaeogeogr. Palaeoclimatol. Palaeoecol.* 388, 81–97. doi:10.1016/j.palaeo.2013.07.026

Stanley, D. J., and Chen, Z. (1996). Neolithic settlement distributions as a function of sea level-controlled topography in the Yangtze Delta[J]. China. *Geology* (12), 1083–1086. CO; 2. doi:10.1130/0091-7613(1996)024<1083:NSDAAF>2.3

Sun, L., and Gao, M. H. (2006). An archeogeographical study on the changes of Jiangnan coastline. *Southeast Culture* 4, 11–17.

Tang, L. Y., Shen, C. M., Zhao, X. T., Xiao, J. Y., Yu, G., and Han, H. Y. (1993). Vegetation and climate since 10000 BP in the qingfeng section, jianhu, Jiangsu. *Sci. China (Series B)* 23 (6), 637–643.

The Archaeological Team of Longqiuzhuang (1999). *Neolithic site excavation report in the Eastern Part of Jiang-Huai area*. Beijing, China: Science Press, 519–520.

Wang, J. M. (2015). The relationship between the pattern of Liangzhu jade and the development-decline of Liangzhu culture. *Heilongjiang Chronicles* 22, 54–56.

Wang, J. T., Guo, X. M., Xu, S. Y., Li, P., and Li, C. X. (1981). Evolution of the Holocene changjiang delta. *Acta Geol. Sin.* 1, 67–81.

Wang, N. Y. (2016). Survey and excavation of the water conservancy system in Liangzhu city and surroundings. *Res. Herit. Preserv.* 1 (5), 102–110.

Wang, W. M., Shu, J. W., Chen, W., and Ding, J. L. (2010). Holocene environmental changes and human impact in the Yangtze River Delta area, east China. *Quat. Sci.* 30 (2), 233–244. doi:10.3969/j.issn.1001-7410.2010.02.01

Wang, Z. H., and Chen, J. (2004). Distribution of the Neolithic sites in the Chang Jiang coastal plains: Holocene transgression impact. *Quat. Sci.* 24 (5), 537–545.

Wu, J. (2012). "Analysis and thinking of the unearthed state of a canoe at Kuahuqiao site. [A]. Kuahuqiao site Museum of Xiaoshan, Hangzhou," in Proceedings of the International Symposium on Kuahuqiao Culture (Beijing: Cultural Relics Publishing House), 125–140.

Wu, J. M. (1988). Distribution of prehistoric sites in the Yangtze River Delta and environmental evolution. *Southeast Cult.* 6, 16–36.

Xiao, J., Shang, Z., Xu, J., Jia, X., and Xiao, S. (2023). The neolithic culture and paleogeographic environment evolution in the eastern Jianghuai area. *Land* 12, 156. doi:10.3390/land12010156

Xie, Z. R., and Yuan, L. W. (2012). Fluctuation characteristics of Holocene sea-level change and its environmental implications. *Quat. Sci.* 32 (6), 1065–1077. doi:10.3969/j.issn.1001-7410.2012.06.02

Yan, Q. S., and Xu, S. Y. (1987). *Recent Yangtze delta deposits*. Shanghai, China: East China Normal University Press, 264–271.

Yancheng MuseumDongtai Museum (2005). Neolithic Kaizhuang site in Dongtai city, Jiangsu province. *Archaeology* 4, 12–26.

Yi, H. (2019). Liangzhu culture and huaxia civilization. *Central Plains Cult. Res.* 5, 5–13.

Zhang, Y. S. (2020). The octogenarian Chen Wenyi: The heroic helmsman of the first ship crossing the Yangtze River. *New Youth* 10, 6–9.

Zhao, Y. (2018). Liangzhu: The paradigm of early civilization in China. *South. Cult. relics* 1, 69–76.

Zhejiang Provincial Institute of Cultural Relics and ArchaeologyXiaoshan Museum (2004).*Kua Hu Qiao*. London, UK: Cultural Relics Publishing House, 222–228.

Zheng, H. B., Zhou, Y. S., Yang, Q., Hu, Z. J., Ling, G. J., Zhang, J. Z., et al. (2018). Spatial and temporal distribution of Neolithic sites in coastal China: Sea level changes, geomorphic evolution, and human adaption. *Sci. China Earth Sci.* 61, 123–133. doi:10.1007/s11430-017-9121-y

Zheng, Y. F. (2018). The social livelihood pattern and rice cultivation in the Liangzhu culture period. *Cult. Relics South. China* 1, 93–101.

Zhu, C., Zheng, C. G., Ma, C. M., Yang, X., Gao, X., Wang, H., et al. (2003). On the Holocene sea-level highstand along the Yangtze delta and ningshao plain, east China. *Chin. Sci. Bull.* 48 (24), 2672–2683. doi:10.1007/BF02901755

Zong, Y., Chen, Z., Innes, J. B., Chen, C., Wang, Z., and Wang, H. (2007). Fire and flood management of coastal swamp enabled first rice paddy cultivation in east China. *Nature* 449, 459–462. doi:10.1038/nature06135

frontiers | Frontiers in Earth Science

TYPE Original Research
PUBLISHED 23 January 2023
DOI 10.3389/feart.2022.1064818

Check for updates

OPEN ACCESS

EDITED BY
Ren Lele,
Lanzhou University, China

REVIEWED BY
Shengli Yang,
Lanzhou University, China
Yiting Liu,
Wuhan University, China

*CORRESPONDENCE
Yue Li,
liyue@nwu.edu.cn
Linlin Zhai,
641055200@qq.com

SPECIALTY SECTION
This article was submitted to Quaternary Science, Geomorphology and Paleoenvironment, a section of the journal Frontiers in Earth Science

RECEIVED 08 October 2022
ACCEPTED 21 November 2022
PUBLISHED 23 January 2023

CITATION
Wang Q, Liu K, Zhai L, Liu B, Sun H and Li Y (2023), Animal resource exploitation in the northern Guanzhong region during the mid-to-late Holocene: A zooarchaeological case study of the Xitou site.
Front. Earth Sci. 10:1064818.
doi: 10.3389/feart.2022.1064818

COPYRIGHT
© 2023 Wang, Liu, Zhai, Liu, Sun and Li. This is an open-access article distributed under the terms of the Creative Commons Attribution License (CC BY). The use, distribution or reproduction in other forums is permitted, provided the original author(s) and the copyright owner(s) are credited and that the original publication in this journal is cited, in accordance with accepted academic practice. No use, distribution or reproduction is permitted which does not comply with these terms.

Animal resource exploitation in the northern Guanzhong region during the mid-to-late Holocene: A zooarchaeological case study of the Xitou site

Qianwen Wang[1,2,3], Kexin Liu[1,2,3], Linlin Zhai[1,2,3]*, Bin Liu[1,2,3], Han Sun[1,2,3] and Yue Li[1,2,3]*

[1]School of Cultural Heritage, Northwest University, Xi'an, China, [2]The Ministry of Education Key Laboratory of Cultural Heritage Research and Conservation Technology, Northwest University, Xi'an, China, [3]China-Central Asia Belt and Road Joint Laboratory on Human and Environment Research, Northwest University, Xi'an, China

Zooarchaeological approach has been effective in providing insights into human subsistence practices, which laid essential economic foundation for social, cultural, and political developments in the past. The Guanzhong region in northern China played a crucial role in the origins and evolution of ancient Chinese civilization. Previous research on subsistence economies of ancient societies in the Guanzhong region, human exploitation of animal resources in particular, has largely focused on the late Neolithic period or the Bronze Age. Insufficient work has been done for historical periods post-dating the end of the first millennium BCE. There is also a dearth of research on the long-term chronological changes. Here, we present a preliminary analysis of animal remains from the Nantou Locale of the Xitou site, a large settlement located in the northern Guanzhong region. Results show that pigs played a dominant role in the site's animal economy during the Neolithic Yangshao and Longshan periods (ca. 5000–2000 BCE). The growing importance of cattle and caprines was documented for the Bronze Age Western Zhou period (ca. 11th-8th centuries BCE). In the Han-Tang periods (ca. second century BCE-tenth century CE), pigs regained their significance in local subsistence practices. Differences in the strategies for animal resource exploitation were possibly associated with changing social and environmental factors. Alongside other relevant archaeological evidence, our zooarchaeological data demonstrate the contribution of diversified animal use strategies to sustained development of subsistence economy in the northern Guanzhong region across millennia. The examination of long-term human-animal interactions in the Guanzhong region allows for a better understanding of changing economic, social, and political landscapes in ancient China.

KEYWORDS

mid-to-late Holocene, China, northern Guanzhong, Nantou Locale, subsistence economy, zooarchaeology

Introduction

Subsistence economy serves as a fundamental material basis for the maintenance and evolution of human societies. The exploitation of animal resources, in particular, played crucial roles in shaping economic, social, and political landscapes in the past. Examining animal remains from archaeological contexts can thus facilitate our understanding of ancient human-animal interactions involving food consumption, ritual practices, trades, and land use strategies, to name but a few (Crabtree, 1990; Zeder, 1991; Davis, 1995; O'Connor, 2000; Reitz and Wing, 2008; de France, 2009; Albarella et al., 2017; Gifford-Gonzalez, 2018; Rowley-Conwy, 2018).

The Guanzhong region, also commonly referred to as the Jing and Wei River valleys in present-day central Shaanxi Province of China (Shi, 1963), is one of the key regions for understanding the origins and development of ancient Chinese civilization. The region experienced population growth and cultural prosperity in prehistoric Yangshao period, and later became the political hinterland of Zhou, Qin, Han, and Tang, several most influential dynasties that contributed to the formation and consolidation of some major cultural traditions and political institutions in Chinese history (Liu, 2004; Liu and Chen, 2012; Underhill, 2013; Shelach-Lavi and Jaffe, 2014; Shelach-Lavi, 2015). Transformations in various aspects in ancient Guanzhong region profited, in large part, from the development and intensification of animal husbandry and crop cultivation, alongside other technological innovations. Investigating subsistence practices is thus beneficial to a more holistic understanding of the economic, social, and political milieu of ancient Guanzhong region.

Previous research on animal remains from archaeological contexts has illustrated the multiple roles of animals in early human subsistence actions in the Guanzhong region (see Hu and Yuan, 2021 for a review). Nevertheless, most of these studies centered on the Wei River valley, with a focus on the late Neolithic period or the Bronze Age. Zooarchaeological data from the Jing River valley remain scarce, particularly those of historical periods post-dating the end of the first millennium BCE. There is also a lack of work on the long-term changes in animal resource exploitation in the prehistory and history of the region.

The northern Guanzhong region generally incorporates the middle and lower reaches of the Jing River. The middle Jing River valley has been considered as where the ancient Bin area was located, an area pertaining to the rise of the Zhou people in historical texts (Niu, 2000; Zhang, 2001; Gong, 2018). Animal remains from excavated sites in this region, such as Nianzipo, Xiaweiluo, Zaolinhetan, and Zaoshugounao were mostly from contexts of a relatively restricted range of time span (Cultural Heritage Archaeology Research Center of Northwest University, andShaanxi Academy of Archaeology, 2006; Institute of Archaeology CASS, 2007; Wang and Chen, 2010; Li et al., 2012; Liang, 1999; Wang et al., 2013; Zhai et al., 2018; Dou et al., 2019; Zhao et al., 2022). Recent archaeological fieldwork at the Nantou Locale of Xitou, a large settlement in the middle Jing River valley, has uncovered animal skeletal elements from contexts dated to a wide range of periods, which facilitate the exploration of chronological changes in past animal use in the region.

Here, we report an analysis of animal remains from the Nantou Locale. Integrating zooarchaeological data with evidence from published archaeobotanical and environmental research, we investigated potential changes in subsistence practices in relation to animal use across millennia in the northern Guanzhong region and the underlying dynamics that might explain these changes.

The site of Xitou

Xitou (35°02′15.56″N, 108°12′59.68″E) is located in modern Xunyi County of western-central Shaanxi Province, 1,125 m above sea level (Wei et al., 2020) (Figure 1). The site sits on a loess platform and sloping edge, approximately 5 km southwest of the Jing River (Dou et al., 2021) (Figure 2). Past field surveys show that the site covers an area of approximately 100 ha, with human occupation spanning from the late Neolithic to historical periods (Dou et al., 2021).

To better understand early settlement patterns and subsistence economies in the middle Jing River valley, the School of Cultural Heritage at Northwest University and partner institutions carried out excavations at the Nantou Locale in 2018, the southern section of the site. The archaeological fieldwork revealed an area of 625 m^2 and recovered cultural remains from more than 200 pits, ditches, hearths, kilns, and burials, dated to the Yangshao (ca. 5000–3000 BCE), Longshan (ca. 3000–2000 BCE), Western Zhou (ca. 1050–771 BCE), Han-Tang (ca. second century BCE-tenth century CE), and Ming-Qing periods (ca. 14th-20th centuries CE).

Materials and methods

In this study, we analyzed a total of 4,786 animal skeletal elements recovered from 103 pits and three ditches at the Nantou Locale (hereafter referred to as Xitou, the name of the site), dated to the Yangshao (YS), Longshan (LS), Western Zhou (WZ), and Han-Tang (HT) periods. The largest proportion of animal remains were unearthed from contexts of the WZ period. All animal specimens were collected by hand. Screening was not applied during excavation, which may have underrepresented bones of small mammals and non-mammals.

We identified animal species using published guides (von den Driesch, 1976; Hillson, 1992; Schmid, 1972) and archaeological

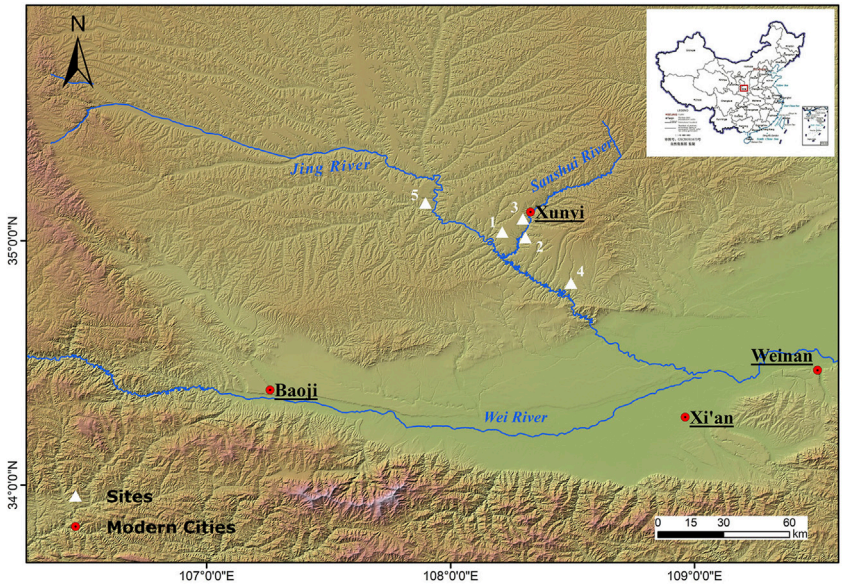

FIGURE 1
The location of archaeological sites in the middle Jing River valley, mentioned in this research. 1) Xitou; 2) Zaolinhetan; 3) Xiaweiluo; 4) Zaoshugounao; 5) Nianzipo.

FIGURE 2
Natural landscape surrounding the Nantou Locale of Xitou.

and modern reference collections in the School of Cultural Heritage, Northwest University. Skeletal elements that can be identified to at least the family level were included in the calculation of NISP (the number of identified specimens) and MNI (the minimum number of individuals). In the following sections, small size deer that cannot be identified to species, such as musk deer and muntjac, were collectively referred to as "small cervids". Similarly, specimens identified as sheep (*Ovis aries*), goat (*Capra hircus*), and sheep/goat (*O. aries/C. hircus*) were grouped as "caprines" where necessary. In addition, we calculated the proportion of NISP or MNI of a given animal species from other relevant sites and used the average value to represent the proportion of this species. The proportion of absolute quantity of charred plant seeds was calculated in the same way during the discussion.

Dental eruption and wear of mandibles on both sides were used to construct mortality profiles of pigs and caprines (Silver, 1969; Payne, 1973; Grant, 1982; Ma, 2007; Li, 2011b). When an age estimate of one specimen covered two age groups, this specimen was counted 0.5 in each age group. Bone epiphyseal fusion (Silver, 1969) was also used to construct mortality profiles of pigs. The mortality profile of cattle younger than 5 years of age was constructed using

TABLE 1 NISP and MNI of animal remains from the YS and LS contexts at Xitou.

Taxon	YS				LS			
	NISP	NISP (%)	MNI	MNI (%)	NISP	NISP (%)	MNI	MNI (%)
Unionidae	0	0.0	0	0.0	1	0.4	1	3.6
Unio douglasiae	1	3.1	1	10.0	0	0.0	0	0.0
Osteichthyes	0	0.0	0	0.0	1	0.4	1	3.6
Zokor, *Eospalax*	0	0.0	0	0.0	3	1.3	2	7.1
Unidentified rodent	0	0.0	0	0.0	4	1.8	1	3.6
Hare, *Lepus*	0	0.0	0	0.0	1	0.4	1	3.6
Dog, *Canis familiaris*	1	3.1	1	10.0	10	4.4	3	10.7
Equus	0	0.0	0	0.0	1	0.4	1	3.6
Pig, *Sus domesticus*	13	40.6	2	20.0	157	69.2	7	25.0
Sika deer, *Cervus nippon*	8	25.0	2	20.0	3	1.3	1	3.6
Roe deer, *Capreolus capreolus*	4	12.5	1	10.0	2	0.9	2	7.1
Medium cervid	0	0.0	0	0.0	5	2.2	1	3.6
Small cervid	0	0.0	0	0.0	3	1.3	2	7.1
Unidentified cervid	1	3.1	1	10.0	2	0.9	1	3.6
Bos	1	3.1	1	10.0	0	0.0	0	0.0
Cattle, *Bos taurus*	0	0.0	0	0.0	19	8.4	1	3.6
Caprinae/Antilopinae	3	9.4	1	10.0	1	0.4	1	3.6
Sheep/goat, *O. aries/C. hircus*	0	0.0	0	0.0	14	6.2	2	7.1
Total	32	100.0	10	100.0	227	100.0	28	100.0

bone epiphyseal fusion (Silver, 1969), while tooth eruption and wear (Silver, 1969; Grant, 1982) was applied for older ones.

We conducted a chi-square test to compare the NISP of wild and domestic animals from contexts of the YS, LS, WZ, and HT periods. Statistical test was performed in IBM SPSS Statistics software.

Taphonomy

A considerable small number of animal remains analyzed suffered from weathering (1.7%) of varying degrees. Approximately 1.8% and 4.6% of the specimens exhibited rodent gnawing and carnivore chewing, respectively. Traces of burning were recorded in 3.2% of all animal remains. Taphonomic effects, in general, had little impact on the animal assemblages.

Animal species representation

In total, 2,621 specimens from Xitou (54.8% of all animal remains analyzed) were identified to at least the family level, representing a minimum number of 169 individuals (Table 1, Table 2). By NISP, wild species constituted the largest proportion of animal remains from the YS contexts, while domestic animals played dominant roles during the LS, WZ, and HT periods. More specifically, pigs were the most important domestic animals at Xitou in prehistory (YS and LS). Caprines and cattle were incorporated into the site's subsistence practices during the LS period, although their proportion was apparently small. This structure of domestic animals changed in the Bronze Age (WZ), during which caprines and cattle outnumbered pigs. Animal species representation at Xitou in historical period (HT) was similar to that of the YS and LS periods, with pigs returning to dominate the animal assemblage.

Wild animals took up 56.3%, 11.9%, 14.8%, and 8.3% of the total NISP for the YS, LS, WZ, and HT periods, respectively. It is worth mentioning that an equine skeletal element was found in animal assemblage of the LS period. Recent ancient DNA analysis suggests that certain wild equine species, such as *Equus ovodovi*, were still present in northern China during the Neolithic period (Zhu, 2020; Hu et al., 2022). Given that genetic data for the equine specimen from Xitou is currently unavailable, we identified this specimen to *Equus*. Chi-square test suggests that the four periods (YS, LS, WZ, and HT) are statistically different in terms of the NISP of wild and domestic animals ($\chi^2 = 79.674$, df = 3, $p < 0.00$).

TABLE 2 NISP and MNI of animal remains from the WZ and HT contexts at Xitou.

Taxon	WZ				HT			
	NISP	NISP (%)	MNI	MNI (%)	NISP	NISP (%)	MNI	MNI (%)
Cypraeidae	3	0.2	3	4.4	0	0.0	0	0.0
Unionidae	39	3.0	3	4.4	12	1.2	4	6.4
Unio douglasiae	4	0.3	1	1.5	0	0.0	0	0.0
Hyriopsis cumingii	0	0.0	0	0.0	1	0.1	1	1.6
Lamprotula	2	0.2	2	3.0	0	0.0	0	0.0
Osteichthyes	2	0.2	1	1.5	0	0.0	0	0.0
Geoemydidae	2	0.2	1	1.5	0	0.0	0	0.0
Trionychidae	1	0.1	1	1.5	0	0.0	0	0.0
Pelecanidae	2	0.2	1	1.5	0	0.0	0	0.0
Phasianidae	4	0.3	1	1.5	1	0.1	1	1.6
Large bird	1	0.1	1	1.5	0	0.0	0	0.0
Medium bird	3	0.2	1	1.5	7	0.7	1	1.6
Unidentified bird	2	0.2	1	1.5	0	0.0	0	0.0
Zokor, *Eospalax*	1	0.1	1	1.5	0	0.0	0	0.0
Field mouse, *Microtus*	0	0.0	0	0.0	9	0.9	1	1.6
Muridae	1	0.1	1	1.5	1	0.1	1	1.6
Unidentified rodent	22	1.7	3	4.4	2	0.2	1	1.6
Hare, *Lepus*	6	0.5	1	1.5	0	0.0	0	0.0
Dog, *C. familiaris*	77	5.9	4	5.9	42	4.0	5	7.9
Mustelidae	1	0.1	1	1.5	0	0.0	0	0.0
Equus	1	0.1	1	1.5	0	0.0	0	0.0
Horse, *Equus caballus*	22	1.7	1	1.5	41	3.9	3	4.8
Boar, *Sus scrofa*	0	0.0	0	0.0	2	0.2	1	1.6
Pig, *S. domesticus*	204	15.5	9	13.2	445	42.5	18	28.6
Sika deer, *C. nippon*	33	2.5	1	1.5	32	3.1	2	3.2
Roe deer, *C. capreolus*	8	0.6	1	1.5	4	0.4	2	3.2
Large cervid	2	0.2	1	1.5	1	0.1	1	1.6
Medium cervid	18	1.4	2	2.9	6	0.6	1	1.6
Small cervid	3	0.2	1	1.5	2	0.2	2	3.2
Unidentified cervid	23	1.8	1	1.5	5	0.5	2	3.2
Bos	0	0.0	0	0.0	1	0.1	1	1.6
Cattle, *B. taurus*	369	28.1	4	5.9	212	20.2	6	9.5
Sheep, *O. aries*	20	1.5	4	5.9	5	0.5	1	1.6
Goat, *C. hircus*	49	3.7	6	8.8	7	0.7	3	4.8
Sheep/goat, *O. aries/C. hircus*	378	28.8	7	10.3	209	19.9	4	6.4
Large artiodactyl	11	0.8	1	1.5	1	0.1	1	1.6
Total	1,314	100.0	68	100.0	1,048	99.9	63	99.9

Note: The total percentages of NISP and MNI for the HT periods are not equal to 100.0% because of scientific notation.

Mortality profiles and animal use at Xitou

Pigs

A total of 49 pig mandibles (YS: $n = 2$; LS: $n = 3$; WZ: $n = 17$; HT: $n = 27$) were available for age estimation using dental wear. Specifically, the two individuals from the YS contexts died at 14–18 and 25–36 months old, while the three individuals of the LS period were culled at 5–8, 9–14, and 37+ months old, respectively. The mortality profiles for pigs of the other two periods (WZ and HT) indicate that the largest kill-off all occurred at the age stage of 1–2 years (Figure 3). In terms of dental eruption of HT periods, two specimens were 6–12 months

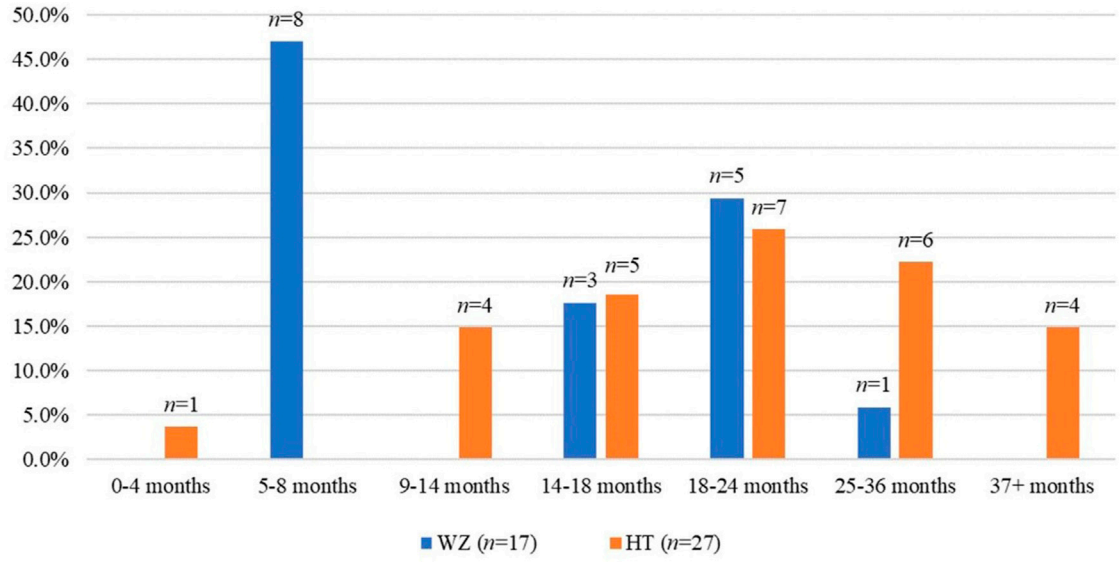

FIGURE 3
Mortality profiles for pigs from the WZ and HT contexts (based on dental wear).

old, two specimens were 12–16 months old, two specimens were younger than 1–1.5 years of age, and 18 specimens were older than 7–22 months old. With respect to bone epiphyseal fusion (LS: $n = 41$; WZ: $n = 64$; HT: $n = 88$), most pigs of the LS and WZ periods died before 2 years of age, with 55.5% of individuals from the WZ contexts being culled before 1 year old (Supplementary Table S1). Bone epiphyseal fusion data for the HT periods were basically consistent with the data on dental wear.

Normally, the major purpose of pig husbandry is for acquiring pork. In order to receive a higher rate of return, 80.0% or higher proportion of juvenile individuals would often be maintained to acquire more meat yields (Ma, 2007). In terms of dental wear and bone epiphyseal fusion, pigs were mainly culled at an optimum slaughter age of 1–2 years old (Li, 2011b) during the WZ and HT periods at Xitou. This suggests that pigs were raised for pork across time. Furthermore, the apparently large proportion of pigs aged 5–8 months old (47.1%) in the WZ assemblage might reflect a preference for tender meat. Existing studies have shown that the consumption of tender pork likely existed in both prehistoric and Bronze Age sites in northern China, such as Zaoshugounao, Zaolinhetan, and Yinxu (Li, 2011a; Li et al., 2020). In addition, pig mortality profile of the WZ period shows an absence of neonatal individuals, and only one individual died at 2–3 years old. Based on field survey results, the scale of Xitou was large during the Bronze Age (Dou et al., 2021). Pork may have been provisioned to Xitou from adjacent areas during the WZ period. That being said, due to the small sample size, future fieldwork and research may help to gain a better understanding of pig consumption and provision at Xitou during the Bronze Age.

Caprines

We documented dental eruption and wear of 42 caprine mandibles (WZ: $n = 28$; HT: $n = 14$). Dental wear data suggest that most caprines from the WZ contexts were culled at the age of 6–12 months, with nearly one quarter (21.7%) of individuals surviving to 6 years old (Figure 4). In terms of the HT periods, 30.0% of caprines survived beyond the age of 6 years and most caprines died at 1–2 years of age. According to dental eruption, two specimens were younger than 21–24 months (WZ: $n = 1$; HT: $n = 1$), and seven were older than 18–24 months (WZ: $n = 4$; HT: $n = 3$). Bone epiphyseal fusion data for the three specimens from the LS contexts suggest that these caprines died before 3 years of age.

Caprines would be culled in large quantity at the optimum slaughter age if the major purpose of herding is for meat consumption, while a pursuit for milk and wool would result in a focused kill-off on individuals younger than 2 months old and a higher mortality rate of elder individuals, respectively (Payne, 1973). Meat yield of caprines normally reached the peak at 1.5–2.5 years of age (Li, 2011a), and a focused culling on individuals of 6–12 months old has been associated with tender meat acquisition (Vigne and Helmer, 2007). In the case of Xitou, the equal death number of caprines aged 6–12 months and 1–3 years of the WZ period might reflect

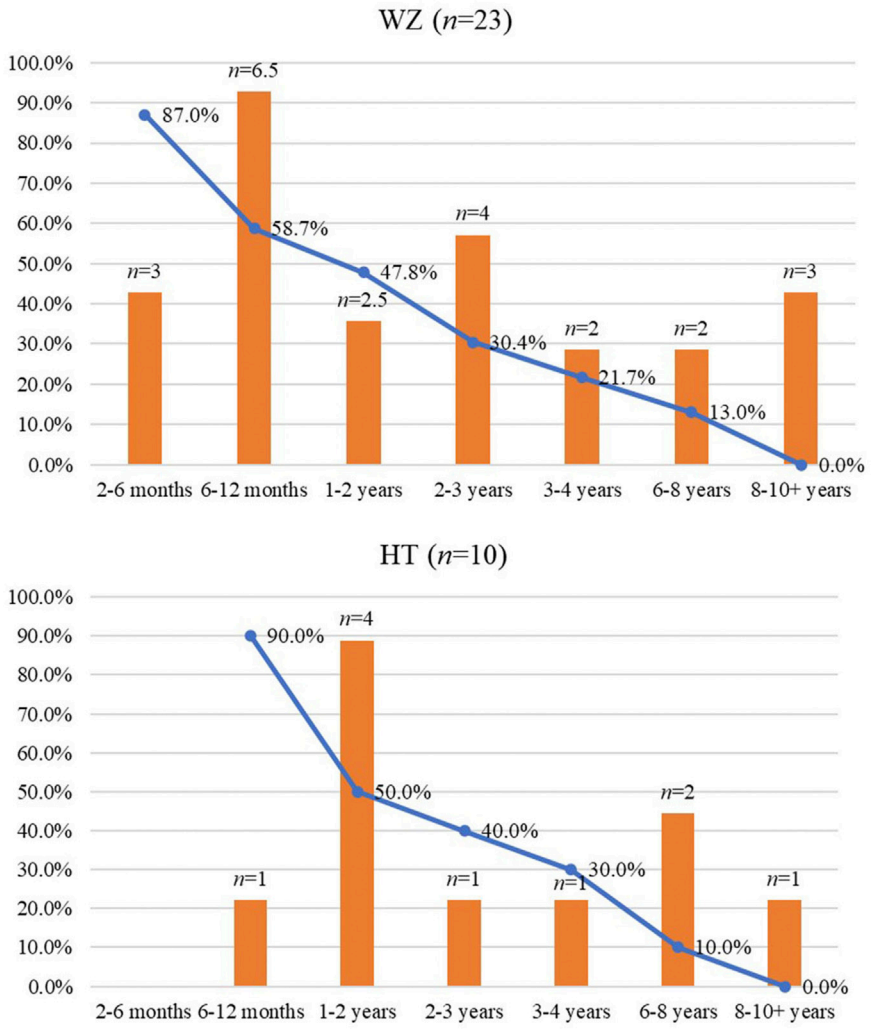

FIGURE 4
Mortality profiles and survivorship curves for caprines from the WZ and HT contexts.

a preference for meat, particularly tender meat. In fact, similar kill-off patterns have been recorded for other Bronze Age sites in the Central Plains, such as the Xiaomintun Locale at Yinxu and the Qijia jade artifact workshop at Zhouyuan, where over one quarter of caprines were killed at the age of 6–12 months (Ma and Hou, 2010; Li, 2011a). Indeed, Chinese historical texts, such as *Shijing (Book of Songs)* (2006), have recorded the sacrifice of lambs and Chinese leeks for the ancestors and the offering of quality lambs and wine in banquets during the Bronze Age. During the HT periods, the mortality profile of caprines at Xitou was similar to those of the late Neolithic sites of Taosi and Xinzhai Phase II (Li et al., 2014; Brunson et al., 2016), and was in between those of the Phase II and Phase IV of the early Bronze Age site of Erlitou (Li et al., 2014). This age structure, with over a quarter of caprines being slaughtered above the age of six, suggests that caprines were primarily raised for meat.

Cattle

We recorded epiphyseal fusion data for 155 cattle skeletal elements (Table 3). Despite the small sample size of the LS assemblage, we can infer that most cattle were supposed to live beyond 18 months of age, of which some may have survived to 3 years old. As for the WZ period, the majority of cattle died before 2 years of age, while most individuals survived past 4 years old. In the HT periods, most cattle survived past

TABLE 3 Bone epiphyseal fusion of cattle from Xitou.

		7–10 months	12–18 months	24–36 months	36–48 months
LS	No. of fused and fusing elements	2	2	1	0
	Percentage	100.0%	100.0%	100.0%	0.0%
	No. of unfused elements	0	0	0	0
	Percentage	0.0%	0.0%	0.0%	0.0%
WZ	No. of fused and fusing elements	6	46	16	14
	Percentage	100.0%	95.8%	69.6%	77.8%
	No. of unfused elements	0	2	7	4
	Percentage	0.0%	4.2%	30.4%	22.2%
HT	No. of fused and fusing elements	3	14	21	10
	Percentage	100.0%	100.0%	95.5%	66.7%
	No. of unfused elements	0	0	1	5
	Percentage	0.0%	0.0%	4.6%	33.3%

Note: Age classes for epiphyseal fusion refer to Silver (1969). 7–10 months: distal scapula, pelvis; 12–18 months: distal humerus, proximal radius, proximal phalanx I, proximal phalanx II; 24–36 months: distal tibia, distal metacarpals, distal metatarsals; 36–48 months: proximal humerus, distal radius, proximal ulna, proximal and distal femur, proximal tibia, calcaneus.

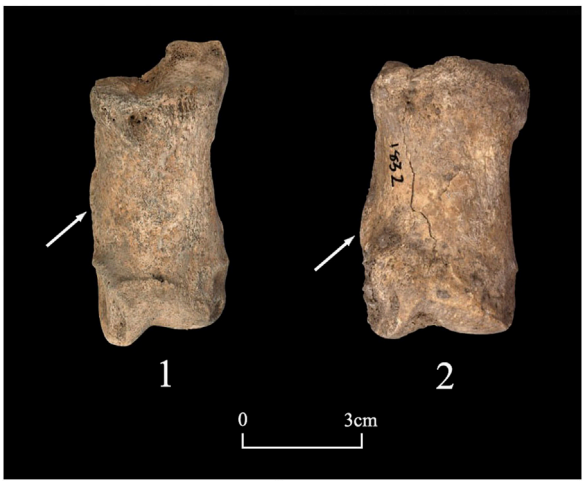

FIGURE 5
Excessive osseous growth found in cattle specimens from the WZ and HT contexts: 1-cattle first phalange (anterior view) of the WZ period; 2-cattle first phalange (anterior view) of the HT period.

18 months of age, with 33.3% of the individuals culled before 3 years of age. Of 10 cattle mandibles (LS: $n = 1$; WZ: $n = 4$; HT: $n = 5$) available for age estimation, only one specimen died at 6–24 months of age, while the other nine lived beyond 24–36 months of age.

Previous zooarchaeological research on the Bronze Age sites of Wangjinglou and Guandimiao in the Central Plains of northern China has suggested two different patterns of cattle use. At Wanjinglou, 83.3% of cattle survived past 4 years old, and was considered reflecting the exploitation of cattle power (You and Wu, 2021). In contrast, only 30.7% of cattle survived to 4 years old at Guandimiao, which shows the use of cattle for food (Hou et al., 2019). The survivorship rates of cattle during the WZ and HT periods at Xitou were similar to that of Wangjinglou, but apparently different from that of Guandimiao. We also identified excessive osseous growth in several cattle specimens from the WZ and HT contexts, respectively, most of which were phalanges (Bartosiewicz et al., 1997) (Figure 5). Alongside other lines of archaeological evidence for the involvement of cattle in agricultural practices (e.g., Lv, 2015; Liu, 2016; Lin et al., 2018), we infer that cattle may have been used as work animals to some extent at Xitou since the Bronze Age. Indeed, Chinese historical records, such as *Zhouli (Rites of Zhou)* (Xu and Chang, 2014), *Hanshu (Book of Han)* (Ban, 1962), and *Xintangshu (New Book of Tang)* (Ouyang and Song, 1975) have documented the use of cattle for pulling military supplies and plowing.

Worked bones

We identified traces of human modification on 198 specimens, accounting for 4.1% of all analyzed animal remains (Table 4). During the prehistoric YS and LS periods, deer antlers and limb bones of deer and pigs were the major raw materials for bone artifact production. A more diverse set of animal species were involved in bone working activities during the WZ and HT periods, with cattle skeletal elements being the most frequently occurring raw materials.

The growing importance of cattle in worked bone production at Xitou in the Bronze Age and historical periods fits into the picture of ancient Guanzhong region. Indeed, at the Neolithic site of Guantaoyuan, two thirds of worked bones unearthed (75.8%) were made of deer species (Yang, 2017). In comparison, cattle were the primary source of worked bones at the Bronze Age sites of Zaolinhetan, Fenghao, and Zhouyuan (Liu, 1980; Xu, 1992; Fu

TABLE 4 Animal taxa for worked bones from Xitou.

Taxon	YS		LS		WZ		HT	
	No.	%	No.	%	No.	%	No.	%
Bovine	0	0.0	0	0.0	38	27.3	16	32.7
Caprine	0	0.0	0	0.0	4	2.9	0	0.0
Pig	0	0.0	1	16.7	2	1.4	3	6.1
Horse	0	0.0	0	0.0	0	0.0	2	4.1
Dog	0	0.0	0	0.0	1	0.7	1	2.0
Deer	2	50.0	0	0.0	11	7.9	7	14.3
Unidentified artiodactyl	0	0.0	0	0.0	6	4.3	1	2.0
Unidentified mammal	2	50.0	5	83.3	61	43.9	16	32.7
Bird	0	0.0	0	0.0	2	1.4	0	0.0
Geoemydidae	0	0.0	0	0.0	2	1.4	0	0.0
Mollusc	0	0.0	0	0.0	12	8.6	3	6.1
Total worked bones	4	100.0	6	100.0	139	99.8	49	100.0

Note: The total percentage for the WZ period is not equal to 100.0% because of scientific notation.

et al., 2014; Huang et al., 2021). Similarly, bone artifacts from the Niejiagou bone workshop, dated to the Qin-Han periods, were mostly made from cattle (Xu et al., 2019). Also, cattle bones took up 41.9% of worked bones from bone workshop at the Western Market of the Tang period (He, 2021).

Ancient subsistence economies in the northern Guanzhong region

Combined with published zooarchaeological and archaeobotanical data, our results from Xitou provide additional insights into the development of subsistence economies in the northern Guanzhong region from prehistoric to historical periods. During the YS period, the animal assemblage from Yangguanzhai comprised domestic animals, such as pigs (by NISP, 77.3%) and wild animals, such as deer (by NISP, 4.0%), with former being the major source of meat (Hu et al., 2011). At the LS period site of Xiaweiluo, pigs (by NISP, 57.9%) and deer (by NISP, 24.2%) were the most frequently occurring animals (Zhang, 2006). Zooarchaeological data from sites in the Wei River valley also suggests that whereas the proportion of domestic animals, particularly pigs, apparently increased in the LS period, wild species continued to play crucial roles (Luo, 2009; Wang et al., 2014; Yuan, 2015; Zong et al., 2021). Indeed, deer were among the most important animal resources from the YS and LS contexts at Xitou. In the Beiluohe River valley on the southern margin of Northern Shaanxi Plateau, pigs dominated the animal assemblages from the late Neolithic sites. When domestic cattle and caprines entered Northern Shaanxi at ca. 4400–4100 B.P., these animals quickly overtook pigs as the primary domestic species in the Wuding and Tuwei River valleys (Hu, 2021; Wang et al., 2022). This seemingly consistency between the Guanzhong Plain-Northern Shaanxi Plateau transition zone and the hinterland of the Guanzhong region during the late Neolithic period may have resulted from the northward expansion of the Miaodigou Culture (Han, 2004; Han, 2013; Dai, 2020). In addition, archaeobotanical data from the late Neolithic contexts at Yangguanzhai and Zaolinhetan suggest that broomcorn millet (by absolute quantity, 39.8% on average) constituted the largest proportion of crops, followed by foxtail millet (by absolute quantity, 24.8% on average) (Wang et al., 2018; Chen et al., 2019). The stable and developing animal husbandry and crop cultivation facilitated social developments in the Guanzhong region and its adjacent areas in prehistory.

In the Bronze Age, the proportions of cattle and caprines in the animal assemblages increased and had exceeded that of pigs. The average NISP and MNI of cattle, caprines, and pigs from contexts of the late second to early first millennium BCE at the sites of Zaoshugounao, Zaolinhetan, and Nianzipo were 35.7% and 10.4%, 16.1% and 23.5%, 26.5% and 23.8%, respectively (Zhou, 2007; Li et al., 2020) (Figure 6, Figure 7). Likewise, cattle became more important than pigs and deer in meat provision and worked bone production at Xitou. This may have been associated with the development of cattle herding and the nature of cattle skeletal elements as quality raw materials. In addition, existing archaeobotanical research shows that foxtail millets (by absolute quantity, 59.8%), broomcorn millets (by absolute quantity, 7.4%), and soybeans (by absolute quantity, 4.4%) were the major crops at the site of Zaolinhetan, with other non-crop plants, such as Leguminosae and Chenopodiaceae, likely being used as feedstuff (Chen et al., 2019). *Shijing (Book of Songs)* described that local residents in the ancient Bin area cultivated crops, such as foxtail millet, broomcorn millet, rice,

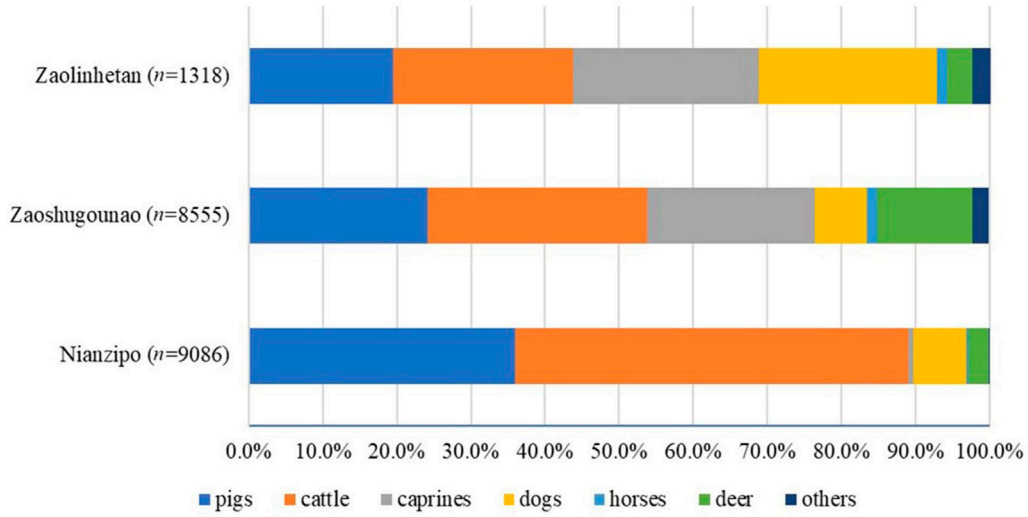

FIGURE 6
NISP% of animal remains from Nianzipo, Zaoshugounao, and Zaolinhetan.

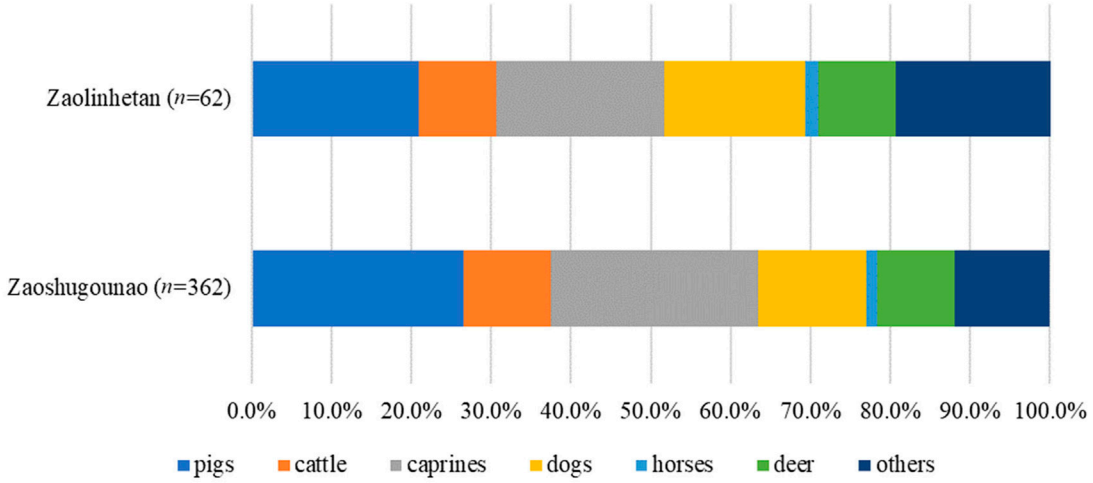

FIGURE 7
MNI% of animal remains from Zaoshugounao and Zaolinhetan.

wheat, and soybean, and consumed vegetables and fruits in different seasons (Wang, 2006). *Shiji (Records of the Grand Historian)* also has records on planting hemps and beans (Sima, 1959). The importance of millet farming was further evidenced by stable isotope analysis, suggesting that the diets of residents in Bronze Age Jing River valley were C_4-based (Lan, 2017). The diversified use of animal and plant resources in Bronze Age Jing River valley reflects an adaption of residents to surrounding natural landscape and cultural exchanges with neighboring areas. The climate in the Jing River valley had gradually turned drier and cooler since the end of the Holocene Megathermal (4500–3100 a. B.P.) (Li, 2009), which resulted in certain degree of soil degradation (Mao, 2003; Wang and Huang, 2002). More favorable conditions were created for the growth of forage grasses (Zhao et al., 2013), thus facilitating cattle and caprine herding, the latter in particular. Located in the southern margin of the Loess Plateau, the Jing River valley is characterized by hills, gullies and terraces (Xun, 2000). The Bronze Age residents in the region took advantage of local ecological conditions by cultivating crops and raising pigs on

loess terraces while herding caprines in gullies and hills (Li, 2005; Li et al., 2020). In addition, the Jing River valley lies in the northern edge of the Guanzhong region, between the Northern Shaanxi Loess Plateau and the Guanzhong hinterland (Xun, 2000; Han, 2005). It served as one of the possible channels through which domestic cattle and caprines entered the Central Plains (Hu, 2020, 2021). As a core area for the pre-dynastic Zhou people, the Jing River valley had maintained its own characteristics of subsistence practices through to the WZ period. This is consistent with the continuation of cultural factors from the late Shang period to the WZ period in the middle Jing River valley (Dou et al., 2021).

During the HT periods, developed agricultural production and pig husbandry laid economic foundation for Chinese dynasties, and also formed the dietary habits of residents in the Guanzhong region (Yuan et al., 2020). Lines of zooarchaeological evidence from the Chang'an City and the Yangling Mausoleum of the Western Han period suggest that pigs and cattle were the major domestic animals in both residential and ritual contexts (Hu et al., 2006; Hu and Yang, 2010; Liu and Jiao, 2019). Since the invention of iron plows in the mid-to-late first millennium BCE, cattle had been increasingly involved in agricultural activities and their role as a source of protein gradually declined (Fan, 1983; Han, 2018). The popularization of cattle plow made these animals crucial part of agricultural production. *Houhanshu (Book of Later Han)* documented the severe adverse impact of the shortage of animal power caused by rinderpest on crop production (Fan, 1965). *Yantielun (Discourses on Salt and Iron)* also recorded the official prohibition of slaughtering cattle at will, implemented by the Han Dynasty rulers (Huan, 1992). Cattle also contributed greatly to transportation during the HT periods. Cattle carts not only were widely used in everyday life, but also fulfilled military tasks, carrying army provisions and weaponry (Zhou, 2002). In addition, cattle continued to be primary raw materials for worked bone production. In general, the dietary structure of residents, in relation to meat consumption, in the Jing River valley during the HT periods was dominated by pigs, supplemented by caprines and cattle. Although archaeobotanical and stable isotope data from the region are currently unavailable, historical texts provided records on crop cultivation. For example, *Hanshu (Book of Han)* mentioned the necessity of planting the "five cereals" (i.e., foxtail millet, broomcorn millet, hemp, wheat, and soybean) for the sake of natural disaster, and the harvest of these cereals was associated with peace and prosperity (Ban, 1962). *Xintangshu (New Book of Tang)* indicated that millet, rice, and wheat were cultivated and that "over 1.9 million *hu* of crops were collected from the fields" (Ouyang and Song, 1975). These texts imply that the system of crop cultivation was well developed, and the yields were significant at the time. Residents in the Jing River valley probably also planted these crops.

To sum up, the Jing River valley experienced diachronic changes in the exploitation of animal resources from prehistoric to historical periods. Domestic pigs played crucial roles in animal economies during the YS and LS periods, while cattle and caprines increased rapidly in number and overtook pigs in the WZ period. Cattle replaced deer as the major raw materials for worked bone production and was possibly exploited as draft animal. In the HT periods, pigs became the primary domestic animal species again. The role of cattle as important draft animals and sources of bone-working raw materials was strengthened. As for plant resources, foxtail millet and broomcorn millet were the major crops during the Neolithic period. Entering the Bronze Age, there were more varieties of crops, especially the wide use of beans. The "five cereals" cultivation system further developed in the HT periods. These diachronic changes were possibly the results of natural factors, such as climate changes since the end of Holocene Megathermal, and social factors, including, but not limited to regulations by the authorities, population structure, and cultural exchanges.

Conclusion

The excavation at the Nantou Locale of Xitou provides a rare opportunity for an investigation of the long-term changes in animal resource exploitation in the Guanzhong region. Our results, along with other relevant lines of evidence, illustrate the changing roles of some major domestic and wild animals in human subsistence practices through time and the various environmental and social factors that contextualized these changes in a region crucial to understanding cultural evolution and social development in ancient China. The zooarchaeological data from the Han-Tang contexts at the site also alleviate current shortage of available datasets of historical periods in the Guanzhong region. Future fieldwork in the region and comparative zooarchaeological research across wider geographic areas may help generate new insights into how diverse human-animal interactions shaped and was modified by the economic, social, and political milieu of ancient China.

Data availability statement

The datasets presented in this study can be found in online repositories. The names of the repository/repositories and accession number(s) can be found in the article/ Supplementary Material.

Author contributions

YL and LZ designed the research. QW, KL, and HS analyzed the data. LZ and BL directed the excavation and provided research

materials. QW and YL wrote the original version of the manuscript. All authors reviewed and approved the submitted version.

Funding

This research was supported by the 111 Project (Grant No: D18004), the National Social Science Fund of China (Grant No: 18CKG024), the Key Research and Development Program of Ningxia Hui Autonomous Region (Grant No: 2020BFG02008), the Key Research Program of Education Department of Shaanxi Provincial Government (Grant No: 21JY042), the Major Project of the Philosophy and Social Sciences of the Ministry of Education of China (Grant No: 2022JZDZ026), and the Professional Support Program for Excellent Young Scholars of Northwest University.

Acknowledgments

We thank the editor and the two reviewers for their critiques and suggestions on the manuscript.

Conflict of interest

The authors declare that the research was conducted in the absence of any commercial or financial relationships that could be construed as a potential conflict of interest.

Publisher's note

All claims expressed in this article are solely those of the authors and do not necessarily represent those of their affiliated organizations, or those of the publisher, the editors and the reviewers. Any product that may be evaluated in this article, or claim that may be made by its manufacturer, is not guaranteed or endorsed by the publisher.

Supplementary material

The Supplementary Material for this article can be found online at: https://www.frontiersin.org/articles/10.3389/feart.2022.1064818/full#supplementary-material

References

Albarella, U., Rizzetto, M., Russ, H., Vickers, K., and Viner-Baniels, S. (2017). *The oxford handbook of zooarchaeology*. Oxford: Oxford University Press.

Ban, G. (1962). *Book of Han*. Beijing: Zhonghua Book Company, 177, 1120, 1139, 4077. (in Chinese).

Bartosiewicz, L., Neer, W. v., Lentacker, A., and Fabiš, M. (1997). *Draught cattle: Their osteological identification and history*. Belgium: Musée royal de l'Afrique centrale Press, 32–72.

Brunson, K., He, N., and Dai, X. (2016). Sheep, cattle, and specialization: New zooarchaeological perspectives on the Taosi Longshan. *Int. J. Osteoarchaeol.* 26 (3), 460–475. doi:10.1002/oa.2436

Campbell, R., Li, Z., He, Y., and Yuan, J. (2011). Consumption, exchange and production at the great settlement Shang: Bone-working at Tiesanlu, Anyang. *Antiquity* 85 (330), 1279–1297. doi:10.1017/S0003598X00062050

Chen, S., Fu, W., Liu, J., Tang, L., Zhai, L., and Zhao, Z. (2019). Study on remains of carbonized plant in Zaolinhetan site in Xunyi, Shaanxi Province. *Cult. Relics South. China* 1, 103–112. (in Chinese). doi:10.3969/j.issn.1004-6275.2019.01.013

Crabtree, P. (1990). Zooarchaeology and complex societies: Some uses of faunal analysis for the study of trade, social status, and ethnicity. *J. Archaeol. Method Theory* 2, 155–205.

Cultural Heritage Archaeology Research Center of Northwest University, and Shaanxi Academy of Archaeology (2006). *Xunyi Xiaweiluo*. Beijing: Science Press. (in Chinese).

Dai, X. (2020). Prehistoric society stages in China and the formation of early states. *Acta Archaeol. Sin.* 3, 309–336. (in Chinese).

Davis, S. (1995). *The archaeology of animals*. New Haven: Yale University Press.

deFrance, S. D. (2009). Zooarchaeology in complex societies: Political economy, status, and ideology. *J. Archaeol. Res.* 17 (2), 105–168. doi:10.1007/s10814-008-9027-1

Dou, H., Li, Y., Yang, L., Yue, L., and Zhao, Y. (2021). Brief report on the excavation of the Shang and Zhou remains at the Yuzuipo location of the Xitou site in Xunyi County, Shaanxi. *Archaeology* 12, 22–39. (in Chinese).

Dou, H., Wang, Z., Zhai, L., Zhao, Y., and Qian, Y. (2019). The excavation of the remains of the Shang and Zhou dynasties at the Zaolinhetan site in Xunyi County, Shaanxi in 2016. *Archaeology* 10, 15–32. (in Chinese).

Fan, C. (1983). Study on stages of the development of Chinese primitive agriculture: Plow and cattle plow. *Agric. Archaeol.* 2, 145–150. (in Chinese).

Fan, Y. (1965). *Book of later Han*. Beijing: Zhonghua Book Company, 132. (in Chinese).

Fu, Z., Li, Z., and Xu, L. (2014). The bone workshop remains of the Western Zhou dynasty to the north of Fengcun village in Chang'an district, Xi'an City. *Archaeology* 11, 29–43. (in Chinese).

Gifford-Gonzalez, D. (2018). *An introduction to zooarchaeology*. Cham: Springer. doi:10.1007/978-3-319-65682-3

Gong, X. (2018). *The preliminary research on archaeological remains of the Sanshui River basin in Shang and Zhou dynasty*. Xi'an: Northwest University. Master's thesis. (in Chinese).

Grant, A. (1982). "The use of tooth wear as a guide to the age of domestic animals," in *Ageing and sexing animal bones from archaeological sites*. Editors B. Wilson, C. Grigson, and S. Payne (Oxford: B.A.R. Publishing), 91–108.

Han, J. (2004). Historical position of Central Plain cultures in Neolithic China. *Jianghan Archaeol.* 1, 59–64. (in Chinese). doi:10.3969/j.issn.1001-0327.2004.01.009

Han, J. (2013). *The Miaodigou period and the "early China"*. Studies in the Early China, 19–35. (in Chinese).

Han, M. (2005). Formation of the interlocking belt of agriculture and husbandry and climatic change in ancient north China. *Archaeology* 10, 57–68. (in Chinese).

Han, Q. (2018). A simple introduction of the diet structure in Shiji—take the diet culture sample in center Guanzhong area. *J. Shaanxi Xueqian Normal Univ.* 34 (9), 104–111. (in Chinese). doi:10.11995/j.issn.2095-770X.2018.09.023

He, S. (2021). New archaeological discoveries and related studies in the Western Market site of Chang'an city in the Tang dynasty. *Cult. Relics South. China* 3, 109–123. (in Chinese). doi:10.3969/j.issn.1004-6275.2021.03.012

He, Y., and Li, Z. (2022). On the excavation of the bone-tool workshop at Huanbei Shang City and its significance. *Cult. Relics Central China* 2, 102–107. (in Chinese).

Hillson, S. (1992). *Mammal bones and teeth: An introductory guide to methods of identification*. 1st ed. London, New York: Routledge. doi:10.4324/9781315425016

Hou, Y., Campbell, R., Li, Z., Zhang, Y., Li, S., and He, Y. (2018). The Guandimiao bone assemblage (and what it says about the Shang economy). *Asian Perspect.* 57 (2), 281–310. doi:10.1353/asi.2018.0018

Hou, Y., Campbell, R., Zhang, Y., and Li, S. (2019). Animal use in a Shang village: The Guandimiao zooarchaeological assemblage. *Int. J. Osteoarchaeol.* 29 (2), 335–345. doi:10.1002/oa.2745

Hu, Q., and Yuan, J. (2021). The formation and development of zooarchaeological research in Shaanxi Province. *Cult. Relics South. China* 4, 189–197. (in Chinese). doi:10.3969/j.issn.1004-6275.2021.04.022

Hu, S. (2021). A preliminary view of the development of animal husbandry from archaeological works in Yulin. *Chin. Soc. Sci. Today*. 2021-09-14(006)(in Chinese).

Hu, S., Liu, Z., and Zhang, J. (2006). Research report on animal bones unearthed from the southwest corner of the city wall of Chang'an city of Han dynasty in Xi'an. *Relics and Museology* 5, 58–60. (in Chinese). doi:10.3969/j.issn.1000-7954.2006.05.013

Hu, S. (2020). *The formation of agro-pastoral ecotone in northern China from a global perspective: A case study of zooarchaeology of the 3rd millennium BC in Yulin*. Guangming Daily. 2020-07-29(in Chinese).

Hu, S., Wang, W., Guo, X., Zhang, W., and Yang, M. (2011). Faunal analysis of the animal remains found near the west gate of the settlement moat at Yangguanzhai site, Gaoling County, Shaanxi Province. *Archaeol. Cult. Relics* 6, 97–107. (in Chinese). doi:10.3969/j.issn.1000-7830.2011.06.012

Hu, S., Yang, T., Yang, M., Shao, J., and Di, N. (2022). Research on faunal remains from the Miaoliang site in Jingbian County, northern Shaanxi on the formation of animal husbandry in China. *Quat. Sci.* 42 (1), 17–31. (in Chinese). doi:10.11928/j.issn.1001-7410.2022.01.02

Hu, S., and Yang, W. (2010). Faunal remains and their significance from the 'Waicangkeng' at the Yang Mausoleum of Han dynasty. *Archaeol. Cult. Relics* 5, 104–110. (in Chinese). doi:10.3969/j.issn.1000-7830.2010.05.019

Huan, K. (1992). *Discourses on salt and iron*. Beijing: Zhonghua Book Company, 556. (in Chinese).

Huang, Z., Cheng, Z., Wang, C., Li, Y., and Dou, H. (2021). The research on bone products of the Shang and Zhou periods from the site of Zaolinhetan in Xunyi, Shaanxi. *Cult. Relics South. China* 4, 183–188. (in Chinese).

Institute of Archaeology CASS (2007). *South Bin Zhou, Nianzipo*. Beijing: World Publishing Corporation. (in Chinese).

Jing-Wei Archaeological TeamIA, CASS (1999). Excavations at the duanjing site, binxian county, Shaanxi. *Acta Archaeol. Sin.* 1, 73122–73195. (in Chinese).

Lan, D. (2017). *Isotope analysis on human and animal's bone unearthed from Zaoshugounao site in Chunhua County, Shaanxi Province*. Xi'an: Northwest University, 18–20. Master's thesis. (in Chinese).

Liang, X. (1999). Excavations at the Duanjing site, Binxian County, Shaanxi. *Acta Archaeol. Sin.* 1, 73–95, 122. (in Chinese).

Li, C., Qian, Y., and Wei, N. (2012). The proto-zhou remains at Zaoshugounao site in Chunhua County, Shaanxi. *Archaeology* 3, 20–34. (in Chinese).

Li, X. (2005). *The climatic change in the middle of the Yellow River and the society vicissitudes in Xi Zhou dynasty*. Xi'an: Shaanxi Normal University, 2–5, 23-24. Master's thesis. (in Chinese).

Li, Y. (2009). *Hydrological study of the Holocene extreme floods and climatic change in the Jinghe River drainage basin*. Xi'an: Shaanxi Normal University, 103–104. Doctor's thesis(in Chinese).

Li, Y., Zhang, C., Wang, Z., Dou, H., Liu, H., Hou, F., et al. (2020). Animal use in the late second millennium BCE in northern China: Evidence from Zaoshugounao and Zaolinhetan in the Jing River valley. *Int. J. Osteoarchaeol.* 30, 318–329. doi:10.1002/oa.2860

Li, Z., Brunson, K., and Dai, L. (2014). The zooarchaeological study of wool exploitation from the Neolithic Age to the early Bronze Age in the Central Plains. *Quat. Sci.* 34 (1), 149–157. (in Chinese). doi:10.3969/j.issn.1001-7410.2014.18

Li, Z. (2011a). The consumption, utilization and supply of sheep and goat of the capital in the late Shang dynasty—the zooarchaeological studies on the sheep and goat remains unearthed in Yinxu area. *Archaeology* 7, 76–87. (in Chinese).

Li, Z. (2011b). A study on death age of domestic pig excavated from Xiaomintun site of Yin dynasty ruins and related issues. *Jianghan Archaeology* 4, 89–96. (in Chinese).

Lin, M., Luan, F., Fang, H., Xu, H., Zhao, H., and Barker, G. (2018). Pathological evidence reveals cattle traction in north China by the early second millennium BC. *The Holocene* 28 (8), 1205–1215. doi:10.1177/0959683618771483

Liu, H., and Jiao, N. (2019). Analysis of faunal remains from the burial pit No.14 in the Yangling Mausoleum. *Archaeol. Cult. Relics* 5, 120–128. (in Chinese). doi:10.3969/j.issn.1000-7830.2019.05.014

Liu, L., and Chen, X. (2012). *The archaeology of China: From the late Paleolithic to the early Bronze Age*. New York: Cambridge University Press. doi:10.1017/CBO9781139015301

Liu, L. (2004). *The Chinese Neolithic: Trajectories to early states*. New York: Cambridge University Press. doi:10.1017/CBO9780511489624

Liu, S. (1980). Brief report on trial excavation of the bone workshop of the Western Zhou period in Fufeng Yuntang. *Cult. Relics* 4, 27–38. (in Chinese).

Liu, X. (2016). Research on the origin of cattle ploughing and its early stages in the ancient China. *Agric. Hist. China* 35 (2), 29–38. (in Chinese).

Luo, Y. (2009). Several problems in prehistoric zooarchaeological research in Guanzhong region. *Archaeol. Cult. Relics* 5, 89–94. (in Chinese). doi:10.3969/j.issn.1000-7830.2009.05.014

Lv, P. (2015). The zooarchaeological observation on the utilization of cattle resources of the people of the Shang dynasty. *Archaeology* 11, 105–111. (in Chinese).

Ma, X. (2007). Age composition of the domestic pigs of the Xipo site in Lingbao and related problems. *Huaxia Archaeol.* 1, 55–74. (in Chinese). doi:10.3969/j.issn.1001-9928.2007.01.004

Ma, X., and Hou, Y. (2010). "Research report on animal bones unearthed from Qijia jade artifact workshop at Zhouyuan site," in *Shaanxi Academy of Archaeology, School of Archaeology and Museology, Institute of Archaeology CASS, Zhouyuan Archaeological Team. Zhou Yuan: Report on archaeological excavation of Qijia jade artifact workshop and Licun site in 2002 season* (Beijing: Science Press), 724–751. (in Chinese).

Mao, L. (2003). *Holocene environmental change of pedogenesis in the middle reaches of the Jinghe River basin*. Xi'an: Shaanxi Normal University, 34–37. Master's thesis. (in Chinese).

Niu, S. (2000). The origination of the predynasty Zhou culture. *Archaeol. Cult. Relics* 2, 48–55. (in Chinese).

O' Connor, T. (2000). *The archaeology of animal bones*. College Station: Texas A&M University Press. doi:10.2307/3557116

Ouyang, X., and Song, Q. (1975). *New book of Tang*. Beijing: Zhonghua Book Company, 1344, 1367, 1371-1372. (in Chinese).

Payne, S. (1973). Kill-off patterns in sheep and goats: The mandibles from Aşvan Kale. *Anatol. Stud.* 23, 281–303. doi:10.2307/3642547

Reitz, E., and Wing, E. (2008). *Zooarchaeology*. 2nd ed. New York: Cambridge University Press.

Rowley-Conwy, P. (2018). Zooarchaeology and the elusive feast: From performance to aftermath. *World Archaeol.* 50 (2), 221–241. doi:10.1080/00438243.2018.1445024

Schmid, E. (1972). *Atlas of animal bones for prehistorians, archaeologists and quaternary geologists*. Amsterdam, London, New York: Elsevier Publishing Company.

Shelach-Lavi, G., and Jaffe, Y. (2014). The arliest states in China: A long-term trajectory approach. *J. Archaeol. Res.* 22, 327–364. doi:10.1007/s10814-014-9074-8

Shelach-Lavi, G. (2015). *The archaeology of early China*. New York: Cambridge University Press.

Shi, N. (1963). *Collection of essays on Chinese historical geography*. Shanghai: SDX Joint Publishing Company, 27. (in Chinese).

Silver, I. (1969). "The ageing of domestic animals," in *Science in Archaeology: A survey of progress and research*. Editors D. Brothwell and E. Higgs (London: Thames and Hudson), 285-286, 296–299.

Sima, Q. (1959). *Records of the Grand historian*. Beijing: Zhonghua Book Company, 112. (in Chinese).

Underhill, A. P. (2013). *A companion to Chinese Archaeology*. New Jersey: Wiley-Blackwell. doi:10.1002/9781118325698

Vigne, J. D., and Helmer, D. (2007). Was milk a "secondary product" in the old world neolithisation process? Its role in the domestication of cattle, sheep and goats. *Anthropozoologica* 42 (2), 9–40.

von den Driesch, A. (1976). *A guide to the measurement of animal bones from archaeological sites*. Massachusetts: Peabody Museum of Harvard University, 27–57.

Wang, H., and Huang, C. (2002). The change of climate and environment in the middle valley of the Yellow River at the end of the Shang dynasty and social changs. *Journal of Historical Science* 1, 13–18. (in Chinese). doi:10.3969/j.issn.0583-0214.2002.01.002

Wang, H., Wang, W., and Hu, S. (2014). Human strategies of hunting sika deers in the Yangshao period: A case study of the wayaogou site, Shaanxi Province. *Acta Anthropol. Sin.* 33 (1), 90–100. (in Chinese). doi:10.16359/j.cnki.cn11-1963/q.2014.01.002

Wang, Q., Wu, Y., Huang, Z., Zhai, L., and Li, Y. (2022). A preliminary study of prehistoric subsistence economy in the southern part of northern Shaanxi: Zooarchaeological evidence from field surveys in the upper Beiluohe River valley. *Quat. Sci.* 42 (6), 1709–1722. (in Chinese). doi:10.11928/j.issn.1001-7410.2022.06.19

Wang, W., Yang, L., Ye, W., An, K., Yin, Y., and Hu, K. (2018). Excavation report of archaeological feature H85 at the Yangguanzhai site in Gaoling, Shaanxi. *Archaeol. Cult. Relics* 6, 3–19. (in Chinese). doi:10.3969/j.issn.1000-7830.2018.06.002

Wang, X. (2006). *Book of songs*. Beijing: Zhonghua Book Company, 220–222. (in Chinese).

Wang, Z., and Chen, H. (2010). The new gains of the third season excavation at Zaoshugounao site, Chunhua County. *Journal of Northwest University (Philosophy and Social Sciences Edition)* 40 (6), 32–36. (in Chinese). doi:10.16152/j.cnki.xdxbsk.2010.06.006

Wang, Z., Qian, Y., and Liu, R. (2013). The excavation of Zaoshugounao site in Chunhua County, Shaanxi in 2007. *Cult. Relics* 2, 55–66. (in Chinese).

Wei, X., Dou, H., Wang, Z., Zhao, Y., and Yang, L. (2020). Brief report on the survey of Xitou site in Xunyi County, Shaanxi Province. *Steppe Cult. Relics* 1, 16–27. (in Chinese). doi:10.3969/j.issn.1001-6406.2020.01.003

Xu, L. (1992). Bone workshop of Western Zhou dynasty in Xinwang village, Fengxi, Chang'an County, Shaanxi Province. *Archaeology* 11, 997–1003. (in Chinese).

Xu, W., He, J., Zhang, Y., Geng, Q., Yao, Y., and Wang, Y. (2019). Preliminary report on the excavation of the bone workshop of the Qin period at the Niejiagou site. *Archaeol. Cult. Relics* 3, 50–62. (in Chinese).

Xu, Z., and Chang, P. (2014). *Rites of Zhou*. Beijing: Zhonghua Book Company, 276. (in Chinese).

Xun, Y. (2000). *County annals of Xun Yi*. Xi'an: San Qin Publishing House, 1–2. 45, 72-73. (in Chinese).

Yang, M. (2017). Research on the working method and raw material selection of bone tools from the Guantaoyuan site in Baoji, Shaanxi. *Archaeol. Cult. Relics* 2, 123–128. (in Chinese). doi:10.3969/j.issn.1000-7830.2017.02.014

You, Y., and Wu, Q. (2021). The uses of domesticated animals at the early Bronze Age city of Wangjinglou, China. *Int. J. Osteoarchaeol.* 31 (5), 789–800. doi:10.1002/oa.2990

Yuan, J., Campbell, R., Castellano, L., and Chen, X. (2020). Subsistence and persistence: Agriculture in the Central Plains of China through the Neolithic to Bronze Age transition. *Antiquity* 94 (376), 900–915. doi:10.15184/aqy.2020.80

Yuan, J. (2015). *Zooarchaeology of China*. Beijing: Cultural Relics Press, 127–132. (in Chinese).

Zeder, M. (1991). *Feeding cities: Specialized animal economy in the ancient Near East*. Washington: Smithsonian Institution Press. doi:10.2307/3085525

Zhai, L., Dou, H., Wang, Z., and Zhao, Y. (2018). Brief report of excavation of Yangshao culture remains of the Zaolinhetan site in Xunyi County, Shaanxi Province. *West. Archaeol.* 2, 1–11. (in Chinese).

Zhang, T. (2001). Surveys of Shang period sites in Binxian and Chunhua Counties, Shaanxi. *Archaeology* 9, 13–21. (in Chinese).

Zhang, Y. (2006). "Report on the identification of animal remains of Xiaweiluo site in Xunyi," in *Cultural Heritage and Archaeology Research Center of Northwest University, Shaanxi Academy of Archaeology*. *Xunyi Xiaweiluo* (Beijing: Science Press), 546–548. (in Chinese).

Zhao, D., Dou, H., and Liu, B. (2022). Research on the physical characteristics of the residents during the Warring States period at Sunjia site in Xunyi County, Shaanxi Province. *North. Cult. Relics* 5, 70–78, 100. (in Chinese).

Zhao, D., Wu, H., Wu, J., and Guo, Z. (2013). C_3/C_4 plants characteristics of the eastern and western parts of the Chinese Loess Plateau during mid-Holocene and last interglacial. *Quat. Sci.* 33 (5), 848–855. (in Chinese). doi:10.3969/j.issn.1001-7410.2013.05.03

Zhou, B. (2007). "Identification of animal remains from Nianzipo site," in *Institute of Archaeology CASS. South Bin Zhou, Nianzipo* (Beijing: World Publishing Corporation), 490–492. (in Chinese).

Zhou, Z. (2002). Animal power and the civilization of Han and Tang dynasties. *J. Fujian Inst. Social.* 2, 20–24. (in Chinese).

Zhu, S. (2020). *Molecular archaeological study of Equus Ovodovi unearthed from three sites in northern China*. Changchun: Jilin University, 30–74. Doctor's thesis. (in Chinese).

Zong, T., Guo, X., Liu, H., Zhang, X., and Li, Y. (2021). Animal remains reveal the development of subsistence economy from prehistory to Qin-Han periods in the Guanzhong region: Evidence from the Gongbeiya site in Xi'an. *Quat. Sci.* 41 (5), 1445–1454. (in Chinese). doi:10.11928/j.issn.1001-7410.2021.05.18

frontiers | Frontiers in Earth Science

TYPE Original Research
PUBLISHED 30 January 2023
DOI 10.3389/feart.2023.1128824

Check for updates

OPEN ACCESS

EDITED BY
Ren Lele,
Lanzhou University, China

REVIEWED BY
Hu Li,
Henan Normal University, China
Fengwen Liu,
Yunnan University, China

*CORRESPONDENCE
Guangliang Hou,
hgl20@163.com

SPECIALTY SECTION
This article was submitted to Quaternary Science, Geomorphology and Paleoenvironment, a section of the journal Frontiers in Earth Science

RECEIVED 21 December 2022
ACCEPTED 17 January 2023
PUBLISHED 30 January 2023

CITATION
Wende Z, Hou G, Chen H, Jin S and Zhuoma L (2023), Dynamic changes in forest cover and human activities during the Holocene on the northeast Tibetan plateau.
Front. Earth Sci. 11:1128824.
doi: 10.3389/feart.2023.1128824

COPYRIGHT
© 2023 Wende, Hou, Chen, Jin and Zhuoma. This is an open-access article distributed under the terms of the Creative Commons Attribution License (CC BY). The use, distribution or reproduction in other forums is permitted, provided the original author(s) and the copyright owner(s) are credited and that the original publication in this journal is cited, in accordance with accepted academic practice. No use, distribution or reproduction is permitted which does not comply with these terms.

Dynamic changes in forest cover and human activities during the Holocene on the northeast Tibetan plateau

Zhuoma Wende[1,2], Guangliang Hou[1,2]*, Hongming Chen[1,2], Sunmei Jin[1,2] and Lancuo Zhuoma[3]

[1]Key Laboratory of Tibetan Plateau Land Surface Processes and Ecological Conservation (Ministry of Education), College of Geographical Science, Qinghai Normal University, Xining, China, [2]Qinghai Province Key Laboratory of Physical Geography and Environmental Process, College of Geographical Science, Qinghai Normal University, Xining, China, [3]School of Finance and Economics, Qinghai University, Xining, China

Human activities strongly influenced the present-day environment of the Tibetan Plateau, especially in the northeastern area. The questions over when and to what extent humans began to utilize the plateau environment have been long investigated, but there are still gaps in our understanding, such as the relationship between forest dynamics and anthropogenic activities. Here, we simulate the potential Holocene geographical distribution of the three dominant coniferous species in the Northeast Tibetan Plateau in response to climate/environment and analyze pollen records and multi-proxies for anthropogenic activities to explore human impact on natural forest dynamics. Simulation results show marked expansion of Picea and Pinus coniferous forests in the Early Holocene (11.5–8.3 ka BP), continuing into the Mid Holocene (8.3–4.0 ka BP). However, there was a slight contraction of forest in the Late Holocene (4.0–2.6 ka BP) in the western part of the region, and near disappearance in the eastern Qaidam Basin, although both Pinus and Picea slightly increased in Hehuang Valley. Pollen analysis confirms the patterns, with an increase in arboreal pollen mainly comprising Pinus and Picea from Early to Early Mid Holocene (11.5–5.3 ka BP), followed by a decrease. Proxies of anthropogenic activities, including carbon concentration, archeological sites, and, synanthropic plants, increased significantly after 5.3 ka BP, with archeological evidence for intensive exploitation of forest and turnover of natural vegetation. We argue that forest retreat at 5.3–4.0 ka BP was due to the expansion of cropland and increasing demand for wood. Significant coniferous forest retreat and degradation from 4.0 to 2.6 ka BP, with forest succession in Hehuang Valley, was driven by the booming population, extensive grazing, and forest exploitation; the drying cooling climate may have aggravated the pace of deforestation at higher elevations. This study presents new insights into the deforestation on the Northeast Tibetan Plateau in the Holocene.

KEYWORDS

coniferous forest, simulation, pollen, human activities, Tibetan plateau

Introduction

A capacity to alter the natural environment is one of the hallmarks of human civilization, and the process of human development and adaptation to the environment is one of modifying the natural environment and rearranging the natural biota (McNeill, 1986; Ellis and Ramankutty, 2008; Harari, 2015; Boivin et al., 2016; Goldewijk et al., 2017; Woodbridge

et al., 2020). This mostly has been true since the Holocene, with an increased rate of species turnover (Mottl et al., 2021), rapid extinction of wildlife (Pimm et al., 2014; Teng et al., 2022), and alteration of the terrestrial vegetation (Pongratz et al., 2008; Qin et al., 2010; Yu et al., 2010). Consequently, the composition and carbon sequestration of the biosphere has been profoundly influenced by the legacies of human activities in the past few thousand years (Broecker and Stocker, 2006; Olofsson and Hicker, 2007; Zhang et al., 2012; McMichael, 2021). Natural forests are essential in carbon cycling, biodiversity conservation, and world climate, organic matter production, water conservation, and soil erosion prevention (Foley and Kutzbach, 1994; IGBP, 1994; Whitney, 1994; Vitousek et al., 1997; Wan, 2017; Tuo et al., 2020). Forest degradation was one of the most apparent land cover changes through the Holocene (McNeill, 1986; Ren, 2000; Kaplan et al., 2009; Kaal et al., 2011; Hou et al., 2013a; Cheng et al., 2018), primarily due to cultivation and grazing, and in some areas may attributing to use of fire for hunting (Ren, 2000; Zhou, 2003; Kirch, 2005; Steffen et al., 2007; Hou et al., 2012; Hou et al., 2013a; Leal et al., 2019; Castilla-Beltrán et al., 2021; Miehe et al., 2021). In the mid and lower reaches of the Yangtze River, anthropogenic disturbance induced deforestation started since Mid Holocene (Ren, 2000; Hou et al., 2012). In Longdong Basin, anthropogenic activities, predominantly agriculture production, caused a decrease in the abundance of shrubs and grassland. In river valleys, the original vegetation has turned into coniferous and broadleaf mixed forests (Zhou et al., 2011). Owing to the human disturbance, the coniferous and broadleaf mixed forests cover decreased markedly after 4.6 cal ka BP in the southeast of Gansu (Li et al., 2012). However, the ways humans may have affected the natural forest on the Tibetan Plateau yet remains to be further studied.

Termed the third pole of the Earth, the Tibetan Plateau is one of the least populated regions in the world. The harsh environment of hypoxia, high altitude, and low temperature, as well as scarce resources have largely constrained mass settlement of people in the area even at the present day (Hou, 2016; Liu et al., 2018; Feng and Li, 2020). Thus there is a knowledge gap in understanding the anthropogenic impact on terrestrial vegetation and especially on the role of humans in natural forest dynamics. The ananlysis of fossile pollen records illustrates past vegetation succession, and the Holocene pollen record is generally well-established. However, whether, when, and to what extent human activity influenced spatial and temporal changes in vegetation and forests on the Tibetan Plateau remains unclear. Some studies suggest that substantial anthropogenic modification of Tibetan landscapes began as early as ~8,000 cal yr BP, with the presence of hunting and possibly grazing and, later, the development of agriculture (Brantingham et al., 2007; Miehe et al., 2014). Supporting evidence includes records of carbon concentration, analysis of wood charcoal, records of grazing related spore pollen and synanthropic plants, expansion of cropland, and human population boom (Miehe et al., 2014; Huang et al., 2017; Miao et al., 2017; Chen F. H et al., 2020; Wei et al., 2020; Wende et al., 2021; Liu et al., 2022). However, other studies argue the plateau, as central Asia's high-altitude heart, was not occupied by the mass human population until the Late Holocene. Therefore, turnover of terrestrial vegetation, including forest retreat in prehistorical time, was mostly driven by climate change (Herzschuh, 2006; Herzschuh et al., 2010; Kramer et al., 2010; Zhou and Li, 2012). However, charcoal records from soils and archeological evidence illustrated utilization of woods in the areas where they believe to be disappeared. More over, the persistence of isolated trees above the current tree line lead to continued speculation of widespread early human-induced forest clearance.

The human footprint on the Tibetan Plateau has steadily grown since the Epipleistocene and followed by the amelioration of climate after the Late Glacial Maximum (LGM), hunters begin to alter the landscape for food, energy, and other resources (Brantingham et al., 2007; 2013; Rhode et al., 2007; Miehe et al., 2014; Miehe et al., 2021). These alterations were especially pronounced on the Northeast Tibetan Plateau, which was at a relatively lower elevation, and occupied by both herders and farmers. Moreover, the area is one of the regions where there was intensive interaction between plateau people and farming communities from lowland China. In this region, use of fire for wild hunting started as early as 8.0 ka BP, when hunters and gatherers made their first sustained use of the plateau (Brantingham et al., 2007; Brantingham et al., 2013). Low intensity but extensive agriculture began at 5 ka BP during the Majiayao Culture, and intensive agricultural land use expanded around 4.3 ka BP during the late Majiayao Culture (Wende et al., 2021). Evidence shows mass grazing began around 3.6 ka BP and grassland degradation around 3.5 ka BP (Huang et al., 2017). As such, the studies on the human dimensions of environmental change are vitally important to explain the current environmental conditions, and to understand and interpret past human-land interactions.

Here, we investigate changes in the distribution of natural coniferous forests in the Holocene on the Northeast Tibetan Plateau and its relationship with human activities. Our objectives are twofold: 1) to map the potential distribution area of the two dominant families of coniferous forest, Picea and Pinus; and 2) to analyze the anthropogenic role in the dynamic change of forest during the Holocene. We use species distribution modeling (SDM) to simulate the fundamental niche of Picea and Pinus, and to map its potential geographic extent through the Holocene. The modeling results are then compared to evidence from archeological sites, carbon concentration, and fossil pollen records to assess actual and potential forest distribution and the role of human disturbance.

Scope of the study

Environmental setting

This study focuses on the northeastern Tibetan Plateau (Figure 1), including the eastern part of the Qinghai Plateau and the southern part of the Gannan Plateau (He et al., 2005), including geographical units of Hehuang Valley, Qinghai Lake area, and Gonghe Basin, between 99°19′–103°12′E and 35°32′–37°47′N, at an elevation of 1700–5,200 m with a west to east decrease in terrain elevations and bounded by the Qilian Mountains in the north and the Loess Plateau in the east. It is at the intersection of the Tibetan alpine region, the northwest arid region, and the eastern monsoon region, which makes it highly sensitive to climate change due to the interaction between the plateau monsoon, the westerly circulation, and the East Asia summer Monsoon.

Hehuang Valley is situated at the eastern margin of the Qinghai Plateau, with a mean annual temperature range of 2.2°C–9.0°C, a mean annual precipitation range of 252–535 mm, and forest-grassland vegetation (Jia et al., 2019). Forests are mainly coniferous, comprising Picea and Pinus; and mixed coniferous and broadleaf, comprising Poplar, Betula, and Salix. Poplar and Salix are mainly secondary forest species (CFEC, 1997). The region is also the most suitable for agricultural production in the Northeast Tibetan Plateau.

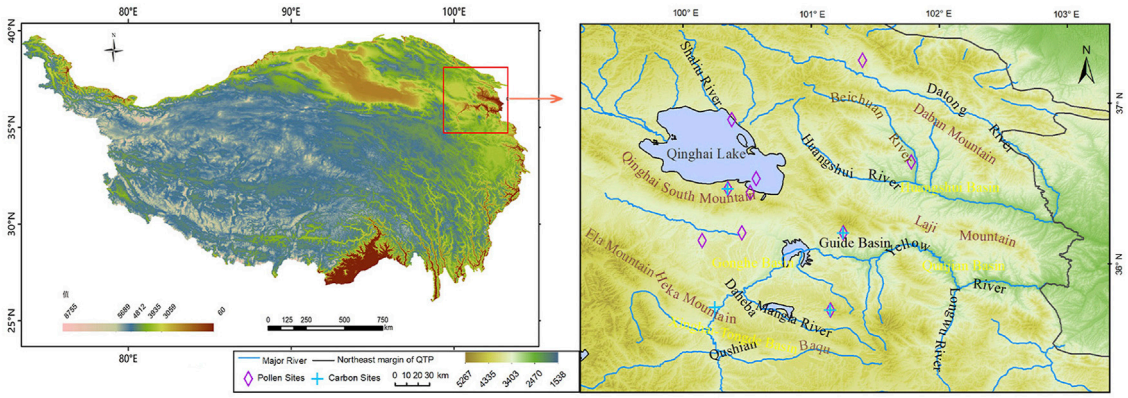

FIGURE 1
Study area and the location of the pollen sites and carbon sites used in this study.

The Qinghai Lake-Gonghe Basin has an average elevation of over 3,000 m and a transitional climate between temperate and sub-frigid, characterized by cold and dry winters, cool and humid summers; mean annual temperature ranges from −0.8°C–0.6°C and mean annual precipitation ranges from 324 to 412 mm. The mode of production is semi-pastrolism, and vegetation includes temperate grassland, alpine meadow, and swamp meadow. The surrounding mountains are mostly covered with alpine shrubs and coniferous forests (Chen and Peng, 1993). Drainage areas of the Yellow River at altitudes below 3,600 m, even in the Gonghe Basin, are occupied by forest-shrubs vegetation (Wu and Wu, 2016).

Cultural sequence

This study focuses on the period from 11.5 to 2.6 ka BP, encompassing the Early Holocene (EH) from 11.5 to 8.3 ka BP, the Mid Holocene (MH) from 8.3 to 4.2 ka BP, and the Late Holocene (LH) from 4.2 to 2.6 ka BP. Early hunter-gatherers were active between 8.3 and 5.3 ka BP, which is referred to as Early Mid Holocene (EMH). The Majiayao Culture was formed between 5.3 and 4.0 ka BP, referred to as Late Mid Holocene (LMH), during this period millet agriculture and pottery production were quite common in the Northeast Tibetan Plateau. In fact, the Majiayao Culture was known for its delicacy in pottery. Three different cultures characterized the LH, the Qijia Culture (4.2–3.6 ka BP), Kayue Culture (3.6–2.7 ka BP), and Xindian Culture (3.6–2.6 ka BP). The Qijia Culture was mainly characterized by agriculture and bronze production. The Xindian and Kayue Cultures occupied this region during the same period, while Xindian Culture mostly lived on farming and partially practiced grazing, the Kayue Culture mainly lived on grazing and practiced agriculture as an alternative source of livelihood.

Materials and methods

Species presence data

Due to the high altitude and harsh environment, coniferous forest, comprising *Picea crassifolia. Kom.* (hereafter referred to as Picea), and *Pinus armandii Franch.* and *Pinus tabulaeformis Carr.* (hereafter referred to as Pinus) accounts for 64.2% of the forested areas on the Northeast Tibetan Plateau (CFEC, 1997; Zhang, 2004; Tang et al., 2019). Thus, the geographical distribution of Picea and Pinus should provide a good indicator of forested land in the Northeast Tibetan Plateau. Both species are cold resistant and tolerate to barren soil conditions, with Picea preferring a cool and humid environment, and Pinus a slightly warmer climate.

In this study, we collated 131 presence localities for Picea and 235 for Pinus, mostly from field research in 2021–2022, and some from the literature and online search engines including the Global Biodiversity Information Facility (http://www.gbif.cn), the Chinese Vitual Herbarium (http://www.cvh.ac.cn), the Teaching Specimen Resource Net (http://mnh.scu.edu.cn), National Specimen Information Infrastructure (www.nsii.org.cn). Samples with unclear localities and artificially planted records were removed. The coordinates of the geographic position of the sampling places were obtained through Baidu coordinate pickup system and the accuracy of the information was checked by Google satellite map. To minimize overfitting of the modeling result and spatial auto-correlation caused by sampling bias, the occurrence data were trimmed using EMtools software so that only a single presence was retained in each 2.5x2.5 km grid cell. This gave a final total of 97 Picea presence samples and 80 Pinus samples (Figure 2).

Climate data

Climate data for the study were obtained from the World Palaeoclimate Database (www.paleoclim.org), focusing on the periods: the LGM (21 ka BP), EH (11.7–8.3 ka BP), MH (8.3–4.2 ka BP), LH (4.2–0.3 ka BP), and present day (1979–2013 AD). The database uses observations from over 4,000 global sites and Shuttle Radar Topography Mission (STRM) 90–30 topography data. Climate data extracted for each period (excluding the LGM) included 19 biological climatic variables (Bios) that were obtained using the thin plate smooth spline interpolation method integrated with ANUSPLIN software (Hijmans et al., 2005). Climate data for the LGM is based on the implementation of the CHELSA algorithm on PMIP3 data (Karger et al., 2021); this is a well-established ocean-

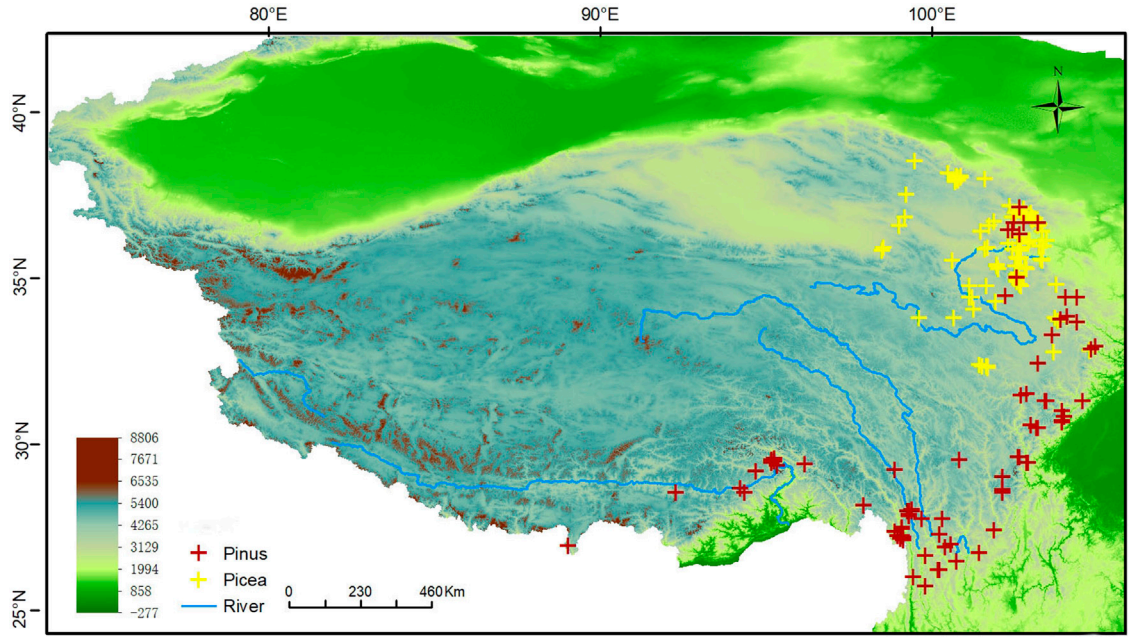

FIGURE 2
Localities of the sampling data.

TABLE 1 Environmental variables for Picea and percent contribution to the model.

Code	Environmental variables	Unit	Percent contribution
Bio1	Annual mean temperature	˚C*10	11.6
Bio2	Mean diurnal range (mean of monthly (maxTP-minTP))	˚C	6.9
Bio4	Temperature seasonality	standard deviation*100	5.2
Bio10	Mean temperature of the warmest month	˚C*10	12.1
Bio14	Precipitation of the driest season	mm/month	5.2
Bio15	Precipitation seasonality	coefficient of variation	1.7
Bio18	Precipitation of the warmest season	mm/season	18.2
Elev	Elevation	m	43.7

atmosphere coupled climate model that has contributed to the last three Intergovernmental Panel on Climate Change (IPCC) Assessment Reports and has been used to simulate climate for nearly 20 years (Fordham et al., 2017).

Climate data were first limited to the boundary of the Tibetan Plateau (Zhang N. M et al., 2021) and converted into ASC format to obtain the climatic layer for each period. As there is multi-collinearity between the 19 Bios, applying all Bios in the calculations may result in overfitting, causing the simulation result to be limited around the presence localities, affecting model accuracy and predictive ability (Warren and Seifert, 2011). To address this, Pearson's Correlation was used to analyze the correlation between the 19 Bios; any pairs with R≥0.80 were considered closely correlated (Kumar and Stohlgren, 2009; Lozier and Mills, 2011). Also, a preliminary SDM was performed using the 19 Bios and the importance of each variable to the model was evaluated using the percent contribution and Jacknife result (Ficetola, 2007). For closely correlated variables, the one that provides the most unique information and the highest contribution to the model was selected and the others were excluded. The model was then rerun using the selected set of variables in a stepwise fashion until all the required variables were determined (Table 1; Table 2).

Model calibration

SDMs have been applied in diverse disciplines, yet overfitting or over parameterize is a major concern, that may lead to severe bias in modeling. In this study we used maximum entropy modeling (MaxEnt) of species geographic distribution (Phillips et al., 2006). We selected MaxEnt over other types of SDM due to its high performance (Elith et al., 2006; McPherson and Jetz, 2007) and extensive use in previous studies, which means there is a robust understanding of its strengths and weaknesses (Elith and Graham, 2009; Phillips et al., 2009; VanDerWal et al., 2009; Veloz 2009; Elith

TABLE 2 Environmental variables for Pinus and percent contribution to the model.

Code	Environmental variables	Unit	Percent contribution
Bio10	Mean temperature of the warmest quarter	˚C*10	10
Bio15	Precipitation seasonality	coefficient of variation	18.8
Bio13	Precipitation of the wettest month	mm/month	21
Bio19	Precipitation of the coldest quarter	mm/quarter	8.6
Elev	Elevation		41.6

et al., 2011). In address to model weaknesses, parameter optimization is essential for model calibration. Feature types and the regularization multiplier are the two crucial parameters that need to be considered. Feature types correspond to environmental variables; these are mathematically transformed so that MaxEnt can use complex mathematical relationships to predict the response of species to various environmental factors. The regularization multiplier is a constraint added to the model based on element parameters that adjusts the response curve of the simulation (Phillips et al., 2009). Here, we used Kuenm, an R package for model calibration. Kuenm selects the best parameters for modeling based on: 1) statistical significance; 2) predictive ability; and 3) model complexity (Cobos et al., 2019). In detail, we used 15 feature types (L, Q, P, H, LQ, LP, LH, QP, QH, PH, LQP, LQH, LPH, QPH, LQPH), 40 regularization multipliers (at intervals of 0.1), giving a total of 600 combinations. Optimal parameters were selected based on omission rates below the statistical significance threshold and delta akaike information criterion (AIC) up to 2 (Warren and Seifert, 2011). AIC is a mathematical method for evaluating how well a model fits the data it was generated from. The best-fit model according to AIC is the one that explains the greatest amount of variation using the fewest possible independent variables. Finally, a combination of feature type and regularization multiplier with AIC of 0 was determined to be the optimal parameter (Milanovich et al., 2012; Zhu et al., 2014).

MaxEnt modeling was performed using the optimized parameters, with 70% of the presence data set as training data for model prediction and 30% used for testing. To reduce the uncertainty of prediction, the process was replicated 10 times, and to avoid model transition pooling, the maximum number of iterations was set to 5,000. The modeling was applied to simulate species distribution for the four periods of interest (LGM, EH, MH, and LH).

Pollen and anthropogenic activity proxies

Nine sites on the Northeast Tibetan Plateau with good palynological data were selected for arboreal pollen analysis, two from Hehuang Valley, namely, Changning site (Dong et al., 2012) and Dashuitang site (Cao et al., 2021), three from Gonghe Basin, namely, Genggahai (Liu, 2016), Dalianhai (Cheng et al., 2010), and Ke section (Miao et al., 2017), three from Qinghai Lake drainage area, namely, Qinghai Lake (Liu et al., 2002), Langgeri (Wei et al., 2020), and YWY(Zhang Y. L et al., 2021), and one along the Qilian Mountains, namely, Luanhaizi (Cao et al., 2021). The data on total amount of arboreal pollen and coniferous trees were extracted from all nine sites to analyze dynamic changes in forest extent and location for comparison with the simulated distributions. The data on carbon concentration was extracted from four sites in Northeast Tibetan Plateau, namely, Nankayan Site (Qi, 2022), Jiangxigou (Jiang et al., 2015) Ke section (Miao et al., 2017), and Langgeri (Wei et al., 2020), along with the synanthropic plants (Chen X. L et al., 2020), number of sites on the Northeast Tibetan Plateau, as indicators of anthropogenic activities in the area. In order to eliminate statistical magnitude variance due to the different units of the collected data, the minimum-maximum normalization method was used in calculations. Finally, archeological evidence for the different periods and cultures on the Northeast Tibetan Plateau was analyzed to further explore the human activities and forest changes.

Results

Geographic distribution of Picea and Pinus since the Late Glacial Maximum

The relative probability of species distribution is expressed on a logistic scale 0–1, with larger values indicating greater species suitability. To derive a map of suitable/unsuitable habitats from the continuous species density distribution, a threshold must be applied. Selection of the optimal threshold is particularly critical because of the binary distribution of species suitability (suitable or unsuitable); small changes in the threshold can result in very different maps (Poirazidis et al., 2019). In previous studies three methods for selecting logistic thresholds for the division of suitable and unsuitable geographical areas that are considered to give greater prediction accuracy have been identified: the minimum training presence (MTP), ten percentile training presence (10P), and equal test sensitivity and specificity (ETSS) (Cao et al., 2013). The MTP method assumes that the least suitable habitat, where the species is known to be present, is the minimum suitability value for that species. The method is prone to exaggerate the geographical distribution range of the species and thus is more suitable for predicting invasive species than native species (Liu et al., 2005). The ETSS method uses a threshold based on where there is the same chance of the habitat being suitable and unsuitable. The 10P method assumes that 10% of the presence localities in the least suitable area are not present in regions that represent the overall habitat of the species and thus should be omitted. This is considered more proper for estimation of native species (Liu et al., 2005; Phillips et al., 2006; Jiménez and Lobo, 2007) and is the approach adopted in this study. The resulting 10P threshold for the binary distribution of Picea is 0.16 and for Pinus is 0.266. As figure two and three illustrates, after the application of the threshold, the area identified as suitable habitat is equally divided into three levels using ArcGIS, namely, low, moderate, and high suitable area. Areas designated moderately and highly suitable are identified as species stable geographical distribution areas.

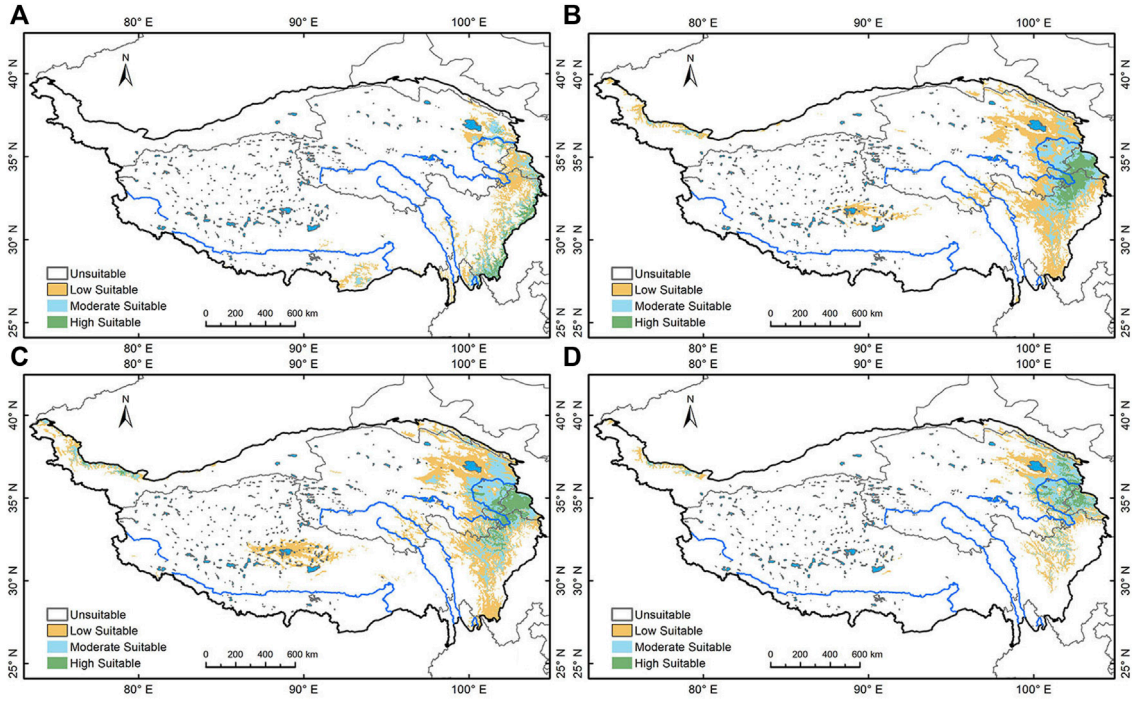

FIGURE 3
Simulation of Picea's geographical distribution. **(A)** Picea's geographical distribution area during LGM; **(B)** during Early Holocene; **(C)** during the Mid Holocene; **(D)** during the Late Holocene.

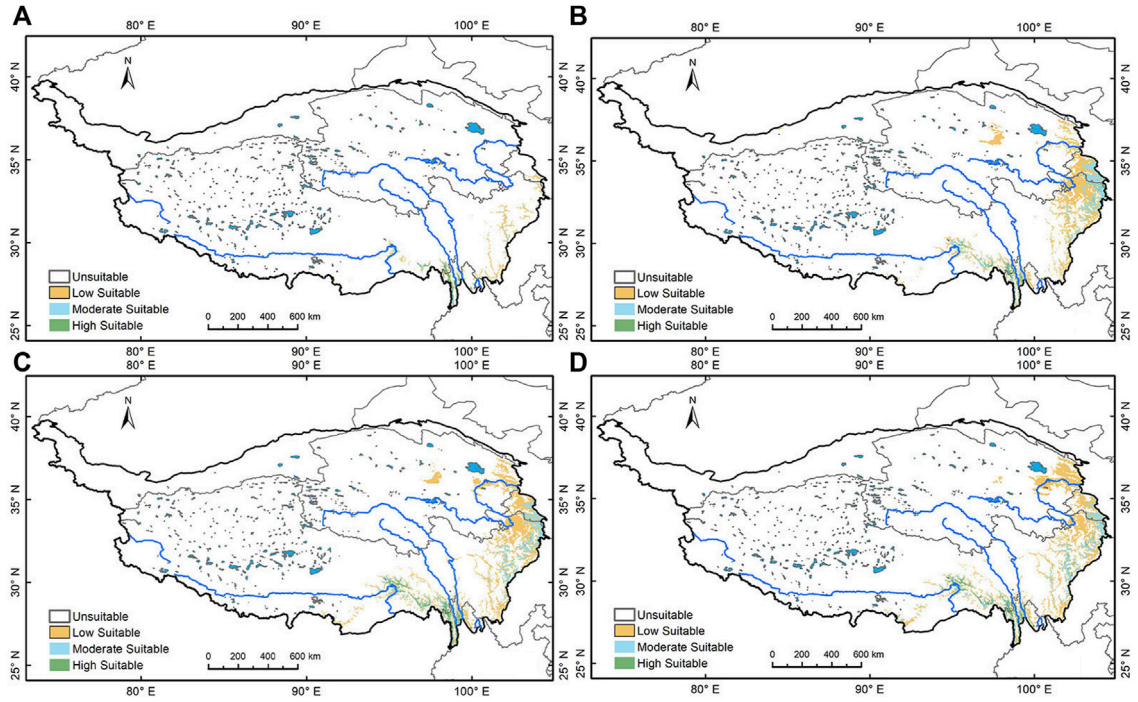

FIGURE 4
Simulation of Pinus' geographical distribution. **(A)** Pinus' geographical distribution area during the LGM; **(B)** during Early Holocene; **(C)** during the Mid Holocene; **(D)** during the Late Holocene.

At the LGM, the coldest period of the Last Glacial, Picea is mostly distributed along the southeast margin of the Tibetan Plateau (Figure 3A); these areas would have provided ecological refugia for Picea during LGM. In the EH, the highly suitable areas for Picea has expanded to the northern part of the Western Sichuan Plateau and southern Gannan Plateau, along the Taohe and Bailong rivers. The moderate and low suitable areas extend to the Huangshui and the Yellow rivers on the Qinghai Plateau and even the eastern margin of Qaidam Basin (Figure 3B). In the MH, the highly suitable areas for Picea have further migrated to the north and enlarged on the northeast Tibetan Plateau, extending along the Yellow and Huangshui rivers and some of their major tributaries. However, most of the highly suitable areas were located on the northern Gannan Plateau, and along the upper reaches of the Dadu River and tributaries on the Western Sichuan Plateau (Figure 3C). By the LH, the highly and moderately suitable areas are concentrated in the northeast Tibetan Plateau, specifically, in the eastern Qinghai Plateau. Low suitable areas include most higher altitude valleys and basins within the northeastern plateau (Figure 3D).

The relatively warm valleys along the eastern and southeastern margins of the plateau may also have provided ecological sanctuary for Pinus during the LGM, according to Hao et al. (2018). Our modeling shows Pinus has very scarcely distributed on the southeastern margin of the Tibetan Plateau at the LGM (Figure 4A). In the EH, the Pinus suitability area expanded significantly; it is sparsely distributed in Hehuang Valley, densely spotted on the Gannan Plateau and the southeastern part of the Western Sichuan Plateau, and extends westward to the eastern margin of the Qaidam Basin (Figure 4B). From EH to MH, Pinus gradually expands to the northern Tibetan Plateau, with a slight expansion in the northeast, and a dwindling of suitable area in the Western Sichuan Plateau (Figure 4C). In the LH, the suitable area contracted in both the Western Sichuan Plateau and Gannan Plateau, expanded in the Northeast Tibetan Plateau, and decreased in Qaidam Basin (Figure 4D).

Overall, both Picea and Pinus show a trend of northward migration and expansion since the LGM. Picea is distributed over a larger area than Pinus on the northeastern Tibetan Plateau, while Hehuang Valley and major drainages of the Yellow River present moderate to high suitability for both families. Therefore, the simulation results suggest that Picea better represents the forested land in the area. Most areas in the Northeast Tibetan Plateau were suitable for coniferous forests in the Holocene. Elevations above 3,000 m could also support sparsely distributed coniferous trees, especially Picea. In the LH, most of the highly suitable areas for Picea are concentrated in the Northeast Tibetan Plateau, indicating the species core distribution area finally reached the Northeast Tibetan Plateau.

Simulation accuracy

Simulation accuracy was quantified by calculating the area under the subject operating characteristic (ROC) curve (AUC). This gives a value range of (0.5–1), and the larger the value, the higher the model prediction accuracy (Hanley and McNeil, 1982). Generally, AUC of <0.6 implies the prediction result has failed, AUC of 0.6≤0.7 implies a poor prediction, AUC of 0.7≤0.8 implies a satisfactory prediction, AUC of 0.8≤0.9 implies a qualified prediction, and 0.9≤1.0 implies an accurate prediction (Swets, 1988). The AUC for Picea is 0.971 (Figure 5A) and the AUC for Pinus is 0.94 (Figure 5B), indicating a high accuracy for the simulation.

Accuracy was also determined by comparing the present day distribution of the Picea and Pinus with the simulation of the contemporary geographical distribution (Figures 6A,B). In terms of present day distribution, the Flora Republiacae Popularis Sinicae of China shows *Picea crassifolia Com.* is mainly found in Datong, Huangzhong, Huangyuan, Minhe, Ledu, Huzhu, Menyuan, Qilian, Haiyan, Tongren, Zeku, Henan, Xinghai, Maqin, Banma, Wulan (Hehuang Valley of Qinghai Plateau, valleys and basins of the upper Yellow River and around Qinghai Lake) in eastern Qinghai Province (ECFC, 1978). Also, in Xiahe, Zhuoni, and Zhouqu on the Gannan Plateau (Xiahe and its tributaries, Taohe and its tributaries, Bailong River and its tributaries). *Pinus armandii Franch.* and *Pinus tabulaeformis Carr.* are mainly found in southern Gansu along the drainage of Taohe and Bailongjiang rivers, Sichuan Province, Yunnan, and the lower reaches of Yalong Zangbu River. Zhang (2004) also indicates that *Picea crassifolia* is mainly found in the eastern Qilian Mountains and the southern Huangnan Mountains and Pinus in the Hehuang Valley in Qinghai Province. The close match between the modern distribution and the simulation for the Picea and Pinus lends additional weight to the simulation accuracy.

In addition, dossil Pollen record indicates that during the LGM, the coniferous forests from north of China retreated to the south (Harrison et al., 2001), and the forests on the plateau mostly retreated to the southeast of the plateau along the Hengduan Mountains and Helan Mountains (Shi et al., 1998; Meng et al., 2007). The molecular phylogeography study of the Picea communities in Qinghai, Gansu and Ningxia showed a recolonization after the LGM from one ecological refugia (Yang et al., 2005; Meng et al., 2007). However, Pinus may had several refugia during the LGM and recolonized to the Tibetan Plateau (Chen, 2008). These findings perfectly matches with the simulation results.

Discussion

Dynamic change of forest and climate from Late Glacial Maximum to Early Mid Holocen (11.7–5.3 ka BP)

During the LGM, both the annual precipitation and annual average temperature in the northeastern Tibetan Plateau were much lower than today, and the region is characterized as dry and cold (Herzschuh, 2006). Following the termination of the LGM, the summer monsoon strengthened and temperature increased, though with some cold events (Anklin et al., 1993; Dykoski et al., 2005) (Figures 7A,B). Pollen concentration in Qinghai Lake Basin gradually increased, and records succession from desert steppe to alpine meadow/sub-alpine shrub at the start of the EH (Shen et al., 2004). At this time, the winter monsoon weakened, but the summer monsoon continued to strengthen (Yang et al., 2019) and total precipitation significantly increased, driving the transition from a cold dry to a relatively warm and humid environment (Chen et al., 2006; Zhao et al., 2006; Chen et al., 2015a; Zhang, 2018). Both the Gonghe Basin and Qinghai Lake areas recorded weakening of aeolian sand activity, increasing vegetation coverage, and enhanced pedogenesis in the EH (Liu et al., 2013). In the MH, solar radiation continued to strengthen and the summer monsoon from the Indian and Pacific oceans gradually increased, with temperatures

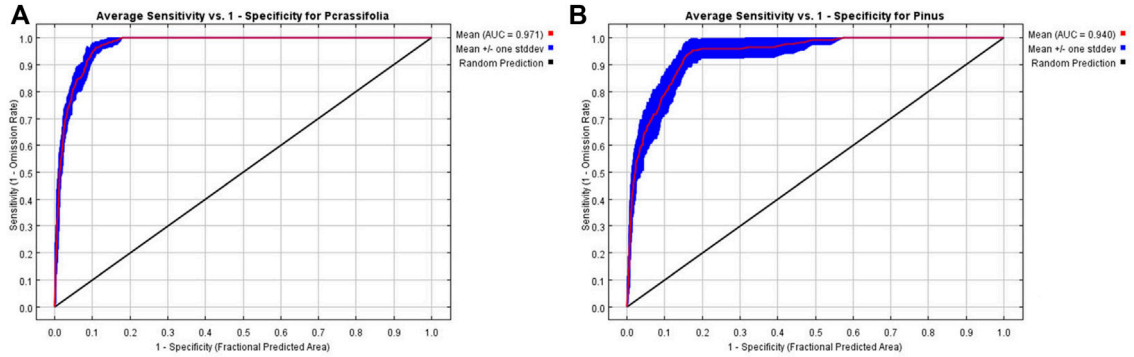

FIGURE 5
AUC rate for Picea **(A)** and Pinus **(B)**.

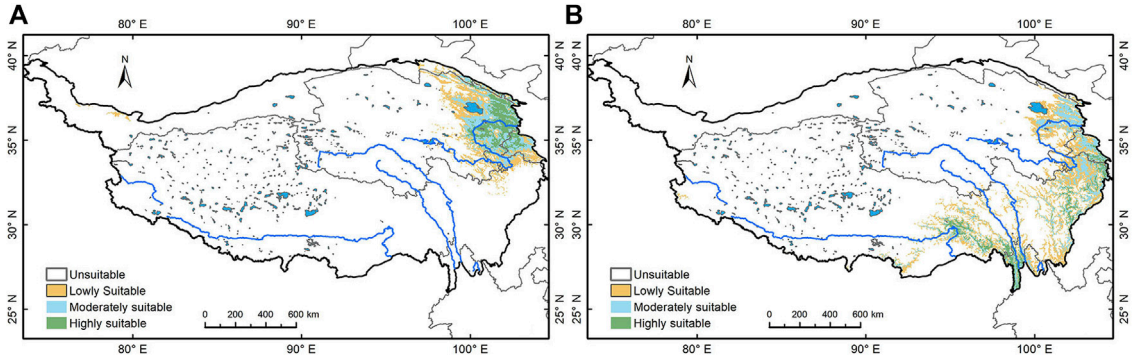

FIGURE 6
Simulation of Picea and Pinus' current geographical distribution. **(A)** Picea and **(B)** Pinus.

peaking about 3°C–4°C higher than present around 6 ka BP (Wang et al., 2002), and precipitation peaking around 6.8 ka BP (Shen and Tang, 1996; Tang et al., 2021); this is thought to be the warmest and wettest period of the Holocene (Chen F. H et al., 2020). The warm and wet conditions are recorded by several proxies, including lake levels at Luanhaizi and Qinghai Lake that increased gradually from EH to MH (Mischke et al., 2004), and humidification degree in Hongyuan peat that shows a gradual increase in the percentage of amorphous humus from EH to MH (Wang et al., 2003).

The warmer and wetter climate trend promoted vegetation productivity on the Tibetan Plateau, especially in reforestation. In Hehuang Valley, coniferous forest with steppe vegetation was recorded in warm periods of the Last Ice Age, and coniferous forest gradually increased from the Last Deglaciation into the EH, while shrubs, herbs, and Artemisia decreased (Zhao et al., 2007). In the Qinghai Lake drainage basin, increasing Picea and Pinus was recorded at approximately 16 ka BP, expansion of Picea-dominated coniferous forest began at approximately 10.8 ka BP, and expanded down slope to the lake shore by approximately 6 ka BP (Liu et al., 2002; Zhang N. M et al., 2021). In the upper reaches of the Yellow River, including Gonghe Basin, pollen records at both Dalianhai and Genggahai show increasing Picea levels from EH to MH (Cheng et al., 2010; Liu, 2016). Moreover, both the arboreal and Picea pollen records in the Northeast Tibetan Plateau showed a gradual increase with the warmer and wetter climate (Figures 6C,D). These trends are consistent with the simulation results in this study that show an expanding area of coniferous forest since the LGM.

A number of archeological sites on the Northeast Tibetan Plateau date to the period from the Last Deglaciation to the EH, including Site 151 (Wang et al., 2020), Jiangxigou 1 and 2, Heimahe 1 (Rhode et al., 2007; Gao et al., 2008; Yi, et al., 2011; Hou et al., 2013b), Hudong Zhongyang Chang (Madsen et al., 2006), Bronze Wire Canyon No. 3, and Yandongtai site (Brantingham and Gao, 2006; Sun et al., 2012; Yi, 2012; Brantingham et al., 2013). Evidence from these sites indicates the presence of early microlithic hunters with temporary camps in the Qinghai Lake Basin since 14 ka BP. It could be judged that increasing vegetation productivity provided a suitable habitat for the wild game which attracted nearby hunters. Animal bone finds at the sites are low at the beginning and gradually increase at around 8–7 ka BP (Hou et al., 2013b), suggesting increasing in wild hunting. By the EMH, archeological sites had expanded to the lower reaches of the Yellow River, as evidenced by early culture layers at the Shalongka (8.5–7.3 ka BP) (Yi et al., 2020) and Layihai sites (6.7 ka BP) (Gai and Wang, 1983). In this period, prehistoric humans mainly adopted short-term foraging activities with small groups focused on the procurement and processing of gazelle-sized ungulates (Brantingham et al., 2007; Wang

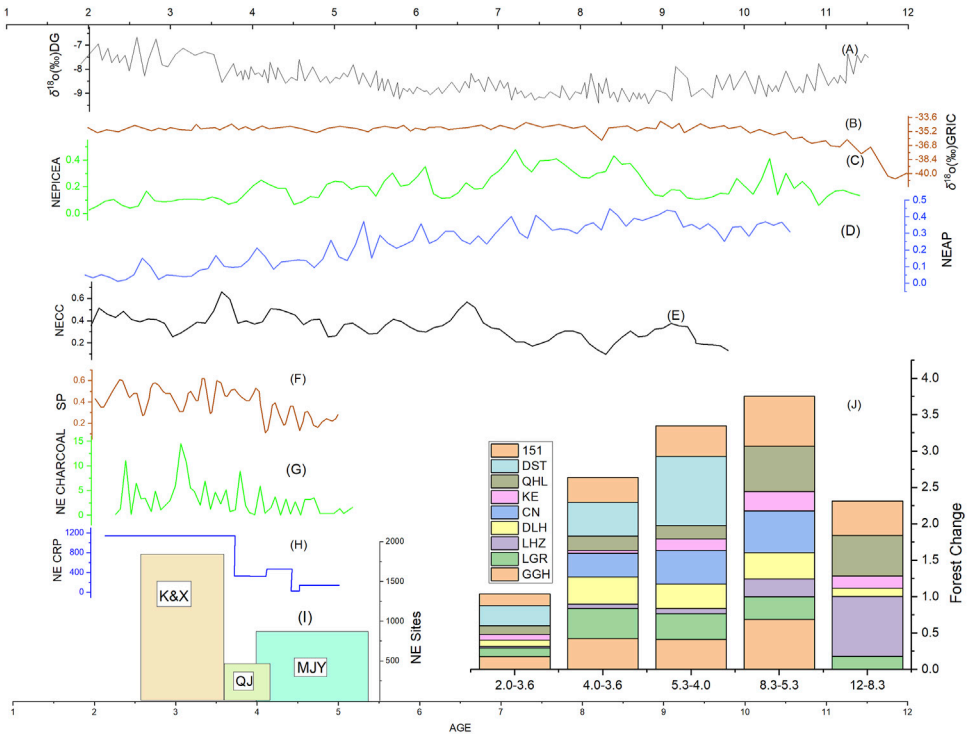

FIGURE 7
Relationships between climate change, forest dynamics, and human activities. **(A)** Greenland ice core oxygen isotope records representing global temperature changes (Anklin et al., 1993); **(B)** Oxygen isotope records of stalagmites in Dongge Cave indicating the intensity of Indian monsoon (Dykoski et al., 2005); **(C)** Normalized Pollen record of Picea from the Northeast Tibetan Plateau; **(D)** Normalized Pollen record of arboreal pollen from the Northeast Tibetan Plateau; **(E)** Normalized Carbon concentration record in the Northeast Tibetan Plateau; **(F)** Record of synanthropic plants through integrative pollen analysis in Northeast Tibetan Plateau during 5.5–2.0 ka BP (Chen X. L et al., 2020); **(G)** Charcoal concentration in different archeological sites in Northeast Tibetan Plateau during Mid-late Holocene (Liu et al., 2022); **(H)** Changes in cropland during the mid to late Holocene in the NETP (Wende et al., 2021); **(I)** Number of archaeological sites in the Northeast Tibetan Plateau. **(J)** Dynamic changes in arboreal pollen from different sites in Northeast Tibetan Plateau indicating change in forested area.

et al., 2020). Due to the relatively small population and high mobility, human activities had no discernable impact on the natural forest.

In summary, forest vegetation began to develop slowly in the northeastern Tibetan Plateau following the LGM, though there was some short-term fluctuation due to cooling events. Humidity and temperature increased significantly Since the LGM, which supported environmental conditions conducive to the growth of forest vegetation. The coniferous forest gradually recovered from the cold climate and expanded from EH to EMH. Relatively, sparse and low-impact human activities in this period did not affect forest growth. Therefore, it could be stated that during the Eh to EMH climate change was essential in the dynamic changes of the forests on the Northeast Tibetan Plateau. It is the warming climate and increasing precipitation that contributed to the regeneration and expansion of the forests in this area.

Forest degradation and human activities in the Late Mid Holocene (5.3–4.2 ka BP)

The East Asia summer Monsoon peaked at around 6 ka BP, and then it declined gradually, but the climate was still warm and humid through the LMH and the Holocene optimum climate lasted until 4 ka BP(Tang et al., 2021). The warm and wet climate conditions encouraged the westward spread of Yangshao culture, bringing millet agriculture to the Northeast Tibetan Plateau and the formation of the Majiayao Culture (Xie, 2002). Both the climate conditions and simulation results show the potential for continuous development of coniferous forests in the study area in the LMH, however, fossil pollen records from archeological sites indicate a gradual decrease in tree pollen: Qinghai Lake (Liu et al., 2002), Genggahai (Liu, 2016), Dalianhai (Cheng et al., 2010), Langgeri (Wei et al., 2020), and Changning (Dong et al., 2012) all show a continuous decrease from 5 ka BP (Figure 7J). At the same time, proxies of anthropogenic activity such as carbon content (Figure 7E), synanthropic plants (Figure 7F), charcoal content (Figure 7G), number of archeological sites (Figure 7I), and area of cultivated land (Figure 7H), increased dramatically, indicating a close relationship between forest degradation and human activities in the LMH.

Evidence from archeological sites indicates the major human activities during this period included millet farming and pottery production. The cultural development of approximately 6.0–5.0 ka BP promoted the spreading of millet crops, and around 5.2 ka BP, millet crops spread from Guanzhong Plain and the eastern Gansu Province to the Hehuang Valley (Jia et al., 2013; Chen et al., 2015b;

Dong et al., 2017). Millet grains have been recovered from archeological remains at Lijiatai, Hongya Zhangjia, Shangduoba, Shalongka, and Gayixianggeng (Jia, 2012). Remains of millet grains dating to around 5.2 ka BP were also unearthed from Zonggri site (5.2–4.1 ka BP), in Gonghe Basin in the upper reaches of the Yellow River. As the agricultural economy developed, the area of millet farming in Hehuang Valley rapidly increased (Wende et al., 2021). Many studies have shown that the expansion of farmland strongly impacts the natural vegetation cover (McNeill, 1986; Pongratz et al., 2008; Hou et al.,; Zhou et al., 2011; Fang et al., 2019; Wende et al., 2021); the prevailing slash-and-burn technique is likely to have greatly contributed to the decrease in forest area in Hehuang Valley. Furthermore, the development of agriculture promotes rapid population increase and expansion in settlement areas. In Hehuang Valley, the number of sites of late Majiayao Culture (Machang type) increased sharply in the LMH and the population reached about 39,000 (Wende et al., 2021). The increasing population inevitably required a great supply of wood resources for firewood, construction, production tools, and living utensils. Charcoal remains from archeological dated to this time comprise 100% Pinus and Picea (Liu et al., 2022), indicating coniferous species were the preferred wood resource used by people on the Northeast Tibetan Plateau, and they were sufficiently abundant to be easily accessed in daily life.

High demand for wood resources in the LMH is evident at many archeological settlements and burial sites. Charcoal remains from hearths indicate the daily use of wood for fire, including the firing of pottery. At Minhe Yangshan site, 96.3% of 218 graves were found to possess burial pottery (Qinghai Institute of Cultural Relics and Archaeology, 1990). In Ledu Liuwan cemetery, on the second level terrace of Huangshui River, 53.3% of 257 mid Majiayao Culture graves contained burial pottery, and more than 10,000 pieces of burial pottery were excavated from the 872 late Majiayao Culture graves (Institute of Archaeology CASS, 1984). In Xunhua Suhusa cemetery, 95.3% of 65 graves excavated contained pottery, and all 64 graves excavated at Zongri site contained burial pottery (Li and Xu, 1994). The pervasive usage of pottery indicates high production rates and a great demand for firewood. The pottery firing process requires a temperature above 800°C to be maintained (Papachristodoulou et al., 2006), and early firing kilns used ground pile burning (Qin and Ju, 2021), which consumes much wood to maintain the high temperature. It is important to note that charcoal remains from dead wood contain a large amount of mycelium (Marguerie and Hunot, 2009; Vidal-Matutano et al., 2017), and analysis of charcoal remains from this period shows very little mycelium (Liu, 2019). This suggests that early people obtained most of their firewood supply through deforestation. In addition, many stone axes have been unearthed from archeological sites and graves of this period, which may also provide strong physical evidence for wood cutting. It is reasonable to assume that the rapid increase in archeological settlement sites in the area consumed a great amount of wood for construction. Most of the settlement buildings at Majiayao are semi-subterranean dwellings (Xie, 2002), and dwelling sites and pillar holes have been excavated at Minhe Yangwapo, Hulijia, and Shalongka sites. Finally, most excavated graves contain wooden coffins (Table 3). In Liuwan Cemetery, 84% of graves had wooden coffins made from four slices of complete wood board (no patches), and in Shang Sunjiazhai, on the west bank of Beichuan River, a tributary of Huangshui River, all the graves had wooden coffins. In summary, a wide range of archeological evidence supports the presence of a rich forest resource in Hehuang Valley in the MH that was heavily exploited by humans. The simulation results and climate evidence both support the archeological findings. Forest retreat in the LMH, indicated by the reduction in arboreal pollen content, was most likely caused by heavy exploitation of the forest resource and cropland expansion. Thus, we argue that human activity is the driving force for forest retreat in the LMH.

Forest retreat and community structure evolution in the Late Holocene (4.2–2.3 ka BP)

The East Asia summer Monsoon greatly weakened around 4.0 ka BP in the Northeast Tibetan Plateau, with both temperature and precipitation decreasing in the LH (An et al., 2012; Chen et al., 2015a; Li et al., 2017). The simulation results showed a contraction of the low suitability area for coniferous trees toward the northeast margin of the plateau, while the high suitable area for Picea and moderate suitable area for Pinus increased markedly in Hehuang Valley. This indicates that through several thousand years of recolonization from the LGM refugia, Picea's core distribution area has finally reached the Northeast Tibetan Plateau, which is also the current core distribution area of the Picea. It also implies that compared to Pinus, Picea is more adapted to the local environment. It is important to note that Picea is a cold and dry-tolerant species. Based on the current distribution, Picea persists with a mean annual temperature of 4.8°C (−4.1–12.3°C) and a mean temperature of the coldest month with −10°C (−17.3–1.1°C), annual precipitation of 351 mm (72–700 mm) and precipitation of the coldest month of 8 mm (1–15 mm) (Fang et al., 2009). While Pinus prefers a warmer climate compared to Picea. Thus, we argue that the LH climate shift alone would not have hindered Picea's existence/distribution in the area. However, the climate shift may have slowed down the growth speed of the Picea, and modern pollen shows that the maximum Picea pollen appears with temperatures ranging from 0°C–8°C and precipitation ranging from 400–850 mm (Lu et al., 2004).

Charcoal remains from archaeological sites also support the distribution of Picea and a climate suitable for Picea. Specifically, ash pits from Jinchankou site (4.2–3.7 ka BP) contain a large quantity of Pinus (Wang et al., 2016). This implies that the climate in Hehuang Valley during the Qijia Culture period must also have been suitable for Picea since Pinus requires a warmer and more humid environment. In the charcoal remains of the Kayue sites in Hehuang Valley, broadleaf trees far exceeded the coniferous in the LH (Liu et al., 2022). Broadleaf trees mostly grow in environments with higher cumulative annual temperatures, while coniferous trees are the dominant species in areas with lower mean annual temperatures (CFEC, 1997). A large amount of charcoal remains from broadleaf trees excavated in the Hehuang Valley indicates that the LH climate was suitable for forest development. However, fossil pollen records for the area show continuously decreasing Picea and total arboreal pollen content in the Northeast Tibetan Plateau (Figures 7C,D). Both the Changning profile (Dong et al., 2012) and Dashuitang pollen record (Cao et al., 2021) show a significant reduction of arboreal pollen content, and pollen records from Qinghai Lake and Gonghe Basin also show a

TABLE 3 Use of wood coffin in the Northeast Tibetan Plateau.

Site	Region	Cultural type	Number of graves	Wooden coffin (%)
Liuwan	Hehuang Valley	Majiayao culture-machang type	872	84%
Liuwa		Qijia Culture	366	78.70%
Liuwan		Xindian Culture	6	None
Upper Sunjiazhai		Majiayao Culture	21	100%
Upper Sunjiazhai		Kayue and Xindian Culture	577	None[a]
Hetaozhuang		Xindian Culture	367	27.80%
Suhasa		Majiayao	65	57%
Suhusa		Kayue	22	63%
Zongri	Gonghe Basin	Zongri Culture	63	100%
Shan Pingtai		Kayue Culture	90	35.50%

[a]Some burial caves were covered with a wooden board.

consistent trend of decreasing arboreal pollen content (Figure 7J). Hence, the pollen records show a very different picture to the results of the simulation and analysis of charcoal remains.

In the LH, there is a significant increase in the proxies indicating human activities (Figures 7E–I). Around 4 ka BP, through cultural exchange barley was introduced to the region from Eurasia (Dodson et al., 2013; Ren and Dong, 2016), which contributed to a shift in subsistence mode from solely millet-based agriculture to a wider range of crops at different altitudes (Ma et al., 2016; Zhang and Dong, 2017). This allowed the expansion of cropland to higher altitudes including Qinghai Lake and Gonghe Basin, and forests were transformed into farmland in the high altitude mountains in Hehuang Valley and middle altitude areas in the upper reaches of the Yellow River (Wende et al., 2021). By the time of the Xindian and Kayue Cultures at approximately 3.6 ka BP, grazing was clearly present in the area. Grazing practices require forest clearance initially, and continued grazing prevents forest regeneration. The Xindian Culture is mainly found in Hehuang Valley, where they practiced farming and livestock herding; the Kayue Culture is mainly at higher elevations, with grazing as their major source of livelihood and cultivation as a secondary source. Grazing seems to have intensified around 3.5 ka BP (Miao et al., 2017), and evidence of overgrazing is recorded in Qinghai Lake and Gonghe Basin (Huang et al., 2017; Wei et al., 2020). Hence, it is likely that the spread of barley and the emergence of grazing resulted in great transformation of native vegetation on a large scale at high altitudes. The new agricultural practices also promoted population development and settlement; by the late LH, there were more than 1,800 settlement sites in the northeastern Tibetan Plateau, with an estimated population of more than 60,000 (Hou et al., 2013a).

Alongside grazing and farming, the production of bronze and pottery was also prevalent in the LH, with the development of a bronze industry seen as the greatest achievement of the Qijia Culture (Xie, 2002). Bronze wares have been excavated from many Qijia sites in the region, including a long bronze spear at Shenna site (Wang et al., 2022), and the earliest bronze mirror at Gamatai site (Qinghai Institute of Cultural Relics and Archaeology and Beijing University, School of Archaeology and Museology, 2015), and the industry continued into the Kayue and Xindian Culture period. Bronze casting requires a temperature of over 1,000°C, especially for producing large wares such as long spears (Mao and Wang, 2019). The pervasive use of bronze wares implies great the consumption of firewood. In addition, pottery production had become a specialized, large scale industry in this period (Xie, 2002), and is likely to have aggravated consumption of the forest resource. Finally, evidence for use of wood for houses at Kayue and Qijia sites, and the dramatic increase in the number of archeological sites, also point to intensive deforestation for infrastructure construction.

Changes in the wood used for coffins over the LH support the persistence of coniferous trees and a declining forest resource. Wooden coffins were used intensively by the Qijia Culture, but their use decreased in most of the sites during the Kayue and Xindian Culture periods (Table 3). Also, most of the Qijia Culture coffins were made from a single log or single plank, but the Kayue and Xindian Culture coffins comprised patchwork boards with a wood diameter of only 10 cm. It is evident that wood utilization was extensive in the early LH and decreased in the late LH, which implies a marked shrinkage in the forest area. In contrast to that, in Suhusa site, located far to the south, the use of wood coffin increased (Xie, 2002). The ample availability of wood at some sites suggests climate was not a limiting factor on forest growth and wood supply. Thus, we argue the high exploitation rate of wood resources in Hehuang Valley and Gonghe Basin since the MH resulted in an extreme shortage of wood by the late LH. However, wood resources were still abundant in less populated areas. In addition, analysis of excavated charcoal shows high rates of broadleaf trees such as Poplar and Salix in the late LH in Hehuang Valley (Liu et al., 2022), which means that primitive coniferous forest in the Northeast Tibetan Plateau was succeeded by secondary forests. Overall, forest retreat in low elevation areas was followed by a secondary succession of the broadleaf forest communities, but intensive grazing and cultivation in higher elevation areas caused forest degradation that, when coupled with the drying and cooling climate, meant the fragile forest ecosystem failed to regenerate.

Conclusion

This study simulated the potential geographical distribution of Picea and Pinus since the LGM to determine the changing area of coniferous forests on the Northeast Tibetan Plateau. Pollen records, carbon concentration, charcoal analysis, archeological evidence, and other proxies for human activities were analyzed to explore human impact on natural forest dynamics. The key results are outlined below.

(1) The simulation shows that climate/environment conditions were suitable for the expansion of coniferous forest on the Northeast Tibetan Plateau from the beginning of the Holocene to the MH. Despite the climate shift in the LH, conditions were still suitable for the pervasive growth of Picea- and Pinus-dominated coniferous forests in Hehuang Valley, as well as the major drainage areas of the Yellow River. Picea showed a strong adaptation to the local environment in the Northeast Tibetan Plateau in the LH.
(2) The pollen record shows rapid forest expansion with optimal climate from EH to EMH, however, this is followed by forest retreat in the LMH, with the formation of the Majiayao Culture, which continued to the LH.
(3) We argue that low population numbers and the low impact of human activities, including short-term encampments for hunting and high mobility wild game, were not sufficient to affect the natural forest in the EH and EMH. However, a demographic boom, extensive cultivation, grazing, and heavy exploitation of the wood resources in the LMH and LH meant that human activities had a stronger influence on forest vegetation than climate on the Northeast Tibetan Plateau.
(4) Our findings also suggest LH climate conditions would not have inhibited forest development at lower elevations, especially coniferous forests, since archeological evidence supports the presence of coniferous and even broadleaf forests in Hehuang Valley. The cold dry climate of the LH may have aggravated the pace of deforestation at high elevations where severe deforestation had already occurred.

Data availability statement

The original contributions presented in the study are included in the article/supplementary material, further inquiries can be directed to the corresponding author.

Author contributions

GH and ZW conceived and designed the paper. GH, ZW, HC, SJ, and ZL participated in the field research. ZW wrote the manuscript and GH, HC, SJ, and ZL revised the manuscript. All authors contributed to the article and approved the submitted version.

Funding

This study wouldn't be possible without the support of National Natural Science Foundation. The grant numbers are 42171165 and 42261030.

Conflict of interest

The authors declare that the research was conducted in the absence of any commercial or financial relationships that could be construed as a potential conflict of interest.

Publisher's note

All claims expressed in this article are solely those of the authors and do not necessarily represent those of their affiliated organizations, or those of the publisher, the editors and the reviewers. Any product that may be evaluated in this article, or claim that may be made by its manufacturer, is not guaranteed or endorsed by the publisher.

References

An, Z. S., Colman, S. M., Zhou, W. J., Li, X. W., Brown, E. T., Jull, T., et al. (2012). Interplay between the westerlies and asian monsoon recorded in lake Qinghai sediments since 32ka. *Sci. Rep.* 1, 619. doi:10.1038/srep00619

Anklin, M., Barnola, J. M., and Beer, J. (1993). Climate instability during the last interglacial period recorded in the GRIP ice core. *Nature* 364 (6434), 203–207. doi:10.1038/364203a0

Boivin, N. L., Zeder, M. A., Fuller, D. Q., Crowther, A., Larson, G., Erlandson, J. M., et al. (2016). Ecological consequences of human niche construction: Examining long-term anthropogenic shaping of global species distributions. *Proc. Natl. Acad. Sci. U. S. A.* 113, 6388–6396. doi:10.1073/pnas.1525200113

Brantingham, P. J., Gao, X., Madsen, D. B., Rhode, D., Perreault, C., Woerd, J., et al. (2013). Late occupation of the high-elevation northern Tibetan plateau based on cosmogenic, luminescence, and radiocarbon ages. *Geoarchaeology* 28 (5), 413–431. doi:10.1002/gea.21448

Brantingham, P. J., Gao, X., Olsen, W., Ma, H. Z., Rhode, D., Zhang, H. Y., et al. (2007). A short chronology for the peopling of the Tibetan Plateau. *Devs. Quat. Sci.* 9, 129–150. doi:10.1016/S15710866(07)090100

Brantingham, P. J., and Gao, X. (2006). Peopling of the northern Tibetan plateau. *World Archaeol.* 38 (3), 387–414. doi:10.1080/00438240600813301

Broecker, W. S., and Stocker, T. F. (2006). The Holocene CO2 rise: Anthropogenic or natural? *EOS* 87, 27–29. doi:10.1029/2006EO030002

Cao, X., Tian, F., Li, K., and Ni, J. (2021). Lake surface-sediment pollen dataset for the alpine meadow vegetation type from the eastern Tibetan Plateau and its potential in past climate reconstructions. National Tibetan Plateau Data Center. doi:10.11888/Paleoenv.tpdc.271191

Cao, Y., Dewalt, E., Robinson, J., Tweddale, T., Hinz, L., and Pessino, M. (2013). Using Maxent to model the historic distributions of stonefly species in Illinois streams: The effects of regularization and threshold selections. *Ecol. Model.* 259, 30–39. doi:10.1016/j.ecolmodel.2013.03.012

Castilla-Beltrán, A., de Nascimento, L., Fernández-Palacios, J. M., Whittaker, R. J., Willis, K. J., Edwards, M., et al. (2021). Anthropogenic transitions from forested to human-dominated landscapes in southern macaronesia. *Proc. Natl. Acad. Sci. USA.* 118, e2022215118. doi:10.1073/pnas.2022215118

CFEC (China Forest Editorial Committee) (1997). *Forests in China. (Volumes I, II and III).* Beijing: China Forestry Publishing House.

Chen, F. H., Cheng, B., Zhao, Y., Zhu, Y., and Madsen, D. B. (2006). Holocene environmental change inferred from a high-resolution pollen record, lake zhuyeze, arid China. *Holocene* 16, 675–684. doi:10.1191/0959683606hl951rp

Chen, F. H., Dong, G. H., Zhang, D. J., Liu, X. Y., Jia, X., An, C. B., et al. (2015b). Agriculture facilitated permanent human occupation of the Tibetan plateau after 3600 BP. *Science* 347, 6219248–6219250. doi:10.1126/science.1259172

Chen, F. H., Xu, Q. H., Chen, J. H., Birks, H. J., Liu, J. B., Zhang, S. R., et al. (2015a). East asian summer monsoon precipitation variability since the last deglaciation. *Sci. Rep.* 5, 11186. doi:10.1038/srep11186

Chen, F. H., Zhang, J. F., Liu, J. B., Cao, X. Y., Hou, J. Z., Xu, L. P., et al. (2020). Climate change, vegetation history, and landscape responses on the Tibetan Plateau during the Holocene: A comprehensive review. *Quat. Sci. Rev.* 243, 106444. doi:10.1016/j.quascirev.2020.106444

Chen, G. C., and Peng, M. (1993). Vegetation and its distribution pattern in Qinghai Lake area. *J. Plant Eco. Geobot.* 17 (1), 73–78.

Chen, K. M. (2008). "Phylogeography of Pinus tabulaeformis Carr. (Pinaceae), a dominant species of coniferous forest in northern China,". Thesis (Lanzhou: Lanzhou University).

Chen, X. L., Hou, G. L., Jin, S. M., Gao, J. Y., and Duan, R. L. (2020). The pollen records of human activities in qinghai-tibet Plateau during the middle and late Holocene. *Earth Envion* 6, 643–651. doi:10.14050/j.cnki.1672-9250.2020.48.074

Cheng, B., Chen, F. H., and Zhang, J. F. (2010). Palaeovegetational and palaeoenvironmental changes since the last deglacial in Gonghe Basin, northeast Tibetan Plateau. *Acta Geogr. Sin.* 65 (11), 136–146. doi:10.1007/s1144201309995

Cheng, Z., Weng, C., Steinke, S., and Mohtadi, M. (2018). Anthropogenic modification of vegetated landscapes in southern China from 6, 000 years ago. *Nat. Geosci.* 11, 939–943. doi:10.1038/s41561-018-0250-1

Cobos, M. E., Peterson, A. T., Barve, N., and Osorio-Olvera, L. (2019). Kuenm: an R Package for detailed development of ecological niche models using maxent. *Peer J.* 6, e6281–e6281. doi:10.7717/peerj.6281

Dodson, J. R., Li, X., Zhou, X., Zhao, K., Sun, N., and Atahan, P. (2013). Origin and spread of wheat in China. *Quat. Sci. Rev.* 72, 108–111. doi:10.1016/j.quascirev.2013.04.021

Dong, G. H., Jia, X., An, C. B., Chen, F. H., Zhao, Y., Tao, S., et al. (2012). Mid-holocene climate change and its effect on prehistoric cultural evolution in eastern Qinghai Province, China. *Quat. Res.* 1, 23–30. doi:10.1016/j.yqres.2011.10.004

Dong, G. H., Yang, Y. S., Han, J. Y., Wang, H., and Chen, F. H. (2017). Exploring the history of cultural exchange in prehistoric Eurasia from the perspectives of crop diffusion and consumption. *Sci. China Earth Sci.* 60, 1110–1123. doi:10.1007/s11430-016-9037-x

Dykoski, A. C., Edwards, R. L., Cheng, H., Yuan, D. X., Cai, Y. J., Zhang, M. L., et al. (2005). A high resolution, absolute-dated Holocene and deglacial Asian monsoon record from Dongge Cave, China. *Earth Planet. Sci. Letts.* 233 (2), 71–86. doi:10.1016/j.epsl.2005.01.036

ECFC (1978). *Flora Republiacae Popularis Sinicae of China*. Beijing: Science Press, 137.

Elith, J., Graham, C. H., Anderson, R. P., Dudik, M., Ferrier, S., Guisan, A., et al. (2006). Novel methods improve prediction of species' distributions from occurrence data. *Ecography* 29, 129–151. doi:10.1111/j.2006.0906-7590.04596.x

Elith, J., and Graham, C. H. (2009). Do they? How do they? WHY do they differ? On finding reasons for differing performances of species distribution models. *Ecography* 32, 66–77. doi:10.1111/j.1600-0587.2008.05505.x

Elith, J., Phillips, S. J., Hastie, T., Dudik, M., Chee, Y. E., and Yates, C. J. (2011). A statistical explanation of MaxEnt for ecologists. *Divers. Distributions* 17, 43–57. doi:10.1111/j.1472-4642.2010.00725.x

Ellis, E. C., and Ramankutty, N. (2008). Putting people in the map: Anthropogenic biomes of the world. *Fron. Ecol. Environ.* 6, 439–447. doi:10.1890/070062

Fang, J. Y., Wang, Z. H., and Tang, Z. Y. (2009). *Atlas of woody plants in China: Distribution and climate, volume 1*. Beijing: Higher Education Press.

Fang, X. Q., Ye, Y., Zhang, C. P., and Tang, C. C. (2019). Cropland cover change and its environmental impacts in the history of China. *J. Paleogeogr.* 21 (1), 160–174. doi:10.4135/9781446247501.n891

Feng, Y. X., and Li, G. D. (2020). Interaction between urbanization and eco-environment in Tibetan plateau. *J. Geogr. Sci.* 31, 298–324. doi:10.1007/s11442-021-1838-8

Ficetola, G. F. (2007). The influence of beach features on nesting of the hawksbill turtle Eretmochelys imbricata in the Arabian Gulf. *Oryx* 41, 402–405. doi:10.1017/S0030605307000543

Foley, J. A., Kutzbach, J. E., Coe, M. T., and Levis, S. (1994). Feed backs between climate and boreal forests during the Holocene epoch. *Nature* 371, 52–54. doi:10.1038/371052a0

Fordham, D. A., Saltré, F., Haythorne, S., Wigley, T. M. L., Otto-Bliesner, B. L., Chan, K. C., et al. (2017). PaleoView: A tool for generating continuous climate projections spanning the last 21000 Years at regional and global scales. *Ecography* 40, 1348–1358. doi:10.1111/ecog.03031

Gai, P., and Wang, G. D. (1983). Excavation report of mesolithic site in laiyihai, upper reaches of Yellow River. *Acta. Anthropol. Sin.* 1, 49–59. doi:10.16359/j.cnki.cn11-1963/q.1983.01.006

Gao, X., Zhou, Z. Y., and Guan, Y. (2008). Human cultural remains and adaptations strategies in the Tibetan plateau margin region in the late pleistocene. 969–977.

Goldewijk, K. K., Beusen, A., Doelman, J., and Stehfest, E. (2017). Anthropogenic land use estimates for the Holocene - hyde 3.2. *Earth Syst. Sci. Data* 9, 927–953. doi:10.5194/essd-9-927-2017

Hanley, J. A., and McNeil, B. J. (1982). The meaning and use of the area under a receiver operating characteristic (ROC) curve. *Radiology* 143, 29–36. doi:10.1148/radiology.143.1.7063747

Hao, Q., de Lafontaine, G., Guo, D., Gu, H., Hu, F. S., Han, Y., et al. (2018). The critical role of local refugia in postglacial colonization of Chinese pine: Joint inferences from DNA analyses, pollen records, and species distribution modeling. *Ecography* 41, 592–606. doi:10.1111/ecog.03096

Harari, Y. N. (2015). *Sapiens: A brief history of humankind*. New York: Harper.

Harrison, S. P., Yu, G., Takahara, H., and Prentice, I. C. (2001). Diversity of temperate plants in East Asia. *Nature* 413 (6852), 129–130. doi:10.1038/35093166

He, F., Li, Y., Xu, Y. N., Zhang, J. H., and Chen, S. B. (2005). Natural environment type, sand environment characteristics in northwest China. *Northwest. Geol.* 38 (3), 93–99.

Herzschuh, U., Birks, H. J., Ni, J., Zhao, Y., Liu, H., Liu, X., et al. (2010). Holocene land cover changes on the Tibetan plateau. *Holocene* 20, 91–104. doi:10.1177/0959683609348882

Herzschuh, U. (2006). Palaeo-moisture evolution in monsoonal Central Asia during the last 50, 000 years. *Quat. Sci. Revs.* 25, 163–178. doi:10.1016/j.quascirev.2005.02.006

Hijmans, R. J., Cameron, S. E., Parra, J. L., Jones, P. G., and Jarvis, A. (2005). Very high resolution interpolated climate surfaces for global land areas. *Int. J. Climatol.* 25, 1965–1978. doi:10.1002/joc.1276

Hou, G. L., Lai, Z. P., Xiao, J. Y., and E, C. Y. (2012). Reconstruction of cultivated land during mid-holocene in the middle and lower reaches of Yellow River and human impact on vegetations. *J. Geogra. Sci.* 22, 933–945. doi:10.1007/s11442-012-0974-6

Hou, G. L., E, C. Y., Zhao, X. H., and Wei, H. C. (2013a). Prehistoric population and cultivated land change in the eastern Qinghai Province and its environmental effects. *Sci. Geogr. Sin.* 03, 299–306. doi:10.13249/j.cnki.sgs.2013.03.010

Hou, G. L. (2016). The prehistoric human activities on the qinghai-tibet plateau. *J. Salt Lake Res.* 24 (2), 68–74.

Hou, G. L., Wei, H. C., E, C. Y., and Sun, Y. J. (2013b). Human activities and environmental change in Holocene in the northeastern margin of Qinghai-Tibet Plateau: A case study of JXG2 relic site in Qinghai Lake. *Acta. Geogr. Sin* 3, 380–388. doi:10.11821/xb201303009

Huang, X. Z., Liu, S. S., Dong, G. H., Qing, M. R., Bai, Z. J., Zhao, Y., et al. (2017). Early human impacts on vegetation on the northeastern Qinghai-Tibetan Plateau during the middle to late Holocene. *Prog. Phys. Geog.* 41, 3286–3301. doi:10.1177/0309133317703035

IGBP (International Geosphere–Biosphere Programme) (1994). *IGBP in action: Work plan* 1994–1998. Stockholm: IGBP, 38–82.

Institute of Archaeology CASS (1984). *Qinghai liuwan*. Beijing: Cultural Relics Press.

Jia, X. (2012). *Cultural evolution process and plant remains during neolithic-bronze Age in Northeast Qinghai Province. Dissertation*. Lanzhou: Lanzhou University.

Jia, X., Dong, G. H., Li, H., Brunson, K., Chen, F. H., Ma, M. M., et al. (2013). The development of agriculture and its impact on cultural expansion during the late neolithic in the western Loess Plateau, China. *Holocene* 23 (1), 85–92. doi:10.1177/0959683612450203

Jia, X., Lee, H. F., Cui, M. C., Chen, G. Q., Zhao, Y., Ding, H., et al. (2019). Differentiations of geographic distribution and subsistence strategies between Tibetan and other major ethnic groups are determined by the physical environment in Hehuang Valley. *Sci. China (Earth Sci. .* 62 (2), 412–422. doi:10.1007/s1143001893015

Jiang, Y. Y., E, C. Y., Hou, G. L., Sun, Y. J., Li, F., Zhao, Y. J., et al. (2015). Charcoal concentration reflecting on environmental changes and human activities in Qinghai Lake JXG2 Relics. *J. Earth Environ.* 2, 98–105.

Jiménez, V. A., and Lobo, J. M. (2007). Threshold criteria for conversion of probability of species presence to either–or presence–absence. *Acta. Oecol* 31, 3361–3369. doi:10.1016/J.ACTAO.2007.02.001

Kaal, J., Carrión, M. Y., Asouti, E., Martín, S. M., Martínez, C. A., Costa, C. M., et al. (2011). Long-term deforestation in NW Spain: Linking the Holocene fire history to vegetation change and human activities. *Quat. Sci. Rev.* 30, 161–175. doi:10.1016/j.quascirev.2010.10.006

Kaplan, J. O., Krumhardt, K. M., and Zimmermann, N. (2009). The prehistoric and preindustrial deforestation of europe. *Quat. Sci. Rev.* 28, 3016–3034. doi:10.1016/j.quascirev.2009.09.028

Karger, D. N., Nobis, M. P., Normand, S., Graham, C. H., and Zimmermann, N. E. (2021). CHELSA-TraCE21k v1. 0. Downscaled transient temperature and precipitation data since the last glacial maximum, doi:10.5194/cp-2021-30

Kirch, P. V. (2005). Archaeology and global change: The Holocene record. *Ann. Rev. Environ. Resour.* 30 (1), 409–440. doi:10.1146/annurev.energy.29.102403.140700

Kramer, A., Herzschuh, U., Mischke, S., and Zhang, C. (2010). Holocene Treeline Shifts and Monsoon Variability in the Hengduan Mountains (Southeastern Tibetan Plateau): Implications from Palynological Investigations. *Palaeogeogr. Palaeocl.* 286 (1–2), 23–41. doi:10.1016/j.palaeo.2009.12.001

Kumar, S., and Stohlgren, T. J. (2009). Maxent Modeling for Predicting Suitable Habitat for Threatened and Endangered Tree Canacomyricamonticola in New Caledonia. *J. Ecol. Nat. Sci.* 1, 94–98. doi:10.5897/JENE.9000071

Leal, A., Gassón, R., Behling, H., and Sánchez, F. (2019). Human-made Fires and Forest Clearance as Evidence for Late Holocene Landscape Domestication in the Orinoco Llanos (Venezuela). *Veget. Hist. Archaeobot.* 28, 545–557. doi:10.1007/s00334-019-00713-w

Li, J. Y., Dodson, J., Yan, H., Cheng, B., Zhang, X. J., Xu, Q. H., et al. (2017). Quantitative Precipitation Estimates for the Northeastern Qinghai-Tibetan Plateau over the Last 18, 000 Years. *J. Geophys. Res. Atmos.* 122, 5132–5143. doi:10.1002/2016jd026333

Li, X., Sun, N., Dodson, J., and Zhou, X. (2012). Human Activity and its Impact on the Landscape at the Xishanping Site in the Western Loess Plateau during 4800-4300 cal yr BP Based on the Fossil Charcoal Record. *J. Archaeol. Sci.* 39, 3141–3147. doi:10.1016/j.jas.2012.04.052

Li, Y. P., and Xu, Y. J. (1994). Qinghai Xunhua Suhusa Cemetary. *Acta. Archaeol. Sin.* 4, 425–469.

Liu, C., Berry, P. M., Dawson, T. P., and Pearson, R. G. (2005). Selecting Thresholds of Occurrence in the Prediction of Species Distributions. *Ecogra* 28 (3), 385–393. doi:10.1111/j.0906-7590.2005.03957.x

Liu, F. W. (2019). "Human Wood Utilization Strategy in the Northeast of Qinghai Tibetan Plateau During Neolithic and Bronze Age,". Dissertation (Lanzhou (China): Lanzhou University).

Liu, F. W., Zhang, S. J., Zhang, H. C., and Dong, G. H. (2022). Detecting Anthropogenic Impact on Forest Succession from the Perspective of Wood Exploitation on the Northeast Tibetan Plateau During the Late Prehistoric Period. *Sci. China Earth Sci.* 65, 2068–2082. doi:10.1007/s11430-021-9911-7

Liu, S. S. (2016). "Vegetation and Climate Change since the Last Deglaciation in the Northeast Qinghai–Tibetan Plateau Genggahai Region,". Dissertation (Lanzhou (China): Lanzhou University).

Liu, X. C., Tang, Q. H., Yin, Y. Y., and Xu, X. C. (2018). Regionalization of Integrated Environmental Risk of China Under Future Climate Change. *Sci. Geogr. Sin.* 38:4. 636–644. doi:10.13249/j.cnki.sgs.2018.04.018

Liu, X. Q., Shen, J., Wang, S. M., Yang, X. D., Tong, G. B., and Zhang, E. L. (2002). Pollen Record and its Paleo Climate, Paleo Environmental Evolution in Qinghai Lake Since 16ka. *Chin. Sics. Bull.* 47, 1351–1355.

Liu, X. X., Song, L., Jin, Y. X., and Wang, Q. (2013). History of Aeolian Deposits in Tibetan Plateau and Climate Change over Holocene. *J. Arid. land Resours. Environ.* 27 (6), 41–47. doi:10.13448/j.cnki.jalre.2013.06.036

Lozier, J. D., and Mills, N. J. (2011). Predicting the potential invasive range of light Brown apple moth (Epiphyas postvittana) using biologically informed and correlative species distribution models. *Biol. Invasions* 13, 2409–2421. doi:10.1007/s10530-011-0052-5

Lu, H. Y., Wang, S. Y., Shen, C. M., Yang, X. D., Tong, G. B., and Liao, K. B. (2004). Spatial Pattern of Modern Abies ans Picea Pollen in the Qinghai-Xizang Plateau. *Chin. Qua. Sci.* 1, 39–49.

Ma, M., Dong, G., Jia, X., Wang, H., Cui, Y., and Chen, F. (2016). Dietary Shift after 3600 cal yr bp and its Influencing Factors in Northwestern China: Evidence from Stable Isotopes. *Quat. Sci. Revs.* 145, 57–70. doi:10.1016/j.quascirev.2016.05.041

Madsen, D. B., Haizhou, M. a., Brantingham, P. J., Xing, G., Rhode, D., Haiying, Z., et al. (2006). The late Upper Paleolithic occupation of the northern Tibetan Plateau margin. *J. Archaeol. Sci.* 33 (10), 1433–1444. doi:10.1016/j.jas.2006.01.017

Mao, W. M., and Wang, K. P. (2019). Analysis of differences between Chinese and Western Bronze Ages. 4. 12-15

Marguerie, D., and Hunot, J. Y. (2009). Charcoal Analysis and Dendrology: Data from Archaeological Sites in North-Western France. *J. Archaeol. Sci.* 34 (10), 1417–1433. doi:10.1016/j.jas.2006.10.032

McMichael, C. N. H. (2021). Ecological Legacies of Past Human Activities in Amazonian Forests. *New Phytol.* 229 (5), 2492–2496. doi:10.1111/nph.16888

McNeill, J. R. (1986). Agriculture, Forests, and Ecological History: Brazil, 1500–1984. *Environ. Hist. Rev.* 10 (2), 122–133. doi:10.2307/3984562

McPherson, M. J., and Jetz, W. (2007). Effects of Species' Ecology on the Accuracy of Distribution Models. *Ecography* 30 (1), 135–151. doi:10.1111/j.0906-7590.2007.04823.x

Meng, L. H., Yang, R., Abbott, R. J., Miehe, G., Hu, T. H., and Liu, J. Q.(2007). Mitochondrial and chloroplast phylogeography of*Picea crassifolia*Kom. (Pinaceae) in the Qinghai-Tibetan Plateau and adjacent highlands. *Mol. Ecol.* 16:19. 4128–4137. doi:10.1111/j.1365-294x.2007.03459.x

Miao, Y. F., Zhang, D. J., Cai, X. M., Li, F., Jin, H. L., Wang, Y. P., et al. (2017). Holocene Fire on the Northeast Tibetan Plateau in Relation to Climate Change and Human Activity. *Quat. Int.* 443, 124–131. doi:10.1016/j.quaint.2016.05.029

Miehe, G., Hasson, S., Glaser, B., Mischke, S., Böhner, J., van der Knaap, W. O., et al. (2021). Föhn, Fire and Grazing in Southern Tibet? A 20, 000-Year MultiProxy Record in an Alpine Ecotonal Ecosystem. *Quat. Sci. Rev.* 256, 106817. doi:10.1016/J.QUASCIREV.2021.106817

Miehe, G., Miehe, S., Böhner, J., Kaiser, K., Hensen, I., Madsen, F. N. M., et al. (2014). How Old is the Human Footprint in the World's Largest Alpine Ecosystem? A Review of Multi-proxy Records from the Tibetan Plateau from the Ecologists' Viewpoint. *Quat. Sci. Rev.* 86, 190–209. doi:10.1016/j.quascirev.2013.12.004

Milanovich, J. R., Peterman, W. E., Barrett, K., and Matthew, E. H. (2012). Do Species Distribution Models Predict Species Richness in Urban and Natural Green Spaces? A Case Study Using Amphibians. *Landsc. Urban Plan.* 107 (4), 409–418. doi:10.1016/j.landurbplan.2012.07.010

Mischke, S., Herzschuh, U., Zhang, C., Bloemendal, J., and Riedel, F. (2004). A Late Quaternary lake record from the Qilian Mountains (NW China): lake level and salinity changes inferred from sediment properties and ostracod assemblages. *Glob. Planet. Change* 46 (1), 337–359. doi:10.1016/j.gloplacha.2004.09.023

Mottl, O. F., Bhatta, K. P., Felde, V. A., Giesecke, T., Goring, S., Grimm, E. C., et al. (2021). Global Acceleration in Rates of Vegetation Change Over the Past 18, 000 Years. *Sci* 372 (6544), 860–864. doi:10.1126/science.abg1685

Olofsson, J., and Hicker, T. (2007). Effects of Human Land-Use on the Global Carbon Cycle During the Last 6000 years. *Veg. Hist. Archaeol.* 17 (5), 605–615. doi:10.1007/s00334-007-0126-6

Papachristodoulou, C., Oikonomou, A., Ioannides, K., and Gravani, K. (2006). A Study of Ancient Pottery by Means of X-Ray Fluorescence Spectroscopy, Multivariate Statistics and Mineralogical Analysis. *Anal. Chim. Acta* 573–574, 347–353. doi:10.1016/j.aca.2006.02.012

Phillips, S. J., Anderson, R. P., and Schapire, R. E. (2006). Maximum Entropy Modeling of Species Geographic Distributions. *Ecol. Model.* 190, 231–259. doi:10.1016/j.ecolmodel.2005.03.026

Phillips, S. J., Dudik, M., Elith, J., Graham, C. H., Lehmann, A., Leathwick, J., et al. (2009). Sample Selection Bias and Presence-only Distribution Models: Implications for Background and Pseudo-absence Data. *Ecol. Appl.* 19, 181–197. doi:10.1890/07-2153.1

Pimm, S. L., Jenkins, C. N., Abell, R., Brooks, T. M., Gittleman, J. L., Joppa, L. N., et al. (2014). The Biodiversity of Species and Their Rates of Extinction, Distribution, and Protection. *Sci* 344, 1246752. doi:10.1126/science.1246752

Poirazidis, K., Bontzorlos, V., Xofis, P., Zakkak, S., Xirouchakis, S., Grigoriadou, E., et al. (2019). Bioclimatic and Environmental Suitability Models for Capercaillie (Tetrao urogallus) Conservation: Identification of Optimal and Marginal Areas in Rodopi Mountain-Range National Park (Northern Greece). *Glob. Ecol. Conserv.* 17, e00526. doi:10.1016/j.gecco.2019.e00526

Pongratz, J., Reick, C., Raddatz, T., and Claussen, M. (2008). A Reconstruction of Global Agricultural Areas and Land Cover for the Last Millennium. *Glob. Biogeochem. Cycles* 22 (3), GB3018. doi:10.1029/2007GB003153

Qi, B. Z., (2022). Environmental Evolution and Human Activities in the Gonghe Basin During the Mid-Late Holocene, A Case Study of Nankayan Site. M.

Qin, L., Dorian, Q. F., and Zhang, H. (2010). Modelling Wild Food resource Catchments Amongst Early Farmers: Case Studies From the Lower Yangtze and Central China. *Quat. Sci.* 30, 2245–2261. doi:10.3969/j.issn.1001-7410.2010.02.02

Qin, X. L., and Ju, X. N. (2021). On The Open Firing Technique and the Neolithic Pottery Firing Technique of the Yangtze River's Lower Reaches with the Cases of Pishan. *Xiaodouli Xindili Sites Zhejiang* 6 (109), 44–57. doi:10.16319/j.cnki.0452-7402.2021.06.005

Qinghai Institute of Cultural Relics and Archaeology and Beijing University (2015). *School of Archaeology and Museology*. Beijing: Science Press.

Qinghai Institute of Cultural Relics and Archaeology (1990). *Minghe yangshan*. Beijing: Cultural Relics Press.

Ren, G. (2000). Decline of the Mid-to Late Holocene Forests in China: Climatic Change or Human Impact? *J. Quat. Sci.* 15, 273–281. doi:10.1002/(sici)1099-1417(200003)15:3<273::aid-jqs504>3.0.co;2-2

Ren, L. L., and Dong, G. H. (2016). The history for origin and diffusion of "Six livestock". *Chin. J. Nat.* 4, 257–262. doi:10.3969/j.issn.0253-9608.2016.04.00

Rhode, D., Zhang, H. Y., Madsen, D. B., Gao, X., Brantingham, P. J., Ma, H. Z., et al. (2007). Epipaleolithic/Early Neolithic Settlements at Qinghai Lake, Western China. *J. Archaeol. Sci.* 34 (4), 600–612. doi:10.1016/j.jas.2006.06.016

Shen, C. M., and Tang, L. Y. (1996). Pollen Evidence for Paleo-Monsoon Changes in Holocene over the Tibetan Plateau. *Acta Micropalaeontological Sin.* 13 (4), 433–436.

Shen, J., Liu, X. Q., Wang, S. M., and Matsumoto, R. (2004). Palaeoclimatic changes in the Qinghai Lake area during the last 18, 000 years. *Quat. Int.* 136 (1), 131–140. doi:10.1016/j.quaint.2004.11.014

Shi, Y. F., Li, J. J., and Li, B. Y. (1998). *Up lift and environmental changes of Qinghai-Tibetan Plateau in the late cenozoic*. Guangzhou: Guangdong Science and Technology Press.

Steffen, W., Crutzen, P. J., and McNeill, J. R. (2007). The Anthropocene: Are Humans Now Overwhelming the Great Forces of Nature. *AMBIO* 36 (8), 614–621. doi:10.1579/0044-7447(2007)36[614:taahno]2.0.co;2

Sun, Y. J., Lai, Z. P., Madsen, D., and Hou, G. L. (2012). Luminescence Dating of a Hearth from the Archaeological site of Jiangxigou in the Qinghai Lake area of the northeastern Qinghai-Tibetan Plateau. *Quat. Geochronol.* 12, 107–110. doi:10.1016/j.quageo.2012.01.010

Swets, J. A. (1988). Measuring the Accuracy of Diagnostic Systems. *Science* 240, 48571285–48571293. doi:10.1126/science.3287615

Tang, L. T., Liu, D., Luo, X. P., Hu, L., and Wang, C. T. (2019). Forest Soil Phosphorus Stocks and Distribution Patterns in Qinghai, China. *Plant Eco* 43 (12), 1091–1103. doi:10.17521/cjpe.2019.0194

Tang, L. Y., Shen, C. M., Lu, H. Y., Li, C. H., and Ma, Q. F. (2021). Fifty Years of Palynology in the Tibetan Plateau. *China. Sci. earth. Sci.* 64, 1825–1843. doi:10.1007/s11430-020-9809-5

Teng, S. Q., Xu, Z. W., Lu, H. Y., and Xu, C. (2022). Megafauna declines and extinctions over the past 40, 000 years in eastern monsoonal China: causes, consequences and implications. *Sci. Sin. Vitae.* 52, 418–431. doi:10.1360/SSV-2021-0212

Tuo, F., Liu, X. D., Liu, R. H., Zhao, W. J., Jin, W. M., Ma, J., et al. (2020). Spatial Pattern and Correlation of Qinghai Spruce Population in Dayekou stream area of Qilian Mountains. *Plant Eco* 11, 1172–1183. doi:10.17521/cjpe.2020.0177

VanDerWal, J., Shoo, L. P., Graham, C., and William, S. E. (2009). Selecting Pseudo-absence Data for Presence-only Distribution Modeling: How Far Should You Stray From What You Know? *Ecol. Model.* 220, 589–594. doi:10.1016/j.ecolmodel.2008.11.010

Veloz, S. D. (2009). Spatially Autocorrelated Sampling Falsely Inflates Measures of Accuracy for Presence-only Niche Models. *J. Biogeogr.* 36, 2290–2299. doi:10.1111/j.1365-2699.2009.02174.x

Vidal-Matutano, P., Henry, A., and Théry-Parisot, I. (2017). Dead Wood Gathering Among Neanderthal Groups: Charcoal evidence from Abric del Pastor and El Salt (Eastern Iberia). *J. Archaeol. Sci.* 80, 109–121. doi:10.1016/j.jas.2017.03.001

Vitousek, P. M., Mooney, H. A., Lubchenco, J., and Melillo, J. M. (1997). Human Domination of Earth's Ecosystems. *Sci* 277, 494–499. doi:10.1126/science.277.5325.494

Wan, Y. F. (2017). *Analysis on transpiration characteristics and influencing factors of Qinghai spruce forest in qilian mountains. [M]*. Lanzhou: Gansu Agricultural University.

Wang, H., Hong, Y. T., Zhu, Y. X., Lin, Q. H., Len, X. T., and Mao, X. M. (2003). The Peat Humification Recors of Holocene Climate Change in Hongyuan Region.

Wang, Y., Li, G. H., Qiao, H., Zhang, Q. M., and Feng, X. (2022). Shenna site, Chengbei district, Xining city, 1992-1993 excavation brief. *Archaeology* 05, 3–23+2.

Wang, J., Xia, H., Yao, J. T., Shen, X. K., Cheng, T., Wang, Q. Q., et al. (2020). Subsistence Strategies of Prehistoric Hunter-Gatherers on the Tibetan Plateau during the Last Deglaciation. *Sci. China Earth Sci.* 63 (3), 395–404. doi:10.1007/s11430-019-9519-8

Wang, S. W., Cai, J. N., Zhu, J. H., and Gong, D. Y. (2002). Studies on Climate Change in China. *Clim. Environ. Res.* 7 (2), 137–145.

Wang, S. Z., Wang, Q. Q., Wang, Z. X., Liang, G. J., Qi, W. Y., and Ren, X. Y. (2016). Utilization and Ecological Environment Indicated by Charcoal Remains of Middle and Late Qijia Culture in Jinchankou Site. *Agri. Archaeo.* 1, 9–15.

Warren, D. L., and Seifert, S. N. (2011). Ecological niche modeling in Maxent: the importance of model complexity and the performance of model selection criteria. *Ecol. Appl.* 21, 335–342. doi:10.1890/10-1171.1

Wei, H. C., E, C. Y., Zhang, J., Sun, Y. J., Li, Q. K., Hou, G. L., et al. (2020). Climate Change and Anthropogenic Activities in Qinghai Lake Basin Over the Last 8500 Years Derived From Pollen and Charcoal Records in an Aeolian Section. *Catena* 193, 104616. doi:10.1016/j.catena.2020.104616

Wende, Z., Hou, G., Gao, J., Chen, X., Jin, S., and Lancuo, Z. (2021). Reconstruction of Cultivated Land in the Northeast Margin of Qinghai–Tibetan Plateau and Anthropogenic Impacts on PalaeoEnvironment During the Mid-Holocene. *Front. Earth Sci.* 9, 681995. doi:10.3389/feart.2021.681995

Whitney, G. G. (1994). *From coastal wilderness to fruited plain: A history of environmental change in temperate North America from 1500 to the present*. Cambridge: Cambridge University Press.

Woodbridge, J., Fyfe, R., Smith, D., Pelling, R., Vareilles, A., Batchelor, R., et al. (2020). What Drives Biodiversity Patterns? Using Long-term Multidisciplinary Data to Discern Centennial-Scale Change. *J. Ecol.* 109 (3), 1396–1410. doi:10.1111/1365-2745.13565,

Wu, Y. H., and Wu, R. H. (2016). Spermatophytes of upper Yellow River Valley in eastern Qinghai. *Acta Bot. Boreali-Occidentalia Sin.* 28 (1), 1–12.

Xie, D. J. (2002). *Gan qing region prehistoric archeology*. Beijing: Cultural Relics Press, 7–167.

Yang, R., Meng, L. H., Zhang, X., and Liu, J. Q. (2005). The Mitochondrial DNA nad1Sequence Variation of Picea crassifolia in the Qinghai-Tibetan Plateau Platform and Adjacent Populations. *Acta ecolo. Sin.* 12, 3307–3313.

Yang, S. L., Dong, X. X., and Xiao, J. L. (2019). The East Asian Monsoon since the Last Glacial Maximum: Evidence from Geological Records in Northern China. *Sci. China Earth Sci.* 49 (8), 1169–1181. doi:10.1360/N072018-00056

Yi, H. L., Song, Y. B., and Xiao, Y. M. (2020). Study of Shalongka Site Animal Relics, Qinghai Huanlong County. Northern Cul. *Relics* 5, 66–77. doi:10.16422/j.cnki.1001-0483.2020.05.007

Yi, M. J., Gao, X., Zhang, X. L., Sun, Y. J., Brantingham, P. J., Madsen, D. B., et al. (2011). A Preliminary Report on Investigations in 2009 of Some Prehistoric Sites in the Tibetan Plateau Marginal Region. 2:124-136.

Yi, M. J. (2012). "The Discovery and Study of Paleolithic in Qinghai Province," in *Proceedings of the 13th annual conference of Chinese vertebrate paleontology* (Beijing: China Ocean Press), 195–202.

Yu, Y. Y., Wu, H., and Guo, Z. T. (2010). A New Simulation Model for Prehistoric Land Use and Carbon Storage(PLCM)- An Application in Yiluo Valleys. *Quat. Sci.* 30 (3), 540–549. doi:10.3969/j.issn.10017410.2010.03.12

Zhang, N. M., Cao, X. Y., Xu, Q. H., Huang, X. Z., Herzschuh, U., Shen, Z. W., et al. (2021). Vegetation Change and Human-Environment Interactions in the Qinghai Lake Basin, Northeastern Tibetan Plateau, since the Last Deglaciation. *Catena* 210, 105892. doi:10.1016/j.catena.2021.105892

Zhang, S. J., and Dong, G. H. (2017). Human Adaptation Strategies to Different Altitude Environment During Mid-Late Bronze Age in Northeast Tibetan Plateau. *Quat. Sci.* 37, 4696–4708. doi:10.11928/j.issn.1001-7410.2017.04.03

Zhang, X. L., Ha, B. B., Wang, S. J., Chen, Z. J., Ge, J. Y., Long, H., et al. (2018). The Earliest Human Occupation of the High-Altitude Tibetan Plateau 40 Thousand to 30 Thousand Years Ago. *Sci* 362, 1049–1051. doi:10.1126/science.aat8824

Zhang, X., Wang, W. C., Fang, X., Ye, Y., and Zheng, J. (2012). Agriculture Development-Induced Surface Albedo Changes and Climatic Implications Across Northeastern China. *Chin. Geogr. Sci.* 22 (3), 264–277. doi:10.1007/s11769-012-0535-z

Zhang, Y. L., Li, B. Y., Liu, L. S., and Zhen, D. (2021). Rediscussion on the extent of the Tibetan Plateau. *Geogr. Res.* 40 (6), 1543–1553. doi:10.11821/dlyj020210138

Zhang, Z. X. (2004). *Qinghai Geography*. Xining: Qinghai people's publishing house.

Zhao, Y., Yu, Z. C., Chen, F. H., and Zhao, C. (2006). Holocene Vegetation and Climate History at Hurleg Lake in the Qaidam Basin, Northwest China. *Rev. Palaeobot.* 145, 275–288. doi:10.1016/j.revpalbo.2006.12.002

Zhao, Y., Yu, Z., Chen, F. H., and An, C. (2007). "Holocene Vegetation and Climate Changes from Fossil Pollen Records in Arid and Semiarid China Late Quat. Climate Change and Human Adaptation in Arid China," in *Developments in quaternary science* (Netherlands: Elsevier), 51–65.

Zhou, Q. Y. (2003). *High-resolution study on the Holocene pedogenic environment evolution and human influence in the weihe river basin. D.* Xi'an: Shanxi Normal University.

Zhou, X., and Li, X. (2012). Variations in Spruce (Picea sp.) Distribution in the Chinese Loess Plateau and Surrounding Areas during the Holocene. *Holocene* 22, 687–696. doi:10.1177/0959683611400195

Zhou, X. Y., Li, X. Q., Zhao, K. L., Dodson, J., Sun, N., and Yang, Q. (2011). Early agricultural development and environmental effects in the Neolithic Longdong basin (eastern Gansu). *Sci. Bull.* 56, 762–771. doi:10.1007/s11434-010-4286-x

Zhu, G. P., Liu, Q., and Gao, Y. B. (2014). Improving Ecological Niche Model Transferability to Predict the Potential Distribution of Invasive Exotic Species. *Biodiv. Sci.* 22 (2), 223–230. doi:10.3724/sp.j.1003.2014.08178

frontiers | Frontiers in Earth Science

TYPE Original Research
PUBLISHED 14 February 2023
DOI 10.3389/feart.2023.1109905

Check for updates

OPEN ACCESS

EDITED BY
Guanghui Dong,
Lanzhou University, China

REVIEWED BY
Fengwen Liu,
Yunnan University, China
Yimin Yang,
University of Chinese Academy of Sciences, China

*CORRESPONDENCE
Junna Zhang,
junnazhang84@163.edu.cn

SPECIALTY SECTION
This article was submitted to Quaternary Science, Geomorphology and Paleoenvironment, a section of the journal Frontiers in Earth Science

RECEIVED 28 November 2022
ACCEPTED 30 January 2023
PUBLISHED 14 February 2023

CITATION
Yin C, Zhang J and Yu X (2023), Mountain valleys, alluvial fans and oases: Geomorphologic perspectives of the mixed agropastoral economy in Xinjiang (3000–200 BC). *Front. Earth Sci.* 11:1109905. doi: 10.3389/feart.2023.1109905

COPYRIGHT
© 2023 Yin, Zhang and Yu. This is an open-access article distributed under the terms of the Creative Commons Attribution License (CC BY). The use, distribution or reproduction in other forums is permitted, provided the original author(s) and the copyright owner(s) are credited and that the original publication in this journal is cited, in accordance with accepted academic practice. No use, distribution or reproduction is permitted which does not comply with these terms.

Mountain valleys, alluvial fans and oases: Geomorphologic perspectives of the mixed agropastoral economy in Xinjiang (3000–200 BC)

Chen Yin[1], Junna Zhang[1,2]* and Xuetong Yu[1]

[1]Institute of Archaeology, Beijing Union University, Beijing, China, [2]School of History, Capital Normal University, Beijing, China

Xinjiang serves as a hub for trans-Eurasian exchange. The Xinjiang hominids are supposed to be greatly influenced by the environment due to the fragile ecology and arid climate. As the territory with the most significant and complex geomorphic units in Inner Asia, Xinjiang features a diverse spectrum of geomorphic forms, including mountains, basins, deserts, river valleys, and oases. This paper presents a systematic summary of the geomorphic locations of 127 Bronze Age to early Iron Age (3000–200 BC) sites and cemeteries in Xinjiang and their economic strategies, exploring the different economic choices of ancient humans who lived in other geomorphic units, and how they adapted to their microenvironments. We have divided Xinjiang into five regions: the Junggar Basin, the Tarim Basin, the Western Tianshan Mountains, the middle Tianshan Mountains, and the Eastern Tianshan Mountains. Our study shows that there were different agropastoral economic modes in different geographical units. Roughly bounded by the Tianshan Mountains, the economy in northern Xinjiang was heavily based on animal husbandry, while oasis farming was popular in the Southern Xinjiang reigon. From the perspective of geomorphology, most sites are situated in mountain valleys, alluvial fans, and oases regions with surface water sources and fine-textured soil cover. Sites near mountains were more likely to develop a mixed pastoral-hunting economy, and oasis communities of a specific size were more likely to build a mixed agricultural-pastoral economy. In large river valleys or alluvial fans, it is expected that settlement clusters and large central settlements will grow, leading to the emergence of social complexity. This study will help to understand the complex "man-land" dynamics between 3000 and 200 BC in Xinjiang.

KEYWORDS

Xinjiang province, bronze age to early iron age, environmental archaeology, geomorphical location, mixed agropastoral economy

1 Introduction

Recent years have witnessed an increase in the acknowledgement of the geographical diversity of the Eurasian steppe's prehistoric economies due to the proliferation of archaeological evidence (Chang, 2002; Frachetti, 2008; Haruda, 2018). Since Frachetti developed the notion of the "Inner Asian Mountain Corridor (IAMC)" (Frachetti, 2008), many scholars have examined the people, cultural exchanges, landscapes, and diversified economies of this region (Frachetti, 2009; Frachetti, 2012; Wang W. et al., 2020). The accumulation of fresh archaeological and Phyto-archaeological data has enhanced scientists'

comprehension of the human lifestyles in this region (Dodson et al., 2013; Doumani et al., 2015; Spengler et al., 2016). Recent research by Spengler et al. (2021) demonstrates the existence of a complex agropastoral economy in Eastern Central Asia between 2000 and 1000 BC, based on nine complementary lines of evidence.

In the IAMC regions, ecology and landscape have long been considered essential to the economy and lifestyle. Frachetti et al. (2017) characterized the entire alpine region of Central Asia as a mobile ecosystem. Li (2020) investigated how ancient Xinjiang farmers adapted to the region's extreme aridity. Important archaeological sites in Central Asia, such as Begash (Frachetti et al., 2010), Tasbas (Spengler et al., 2014), and Sarazm (Spengler and Willcox, 2013), have provided cases of the adaptability of humans to their landscape. In eastern Central Asia, archaeological sites are dispersed across a landscape characterized by mountains, river basins and lakes, alluvial fans, desert oases, and immense steppes. Ancient communities had multiple opportunities to make economic decisions about the farming, herding, and foraging in each region and ecosystem. To fully comprehend the IAMC region's complex mixed agropastoral economy system, extensive research on the relationship between landform position and economic pattern is required.

In the third millennium BC, Xinjiang began to play a pivotal role in Inner Asia. Studies into Xinjiang's prehistoric cultures have made significant strides over the past decades. A preliminary chronology of prehistoric cultures in Xinjiang has been compiled by Han (2007), Guo (2012), and Shao (2018). Wang and Xi proposed that certain nomads may not have lived a nomadic lifestyle and may have established permanent communities based on their fieldwork at the eastern Tianshan Mountains (Wang and Xi, 2009). The ethnographic research of the Adonqolu and Husta Sites showed that seasonal transhumance had existed in the western Tianshan Mountains throughout the early Bronze Age (Jia, 2018). Studies of the Subeixi population (Shevchenko et al., 2014), the Chawuhu population (An and Yuan, 1998; Zhang et al., 2005), and the Tianshanbeilu population (Zhang et al., 2010) revealed the economic strategies in oasis basins. Li (2020) and Dong (2021) respectively summarized the results of archaeobotanical and zooarchaeological studies of Xinjiang, demonstrating the complex mixed agropastoral economy from the Bronze Age to the early Iron Age.

Xinjiang has a dry climate influenced by westerlies, and its ecological environment is fragile and sensitive to climate change. Therefore, the environment significantly affected ancient humans' lifestyles and economies. Chen et al. (2008) found that the climate was arid during the early Holocene, but it became more humid in the middle and late Holocene (6–1.5 cal ka BP), as evidenced by the high lake surface. This result is supported by a later review based on sporopollen data (Wang and Feng, 2013). The loess-paleosol records also showed that since 6 ka BP, the climate had a trend toward humidity; four paleosol layers were developed, the thickest of which developed in the late Holocene (Chen et al., 2016). The eleven lakes' aridity and temperature index curves show a spatial variation of the Holocene climate in Xinjiang. It is suggested that the climate became cooler and wetter in the northern Xinjiang region; however, the western Tianshan Mountains region has shown a dry and cold trend (Feng, 2017). Scholars have recently investigated the spatial and temporal processes of changing human subsistence patterns in Xinjiang (Dong G. H. et al., 2022) and the environmental factors forming the agropastoral economy (An et al., 2020). Although significant progress has been made to understand the mixed pastoral-hunting economy in Xinjiang, the discussion between environmental and economic patterns is still limited to macroscopic perspectives of climatic context and geospatial distribution, while in-depth examinations of the landforms and microenvironments that heavily influenced the economic choices are still lacking.

As the region with the most complex geomorphic units in Inner Asia, Xinjiang contains complex landforms such as mountains, basins, deserts, river valleys, and oases, but also a unique landform pattern of "three mountains sandwiched by two basins." This study examines the landforms and mixed agropastoral economy in Xinjiang and analyzes the economic patterns of ancient humans inhabiting distinct geomorphic units and their adaptations to the environment.

2 Study areas

The Xinjiang Province is located on the southeast edge of the Eurasian steppe, serving as a link for trans-Eurasian trade. The main geologic units in Xinjiang are the relatively stable Tarim and Junggar platforms and the highly active geosynclinal zone around them, which is, the Altai, Tianshan, Kunlun, and Karakoram Mountains (Xinjiang Comprehensive Expedition Team et al., 1978). There are 45 major mountain systems in the Altai, Tianshan, and Kunlun Mountains, which account for 53.64% of the total area (Yang, 2011). Basins or valleys are distributed among the continuous mountains, and oases of different sizes are located in the foothills where the mountains and basins meet, forming a combination of alpine, oasis, basin, and the Gobi Desert. In Xinjiang, the areas of aeolian landform account for 52.17%, and the flowing landform only accounts for 27.07% (Yang, 2011). The desert area is large; however, the quality lands are insufficient.

As part of the arid area of Inner Asia, Xinjiang is far from the sea, forming a temperate continental climate. The temperature in Xinjiang ranges from 20°C to 27°C in the summer and from −10°C to −22°C in the winter. The average annual precipitation is less than 200 mm, affected by geomorphology, altitude, and whether it is on a windward slope (Yang, 2011). The water sources are different in various geomorphic locations: the mountain valley is fed by precipitation; the oasis is supplied by mountain water; and the desert basin is supplied by surface rivers and underground water (An et al., 2020).

The vertical vegetational zonation of the Tianshan Mountains is remarkable. On the Northern slope, there is alpine and subalpine meadow between 2,900 and 3,600 m asl, forming good summer pasture; between 2,200 and 2,900 m asl is the mountainous coniferous forest; between 1,800 and 2,200 m asl is the middle-temperate mountain steppe, suitable for pasture and crop growth; and from 1,500 to 1,800 m asl, the Gobi Desert forest is widely distributed with various desert trees and shrubs. On the Southern slope, between 2,500 and 3,800 m asl is the alpine sub-alpine mountain steppe; between 2,200 and 2,500 m asl is the mountain grassland; from 1,700 to 2,200 m asl is the weathered rock desert; between 1,000 and 1,700 m asl is the Gobi Desert forest; and from 500 to 1,000 m asl is the oasis.

Recent archaeological discoveries show that both Western (wheat) and eastern (millet) crops were present in the Junggar region as early as 3000 BC (Zhao, 2009; Zhou et al., 2020). During the Bronze Age, the spread of the Seima-Turbino and the Andronovo cultures significantly impacted neighboring regions. The Andronovo culture mainly

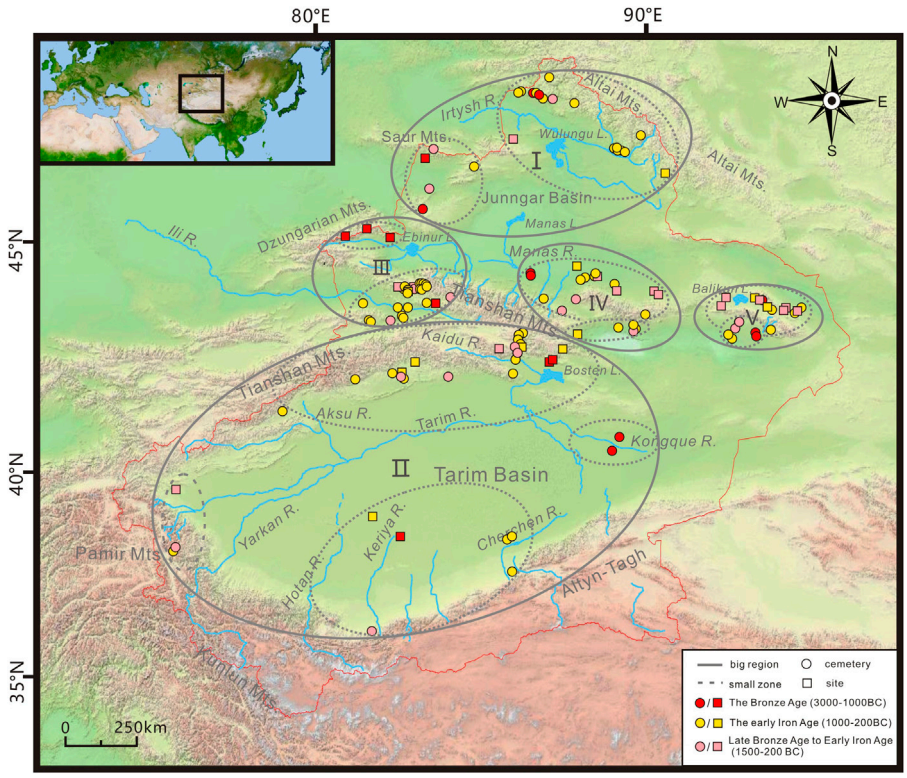

FIGURE 1
Map of Xinjiang, with the sites and the subregions of this study. I. Junggar Basin; II. Tarim Basin; III. Western Tianshan Mountains; IV. Middle Tianshan Mountains; V. Eastern Tianshan Mountains.

influenced the western region of Xinjiang (Chan and Shao, 2018). Seima-Turbino cultural remains are found in the northern Junggar Basin, northern Tianshan Mountains, and the eastern Tarim Basin, etc., (Lin, 2016). By the late Bronze Age, East-West interactions had intensified (Han, 2021). The early Iron Age was a mature time of East-West exchange, with increasingly close regional connections between cultures within the Xinjiang region from the mid-1000 BC onward (Shao, 2009).

3 Material and methods

We systematically studied the geomorphic location and economic strategies of the archaeological sites and cemeteries from the Bronze Age to the early Iron Age (3000-200 BC) in Xinjiang. There are two criteria: 1) All the sites have been systematically excavated or investigated, and the archaeological reports have been published; 2) Reliable dates have been obtained from radiocarbon dating or typology analysis. A total of 127 sites (including 91 cemeteries) were selected for analysis, of which 79 sites (including 45 cemeteries) had AMS ^{14}C dates (Figure 1).

Due to the vast area and numerous remains in Xinjiang, it is difficult to conduct field investigations of each site and cemetery. Therefore, we used the geographic coordinates to locate most sites (66 sites). For the sites whose coordinates were not published, we located them according to the map and description of the location from the archaeological report (61 sites). We use the Baidu topographic map to identify the geomorphic location of each site. Besides, we conducted three field investigations in the Bortala River Valley, Ili River Valley, and Kashi region, respectively, in the years 2018, 2020, and 2021, and investigated the landform positions of the Quanshuigou, Jirentaigoukou, Adonqolu, Husta, and Wupaer Sites.

Spengler et al. (2021) put forward nine categories of evidence to study the mixed agropastoral economies in Central Asia. This study considered all the evidence as thoroughly as possible, including: archaeological excavated materials, plant remains (large fossils and microfossils such as phytoliths, starch grains, and sporopollens), zooarchaeological evidence (animal bones and isotope data). We classify the bones of cattle, sheep, and horses, fur and dairy products, and horse harness as the evidence of pastoralism practices; while the crop remains, the tools of the sickle, pestle, millstone, spinning wheel, grinding rod are classified as evidence of farming or gathering activities; the arrowheads, bows, and fish hooks are considered to be hunting or fishing tools. However, as food exchanges might have frequently happened between "farmers" and "herders" (Dong et al., 2022a), the unearthed plant remains can not be used as conclusive evidence of farming activities, as they might have been exchanged with other agricultural populations.

Carbon and Nitrogen isotope data provide an important index for studying the diets of people. The δ^{15}N values of carnivores that feed on herbivores and fish range from 9‰ to 12‰, among which the δ^{15}N values of herbivores are about 3‰–7‰, the δ^{15}N values of first-level carnivores and fish are generally higher than 10‰; the δ^{15}N values of omnivores range from 7‰ to 9‰ (Cong et al., 2021). The mean

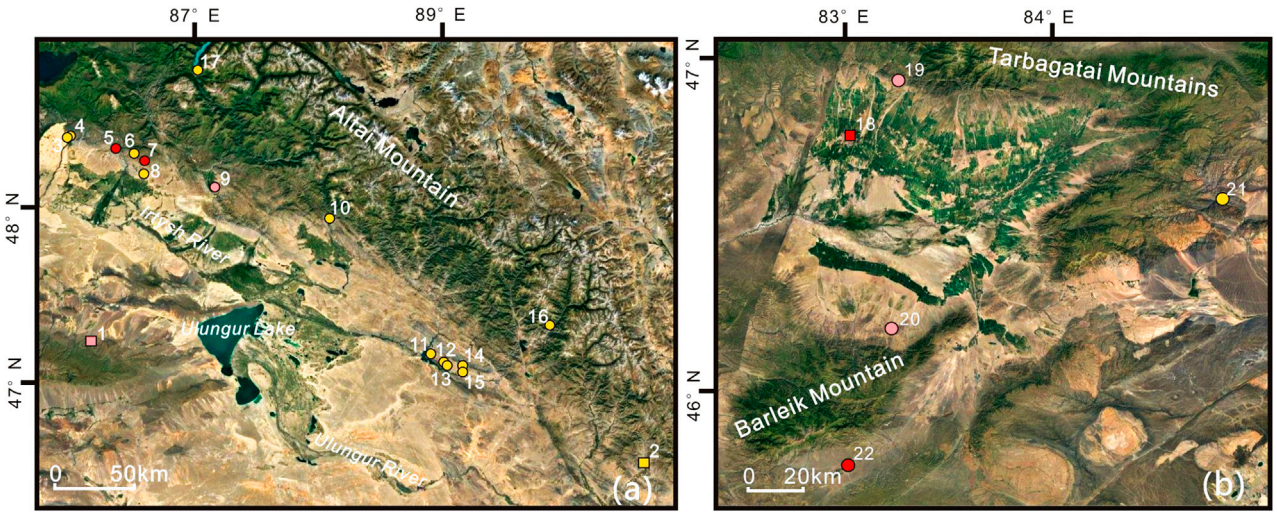

FIGURE 2
Topographic map of Junggar Basin and the sites mentioned in this study. **(A)** Northern margin area of Junggar Basin. 1. Tongtian Cave; 2. Huahaizi No.3; 3. Jialanggashi; 4. Habahan; 5. Ayituohan No.1;6. Dongtalede; 7. Tuoganbai No. 2; 8. Kalasu; 9. Shankoushuidian in Burqin County; 10. Wulasite; 11. Taledesayi; 12. Qilikete; 13. Sawudiegeer; 14. Sukeerte; 15. Saerbulake; 16. Zhelegabashi; 17. Tuwaxincun. **(B)** Western margin area of Junggar Basin 18. Xiakalangguer; 19. Abudulashuiku; 20. Aletengyemuleshuiku; 21. Baiyanghe; 22. Sazicun.

Corbon isotope values of C_3 plants is reported to be around −26.5‰ with a range of −35‰ to −20‰; C_4 plants is reported to be around −12.5‰ with a range of −16‰ to −7‰ (Marino and McElroy, 1991). However, the isotope data should be carefully analyzed. For example, high $\delta^{15}N$ values may be related to dairy diets. There is a dietary habit even among modern farmers in Xinjiang. As a result, a high $\delta^{15}N$ value does not definitely indicate a meat-based diet, nor does it indicate a herding-based economy. Besides, the $\delta^{15}N$ value is affected by the enrichment law of trophic level, environment, and animal situation (Hedges and Reynard, 2007; Chen, 2017). As the $\delta^{15}N$ value is generally higher in arid environments, the high $\delta^{15}N$ value at most sites in Xinjiang cannot rule out by the possibility that they are affected by the drought climate (Hartman, 2011). Similarly, due to the concentration of carbon isotopes in herbivorous livestock, the content of $\delta^{13}C$ in the bones of the man who ingested cattle and sheep will also be raised. As a result, using ^{13}C to determine whether humans consume C_3 or C_4 plants should be done with caution.

In this paper, the Bronze Age (BA) ranges from 3000–1000 BC, and the early Iron Age (EIA) ranges from 1000–200 BC (Shao, 2018). All the dates are calibrated in BC. We divide Xinjiang into five regions according to the geographical zones: the Junggar Basin, Tarim Basin, Western Tianshan Mountains, middle Tianshan Mountains, and Eastern Tianshan Mountains. Each region is segmented into several smaller zones, according to the geographical zones and Shao's archaeological culture partition (Shao, 2018) (Figure 1).

It should be noted that our study is built on two assumptions: 1) The cemeteries are close to the sites where people have lived (Cong et al., 2013; Jiang et al., 2013; Xinjiang Institute of Cultural Relics and Archaeology, 2016a). Archaeological excavations have shown that the sites and tombs are usually close to each other in most cases in Xinjiang (Liu and Guan, 2002; Jiang et al., 2014; Yu et al., 2016). Although special cases may exist, we presume they are not common and will not influence the results. 2) Replace ancient landforms with modern landforms. Geomorphologic evolution has been known to happen over millennia. However, our field investigations have shown that the landforms in Xinjiang did not change much due to the lack of thick sediments and strong transporting forces, especially during the late Holocene (Zhang Y. P. et al., 2021; Zhang et al., 2022). Moreover, we will pay special attention to the sites with geomorphic changes in our discussion.

4 Results

4.1 Junggar Basin

4.1.1 Northern margin area of Junggar Basin

This region consists primarily of the Altai piedmont plain, Ulungur Lake, and Junggar's western piedmont plain. In front of the Altai Mountains, sloping alluvial plains are formed by the Kelan River, Burqin River, Haba River, and some other short seasonal rivers. These plains are made up of alluvial fans and terraces with sand and gravel sediments. The southern bank of the Irtysh River is mainly composed of Neogene and early Quaternary sandstone, which is covered by sand dunes. There are seventeen sites, including fifteen cemeteries, in this area (Figure 2A).

4.1.1.1 Altai mountain valleys and alpine lakes

There are four sites (Figures 2A, 2.10.16.17), including three cemeteries on the terraces or oases around the mountain valleys and alpine lakes of Altai Mountain. The excavated stiff-bits, iron knives, arrowheads, and arrows suggest a pastoral economy and hunting activities (Figures 2A, 10.16.17) (Xinjiang Institute of Cultural Relics and Archaeology, 2013a; 2015a; Yu et al., 2014a). The $\delta^{15}N$ (10.2‰ and 10.8‰) and $\delta^{13}C$ (−18.7‰ and −17.8‰) values of two human bones from Tuwaxincun Cemetery (Figures 2A, 17)

show that the resident consumed a large number of animal proteins but hardly any C_4 crops (Dong et al., 2022b). Deer stones, stone circles, and stone cairns were discovered at Huahaizi No. 3 Site in Sandaohaizi (900–500 BC; Figures 2A, 2), which is speculated as the ceremonial and sacrificial center of early nomadic society (Guo et al., 2016).

4.1.1.2 Planation surfaces in the South of altai mountain or platforms on both sides of the North-South river

The tributaries of the Irtysh River flow from the Altai Mountains' southern foothills. This area is near the mountains, with abundant grassland and water.

There are seven cemeteries (Figures 2A, 3–9) on the planation surfaces. Isotopic analysis of two BA cemeteries (Figures 2A, 5.7) shows the inhabitants relied heavily on animal protein (Yu et al., 2014b; Dong et al., 2022b). However, the strong C_4 signatures at Ayituohan No. 1 Cemetery (2836–2490 BC) indicate that the inhabitants probably consumed the millet (Qu et al., 2020). One cemetery of mid-late BA to EIA (Figures 2A, 9) discovered iron knives, stiff-bits, and the burying horse, showing a nomadic economy. Human bones from Kalasu (EIA) with $\delta^{15}N$ values ranging from 10.9‰ to 12.6‰ and $\delta^{13}C$ values ranging from −17.2‰ to −16.1‰ indicate that inhabitants relied heavily on meat- or -dairy - based diets (Chen et al., 2017). This evidence shows a mainly pastoral economy.

Five EIA cemeteries (Figures 2A, 11.12.13.14.15) lie on the platform along the river. Stirrups, stiff-bits, copper fish hooks, and arrowheads identified at these cemeteries indicate a mixed pastoral -hunting economy.

The Tongtian Cave, a rock shelter site in the deep valley of the low hills north of Saur Mountain, dates from the Paleolithic to the Bronze Age (Figures 2A, 1). In the BA layer (3250–1250 BC), plant macrofossils of wheat, barley, foxtail millet (*Setaria italica*), and broomcorn millet (*Panicum miliaceum*) were identified, providing evidence of crop planting (Zhou et al., 2020). The pikas, voles, and small bird remains were unearthed, indicating hunting activities (Zhou et al., 2020).

4.1.2 Western margin area of Junggar Basin

The western margin of the Junggar Basin is mostly located in Xinjiang's northwest corner. The main geomorphic unit is the Tacheng-Tuoli alluvial plain. There is a high-coverage semi-desert steppe inside the flat plain of the Tuoli Basin, and the sediments are made up of sand and fine soil. The low-lying, flat floodplain in the abdomen of Tacheng Basin is inset with many meandering streams and swamps, where thermophilic plants such as Phragmites australis and Splendens are flourishing. The margin area of the basin is the alluvial plain, composed of gravel and loess-like soil, showing a desert environment with sparse vegetation. There are five sites, including four cemeteries, in this area (Figure 2B).

4.1.2.1 Mountain valleys

The Baiyanghe Cemetery of EIA (Figures 2B, 21) is located in the Baiyang River Valley. Bronze and iron swords, bows, arrowheads, and millstones were excavated, indicating herding and hunting activities (Wang and Tian, 2012).

4.1.2.2 On the alluvial fans

The gully on the alluvial fan in this area is well developed. On the top of the fan, small oases are often developed between the edges of the fans. Two cemeteries of mid-late BA to EIA (Figures 2B, 19.20) excavated relics of sheep and horse bones, arrowheads, iron swords, and bone buckles (Xinjiang Institute of Cultural Relics and Archaeology, 2016b; Wu et al., 2017).

4.1.2.3 Alluvial fan margin oases

One site (1450–1300 BC; Figures 2B, 18) lies in the oasis at the front of the alluvial fan in the south of Taerbahatai Mountain (Yuan et al., 2017). Charcoal, pottery pieces, and broken bones of cattle, horses, and sheep were unearthed in the kiln's layer. Wheat was identified, too (Dodson et al., 2013).

4.2 Tarim Basin

4.2.1 Northern margin area of Tarim Basin

On the North margin of is the flood-alluvial-lacustrine plain is located on the Tarim Basin's northern margin. The main rivers originate from the Tianshan Mountains' Southern slope, such as the Kongque River, Kuche River, Weigan River, and Aksu River. They carry the sediments to the foothills, forming alluvial fans. The alluvial plains are composed of fluviological deposits and debris flows, forming some large delta plains and oases that have become important agricultural districts of southern Xinjiang. There are 22 sites, including fifteen cemeteries, in this area (mainly EIA remains) (Figure 3A).

4.2.1.1 Mountain valleys

There are seven sites (Figures 3A, 12.13.14.15.16.17.22), including five cemeteries (Figures 3A, 13.14.15.16.17), in the mountain valleys. Mohuchahan (950–850 BC; Figures 3A, 12) is located between the piedmont alluvial fans on the East bank of the Mohuchahan River (Xinjiang Institute of Cultural Relics and Archaeology, 2016a). The mean $\delta^{13}C$ values (−18.2‰ ± 0.7‰) and mean $\delta^{15}N$ values (12.6‰ ± 0.6‰) of nine human bones, as well as the mean $\delta^{13}C$ values (−18.6‰ ± 1.0‰) and mean $\delta^{15}N$ values (5.0‰± 2.1‰) of 20 animal bones, indicate the heavily meat-based diet and mainly C_3 diets (Dong et al., 2022a). Moreover, the unearthed weapons, life appliances, and horse harnesses without farming tools showed that animal herding is an important way for people to live. The isotope data of a few bones show that C_4 plant sources may result from communication with the surrounding oasis population (Dong et al., 2022a). Hongshangou of the EIA (Figures 3A, 22) is located at the small basin at the southern foot of the Tianshan Mountains, where the sacrificial remains, including stone relics, residential remains, and tombs, were unearthed (Hou, 2016). The unearthed copper knives, arrows, and bones of sheep and horses in five cemeteries (Figures 3A, 13.14.15.16.17) suggest a pastoral economy and hunting activity (Xinjiang Institute of Cultural Relics and Archaeology, 2015b).

4.2.1.2 On the alluvial fans

Three EIA sites (Figures 3A, 2.3.20) are in this area. Duogang (900–500 BC; Figures 3A, 3) is located near the oasis of the alluvial fan (Zhang X. L. et al., 2014). The mean $\delta^{15}N$ values (12.56‰) and mean $\delta^{13}C$ values (−14.77‰) of 39 human bones indicate a meat-based heavy diet and mixed C_3 and C_4 diets in this cemetery (Zhang X. L. et al., 2014).

4.2.1.3 Alluvial fan margin (river valley) oases

Eleven sites (Figures 3A, 1.4.5.6.7.8.9.10.11.18.19), including seven cemeteries (Figures 3A, 1.5.6.8.9.18.19), are situated in this

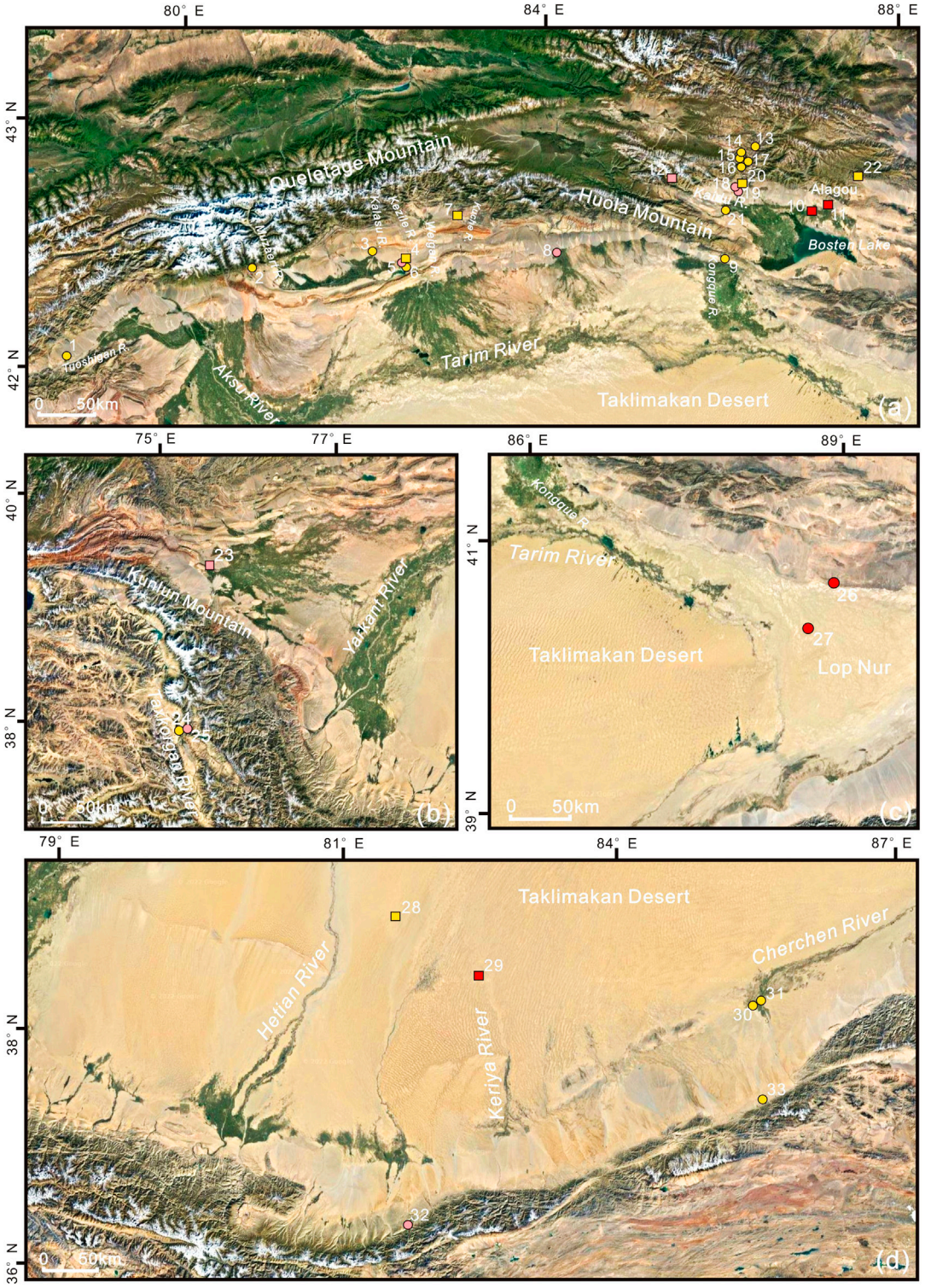

FIGURE 3
Topographic map of Tarim Basin and the sites mentioned in this study. **(A)** Northern margin area of Tarim Basin. 1. Kulansarike; 2. Baozidong M41; 3. Duogang; 4. Kezier; 5. Keziertuershuiku; 6. Karigayi; 7. Tikemaike; 8. Qunbake; 9. Shanghuxiang; 10. Xintala; 11. Quhui; 12. Mohuchahan; 13. Habuqihan I and II; 14. Narenhabuqihangou; 15. Daxigou No.1; 16. Qiaoenqiakeledeke; 17. Daxigou No.4; 18. Chawuhu No.4; 19. Chawuhu No.1; 20. Hejingzhonggongyeyuanqu; 21. Baileqier; 22. Hongshangou. **(B)** Southwestern margin area of Tarim Basin. 23. Wupaer; 24. Jierzankale; 25. Xiabandi. **(C)** Eastern margin area of Tarim Basin. 26. Gumugou; 27. Xiaohe. **(D)** Southern margin area of Tarim Basin. 28. Yuansha Gucheng; 29. Northern Niya; 30. Zhagunluke; 31. Jiawaairike; 32. Liushui; 33. Gudaqi.

geomorphic location. Two BA sites (Figures 3A, 10.11) are located at the fan margin oasis area on the north bank of Bosten Lake. The oasis is large and has abundant water. Farming tools and botanical remains (wheat, naked barley, and broomcorn millet) were excavated at Xintala Site (1950–1650 BC; Figures 3A, 10) (Zhao et al., 2013).

Four cemeteries of mid-late BA to EIA (Figures 3A, 5.8.18.19) were discovered. Qunbake (mainly 950–600 BC; Figures 3A, 8) is located in the fan-margin oasis at the southern foot of Huola Mountain. Millstones and plant remains (wheat and broomcorn millet) were found here; horse and sheep bones, leather, iron knives, and arrowheads were also excavated. The evidence points to an agropastoral economy supplemented by hunting activities (Sun and Chen, 1987; Cong and Chen, 1991). The two Chawuhu cemeteries (Figures 3A, 18.19) lie on the first terrace and sloping platform of Chawuhu valley, respectively, in the northwest of the Yanqi Basin. Both of them are near the fan margin oasis. Stiff-bits, horse bounders, and arrowheads were unearthed from Chawuhu No. 1 (Figures 3A, 19) (Xinjiang Institute of Cultural Relics and Archaeology, 1992). Because the number of horse bones accounted for a large proportion, students speculate that horse bones stem from domestic horses (An and Yuan, 1998). Besides, the evidence of residues and physical anthropology analysis suggests that the Chawuhu population at Chawuhu No. 4 (Figures 3A, 18) relied on meat- or dairy-heavy diets and consumed wheat and barley (Zhang et al., 2005).

Five EIA sites (Figures 3A, 1.4.6.9.7), including three cemeteries (Figures 3A, 1.6.9), were discovered in the southern Queletage and Huola Mountains. Tikemaike (Figures 3A, 7) lies on the oasis of the Kuche River. Slag smelting, flow pipes, and pottery pieces were discovered at this site, showing metallurgical elements (Ruan et al., 2016). The unearthed iron arrowheads from Shanghuxiang (Figures 3A, 9) suggest hunting activities (He, 1999).

4.2.2 Southern margin area of Tarim Basin

The topography of this region is high in the South and West and low in the North and East. The main geomorphological unit is the piedmont gravel plain on the north of the Kunlun Mountains and Altun Mountains, which is composed of alluvial fans of different sizes. The sites and cemeteries are distributed along the Hetian River, Keriya River, and Cherchen River from West to East. The Hetian River is the largest river on the Northern slope of the Kunlun Mountains. It flows through the Taklimakan Desert and is supplied by mountain precipitation and glacial meltwater. Big oases and alluvial plains along the Keriya River have a large amount of water. The Cherchen River has a small amount of water and a deeply cut valley. The lower part of the plain is composed of sandy, loamy soil, on which fixed or semi-fixed dunes are distributed. The fine soil plain is supplied by springs and floods, which is favorable for developing agriculture. There are six sites, including four cemeteries, in this area (Figure 3D).

4.2.2.1 On low hills and alluvial fans

In this geomorphic area, there are two cemeteries (Figures 3D, 32.33). Liushui (1108–493 BC; Figures 3D, 32) is located on the lower hills. Combined with paleopathological analysis, stiff-bits, bridle-bits, and arrowheads were unearthed from this cemetery, providing evidence for animal herding and hunting (Zhang X. et al., 2014; Wu et al., 2016). Gudaqi (500–300 BC; Figures 3D, 33) lie on an alluvial fan. Horse and sheep head remains were found in almost all burials here, probably indicating developed animal husbandry (Xinjiang Institute of Cultural Relics and Archaeology, 2013b).

4.2.2.2 Alluvial fan margin oases

Two EIA cemeteries (Figures 3D, 30.31) lie on the alluvial fan margin oasis area along the Cherchen River. Wheaten food, arrowheads, bows, horse and sheep bones, and leather products were excavated at Zhagunluke (1050 BC–500 AD; Figures 3D, 30), indicating an agropastoral economy and hunting activities (Xinjiang Institute of Cultural Relics and Archaeology, 1998a; Wang et al., 2003).

4.2.2.3 River oases in the desert

Two sites (Figures 3D, 28.29) were discovered in the Taklimakan Desert and were presumed to be located in the ancient river oasis. Yuansha Gucheng of EIA (Figures 3D, 28) lies on an oasis near the Keriya River. Wheat, barley, broomcorn millet, and the irrigation system were found (Debaine et al., 2010; Li, 2020); domesticated animals (*Capra* sp., *Ovis* sp., *Bos taurus*, and *Camelus bactrianus, etc.*) and wild animal remains (*Lepus* sp., *Nesokia indica*, and *Aves*, *etc.*) were also unearthed here (Huang, 2008). These remains point to the agropastoral economy and hunting activities.

4.3.3 Southwestern margin area of Tarim Basin

The Tarim Basin's Southwestern margin is located East of the Pamir Plateau. The terrain slopes from Southwest to Northeast, with the Karakorum Mountains in the Southwest, the Yarkant River alluvial plain in the middle, and the Taklimakan Desert in the East. Most of the terrain is relatively flat, and there is a large amount of sand and gravel in the Taxkorgan Valley. Plants grow well in the valley but are rare or scarce on the bilateral slopes. There is a small amount of forest on the windward slope of the Western mountain. Three sites, including two cemeteries, are found in this area (Figure 3B).

4.3.3.1 Mountain valleys

Two cemeteries (Figures 3B, 24.25) lie in the Taxkorgan River Valley on the eastern margin of the Pamir Plateau. The mean $\delta^{13}C$ values (−18.2‰ ±0.8‰) and mean $\delta^{15}N$ values (12.3‰ ±1.0‰) of 26 human bones at Xiabandi (1500–600 BC; Figures 3B, 25) show heavy meat-based diets mixed with a few C_4 diets (Wu, 2005; Zhang et al., 2016).

4.3.3.2 Alluvial fan margin oases

The Wupaer Site of mid-late BA to EIA (1500–400 BC; Figures 3B, 23) lies on the alluvial fan margin oasis of Konggur Mountain. Some farming tools (such as sickles, pestles, millstones, *etc.*) and plant remain (barley, wheat, millet, and *Fabaceae*) were identified, indicating an agricultural economy (Yang et al., 2020).

4.3.4 Eastern margin area of Tarim Basin

This region mainly refers to the Lop Nur, including the alluvial plains of the lower reaches of the Kongque River and Tarim River. Most of the landforms are composed of salt crust. Through long-term drying, denudation, and wind erosion, the ancient lake plain was transformed into various landforms such as Yadan, wind erosion depressions, and wind erosion plains (Figure 3C).

River oases in the desert

Xiaohe (Figures 3C, 27) is located in the ancient oasis near the Kongque River in the Lop Nur desert. Paleoenvironment research showed that during Bronze Age, there was a well-developed oasis around the Xiaohe area (Li et al., 2013; Yang et al., 2014). Common millet and wheat were identified, suggesting a farming economy at

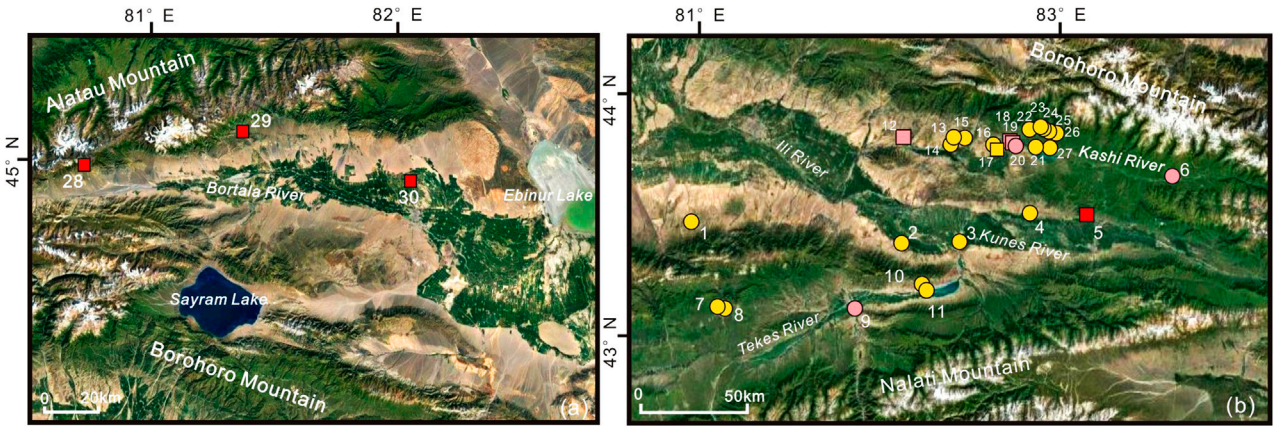

FIGURE 4
Topographic map of Western Tianshan Mountains and the sites mentioned in this study. **(A)** Bortala River Basin. 28. Adonqolu; 29. Husta; 30. Quanshuigou. **(B)** Ili River Basin. 1. Suodunbulake; 2. Fanliuyilegedai; 3. Shankoushuiku in Gongliu County; 4. Tiemulike; 5. Ayousaigoukou; 6. Tangbalesayi; 7. Biesikalagai; 8. Saerhuobu; 9. Koksu West Cemetery No.2; 10. Plot XV and Plot X, Area A, Qiafuqihai; 11. Yeshikelieke site A; 12. Kalasu; 13. Shibukeqi No.1 14. Shibukeqi No.2; 15. Taerketebei; 16. Dongmaili; 17. Qiongkeke; 18. Qialegeer; 19. Jirentaigoukou; 20. Wutulan; 21–26. Jialekesikayinte; 27. Qirentuohai.

Xiaohe (1884-1736 BC) (Yang et al., 2014; Zhang F. et al., 2021). Domesticated cattle, dairy products, and arrows unearthed here show a husbandry economy and hunting activities (Zhang Y. F. et al., 2017).

Gumugou (ca. 1850 BC; Figures 3C, 26) is located at the ancient oasis on the north bank of the lower reaches of the Kongquehe River, which is close to the mountain. The $\delta^{13}C$ values (ranging from −18.39‰ to −17.85‰) and $\delta^{15}N$ values (ranging from 13.58‰ to 15.33‰) of ten human bones suggest that the people relied heavily on animal products and also consumed C_3 plant (Zhang and Zhu, 2011; Zhang et al., 2015).

4.3 Western Tianshan Mountains

4.3.1 Bortala River Basin

The terrain of this region slopes from west to east and consists of three large landform units: the Alatau in the North, the Borohoro Mountains in the South, and the Bortala Valley and Ebi Lake Basin in the middle. The high and middle mountains, low hills, plains, and valleys line up in a ladder shape. In the North of Bortala valley, there are huge alluvial fans in front of the Alatau Mountain, the upper sediment is loess, and the lower is gravel. There are four terraces along the North bank of the Bortala River. Three sites were found in this area (Figure 4A).

4.3.1.1 On the alluvial fans

Adonqolu (1743–1680 BC; Figures 4A, 28) lies on the top of the alluvial fan, where a small oasis emerges at the junction of the two nearby fans (Cong et al., 2013). Husta (1370–1175 BC; Figures 4A, 29) lies on the fans with many gullies; some small oases are exposed near the fan edge (Cong et al., 2018). The phytoliths of wheat, barley, common millet, and foxtail millet were identified at Adonqolu, and the starch grains of millet were identified at Husta, indicating agricultural elements (Cong et al., 2018; Shao et al., 2019). The isotopic analysis of human dental calculus at Adonqolu (mean $\delta^{13}C$ values of −19.528‰ ± 0.2‰ and mean $\delta^{15}N$ values of 11.6‰ ± 0.2‰) suggests predominantly C_3 diets and heavily meat-based diets (Cong et al., 2021). Besides, strontium isotopic analysis of human enamel and bones shows that Adonqolu residents experienced migrations (Cong et al., 2021). Archaeologists speculated that seasonal transhumance probably played a vital role in the inhabitants' lives at Adonqolu and Husta (Jia, 2018).

4.3.1.2 Alluvial fan margin oases

Quanshuigou (1550–1050 BC; Figures 4A, 30) is located at the alluvial fan margin oasis on the southern foot of Alatau Mountain (Zhang et al., 2022). Unambiguous evidence of the metallurgical site, such as copper slag and ore, was found. The animal remains (cattle and sheep bones) and the production tools (such as bronze sickles) were excavated at the site. It is speculated that the site is a bronze metallurgical settlement with mixed agropastoral economy (Han and Chen, 2017).

4.3.2 Ili River Basin

The alluvial plain of Ili Valley, which consists of the Ili Basin and the Kunes Basin, has an altitude of 540–700 m asl. The riverbed slopes gently, so the floodplain and marshland are well developed. Twenty-seven sites, including twenty-two cemeteries (Figure 4B).

4.3.2.1 Loess platforms on both sides of the river valley

Three sites (Figures 4B, 12.18.19) are located at the loess platform on the north bank of the Kashi River, the first-grade tributary of the upper reaches of the Ili River. In Jirentaigoukou (2631–1020 BC; Figures 4B, 19), charred broomcorn millet seeds were identified (Wang Q. et al., 2020). The isotope analysis suggests a pattern of feeding sheep and cattle and a mixed C_3 and C_4 diet (Wang et al., 2019).

This area has one BA cemetery (Figures 4B, 9) and seven EIA cemeteries (Figures 4B, 2.3.4.13.14.15.20). Painted pottery, mutton, and iron knives were excavated at Wutulan (Figures 4B, 20), and iron knives and arrowheads were found at Koksu West Cemetery No. 2 (Figures 4B, 9), indicating the mixed husbandry and hunting economy (Ruan et al., 2012; Ruan et al., 2014).

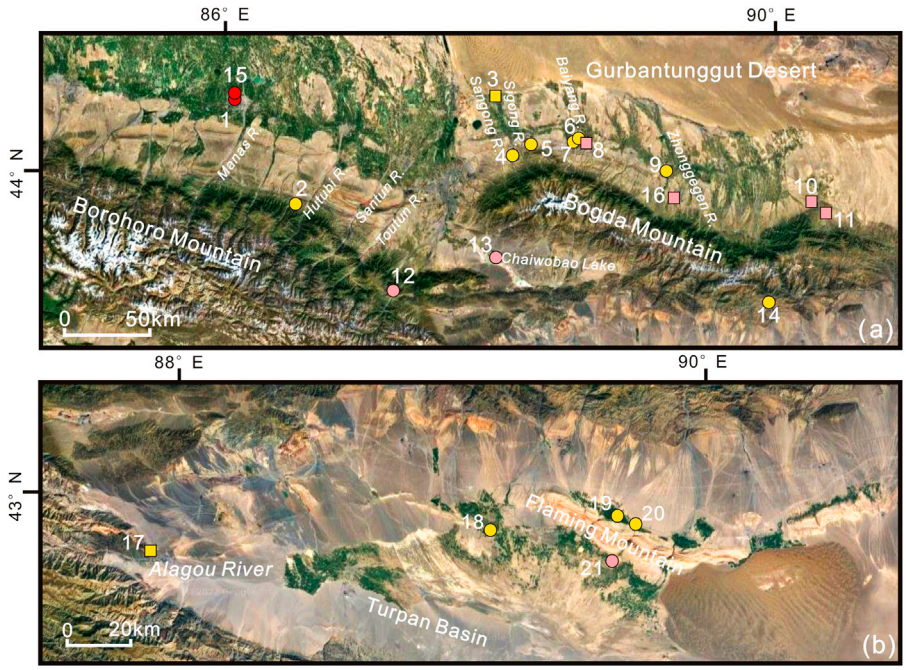

FIGURE 5
Topographic map of middle Tianshan Mountains and the sites mentioned in this study. **(A)** Areas on both sides of the middle Tianshan Mountains. 1. Liangzhongchangyilian; 2. Shimenzi; 3. Fukangfubeinongchangjijiandui; 4. Sangongxiang; 5. Choumeigou; 6. Xigou II area; 7. Baiyanghe; 8. Xigou I area; 9. Dalongkou; 10. Sidaogou; 11. Gangou; 12. Saensayi; 13. Chaiwobao; 14. Ertanggou; 15. Shuinichang; 16. Luanzagangzi. **(B)** Turpan Basin. 17. Yuergou; 18. Jiayi; 19. Shengjindian; 20. Subeixi; 21. Yanghai.

4.3.2.2 River valley oases

Four sites (Figures 4B, 5.10.11.17), including two cemeteries (Figures 4B, 10.11), provide evidence of animal husbandry and hunting. An abundance of horse and sheep bones and saddle-shaped millstones was unearthed at Ayousaigoukou (1410–1260 BC; Figures 4B, 5) on the bank of the Kashi River (Xinjiang Institute of Cultural Relics and Archaeology, 2013c; Wang et al., 2019). The $\delta^{13}C$ values (ranging from −16.02‰ to −16.47‰) and $\delta^{15}N$ values (ranging from 12.08‰ to 13.33‰) from eight human bones at Qiongkeke (1000–500 BC; Figures 4B, 17) suggest that ancient inhabitants relied on meat-based diets and had a mixed C_3 and C_4 diet (Liu and Guan, 2002; Zhang and Li, 2006).

4.3.2.3 On the alluvial fans

There are three EIA cemeteries (Figures 4B, 1.7.8) in this area. Combined with excavated iron knives and sheep bones, it is presumed to be an animal husbandry economy at Suodunbulake Cemetery (Xinjiang Institute of Cultural Relics and Archaeology, 1995).

4.3.2.4 Mountain valleys

There are eight cemeteries in the valley. Tangbalesayi (Figures 4B, 6) is located near the mouth of the Tangbalesayi gully. Seven cemeteries (Figures 4B, 21–27) lie in the valley of the Jialekesikayinte mountain. Arrow shafts and quivers were discovered at Qirentuohai (Figures 4B, 27) (Xinjiang Institute of Cultural Relics and Archaeology, 2004). Arrowheads were discovered at the burials (Figures 4B, 21–26), indicating a hunting activity (Xinjiang Institute of Cultural Relics and Archaeology et al., 2007).

4.4 Middle Tianshan Mountains

4.4.1 Areas on both sides of the middle Tianshan Mountains

Anticline hills and valleys were distributed at the Northern foot of the Tianshan Mountains below 1,500 m asl between the city of Wusu and Urumqi. Thick alluvial sand and gravel layers are deposited in the valley from South to North. The hills with rounded tops are cut into canyons, developing multilevel terraces. The alluvial fans of the Manas River have relatively flat terrain. The deposits gradually tapered from the top to the edge of the fan and transitioned from sandy pebbles to fine soil. The groundwater level is high, resulting in swamping and salinization. There are sixteen sites, including eleven cemeteries, in this area (Figure 5A).

4.4.1.1 Mountain valleys

There are nine sites (Figures 5A, 2.4.5.6.8.10.11.12.14), including six cemeteries (Figures 5A, 2.4.5.6.12.14) in this area. Wheat and barley were identified in the early BA layers at the Saensayi (2480–530 BC; Figures 5A, 12), suggesting a farming economy (Liu et al., 2021). Large pottery for grain storage, agricultural tools carbonized grain particles, and large animal bones were unearthed at Sidaogou (975–451 BC; Figures 5A, 10), showing an agropastoral

economy (Du and Ren, 2017; Tian et al., 2021). Horse and sheep bones, harnesses, and arrows were found at two cemeteries (Figures 5A, 2.14), suggesting a pastoral economy and hunting activity (Xinjiang Institute of Cultural Relics and Archaeology, 2012; Zhang Y. Z. et al., 2014).

Stiff-bits and arrowheads were unearthed at Ertanggou (700–500 BC; Figures 5A, 14), showing hunting activities (Xinjiang Institute of Cultural Relics and Archaeology, 2012). Iron knives, harnesses, and arrowheads were found at Shimenzi (Figures 5A, 2). Paleoanthropological research indicates that the residents relied heavily on animal products and also engaged in hunting (Zhang Y. Z. et al., 2014).

4.4.1.2 On the alluvial fans

There is one site (Figures 5A, 16) and two EIA cemeteries (Figures 5A, 7.9). Broomcorn millet, foxtail millet, and wheat/barley were identified in Figures 5A, 16 (1372–890 BC), indicating a farming economy (Zhang J. P. et al., 2017).

4.4.1.3 Alluvial fan margin oases

One site (Figures 5A, 3) and three cemeteries (Figures 5A, 1.13.15) are located in this area. Chaiwobao (Figures 5A, 13) is near the lake at the lowest part of the basin between two mountains. Large potteries, arrowheads, and horse and sheep bones were excavated here, suggesting an animal husbandry economy supplemented by hunting (Xinjiang Institute of Cultural Relics and Archaeology, 1998b).

4.4.2 Turpan Basin

The Turpan Basin can be divided into three areas: 1) The high basin in the north of Huoyanshan-Yanshan Mountains. Various sizes of channels originating from the South slope of Bogda Mountain carry sediments to accumulate alluvial fans. The sediments are composed of sand, gravel, and pebbles. The fine silt and clay have been eroded by the wind, so there is no vegetation on the fans. However, the fine soil belt at the edge of the fan forms oases where the plant grows well. 2) The mountain systems are across the central of the basin, where bare rocks are exposed to the air, and no vegetation is growing. 3) Low intermountain basins on the South of Huoyanshan and other mountains. Oases developed in the north and west of Aiding Lake. In the South of the lake is the diluvial plain of the Jueluotage Mountains. The sediments are mainly composed of angular gravel, and the vegetation is rare. In the east of Aiding Lake is the Kumtag Desert. The river system from the Tianshan Mountains to the basin formed numerous oases in Turpan Basin. Five cemeteries of Subeixi culture were found in this area (Figure 5B).

4.4.2.1 Alluvial fan margin oases

There are three cemeteries (Figures 5B, 19.20.21) near Huoyanshan Mountain in Turpan Basin and one cemetery (Figures 5B, 18) on the Gobi platform in the south of Turpan Oasis.

Plant remains (such as wheat, millet, and naked barley), harness, leather, and wool clothing were discovered at Yanghai (1300 BC–200 AD; Figures 5B, 21) (Jiang et al., 2021). The low $\delta^{13}C$ and high $\delta^{15}N$ values at the EIA of this cemetery suggest the consumption of huge amounts of animal protein (Si et al., 2013; Jiang et al., 2021). Desiccated noodles, cakes, porridge, and sourdough bread made of barley and broomcorn millet were identified at Subeixi (500–300 BC; Figures 5B, 20) (Gong et al., 2011). Leather, wool clothing, and sheep remains were also found here, reflecting animal husbandry and farming (Shevchenko et al., 2014). Plant remains (such as cereal remains, grape seeds, *etc.*) were identified at Shengjindian (ca. 500 BC–1 AD; Figures 5B, 19) (Jiang et al., 2014). Combining the buccal surfaces of the 13 molars for analysis, researchers agree that the inhabitant engaged in herding, farming, and hunting (Yang et al., 2022). Isotope analysis of tooth enamel from Jiayi (800–500 BC; Figures 5B, 18) shows that the residents relied heavily on meat- or dairy-based diets and mixed C_3 and C_4 plants (Xiao, 2018; Wu et al., 2021). Besides, bows and arrows are excavated here, indicating hunting activity (Wang L. et al., 2014).

4.4.2.2 Piedmont alluvial fans

Yuergou (ca. 450–350 BC; Figures 5B, 17) is located on the alluvial fan oasis in the junction between Aiweiergou and Alagou Valleys. Naked barley, broomcorn millet, and foxtail millet were excavated from this site, suggesting a farming economy (Jiang et al., 2013).

4.5 Eastern Tianshan Mountains

4.5.1 Areas on both sides of the Eastern Tianshan Mountains

The middle mountains in this region include MoQinulla, Bogda, Barkual, and Kalik. The areas on the north and south slopes of the Barkual and Kalik Mountains can be divided into three natural vertical zones: 1) The midmountain belt between 1,800 and 3,000 m asl on the North slope and 2,000–3,200 m asl on the South slope is controlled by fluviation. On the North-windward slope, the precipitation is abundant, resulting in a dense river network and spruce forest. However, the precipitation on the South leeward slope is less, so the river network is scarce. The shady slope or river valley has only scattered forests, while the sunny slope has semi-desert grassland. 2) The mountains above 3,000–3,200 m asl are controlled by frost action. Alpine meadows grow in gullies on gentle slope. Only bare bedrock and frozen soil are on the steep slopes. 3) The valley glacier, cirque glacier, hanging glacier, and mountain ice cap can be seen above the slow line of 3,900–4,000 m asl. On the horn and knife-edge crest, the bedrock is exposed. There are fifteen sites, including five cemeteries, in this area (Figure 6A).

4.5.1.1 On the alluvial fans

Eight sites (Figures 6A, 2.3.4.7.9.10.14.15) lie on the foothills of the Eastern Tianshan Mountains. Three sites of mid-late BA to EIA (Figures 6A, 3.4.9) and two EIA sites (Figures 6A, 2.7) are located on the alluvial fans. Two sites of mid-late BA to EIA (Figures 6A, 10.14) and one EIA cemetery (Figures 6A, 15) are located on top of the alluvial fan.

Botanical and isotope analysis indicates that the ancestors on the alluvial fans were engaged in animal herding, supplemented by farming and hunting. Cattle, horse, and sheep bones were unearthed at seven sites (Figures 6A, 2.3.4.7.9.10.14). Wild animal remains such as boar, deer, and antelope were unearthed at Liushugou (1400–400 BC; Figures 6A, 14) (Dong, 2021). The naked barley was identified at five sites (Figures 6A, 1.3.4.9.10); a few grains of wheat were unearthed at two sites (Figures 6A, 1.3.4), and a few millet were discovered at three sites (Figures 6A, 1.3.10) (Tian, 2018). Millstones and pestles were unearthed at several sites (Figures 6A, 1.3.9.10.14) (Tian, 2018; Ren et al., 2020; Tang et al., 2020; Xi et al., 2020; Dong, 2021). The abnormal phenomenon of horse vertebrae was identified at

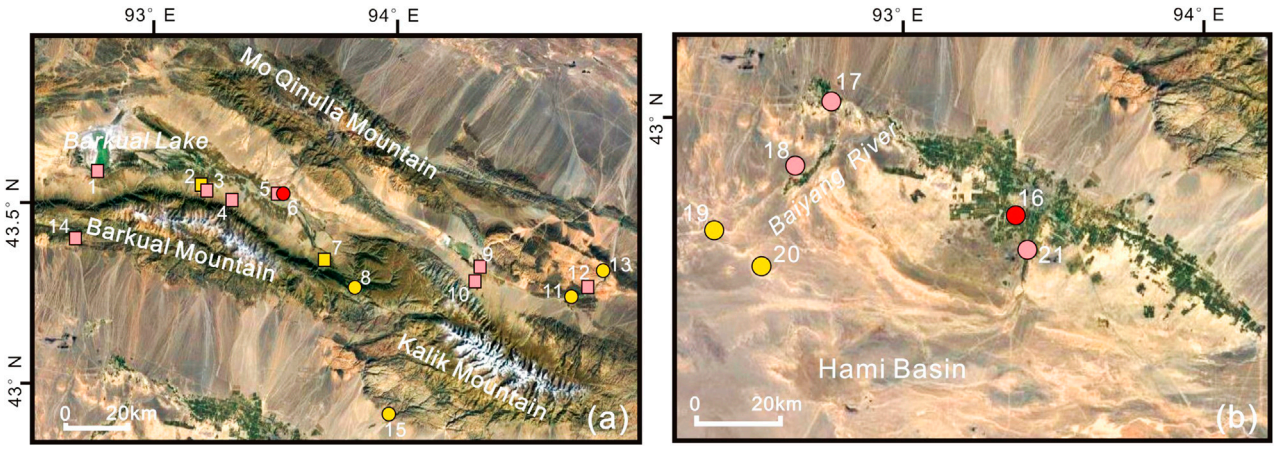

FIGURE 6
Topographic map of Eastern Tianshan Mountains and the sites mentioned in this study. **(A)** Areas on both sides of the Eastern Tianshan Mountains. 1. Haiziyan; 2. Xigou; 3. Dongheigou (Shirenzigou); 4. Hongshankou; 5. Qinggeda; 6. Nanwan; 7. Heigouliang; 8. Hanqigou; 9. Yanchi Gucheng; 10. Kuola; 11. Tuobeilang; 12. Baiqier 13. Xiagou; 14. Liushugou; 15. Huangtianshangmiaoergou I plot. **(B)** Hami Basin. 16. Tianshanbeilu; 17. Yanbulake; 18. Wupu; 19. Aisikexiaer; 20. South Aisikexiaer; 21. Sayituer.

Dongheigou, suggesting that the residents had mastered equestrian riding (Li et al., 2016). The high $\delta^{15}N$ values at Shirenzigou and Heigouliang suggest that the local population relied on a meat- or dairy-heavy diet (Li, 2020).

4.5.1.2 Mountain valleys

One site of mid-late BA to EIA (Figures 6A, 12) and three EIA cemeteries (Figures 6A, 8.11.13) have been found in this area. Sheep and horse bones, iron knives, and arrowheads were found at Tuobeiliang (Figures 6A, 11) (Wang J. X. et al., 2014). Sheep bones, bridle-bits, and arrowheads were found at Hanqigou (Figures 6A, 8) (Xi, 2014). Those remains show nomadic and hunting activities.

4.5.1.3 Alluvial fan margin oases

There are two sites from mid-late BA to EIA (Figures 6A, 1.5) and one BA cemetery (Figures 6A, 6). Qinggeda (1380–1127 BC; Figures 6A, 5) and Nanwan (1300-500 BC; Figures 6A, 6) were located in alluvial fan margin oasis areas near the river valley (Xi, 2014; Tian, 2018). Haiziyan (1300–800 BC; Figures 6A, 1) is located near an oasis around Barkual Lake. The archaeologists have excavated naked barley and bridle-bits of the late BA and iron knives and buckles, arrowheads, and ornaments of the EIA (Ren et al., 2020).

4.5.2 Hami Basin

The Hami Basin is between Barkual Mountain, Kalik Mountain, and the Gaxun Gobi. It is tectonically connected with the Turpan Basin. The terrain slopes from northeast to southwest, and the small rivers that originated in the Barkual-Karlik Mountains carry many sediments and form the alluvial fans, which constitute the sloping piedmont plain. The middle and upper plains are covered by gravel, with few plants growing. The lower part has more fine soil material, the terrain is gentle, and the diving depth is 5–7 m asl, forming Hami Oasis. The lowest area of the basin is Shar Lake, only 81 m asl above sea level. There is no water in the lake, only the salt shell. Six cemeteries lie on these alluvial plains and fan edge oases (Figure 6B).

4.5.2.1 Alluvial fan margin oases

Four cemeteries (Figures 6B, 16.17.18.21) are located on the alluvial fan margin oasis. Two BA cemeteries (Figures 6B, 16.21) are located in the Gobi Desert near the oasis. The $\delta^{15}N$ values (ranging from 14.34‰ to 16.49‰) and the $\delta^{13}C$ values (ranging from −13.97‰ to −16.40‰) of ten human bones at Tianshanbeilu (1940-1215 BC; Figures 6B, 16) show a heavy meat diet mixed with C_3 and C_4 plants (Zhang et al., 2010; Wang et al., 2017). Two cemeteries of mid to late BA to EIA (Figures 6B, 17.18) lie on an oasis surrounded by the Gobi in the Baiyang River Basin. Crops, pastries, and woolen fabrics were found in the Yanbulake (1000–500 BC; Figures 6B, 17) (Zhang et al., 1989; Chen, 1990). Leathers, millets, and wheat were discovered at Wupu (1050–450 BC; Figures 6B, 18) (Wang L. J. et al., 2020). Isotope analysis showed that the inhabitants consumed C_4 plants (Dong, 2021).

4.5.2.2 Alluvial plains

Two EIA cemeteries (Figures 6B, 19.20) are located on the alluvial plain near the paleochannel of the Baiyang River. Many arrowheads and cereal processing remains were unearthed at South Aisikexiaer (650–350 BC), indicating hunting and probably farming activities (Wang and Dang, 2011; Dong, 2021). The mean $\delta^{13}C$ values (−17.3‰ ± 0.9‰) and mean $\delta^{15}N$ values (14.5‰ ± 1‰) of forty-three human bones show that the population relied heavily on animal products and consumed C_3 plants here (Dong, 2021).

5 Discussion

5.1 Mixed agropastoral economy under grand geographical settings: The differentiation in Northern and Southern Xinjiang

The Tianshan range divides Xinjiang into two large geographical units. Northern Xinjiang mainly includes the Junggar Basin, the Bortala and Ili River Valleys, and northern areas of the middle and

eastern Tianshan Mountains. Southern Xinjiang mainly includes Tarim Basin, as well as Turpan Basin and Hami Basin, respectively, in the middle and eastern Tianshan Mountains. In general, the Bronze Age to the early Iron Age in Xinjiang was characterized by various economic systems, including a diverse combination of pastoralism, agriculture, and hunter-gathering. However, the economic strategies are significantly different between northern Xinjiang and southern Xinjiang.

5.1.1 Northern Xinjiang

The Junggar Basin was deeply influenced by Scythian culture (Shui, 2016). Iron knives, harnesses, animal ornaments, and other artifacts of the steppe nomadic style were excavated in the early Iron Age tombs. Sheep bones and horse bones were unearthed, and the horse sacrifice behavior was evidenced (e.g., Figures 2A, 2.8.10.17, *etc.*), indicating a highly mobile animal husbandry economy.

The Western Tianshan Mountains region was deeply influenced by the Andronovo culture, which had a well-developed animal husbandry tradition (Guo, 2012). Evidence of migration (Cong et al., 2021) and seasonal transhumance (Jia, 2018) had been found at the Adonqolu and Husta Site (Figure 4A). In the Ili River Basin, sheep and horse bones, stone pestles, millstones, and arrowheads were unearthed in the sites and tombs (e.g., Figures 4B, 3.5.17.19.21–26.27). In short, the economy of the western Tianshan Mountains area was mainly animal husbandry, but evidence of plant remains has also been found in several sites (Figures 4A, 28; Figures 4B, 12.19).

The middle Tianshan Mountains area was influenced by many archaeological cultures from different directions. Sheep and horse bones were found at the northern foot of the middle Tianshan Mountains. Stone pestles, millstones, hoes (e.g., Figures 5A, 3.10.11), and plant remains (e.g., Figures 5A, 10.16) were also unearthed at the sites of this area. Large settlements, of ancient nomads, such as Shirenzigou, Hongshankou, and Dongheigou, were found at the northern foot of the eastern Tianshan Mountains. Wore horse vertebrae and high $\delta^{15}N$ values of human bones showed nomadic activities (Li, 2020). Naked barley/wheat-millet plant remains were also unearthed at some sites (Figures 6A, 1.3.4.9.10). Furthermore, scattered remains were discovered in the southern Tianshan Mountains (e.g., Figures 5A, 14; Figures 6A, 14), indicating an animal husbandry economy.

5.1.2 Southern Xinjiang

The Xiaohe culture, which is in the Lop Nur Oasis on the eastern edge of the Tarim Basin, showed a mixed agropastoral economy (Shao, 2018). Sheep bones were discovered on Tarim Basin's Northern edge sites (Figures 3A, 1.3.4.5.6.7.8.9), and stone sickle, stone pestle, wheat, and millet were discovered in oases on the edge of alluvial fans (Figures 3A, 4.8). In the oasis area near Bosten Lake, the remains of naked barley, wheat, and broomcorn from the Xintala Site indicate a predominantly agricultural economy. Irrigation systems were found at the Yuansha Gucheng Site (Figures 3D, 28). Food made from wheat and millet was discovered in Zhagunluke Cemetery on the Tarim Basin's Southern edge (Figures 3D, 30).

The Subexi culture, with well-developed painted pottery, emerged in the oasis area of Turpan Basin (Shao, 2018). The animal remains (cattle, sheep, and horses), bows, arrows, and harness were unearthed from tombs in this area (Figure 5B). The seeds, including naked barley, wheat (Figures 5B, 17.19.21), broomcorn millet (Figures 5B, 17.19.20.21), and foxtail millet (Figures 5B, 17.19) were found in most tombs in Turpan Basin.

In the oasis area of Hami Basin, the Tianshanbeilu culture originated from the mix of Eastern and Western ancestors, which gradually developed into the Yanbulake culture (Shao, 2009; Shao, 2018). Bones of cattle, horses, and sheep (Figures 6A, 16.18.20); plant remains of naked barley, wheat, and millet (Figures 6A, 18); and tools such as stone pestles and millstones were found in this area (Figures 6A, 17.19.20). This evidence indicates that people in the Turpan and Hami Basins have worked in a mixed agropastoral economy.

To summarize, the Northern Xinjiang economy is primarily based on animal husbandry. The mixed agropastoral economy, which is primarily based on animal husbandry and supplemented by agriculture, has developed along the Tianshan Mountains. In Southern Xinjiang, however, there is an oasis agricultural economy or mixed agropastoral economy that is heavily based on agriculture. We believe there are two possible explanations. One is the difference in cultural traditions. Northern Xinjiang was strongly influenced by the Scythian culture, Andronovo culture, Northern steppe culture, and other nomadic cultures, so there are some animal husbandry traditions. But the Southern Xinjiang was strongly influenced by agricultural groups from Western and Central Asia. The other is the geographic and geomorphic setting. The sites in Northern Xinjiang are mainly located in mountain valleys, river valleys, and alluvial fans, which are more suitable for raising livestock. However, the sites and tombs in Southern Xinjiang are typically located in oases on the edges of alluvial fans, in basins, or around rivers and lakes in deserts, which are more suitable for cultivating crops.

5.2 Mountain valleys, alluvial fans and oases: The landforms where people choose to live

Previous research has shown that Xinjiang's late Holocene palaeoenvironment was similar to modern times. That is, the climate was dry from the Bronze Age to the early Iron Age, and a lack of water rendered the vast deserts and Gobi uninhabitable. Our detailed examination of the geomorphic locations reveals that the sites in Xinjiang are mainly distributed in mountain valleys, alluvial fans, and oases (Table 1). There are two necessary environmental conditions: 1) Surface water sources, primarily rivers, lakes, gullies, springs, and so on, which are required for humans and livestock; 2) Fine-grained soil, including hydatogen sediments (alluvial or diluvial deposits) and eolian sediments (fine-grained weathering crust or loess), which are required for growing pasture or crops.

5.2.1 Mountain valleys and alluvial fans

The mountain valley includes the region near the lakes, rivers, and springs inside the mountains. Our analysis showed that many sites are located in the mountain valleys in the Altai Mountains, the Alatau-Borohoro Mountains, the middle and eastern Tianshan Mountains, and the Western and Southern Kunlun Mountains (Table 1). The ancient humans usually lived on platforms, terraces, or oases along alpine lakes or rivers. Most of these areas belong to the forest-grassland junction band.

An alluvial fan is a fan-shaped accumulation at the Mountain Pass (Yang, 2011). The piedmont alluvial fans are well-developed and of various shapes in arid Xinjiang. Groundwater is usually exposed between fans, forming spring water or a small oasis. There are also many gullies on the fans, providing abundant water sources for people and livestock. Our field investigation showed that the sites at the top of

TABLE 1 The geomorphic location of the sites mentioned in this study.

Area	Zone	Mountain vallys	Alluvial fans	Oases
Junggar Basin	Northern margin area of Junggar Basin	Tongtian Cave; Huahaizi No. 3; Wulasite; Zhelegabashi; Tuwaxincun	—	—
	Western margin area of Junggar Basin	Baiyanghe	Abudulashuiku; Aletengyemushuiku; Sazicun	Xiakalangguer
Tarim Basin	Northern margin area of Tarim Basin	Mohuchahan; Habuqihan I and II; Narenhabuqihangou; Daxigou No. 1; Daxigou No. 4; Qiaoenqiakeledeke	Baozidong M41; Duogang; Hejingzhonggongyeyuan	Kulansarike; Kezier; Keziertuershuiku; Karigayi; Tikemaike; Qunbake; Shanghuxiang; Xintala; Quhui
	Southern margin area of Tarim Basin	—	Liushui; Gudaqi	Yuansha Gucheng; Northern-Niya; Zhagunluke; Jiawaairike
	Southwestern margin area of Tarim Basin	Jierzankale; Xiabandi	—	Wupaer
	Eastern margin area of Tarim Basin	—	—	Gumugou; Xiaohe
Western Tianshan Mountains	Bortala River Basin	—	Adonqolu; Husta	Quanshuigou
	Ili River Basin	Tangbalesayi; Jialekesikayinte; Qirentuohai	Suodunbulake; Biesikalagai; Saerhuobu	Ayousaigoukou; Qiafuqihai Area A Plot XV and Plot X; Yeshikelieke Cemetery A site; Qiongkeke
Middle Tianshan Mountains	Areas on both sides of the middle Tianshan Mountains	Shimenzi; Sangongxiang; Xigou I area; Xigou II area; Sidaogou; Gangou; Saensayi; Ertanggou	Luanzagangzi; Baiyanghe; Dalongkou	Liangzhongchangyilian; Fukangfubeinongchangjijiandui; Chaiwobao; Shuinichang
	Turpan Basin	—	Yuergou	Jiayi; Shengjindian; Subeixi; Yanghai
Eastern Tianshan Mountains	Areas on both sides of the Eastern Tianshan Mountains	Hanqigou; Tuobeiliang; Baiqier; Xiagou	Xigou; Dongheigou (Shirenzigou); Hongshankou; Heigouliang; Yanchi Gucheng; Kuola; Liushugou; Huangtianshangmiaoergou I plot	Haiziyan; Qinggeda; Nanwan
	Hami Basin	—	—	Tianshanbeilu; Yanbulake; Wupu;Sayituer

the alluvial fans are usually near small oases between fans, such as Adonqolu at the southern foot of the Alatau Mountains, Baiyanghe in the middle Tianshan Mountains, and Kuola in the eastern Tianshan Mountains. Some other sites are near the streams on the alluvial fan, including Husta in the Alatau Mountains, Luanzhanggangzi in the middle Tianshan Mountains, and Shirenzigou, Hongshankou, and Liushugou in the Eastern Tianshan Mountains.

The alluvial fan is often adjacent to the foothill meadow. The fine sediment transported by flowing water will provide suitable soil for pasture growth. Thus, there are favorable conditions for animal husbandry on the alluvial fans. The sites located in the valleys and alluvial fans showed a primarily pastoral economy supplemented by agriculture. Furthermore, sites with hunter components are mostly located in valleys or on alluvial fans that are adjacent to the mountains. Such as the Tuoganbai No. 2 and Tuwaxincun Cemeteries at the southern foot of the Altai Mountains; the Husta Site in the Bortala River Basin; the Mohuchahan Site on the Northern edge of the Tarim Basin; and the Liushui Cemetery on the Southern edge of the Tarim Basin; the Shimenzi Cemetery at the foothills of the middle Tianshan Mountains; and the Yuergou Site on the edge of the Turpan Basin. The nearby mountains are important for hunting activities. In Xinjiang, mountain forests and steppes are usually distributed between 1,000 and 2,000 m asl. This region always coincides with the maximum precipitation zone and is usually distributed in the mid-mountain zone cut by the river valley (Xinjiang Comprehensive Expedition Team et al., 1978). Therefore, this region is rich in pasture and often becomes an ideal place for herding activities. As it is usually adjacent to the mountainous forests, there are abundant wild animals and plants for hunting and gathering, which is a beneficial supplement to animal husbandry.

5.2.2 Various oases

Oases are areas with a good combination of soil and water in arid areas (Yang, 2011). There are alluvial fan edge oases, river valley oases, and desert oases in Xinjiang. The sites located at the fan edge oases along the Tianshan Mountains include Quanshuigou, Chaiwobao, Haiziyan, *etc.* The sites in the Grand River Valley are mainly distributed in the Ili Basin, such as Qiongkeke, Ayousaigoukou, *etc.* The sites at the desert oases are often adjacent to ancient river channels or lakes. They are mainly distributed around the Tarim Basin, such as Zhagunluke, Yuansha Gucheng, Xiaohe, *etc.*

In some cases, the landforms of the sites changed from oases to arid deserts or dry platforms over time. For example, studies of the Lop Nor showed that ancient people had lived in the oases deep in the desert 3,800 years ago. Research on the Xiaohe Cemetery indicates several lake development periods around the site (Zhang et al., 2015; Zhang Y. F. et al., 2017). The sporopollen and phytolith results indicate that the Xiaohe people lived in an oasis, growing plants such as *Populus euphratica*, *Phragmites australis*, and *Typha*, while some drought plants such as *Ephedra*, *Salix*, *Artemisia,* and *Chenopodiaceae* grew in the surrounding desert (Li et al., 2013; Qiu et al., 2014). Recently published research showed that a genetically isolated local population adopted neighboring pastoralist and agriculturalist practices in the early Bronze Age, which allowed

TABLE 2 Geomorphic area and economic strategy of important sites and cemeteries.

Period	Zone	Site	Geomorphic area				Economic strategy			Others
			Mountain vallys	Alluvial fans	Oases	Others	Agriculture	Husbandry	Hunting	
Bronze Age	Northern margin area of Junggar Basin	Tongtian Cave	√				√		√	
		Ayituohan No.1				Planation surface in the south of Altai Mountain	√	√	√	
		Tuoganbai No.2					√	√	√	Existing Sacrificial remains
	Western margin area of Junggar Basin	Xiakalangguer			√		√	√		
	Northern margin area of Tarim Basin	Xintala			√		√			
	Eastern margin area of Tarim Basin	Xiaohe			√		√	√	√	Existing Sacrificial remains
		Gumugou			√		√	√	√	
	Bortala River Basin	Adonqolu		√			√	√		Winter camps
		Husta		√			√	√	√	High-grade residential or sacrificial site
		Quanshuigou			√		√	√		Metalurgical sites
	Hami Basin	Tianshanbeilu			√		√	√	√	
Mid-late Bronze Age to Early Iron Age	Northern margin area of Tarim Basin	Chawuhu No.1			√		√	√	√	
		Chawuhu No.4			√		√	√		
		Mohuchahan	√					√	√	
	Southern margin area of Tarim Basin	Liushui				On low hills and alluvial fans		√	√	Existing Sacrificial remains
	Southwestern margin area of Tarim Basin	Wupaer			√		√			
	Ili River Basin	Jirentaigoukou				Loess platforms on both sides of the river valley	√	√		Surrounded by metallurgical remains
		Qialegeer						√		
		Kalasu						√		
	Middle Tianshan Mountains	Luanzagangzi		√			√			
		Sidaogou	√				√	√		
		Saensayi	√				√	√		
	Turpan Basin	Yanghai			√		√	√	√	

(Continued on following page)

10.3389/feart.2023.1109905

TABLE 2 (*Continued*) Geomorphic area and economic strategy of important sites and cemeteries.

Period	Zone	Site	Geomorphic area				Economic strategy			Others
			Mountain vallys	Alluvial fans	Oases	Others	Agriculture	Husbandry	Hunting	
	Eastern Tianshan Mountains	Haiziyan			√		√	√		
		Shirenzigou		√			√	√		
		Liushugou		√			√	√	√	
		Kuola		√			√	√		Existing Sacrificial remains
		Yanchi Gucheng		√			√	√		
	Hami Basin	Yanbulake			√		√	√	√	
Early Iron Age	Northern margin area of Junggar Basin	Huahaizi No.3	√							Ceremonial center of early nomadic society
		Tuwaxincun	√					√	√	Existing Sacrificial remains
		Kalasu				planation surface in the south of Altai Mountain		√	√	
	Northern margin area of Tarim Basin	Duogang		√			√	√	√	
		Tikemaike			√					Metallurgical sites
		Qunbake			√		√	√	√	
	Southern margin area of Tarim Basin	Yuansha Gucheng			√		√	√	√	
		Zhagunluke			√		√	√	√	
	Ili River Basin	Qiongkeke			√		√	√		Existing Sacrificial remains
	Middle Tianshan Mountains	Shimenzi	√					√	√	
	Turpan Basin	Yuergou		√			√	√	√	
		Shengjindian			√		√	√	√	
		Subeixi			√		√	√	√	
		Jiayi			√		√	√	√	
	Eastern Tianshan Mountains	Heigouliang		√			√	√		Existing Sacrificial remains
	Hami Basin	South Aisikexiaer				Alluvial plain	√	√	√	Existing Sacrificial remains

10.3389/feart.2023.1109905

them to settle and thrive along the shifting riverine oases of the Taklamakan (Zhang F. et al., 2021). Our field investigation at the Wupaer Site showed that the remains were buried in lacustrine sediments, indicating that the ancient people lived near a lake or in an oasis, which is quite different from nowadays.

Oases are generally groundwater outcropping zones with fine-grained and fertile soils. With excellent water and soil conditions, oases are suitable for planting crops and establishing settlements. As a result, agricultural activities are usually carried out in the oases, forming a mixed agropastoral economy. The materials in this paper show that the sites with a heavy proportion of agriculture are mainly distributed near oases. For example, tools such as a sickle, pestle, millstone, and hoe were found in the oases in the Turpan Basin, the Hami Basin, and on the Northern margin of the Tarim Basin (Figures 3A, 4.8.10.20; Figures 5B, 17.21; Figures 6B, 17.19.20). The barley, wheat, and millet were discovered in the Northern Tarim Basin alluvial fan margin oases (Figures 3A, 8.10). Barley (naked), wheat, and millet were unearthed in some oases of the Turpan Basin (Figures 5A, 17.19.20.21). In the desert oases inside the Tarim Basin, Xintala and Yuansha Gucheng also developed oasis agriculture. Isotopic results evidence that the people ate millet (Figures 5B, 18; Figures 6B, 16.18).

In general, the valleys or alluvial fans close to the mountains have shown a mixed herding-hunting economy, and the sites near the large oases have shown a mixed agropastoral economy with a high proportion of agriculture (Table 2).

It should be noted that people have most likely lived in different geomorphic areas during different seasons since the Bronze Age (Jia, 2018). Therefore, the sites showing different economic strategies in various landforms probably also indicate that people will engage in different economic activities along with their seasonal migration. The complex combination of stock raising, crop planting, and hunting depends largely on different landforms, microenvironments, and local ecology.

5.3 Special site, social complexity and the trend of nomadism

Sites of special nature in Xinjiang include ritual sites and metallurgical sites. Six ritual sites were found, including Huahaizi No.3 in the northern margin of Junggar Basin; Qiongkeke in the Ili River Valley; Hongshangou on the northern edge of Tarim Basin; Dongheigou, Hongshankou, and Kuola Site in the eastern Tianshan Mountains. Because these ritual sites are all close to certain large center settlements, we believe they probably serve some special purpose. One of the most typical ritual sites is Huahaizi No. 3. This location is on the lakeshore in a valley surrounded by the Altai Mountains. There are three alpine lakes formed by melting alpine snow, and surrounded by some small rivers and lakes. Deer-stone remains were found on this site. The excavators speculated that it would probably be a nomadic ceremonial center to hold the summer rituals (Guo et al., 2016). The nomads might have chosen this special landform to hold regular ritual activities because it is around the alpine lake at the top of the high mountain; it is easy to communicate with heaven and strengthen people's cohesion.

The metallurgical sites are mainly distributed in the Ili Valley and the Hami Basin. The metallurgical site in the Western Tianshan Mountains includes Quanshuigou and Jirentaigoukou. There are three ancient copper mine sites near the Jirentaigoukou: Nulasai, Yuantoushan, and Kezilekezangbei (Wang et al., 2019). The flat terrain of Bortala Valley and Kashi Valley provides the possibility of East-West communication. The favorable environmental conditions of the fan margin oasis and the loess platform lay the foundation for developing a stable mixed agropastoral economy, which probably gave rise to metallurgical behavior (Zhang Y. P. et al., 2021). The Tikemaike is located in the river valley between the Queletage Mountain and the Kuche River, with a rich iron ore mine nearby. The relics, such as refining slag, flow pipes, and pottery pieces, are distributed on the slopes of the mountain range, visible on the surface (Ruan et al., 2016). In the eastern Tianshan Mountains region, the archaeological investigation has found ancient turquoise mines, turquoise debris, and house relics in both the Heishanling and Tianhudong Sites (Li et al., 2019). It could be concluded that the metallurgical sites are generally located in landforms with good transportation and favorable soil and water conditions, such as river valleys or oases. Besides, there is also evidence to show that some metallurgical sites are close to mining sources. From the perspective of spatial distribution, the metallurgical sites in the western Tianshan Mountains may be more affected by western metallurgical technology (Tan, 2022). The Ili Valley consists of three mountain ranges that gradually contracted from west to east, to the west it is connected with the Zhetysu region of Kazakhstan (Tan, 2022). Multiple east-west river systems provide transportation routes for people to communicate and spread metallurgical technology. The turquoise metallurgy technology in the Hami Basin of the Eastern Tianshan Mountains is more likely to be influenced by the eastern central plain culture (Li et al., 2020; Xian et al., 2020).

There are six large settlements with an area of more than 7 km^2. Archaeologists have excavated high-level burials at the Jirentaigoukou Site, indicating the emergence of social complexity in the Bronze Age (Yuan, 2022). Husta, Adonqolu, Shirenzigou, Hongshankou, and Kuola are among the other major central settlements. These sites are located in large river valleys or alluvial fans with abundant water and pastures. These microenvironments with favorable soil-water composition and high land-bearing capacity often have homogeneity in a large region. That is to say, there are many similar microenvironments around. As a result, there are usually many homochronous sites around the central site. Under similar ecological conditions, these people developed similar cultures and probably communicated frequently with each other. As the population density increased, social complexity arose, and the central settlement appeared.

The sites that lasted a long time have shown signs of normalization. For example, the excavations at Jirentaigoukou and Haiziyan revealed an obvious tendency from large and complex houses in the late Bronze Age to small and simple dwellings in the early Iron Age. The remains of grain storage, processing, and cooking functions are gradually disappearing (Haiziyan) (Ren et al., 2020). Most scholars believe that the early nomadic economy developed from the pastoralism of the Bronze Age (Shao and Wu, 2020). Ethnological studies suggested that the Husta and Adonqolu had developed a seasonal transhumance economy and that summer pasture and winter pasture had appeared (Cong et al., 2018; Jia, 2018; Jia, 2019). However, the highly mobile grassland nomadic economy was not formed until the early Iron Age (Shao and Wu, 2020).

Although it is necessary to consider the economy, technology, society, politics, and other factors, scholars believe that the final appearance of nomadism needs to be stimulated by a specific motivator, and most of the cases are related to environmental changes (Gumilev, 1996; Tairov, 2003). Vinogradov (Vinogradov and Epimakhov, 2000) and Xi (2014) et al. believed that the

changes in economic organization, environmental resources, and related metallurgical production caused by drought or cold climate events were the causes of nomadism. According to An et al. (2020), the humidity has caused pastures to thrive for the past 4,000 years, hastening the process of nomadism. Based on the materials we have sorted out, both animal husbandry and agriculture were greatly developed from the Bronze Age to the early Iron Age. During the Bronze Age, the differentiation between animal husbandry and agriculture did not occur because of an undeveloped economy and technology (Shao and Wu, 2020). Since 4,000 BP, the ancient climate in Xinjiang has become wetter, which probably promoted the growth of pasture and crops, resulting in animal husbandry and agriculture development. Thus, the scale and specialization of animal husbandry increased, which led to the differentiation of herding and farming activities. Finally, specialized and highly mobile nomadism emerged in the early Iron Age.

6 Conclusion

We have drawn the three tentative conclusions listed below based on analyzing the geomorphic patterns and subsistence modes of Xinjiang's Bronze Age and early Iron Age sites.

(1) There are different economic strategies between southern and northern Xinjiang. Northern Xinjiang's economy was primarily based on animal husbandry; areas along the Tianshan Mountains had a mixed agropastoral economy that was primarily based on animal husbandry and supplemented by agriculture. In southern Xinjiang, there is an typical oasis agricultural economy or mixed agropastoral economy heavily based on agriculture.
(2) Certain regions of the landscape with surface water sources and fine-grained soil cover were inhabited by ancient humans. This consists primarily of mountain valleys, alluvial fans, and various oases. The presence of hunting activities is heavily influenced by the distance to the mountains, whereas adequately sized oases favor agriculture. Accordingly, sites near mountains are more likely to have developed a mixed pastoral-hunting economy, sites in mountain valleys or on alluvial fans are more likely to have developed a livestock-based economy, and oases of large size are more likely to have developed a mixed agropastoral economy.
(3) Some unique ritual sites are found in specific geomorphic regions (e.g., near alpine lakes); metallurgical sites are more likely along the geographical channel. Large settlements are usually situated in vast river valleys or alluvial fans with ample water and pasture. Under similar microenvironmental conditions, more similar cultural and economic patterns tend to evolve amongst sites within the same area, resulting in more significant central settlements and social complexity.

This paper presents a preliminary discussion on the economic strategy and its differentiation between geographic units and landforms, which is helpful to comprehend the "man-land" dynamics in Xinjiang. More detailed case studies, however, are still required to promote an in-depth understanding of the complex mixed agropastoral economy from the Bronze Age to the early Iron Age.

Data availability statement

The original contributions presented in the study are included in the article/Supplementary Material, further inquiries can be directed to the corresponding author.

Author contributions

JZ designed the research. JZ and CY performed the research. JZ and CY analyzed the data. CY and JZ completed writing. XY edited the figures.

Funding

This research was funded by the National Natural Science Foundation of China (41971114) and the important project of National Social Science Foundation of China (21&ZD223, 18ZDA172).

Acknowledgments

The authors are greatful to Yixian Lin for helping to edit the manuscript.

Conflict of interest

The authors declare that the research was conducted in the absence of any commercial or financial relationships that could be construed as a potential conflict of interest.

Publisher's note

All claims expressed in this article are solely those of the authors and do not necessarily represent those of their affiliated organizations, or those of the publisher, the editors and the reviewers. Any product that may be evaluated in this article, or claim that may be made by its manufacturer, is not guaranteed or endorsed by the publisher.

References

An, C. B., Zhang, M., Wang, W., Liu, Y., Duan, F. T., and Dong, W. M. (2020). The characteristics of Xinjiang's geographical environment and the formation of the pattern of agriculture and animal husbandry. *Sci. China Earth Sci.* 50 (2), 295–304.

An, J. Y., and Yuan, J. (1998). Research report on animal skeletons at Chawuhu goukou cemetery No. 1 and 3, hejing county. *Xinjiang. Archaeol.* 7, 63–68.

Chan, A., and Shao, H. Q. (2018). Современные решения актуальныч Проблем евразийской арчеолоГии. Сборник научныч трудов 2. *Contemp. Solutions Curr. Problems Eurasian Archaeol. Collect. Sci. Pap.* 2, 55–59.

Chang, C. (2002). *The evolution of steppe communities from the bronze Age through medieval periods in southeastern Kazakhstan (Zhetysu): The Kazakh-American talgar project 1994-2001*. Sweet Briar, Virginia: Sweet Briar College.

Chen, F. H., Jia, J., Chen, J. H., Li, G. Q., Zhang, X. J., Xie, H. C., et al. (2016). A persistent Holocene wetting trend in arid central Asia, with wettest conditions in the late Holocene, revealed by multi-proxy analyses of loess-paleosol sequences in Xinjiang, China. *Quat. Sci. Rev.* 146, 134–146. doi:10.1016/j.quascirev.2016.06.002

Chen, F. H., Yu, Z. C., Yang, M. L., Ito, E., Wang, S. M., Madsen, D. B., et al. (2008). Holocene moisture evolution in arid central Asia and its out-of-phase relationship with Asian monsoon history. *Quat. Sci. Rev.* 27 (3-4), 351–364. doi:10.1016/j.quascirev.2007.10.017

Chen, G. (1990). A little discussion of Yanbulake culture. *West. Regions Stud.* 1, 81–96.

Chen, X. L. (2017). New progress in analysis methods of carbon and nitrogen stable isotopes and agricultural archaeology. *Agric. Archaeol.* 154 (6), 13–25.

Chen, X. L., Yu, J. J., and You, Y. (2017). Horse burial customs in Kalasu cemetery of Xinjiang seen from stable carbon and nitrogen isotope. *West. Regions Stud.* 108 (4), 89–143. doi:10.16363/j.cnki.xyyj.2017.04.008

Cong, D. X., and Chen, G. (1991). Brief report on the second and third excavations of qunbake cemetery in luntai county, Xinjiang. *Archaeology* 8, 684–771.

Cong, D. X., Jia, X. B., Guo, W., Shang, G. J., and Ge, L. (2013). The Adonqolu site and cemetery in wenquan county, Xinjiang. *Archaeology* 550 (7), 25–32.

Cong, D. X., Jia, X. B., Jia, W. M., Alison, B., and Paula, D. M. (2018). Mountaintop remains of the bronze age by the Bortala River Valley, Xinjiang. *West. Regions Stud.* 110 (2), 138–150. doi:10.16363/j.cnki.xyyj.2018.02.013

Cong, D. X., Zhao, C. Y., and Jia, W. M. (2021). Human migration and dietary structure of the adunqiaolu site in Xinjiang: A pilot study. *Jianghan Archaeol.* 177 (6), 233–239.

Debaine, F. C., Debaine, F., and Idriss, A. (2010). "The Taklimakan oases: An environmental evolution shown through geoarchaeology," in *Water and sustainability in arid regions*. Editors G. Schneier-Madanes and M. F. Courel (Dordrecht: Springer), 181–202. doi:10.1007/978-90-481-2776-412

Dodson, J. R., Li, X., Zhou, X., Zhao, K., Sun, N., and Atahan, P. (2013). Origin and spread of wheat in China. *Quat. Sci. Rev.* 72, 108–111. doi:10.1016/j.quascirev.2013.04.021

Dong, G. H., Du, L. Y., Yang, L., Lu, M. X., Chou, M. H., Li, H. M., et al. (2022). Dispersal of crop-livestock and geographical-temporal variation of subsistence along the Steppe and Silk Roads across Eurasia in prehistory. *Sci. China Earth Sci.* 52 (8), 1476–1498.

Dong, W. M., An, C. B., Zhang, T. N., and Alifujiang, N. Z. (2022a). Subsistence strategies of people from Chawuhu culture in the middle of tianshan mountains: A case study of mohuchahan site from hejing county. *Quat. Sci.* 42 (1), 80–91. doi:10.11928/j.issn.1001-7410.2022.01.07

Dong, W. M., An, C. B., Yu, J. J., and Chen, X. L. (2022b). The subsistence strategy of the residents in the bronze-early altay region and its implications-evidence from bone stable isotopes. *West. Regions Stud.* 125 (1), 45–170. doi:10.16363/j.cnki.xyyj.2022.01.005

Dong, W. M. (2021). *Recipes of the prehistoric residents of the Hami Basin*. Shanghai: Fudan University Press.

Doumani, P., Frachetti, M. D., Beardmore, R., Schmaus, T. M., Spengler, R. N., III, and Mar'yashev, A. N. (2015). Burial ritual, agriculture, and craft production among Bronze Age pastoralists at Tasbas (Kazakhstan). *Archaeol. Res. Asia* 1-2, 17–32. doi:10.1016/j.ara.2015.01.001

Du, S. Q., and Ren, M. (2017). A preliminary study on the archaeological and cultural remains from the bronze age to the early iron age in changji, Xinjiang. *West. Regions Stud.* 106 (2), 48–56. doi:10.16363/j.cnki.xyyj.2017.02006

Feng, Z. D. (2017). *Climate and hydrological changes in northern Xinjiang and its surrounding areas in the past 10,000 years*. Lanzhou: Lanzhou University Press.

Frachetti, M. D. (2009). Differentiated landscapes and non-uniform complexity among bronze age societies of the eurasian steppe. *Soc. Complex. Prehist. Eurasia* 3, 19–46. doi:10.1017/CBO9780511605376.004

Frachetti, M. D. (2012). Multiregional emergence of mobile pastoralism and nonuniform institutional complexity across eurasia. *Curr. Anthropol.* 53 (1), 2–38. doi:10.1086/663692

Frachetti, M. D. (2008). *Pastoralist landscapes and socialinteraction in bronze Age eurasia*. Berkeley: University of California Press.

Frachetti, M. D., Smith, C. E., Traub, C. M., and Williams, T. (2017). Nomadic ecology shaped the highland geography of Asia's Silk Roads. *Nature* 543 (7644), 193–198. doi:10.1038/nature21696

Frachetti, M. D., Spengler, R. N., Fritz, G. J., and Mar'yashev, A. N. (2010). Earliest direct evidence for broomcorn millet and wheat in the central Eurasian steppe region. *Antiquity* 84 (326), 993–1010. doi:10.1017/s0003598x0006703x

Gong, Y. W., Yang, Y. M., Ferguson, D. K., Tao, D. W., Li, W. Y., Wang, C. S., et al. (2011). Investigation of ancient noodles, cakes, and millet at the Subeixi Site, Xinjiang, China. *J. Archaeol. Sci.* 38 (2), 470–479. doi:10.1016/j.jas.2010.10.006

Gumilev, L. N. (1996). Isioki ritma kochevoi kultury sredinnoi aziyi: Opyt istorikogeographicheskogo sinieza. *Nar. I Afriki* 4, 25–46.

Guo, W. (2012). *Archaeological research on late prehistoric society in Xinjiang*. Shanghai: Shanghai Ancient Books Press.

Guo, W., Zhang, H. L., Lv, E. G., Wu, D. J., Zheng, J., Yao, R. W., et al. (2016). The excavation of the Huahaizi No. 3 site in qinghe county, Xinjiang. *Archaeology* 588 (9), 25–37.

Han, J. Y. (2007). *Bronze Age and early iron Age culture in Xinjiang*. Beijing: Heritage Press.

Han, J. Y., and Chen, X. L. (2017). The discovery and preliminary understanding of the bronze age remains in Quanshuigou, shuanghe city, Xinjiang. *West. Regions Stud.* 105 (1), 142–143. doi:10.16363/j.cnki.xyyj.2017.01.014

Han, J. Y. (2021). The three stages of early sino-western cultural interactions. *Acta Archaeol. Sin.* 222 (3), 317–338.

Hartman, G. (2011). Are elevated $\delta^{15}N$ values in herbivores in hot and arid environments caused by diet or animal physiology? *Funct. Ecol.* 25 (1), 122–131. doi:10.1111/j.1365-2435.2010.01782.x

Haruda, A. (2018). Regional pastoral practice in central and southeastern Kazakhstan in the Final Bronze Age (1300–900 BCE). *Archaeol. Res. Asia* 15, 146–156. doi:10.1016/j.ara.2017.09.004

He, D. X. (1999). Ancient tombs in Shanghuxiang, kuerle city, Xinjiang. *Cult. Relics* 2, 32–40.

Hedges, R. E. M., and Reynard, L. M. (2007). Nitrogen isotopes and the trophic level of humans in archaeology. *J. Archaeol. Sci.* 34 (8), 1240–1251. doi:10.1016/j.jas.2006.10.015

Hou, Z. J. (2016). Archaeological discovery of hongshan tombs in heshuo county, Xinjiang in 2015. *West. Regions Stud.* 103 (3), 132–135+2. doi:10.16363/j.cnki.xyyj.2016.03.017

Huang, Y. P. (2008). Animal bone analysis of Yuansha Gucheng site in Keriya River, yutian county, Xinjiang. *A Collect. Stud. Archaeol.* 0, 532–540.

Jia, W. M. (2018). Archaeological observations on prehistoric nomadic activities: Analysis of prehistoric settlements in the western tianshan mountains of Xinjiang. *West. Regions Stud.* 111 (3), 63–145.

Jia, X. B. (2019). Major discoveries of the excavation at Husta, wenquan county, Xinjiang, China. *West. Regions Stud.* 113 (1), 139–141. doi:10.16363/j.cnki.xyyj.2019.01.012

Jiang, H. E., Lv, E. G., and Zhang, Y. N. (2021). A consideration of the lifestyle of the ancient Yanghai people in turfan. *Turfanological Res.* 27 (1), 41–154. doi:10.14087/j.cnki.65-1268/k.2021.01.005

Jiang, H. G., Wu, Y., Wang, H. H., Ferguson, D. K., and Li, C. S. (2013). Ancient plant use at the site of Yuergou, Xinjiang, China: Implications from desiccated and charred plant remains. *Veg. Hist. Archaeobotany* 22 (2), 129–140. doi:10.1007/s00334-012-0365-z

Jiang, H. G., Zhang, Y. B., Lv, E. G., and Wang, C. S. (2014). Archaeobotanical evidence of plant utilization in the ancient turpan of Xinjiang, China: A case study at the shengjindian cemetery. *Veg. Hist. Archaeobotany* 24 (1), 165–177. doi:10.1007/s00334-014-0495-6

Li, J. F., Abuduresule, I., Hueber, F. M., Li, W. Y., Hu, X. J., Li, Y. Z., et al. (2013). Buried in sands: Environmental analysis at the archaeological site of Xiaohe cemetery, Xinjiang, China. *PLoS ONE* 8 (7), e68957. doi:10.1371/journal.pone.0068957

Li, Y. Q. (2020). Agriculture and palaeoeconomy in prehistoric Xinjiang, China (3000–200 BC). *Veg. Hist. Archaeobotany* 30, 287–303. doi:10.1007/s00334-020-00774-2

Li, Y. X., Tan, Y. C., Jia, Q., Zhang, D. Y., Yu, J. J., Duan, C. W., et al. (2019). Preliminary investigation of two turquoise mining sites in Hami, Xinjiang. *Archaeol. Cult. Relics* 236 (6), 22–27.

Li, Y. X., Yu, J. J., Xian, Y. H., Tan, Y. C., Zhu, Z. Z., Cao, K., et al. (2020). A survey of the ancient turquoise mining sites at heishanling in ruoqiang, Xinjiang. *Cult. Relics* 771 (8), 4–13. doi:10.13619/j.cnki.cn11-1532/k.2020.08.001

Li, Y., You, Y., Liu, Y. T., Xu, N., Wang, J. X., Ma, J., et al. (2016). The study on the vertebrae abnormality of the Shirenzigou and xigou sites in Xinjiang. *Archaeology* 580 (1), 108–120.

Lin, M. C. (2016). Seima-turbino culture and the proto-silk road. *Chin. Cult. Relics* 1-2, 241–262. doi:10.21557/ccr.48032340

Liu, X. T., and Guan, B. (2002). Important harvests of prehistoric archaeology in the Ili River Valley in Xinjiang. *West. Regions Stud.* 4, 106–108. doi:10.16363/j.cnki.xyyj.2002.04.019

Liu, Y., Liu, L. Y., Zhang, M., Zhang, Y., and An, C. B. (2021). A preliminary study on the estimation of the population size of the Saensayi and Yanghai sites in Xinjiang in different times. *Quat. Sci.* 41 (1), 267–275.

Marino, B. D., and McElroy, M. B. (1991). Isotopic composition of atmospheric CO_2 inferred from carbon in C_4 plant cellulose. *Nature* 349 (6305), 127–131. doi:10.1038/349127a0

Qiu, Z. W., Yang, Y. M., Shang, X., Li, W. Y., Abuduresule, Y., Hu, X. J., et al. (2014). Paleo-environment and paleo-diet inferred from early bronze age cow dung at Xiaohe cemetery, Xinjiang, NW China. *Quat. Int.* 349, 167–177. doi:10.1016/j.quaint.2014.03.029

Qu, Y. T., Hu, X. J., Wang, T. T., and Yang, Y. M. (2020). Early interaction of agropastoralism in eurasia: New evidence from millet-based food consumption of afanasyevo humans in the southern Altai mountains, Xinjiang, China. *Archaeol. Anthropol. Sci.* 12 (8), 195–207. doi:10.1007/s12520-020-01094-2

Ren, M., Ma, J., Xi, T. Y., Tian, Y. L., and Jiang, X. L. (2020). Brief report on the excavation of the haiziyan site in balikun, Xinjiang in 2017. *Cult. Relics* 775 (12), 21–36. doi:10.13619/j.cnki.cn11-1532/k.2020.12.002

Ruan, Q. R., Hu, W. L., Zhang, J., Guan, B., Liu, Y. S., Wang, Y., et al. (2014). Brief report on the excavation of the wutulan cemetery in nileke county, Xinjiang. *Cult. Relics* 703 (12), 50–63. doi:10.13619/j.cnki.cn11-1532/k.2014.12.002

Ruan, Q. R., Wang, Y. Q., and Alifu, N. Z. (2012). Excavation of Koksu West Cemetery No. 2 in tekes county, Xinjiang. *Archaeology* 540 (9), 3–101.

Ruan, Q. R., Wang, Y. Q., Ni, J. T., Yu, Y. J., and Liu, Y. S. (2016). Brief report on excavation of the kuche-ehuobulake railway area, Kuche county, Xinjiang. *West. Archaeol.* 1, 29–50.

Shao, H. Q. (2009). Early collision and fusion of Eastern and Western cultures - from the evolution of cultural pattern in Xinjiang's prehistoric period. *Soc. Sci. Front* 171 (9), 146–150.

Shao, H. Q. (2018). *The evolution of the prehistoric cultural pattern in Xinjiang and its relationship with the surrounding culture*. Beijing: Science Press.

Shao, H. Q., and Wu, Y. T. (2020). An analysis of the origin of early nomadic culture. *North. Cult. Relics* 141 (1), 28–37. doi:10.16422/j.cnki.1001-0483.20200319.004

Shao, K. L., Zhang, J. P., Cong, D. X., Jia, W. M., Cui, A. N., and Wu, N. Q. (2019). Analysis of plant microfossils reveals the ancient survival strategy of the Adunqiaolu site in Xinjiang, China. *Quat. Sci.* 39 (1), 37–47. doi:10.11928/j.issn.1001-7410.2019.01.04

Shevchenko, A., Yang, Y. M., Knaust, A., Thomas, H., Jiang, H. E., Lu, E. G., et al. (2014). Proteomics identifies the composition and manufacturing recipe of the 2500-year old sourdough bread from Subeixi cemetery in China. *J. Proteomics* 105, 363–371. doi:10.1016/j.jprot.2013.11.016

Shui, T. (2016). The formation and influence of the interaction circle in the Altai Region during the Bronze Age - with the discovery of China as the main line. *Anc. Civilizations Period.* 10 (0), 262–267.

Si, Y., Lv, E. G., Li, X., Jiang, H. G., Hu, Y. W., and Wang, C. S. (2013). Exploration of human diets and populations from the Yanghai tombs, Xinjiang. *Sci. Bull.* 58 (15), 1422–1429. doi:10.1360/972012-1007

Spengler, R. N., III, Frachetti, M. D., and Doumani, P. N. (2014). Late bronze age agriculture at Tasbas in the Dzhungar mountains of eastern Kazakhstan. *Quat. Int.* 348, 147–157. doi:10.1016/j.quaint.2014.03.039

Spengler, R. N., III, Miller, A. V., Schmaus, T., Matuzevičiūtė, G. M., Miller, B. K., Wilkin, S., et al. (2021). An imagined past?: Nomadic narratives in central asian archaeology. *Curr. Anthropol.* 62, 251–286. doi:10.1086/714245

Spengler, R. N., III, Ryabogina, N., Tarasov, P. E., and Wagner, M. (2016). The spread of agriculture into northern central Asia: Timing, pathways, and environmental feedbacks. *Holocene* 26 (10), 1527–1540. doi:10.1177/0959683616641739

Spengler, R. N., III, and Willcox, G. (2013). Archaeobotanical results from Sarazm, Tajikistan, an early bronze age settlement on the edge: Agriculture and exchange. *Environ. Archaeol.* 18 (3), 211–221. doi:10.1179/1749631413y.0000000008

Sun, B. G., and Chen, G. (1987). Brief report on the first excavation of the qunbake cemetery in luntai, Xinjiang. *Archaeology* 11, 987–1061.

Tairov, A. D. (2003). *Izmeneniya klimata stepei i lesostepei Tsentral'noi Evrazii vo II–I tys. do n.e. Materialy k istoricheskim rekonstruktsiyam.Chelyabinsk. Krokus*.

Tan, Y. C. (2022). "The study on early bronze metallurgy within the regins of west tianshan mountains in Xinjiang during the 2nd mellenium BC,". PhD dissertation (Beijing: University of Science and Technology Beijing).

Tang, Y. P., Fu, Y. H., Xi, T. Y., Wang, W. Z., Rouzi, M., Ma, J., et al. (2020). Brief report on archaeological excavation of Kuola site in yiwu county, Xinjiang, from 2017 to 2018. *Archaeology* 771 (8), 14–28. doi:10.13619/j.cnki.cn11-1532/k.2020.08.002

Tian, D., Ma, J., Ren, M., Xi, T. Y., Wang, J. X., and Zhao, Z. J. (2021). Barley production in early Xinjiang: Evidence from archaeobotanical remains in the Shirenzigou site, northern tianshan mountains. *Agric. Hist. China* 40 (3), 44–55.

Tian, D. (2018). "Phytoarchaeological research in the Eastern Tianshan area in the 1st millennium BC,". PhD dissertation (Xi'an: Northwestern University).

Vinogradov, N., and Epimakhov, A. (2000). *From a settled way of life to nomadism. Variants in models of transition. (Kurgans, ritual sites, and settlements eurasian bronze and iron Age)*. Oxford: Archaeopress, 240–246.

Wang, B., Lu, L. P., Xu, H. H., Ai, A. N. W. E., and Mai, Y. S. F. (2003). Excavation of Zhagunluke No.1 in charchan, xingjiang. *Acta Archaeol. Sin.* 148 (1), 89–176.

Wang, J. X., and Xi, L. (2009). Archaeological research on early nomadic cultural settlements in the Eastern Tianshan Mountains area. *Archaeology* 496 (1), 28–114.

Wang, J. X., Zhou, X. M., Xi, T. Y., Ye, Q., Li, M. Y., and Ma, J. (2014). A preliminary report on the 2009 excavation of the Tuobeiliang cemetery in yiwu county, Xinjiang. *Archaeol. Cult. Relics* 204 (4), 24–121.

Wang, L. J., Wang, Y. Q., Li, W. Y., Spate, M., Reheman, K., Sun, Q. L., et al. (2020). Inner Asian agropastoralism as optimal adaptation strategy of Wupu inhabitants (3000–2400 cal BP) in Xinjiang, China. *Holocene* 31 (2), 203–216. doi:10.1177/0959683620941139

Wang, L., Xiao, G. Q., Liu, Z. J., Lv, E. G., and Wu, Y. (2014). Brief report on excavation of Jiayi cemetery in turpan, Xinjiang. *Turfanological Res.* 13 (1), 19–161. doi:10.14087/j.cnki.65-1268/k.2014.01.015

Wang, Q., Ma, Z. K., Chen, Q. H., Ma, Y. C., Ruan, Q. R., Wang, Y. Q., et al. (2020). Microbotanical remains provide direct evidences for the functional study of stone tools from Jartai Pass site in Nilka County, Xinjiang. *Quat. Sci.* 40 (2), 450–461. doi:10.11928/j.issn.1001-7410.2020.02.15

Wang, T. T., Dong, W., Chang, X. E., Yu, Z. Y., Zhang, X. Y., Wang, C. S., et al. (2017). Tianshanbeilu and the isotopic millet road: Reviewing the late neolithic/bronze age radiation of human millet consumption from north China to europe. *Natl. Sci. Rev.* 6 (5), 1024–1039. doi:10.1093/nsr/nwx015

Wang, W., and Feng, Z. D. (2013). Holocene moisture evolution across the Mongolian plateau and its surrounding areas: A synthesis of climatic records. *Earth Sci. Rev.* 122, 38–57. doi:10.1016/j.earscirev.2013.03.005

Wang, W., Liu, Y., Duan, F. T., Zhang, J., Liu, X. Y., Reid, R. E. B., et al. (2020). A comprehensive investigation of Bronze Age human dietary strategies from different altitudinal environments in the Inner Asian Mountain Corridor. *J. Archaeol. Sci.* 121, 105201–201. doi:10.1016/j.jas.2020.105201

Wang, Y. Q., and Dang, Z. H. (2011). New archaeological discovery of the south Aisikexiaer cemetery in wubao, Hami, Xinjiang. *West. Regions Stud.* 82 (2), 134–137. doi:10.16363/j.cnki.xyyj.2011.02.017

Wang, Y. Q., and Tian, X. H. (2012). Brief report on the excavation of Baiyanghe cemetery in Tacheng area, Xinjiang. *Archaeology* 540 (9), 17–105.

Wang, Y. Q., Yuan, X., and Ruan, Q. R. (2019). The achievement and preliminary study on the excavation during 2015-2018 at Jirentai Goukou site, Nileke County, Xinjiang,China. *West. Regions Stud.* 113 (1), 133–138. doi:10.16363/j.cnki.xyyj.2019.01.011

Wu, X. H., Ma, S., and Ai, L. J. (2016). Archaeological excavation of Liushui cemetery of bronze age in yutian county. *Xinjiang Cult. Relics* 12, 19–36.

Wu, X. T., Zhang, X. X., Li, Y., Jin, Z. Y., Wang, L., and Wang, B. H. (2021). Analysis on human migration and dietary structure of the Jiayi cemetery in Turpan,Xinjiang. *West. Regions Stud.* 123 (3), 83–171. doi:10.16363/j.cnki.xyyj.2021.03.010

Wu, Y., Hu, X. J., Ai, T., Ni, J. T., Yu, Y. J., Sai, L. K., et al. (2017). The excavation of Aletengyemulei water control cemetery. *Res. China's Front. Archaeol.* 1, 13–42.

Wu, Y. (2005). New harvest from the archaeological excavation of the Xiabandi cemetery in Kashgar, Xinjiang. *West. Regions Stud.* 1, 109–113. doi:10.16363/j.cnki.xyyj.2005.01.015

Xinjiang Comprehensive Expedition Team; Chinese Academic of Science; Institute of Geography, Chinese Academy of Sciences; Department of Geography Beijing Normal University; Geomorphology Group of Xinjiang, Comprehensive Expedition Team (1978). *Xinjiang geomorphology*. Beijing: Science Press.

Xi, T. Y., Fu, Y. H., Wang, W. Z., Tang, Y. P., Tian, D., Rozi, M., et al. (2020). Brief report on investigation of yanchigucheng site in yiwu, Xinjiang in 2017. *West. Archaeol.* 1, 26–38.

Xi, T. Y. (2014). "Study on settlement sites in eastern tianshan mountains from bronze age to early iron age,". PhD dissertation (Xi'an: Northwestern University).

Xian, Y. H., Li, X. T., Zhou, X. Q., Ma, J., Li, Y. X., and Wen, R. (2020). Study on chemical composition and provenience differentiation of turquoises excavated from two sites in Xinjiang. *Spectrosc. Spectr. Analysis* 40 (3), 967–970.

Xiao, G. Q. (2018). "The review and study of Jia yi cemetery in turfan, Xinjiang,". Master dissertation (Xi'an: Northwestern University).

Xinjiang Institute of Cultural Relics and Archaeology (2015a). Archaeological excavation report of wulasite cemetery in Altai region. *Xinjiang Cult. Relics* 2, 59–64.

Xinjiang Institute of Cultural Relics and Archaeology (2012). Brief report on the archaeological excavation of Ertanggou cemetery in shanshan county. *Xinjiang Cult. Relics* 1, 92–99.

Xinjiang Institute of Cultural Relics and Archaeology (2016b). Brief report on the archaeological excavation of the Abudulashuiku cemetery in Tacheng County. *Xinjiang Cult. Relics* 1, 50–60.

Xinjiang Institute of Cultural Relics and Archaeology (2013c). Brief report on the archaeological excavation of the Ayousaigoukou site in Xinyuan County. *Xinjiang Cult. Relics* 2, 4–10.

Xinjiang Institute of Cultural Relics and Archaeology (2013b). Brief report on the archaeological excavation of the gudaqi cemetery in qiemo county. *Xinjiang Cult. Relics* 3-4, 67–74.

Xinjiang Institute of Cultural Relics and Archaeology (2013a). Brief report on the archaeological excavation of the zhelegabashi cemetery in fuyun county. *Xinjiang Cult. Relics* 2, 43–51.

Xinjiang Institute of Cultural Relics and Archaeology; Culture Heritage and Archaeology Research Center of North-West University; Yili Prefectural Bureau of Culture Heritage (2007). Excavation report of jialekesikayin cemetery in nileke county. *Xinjiang Cult. Relics* 4, 1–14.

Xinjiang Institute of Cultural Relics and Archaeology (1992). Chawuhu cemetery No. 1, hejing county, Xinjiang. *Xinjiang Cult. Relics* 4, 11–68.

Xinjiang Institute of Cultural Relics and Archaeology (1998b). Excavation report of chaiwopu cemetery, urumqi. *Xinjiang Cult. Relics* 1, 11–31.

Xinjiang Institute of Cultural Relics and Archaeology (1998a). Excavation report of five tombs in Zhagunluke, qiemo county. *Xinjiang Cult. Relics* 2, 2–18.

Xinjiang Institute of Cultural Relics and Archaeology (2004). Excavation report of Qirentuohai cemetery in tekesi county. *Xinjiang Cult. Relics* 3, 60–96.

Xinjiang Institute of Cultural Relics and Archaeology (2015b). First archaeological excavation report of habuqihansala cemetery in heijing county. *Xinjiang Cult. Relics* 2, 34–57.

Xinjiang Institute of Cultural Relics and Archaeology (2016a). *Mohuchahan cemetery in Xinjiang*. Beijing: Science Press.

Xinjiang Institute of Cultural Relics and Archaeology (1995). Suodunbulak cemetery in chabuchaer county. *Xinjiang Cult. Relics* 2, 1–19.

Yang, F. X. (2011). *Xinjiang landform and its environmental effects*. Beijing: Geological Press.

Yang, Q. J., Zhou, X. Y., Spengler, R. N., Zhao, K. L., Liu, J. C., Bao, Y. G., et al. (2020). Prehistoric agriculture and social structure in the southwestern Tarim Basin: Multiproxy analyses at wupaer. *Sci. Rep.* 10 (1), 14235. doi:10.1038/s41598-020-70515-y

Yang, R. P., Yang, Y. M., Li, W. Y., Abuduresule, Y., Hu, X. J., Wang, C. S., et al. (2014). Investigation of cereal remains at the Xiaohe cemetery in Xinjiang, China. *J. Archaeol. Sci.* 49, 42–47. doi:10.1016/j.jas.2014.04.020

Yang, S. Y., Zhang, Q., Wang, L., and Zhang, Q. H. (2022). Dental microwear analysis of human teeth in Shengjindian cemetery, Turpan, Xinjiang. *Acta Anthropol. Sin.* 41 (2), 218–225. doi:10.16359/j.1000-3193/aas.2021.0029

Yu, J. J., Hu, X. J., Yu, Y. J., A, B. S., Tuo, H. S., A, Y. D., et al. (2014b). Brief report on the archaeological excavation of Tuoganbai cemetery No.2 in Habahe County. *Cult. Relics* 703 (12), 18–28. doi:10.13619/j.cnki.cn11-1532/k.2014.12.001

Yu, J. J., Hu, X. J., Yu, Y. J., Liu, Y. S., He, X., Zhang, J., et al. (2014a). The excavation of the cemetery in the tuva new village at the lower outlet of kanas lake in Burqin county, Xinjiang. *Cult. Relics* 698 (7), 4–16. doi:10.13619/j.cnki.cn11-1532/k.2014.07.001

Yu, Z. Y., Hu, W. L., Wang, Y. Q., Feng, C., Yu, Y. J., Dang, Z. H., et al. (2016). Brief report on the excavation of xigou cemetery and ruins in fukang, changji, Xinjiang. *Archaeol. Cult. Relics* 217 (5), 3–30.

Yuan, X. (2022). The upper Ili River society in the middle bronze age. *West. Regions Stud.* 126 (2), 99–107+171. doi:10.16363/j.cnki.xyyj.2022.02.008

Yuan, X., Wang, P. D., and Zeng, B. D. (2017). New archaeological discoveries from the XiaKalangguer site in Tacheng. *Xinjiang Cult. Relics* 2, 40–42.

Zhang, F., Ning, C., Scott, A., Fu, Q. M., Bjørn, R., Li, W. Y., et al. (2021). The genomic origins of the bronze age Tarim Basin mummies. *Nature* 599, 256–261. doi:10.1038/s41586-021-04052-7

Zhang, G. L., Wang, S. Z., Ferguson, D. K., Yang, Y. M., Liu, X. Y., and Jiang, H. E. (2015). Ancient plant use and palaeoenvironmental analysis at the gumugou cemetery, Xinjiang, China: Implication from desiccated plant remains. *Archaeol. Anthropol. Sci.* 9 (2), 145–152. doi:10.1007/s12520-015-0246-3

Zhang, J. N., Han, J. Y., Xia, Z. K., Chen, X. L., Ren, X. L., Yu, X. T., et al. (2022). Preliminary analysis on the paleoenvironment of the Quanshuigou site, which is located on the oasis area in front of diluvial fan at southern piedmont of Alatao Mountain, Xinjiang. *Quat. Sci.* 42 (1), 206–222. doi:10.11928/j.issn.1001-7410.2022.01.17

Zhang, J. P., Lu, H. Y., Jia, P. W., Flad, R., Wu, N. Q., and Betts, A. (2017). Cultivation strategies at the ancient Luanzagangzi settlement on the easternmost Eurasian steppe during the late Bronze Age. *Veg. Hist. Archaeobotany* 26 (5), 505–512. doi:10.1007/s00334-017-0608-0

Zhang, P., Mijiti, E., Tian, Z. X., Feng, X., Zhang, T. N., Yao, S. W., et al. (1989). Yanbulake cemetery in Hami, Xinjiang. *Acta Archaeol. Sin.* 3, 325–402.

Zhang, Q. C., Chang, X., and Liu, G. R. (2010). Stable isotope analysis of human bones unearthed from the tianshan beilu cemetery in Hami. *Xinjiang. West. Regions Stud.* 78 (2), 38–123. doi:10.16363/j.cnki.xyyj.2010.02.013

Zhang, Q. C., and Li, S. Y. (2006). Analysis of food structure of ancient inhabitants in No. 1 cemetery of Qiongkeke at nilka county, Xinjiang. *West. Regions Stud.* 4, 78–118. doi:10.16363/j.cnki.xyyj.2006.04.011

Zhang, Q. C., Wang, M. H., Jin, H. Y., and Zhu, H. (2005). Analysis of chemical elements in human bones unearthed from the No. 4 cemetery in Chawuhugoukou, Hejing County, Xinjiang. *Acta Anthropol. Sin.* 4, 328–333. doi:10.16359/j.cnki.cn11-1963/q.2005.04.009

Zhang, Q. C., and Zhu, H. (2011). Carbon and nitrogen stable isotope analysis of the human bones from the gumugou cemetery in Xinjiang: A preliminary exploration of the early population dietary in Lop nor. *West. Regions Stud.* 83 (3), 91–96+142. doi:10.16363/j.cnki.xyyj.2011.03.005

Zhang, X. L., Qiu, S. H., Zhang, J., and Guo, W. (2014). Carbon and nitrogen stable isotope analysis of human bones unearthed from Duogang cemetery in Xinjiang. *Cult. Relics South. China* 3, 79–91.

Zhang, X. Y., Wei, D., Wu, Y., Nie, Y., and Hu, Y. W. (2016). Carbon and nitrogen stable isotope ratio analysis of Bronze Age humans from the Xiabandi cemetery, Xinjiang, China: Implications for cultural interactions between the East and West. *Chin. Sci. Bull.* 61 (32), 3509–3519. doi:10.1360/n972016-00514

Zhang, X., Zhu, H., Wang, M. H., and Wu, X. H. (2014). Bioarchaeological analysis of bronze age population of the Liushui cemetery using dental nonmetric traits. *Acta Anthropol. Sin.* 33, 460–470. doi:10.16359/j.cnki.cn11-1963/q.2014.04.005

Zhang, Y. F., Mo, D. W., Hu, K., Bao, W. B., Li, W. Y., Idris, A., et al. (2017). Holocene environmental changes around Xiaohe Cemetery and its effects on human occupation, Xinjiang, China. *J. Geogr. Sci.* 27, 752–768. doi:10.1007/s11442-017-1404-6

Zhang, Y. P., Zhang, J. F., Ruan, Q. R., Wang, Y. Q., Zhang, J. N., Zhou, L. P., et al. (2021). Geomorphological background and formation process of the goukou site in jirentai, Xinjiang. *Quat. Sci.* 41 (5), 1376–1393. doi:10.11928/j.issn.1001-7410.2021.05.13

Zhang, Y. Z., Wen, K., Ai, K. B. E., Zhang, F. Z., Yu, Y. J., Liu, Y. S., et al. (2014). The excavation of Shimenzi cemetery in hutubi, Xinjiang. *Cult. Relics* 12, 4–17. doi:10.13619/j.cnki.cn11-1532/k.2014.12.010

Zhao, K. L., Li, X. Q., Zhou, X. Y., Dodson, J., and Ji, M. (2013). Impact of agriculture on an oasis landscape during the late Holocene: Palynological evidence from the Xintala site in Xinjiang, NW China. *Quat. Int.* 311, 81–86. doi:10.1016/j.quaint.2013.06.035

Zhao, Z. J. (2009). Eastward spread of wheat into China – new data and new issues. *Chin. Archaeol.* 9, 1–9. doi:10.1515/char.2009.9.1.1

Zhou, X. Y., Yu, J. J., Spengler, R. N., Shen, H., Zhao, K. L., Ge, J. Y., et al. (2020). 5,200-year-old cereal grains from the eastern Altai Mountains redate the trans-Eurasian crop exchange. *Nat. plants* 6, 78–87. doi:10.1038/s41477-019-0581-y

frontiers | Frontiers in Earth Science

TYPE Original Research
PUBLISHED 17 March 2023
DOI 10.3389/feart.2023.1135395

Check for updates

OPEN ACCESS

EDITED BY
Ren Lele,
Lanzhou University, China

REVIEWED BY
Jie Fei,
Fudan University, China
Haipeng Wang,
Northwest Institute of Eco-Environment and Resources (CAS), China

*CORRESPONDENCE
David D. Zhang,
dzhang@gzhu.edu.cn

SPECIALTY SECTION
This article was submitted to Quaternary Science, Geomorphology and Paleoenvironment, a section of the journal Frontiers in Earth Science

RECEIVED 31 December 2022
ACCEPTED 01 March 2023
PUBLISHED 17 March 2023

CITATION
Zhang S and Zhang DD (2023), Centralization or decentralization? A spatial analysis of archaeological sites in northern China during the 4.2 ka BP event.
Front. Earth Sci. 11:1135395.
doi: 10.3389/feart.2023.1135395

COPYRIGHT
© 2023 Zhang and Zhang. This is an open-access article distributed under the terms of the Creative Commons Attribution License (CC BY). The use, distribution or reproduction in other forums is permitted, provided the original author(s) and the copyright owner(s) are credited and that the original publication in this journal is cited, in accordance with accepted academic practice. No use, distribution or reproduction is permitted which does not comply with these terms.

Centralization or decentralization? A spatial analysis of archaeological sites in northern China during the 4.2 ka BP event

Shengda Zhang and David D. Zhang*

School of Geography and Remote Sensing, Guangzhou University, Guangzhou, China

The phenomenon of centralization or decentralization has been widely observed in archaeological research. Studies are usually related to the evolution and dynamics of culture or civilization, but less pertinent to the temporal–spatial pattern and variation of human settlement, especially the insufficient applications of statistics and spatial analyses; also, their relationship with climate change is unclear. In this study, using the one-way analysis of variance (one-way ANOVA) and standard deviational ellipse (SDE) with its parameters and frequency histogram, with thousands (>4,000) of document-based data on archaeological sites (the indicator of human settlement), two pairs of successive cultural types, i.e., Majiayao–Qijia cultures and Longshan–Yueshi cultures in both ends of northern China were compared as cross-regional cases to uncover whether the locations of prehistoric settlements with ended or started ages were (de-) centralized under the impacts of climate cooling and aridification during the well-known "4.2 ka BP event" (4200–3900 BP). The results illustrate that the "inherited" sites become more decentralized. Such a pattern embodies human resilience (including adaptation and migration) for pursuing better living conditions under the circumstances of climatic and environmental deterioration over the mid–late Holocene cultural transition, which provides some implications for the response to contemporary climate change.

KEYWORDS

(de-) centralization, spatial pattern, archaeological site, northern China, 4.2 ka BP event

1 Introduction

Over the past decades, centralization/decentralization in archaeological research is commonly linked to the rise of chiefdom/state, emergence of elites/stratification, and social complexity (Earle, 1989; Gledhill et al., 1995; Drennan and Peterson, 2008). Also, it is associated with the size, number, structure/hierarchy, and landscape of human settlement (Liu, 1996; Gao et al., 2009; Rajala, 2013; Li et al., 2021; Yan et al., 2021). However, the temporal–spatial patterns of centralization or decentralization revealed by human settlements based on archaeological sites in prehistoric China vary with different studies (Liu, 1996; Gao et al., 2009; Li et al., 2021; Yan et al., 2021). Specifically, Liu (1996) and Yan et al. (2021) suggested that the settlements in North China decentralized during the Yangshao–Longshan period and became centralized in the Xia and Shang dynasties. In comparison, taking the Gansu–Qinghai region as the study area, Li et al. (2021) presented the spatiotemporal variations of settlements from the Yangshao–Majiayao period to the Qijia period, during which the centralized distributions of settlements persisted. By contrast, the

Neolithic sites on the western shore of the Chaohu Lake, Anhui, showed a decentralized pattern (Gao et al., 2009). Such disparities, which are possibly derived from different sample sizes, focused regions and analytical methods, and more importantly, the lack of spatial statistics and the absence of the possible influence of climate change, undoubtedly hinder the clear and comprehensive understanding of the dynamics and mechanisms of cultures and civilizations in prehistoric China.

Therefore, this study is aimed at figuring out whether and why the archaeological sites were concentrated or decentralized in prehistoric northern China, the cradle of the Chinese civilization, using statistical approaches and geographical information technology. The study period is set between 4200 and 3900 BP, when the abrupt climate cooling and aridification in circa 4200 BP (also known as the "4.2 ka BP event") played a crucial role in the cultural transition (i.e., changing from one cultural type to another) from the Neolithic Age to the Bronze Age, the increase of social complexity, and the birth of the Chinese civilization (Wu and Liu, 2001; Wu and Ge, 2014). Scholars prevailingly opined that the cultures in the Central Plain "survived" in climatic deterioration and environmental degradation during this event and finally evolved into the first dynasty of the Chinese history, whereas the peripheral ones experienced widespread "collapse" (Wu and Liu, 2001; Chen and Wang, 2012; Wu and Ge, 2014; Xu, 2016; Xiao et al., 2019; An et al., 2021; Zhang H et al., 2021). However, not all cultures beyond the Central Plain collapsed (Huang et al., 2004; Wen et al., 2013; Huang et al., 2021); moreover, the term *per se* is to some extent overused, which oversimplifies the complexity of human societies and has been broadly criticized as environmental determinism (Butzer and Endfield, 2012; Butzer, 2012; Correia, 2013; Haldon et al., 2020) and state-centric climate historiography (Fitzsimons, 2022). Instead, cultural "transition" is prioritized in this study. Accordingly, neutral expressions such as the "start" and "end" will be used to refer to the maximum and minimum age of a certain culture or archaeological site, respectively.

To better and fully identify the characteristics of (de-) centralization in the cultural transition, cross-regional comparisons were carried out in this study. With a large sample size, a document-retrieved site dataset published by Hosner et al. (2016) was employed, in which province was regarded as the basic unit of data collection. In the two ends of northern China, where different geographical settings and land carrying capacities may determine the regional differences in the cultural transition, two pairs of successive cultures (i.e., the Majiayao–Qijia cultures in the west and the Longshan–Yueshi cultures in the east) spread in three provinces (i.e., Gansu, Qinghai, and Shandong) were compared as cases since the Qijia (4–3.6 ka BP, according to Hosner et al., 2016, the same given as follows) and Yueshi (3.9–3.5 ka BP) cultures "inherited" some features from the Majiayao (5.8–4 ka BP) and Longshan (4.6–3.9 ka BP) cultures, respectively, and survived through climate disasters. Here, we hypothesize that the original sites were abandoned due to the uninhabitable environment resulting from drastic climate change, whereas the spatial distributions of the new sites became decentralized as a response (i.e., adaptation and migration for survival) to the 4.2 ka BP event.

2 Materials and methods

2.1 Physical geography of the study area and its evolution

The study regions are located in two ends of northern China, i.e., Gansu–Qinghai and Shandong provinces. The archaeological sites for the two pairs of cultural types range between 99°E and 122°E and between 33°N and 40°N (Supplementary Figures S1–S2), the majority of which belongs to temperate and semi-arid/semi-humid climate, with the present-day annual average precipitation falling between 200 mm and 800 mm. The western end is mainly situated on the second step of topography in China, i.e., the Loess Plateau and partly on the northeastern edge of the Qinghai–Tibetan Plateau. By running through and cutting these plateaus, which are interspersed with abundant valleys/basins, the upper reaches of the Yellow River and its tributaries, e.g., the Huangshui River, the Tao River, and the Wei River, provided a diversified environment (including grassland, forest, and farmland) for our ancestors to live in the current Gansu–Qinghai region. Benefitting from the megathermal effect in the mid-Holocene, the millet farming systems expanded more inland and boosted the prosperity of the Majiayao culture (Dong et al., 2013; Jia et al., 2013). By contrast, the physical geographical condition in the eastern part, the Shandong Peninsula, is relatively homogeneous. It is located on the third step of topography; its northern and western sides belong to the North China Plain, which is basically low, flat, and prone to flooding. The shifting channels of the lower reaches of the Yellow River have been of significant threat to the livelihood and civilizational development of ancient Chinese. Meanwhile, the coastline of North China was much closer to the inland area four millennia ago due to the megathermal effect (Wang K et al., 2022; also see the map with ancient coastline/river courses given as follows), that is why large amounts of sites are distributed in the south of the ancient Jishui River and encircle the Shandong Hills with higher altitude, where the Longshan culture flourished throughout the late Neolithic (Han et al., 2021; Wang and Wang, 2022). The termination of such a mild climate at circa 4.2 ka BP was preserved by multi-proxy geological records *via* pollen, loess–paleosol, marine sediment, etc., all of which indicate an abrupt cooling and aridification trend that incurs widespread environmental deterioration/degradation in both ends of northern China (An et al., 2005; Chen and Wang, 2012; Han et al., 2021; Wang K et al., 2022).

2.2 Data source, processing, and evaluation

2.2.1 Climate data

Climate data containing temperature and precipitation reconstruction records were used in this study as a reference for demonstrating the backdrop of climate change during the 4.2 ka BP event. The annual temperature series is taken from Pei et al. (2019), in which the data of multi-proxies such as historical documents, ice core, pollen, peat deposit, lake sediment, coral, loess, and stalagmite from 31 records across China over the past 12,000 years were integrated using three statistical methods (empirical orthogonal function, composite–plus–scale, and simple arithmetic average). The majority of these records come from northern China, which

means the temperature reconstruction is suitable for the scope of this study.

The precipitation data were taken from two sources because unlike temperature, which may remain consistent for regions with similar latitudes, the spatial pattern of precipitation varies substantially across such a large area of northern China. The first is the so far longest precisely dated and well-calibrated tree-ring stable isotope (^{18}O) chronology in Asia with nearly 6,700 years (from 4680 BCE to 2011 CE) based on the samples retrieved from Delingha on the northeastern Qinghai–Tibetan Plateau (Yang et al., 2021). A total number of 9,526 individual samples were measured to obtain the full $\delta^{18}O$ series, which was converted into a precipitation sequence. With the high resolution of 1–5 years together with the sampling location that is close to the present-day northwestern fringe of the Asian summer monsoon region, this record sensitively captures the variation in the intensity of the Asian summer monsoon and could be utilized to denote the precipitation pattern in northern China (at least in the Gansu–Qinghai region).

The second is the simulated precipitation reconstruction in northern China over 11,000 years using the NCAR Community Earth System Model, in which two sets of transient experiments (with and without dynamic vegetation) were performed (Li et al., 2022). The spatial range of this dataset (100–120°E, 35–45°N) basically covers the archaeological sites of the two pairs of successive cultures, and the resolution (20 years) is relatively satisfactory. According to the description by Li et al. (2022), the experimental result with dynamic vegetation was better and could be adopted in this study.

Data processing was divided into three steps. 1) The precipitation sequences were linearly interpolated into annual ones identical to the temperature series; 2) all data were detrended to remove the long-term effect; and 3) smoothed by a 300-year Butterworth low-pass filter to gain the low-frequency (i.e., long-cycle) signal of the series. Hence, both long- and short-term data represent climatic anomalies. The detrending and smoothing procedures were conducted using MATLAB (version R2020b).

2.2.2 Archaeological site data

The data on archaeological sites in prehistoric northern China were obtained from Hosner et al. (2016). The original data were actually retrieved from the voluminous *Atlas of Chinese Cultural Relics* edited by the National Cultural Heritage Administration, which has been widely utilized by many researchers (Liu, 1996; Dong et al., 2012; Dong et al., 2013; Shi et al., 2019; Li et al., 2021; Yan et al., 2021; Wang and Wang, 2022; Wang Y et al., 2022). Until now, 28 volumes (each corresponding to one province) have been published, except on the southern provinces of Guizhou, Jiangxi, Hainan, and Taiwan, which will not affect this study because the area of study is in the north. The published dataset sorted out by Wagner et al. (2013) and Hosner et al. (2016), which could be downloaded from the open-access PANGAEA Data Publisher for Earth and Environmental Science (https://doi.pangaea.de/10.1594/PANGAEA.860072), contains cultural types, the maximum/started and minimum/ended ages, and the locations/coordinates (including longitude and latitude) of the sites that are taken as the object of this study.

It should be noted that only two inherited cultures in both ends of northern China, i.e., the Majiayao–Qijia cultures in the northwest as well as the Longshan–Yueshi cultures in Shandong were employed as study cases in this research, as there are no specific and successive cultural types in other major provinces of northern China, e.g., Shaanxi, Shanxi, Henan, and Hebei, during the study period for the original data from Hosner et al. (2016). The details are listed in Table 1. All these sites with unspecific cultural types cannot be clearly compared, and the related cultures in the middle of northern China were, thus, not considered.

Even so, with the huge number and detailed information of archaeological sites in mainland China, Hosner et al. (2016)'s dataset offers a great opportunity for statistical and spatial analysis. Moreover, it is the most complete collection of the sites so far, all of which were the results of detailed and long-time investigations by the local archaeological authorities. Although no precise date of ^{14}C or other dating technology in each site was given, the dates of the started and ended times of the four cultural types involved in this study have been identified by a large amount of archaeological surveys with modern dating technology. Also, the locations of these sites are accurate to three decimal places. In summary, although the temporal resolution of this dataset is at a centennial scale of these dates, the correct cultural type with generally agreed start and end times and accurate location of each site provides reliable information for this study.

2.3 Methods

2.3.1 One-way analysis of variance

The differences in the coordinates of archaeological sites between the ended and started ages can be compared by one-way ANOVA, which evaluates the equality of two or more group means *via* the variances (De Vaus, 2002). The null hypothesis states that the means of different groups are equal, and the alternative hypothesis states that at least one of the group means is different from the others (Lee, 2008). It has been widely used in previous studies to determine the significant differences of population dynamics, frequencies of Malthusian population checks (Lee and Zhang, 2010; Lee and Zhang, 2013; Lee et al., 2016), and battle coordinates with a few categories of war defined (Zhang S et al., 2021) between warm and cold periods. In this study, the cultural end or start rather than the climatic phase was chosen as the independent ANOVA factor, while the coordinates of archaeological sites were input as the dependent ANOVA factor. In addition, data dispersion could be measured by the value of variance, and the larger the variance, the more dispersed (i.e., decentralized) the sites.

2.3.2 Standard deviational ellipse and its parameters

The comparison of the mean coordinates between ended and started sites by one-way ANOVA is insufficient, as it cannot elaborate the spatial patterns of archaeological sites during the 4.2 ka BP event. The site distributions and from which whether any regular pattern is unveiled can be solved by the tool, the SDE in ArcGIS. Put forward by Lefever (1926), it is a common method

TABLE 1 Categorization of the ended and started sites in the four major provinces of northern China during the study period (by Hosner et al., 2016).

Province	Ended site categorization	Started site categorization	Original source
Shaanxi	Late Neolithic	Xia dynasty period	National Cultural Heritage Administration (1998)
Shanxi	Longshan culture	Undistinguished Xia–Shang dynasty period and Xia dynasty period	National Cultural Heritage Administration (2006)
Henan	Longshan culture	Not mapped	National Cultural Heritage Administration (1991)
Hebei	Undistinguished Neolithic age cultures	Undistinguished Xia–Shang–western Zhou dynasty period	National Cultural Heritage Administration (2013)

used to measure the trend for a set of points and to separately calculate the standard distance along the *x*- and *y*-directions, and it is taken as a proxy of the main range of culture in this study. The ellipse is referred to as the SDE because the standard deviation (1σ by default) of the *x*- and *y*-coordinates from the mean center is calculated to define the axes of the ellipse. The information on central tendency, dispersion of sites, and whether the site distributions are elongated with a specific direction can be obtained from the output. Furthermore, when an ellipse is calculated, a few elliptical parameters are generated as well, and their definitions are outlined as follows.

2.3.2.1 Area

The elliptical area (*s*), showing the major coverage of sites, is calculated *via* the following equation:

$$S = \pi ab, \quad (1)$$

where *a* and *b* denote the length of the semi-major and semi-minor axis, respectively. The unit of *s* is 10^4 km^2.

2.3.2.2 Eccentricity

Eccentricity (*e*) determines whether an ellipse is oblate or close to a circle. It ranges between 0 and 1 (dimensionless), and the smaller the rounder, the larger the flatter. The formula of *e* is given as follows:

$$e = c/a, \quad (2)$$

where *c* is the semi-focal distance and can be obtained from the formula:

$$c = \sqrt{a^2 - b^2}. \quad (3)$$

Compared with a geographic coordinate system, in which the spatial unit is expressed as degree or degree–minute–second, a projected coordinate system is required for the SDE so that the parameters can be accurately calculated. *a* and *b* (in kilometer) are automatically generated with an attribute table in ArcGIS, and they can be substituted into the aforementioned formulas to obtain *e*. The three parameters, *a*, *s*, and *e* were combined to measure the cultural decentralization in this study. The longer the semi-major axis (*a*), the larger the elliptical area (*s*), and the larger the eccentricity (*e*), the more decentralized the archaeological sites.

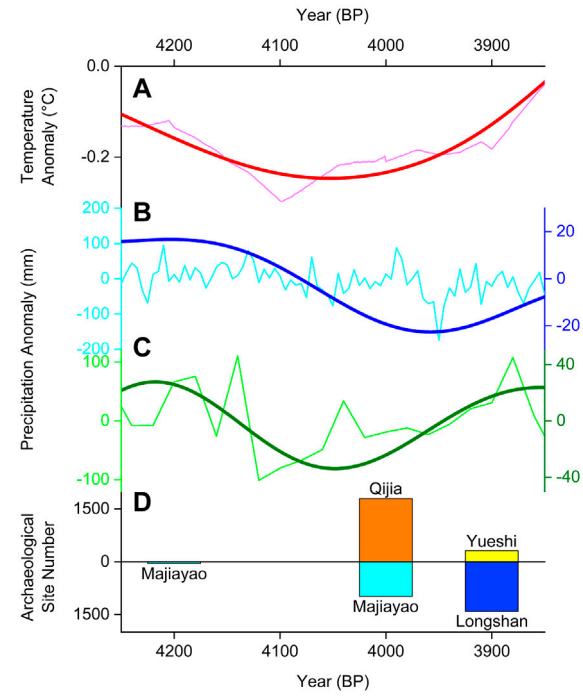

FIGURE 1
Time-series of climate change and the number of archaeological sites in northern China during 4200–3900 BP. Note: **(A)** temperature anomaly (red) reconstructed by Pei et al. (2019); **(B)** precipitation anomaly (blue) calculated by Yang et al. (2021); **(C)** precipitation anomaly (green) simulated by Li et al. (2022); these data were detrended (thin line with light color) and smoothed by a 300-year Butterworth low-pass filter (thick line with deep color); and **(D)** archaeological site numbers (started site—the Qijia culture: orange; the Yueshi culture: yellow; ended sites—the Majiayao culture: cyan; the Longshan culture: blue) from Hosner et al. (2016).

2.3.3 Frequency histogram

Except the one-way ANOVA and SDE, frequency histogram was also applied to show the frequency distributions of site coordinates and central tendency. The longitude and latitude were divided by one-degree intervals. The more concentrated the sites, the higher the frequencies with fewer intervals, and the larger the differences between them and other frequencies of intervals. If the sites have more decentralized distributions, such

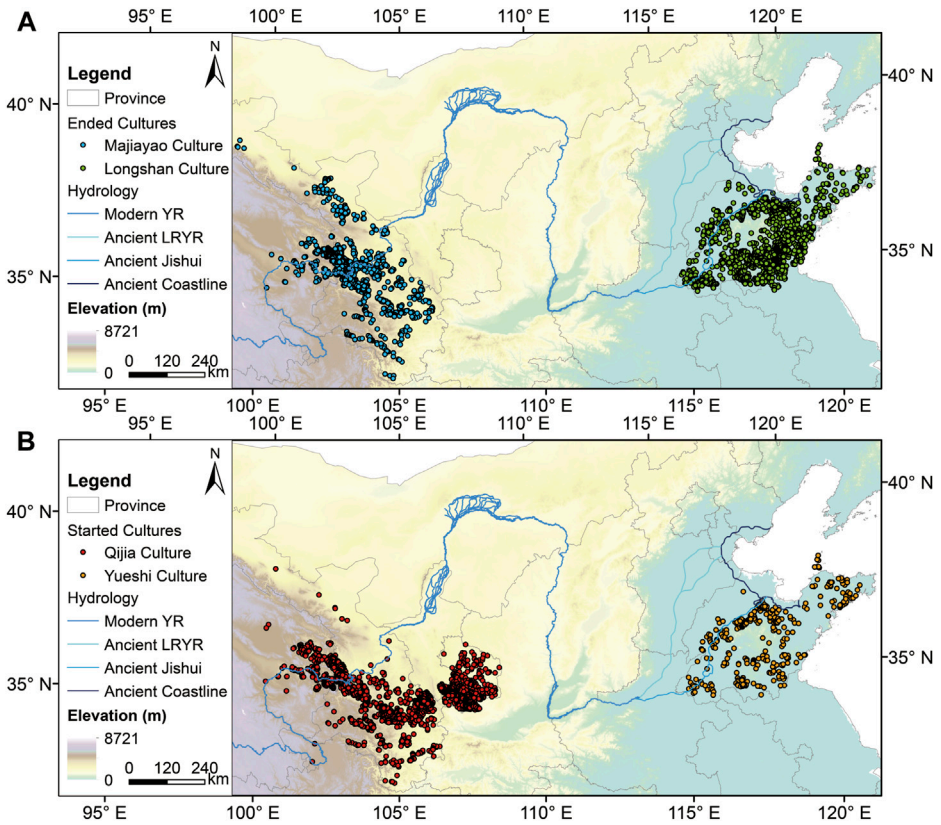

FIGURE 2
Distributions of archaeological sites between different cultures during 4200–3900 BP. Note: **(A)** ended cultures, including the Majiayao culture (blue) and the Longshan culture (green); **(B)** started cultures, including the Qijia culture (red) and the Yueshi culture (orange). The courses of the modern Yellow River (YR), the ancient lower reaches of the Yellow River (LRYR) plus the ancient Jishui River, and the ancient coastline of the North China Plain were depicted from Tan (1982) as references.

differences are smaller, while two or more peaks of frequencies may exist.

3 Results

Before visualizing the spatial patterns of archaeological sites in two ends of northern China during 4200–3900 BP, the time-series of climate change and the started/ended site number are presented and compared in Figure 1. It clearly exhibits the climate cooling in the 4.2 ka BP event (Figure 1A), which symbolizes the termination of the Holocene Optimum/Megathermal Period and the transition of the mid–late Holocene (Walker et al., 2018). Looking from the long-term (300-yr-filtered thick line) trends, the precipitation anomaly by tree-ring $\delta^{18}O$ (Yang et al., 2021) reaches the minimum at circa 3950 BP (Figure 1B), while the troughs of the model-derived precipitation anomaly (Li et al., 2022; Figure 1C) and the temperature anomaly are consistent during 4100–4000 BP. Correspondingly, in Figure 1D, large numbers of archaeological sites (2,445) ended in this period, while 2,109 new sites emerged. Specifically, the numbers increase from 1,036 for the Majiayao culture to 1,795 for the Qijia culture, which almost doubles; by contrast, the numbers drastically decrease from the Longshan culture (1,409) to the Yueshi culture (314) by nearly 80%. Since the total number of the started sites only reduced by about 14% compared with that of the ended sites, the abandonment of human settlements possibly caused by climatic exacerbation and concurrent environmental degradation in northern China throughout the 4.2 ka BP event was by no means equal to societal "collapse" yet transition instead (e.g., people just out-migrated to better living conditions for survival and/or gradually adapted).

In this study, two pairs of successive regional cultures were compared as cases, and spatial analyses were carried out to investigate any possible pattern that could be related to cultural decentralization during the 4.2 ka BP event. As shown in Figure 2, the distributions of archaeological sites for different cultures are presented and overlaid with river channels. In Shandong, compared with the extensive concentration of the sites of the Longshan culture that drastically declined during the study period (Figure 2A), the sites of the Yueshi culture with decreased number become relatively sparse (Figure 2B). In Gansu and Qinghai, as the started Qijia culture preserved some features from the previous Majiayao culture, they were compared as another case (Figure 2A). The region where the Qijia sites occupy is obviously "wider" than that for the Majiayao culture with respect to the range of longitude (Figure 2B).

The regional site distributions were further examined by dividing the site coordinates into longitude and latitude with frequency histograms (Figure 3), in which two key findings could

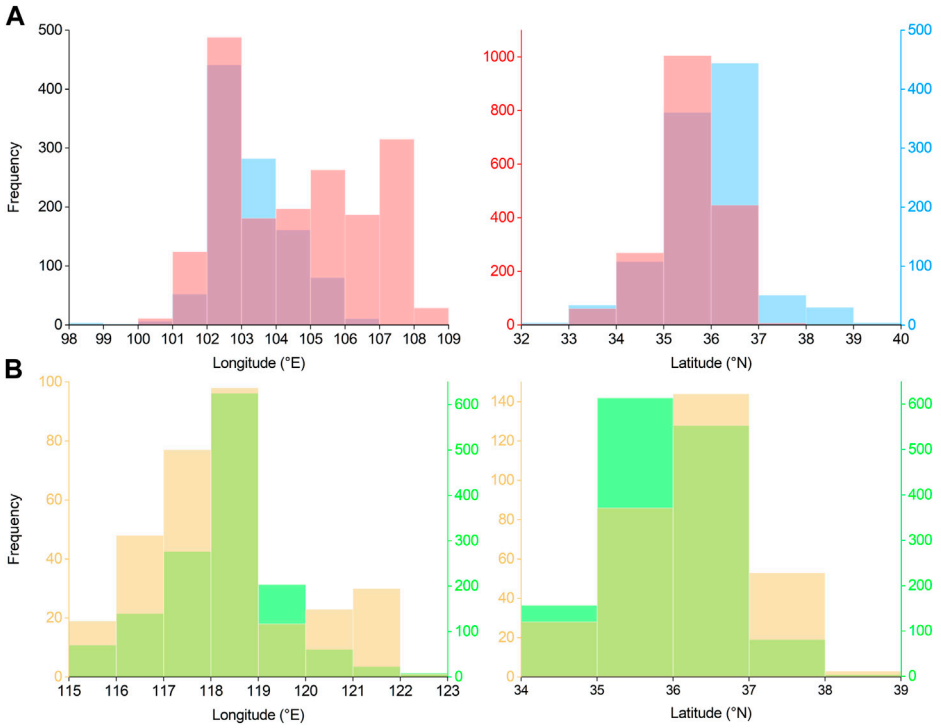

FIGURE 3
Frequency histograms showing the coordinates between the ended and started cultures. Note: **(A)** the Majiayao culture (blue) *vs.* the Qijia culture (red); **(B)** the Longshan culture (green) *vs.* the Yueshi culture (earthy yellow). The color of the *y*-axis follows the cultural type.

TABLE 2 One-way ANOVA of the coordinates of archaeological sites between different cultures. Panel (A): the Majiayao culture *vs.* the Qijia culture. Panel (B): the Longshan culture *vs.* the Yueshi culture.

Coordinate	Majiayao		Qijia		df[a]	df[b]	*F*	*P*	*F crit*
	Mean	Variance	Mean	Variance					
Longitude	103.319	1.104	104.619	4.113	1	2,829	368.129	0.000	3.845
Latitude	35.930	0.843	35.520	0.484	1	2,829	179.535	0.000	
Coordinate	Longshan		Yueshi		df[a]	df[b]	*F*	*P*	*F crit*
	Mean	Variance	Mean	Variance					
Longitude	118.290	1.564	118.301	2.619	1	1,721	0.018	0.892	3.847
Latitude	35.944	0.601	36.273	0.702	1	1,721	44.883	0.000	

[a] between groups; [b] within groups.

be noted. First, the cultural decentralization mainly embodies a longitudinal extension, i.e., the longitudinal range of the high-frequency interval of the started culture becomes wider. As shown in Figure 3A (left panel), the sites of the ended Majiayao culture chiefly range between 102°E and 104°E, whereas those of the started Qijia culture are concentrated in 102–108°E, with the frequency in 102–103°E being the most prominent. Similarly, as shown in Figure 3B (left panel), the sites of the ended Longshan culture dominantly cluster in 118–119°E solely, yet the counterparts of the started Yueshi culture fall into 117–119°E with 116–117°E to a lesser extent. Second, the latitudinal distribution of sites during the cultural transition manifests a shifted trend. Among these cultures, the sites of the Majiayao culture (Figure 3A, right panel) stand out from the interval of 36–37°N, with 35–36°N taken as the second place, while the counterparts of the Qijia culture largely cluster in 35–36°N. For the Longshan culture (Figure 3B, right panel), the frequency values of latitude between 35°N and 37°N are close and the value in the interval of 35–36°N is the largest, yet 36–37°N is the

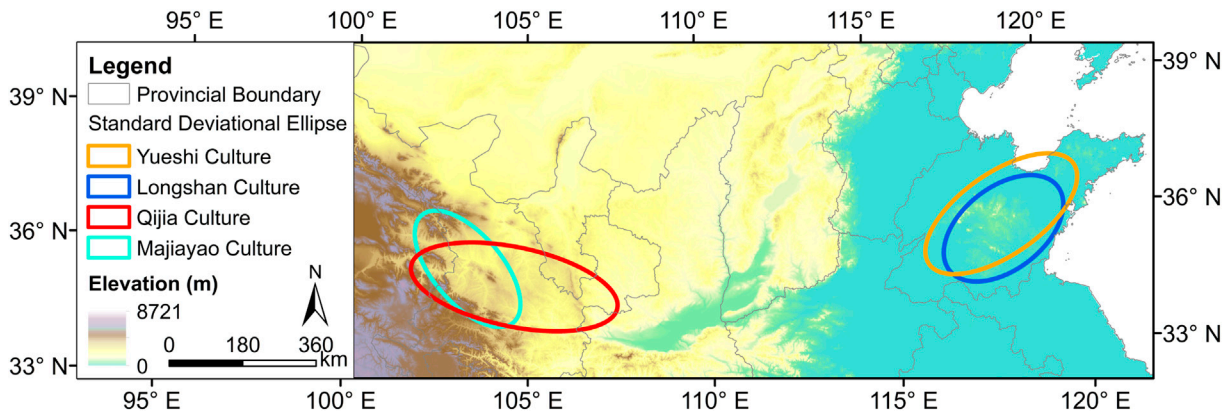

FIGURE 4
Comparison of standard deviational ellipses (SDEs) for the successive ended and started cultures. Note: the Majiayao culture (cyan) *vs.* the Qijia culture (red); the Longshan culture (blue) *vs.* the Yueshi culture (orange).

TABLE 3 Parameters of SDEs for archaeological sites of different cultures.

Culture	Area (10^4 km^2)	Semi-major axis (km)	Eccentricity
Majiayao	4.598	172.721	0.871
Qijia	7.866	257.915	0.926
Longshan	5.331	167.763	0.798
Yueshi	6.779	215.494	0.885

major interval of latitudinal distribution for the Yueshi sites. This finding indicates that compared with the previous cultures, the Qijia culture in the west and the Yueshi culture in the east generally shifted toward lower and higher latitude by one degree, respectively. The reason why the moving directions are different will be given in the following section.

The differences in coordinates between different ended and started cultures reflected by one-way ANOVA are shown in Table 2. Except the longitude between the Longshan culture and the Yueshi culture (Panel B), which fails to pass the significance test (p = 0.892), others are significant at the 0.001 level. Regarding the mean longitudes for the ended cultures (the Majiayao culture and the Longshan culture), they are situated slightly more westward than the ones for the started cultures (the Qijia culture and the Yueshi culture), but there is no consistency for the latitudinal mean. As for longitude, the variances of the started cultures are larger than those of the ended cultures; moreover, for the same culture, the variances of longitude are always larger than those of latitude. Therefore, the coordinates (especially for longitude) of the started cultures are more decentralized.

The directional characteristics of archaeological sites for different cultures are also revealed by the SDEs (Figure 4) and their parameters (Table 3). In Figure 4, evidently, the orientations of the SDEs for the successive ended and started cultures are relatively in agreement. Specifically, the SDE directions for the Majiayao culture (cyan) and the Qijia culture (red) are both northwest–southeast, along the basins/valleys of the Yellow River and its tributaries in Gansu and Qinghai, while the SDEs for the Longshan culture (blue) and the Yueshi culture (orange) elongate northeast–southwestward, which is possibly regulated by the central Shandong Hills where the sites surrounded, and such a direction is also identical to the counterpart of the Shandong Peninsula. Additionally, based on the data in Table 3, the areas, semi-major axes, and shapes of the SDEs for the started cultures are larger, longer, and flatter than their counterparts for the previous ended cultures, respectively. For example, the values of the area, semi-major axis, and eccentricity of the SDE for the Qijia culture are around 7.9×10^4 km^2, 258 km, and 0.93, respectively, compared with 4.6×10^4 km^2, 173 km, and 0.87 for the Majiayao culture. In short, these SDEs and their parameters indicate that the decentralization trend of the started cultures after 4.2 ka BP is valid on the regional scale.

4 Discussion

4.1 Decentralization and adaptation differences of cultural cases in different regions

When ancient people encountered drastic climate change, there were two choices, migration and cultural adaption. Short-term and short-distance migration is preferable since cultural adaptation is usually a considerably long process, in particular technological progress, for example. As there is no instant effect for cultural adaption, people had to abandon their original settlements and out-migrate for more resources under the impacts of cooling and aridification during the 4.2 ka BP event, and thus settlement decentralization became the major trend for survival. In addition, the decentralized spatial patterns of the cross-regional cases reflect the differences in latitudinal variations of sites and the orientations of the SDEs (Figures 3, 4). As shown previously, the north-to-south movement from the Majiayao culture to the Qijia culture and the south-to-north shift

TABLE 4 Statistics of the distance (km) between the archaeological site and the water body (including rivers and lakes) for different cultures. Note: the sites on the islands were excluded.

Culture	Mean distance	90th percentile distance	Maximum distance
Majiayao	7.722	17.323	55.960
Qijia	6.613	15.330	28.003
Longshan	6.276	13.370	32.878
Yueshi	5.618	11.454	30.517

from the Longshan culture to the Yueshi culture are possibly pertinent to water intake, as agriculture played an important part in people's livelihood at that time (Jia et al., 2013; An et al., 2021). Since the climate turned colder and (foremost) drier during the study period (Figure 1), it is understandable that dryland farming systems in northern China were severely hit. Therefore, people had to migrate to the areas closer to rivers or lakes for getting water for irrigation, especially toward the Yellow River with the largest runoff in North and Northwest China. From Table 4, it is apparent that the distances between water bodies and the started sites, including the mean, 90th percentile (i.e., the shorter the distance, the faster the cumulative frequency curve reaches 90%), and maximum ones, are shorter than the counterparts of the ended sites, which means the started cultures became more water-dependent. In the west, the majority of the Qijia sites are still concentrated near the border between Qinghai and Gansu and distributed along the Yellow River and its tributaries, yet the originally marked sites located in the reaches of the Shiyang River (an inland river) of the Hexi Corridor during the Majiayao period were mostly uninhabited. Meanwhile, part of dense sites shifted toward the eastern Gansu/Longdong Plateau (i.e., central Loess Plateau) and distributed along the Jing River, the largest tributary of the Wei River (Supplementary Figure S1). Such a spatial disparity may imply the aridification of Northwest China around 4000 BP (An et al., 2005). With regard to the eastern area, during the Longshan era, many sites were situated in the south of the central Shandong Hills, where the most remarkable ones were distributed along the Yi–Shu rivers (tributaries of the Huai River) and the Mi River (flowing through present-day Weifang city). By contrast, during the Yueshi period, the sites only clustered in the reaches of the Xiaoqing River (located in the north of the Hills, probably the ancient Jishui River according to historical records), yet the high-density sites for the previous Longshan culture disappeared, with scattered sites left, particularly in the southeast of the Hills (Figure 2 and Supplementary Figure S2).

In fact, as Hosner et al. (2016) also pointed out in their paper, the changes in site numbers of these two cases are rather contrasting. However, whether the new cultures were more advanced or not may not be deduced by the changes in site numbers since bronze artifacts were found in both sites of Yueshi and Qijia cultures (Cohen, 2001; Yang et al., 2017; Zhang et al., 2017). Granted, compared with the Yueshi culture, the Qijia culture developed more rapidly and became more sophisticated. Owing to the trans-Eurasian material exchange during 5000–4000 BP, large number of specimens of crop (wheat and barley) and livestock (cattle, goat, sheep, or horse) were identified in the Qijia sites, while the bronze metallurgy was introduced and the bronze products were excavated during this period (Dong et al., 2017; Yang et al., 2017; Zhang et al., 2017; Dong et al., 2020; Dong et al., 2021; Dong et al., 2022; Ren et al., 2022). Also, the diversified environments benefited from semi-arid temperate continental climate to semi-humid temperate monsoon climate, which were in favor of such an emergence/transition of new culture and the inhabitants for adaptation and survival in the Gansu–Qinghai region. By contrast, the relatively homogeneous environment in the Shandong Peninsula seems the bane of decentralization. As mentioned previously, the northern and western sides belong to the low-lying and flood-prone North China Plain, through which the channel of the Yellow River shifts erratically. Also, the central Shandong Hills are not very high but steep, which may not well-conserve water or control floods. Furthermore, the open topography toward the surroundings makes the security worse, especially when intertribal–chiefdom conflicts became increasingly frequent since the Longshan era (Han, 2020a; Han, 2020b). Consequently, possibly because of the wars against the cultures in the Central Plain or the Xia Dynasty and/or the legendary flood, the site numbers from the Longshan culture to the Yueshi culture dramatically decreased. Researchers even inferred that people who migrated from the northeast conquered the Longshan culture and created the Yueshi culture, which did not originate from the former, or at least the mix in between (Zhang, 1989). Nevertheless, compared with their predecessors, especially their neighbors who primarily depended on rice cultivation in the south and southeast of the Hills, the Yueshi societies, which relied more on drought-resistant millet farming and extensive exploitation of previously uncultivated lands, no doubt displayed stronger resilience against climatic deterioration during the 4.2 ka BP event (An et al., 2021).

In brief, different geographical settings and land carrying capacities between the western and eastern sides of northern China may lay a foundation for different patterns of the cultural transition from the Neolithic Age to the Bronze Age; additionally, equipped with collective wisdom, humans are not just gregarious animals but their adaptability, flexibility, and activeness in response to climate cooling and drying (and related environmental pressure) should not be ignored.

4.2 Cultural transition in prehistoric northern China and its implications on the climate–society nexus

The transition from the middle to late Holocene in China underwent fundamental changes such as political (re-)

organization (from chiefdom to kingdom) and social structure (from egalitarian clans to stratified classes). In comparison to the state formation in the Central Plain (more specifically, the core area crosses the borders among western Henan, eastern Shaanxi, and southern Shanxi), and the cultures surrounding this area were deemed declined (Wu and Liu, 2001). Scholars have explained that environment constraint together with population stress, which were superimposed on the abrupt climatic deterioration during 4.5–4.0 ka BP, accounted for such a peripheral cultural decline and the rise of states in the Central Plain (Wu and Liu, 2001; Wu and Ge, 2014). Others blamed such a decline of the Neolithic cultures beyond the Central Plain for frequent tribal conflicts or the legendary great flood (Wei, 2010; Guo et al., 2013; Wu et al., 2016), yet the authenticity of the latter and (if yes) its possibility that covers such a wide range are still questionable (Dong et al., 2018).

The cultural transition reflected from the spatial patterns of archaeological sites (i.e., the indicator of human settlements) in northern China during the 4.2 ka BP event indicates that the started cultures inherited from the ended ones survived and even thrived through decentralization, which implies the possibility of the periodicity of concentration and decentralization, or coexistence similar to spatial heterogeneity (i.e., concentration occurred in some places but decentralization happened somewhere else). Such a possibility has been corroborated by the experts who focus on the cases in ancient Mesopotamia, Europe, and East Africa (Stein and Wattenmaker, 1990; Fernández-Götz, 2018; Fitzsimons, 2022). Among them, the climate–settlement nexus (i.e., decentralization in the cold phase) has been confirmed (Fernández-Götz, 2018), which is consistent with the spatial pattern of the cultural transition in northern China under the 4.2 ka BP climatic shock in our study. Specifically, during this event, the deteriorated climate dramatically reduced the available resources and, hence, weakened the once prosperous Longshan and Majiayao cultures, with human settlements abandoned in a concentrated way. Meanwhile/subsequently, settlement diffusion and/or adaptation had to be adopted for survival, during which new types of cultures (e.g., the Qijia and Yueshi cultures) were born and the cultural transition was completed accordingly. On one hand, they all decentralized in space/longitude and survived under the extreme climate change and environmental pressure throughout this event. On the other hand, with different response modes, the Qijia culture thrived on the western and central Loess Plateau, while the Yueshi culture in Shandong, though with a simpler pattern, had its own characteristics. It seems different adaptation strategies to climatic and environmental degradation determined different dynamics, mechanisms, processes, and features of the cultural transition in prehistoric China, thus emphasizing the importance of human resilience in the narrative of archaeological studies. By introducing exogenous material "packages", the more successful case of the Qijia culture undoubtedly implies the benefit of cultural diversity, which is similar to biodiversity (Burke et al., 2021). Such diversity nonetheless deserves further investigations with more cases and evidence in the near future.

5 Conclusion

In this study, with two pairs of successive (i.e., ended and then started) cultural types compared as cases, the phenomenon of decentralization for the "inherited" sites in two ends of northern China during the 4.2 ka BP event (4200–3900 BP) has been unveiled. The consistent spatial patterns of the started cultures support the validity of such decentralization on the regional scale, in which the longitudinal expansion of the sites becomes most striking. Moreover, the different directions of latitudinal movements of the sites between the Majiayao culture and the Qijia culture (from north-to-south) and the Longshan culture and the Yueshi culture (from south-to-north) are observed, which are explained by a shortened distance between the human settlement and the water body for adapting to the prolonged drought. Combined with our findings and those of the previous research on different adaptation strategies adopted by the inherited Qijia and Yueshi cultures, we conclude that prehistoric societies who suffered from climate disasters in northern China during this event had to adapt and even out-migrate for survival through different solutions, which depended upon different geographical settings and land carrying capacities, hence realizing the essential cultural diversity over the mid–late Holocene transition. As cultural diversity is the source of climate adaptation–mitigation strategies and human resilience (Burke et al., 2021), our work may potentially offer new insights into the research on the climate–society nexus and provide some implications for policymakers in response to the impending threat on social and cultural sustainability brought on by contemporary climate change.

Data availability statement

Publicly available datasets were analyzed in this study. These data can be found here: Hosner, D et al. (2016); PANGAEA, https://doi.org/10.1594/PANGAEA.860072.

Author contributions

DZ contributed to the conception and design of the research. SZ and DZ performed the research. SZ analyzed the data. SZ wrote the first draft of the manuscript. Both authors contributed to the revision and approved the submitted version of the manuscript.

Funding

This research was supported by the Second Tibetan Plateau Scientific Expedition and Research Program from the Institute of Tibetan Plateau Research, Chinese Academy of Sciences (2019QZKK0601) and the National Natural Science Foundation of China (41971110).

Acknowledgments

The authors thank the reviewers for their valuable comments on this manuscript.

Conflict of interest

The authors declare that the research was conducted in the absence of any commercial or financial relationships that could be construed as a potential conflict of interest.

Publisher's note

All claims expressed in this article are solely those of the authors and do not necessarily represent those of their affiliated organizations, or those of the publisher, the editors, and the reviewers. Any product that may be evaluated in this article, or claim that may be made by its manufacturer, is not guaranteed or endorsed by the publisher.

Supplementary material

The Supplementary Material for this article can be found online at: https://www.frontiersin.org/articles/10.3389/feart.2023.1135395/full#supplementary-material

References

An, C., Tang, L., Barton, L., and Chen, F. H. (2005). Climate change and cultural response around 4000 cal yr BP in the Western part of Chinese Loess Plateau. *Quat. Res.* 63 (3), 347–352. doi:10.1016/j.yqres.2005.02.004

An, J., Kirleis, W., and Jin, G. (2021). Understanding the collapse of the Longshan culture (4400-3800 BP) and the 4.2 ka event in the Haidai Region of China - from an agricultural perspective. *Environ. Archaeol.* doi:10.1080/14614103.2021.2003583

Burke, A., Peros, M. C., Wren, C. D., Pausata, F. S. R., Riel-Salvatore, J., Moine, O., et al. (2021). The archaeology of climate change: The case for cultural diversity. *Proc. Natl. Acad. Sci. U. S. A.* 118 (30), e2108537118. doi:10.1073/pnas.2108537118

Butzer, K. W. (2012). Collapse, environment, and society. *Proc. Natl. Acad. Sci. U. S. A.* 109 (10), 3632–3639. doi:10.1073/pnas.1114845109

Butzer, K. W., and Endfield, G. H. (2012). Critical perspectives on historical collapse. *Proc. Natl. Acad. Sci. U. S. A.* 109 (10), 3628–3631. doi:10.1073/pnas.1114772109

Chen, W., and Wang, W. (2012). Middle-Late Holocene vegetation history and environment changes revealed by pollen analysis of a core at Qingdao of Shandong province, East China. *Quat. Int.* 254, 68–72. doi:10.1016/j.quaint.2011.04.005

Cohen, D. J. (2001). *The Yueshi culture, the Dong Yi, and the archaeology of ethnicity in early bronze age China*. Cambridge: Harvard University.

Correia, D. (2013). F**k jared diamond. *Capital. Nat. Social.* 24 (4), 1–6. doi:10.1080/10455752.2013.846490

De Vaus, D. A. (2002). *Analyzing social science data*. London: SAGE.

Dong, G., Jia, X., An, C., Chen, F., Zhao, Y., Tao, S., et al. (2012). Mid-Holocene climate change and its effect on prehistoric cultural evolution in eastern Qinghai province, China. *Quat. Res.* 77 (1), 23–30. doi:10.1016/j.yqres.2011.10.004

Dong, G., Wang, L., Cui, Y., Elston, R., and Chen, F. (2013). The spatiotemporal pattern of the Majiayao cultural evolution and its relation to climate change and variety of subsistence strategy during late Neolithic period in Gansu and Qinghai provinces, Northwest China. *Quat. Int.* 316, 155–161. doi:10.1016/j.quaint.2013.07.038

Dong, G., Yang, Y., Han, J., Wang, H., and Chen, F. (2017). Exploring the history of cultural exchange in prehistoric Eurasia from the perspectives of crop diffusion and consumption. *Sci. China Earth Sci.* 60 (6), 1110–1123. doi:10.1007/s11430-016-9037-x

Dong, G., Zhang, F., Liu, F., Zhang, D., Zhou, A., Yang, Y., et al. (2018). Multiple evidences indicate no relationship between prehistoric disasters in Lajia site and outburst flood in upper Yellow River valley, China. *Sci. China Earth Sci.* 61 (4), 441–449. doi:10.1007/s11430-017-9079-3

Dong, G., Li, R., Lu, M., Zhang, D., and James, N. (2020). Evolution of human–environmental interactions in China from the late paleolithic to the bronze age. *Prog. Phys. Geogr.* 44 (2), 233–250. doi:10.1177/0309133319876802

Dong, G., Du, L., and Wei, W. (2021). The impact of early trans-Eurasian exchange on animal utilization in northern China during 5000–2500 BP. *Holocene* 31 (2), 294–301. doi:10.1177/0959683620941169

Dong, G., Du, L., Yang, L., Lu, M., Qiu, M., Li, H., et al. (2022). Dispersal of crop-livestock and geographical-temporal variation of subsistence along the Steppe and Silk Roads across Eurasia in prehistory. *Sci. China Earth Sci.* 65, 1187–1210. doi:10.1007/s11430-021-9929-x

Drennan, R. D., and Peterson, C. E. (2008). "Centralized communities, population, and social complexity after sedentarization," in *The neolithic demographic transition and its consequences*. Editors J. -P. Bocquet-Appel and O. Bar-Yosef (Dordrecht: Springer), 359–386.

Earle, T. (1989). The evolution of chiefdoms. *Curr. Anthropol.* 30 (1), 84–88. doi:10.1086/203717

Fernández-Götz, M. (2018). Urbanization in iron age Europe: Trajectories, patterns, and social dynamics. *J. Archaeol. Res.* 26 (2), 117–162. doi:10.1007/s10814-017-9107-1

Fitzsimons, W. (2022). "Social responses to climate change in a politically decentralized context: A case study from east african history," in *Perspectives on public policy in societal-environmental crises*. Editors A. Izdebski, J. Haldon, and P. Filipkowski (Cham: Springer), 145–159.

Gao, C., Wang, X., Jiang, T., and Jin, G. (2009). Spatial distribution of archaeological sites in lakeshore of Chaohu Lake in China based on GIS. *Chin. Geogr. Sci.* 19 (4), 333–340. doi:10.1007/s11769-009-0333-4

Gledhill, J., Bender, B., and Larsen, M. T. (1995). *State and society: The emergence and development of social hierarchy and political centralization (vol. 4)*. East Sussex: Psychology Press.

Guo, Y., Mo, D., Mao, L., Wang, S., and Li, S. (2013). Settlement distribution and its relationship with environmental changes from the Neolithic to Shang-Zhou dynasties in northern Shandong, China. *J. Geogr. Sci.* 23 (4), 679–694. doi:10.1007/s11442-013-1037-3

Haldon, J., Chase, A. F., Eastwood, W., Medina-Elizalde, M., Izdebski, A., Ludlow, F., et al. (2020). Demystifying collapse: Climate, environment, and social agency in pre-modern societies. *Millennium* 17 (1), 1–33. doi:10.1515/mill-2020-0002

Han, D., Ding, M., Peng, S., Zhu, L., Zhao, Q., Jin, H., et al. (2021). Holocene climate evolution and Neolithic cultural evolution recorded in the loess profile in central Shandong province, China. *Earth Sci.* 10 (6), 315–324. doi:10.11648/j.earth.20211006.17

Han, J. (2020a). Neolithic wars and the course of early Chinese civilization. *Soc. Sci. Front.* 10, 99–107, 282. (in Chinese with English abstract).

Han, J. (2020b). Violent cultural changes in Longshan period and tribal warfare in Chinese legendary era. *J. Soc. Sci.* 1, 152–163. (in Chinese with English abstract). doi:10.13644/j.cnki.cn31-1112.2020.01.015

Hosner, D., Wagner, M., Tarasov, P. E., Chen, X., and Leipe, C. (2016). Spatiotemporal distribution patterns of archaeological sites in China during the Neolithic and Bronze Age: An overview. *Holocene* 26 (10), 1576–1593. doi:10.1177/0959683616641743

Huang, C., Pang, J., Zhou, Q., and Chen, S. (2004). Holocene pedogenic change and the emergence and decline of rain-fed cereal agriculture on the Chinese Loess Plateau. *Quat. Sci. Rev.* 23 (23), 2525–2535. doi:10.1016/j.quascirev.2004.06.003

Huang, X., Xiang, L., Lei, G., Sun, M., Qiu, M., Storozum, M., et al. (2021). Sedimentary Pediastrum record of middle-late Holocene temperature change and its impacts on early human culture in the desert-oasis area of northwestern China. *Quat. Sci. Rev.* 265, 107054. doi:10.1016/j.quascirev.2021.107054

Jia, X., Dong, G., Li, H., Brunson, K., Chen, F., Ma, M., et al. (2013). The development of agriculture and its impact on cultural expansion during the late Neolithic in the Western Loess Plateau, China. *Holocene* 23 (1), 85–92. doi:10.1177/0959683612450203

Lee, H. F. (2008). *Climate change and Chinese population growth dynamics over the last millennium*. [dissertation]. Hong Kong (China): The University of Hong Kong.

Lee, H. F., and Zhang, D. D. (2010). Changes in climate and secular population cycles in China, 1000 CE to 1911. *Clim. Res.* 42 (3), 235–246. doi:10.3354/cr00913

Lee, H. F., and Zhang, D. D. (2013). A tale of two population crises in recent Chinese history. *Clim. Change* 116 (2), 285–308. doi:10.1007/s10584-012-0490-9

Lee, H. F., Zhang, D. D., Pei, Q., Jia, X., and Yue, R. P. (2016). Demographic impact of climate change on northwestern China in the late imperial era. *Quat. Int.* 425, 237–247. doi:10.1016/j.quaint.2016.06.029

Lefever, D. W. (1926). Measuring geographic concentration by means of the standard deviational ellipse. *Am. J. Sociol.* 32 (1), 88–94. doi:10.1086/214027

Li, Y., Lu, P., Mao, L., Chen, P., Yan, L., and Guo, L. (2021). Mapping spatiotemporal variations of Neolithic and Bronze Age settlements in the Gansu-Qinghai region, China: Scale grade, chronological development, and social organization. *J. Archaeol. Sci.* 129, 105357. doi:10.1016/j.jas.2021.105357

Li, X., Liu, X., Pan, Z., Xie, X., Shi, Z., Wang, Z., et al. (2022). Orbital-scale dynamic vegetation feedback caused the Holocene precipitation decline in northern China. *Commun. Earth Environ.* 3 (1), 257. doi:10.1038/s43247-022-00596-2

Liu, L. (1996). Settlement patterns, chiefdom variability, and the development of early states in North China. *J. Anthropol. Archaeol.* 15 (3), 237–288. doi:10.1006/jaar.1996.0010

National Cultural Heritage Administration (1991). *Atlas of Chinese cultural Relics: Henan volume*. Beijing: Sinomaps Press. (in Chinese).

National Cultural Heritage Administration (1998). *Atlas of Chinese cultural Relics: Shaanxi volume*. Xi'an: Xi'an Cartographic Publishing House. (in Chinese).

National Cultural Heritage Administration (2006). *Atlas of Chinese cultural Relics: Shanxi volume*. Beijing: Sinomaps Press. (in Chinese).

National Cultural Heritage Administration (2013). *Atlas of Chinese cultural Relics: Hebei volume*. Beijing: Sinomaps Press. (in Chinese).

Pei, Q., Zhang, D. D., Li, J., and Fei, J. (2019). Proxy-based temperature reconstruction in China for the Holocene. *Quat. Int.* 521, 168–174. doi:10.1016/j.quaint.2019.06.032

Rajala, U. (2013). The concentration and centralization of late prehistoric settlement in central Italy: The evidence from the nepi survey. *Pap. Br. Sch. Rome* 81, 1–38. doi:10.1017/s0068246213000032

Ren, L., Yang, Y., Qiu, M., Brunson, K., Chen, G., and Dong, G. (2022). Direct dating of the earliest domesticated cattle and caprines in northwestern China reveals the history of pastoralism in the Gansu-Qinghai region. *J. Archaeol. Sci.* 144, 105627. doi:10.1016/j.jas.2022.105627

Shi, Z., Chen, T., Storozum, M. J., and Liu, F. (2019). Environmental and social factors influencing the spatiotemporal variation of archaeological sites during the historical period in the Heihe River basin, Northwest China. *Quat. Int.* 507, 34–42. doi:10.1016/j.quaint.2018.12.016

Stein, G. J., and Wattenmaker, P. (1990). "Settlement trends and the emergence of social complexity in the Leilan Region of the Habur Plains (Syria) from the fourth to the third millennium B.C," in *The origins of North mesopotamian civilization: Ninevite 5 chronology, economy, society*. Editor H. Weiss (New Haven, CT: Yale University Press), 361–386.

Tan, Q. (1982). *Historical Atlas of China, vol. 1*. Beijing: Sinomaps Press. (in Chinese).

Wagner, M., Tarasov, P., Hosner, D., Fleck, A., Ehrich, R., Chen, X., et al. (2013). Mapping of the spatial and temporal distribution of archaeological sites of northern China during the Neolithic and Bronze Age. *Quat. Int.* 290–291, 344–357. doi:10.1016/j.quaint.2012.06.039

Walker, M., Head, M. J., Berkelhammer, M., Björck, S., Cheng, H., Cwynar, L., et al. (2018). Formal ratification of the subdivision of the Holocene series/epoch (quaternary system/period): Two new global boundary stratotype sections and points (GSSPs) and three new stages/subseries. *Episodes J. Int. Geosci.* 41 (4), 213–223. doi:10.18814/epiiugs/2018/018016

Wang, X., and Wang, L. (2022). Holocene environmental evolution and human adaptability in a coastal area: A case study of the jiaodong Peninsula in Shandong province, eastern China. *Anthropol. Sci.* 220528, 45–53. doi:10.1537/ase.220528

Wang, K., Yu, X., Xia, J., Xu, S., Zhang, T., Xu, Y., et al. (2022). Holocene environmental evolution history based on sporopollenin and micropaleontological reconstruction of KY-01 in the Yellow River Delta. *J. Water Clim. Chang.* 13 (1), 206–223. doi:10.2166/wcc.2021.144

Wang, Y., Wang, N., Zhao, X., Liang, X., Liu, J., Yang, P., et al. (2022). Field model-based cultural diffusion patterns and GIS spatial analysis study on the spatial diffusion patterns of Qijia culture in China. *Remote Sens.* 14 (6), 1422. doi:10.3390/rs14061422

Wei, X. (2010). Discussion of the age of Longshan city sites in the Central Plain and the reason of their rise and abandonment. *Huaxia Archaeol.* 1, 49–60. (in Chinese). doi:10.16143/j.cnki.1001-9928.2010.01.004

Wen, X., Bai, S., Zeng, N., Chamberlain, C. P., Wang, C., Huang, C., et al. (2013). Interruptions of the ancient shu civilization: Triggered by climate change or natural disaster? *Int. J. Earth Sci.* 102 (3), 933–947. doi:10.1007/s00531-012-0825-9

Wu, Q., Zhao, Z., Liu, L., Granger, D. E., Wang, H., Cohen, D. J., et al. (2016). Outburst flood at 1920 BCE supports historicity of China's Great Flood and the Xia dynasty. *Science* 353 (6299), 579–582. doi:10.1126/science.aaf0842

Wu, W., and Ge, Q. (2014). 4.5-4.0kaB.P. Climate change, population growth, circumscription and the emergence of chiefdom-like societies in the middle-lower Yellow River valley. *Quat. Sci.* 34 (1), 253–265. (in Chinese with English abstract). doi:10.3969/j.issn.1001-7410.2014.01.29

Wu, W., and Liu, T. (2001). 4000a B.P. event and its implications for the origin of ancient Chinese civilization. *Quat. Sci.* 21 (5), 443–451. (in Chinese with English abstract).

Xiao, J., Zhang, S., Fan, J., Wen, R., Xu, Q., Inouchi, Y., et al. (2019). The 4.2 ka event and its resulting cultural interruption in the Daihai Lake basin at the East Asian summer monsoon margin. *Quat. Int.* 527, 87–93. doi:10.1016/j.quaint.2018.06.025

Xu, H. (2016). *China: 2000 B.C.* Beijing: SDX Joint Publishing Company. (in Chinese).

Yan, L., Yang, R., Lu, P., Teng, F., Wang, X., Zhang, L., et al. (2021). The spatiotemporal evolution of ancient cities from the late Yangshao to Xia and Shang dynasties in the central plains, China. *Herit. Sci.* 9 (1), 124. doi:10.1186/s40494-021-00580-7

Yang, Y., Dong, G., Zhang, S., Cui, Y., Li, H., Chen, G., et al. (2017). Copper content in anthropogenic sediments as a tracer for detecting smelting activities and its impact on environment during prehistoric period in Hexi Corridor, Northwest China. *Holocene* 27 (2), 282–291. doi:10.1177/0959683616658531

Yang, B., Qin, C., Bräuning, A., Osborn, T. J., Trouet, V., Ljungqvist, F. C., et al. (2021). Long-term decrease in Asian monsoon rainfall and abrupt climate change events over the past 6,700 years. *Proc. Natl. Acad. Sci. U. S. A.* 118 (30), e2102007118. doi:10.1073/pnas.2102007118

Zhang, G. (1989). A preliminary study on the origin of the Yueshi culture. *J. Zhengzhou Univ. Philos. Soc. Sci. Ed.)* 1, 5–10. (in Chinese).

Zhang, S., Yang, Y., Storozum, M. J., Li, H., Cui, Y., and Dong, G. (2017). Copper smelting and sediment pollution in bronze age China: A case study in the Hexi corridor, northwest China. *Catena* 156, 92–101. doi:10.1016/j.catena.2017.04.001

Zhang, H., Cheng, H., Sinha, A., Spötl, C., Cai, Y., Liu, B., et al. (2021). Collapse of the Liangzhu and other Neolithic cultures in the lower Yangtze region in response to climate change. *Sci. Adv.* 7 (48), eabi9275. doi:10.1126/sciadv.abi9275

Zhang, S., Zhang, D. D., and Pei, Q. (2021). Spatiotemporal shifts of population and war under climate change in imperial China. *Clim. Change* 165, 11. doi:10.1007/s10584-021-03042-y

frontiers | Frontiers in Earth Science

TYPE Original Research
PUBLISHED 24 March 2023
DOI 10.3389/feart.2023.1144805

Check for updates

OPEN ACCESS

EDITED BY
Harry F. Lee,
The Chinese University of Hong Kong, China

REVIEWED BY
Yi Guo,
Zhejiang University, China
Liangliang Hou,
Shanxi University, China

*CORRESPONDENCE
Minmin Ma,
mamm@lzu.edu.cn

†These authors have contributed equally to this work and share first authorship

SPECIALTY SECTION
This article was submitted to Quaternary Science, Geomorphology and Paleoenvironment, a section of the journal Frontiers in Earth Science

RECEIVED 15 January 2023
ACCEPTED 15 March 2023
PUBLISHED 24 March 2023

CITATION
Lu M, Lu Y, Yang Z, Cili N and Ma M (2023), Diverse subsistence strategies related to the spatial heterogeneity of local environments in the Hengduan Mountain Region during the Bronze Age. *Front. Earth Sci.* 11:1144805. doi: 10.3389/feart.2023.1144805

COPYRIGHT
© 2023 Lu, Lu, Yang, Cili and Ma. This is an open-access article distributed under the terms of the Creative Commons Attribution License (CC BY). The use, distribution or reproduction in other forums is permitted, provided the original author(s) and the copyright owner(s) are credited and that the original publication in this journal is cited, in accordance with accepted academic practice. No use, distribution or reproduction is permitted which does not comply with these terms.

Diverse subsistence strategies related to the spatial heterogeneity of local environments in the Hengduan Mountain Region during the Bronze Age

Minxia Lu[1†], Yongxiu Lu[1†], Zhijian Yang[2], Nongbu Cili[3] and Minmin Ma[1*]

[1]MOE Key Laboratory of Western China's Environmental Systems, College of Earth & Environmental Sciences, Lanzhou University, Lanzhou, China, [2]Yulong County Cultural Relics Management Institute, Lijiang, China, [3]Deqin County Cultural Relics Management Institute, Diqing Tibetan Autonomous Prefecture, China

Human subsistence strategies in East Asia changed significantly during the Bronze Age. The notable spatial variability in these strategies has been mainly attributed to the asynchronous introduction and adoption of new crops and livestock, as well as climate changes. However, the impact of differential local environments on spatial patterns of subsistence strategies in diverse geomorphic areas, such as the Hengduan Mountain Region (HMR), is poorly understood. In this study, we present new carbon and nitrogen isotopic data of human bone collagen from the Adong and Gaozhai tombs in the HMR. Adong is located in a mountain area, and Gaozhai is located on a river terrace. Both sites were dated to the early third Millennium BP (before the present). Our results suggest that human diets at Gaozhai were dominated by C_3 foods. Human diets at Adong, alternatively, displayed more differentiation, with greater consumption of C_4 foods. Further evidence is needed to discuss the significant differences in $\delta^{15}N$ values of human bone collagen between the Gaozhai and Adong tombs. By comparing published isotopic, archaeobotanical, and zooarchaeological data, as well as the altitude and precipitation at the archaeological sites, we propose that precipitation may have affected the diversity of human dietary strategies in the Bronze Age HMR. We conclude that at higher altitudes, humans adopted diverse subsistence strategies and obtained meat resources by hunting. Some of this preferential behavior is likely explained by the survival pressure in the highlands of the HMR during the Bronze Age.

KEYWORDS

isotopic analysis, subsistence strategies, regional landform, hydrothermal conditions, Bronze Age, Hengduan Mountain Region

1 Introduction

Spatio-temporal patterns of subsistence strategies transformed significantly throughout Eurasia during the late Neolithic and Bronze periods (Jones et al., 2011; Liu et al., 2019; Dong et al., 2022a; Ma et al., 2022a). These patterns' relationship to transcontinental exchange and climate change have been intensively discussed in the past two decades (Chen et al., 2015; Yang et al., 2021; Dong et al., 2022b; He et al., 2022; Li et al., 2022; Yang et al., 2022), with the rapid accumulation of archaeobotanical, zooarchaeological, and stable isotopic data from archaeological sites, as well paleoclimatic studies across the continent (Outram et al., 2012; Brunson et al., 2016; Jia et al., 2016; Dong et al., 2017; Hanks et al., 2018; Du et al., 2020; Zhou et al., 2020; Zhang et al., 2021; Wang et al., 2022). The introduction and utilization of new crops and livestock brought by early trans-Eurasian exchange profoundly influenced the spatial features of human livelihoods on both continental and regional scales (Chen et al., 2015; Dong et al., 2018; Liu et al., 2019; Dong et al., 2021). Some researchers have also suggested that rapid and drastic climatic fluctuations triggered the transformation of human subsistence strategy in local and regional scales during the late Neolithic and Bronze Age (d'Alpoim Guedes and Bocinsky, 2018; Sun et al., 2019; Chen et al., 2020; Li et al., 2022). Despite such studies, not much is known about the influence of diverse local environments (e.g., landform and hydrothermal conditions) on the spatial patterns of human subsistence strategies during the late Neolithic and Bronze periods, especially around high plateau margin areas with significant differences in altitude.

The Hengduan Mountain Region (HMR) lies in the southeast of the Tibetan Plateau and has acted as an essential passageway for human migration and cultural exchange since the late Paleolithic period (Hein, 2014; Gao et al., 2021; Ma et al., 2022b; Huan et al., 2022). Humans engaged in hunting-gathering in the HMR until the arrival of Neolithic farming groups from the Yellow River Valley during the sixth Millennium BP (Chen and Chen, 2006; Zhao and Chen, 2011; Huan et al., 2022). Following this introduction to agriculture, human strategies for food production transformed with notable spatial variability in the subsequent thousands of years (Lu et al., 2021; Ma et al., 2022a). According to the radiocarbon dates of the crop remains, millets, rice, and wheat/barley first spread to the HMR around 5,300 BP, 5,000 BP, and 3,400 BP, respectively (d'Alpoim Guedes et al., 2015; Huan et al., 2022). Archaeobotanical studies suggest that foxtail and broomcorn millet might have served as essential crops in the highlands of the Western Sichuan Plateau during ~5,300 BP–3,700 BP (Chen and Chen, 2006; d'Alpoim Guedes, 2011; Zhao and Chen, 2011; Yan et al., 2016a; Chen et al., 2022). These same crops were utilized in the comparatively low-lying areas of southern HMR until ~4,600 BP (Dal Martello et al., 2018). Cropping patterns in the HMR during the late Neolithic and especially during the Bronze period (~3,400–2,200 BP) demonstrated diverse characteristics across different landforms (e.g., mountain areas, dry-hot valleys) (Lu et al., 2021; Ma et al., 2022a). However, the importance of different crops in plant subsistence and their relation to local environments throughout the HMR remains unclear, mainly due to the absence of human bone collagen stable isotopic data from different geomorphological positions.

Recent archaeological investigations provided new radiocarbon data from Bronze Age sites in the HMR: Adong tombs (2,517 masl, 2,750 BP–2,450 BP) in mountain areas and Gaozhai tombs (2,080 masl, 2,850 BP–2,450 BP) in river terraces (Figure 1; Ma et al., 2022b). Thirty-one human bones were collected from these two contemporaneous sites, providing an excellent opportunity to examine human diet patterns across different HMR Bronze Age landforms. We analyzed carbon and nitrogen isotopes of human bone collagen from these sites and compared them with published carbon isotopic data of human bone collagen and archaeobotanical and zooarchaeological data from HMR sites during the Bronze Age. Moreover, we explored the relationship between human subsistence strategy and local environments during the third Millennium BP by comparing the altitude and precipitation values of HMR sites, which is valuable to understand human-land relations during the Bronze Age in the HMR with high geomorphic diversity.

2 Study area

The Hengduan Mountain Region (HMR, 24.65°N–33.57°N, 96.97°E–104.45°E)is located in the southeast of the Qinghai–Tibet Plateau (Figure 1), covering a total area of about 5.0 $km^2 \times 10^5$ km^2 (Yang and Zheng, 1989; Bian et al., 2018; Wang et al., 2018). The altitude of HMR is 300–7,000 masl, with higher terrain in the northwest and lower terrain in the southeast. The geography is complex and diverse, with parallel mountains and deep, river-carved gorges (e.g., Jinsha River, Nujiang River, and Lancang River). The climate varies, crossing the subtropical zone, plateau temperate zone, and plateau subfrigid zone from south to north. HMR southern and northern areas are mainly dominated by monsoon climate and paramos climate, respectively (Bian et al., 2018). The vertical zones of vegetation in HMR vary significantly, with shrubs, coniferous forests, and meadows total accounting for 76% (Wang et al., 2017).

Gaozhai sarcophagus tombs (100.26°E, 27.27°N, 2080 masl)—found in 2020—are located in Daju Town, Yulong County, Yunnan Province. The average annual temperature is 13.3°C, annual precipitation is 968.1 mm, and annual sunshine time is 2,411.7 h. Daju Town is in the dry-hot valley of the Jinshajiang River, with high annual accumulated temperature and significant diurnal temperature variation (Zi, 2011). Shrubs and meadows dominate the vegetation. Modern-day crops include wheat, rice, and corn. A total of four tombs were excavated, and some human bones were unearthed. Human bones allowed researchers to date the tombs to 2,850–2,450 BP (Ma et al., 2022b).

Adong sarcophagus tombs (28.56°E, 98.86°N, 2,517 masl) are located in Adong village, Deqin County, Yunnan Province. The average annual temperature is 5.9°C, annual precipitation is 639.9 mm, and annual sunshine time is 1,964.8 h. The Adong village is a typical Tibetan village located in the high-mountain gorge areas of the HMR. Modern-day residents mainly survive on agriculture and livestock (Haynes et al., 2013; Li, 2020): they plant (e.g., naked barley, wheat, corn) along the river banks and gentle slopes below 2,600 masl, and graze (e.g., yak, cattleyak) above 2,600 masl (Li, 2020). The Adong sarcophagus tombs were found by the Deqin County Cultural Relics Management Institute in 2020 and were dated to 2,750 BP –2,450 BP with human bones (Ma et al., 2022b).

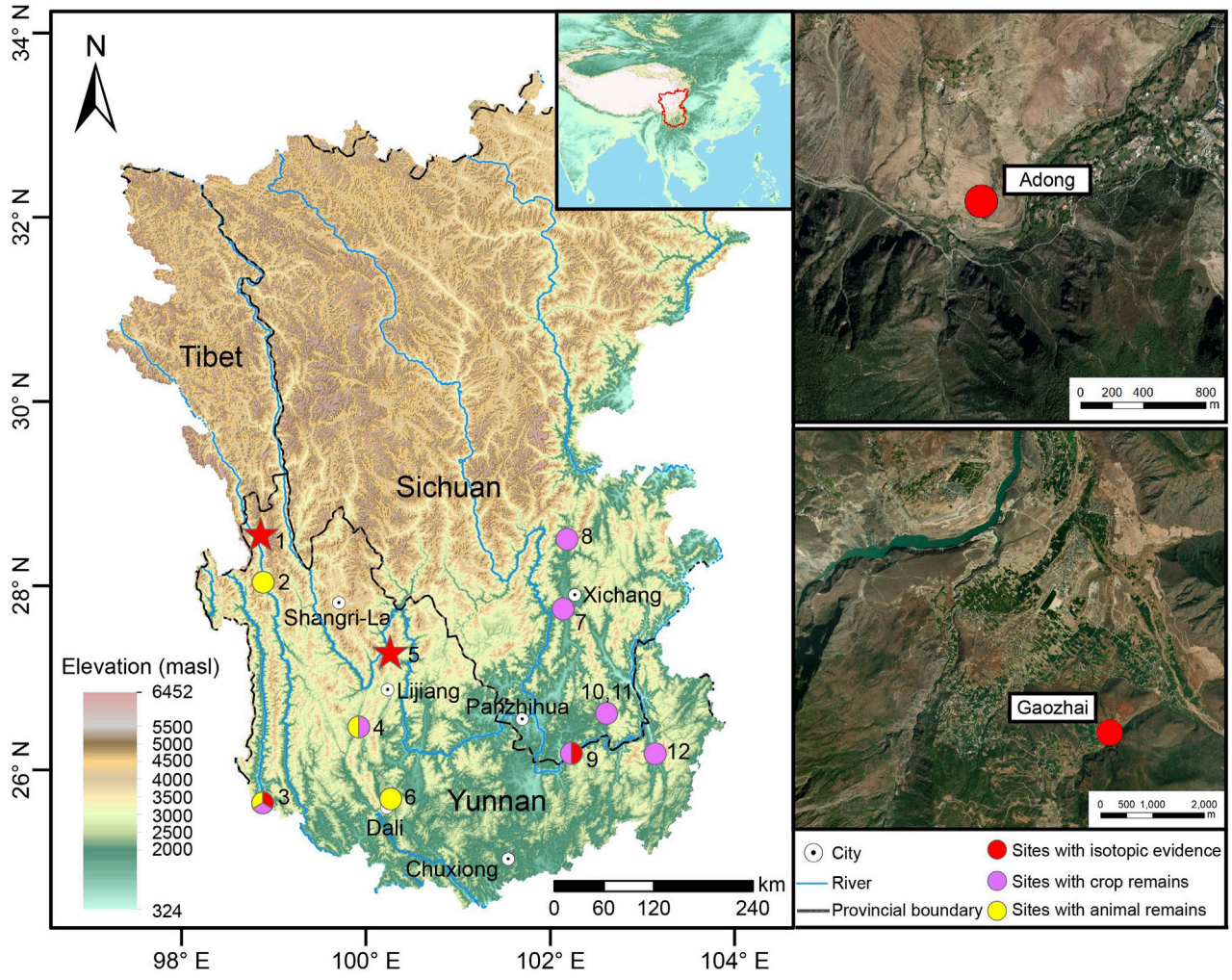

FIGURE 1
Archaeological sites with isotopic data of human bone collagen and remains of crops and animals in the HMR during the Bronze Age; (1) Adong; (2) Zongzan; (3) Shilinggang; (4) Haimenkou; (5) Gaozhai; (6) Yinsuodao; (7) Shapingzhan; (8) Gaopo; (9) Jiangxifen; (10) Dashanbao; (11) Tuanshanbao; (12) Yubeidi.

3 Materials and methods

3.1 Collagen preparation and isotopic measurements

Carbon and nitrogen isotopes of bone collagen can reflect an individual's diet before death (Ambrose and Norr, 1993), so it is one of the useful tools to reconstruct human subsistence strategies in prehistory. Various photosynthetic pathways lead to different $\delta^{13}C$ values of plants (Van der Merwe, 1982; van der Merwe and Medina, 1989), which makes the $\delta^{13}C$ values of bone collagen can distinguish the plant species that an individual consumes. The $\delta^{15}N$ values of bone collagen usually reflect the nutritional level of an individual, but it is also affected by metabolism (Chen, 2017). Various factors need to be considered when reconstructing the paleodiet with nitrogen isotope.

We collected a total of 31 human bones from the Gaozhai and Adong tombs: 25 bones from four Gaozhai tombs (25 human individuals) and six bones from three Adong tombs (at least three human individuals, Table 1).

According to the method described by Richards and Hedges. (1999), we further removed humic acid with NaOH (Ma et al., 2016) to extract bone collagen samples at the Key Laboratory of Western China's Environmental Systems (MOE), Lanzhou University. We demineralized 0.5 g–1.5 g of bone samples (according to the preserved condition of bones) with 0.5 mol/L hydrochloric acid after cleaning sediment on bone fragments. It took about two weeks of refreshing the hydrochloric acid for bubbles to stop appearing. Next, we placed bones into 0.125 mol/L NaOH for 20 h to remove the humic acid. A 4°C environment housed all of these steps. We gelatinized the bone samples with hydrochloric acid (pH = 3) for 48 h in a 75°C environment. Finally, we obtained the collagen samples by filtering and freeze-drying.

TABLE 1 The collagen isotopic results of human bones at the Gaozhai and Adong tombs.

Site	Sample no.	Skeletal element	Col wt%	C wt%	N wt%	C/N	$\delta^{13}C$ (‰)	$\delta^{15}N$ (‰)
Gaozhai	2021YDGM1R1①	Tibia	3.2	43.2	15.8	3.2	−18.2	7.5
Gaozhai	2021YDGM1R2①	Skull	4.9	43.5	15.8	3.2	−18.1	9.7
Gaozhai	2020YDGM1②R4	Skull	4.2	43.7	15.9	3.2	−18.7	8.3
Gaozhai	2020YDGM1②R5	Skull	4.3	42.8	15.7	3.2	−18.1	6.9
Gaozhai	2020YDGM1③R6	Phalanx	4.5	43.3	15.8	3.2	−17.8	8.0
Gaozhai	2020YDWGM2R1	Femur	3.0	42.8	15.5	3.2	−18.8	8.2
Gaozhai	2020YDWGM3R1	Long bone	13.3	43.2	15.7	3.2	−18.4	9.5
Gaozhai	2020YDWGM4R1	Skull	5.1	41.9	15.3	3.2	−18.7	7.4
Gaozhai	2020YDWGM4R2	Skull	1.8	43.5	15.8	3.2	−19.1	8.2
Gaozhai	2020YDWGM4R3	Skull	3.9	43.4	15.9	3.2	−18.7	9.1
Gaozhai	2020YDWGM4R4	Skull	3.9	43.6	15.9	3.2	−18.2	8.3
Gaozhai	2020YDWGM4R5	Skull	3.9	43.6	15.9	3.2	−18.0	8.2
Gaozhai	2020YDWGM4R6	Skull	4.7	42.4	15.5	3.2	−18.4	8.5
Gaozhai	2020YDWGM4R7	Skull	7.1	42.6	15.6	3.2	−18.8	9.3
Gaozhai	2020YDWGM4R8	Skull	4.1	43.4	15.8	3.2	−18.2	7.9
Gaozhai	2020YDWGM4R10	Maxilla	8.3	43.7	16.0	3.2	−17.8	9.4
Gaozhai	2020YDWGM4R11	Skull	4.6	43.6	16.0	3.2	−19.2	8.3
Gaozhai	2020YDWGM4R13	Rib	7.8	43.0	15.7	3.2	−18.6	7.6
Gaozhai	2020YDWGM4R14	Humerus	1.8	44.1	16.2	3.2	−18.2	7.9
Gaozhai	2020YDWGM4R15	Skull	3.3	43.7	15.9	3.2	−17.7	10.1
Gaozhai	2020YDWGM4R17	Mandible	5.3	43.9	16.0	3.2	−18.4	8.9
Gaozhai	2020YDWGM4R20	Skull	5.0	43.9	15.9	3.2	−19.0	8.5
Gaozhai	2020YDWGM4R21	Clavicle	5.9	43.9	16.1	3.2	−18.3	8.4
Gaozhai	2020YDWGM4R22	Tibia	5.1	43.9	15.8	3.2	−17.8	7.9
Adong	AD-M1-B1	Long bone	8.4	44.0	16.1	3.2	−15.2	12.4
Adong	AD-M1-B2	Long bone	13.9	44.5	16.3	3.2	−15.4	12.0
Adong	AD-M2-B1	Metacarpus	16.5	44.5	16.4	3.2	−15.7	12.2
Adong	AD-M3-B1	Mandible	4.0	43.4	15.8	3.2	−17.8	11.4
Adong	AD-M3-B2	Radius	17.4	44.0	16.1	3.2	−18.5	9.7
Adong	AD-M3-B3	Tooth	13.3	43.5	16.0	3.2	−18.4	10.1

We measured C% and N% of bone collagen samples on Elementar Vario EL Cube elemental analyzer at the State Key Laboratory of Applied Organic Chemistry, Lanzhou University, and measured carbon and nitrogen stable isotopic values on Thermo Fisher Flash EA1112–MAT253 mass spectrometer at the Key Laboratory of Western China's Environmental Systems (MOE), Lanzhou University. The carbon and nitrogen isotope ratios were measured relative to VPDB (Vienna Pee Dee Belemnite) and AIR (Ambient lnhalable Reservoir) with 0.2‰ analytical precision, respectively.

3.2 Data collection

We collected the quantity of crop remains, the number of identified specimens (NISP) of animal remains, and carbon isotopic data of human bone collagen to compare the human subsistence strategies in diverse geomorphic areas in HMR during the Bronze Age. Precipitation data were obtained from http://data.cma.cn, and we calculated the average precipitation from 1981 to 2010 of weather stations adjacent to the archaeological sites.

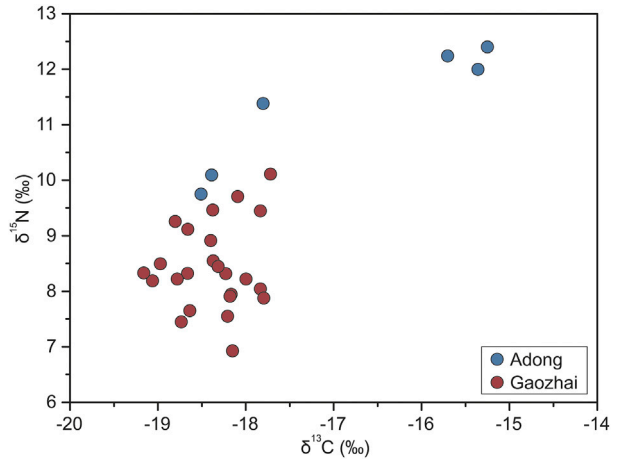

FIGURE 2
Scatter diagram of isotopic values from Gaozhai and Adong tombs.

4 Results

We obtained 30 bone collagen samples; we could not obtain collagen from one human bone from a Gaozhai tomb (Figure 2; Table 1). We believe the bone collagen samples were well-preserved as the ranges of C%, N%, and C: N atomic ratios were 41.9%–44.5%, 15.3%–16.4%, and 3.2, respectively (Table 1). Additionally, collagen yields exceeded 1% (Table 1; DeNiro, 1985; Ambrose, 1990). All bone collagen samples could be further analyzed.

The $\delta^{13}C$ and $\delta^{15}N$ values of bone collagen samples from the Gaozhai tombs are −19.2‰—−17.7‰ (mean = −18.4‰ ± 0.4‰, n = 24) and 6.9‰—10.1‰ (mean = 8.4‰ ± 0.8‰, n = 24), respectively (Figure 2; Table 2). The $\delta^{13}C$ and $\delta^{15}N$ values from the Adong tombs are −18.5‰—−15.2‰ (mean=−16.8‰ ± 1.6‰, n = 6) and 9.7‰–12.4‰ (mean = 11.3‰ ± 1.1‰, n = 6), respectively (Figure 2; Table 2). It should be noted that the $\delta^{13}C$ and $\delta^{15}N$ values of M1 and M2 are significantly different from those of M3 (Figure 2; Table 1). The $\delta^{13}C$ and $\delta^{15}N$ values of M1 and M2 are −15.7‰—−15.2‰ (mean = −15.4‰ ± 0.3‰, n = 3) and 12.0‰–12.4‰ (mean = 12.2‰ ± 0.2‰, n = 3), respectively, and the $\delta^{13}C$ and $\delta^{15}N$ values of M3 are −18.5‰—−17.8‰ (mean = −18.2‰ ± 0.4‰, n = 3) and 9.7‰–11.4‰ (mean = 10.4‰ ± 0.9‰, n = 3), respectively.

5 Discussion

5.1 Spatial pattern of human dietary strategies in the HMR during the Bronze Age

Stable isotopic data of human bone collagen from the Adong and Gaozhai tombs reveal that humans living in the highlands consumed different foodstuffs during the early third Millennium BP than those living in the dry-hot valley of the Jinsha River. Two groups can be detected from the C-N isotopes of human bone collagen at the Adong tombs. The $\delta^{13}C$ values (−15.7‰—−15.2‰) from M1 and M2 (at least two human individuals) indicate that humans consumed a mixed C_3 and C_4 diet and the $\delta^{13}C$ values (−18.5‰—−17.8‰) from M3 (at least one human individuals) indicate a C_3-based diet (Figure 2; Table 1). Three radiocarbon dates of human bones from those tombs ranged between 2,750 and 2,450 BP, indicating that these two groups (C_3-based and C_3-C_4 mixed) lived in the Adong area concurrently (Ma et al., 2022b). Previous studies indicated that C_4 plants in the flora gradually decreased or even disappeared when the altitude exceeds 2,000 m–3,000 m (Chazdon, 1978; Boutton et al., 1980; Rundel, 1980; Cavagnaro, 1988; Wang et al., 2004; Li et al., 2009), which suggests that individuals from M1 and M2 might consume a certain amount of C_4 crops. No archaeobotanical evidence was reported from the Adong tombs or other Bronze Age sites above 2,500 masl in the HMR. Archaeobotanical studies from late Neolithic sites in the highlands of the HMR, including Haxiu, Guijiabao, and Karuo, demonstrate that humans utilized foxtail and broomcorn millet in the mountain areas since ~5,300 BP (Chen and Chen, 2006; Yan et al., 2016a; Song et al., 2021). These indigenous crops were also widely cultivated in the HMR during the Bronze Age (Yang, 2016; Xue et al., 2022). Based on this information and our analysis, we conclude that the individuals from Adong M1 and M2 (at least two individuals) likely both consumed millet crops and C_3 food, while those from M3 mainly consumed C_3 foods. Moreover, $\delta^{15}N$ values of M1 and M2 (12.2‰ ± 0.2‰) are higher than those of M3 (10.4‰ ± 0.9‰, Figure 2; Table 1). The possible reason is that individuals from M1 and M2 consumed more animal protein, but the $\delta^{15}N$ value of millet remains at Jiagezi cemetery suggests that the intake of millet might also be the reason for the high nitrogen isotope of human collagen (Ren et al., 2020). In addition, it is not excluded that individuals from M1 and M2 might migrate from other areas. More samples are needed for further discussion.

The $\delta^{13}C$ values of human bone collagen from the Gaozhai tombs are relatively clustered compared to those from the Adong tombs (Figure 2). The $\delta^{13}C$ value (−18.4‰ ± 0.4‰) indicates that humans at Gaozhai primarily consumed C_3 foods (Figure 2; Table 2).

TABLE 2 Summary of human isotopic values from the Gaozhai and Adong tombs.

Site	Region	Elevation (masl)	Age (BP)	Number	$\delta^{13}C$ (‰)			$\delta^{15}N$ (‰)		
					Mean	SD	Range	Mean	SD	Range
Gaozhai	Yulong	2,080	~2,850–2,450	24	−18.4	0.4	−19.2–−17.7	8.4	0.8	6.9–10.1
Adong	Deqin	2,517	~2,750–2,450	6	−16.8	1.6	−18.5–−15.2	11.3	1.1	9.7–12.4

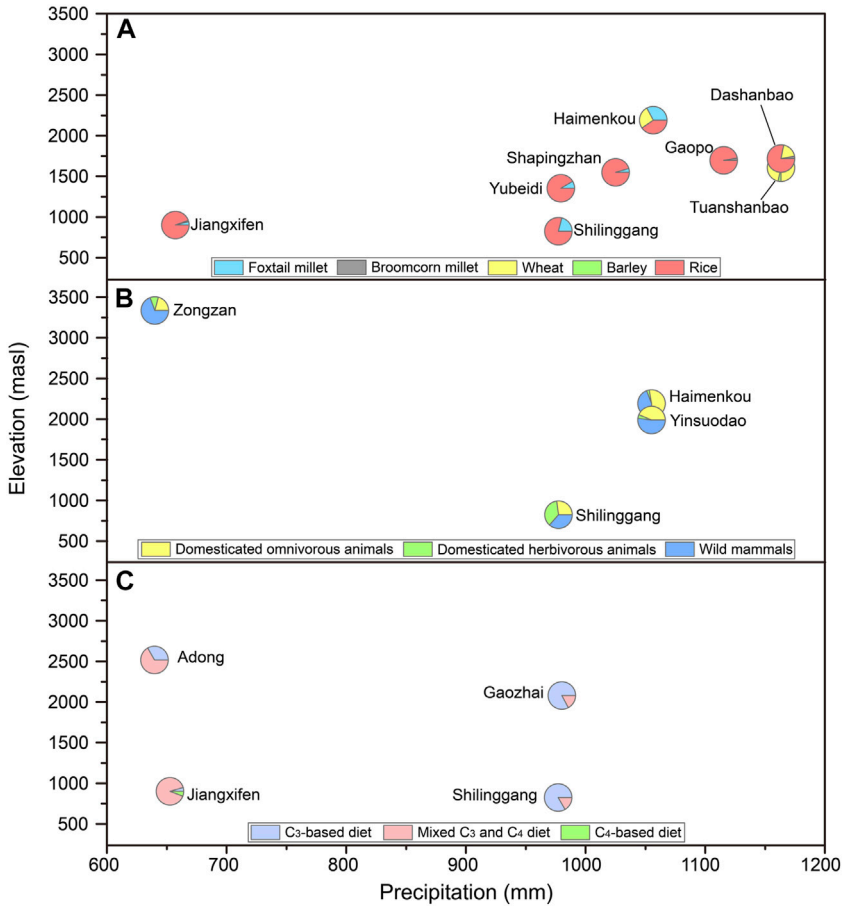

FIGURE 3
Elevation and precipitation variation in the distribution of sites with **(A)** crop remains; **(B)** animal remains; and **(C)** carbon isotopic signals of human bone collagen in HMR during the Bronze Age.

Archaeobotanical studies from contemporaneous sites on the terraces of rivers and lakes in the HRM, such as Yubeidi, Shilinggang, and Jiangxifen, suggest that rice served as the dominant crop (Figure 3A; Yang, 2016; Li et al., 2016; Lu et al., 2021). At the same time, wheat/barley and millets served as auxiliary crops in these areas during the early third Millennium BP. It suggests that rice was the primary crop, though wheat may have served as another staple food at Gaozhai. Further archaeobotanical analysis is needed to ascertain this assumption. $\delta^{15}N$ values (8.4‰ ± 0.8‰) of human bone collagen from the Gaozhai tombs are significantly lower than those of the Adong tombs (11.3‰ ± 1.1‰, $t = 0.000$, Figure 2; Table 2). Due to the lack of vegetation isotopic data and the different opinions on the relationship between vegetation $\delta^{15}N$ values and altitude (Sah and Brumme, 2003; Yi and Yang, 2006; Liu et al., 2009), it is difficult to determine the reasons for the differences in $\delta^{15}N$ values between Gaozhai and Adong sites. The differences in animal protein intake and the natural environment are both possible reasons.

Previous studies analyzed human bone collagen's carbon and nitrogen isotopic data from Jiangxifen and Shilinggang Bronze sites in the HMR (Liu, 2016; Lu et al., 2021). The human $\delta^{13}C$ signals in the Shiligang site are almost similar to those in the Gaozhai tombs (Liu, 2016): in both sites, the human diet appears to have been dominated by C_3 foods (likely rice and rice byproducts), and auxiliary with mixed C_3 and C_4 foods (Figure 3C). The Shilinggang and Gaozhai sites are on river terraces in south HMR. The average annual precipitation of these sites is roughly the same, though the elevation of Gaozhai is ~1,200 masl higher than Shilinggang. The Jiangxifen site and the Shilianggang site lie at roughly the same elevation, though the average annual precipitation of Shilianggang is ~300 mm higher. Jiangxifen data suggests that the consumption of C_4 foods exceeded that of Shilinggang and Gaozhai (Figure 3C; Liu, 2016; Lu et al., 2021). Based on such data, we infer that human dietary strategies in the HRM during the Bronze Age were related to precipitation to a certain extent, though more information regarding the specific variation in subsistence strategies is needed.

5.2 Relationship between the spatial pattern of human subsistence strategies during the Bronze Age and local environments in the HMR

Numerous environmental features, including precipitation, temperature, landscape, and vegetation cover, are considered critical influencing factors for cultural evolution, subsistence

strategy transformation, and massive human migration during the Neolithic and Bronze periods (Liu et al., 2009; Preston et al., 2012; Wang et al., 2017; Liao et al., 2019; Dong et al., 2022c; Li et al., 2022). The HMR in particular possesses significant spatial differences in altitude and precipitation. In addition, the average annual temperature in the HMR is closely related to the variation in altitude. To explore the relationship between human subsistence strategies and the spatial heterogeneity of local environments in HMR during the Bronze Age, we compared carbon isotopic data of human bone collagen, archaeobotanical and zooarchaeological data from Bronze Age sites in the HMR, and then assessed those data against the backdrop of altitude and precipitation in those sites (Figure 3).

According to published archaeobotanical data from Bronze Age sites in the HMR, rice dominated the human diet, followed by foxtail millet in most Bronze Age sites below ~1,700 masl in the HMR (Jiang et al., 2013; Yan et al., 2016b; Li et al., 2016; Yang, 2016; Lu et al., 2021). Two exceptions to this trend are the Tuanshanbao and Dashanbao sites, both of which lie at ~1,700 masl (Figure 3A; Yan et al., 2016c). The Tuanshanbao and Dashanbao sites were dated to ~2,700 BP–2,400 BP and 2,400 BP–2,200 BP, respectively (Yan et al., 2016c). Other sites, such as the Gaopo and Shapingzhan sites, were settled during the early third Millennium BP (Jiang et al., 2013; Yan et al., 2016b). This temporal difference might suggest that the cropping pattern of the Tuanshanbao and Dashanbao sites was affected by increasing cultural exchange from the surrounding regions. However, the small number of the crop remains at these sites makes it difficult to understand the crops' cultivated structure well at the Tuanshanbao and Dashanbao sites (Yan et al., 2016c). In the Bronze Age sites above ~1,700 masl, rice was also the primary crop, while foxtail millet and wheat were also important. The cropping pattern of the Haimenkou site was more diverse than the crop remains discovered in sites at lower elevations, typically below ~1,700 masl (Figure 3A; Xue et al., 2022). This suggests that cropping patterns in the HMR during the Bronze Age were primarily affected by the altitude of human settlements. The relationship between cropping patterns and precipitation is difficult to ascertain, likely because the average annual precipitation in each site exceeded 600 mm (Figure 3A), which is sufficient for the growth of different crops.

We obtained zooarchaeological data from only four Bronze sites in the HMR. In the Shilinggang site (~800 masl), omnivorous livestock (e.g., pig and dog), herbivorous livestock (e.g., cattle, sheep/goat), and wild mammals appear to be of similar significance in human diets (Liu, 2016). This suggests that humans in the Nujiang River valley adopted a diverse strategy with various animal utilization to adequately exploit their surrounding natural resources and rice and millet byproducts. In the Yinsuodao and Haimenkou sites (~2,000 masl), the proportion of wild mammals and omnivorous livestock ranged between 44%–52% and 44%–53%, respectively, and the proportion of herbivorous livestock fell below 5% (Figure 3B; Zhao, 2011; Wang, 2012). This suggests that humans mainly hunted game and fed pigs/dogs to obtain animal protein during the Bronze Age. In contrast, the importance of herbivorous livestock herding in livelihoods was limited, possibly due to the absence of contiguous grasslands. In the Zongzan site (~3,300 masl), the proportion of wildlife remains was roughly 70%, while omnivorous and herbivorous livestock remains accounted for 21% and 10%, respectively (Chen et al., 2019). This suggests that in this site, humans mainly relied on hunting, and only supplemented with livestock to obtain meat resources in mountain areas of the HMR during the Bronze Age.

As shown in Figure 3, the diversity of human dietary strategies and the importance of hunting in the HMR during the Bronze Age increased with altitude: limited agricultural production forced humans to exploit more diverse food resources in high-altitude areas. This relationship is likely due to the decrease in arable land and suitable hydrothermal conditions for the high-yielding rice cultivation at higher elevations, which also limits livestock feeding, while the resources of wild animals are relatively abundant in high-altitude areas. These factors resulted in increased survival pressure in the highlands, which possess lower accumulated temperature and precipitation compared to the river valleys in the lowlands. The relationship between average annual precipitation and cropping patterns or animal utilization strategies in the HMR during the Bronze Age is difficult to evaluate. It seems that humans consumed more diverse diets at the Jiangxifen and Adong sites, both of which experienced relatively low average annual precipitation (~650 mm) than they did at the Shilinggang and Gaozhai sites, which both experienced relatively high average annual precipitation (~1,000 mm) (Figure 3C; Liu, 2016; Lu et al., 2021). Compared to the late Neolithic period, the Bronze Age saw the introduction and utilization of more crops and livestock in the HMR. This facilitated the development of diverse subsistence strategies across different altitudes. Furthermore, the large rivers and mountains resulted in highly fragmented and isolated habitats, which mitigated opportunities for the formation of a dominant subsistence strategy in late Neolithic China (Lu et al., 2021; Ma et al., 2022a), but which supported the emergence of diverse subsistence strategies in the Bronze Age HMR.

6 Conclusion

Carbon and nitrogen isotopes of human bone collagen from the Adong and Gaozhai tombs indicate that human dietary patterns differed across HMR mountain areas and river terraces during the early third Millennium BP. Humans may have consumed diverse mixed C_3/C_4 foods at Adong during ~2,750 BP–2,450 BP. Humans at Gaozhai mainly relied on C_3 foods, supplemented only by a few C_4 foods. The difference in animal protein intake between the two sites needs more evidence for discussion. By comparing published isotopic, archaeobotanical, and zooarchaeological studies, as well as analyzing the altitude and precipitation of investigated sites, we deduce that, in general, humans engaged in more diverse subsistence strategies and hunted more wildlife with the increase of altitude. This is likely due to the severe survival pressure in the HMR highlands during the Bronze Age. In addition, cropping patterns throughout the Bronze Age HMR were likely affected by various factors, such as the introduction and utilization of wheat/barley, localized landform, and hydrothermal conditions. The diverse subsistence strategies in the HMR during the Bronze period were rooted in the convergence of numerous crops and livestock in the critical passageways for culture exchange, the relatively abundant wild resources, and the highly fragmented habitats cut by large mountains and rivers in the southeast margin of the Tibetan Plateau.

Data availability statement

The original contributions presented in the study are included in the article/Supplementary Material, further inquiries can be directed to the corresponding author.

Author contributions

MM designed the study. ZY and NC provided archaeological samples. YL experimented. ML, MM, and YL participated in the discussion. ML and YL wrote the manuscript.

Funding

This work was supported by the Second Tibetan Plateau Scientific Expedition and Research Program (STEP) (Grant No. 2019QZKK0601), National Natural Science Foundation of China (Grant No. 42271160), and International Partnership Program of Chinese Academy of Sciences (Grant No. 131C11KYSB20190035).

Conflict of interest

The authors declare that the research was conducted in the absence of any commercial or financial relationships that could be construed as a potential conflict of interest.

Publisher's note

All claims expressed in this article are solely those of the authors and do not necessarily represent those of their affiliated organizations, or those of the publisher, the editors and the reviewers. Any product that may be evaluated in this article, or claim that may be made by its manufacturer, is not guaranteed or endorsed by the publisher.

References

Ambrose, S. H., and Norr, L. (1993). "Experimental evidence for the relationship of the carbon isotope ratios of whole diet and dietary protein to those of bone collagen and carbonate," in *Prehistoric human bone: Archaeology at the molecular level*. Editors J. B. Lambert and G. Grupe (Berlin, Heidelberg: Springer), 1–37. doi:10.1007/978-3-662-02894-0_1

Ambrose, S. H. (1990). Preparation and characterization of bone and tooth collagen for isotopic analysis. *J. Archaeol. Sci.* 17, 431–451. doi:10.1016/0305-4403(90)90007-R

Bian, J. H., Li, X. Z., and Hu, K. H. (2018). Study on distribution characteristics and dynamic evolution of mountain hazards in Hengduan Mountains Area (in Chinese with English abstract). *J. Eng. Geol.* 26, 6–13. doi:10.13544/j.cnki.jeg.2018030

Boutton, T. W., Harrison, A. T., and Smith, B. N. (1980). Distribution of biomass of species differing in photosynthetic pathway along an altitudinal transect in southeastern Wyoming grassland. *Oecologia* 45, 287–298. doi:10.1007/BF00540195

Brunson, K., He, N., and Dai, X. (2016). Sheep, cattle, and specialization: New zooarchaeological perspectives on the taosi longshan. *Int. J. Osteoarchaeol.* 26, 460–475. doi:10.1002/oa.2436

Cavagnaro, J. B. (1988). Distribution of C_3 and C_4 grasses at different altitudes in a temperate arid region of Argentina. *Oecologia* 76, 273–277. doi:10.1007/BF00379962

Chazdon, R. L. (1978). Ecological aspects of the distribution of C_4 grasses in selected habitats of Costa Rica. *Biotropica* 10, 265–269. doi:10.2307/2387678

Chen, F. H., Dong, G. H., Zhang, D. J., Liu, X. Y., Jia, X., An, C. B., et al. (2015). Agriculture facilitated permanent human occupation of the Tibetan Plateau after 3600 BP. *Science* 347, 248–250. doi:10.1126/science.1259172

Chen, J., Chen, Q. J., and Zhu, Z. H. (2019). A Research of faunal remains excavated from the Zongzan site, Yunnan, South China (in Chinese with English abstract). *Res. China's Front. Archaeol.* 26, 247–263.

Chen, J., and Chen, X. Z. (2006). The prehistoric cultures in the upper Dadu River (in Chinese). *J. Chin. Cult.* 3, 5–10.

Chen, T., Qiu, M., Liu, R., Li, H., Hou, H., Howarth, P., et al. (2020). Human responses to climate change in the late prehistoric Western loess plateau, northwest China. *Radiocarbon* 62, 1193–1207. doi:10.1017/RDC.2020.32

Chen, W., Ren, R. B., He, Q., Wan, J., Zhang, L., Yuan, R., et al. (2022). Brief report on the 2012 excavation of the Liujiazhai site in Jinchuan county, Sichuan (in Chinese with English abstract). *Archaeology* 4, 3–21.

Chen, X. L. (2017). New progress in the analysis of stable carbon and nitrogen isotopes and agricultural archaeology (in Chinese). *Agric. Archaeol.* 6, 13–25.

Dal Martello, R., Min, R., Stevens, C., Higham, C., Higham, T., Qin, L., et al. (2018). Early agriculture at the crossroads of China and southeast Asia: Archaeobotanical evidence and radiocarbon dates from baiyangcun, yunnan. *J. Archaeol. Sci. Rep.* 20, 711–721. doi:10.1016/j.jasrep.2018.06.005

d'Alpoim Guedes, J. A., Lu, H., Hein, A. M., and Schmidt, A. H. (2015). Early evidence for the use of wheat and barley as staple crops on the margins of the Tibetan Plateau. *Proc. Natl. Acad. Sci.* 112, 5625–5630. doi:10.1073/pnas.1423708112

d'Alpoim Guedes, J., and Bocinsky, R. K. (2018). Climate change stimulated agricultural innovation and exchange across Asia. *Sci. Adv.* 4, eaar4491. doi:10.1126/sciadv.aar4491

d'Alpoim Guedes, J. (2011). Millets, rice, social complexity, and the spread of agriculture to the chengdu plain and southwest China. *Rice* 4, 104–113. doi:10.1007/s12284-011-9071-1

DeNiro, M. J. (1985). Postmortem preservation and alteration of *in vivo* bone collagen isotope ratios in relation to palaeodietary reconstruction. *Nature* 317, 806–809. doi:10.1038/317806a0

Dong, G., Du, L., and Wei, W. (2021). The impact of early trans-Eurasian exchange on animal utilization in northern China during 5000–2500 BP. *Holocene* 31, 294–301. doi:10.1177/0959683620941169

Dong, G., Du, L., Yang, L., Lu, M., Qiu, M., Li, H., et al. (2022a). Dispersal of crop-livestock and geographical-temporal variation of subsistence along the Steppe and Silk Roads across Eurasia in prehistory. *Sci. China Earth Sci.* 65, 1187–1210. doi:10.1007/s11430-021-9929-x

Dong, G., Lu, Y., Liu, P., and Li, G. (2022c). Spatio-temporal pattern of human activities and their influencing factors along the ancient Silk Road in Northwest China from 6000 a B.P. to 2000 a B.P. (in Chinese). *Quat. Sci.* 42, 1–16. doi:10.11928/j.issn.1001-7410.2022.01.01

Dong, G., Lu, Y., Zhang, S., Huang, X., and Ma, M. (2022b). Spatiotemporal variation in human settlements and their interaction with living environments in Neolithic and Bronze Age China. *Prog. Phys. Geog.* 46, 949–967. doi:10.1177/03091333221087992

Dong, G., Yang, Y., Liu, X., Li, H., Cui, Y., Wang, H., et al. (2018). Prehistoric trans-continental cultural exchange in the Hexi Corridor, northwest China. *Holocene* 28, 621–628. doi:10.1177/0959683617735585

Dong, Y., Morgan, C., Chinenov, Y., Zhou, L., Fan, W., Ma, X., et al. (2017). Shifting diets and the rise of male-biased inequality on the central plains of China during eastern Zhou. *Proc. Natl. Acad. Sci.* 114, 932–937. doi:10.1073/pnas.1611742114

Du, L., Ma, M., Lu, Y., Dong, J., and Dong, G. (2020). How did human activity and climate change influence animal exploitation during 7500-2000 BP in the Yellow River Valley, China. *Front. Ecol. Evol.* 8, 161. doi:10.3389/fevo.2020.00161

Gao, Y., Yang, J., Ma, Z., Tong, Y., and Yang, X. (2021). New evidence from the qugong site in the central Tibetan plateau for the prehistoric highland silk road. *Holocene* 31, 230–239. doi:10.1177/0959683620941144

Hanks, B., Miller, A. V., Judd, M., Epimakhov, A., Razhev, D., and Privat, K. (2018). Bronze Age diet and economy: New stable isotope data from the Central Eurasian steppes (2100-1700 BC). *J. Archaeo. Sci.* 97, 14–25. doi:10.1016/j.jas.2018.06.006

Haynes, M. A., Fang, Z., and Waller, D. M. (2013). Grazing impacts on the diversity and composition of alpine rangelands in Northwest Yunnan. *J. Plant Ecol.* 6, 122–130. doi:10.1093/jpe/rts021

He, K., Lu, H., Jin, G., Wang, C., Zhang, H., Zhang, J., et al. (2022). Antipodal pattern of millet and rice demography in response to 4.2 ka climate event in China. *Quat. Sci. Rev.* 295, 107786. doi:10.1016/j.quascirev.2022.107786

Hein, A. M. (2014). Interregional contacts and geographic preconditions in the prehistoric Liangshan Region, Southwest China. *Quat. Int.* 348, 194–213. doi:10.1016/j.quaint.2013.12.011

Huan, X., Deng, Z., Zhou, Z., Yan, X., Hao, X., Bu, Q., et al. (2022). The emergence of rice and millet farming in the zang-yi corridor of southwest China dates back to 5000 Years ago. *Front. Earth Sci.* 10, 874649. doi:10.3389/feart.2022.874649

Jia, X., Sun, Y., Wang, L., Sun, W., Zhao, Z., Lee, H. F., et al. (2016). The transition of human subsistence strategies in relation to climate change during the Bronze Age in the West Liao River Basin, Northeast China. *Holocene* 26, 781–789. doi:10.1177/0959683615618262

Jiang, M., Gen, P., Liu, L. H., Sun, C., and Zuo, Z. Q. (2013). "Brief report and preliminary analysis on flotation results of Gaopo site in Mianning County in 2011 (in Chinese)," in *Chengdu Institute of cultural Relics and archaeology* (Beijing: Science Press), 331–337.

Jones, M., Hunt, H., Lightfoot, E., Lister, D., and Liu, X. (2011). Food globalization in prehistory. *World Archaeol.* 43, 665–675. doi:10.1080/00438243.2011.624764

Li, H., Cui, Y., James, N., Ritchey, M., Liu, F., Zhang, J., et al. (2022). Spatiotemporal variation of agricultural patterns in different geomorphologic and climatic environments in the eastern Loess Plateau, north-central China during the late Neolithic and Bronze Ages. *Sci. China Earth Sci.* 65, 934–948. doi:10.1007/s11430-021-9879-x

Li, H., Zuo, X., Kang, L., Ren, L., Liu, F., Liu, H., et al. (2016). Prehistoric agriculture development in the Yunnan-Guizhou Plateau, southwest China: Archaeobotanical evidence. *Sci. China Earth Sci.* 59, 1562–1573. doi:10.1007/s11430-016-5292-x

Li, J. J. (2020). A study on the changes of livelihoods in the traditional Tibetan area of Yunnan (in Chinese). *Theor. Obs.* 4, 85–88.

Li, J., Wang, G., Liu, X., Han, J., Liu, M., and Liu, X. (2009). Variations in carbon isotope ratios of C_3 plants and distribution of C 4 plants along an altitudinal transect on the eastern slope of Mount Gongga. *Sci. China Ser. D-Earth Sci.* 52, 1714–1723. doi:10.1007/s11430-009-0170-4

Liao, Y., Lu, P., Mo, D., Wang, H., Storozum, M. J., Chen, P., et al. (2019). Landforms influence the development of ancient agriculture in the Songshan area, central China. *Quat. Int.* 521, 85–89. doi:10.1016/j.quaint.2019.07.015

Liu, H. G. (2016). Human activities and agriculture resources utilization from Paleolithic to Bronze Age in northwest Yunnan province. [doctor dissertation]. Lanzhou: Lanzhou University.

Liu, X. Z., Wang, G. A., Li, J. Z., and Wang, Q. (2009). Nitrogen isotope composition characteristics of modern plants and their variations along an altitudinal gradient in Dongling Mountain in Beijing (in Chinese). *Sci. China Ser. D-Earth Sci.* 39, 1347–1359. doi:10.1007/s11430-009-0175-z

Liu, X., Jones, P. J., Matuzeviciute, G. M., Hunt, H. V., Lister, D. L., An, T., et al. (2019). From ecological opportunism to multi-cropping: Mapping food globalisation in prehistory. *Quat. Sci. Rev.* 206, 21–28. doi:10.1016/j.quascirev.2018.12.017

Liu, X., Hunt, H. V., and Jones, M. K. (2009). River valleys and foothills: Changing archaeological perceptions of North China's earliest farms. *Antiquity* 83, 82–95. doi:10.1017/S0003598X00098100

Lu, M., Li, X., Wei, W., Lu, Y., Ren, L., and Ma, M. (2021). Environmental influences on human subsistence strategies in southwest China during the Bronze Age: A case study at the jiangxifen site in yunnan. *Front. Earth Sci.* 9, 662053. doi:10.3389/feart.2021.662053

Ma, M., Lu, M., Zhang, S., Min, R., and Dong, G. (2022a). Asynchronous transformation of human livelihoods in key regions of the trans-Eurasia exchange in China during 4000-2200 BP. *Quat. Sci. Rev.* 291, 107665. doi:10.1016/j.quascirev.2022.107665

Ma, M., Lu, Y., Dong, G., Ren, L., Min, R., Kang, L. H., et al. (2022b). Understanding the transport networks complex between south Asia, southeast Asia and China during the late neolithic and Bronze Age. *Holocene* 33, 147–158. doi:10.1177/09596836221131698

Ma, M. M., Dong, G. H., Jia, X., Wang, H., Cui, Y. F., and Chen, F. H. (2016). Dietary shift after 3600 cal yr BP and its influencing factors in northwestern China: Evidence from stable isotopes. *Quat. Sci. Rev.* 145, 57–70. doi:10.1016/j.quascirev.2016.05.041

Outram, A. K., Kasparov, A., Stear, N. A., Varfolomeev, V., Usmanova, E., and Evershed, R. P. (2012). Patterns of pastoralism in later Bronze Age Kazakhstan: New evidence from faunal and lipid residue analyses. *J. Archaeol. Sci.* 39, 2424–2435. doi:10.1016/j.jas.2012.02.009

Preston, G. W., Parker, A. G., Walkington, H., Leng, M. J., and Hodson, M. J. (2012). From nomadic herder-hunters to sedentary farmers: The relationship between climate change and ancient subsistence strategies in south-eastern Arabia. *J. Arid. Environ.* 86, 122–130. doi:10.1016/j.jaridenv.2011.11.030

Ren, M., Yang, Y. M., Tong, T., Li, L. H., Cilie, C. L., and Wu, R. (2020). Scientific analysis of plant remains and food residue from the Chuvthag cemetery and Jiagezi cemetery (in Chinese with English abstract). *Archaeol. Cult. Relics* 1, 122–128.

Richards, M. P., and Hedges, R. E. M. (1999). Stable isotope evidence for similarities in the types of marine foods used by Late Mesolithic humans at sites along the Atlantic coast of Europe. *J. Archaeol. Sci.* 26, 717–722. doi:10.1006/jasc.1998.0387

Rundel, P. W. (1980). The ecological distribution of C_4 and C_3 grasses in the Hawaiian Islands. *Oecologia* 45, 354–359. doi:10.1007/BF00540205

Sah, S. P., and Brumme, R. (2003). Altitudinal gradients of natural abundance of stable isotopes of nitrogen and carbon in the needles and soil of a pine forest in Nepal. *J. For. Sci.* 49, 19–26. doi:10.17221/4673-jfs

Song, J., Gao, Y., Tang, L., Zhang, Z., Tang, M. H., Xu, H., et al. (2021). Farming and multi-resource subsistence in the third and second millennium BC: Archaeobotanical evidence from Karuo. *Archaeol. Anthropol. Sci.* 13, 47. doi:10.1007/s12520-021-01281-9

Sun, Q., Liu, Y., Wünnemann, B., Peng, Y., Jiang, X., Deng, L., et al. (2019). Climate as a factor for Neolithic cultural collapses approximately 4000 years BP in China. *Earth Sci. Rev.* 197, 102915. doi:10.1016/j.earscirev.2019.102915

Van der Merwe, N. J. (1982). Carbon isotopes, photosynthesis, and archaeology: Different pathways of photosynthesis cause characteristic changes in carbon isotope ratios that make possible the study of prehistoric human diets. *Am. Sci.* 70, 596–606. Avaliable At: https://www.jstor.org/stable/27851731.

van der Merwe, N. J., and Medina, E. (1989). Photosynthesis and $^{13}C/^{12}C$ ratios in Amazonian rain forests. *Geochimica Cosmochimica Acta* 53, 1091–1094. doi:10.1016/0016-7037(89)90213-5

Wang, Q., Zhang, T. B., Yi, G. H., Chen, T. T., Bie, X. J., He, Y. X., et al. (2017). Tempo-spatial variations and driving factors analysis of net primary productivity in the Hengduan mountain area from 2004 to 2014. *Acta Ecol. Sin* 37, 3084–3095. doi:10.5846/stxb201602030248

Wang, J. (2012). A zooarchaeological study of the Haimenkou site, Yunnan province, China. [doctor dissertation]. Bundoora: La Trobe University.

Wang, L., Lv, H. Y., Wu, N. Q., Chu, D., Han, J. M., Wu, Y. H., et al. (2004). Discovery of C4 plants in high altitude areas of Tibet Plateau (in Chinese). *Chin. Sci. Bull.* 49, 1290–1293.

Wang, C., Lu, H., Gu, W., Wu, N., Zhang, J., and Zuo, X. (2017). The spatial pattern of farming and factors influencing it during the Peiligang culture period in the middle Yellow River valley, China. *Sci. Bull,* 62, 1565–1568. doi:10.1016/j.scib.2017.10.003

Wang, T., Li, D., Cheng, X., Lan, J., Edwards, R. L., Cheng, H., et al. (2022). Hydroclimatic changes in south-central China during the 4.2 ka event and their potential impacts on the development of Neolithic culture. *Quat. Res.* 109, 39–52. doi:10.1017/qua.2022.11

Wang, Y., Dai, E., Yin, L., and Ma, L. (2018). Land use/land cover change and the effects on ecosystem services in the Hengduan Mountain region, China. *Ecosyst. Serv.* 34, 55–67. doi:10.1016/j.ecoser.2018.09.008

Xue, Y., Dal Martello, R., Qin, L., Stevens, C. J., Min, R., and Fuller, D. Q. (2022). Post-neolithic broadening of agriculture in yunnan, China: Archaeobotanical evidence from Haimenkou. *Archaeol. Res. Asia* 30, 100364. doi:10.1016/j.ara.2022.100364

Yan, X., Jiang, M., Liu, X. Y., Liu, L. H., Bu, Q., and Li, T. (2016a). "Analysis report of plant remains unearthed from the Guijiabao and Daozuomiao site in Yanyuan County in 2015 (in Chinese)," in *Chengdu Institute of cultural Relics and archaeology* (Beijing: Science Press), 147–154.

Yan, X., Jiang, M., Zuo, Z. Q., and Bu, Q. (2016b). "Analysis report of plant remains unearthed from Shapingzhan site in Xichang in 2015 (in Chinese)," in *Chengdu Institute of cultural Relics and archaeology* (Beijing: Science Press), 155–162.

Yan, X., Jiang, M., Zuo, Z. Q., Liu, X. Y., Sun, C., Liu, L. H., et al. (2016c). "Analysis report of plant remains unearthed from Huili and Huidong County in 2015 (in Chinese)," in *Chengdu Institute of cultural Relics and archaeology* (Beijing: Science Press), 135–144.

Yang, L., Ma, M., Chen, T., Cui, Y., Chen, P., Zheng, L., et al. (2021). How did trans-Eurasian exchanges affect spatial-temporal variation in agricultural patterns during the late prehistoric period in the Yellow River valley (China)? *Holocene* 31, 247–257. doi:10.1177/0959683620941140

Yang, Q. Y., and Zheng, D. (1989). An outline of physico-geographic regionalization of the Hengduan Mountainous Region (in Chinese). *Mt. Res.* 7, 56–64.

Yang, W. (2016). The analysis of charred plant remains at Hebosuo site and Yubeidi site in Yunnan Province. [master's thesis]. Jinan: Shandong University.

Yang, Y., Wang, J., Li, G., Dong, J., Cao, H., Ma, M., et al. (2022). Shift in subsistence crop dominance from broomcorn millet to foxtail millet around 5500 BP in the Western Loess Plateau. *Front. Plant Sci.* 13, 939340. doi:10.3389/fpls.2022.939340

Yi, X. F., and Yang, Y. Q. (2006). Enrichment of stable carbon and nitrogen isotopes of plant populations and plateau pikas along altitudes. *J. Anim. Feed Sci.* 15, 661–667. doi:10.22358/jafs/66937/2006

Zhang, H., Cheng, H., Sinha, A., Spötl, C., Cai, Y., Liu, B., et al. (2021). Collapse of the Liangzhu and other Neolithic cultures in the lower Yangtze region in response to climate change. *Sci. Adv.* 7, eabi9275. doi:10.1126/sciadv.abi9275

Zhao, Y. (2011). A research of faunal remains excavated from Yinsuodao site in Yunnan province. [master's thesis]. Changchun: Jilin University.

Zhao, Z., and Chen, J. (2011). Flotation results and analysis on yingpanshan site in mao county, sichuan (in Chinese). *Cult. Relics South* 3, 60–67.

Zhou, X., Yu, J., Spengler, R. N., Shen, H., Zhao, K., Ge, J., et al. (2020). 5,200-year-old cereal grains from the eastern Altai Mountains redate the trans-Eurasian crop exchange. *Nat. Plants* 6, 78–87. doi:10.1038/s41477-019-0581-y

Zi, G. C. (2011). Preliminary study on olive introduction and cultivation experiment in Lijiang (in Chinese with English abstract). *For. Inventory Plan.* 36, 122–124. doi:10.3969/j.issn.1671-3168.2011.04.031

frontiers | Frontiers in Earth Science

TYPE Original Research
PUBLISHED 05 May 2023
DOI 10.3389/feart.2023.1134677

Check for updates

OPEN ACCESS

EDITED BY
Ren Lele,
Lanzhou University, China

REVIEWED BY
Yu Gao,
Institute of Tibetan Plateau Research (CAS), China
Haiming Li,
Nanjing Agricultural University, China

*CORRESPONDENCE
Fei Peng,
pengfei@muc.edu.cn
Shuzhi Wang,
shuzhiwang@163.com
Zhijun Zhao,
zjzhao@cass.org.cn

SPECIALTY SECTION
This article was submitted to Quaternary Science, Geomorphology and Paleoenvironment, a section of the journal Frontiers in Earth Science

RECEIVED 30 December 2022
ACCEPTED 29 March 2023
PUBLISHED 05 May 2023

CITATION
Zheng X, Peng F, Wang S, Guo J, Wang H, Gao X and Zhao Z (2023), Plant exploitation and subsistence patterns of the Mesolithic in arid China: New evidence of plant macro-remains from the Pigeon Mountain site.
Front. Earth Sci. 11:1134677.
doi: 10.3389/feart.2023.1134677

COPYRIGHT
© 2023 Zheng, Peng, Wang, Guo, Wang, Gao and Zhao. This is an open-access article distributed under the terms of the Creative Commons Attribution License (CC BY). The use, distribution or reproduction in other forums is permitted, provided the original author(s) and the copyright owner(s) are credited and that the original publication in this journal is cited, in accordance with accepted academic practice. No use, distribution or reproduction is permitted which does not comply with these terms.

Plant exploitation and subsistence patterns of the Mesolithic in arid China: New evidence of plant macro-remains from the Pigeon Mountain site

Xuefang Zheng[1], Fei Peng[2]*, Shuzhi Wang[3]*, Jialong Guo[4], Huiming Wang[4], Xing Gao[5,6,7] and Zhijun Zhao[3]*

[1]University of Chinese Academy of Social Sciences (UCASS), Beijing, China, [2]Department of Archaeology and Museology, Minzu University of China, Beijing, China, [3]Institute of Archaeology, Chinese Academy of Social Sciences, Beijing, China, [4]Ningxia Institute of Cultural Relics and Archaeology, Yinchuan, China, [5]Key Laboratory of Vertebrate Evolution and Human Origins, Institute of Vertebrate Paleontology and Paleoanthropology, Chinese Academy of Sciences (CAS), Beijing, China, [6]CAS Center for Excellence in Life and Paleoenvironment, Beijing, China, [7]University of Chinese Academy of Science, Beijing, China

The nature of the Mesolithic in China has not been studied much due to the few well-context sites discovered and excavated during this period. The situation also restricts the understanding of human subsistence in the Mesolithic period in China, especially in the arid region. The present paper reports the flotation results at Locality 10 of the Pigeon Mountain site in Northwest China. Ten species of plants belonging to six families were identified, dominated by *Agriophyllum squarrosum* and *Artemisia sieversiana*. No firm evidence proves the domestication. Combined with the lithic artefacts in QG10, ancient people could utilize plant resources by constructing or expanding the food spectrum. It is the first systematic archaeobotany work in the Paleolithic site of Northwest China. The result reminds us that the enhanced utilization of wild plant resources is a vital subsistence for Mesolithic people in arid regions.

KEYWORDS

Pigeon Mountain site, macro-remains, ancient plant utilization, arid and semi-arid, Northwest China

Introduction

The Paleolithic period, also known as the Old Stone Age, was a time in human history marked by the development of stone tools. On the other hand, the Neolithic period was characterized by the emergence of agriculture and polished stone tools (Fagan, 2010). The transition from the Paleolithic to Neolithic was marked by the domestication of animals, manufacture of pottery, and intensified utilization of plants (Liu and Chen, 2017). Due to climate fluctuations, ancients frequently adjusted their subsistence strategies by equipping them with portable and flexible composite tools made of organic material and microblades, grinding stone tools, and pottery (Price, 1987). These tools strengthened the ability of ancient humans to hunt animals and exploit plant resources. The trajectory became significant during the Mesolithic. The ancients gradually increased the utilization of plant resources, such as seeds and fruits. Plant exploitation and subsistence patterns during these periods have been inferred from the study of plant macro-remains or the physical remains of plants

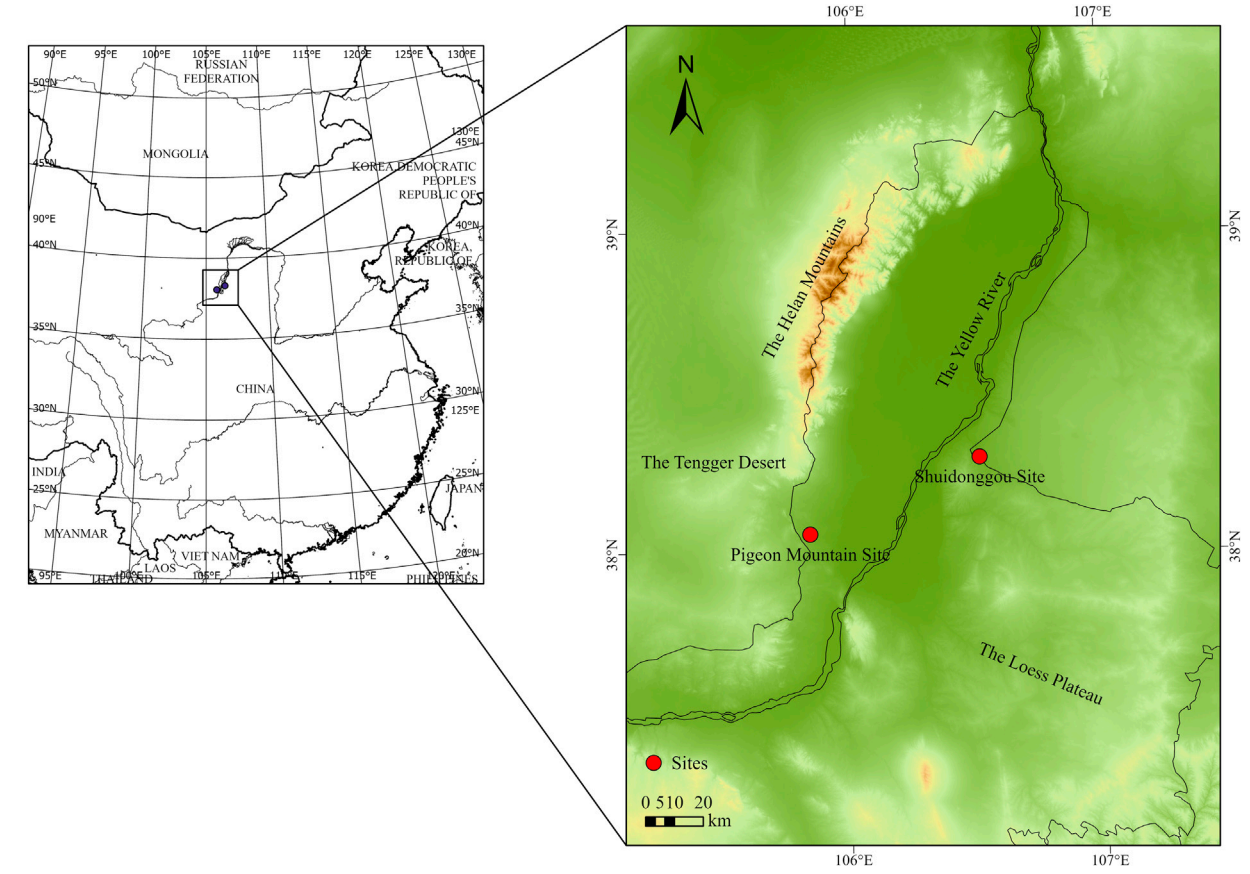

FIGURE 1
Geographical location of the Pigeon Mountain site.

that can be analyzed and identified. These remains include seeds, fruits, nuts, and other plant parts preserved in the archaeological record.

In the 1960s and 1970s, Binford and Flannery proposed the "Broad Spectrum Revolution" concept, which indicates that hunter–gatherers significantly improved their ability to adapt to the environment by expanding their diets in the late Paleolithic (Binford, 1968; Flannery, 1973). Climate change resulted in worse environmental conditions, and the quantity of food resources decreased drastically. Ancient people had to exploit more kinds of food and rely more on plant resources than before in this situation. Though the climate steadily warmed up after the Last Glacial Maximum, some cooling events still occurred irregularly (Lu, 1999; Lu, 2006). The transitions occurred at different times in different places worldwide and were called the Mesolithic period someplace. In Europe, using wild plant food was accepted as a norm for the Mesolithic period (Zvelebil, 1994). However, the transition dynamics of the Mesolithic period in China are still unclear. The main reason is few archaeological sites in the Mesolithic period, ranging from terminal Pleistocene to early Holocene about 13–9 ka BP, have been discovered and systematically excavated. Most discovered sites include the Longwangchan site (The Institute of ArchaeologyCASS, 2021) in Shaanxi, the Xiachuan site (Du, 2021), the Shizitan site (Liu et al., 2011) in Shanxi, Yujiagou in Hebei, the Lijiagou site (Wang et al., 2011) in Henan, and the Donghulin site (Zhao et al., 2020) in Beijing, concentrated in North and Northeast China.

The present paper provides the latest utilization of plant resource evidence from the Pigeon Mountain site, a Mesolithic site in China's arid and semi-arid regions, mainly in Northwest China. The research aims to explore the types of plants and subsistence patterns in the Pigeon Mountain site and shed light on the strategy and subsistence of people during the Mesolithic period in arid China.

Archaeological background and study sites

Before the emergence of agriculture and permanent settlement, seasonal variations in precipitation and temperature challenged the survival of ancient people in higher-latitude areas in the northern region of China. China's vast territory is described as the Three Steps or the Three Gradient Terrains based on the average altitude from west to east and the relief amplitude (Guan et al., 2020). The first gradient terrain is the Qinghai–Tibetan Plateau. The second gradient terrain includes the Inner Mongolian Plateau, Xinjiang Autonomous Region, Yunnan–Guizhou Plateau, Loess Plateau, and Sichuan Basin. The third gradient terrain comprises plains and hills

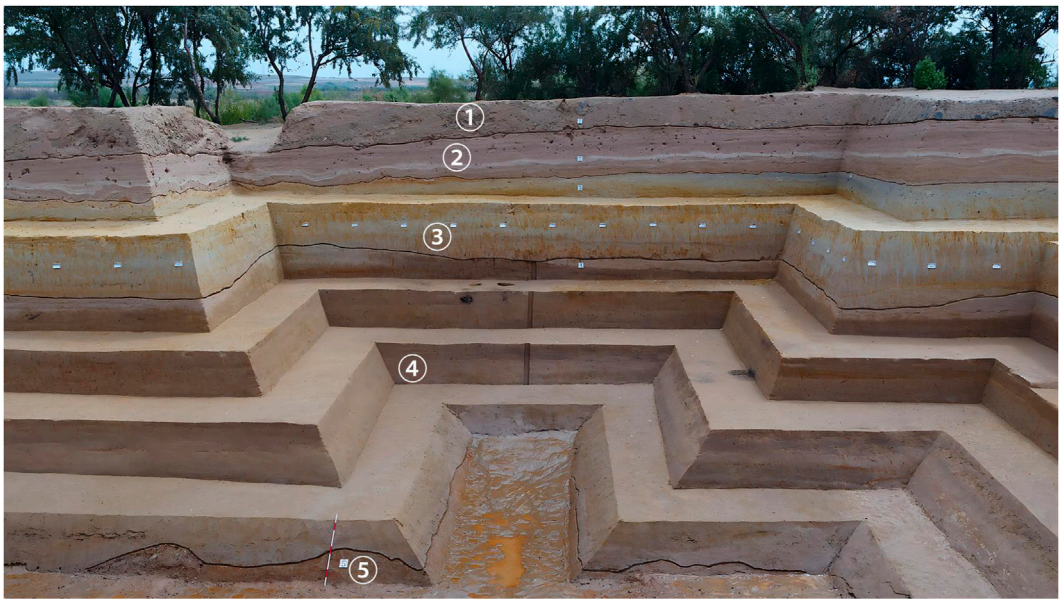

FIGURE 2
Stratigraphic profile of QG10.

below 500 m above the sea level (Guan et al., 2020). Most Paleolithic–Neolithic sites are found on the second- and third-gradient terrain where the environment is suitable for animal–plant domestication, permanent occupation, and human survival. Figure 1 shows the geographical location of the Pigeon Mountain site, which is in Northwest China, characterized by an arid and semi-arid climate.

The Pigeon Mountain site (QG) is located in northwest of Qingtongxia City, Ningxia Hui Autonomous Region, China. It is composed of 15 localities. In the literature, the site is either referred to as "Pigeon Mountain Loc. 10" or it is Chinese pinyin equivalent, i.e., "Gezishan Loc. 10" (Zhang et al., 2022). In the 1990s, QG3 and QG4 were excavated by a joint team of Chinese and American scholars. Evidence of microblades, grindstones, and flakes had been yielded (Elston et al., 1997). These remains provide valuable insights into the subsistence patterns of those who lived there during these periods. The ^{14}C age indicates that it is a Mesolithic period site less commonly discovered in the arid region. Meanwhile, the site is situated in a transition zone between the northwest desert and the Loess Plateau, with a presently mid-temperate continental climate and proximity to the edge of the East Asian monsoon climate zone (Madsen et al., 1996). The mean annual temperature and precipitation are approximately 8.5°C and 260 mm, respectively. The frost-free period is 176 days, the annual sunshine is 2,955 h, and the temperature difference between day and night is significant (Madsen et al., 1996).

The locality 10 of the Pigeon Mountain site (known as QG10, N38°03′33.1″, E105°50′30.3″, altitude ca. 1,200 m) is located on the foothills of the Helan Mountains and the southeast edge of the Tengger Desert, which is about 20 km from Qingtongxia City, Ningxia Hui Autonomous Region, China (Madsen et al., 1996). It is the most important locality in the site complex because of its rich discoveries. QG10 was discovered in the 1990s. However, just sporadic artifacts were collected at that time. In 2013, the Institute of Vertebrate Paleontology and Paleoanthropology, Chinese Academy of Sciences (IVPP-CAS), and the Ningxia Institute of Cultural Relics and Archaeology launched a new investigation in this region. Two new localities were discovered: QG14 and QG15 (Guo et al., 2019). From 2014 to 2017, a formal excavation was conducted at QG10. The new excavation of QG10 unearthed multiple sets of archaeological data with a well-stratigraphic context. This work provides a reliable chronological framework for site research and an opportunity to explore ancient humans' technological adaptation, resource utilization, and environmental adaptation behavior in the desert fringe area. Latest 14C dating display the excavated area covers c. 200 m^2 and reaches a depth of c. 3.5 m (Madsen et al., 1998). The map in Figure 2 shows the QG10 stratigraphic sequence comprising five geological layers from 1 on the top to 5 at the bottom.

Three archaeological horizons were identified in layers 2, 3, and 4 separately. They were named CL1 in Layer2, CL2 in Layer3, and CL3 in Layer4. CL3 yielded the richest archaeological assemblage, including architectural structures, hearth, grinding discs, grinding rods, typical amphibians, Helan pointed implements, animal skeletons, macro-remains, micro-remains, and small ornaments made of ostrich egg skins, especially animal skeletons, macro-remains, micro-remains, fire ponds, architectural structures, and others remains indicating that ancient humans exploited more diverse food resources, widening their recipe, closely related to the Broad Spectrum Revolution and society complexities increased.

A total of 361 starch grains and a small amount of plant organ debris were found in 19 stone artifacts from CL2 and CL3. The starch grains include Triticeae, Panicoideae, possibly Fagopyrum, beans (Fabaceae), acorns (Quercus), possibly Typha, Dioscorea or Fritillaria, underground storage organs of other plants, lotus seed and a small number of unidentifiable starch granules and broken

TABLE 1 Soil sample record of Locality 10.

Sample background	CL1		CL2		CL3		Total	
	Liter	Number	Liter	Number	Liter	Number	Liter	Number
Layer	1,640	164	3,765	379	5,078	476	10,483	1,019
Remains	0	0	456	26	2,623	83	3,079	109
Total	1,640	164	4,221	405	7,701	559	13,562	1,128

TABLE 2 Radiocarbon age for the seed in this study.

Lab code	Sample type	^{14}C date (BP)	Calibrated age (cal. BP)	
			1σ (68%)	2σ (95%)
Beta-450602	Seed	10400 ± 30 BP	12395–12225	12410–12120
			12215–12155	

granules. Among them, grasses occupy an absolute advantage, while legumes, nuts, and tubers account for a smaller proportion (Guan et al., 2020). More than 2,000 animal remains were unearthed from CL3. In decreasing order of the identified specimens, animal skeletons are represented by *Lepus* sp., *Equus przewalskyi*, *Procapra przewalskii*, *Vulpes* sp., and Cervids (Zhang et al., 2022).

Materials and methods

During the 2016–2017 field season, two systematic samplings were carried out from 1,128 soil samples, and 13,562 L was collected and floated at CL1, CL2, and CL3 of T5 at the QG10 based on Table 1.

Conducting flotation in the current study has been an effective way of developing subsistence knowledge in a specific region and time. The interpretations and limitations of the data are contextualized based on the type and size. The flotation for extracting the samples was carried out on the Pigeon Mountain site. The flotation samples were sent to the Laboratory of Paleoethnobotany, Institute of Archaeology, Chinese Academy of Social Sciences, for identification and analysis after drying in the local shade. The primary method for identifying carbonized plant seeds is to compare the samples unearthed from the archaeological site with the existing species based on researchers' experience and refer to the relevant atlas. At counting, the seed fragments with less than 50% of the seed sizes were omitted. The key to seed identification is its shape and size. The method was favorable for the current study to avoid artificial inflation of the total and follow the principle of the minimum number of samples. The morphology of seeds varies greatly depending on the family and genus they belong to, but there is also the phenomenon that the same plant produces seeds of different shapes. More accurate judgments can be made based on experience and comparison when classifying and identifying. Size is one of the most obvious characteristics of seeds and can be expressed by length, width, and thickness.

In the laboratory, wood charcoal specimens were fractured manually with a razor blade along the three anatomical planes (transverse, radial longitudinal, and tangential longitudinal) and were analyzed under a Nikon LV150 reflected-light bright/darkfield microscope at magnifications of ×50, ×100, ×200, and ×500. Identifications were checked by comparison to wood anatomy atlases (Cheng et al., 1992) and specimens held in the modern microscopic wood anatomy slide reference collection of CASS. A Quanta 650 SEM was used to observe finer anatomical details and to take photos. The description of wood anatomical features follows the definitions given in the published literature (IAWA Committee, 1989; IAWA Committee, 2004; Schweingruber, 1990).

Results

To get an absolute age of the recovered macro-remains, the research focused on 30 seeds of *Agriophyllum squarrosum* from CL3, with a 95% confidence interval of the calibrated ages bounded between 12410 and 12120 Cal BP. Table 2 shows the calibration of radiocarbon age to calendar years with a probability of 95%.

The 10 species of plants belonging to six families were identified (Figure 3): *Agriophyllum squarrosum* (Figure 3A), *Corispermum declinatum* (Figure 3B), *Kochia scoparia* (Figure 3C), *Salsola collina* (Figure 3D), *Artemisia sieversiana* (Figure 3E), *Poa annua* (Figure 3F), *Sclerochloa dura* (Figure 3G), *Allium mongolicum* (Figure 3H), *Viola verecunda* (Figure 3I), and *Lagopsis supina* (Figure 3J).

The average weight of charcoal >1 mm contained in each flotation sample (10 L of each) is 0.038 g, while CL2 and CL3 contain 0.052 and 2.48 g, respectively, as shown in Figure 4. Concerning the three types of relic units, the average number of charcoals and seeds unearthed (each 100 L soil samples) in outlines and holes is the smallest. In contrast, the hearth contains the highest number of charcoals and seeds. In consideration of the weight of charcoals, outlines only yield about

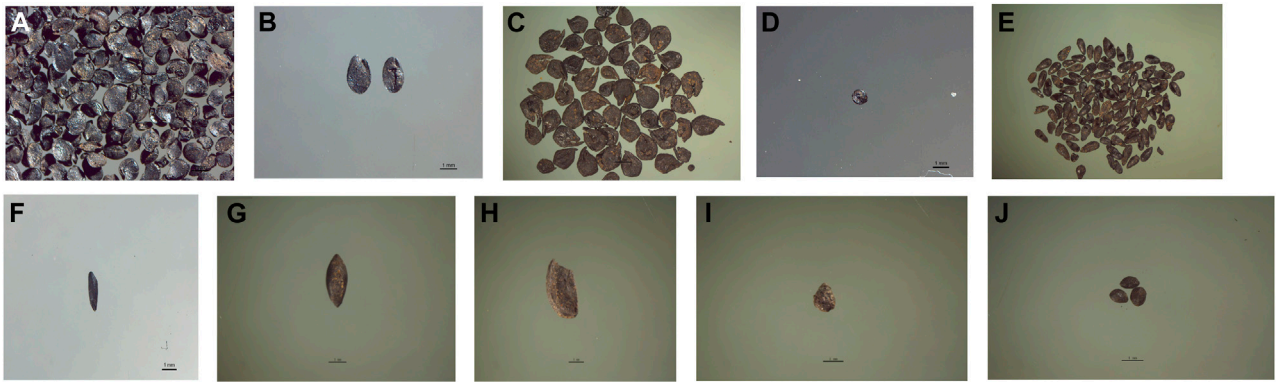

FIGURE 3
Seeds discovered from QG10: **(A)** *Agriophyllum squarrosum*; **(B)** *Corispermum declinatum*; **(C)** *Kochia scoparia*; **(D)** *Salsola collina*; **(E)** *Artemisia sieversiana*; **(F)** *Poa annua*; **(G)** *Sclerochloa dura*; **(H)** *Allium mongolicum*; **(I)** *Viola verecunda*; **(J)** *Lagopsis supina*.

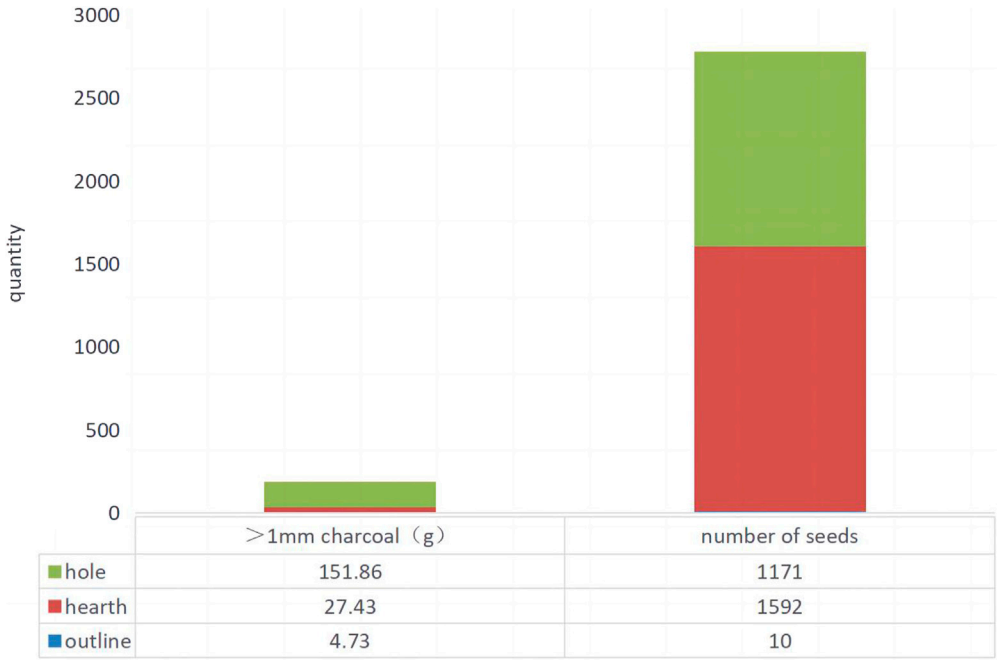

	>1mm charcoal（g）	number of seeds
hole	151.86	1171
hearth	27.43	1592
outline	4.73	10

FIGURE 4
Comparison diagram of charcoal weight and plant seed quantity per 100 L soil sample unearthed in different relic phenomena, PM.

one-fifth of that unearthed in the hole. This may be related to the different functions of the remains.

Compared to the types of carbonized plant seeds unearthed from most Neolithic and historical, archaeological sites, the types of plant seeds unearthed from the Pigeon Mountain site are relatively few. The six families identified were: *Agriophyllum* spp., *Corispermum* spp., *Kochia* spp., and *Salsola* spp. of the Chenopodiaceae, *Artemisia* spp. of Compositae, *Poa* spp. and *Sclerochloa* spp. of Poaceae, *Allium* spp. of Liliaceae, *Viola* spp. of Violaceae, and *Lagopsis* spp. of Lamiaceae.

Only two carbonized seeds were unearthed in CL1: *Lagopsis supina* of the Lamiaceae. The species of carbonized plant seeds unearthed in CL2 and CL3 were similar. The ubiquity and proportion of plant seeds in CL2 and CL3 were counted, respectively. Figures 5, 6 indicate that the proportion and ubiquity of *Agriophyllum squarrosum* were the highest, followed by *Artemisia sieversiana*, and no significant difference found between CL2 and CL3 in the Pigeon Mountain site. *Agriophyllum squarrosum* showed no signs of domestication. The size of *Artemisia sieversiana* unearthed was only about half compared to that of living *Artemisia sieversiana*. To estimate the importance of *Agriophyllum squarrosum* and *Artemisia sieversiana*, the calculation included the ubiquity of the taxa using the available botanical remains as a measure of

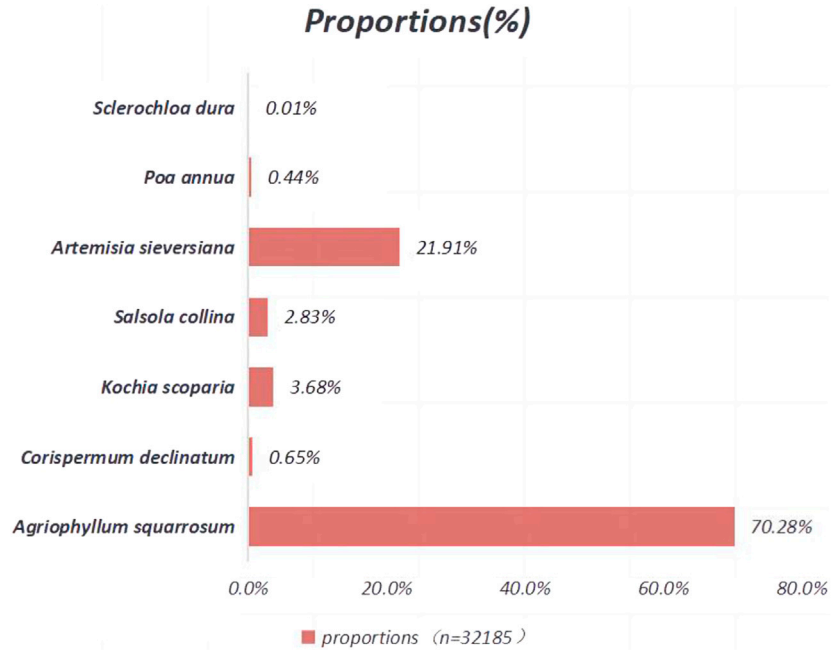

FIGURE 5
Proportions of species within the Pigeon Mountain site, CL3.

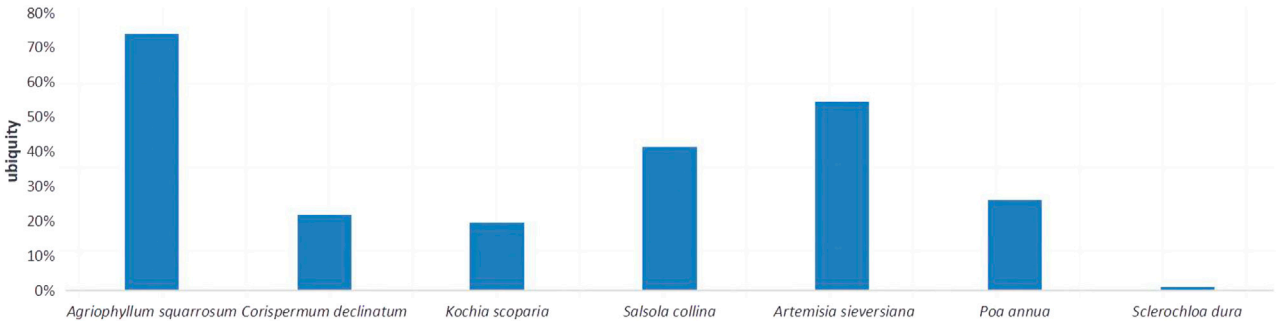

FIGURE 6
Ubiquity of species within the Pigeon Mountain site, CL3.

aggregation. This showed the high frequencies of the seeds at 70.28% and 21.91%, respectively.

Discussion

Paleo-environment and plant utilization in Mesolithic Northwest China

The proportion of *Tamarix* spp. in the Pigeon Mountain site is very high, which is the most widely distributed regional vegetation. The plants of Tamariaceae are all xerophytes, indicating that the climate is arid. The ubiquity of *Agriophyllum squarrosum* is also very high. *Agriophyllum squarrosum* is an annual summer and autumn plant that rarely develops in drought years. The appearance of the large number of *Agriophyllum squarrosum* indicates significant precipitation in summer. In addition, *Corispermum declinatum*, *Kochia scoparia*, and *Salsola collina* are also annual plants that develop in summer and autumn. According to the climatic characteristics of this study area, the rainfall season is conceived in summer. In the terrestrial ecosystem, the microenvironment plays a fundamental role in plant species' growth, germination, mortality, and reproduction (Cao et al., 2009). This role is essential because of the direct and indirect influence on essential processes such as nutrient cycles, evapotranspiration, and photosynthesis (Figures 7A–C). The changes in the vegetation composition and structure due to human activities and natural disturbances alter local conditions (Gehlhausen).

As *Corispermum declinatum*, *Kochia scoparia*, and *Agriophyllum squarrosum* show changes based on the

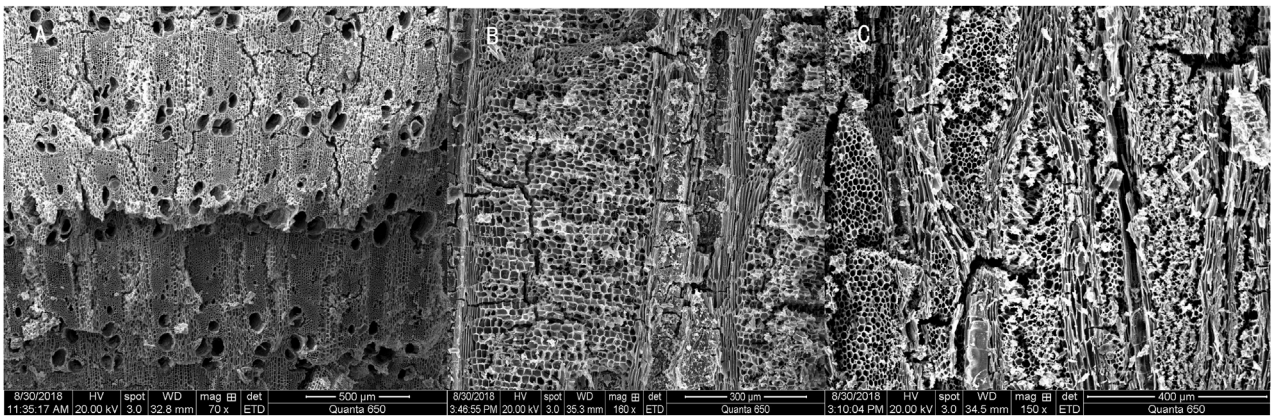

FIGURE 7
SEM microphotographs of *Tamarix*. **(A)** TS; **(B)** RLS; and **(C)** TLS.

environment, it demonstrates how the interaction of biotic and abiotic factors influences the microenvironment. This means that a change in the microenvironment influences the ecosystem and structural processes (Behera). Among the changes observed at the Pigeon Mountain site, the changes in the ecosystem are increased air and soil pressure, solar radiation levels, and decreased relative humidity, soil moisture, and vapor pressure. The Pigeon Mountain site has provided an exciting system for analyzing the relationship between variations in plant composition and structure and the microenvironment. This shows that the ecosystem has specific environmental conditions for plants to grow despite the climatic conditions. The topography of the Pigeon Mountain Site shows that the most common species found are mainly flowery plants such as *Artemisia sieversiana*. The number of plant species in the region shows the variation in environmental conditions based on the topography, moisture, and degree of disturbances.

Plants are essential to our well-being and they are included in people's food, religions, cultures, and medicines. The vital component of plants results in plant species' coevolution and domestication (Guo and Li, 2014). The archaeological practices to identify ancient practices ensure that indigenous plants do not become extinct because of environmental changes and human adaptation to modern plantation. Ancient people of the Pigeon Mountain site strengthened their utilization of herbal plants for a long time. The use of plant resources by ancient ancestors mainly includes two aspects: wooden tools and edible resources (Guo and Li, 2014). Wooden tools are commonly used for building materials, firewood, and tool-making. At the same time, edible resources focused on collecting seeds, fruits, roots, stems, and leaves of various plants. Almost all the remains of carbonized seeds unearthed in and around the archaeological site remain in the Pigeon Mountain site appearance (Cao et al., 2009). The ancient ancestors of the Pigeon Mountain site used fire frequently, and firewood resources, such as *Tamarix* spp., *Myricaria* spp., *Tetraena mongolia*, *Zygophyllum* spp., and *Caragana korshinskii*, were abundantly found. Therefore, the occupants of the Pigeon Mountain site did not have to collect the stems of herbs for fuel.

The community-staggered zone is also named the ecological or ecological transition zone. The environmental conditions of the community-staggered zone are relatively complex, which can provide growth conditions for plants of different ecological types, even species unique to the staggered region (Cao et al., 2009). The QG10 is located in a transitional area from grassland to the desert. It is also a community-interlaced area, providing conditions for human development and selecting a wider variety of food resources.

Diet structure and subsistence patterns of ancestors at the Pigeon Mountain site

Related theories, such as the optimal foraging theory (Smith, 1983; Pyke, 1984; Yi et al., 2013), Niche construction theory (Odling-Smee, 1988; Smith, 2011), and adaptation cycle theory, all explain the adjustment of the survival strategies of ancient humans to a specific period, such as the transition from a hunter–gatherer economy to an agricultural economy. According to the cost and return rate in development and utilization, natural resources can be divided into different grades. Ancient humans always preferred natural resources at higher rates of return. However, when specific high-return resources were scarce or difficult to obtain due to climate change or over-exploitation of specific resources, ancient humans had to include natural resources with relatively low returns to expand food sources (Piperno and Pearsall, 1998). Among all kinds of natural resources, the return rate of plant resources is usually lower than animal resources (Piperno, 2011). Therefore, ancient humans likely used animal resources first and then various plant resources.

Even the animal bones unearthed at QG10 are the highest (Zhang et al., 2019). The number of plant remains obtained by flotation and residue analysis is exceptionally abundant, which may indicate adaptions made by the ancestors of the QG10 in exploiting natural resources. Herb-seed plants, such as *Agriophyllum squarrosum* and *Artemisia sieversiana*, are primarily annual plants with solid recovery ability, which can meet the needs of

the continuous utilization of ancient humans. In addition, grass-seed plants are productive and can be stored; this can also help the Pigeon Mountain site populations get through the harsh condition and food-scarce winter. In summary, grass-seed plants have been strengthened in the selection and utilization at the Pigeon Mountain site, indicating the ancient humans' adaption strategy to the living environment.

The current research and various relic phenomena and relics unearthed can provide valuable information about ancient ancestors' survival and adaptation ability in arid areas. First, grinding tools such as stone grinding discs and grinding rods were unearthed at Locality 10 (Guo et al., 2017). The residue analysis identified many starches of grasses, tubers, and other plant types on the surface (Guan et al., 2020). The existence of the ancestors' grinding behavior indicates that plant processing and utilization frequency were improved and strongly dependent on plant resources. Second, the suspected column–hole remains found in Layer4 are characterized by uniform horizontal distribution, strip-like, similar inner diameters, and similar internal contents. They contain much large amounts of *Tamarindaceae* charcoal, indicating the possibility of early attempts to build huts at the Pigeon Mountain site, though it still needs further discussion. The rich relic phenomenon and the continuous distribution of the culture layer indicate that ancient humans lived in this area for a long time. In addition, plenty of fire remains were found on the site, including many fire ponds with clear structures, indicating the ancestors of the site had behaviors such as heating and even cooking animal and plant resources and adapted to changes in the environment.

In the QG10, *Agriophyllum squarrosum* dominated the unearthed plants in number and ubiquity. Thus, the seeds of *Agriophyllum squarrosum* seem to be one of the most important food sources for the ancient people at the Pigeon Mountain site. However, according to textual research studies, there is no cultivation tradition of *Agriophyllum squarrosum* in China or other countries. In our observation, seeds unearthed in the Pigeon Mountain site did not show domestication characteristics, so further research is needed.

The dried seeds of *Artemisia sieversiana* can be ground into *Artemisia* powder, which is sticky when exposed to water. When kneaded with flour and water, the *Artemisia* powder can refine the flour and be kneaded into the soft and flexible dough to make *Artemisia* seed noodles. The seeds of *Artemisia sieversiana* could improve the digestion in humans. Therefore, we speculate that the ancestors of the Pigeon Mountain site used the seeds of *Artemisia sieversiana* to bind the powder made by other seeds (or fruits) and then ate them. Among the plant food resources unearthed from the Pigeon Mountain site, the resources that can be ground into powder include *Agriophyllum squarrosum* and *Elaeagnus angustifolia*. In addition, the tender leaves of *Artemisia sieversiana* are edible, and *Artemisia sieversiana* seeds were used as a source of oil by ancient ancestors.

Conclusion

Some scholars believe that in the Mesolithic in North China, hunter–gatherers experienced a shift from a "forager" to a "gatherer" strategy, which means an intensification of sedentism began to take advantage of seasonally growing wild animals. Plant resources unearthed from QG10 first provided good context evidence for human adaptation in the arid paleoenvironment. Plentiful seeds and remains illustrated that the ancient people in QG10 has explored a broader food spectrum, especially plant resources.

The taxa represented in the macro-botanical evidence of QG10 indicate in terms of land use and utilization of wild plant resources. The macro-botanical species, i.e., *Agriophyllum squarrosum*, as the most prosperous species, could be the most crucial food resource of ancient people in this region, even with no evidence of domestication. Abundance of *Artemisia sieversiana* floating from the sediments with a large number of grindstones of QG10 displays the possibility of reprocessing behavior for the seeds.

The existence of the Mesolithic is still under debate in China. In eastern China, some clues of the earliest pottery and agriculture were seen as the landmark of the transition period from Paleolithic to Neolithic. Nonetheless, the scenario was unclear in Western China, particularly in the northwest arid region. Archaeobotany evidence from QG10 provided reliable and AMS-dated *in situ* evidence to give rise to a possible answer to the Mesolithic in this region. Meanwhile, this new finding shed light on the possibility that the subsistence patterns of hunter–gatherers in arid environments underwent a severe shift during the Mesolithic, marked by the extensive use of wild plant resources.

Data availability statement

The raw data supporting the conclusion of this article will be made available by the authors, without undue reservation.

Author contributions

ZZ, FP, and XZ designed the study. XZ, FP, SW, JG, HW, XG, and ZZ conducted the study. XZ and FP wrote an initial version of the manuscript. All co-authors reviewed and made modifications to the final version of the manuscript.

Funding

This work was funded by grants from the National Social Science Foundation of China (Nos.19AKG001) and the Fundamental Research Funds for the Central Universities (Nos.2022QNYL03).

Acknowledgments

We thank the colleagues and volunteers for their participation in the fieldwork at QG10. We also thank the editor and reviewers for their constructive comments which help improve the manuscript.

Conflict of interest

The authors declare that the research was conducted in the absence of any commercial or financial relationships that could be construed as a potential conflict of interest.

Publisher's note

All claims expressed in this article are solely those of the authors and do not necessarily represent those of their affiliated organizations, or those of the publisher, the editors, and the reviewers. Any product that may be evaluated in this article, or claim that may be made by its manufacturer, is not guaranteed or endorsed by the publisher.

References

Binford, L. R. (1968). "Post-Pleistocene adaptations," in *New perspectives in archeology*. Editors L. R. Binford and S. R. Binford (Chicago: Aldine), 313–341.

Cao, S., Chen, L., and Yu, X. (2009). Impact of China's grain for green project on the landscape of vulnerable arid and semi-arid agricultural regions: A case study in northern Shaanxi province. *J. Appl. Ecol.* 46 (3), 536–543. doi:10.1111/j.1365-2664.2008.01605.x

Cheng, J., Yang, J., and Liu, P. (1992). *Chinese wood (in Chinese)*. Beijing: Chinese Forestry Publishing House, 1–820.

Du, S. (2021). Cotinuity and break: Rethinking the significance of xiachuan site in Chinese paleolithic research(in Chinese). *Acta Anthropol. Sin.* 41 (01), 153–163.

Elston, R. G., Cheng, X., Madsen, D. B., Kan, Z., Bettinger, R. L., Jingzen, L., et al. (1997). New dates for the north China Mesolithic. *Antiquity* 71, 985–993. doi:10.1017/s0003598x00085872

Fagan, B. M. (2010). *World prehistory: A brief introduction*. New York, U.S.: Harper Collins College Publisher.

Flannery, K. V. (1973). The origins of agriculture. *Rev. Anthropol. Res.* 2, 271–310. doi:10.1146/annurev.an.02.100173.001415

Guan, Y., Tian, C., Peng, F., Guo, J., Wang, H., Zhou, Z., et al. (2020). Plant diet during the Pleistocene-Holocene transition in northwest China: Evidence from starch remains from pigeon mountain site in Ningxia province. *Quat. Int.* 559, 110–118. doi:10.1016/j.quaint.2020.03.016

Guo, J., Wang, H., and Qiao, Q. (2017). New archaeological discoveries of the Pigeon Mountain Site in Ningxia province. *Xixia Res.* 30 (02), 2+129.

Guo, J., Yao, Y., and Wang, H., (2019). A report on 2019 excavation of the gezishan locality 15 in Qingtongxia of Ningxia Hui autonomous region(in Chinese). *Acta Anthropol. Sin.* 38 (2), 182–190. doi:10.16359/j.cnki.cn11-1963/q.2019.0030

Guo, R., and Li, F. (2014). Agroecosystem management in arid areas under climate change: Experiences from the Semiarid Loess Plateau, China. *World Agric.* 4 (2), 19–29.

IAWA Committee (1989). IAWA list of microscopic features for hardwood identification. *IAWA Int. Assoc. Wood Anat.) Bull.* 10, 219–332.

IAWA Committee (2004). Standard list of microscopic features for softwood identification. *IAWA J.* 25, 1–70.

Liu, L., Ge, W., SbestelJones, D., Shi, J., and Song, Y. (2011). Plant exploitation of the last foragers at shizishan site in the middle yellow river vally China: Evidence from grinding stones. *J. Archaeol. Sci.* 38, 3524–3532.

Liu, L., and Chen, X. (2017). "The Archaeology of China:from the late paleolithic to the early bronze age," in *Chinese* (Beijing: SDX Joint Publishing Company), 49–51.

Lu, T. (2006). The occurrence of cereal cultivation in China. *Asian Perspect.* 45 (2), 129–158. doi:10.1353/asi.2006.0022

Lu, T. (1999). "The transition from foraging to farming and the origin of agriculture in China," in *British archaeological report international series* (Oxford: Hadrian Books), 774.

Madsen, D., Elston, R., Bettinger, R., Cheng, X., and Kan, Z. (1996). Settlement patterns reflected in assemblages from the Pleistocene/Holocene transition of north central China. *J. Archaeol. Sci.* 23 (2), 217–231. doi:10.1006/jasc.1996.0019

Madsen, D. B., Li, J., Elston, R. G., Cheng, X., Bettinger, R. L., Kan, G., et al. (1998). The loess/paleosol record and the nature of the Younger Dryas climate in Central China. *Geoarchaeology* 13 (8), 847–869. doi:10.1002/(sici)1520-6548(199812)13:8<847::aid-gea4>3.0.co;2-6

Odling-Smee, F. J. (1988). "Niche-constructing phenotypes," in *The role of behavior in evolution*. Editor H. C. Plotkin (Massachusetts, United States: MIT Press), 73–132.

Piperno, D. R., and Pearsall, D. M. (1998). *The origins of agriculture in the lowland neotropics*. SanDiego: Academic Press, 400.

Piperno, D. R. (2011). The origin of plant cultivation and domestication in the new world tropics: Patterns, process, and new developments. *Curr. Anthropol.* 52, 453–470. doi:10.1086/659998

Price, T. D. (1987). The mesolithic of Western Europe. *J. World Prehistory* 3, 225–305. doi:10.1007/bf00975322

Pyke, G. H. (1984). Optimal foraging theory: A critical review. *Annu. Rev. Ecol. Syst.* 15, 523–575. doi:10.1146/annurev.es.15.110184.002515

Schweingruber, F. H. (1990). *Anatomy of European woods – an atlas for the identification of European trees, shrubs and dwarf shrubs*. Stuttgart: Paul Haupt Berne and Stuttgart Publishers, 1–800.

Smith, B. D. (2011). General patterns of niche construction and the management of"wild"plant and animal resources by small -scale pre -industrial societies. *Philosophical Trans. R. Soc. B* 366, 836–848. doi:10.1098/rstb.2010.0253

Smith, E. A., Bettinger, R. L., Bishop, C. A., Blundell, V., Cashdan, E., Casimir, M. J., et al. (1983). Anthropological applications of optimal foraging theory: A critical review [and comments and reply]. *Curr. Anthropol.* 24 (5), 625–651. doi:10.1086/203066

The Institute of Archaeology, CASS (2021). *Locality 1 of the longwangchan site: Longwangchan site: Excavation report of the late paleolithic site*. Beijing: Cultural Relics Press.

Wang, F., Liu, S., and Gao, D., 2011, Brief report of excavation on Lijiagou site in xinmi city, henan province(in Chinese), *Archaeology*, 4,3–99.

Yi, M., Gao, X., and Bettinger, R. (2013). Hunter-gatherer foraging models: Review and prospect in paleolithic Archaeology (in Chinese). *Acta Anthropol. Sin.* 32 (02), 156–168. doi:10.16359/j.cnki.cn11-1963/q.2013.02.003

Zhang, S., Peng, F., and Zhang, Y. (2019). Taphonomic observation of faunal remains from the gezishan locality 10 in Ningxia Hui autonomous region(in Chinese). *Acta Anthropol. Sin.* 38 (2), 232–244. doi:10.16359/j.cnki.cn11-1963/q.2019.0019

Zhang, Y., Doyon, L., Peng, F., Wang, H., Guo, J., Gao, X., et al. (2022). An upper paleolithic perforated red deer canine with geometric engravings from QG10, Ningxia, northwest China. *Front. Earth Sci.* 10, 814761. doi:10.3389/feart.2022.814761

Zhao, Z., Guo, S., and Liu, Y. (2020). Analysis on flotation results from the Donghulin site in beijing (in Chinese). *Archaeology* 7, 99–106.

Zvelebil, M. (1994). Plant use in the Mesolithic and its role in the transition to farming. *Proc. Prehist. Soc.* 60, 35–74. doi:10.1017/S0079497X00003388

frontiers | Frontiers in Earth Science

TYPE Original Research
PUBLISHED 09 May 2023
DOI 10.3389/feart.2023.1143231

Check for updates

OPEN ACCESS

EDITED BY
Ren Lele,
Lanzhou University, China

REVIEWED BY
Yan Liu,
East China Normal University, China
Kai Li,
Zhejiang Normal University, China
Yongbo Wang,
Capital Normal University, China

*CORRESPONDENCE
Chunmei Ma,
chunmeima@nju.edu.cn

SPECIALTY SECTION
This article was submitted to Quaternary Science, Geomorphology and Paleoenvironment, a section of the journal Frontiers in Earth Science

RECEIVED 12 January 2023
ACCEPTED 29 March 2023
PUBLISHED 09 May 2023

CITATION
Deng Z, Ma C, Wu L, Tan Y, Wang K, Lin L, Zhao D, Shui T and Zhu C (2023), Asynchronous destruction of marsh and forest in Neolithic age: An example from Luotuodun site, Lower Yangtze. *Front. Earth Sci.* 11:1143231. doi: 10.3389/feart.2023.1143231

COPYRIGHT
© 2023 Deng, Ma, Wu, Tan, Wang, Lin, Zhao, Shui and Zhu. This is an open-access article distributed under the terms of the Creative Commons Attribution License (CC BY). The use, distribution or reproduction in other forums is permitted, provided the original author(s) and the copyright owner(s) are credited and that the original publication in this journal is cited, in accordance with accepted academic practice. No use, distribution or reproduction is permitted which does not comply with these terms.

Asynchronous destruction of marsh and forest in Neolithic age: An example from Luotuodun site, Lower Yangtze

Zeyu Deng[1], Chunmei Ma[1,2]*, Li Wu[3], Yan Tan[1], Kunhua Wang[1], Liugen Lin[4], Dongsheng Zhao[5], Tao Shui[5] and Cheng Zhu[1]

[1]School of Geography and Ocean Science, Nanjing University, Nanjing, China, [2]Jiangsu Collaborative Innovation Center for Climate Change, Nanjing, China, [3]School of Geography and Tourism, Anhui Normal University, Wuhu, China, [4]School of Art and Archaeology, Zhejiang University, Hangzhou, China, [5]School of History, Nanjing University, Nanjing, China

The natural marshland and forest landscapes in the Lower Yangtze region have undergone a long history of human-induced destruction; however, little is known about the beginning and process of this destruction. In this study, we investigate the anthropogenic impact on the marsh and forest using cores collected from the vicinity of the Neolithic Luotuodun site, employing palaeoenvironmental and palaeovegetation methods. Our results indicate that the marsh was disturbed by the Neolithic community at 7500 cal yr BP and was completely destroyed at 6500 cal yr BP. Deforestation began at 6500 cal yr BP, and the original mixed broadleaf evergreen and deciduous forest was completely cleared at 4800 cal yr BP. Our findings demonstrate that the Neolithic community in the Luotuodun site prioritized the transformation of marsh in low-lying areas before deforestation. Given that most recent research has focused on pollen-based forest dynamics to study terrestrial landscape changes, the emergence and evolution of anthropogenic landscapes may be greatly underestimated.

KEYWORDS

land use, anthropogenic landscape, marsh degradation, deforestation, Neolithic

1 Introduction

As part of a planetary transition to the Anthropocene, land use is dramatically changing the world's landscapes (Foley et al., 2005). However, human transformation of the Earth is not a recent phenomenon but has been extensive and sustained for millennia (Ellis et al., 2013; Ellis et al., 2021). To understand the causes and consequences of terrestrial landscape change, it is necessary to examine the land use history from prehistoric times to compile a continuous record.

The Lower Yangtze provides an example of long-term human-environment interactions. The successful development of Neolithic communities, characterized by rice domestication and intensification (Fuller et al., 2009), coincident with swamp management (Zong et al., 2007), deforestation (Atahan et al., 2008), construction of hydraulic enterprise (Liu et al., 2017) and urbanization (Fuller and Stevens, 2019), all of which resulted in large-scale landscape change. Deforestation is often regarded as the most significant human-induced landscape change and has been extensively studied using mature pollen-based methods (He et al., 2022; Liu et al., 2023). However, it is unclear whether deforestation marks the beginning of anthropogenic landscape change. Based on the regional characteristics of the

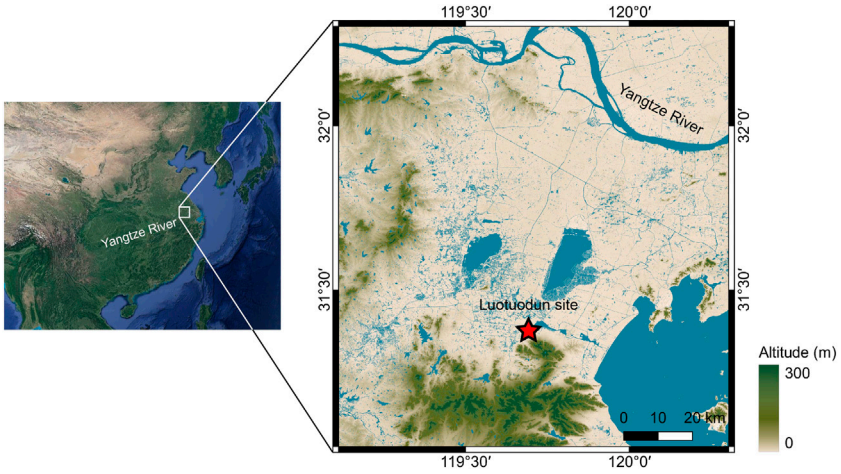

FIGURE 1
Map showing the location of the Luotuodun site (red star).

Lower Yangtze, we propose a hypothesis that the marshlands, non-forest-covered areas, may have been subjected to earlier human disturbances in certain locations.

Here, we assess the response of the marshlands and forests to human impact during the Neolithic period, on the temporal sequence of different landscapes under human disturbance. We present a detailed analysis of a 386-cm sediment core from the Lower Yangtze region, near the Neolithic Luotuodun site, using a range of proxies, including total organic carbon (TOC) values, carbon-to-nitrogen ratio (C/N), grain size, Rubidium-to-Strontium ratio (Rb/Sr), and palynological analysis.

2 Study site

The Luotuodun site (119°42′E, 31°21′N), 10 km away from Yixing City to the east, lies on the transitional zone from the Yili mountains to the deltaic plains in the Lower Yangtze (Figure 1). This site was excavated by the Institute of Archaeology, Nanjing Museum from November 2001 to July 2002 with a distribution area of about 250,000 m^2. Excavations revealed a large central settlement of the Majiabang Culture, as well as cultural relics of the Songze, Liangzhu and Guangfulin Culture in the Luotuodun site (Nanjing Museum Archaeological Research Institute, 2003; Nanjing Museum and Yixing Cultural Heritage Administration Committee, 2009). Previous studies have found that there is a 50-centimetre-thick peat layer with pottery pieces under the Majiabang cultural layer (Supplementary Figure S1) (Li et al., 2009; Li, 2011).

Meteorological data collected from 1981 to 2010 at the nearby Yixing station show the mean annual temperature and precipitation are 16.2°C and 1294.3 mm, respectively (China Meteorological Data Service Center, http://data.cma.cn). Approximately 40% of the precipitation occurs in summer, which means a strong effect of the East Asian Summer Monsoon on local precipitation. The natural vegetation types include subtropical broadleaf evergreen forest and mixed broadleaf evergreen and deciduous forest, but nowadays they are almost replaced by cultural vegetation such as *Oryza sativa* and *Triticum aestivum* (Su et al., 2020).

3 Materials and methods

3.1 Sample collection

We obtained a 386-cm sediment core (core LTD-12) in May 2013 from a rice field located outside the Luotuodun site (119°42′9.96″E, 31°21′44.82″N, 6 m a.s.l.). Core LTD-12 was sampled from a location 650 m away from the archaeological excavation area of the Luotuodun site. This location is close enough to record the environmental effects of human activity clearly, but far enough away from the main occupation area to avoid disturbance of the deposits' stratigraphy. Core LTD-12 has yellowish-grey silt deposits that gradually darken upwards (386–251 cm), followed by a black peat layer (251–200 cm), dense blackish-grey silt deposits (200–128 cm), finer brownish-grey clayey silt deposits (128–47 cm), and taupe paddy soil with plant roots (47–0 cm). Core LTD-5 has similar lithology, with a black peat layer in the 240–210 cm interval. Upon returning to the laboratory, we sampled the cores at a resolution of 1 cm and stored them in a refrigerator at 4°C before analysis.

3.2 Radiocarbon dating

Five accelerator mass spectrometry (AMS) radiocarbon (^{14}C) dates were obtained *via* organic sediments collected from core LTD-12, four of which have been published by Lu et al. (2019). For this study, we provide two new AMS ^{14}C dates from the upper and lower bounds of the peat layer in core LTD-5 and convert them to the corresponding depths of core LTD-12. All samples were processed by the laboratory of Guangzhou Institute of Geochemistry, Chinese Academy of Sciences and measured by the State Key Laboratory of

TABLE 1 AMS^{14}C dates for core LTD-12 and LTD-5.

Core	Lab. code	Depth (cm)	^{14}C date (yr BP)	Calibrated age (cal yr BP, 2σ-range)	References
LTD-12	GZ6724	51	2,120 ± 25	2,148–2,001	Lu et al. (2019)
LTD-12	GZ6725	101	2,020 ± 25	2,041–1,884	This study
LTD-5	GZ6727	201	5,995 ± 30	6,936–6,743	This study
LTD-5	GZ6728	251	8,255 ± 30	9,406–9,035	This study
LTD-12	GZ6730	300	7,310 ± 30	8,177–8,030	Lu et al. (2019)
LTD-12	GZ6731	340	9,060 ± 45	10,335–10,159	Lu et al. (2019)
LTD-12	GZ6732	386	11,135 ± 45	13,159–12,921	Lu et al. (2019)

Nuclear Physics and Technology, Peking University, using standard procedures (acid–alkali–acid treatment).

3.3 Organic analysis

The TOC and TN (total nitrogen) contents were conducted on 126 samples from core LTD-12 and performed with a Vario EL cube elemental analyzer (Elementar, Germany). All the samples were dried at 25°C. We then tested the samples with 10% HCl, processed them with distilled water, and dried them at 50°C for 24 h to attain a pH of 7. The sample was ground in an agate mortar and passed through a 200-mesh sieve. The C/N ratio was calculated using the ratio of TOC to TN.

3.4 Grain-size analysis

Grain-size analysis was conducted on 126 samples from core LTD-12 and performed with a Malvern Mastersizer 2000 laser analyzer (Malvern, UK). We removed organic matter and carbonates before the examination by adding 10% H_2O_2 and 10% HCl, and then performed ultrasonic pre-treatment in a 0.05 mol/L $(NaPO_3)_6$ solution to disperse the samples for grain size determination.

3.5 Elemental analysis

The Rb and Sr contents were conducted on 126 samples from core LTD-12 and determined using an ARL 9800 XP+ (Thermo ARL, Switzerland). All samples were dried at 25°C. Each sample (no less than 5 g) was grounded with a <200 mesh in an agate mortar and then compacted the sample into a disc.

3.6 Palynological analysis

127 samples were extracted from core LTD-12 and processed following standard palynological techniques (Faegri et al., 1989), including treatment with HCl, KOH, HF and acetolysis treatment. One tablet of *Lycopodium* spores (27,637 ± 563 grains) was added to each sample for calculation of pollen concentrations. Identification followed pollen morphological atlases (Wang et al., 1995) aided by modern reference slides. Terrestrial pollen and fern spore data were previously presented (Lu et al., 2019). Terrestrial pollen percentages are calculated based on the pollen sum of trees, shrubs and upland herbs, while fern spores are calculated based on all the pollen. Here we present new wetland herb pollen data, expressed in terms of concentration (grains/g). Limited pollen remains were found in the lower part of core LTD-12, so this study focuses on the upper part (1–300 cm) and removes samples with less than 50 grains of terrestrial pollen. The pollen diagrams were plotted using Tilia software (Grimm, 1993) based on the remaining 91 data, and pollen assemblage zones were defined using CONISS (Grimm, 1987) based on all terrestrial pollen.

4 Results

4.1 Chronology

All 7 AMS ^{14}C determinations are shown in Table 1. We rejected one ^{14}C date from the 300 cm depth of core LTD-12 (sample GZ6730), as it is too young based on the dates from the bottom of the peat layer of core LTD-5 and profile T5033. Both suggest a likely age of 9,000 cal yr BP for the beginning of peat formation. Based on 6 ^{14}C dates, we generated an age-depth model for core LTD-12 using rbacon package 2.5.8 (Blaauw and Christen, 2011). The ^{14}C dates were calibrated with reference to the IntCal20 (Reimer et al., 2020). Ages are expressed as calendar years before the present (cal yr BP, defined the present as 1950 CE). The age-depth model (Figure 2) shows the age coverage ranges from 12,800 to 2,100 cal yr BP for the 386–51 cm layer.

4.2 Palaeoenvironmental proxies

We present the mean grain size (Mz), Rb and Sr contents, Rb/Sr ratio, TOC, and C/N ratio in Figure 3. According to the lithology and multi-proxy records, we divided core LTD-12 into four environmental units.

Mz in Units 1 and 3 from depths of 377–301 and 206–47 cm, respectively, were fine and remained constant, ranging between 4.01 and 7.85 μm. The middle section (Unit 2, 300–207 cm) was characterized by coarser Mz and considerably fluctuated, ranging between 6.63 and 31.35 μm. The upper section (Unit 4, 46–1 cm) was a cultivated layer disturbed by humans, and its Mz increased from 5.25 to 21.22 μm.

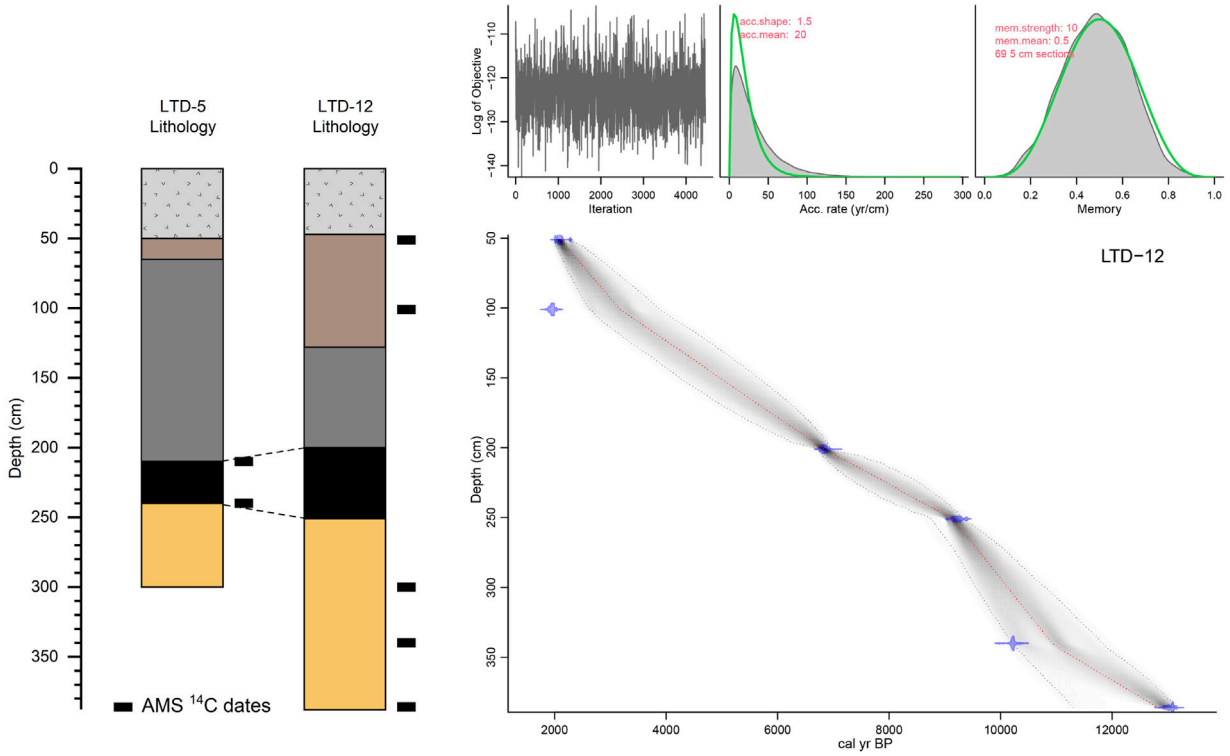

FIGURE 2
Lithology of cores LTD-5 and LTD-12, and age-depth model of core LTD-12. Locations of the dating samples are shown on the right side of the lithology pictures by black rectangles. The colours represent different lithologies: From top to bottom are yellowish-grey silt deposits, black peat, dense blackish-grey silt deposits, finer brownish-grey clayey silt deposits and taupe paddy soil.

The Rb and Sr contents variations exhibited roughly opposite trends, except for some rapid fluctuations. The Rb contents fluctuate widely, averaging 103.6 ppm. Comparatively, the Sr contents exhibited relatively high values in 287–227 cm averaging 114.5 ppm, whereas relatively lower values in 377–288 and 226–1 cm averaging 78.5 ppm. The Rb/Sr ratio averages 1.27, with a distinct peak between 224 and 206 cm.

In Unit 1, the TOC content and C/N ratio remained stable, ranging from 0.21% to 0.50% and 5.10 to 11.45, respectively. In Unit 2, the TOC content increased and reached a maximum value of 10.22% at a depth of 215 cm. We observed distinct changes in the C/N ratio in this unit, ranging from 13.19 to 24.18, with an average of 18.07. In Unit 3, the TOC content and C/N ratio showed the same changes: TOC content decreased to a low and stable state ranging from 0.43% to 3.31%; the C/N ratio gradually decreased and ranged from 7.03 to 16.98 with an average value of 10.66. In Unit 4, the TOC content and C/N ratio gradually increased, ranging from 0.49% to 2.88% and 8.41 to 11.40, respectively.

4.3 Palaeovegetation proxies

Forty-two terrestrial pollen taxa were identified from core LTD-12 (Lu et al., 2019). The main tree pollen taxa are *Pinus*, *Quercus* evergreen, *Quercus* deciduous, and *Liquidambar*; and the main herb pollen taxa are *Artemisia*, Cruciferae, and Poaceae. Four palaeovegetation zones (1–4) were recognized according to CONISS analysis (Figure 4).

Zone 1 (298–191 cm, 10,100–6,500 cal yr BP), pollen data show a high percentage of broadleaved content, with a decrease in *Pinus*. Additionally, fern content remains low except at the bottom.

Zone 2 (190–146 cm, 6,500–4,800 cal yr BP), the pollen percentages of both *Quercus* evergreen and *Quercus* deciduous decline in abundance (with fluctuations) throughout this zone, but *Liquidambar* remains at the highest level (18.8% on average). *Pinus* expansion is observed, accompanied by the rising proportions of ferns.

Zone 3 (145–20 cm, 4,800–2,100 cal yr BP), this zone was characterized by the absolute dominance in the pollen percentage of *Pinus* (88.8% on average) and the almost disappearance of *Quercus* and *Liquidambar* at the start of this period, coincident with an abundance of fern content.

Zone 4 (19–1 cm, after 2,100 cal yr BP), this zone is characterized by increases in the pollen percentages of Cruciferae (5.9% on average) and Poaceae (9.6% on average), which are the two most abundant agricultural-associated taxa. On the contrary, the pollen percentages of *Pinus* decrease slightly.

Wetland herb pollen taxa include Cyperaceae, *Typha*, and *Polygonum*. Pollen data show that wetland herbs occur mainly in Zone 1 with an average concentration of 92.4 grains/g, while almost no wetland herb pollen exists in Zone 2–4.

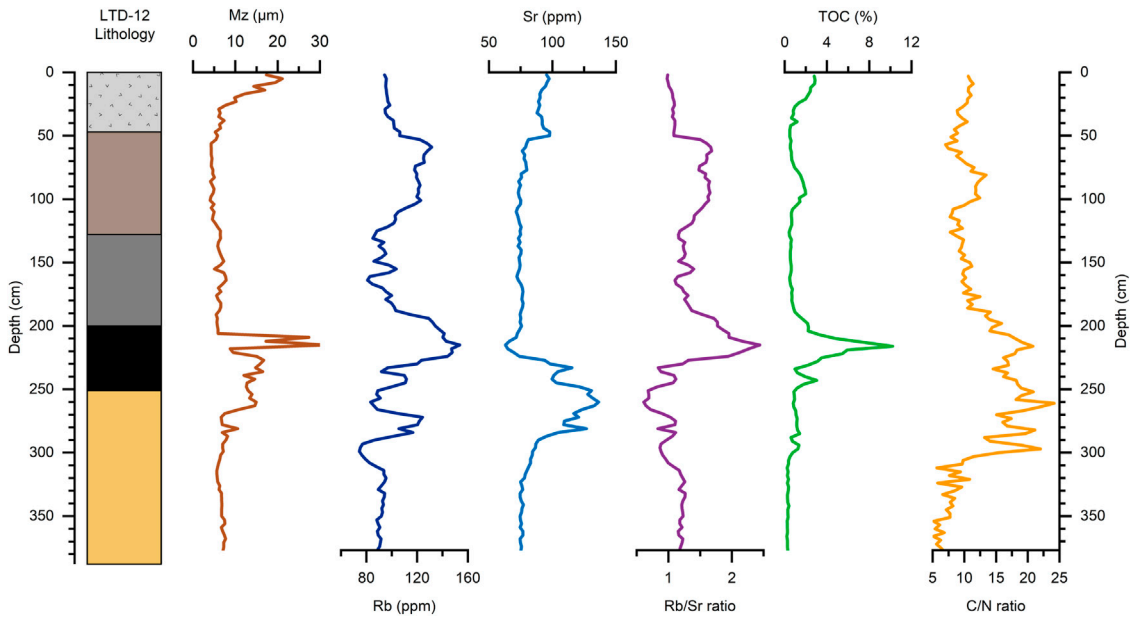

FIGURE 3
Multi-proxy record of core LTD-12. From left to right: lithology, mean grain size (Mz), Rb and Sr contents, Rb/Sr ratio, total organic carbon (TOC), C/N ratio.

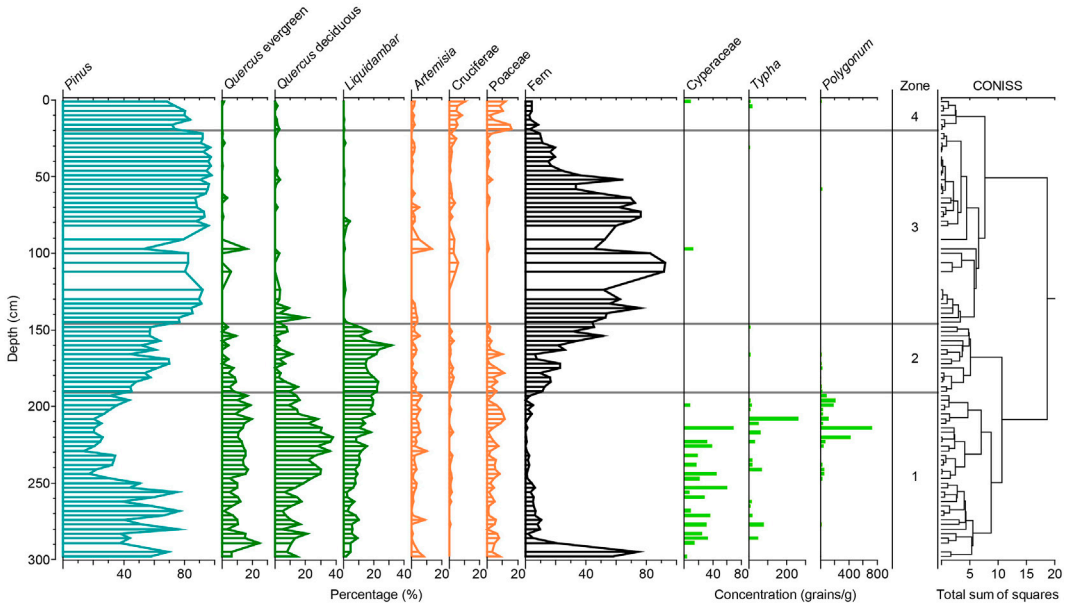

FIGURE 4
Pollen diagram for core LTD-12. The results of CONISS are shown on the right.

5 Discussion

5.1 Marsh dynamic

The C/N ratio and wetland herb pollen record are reliable indicators of marshland existence. In the Lower Yangtze region, the dominant pollen taxa in freshwater wetland habitats are Cyperaceae and *Typha*, which are often used to indicate marsh/wetland environments (Zong et al., 2007; Tang et al., 2019). *Polygonum* is also an important taxon in marshland environments (Ge et al., 2019). Li et al. (2009) identified a total of 413 plant fossils in the peat layer at the Luotuodun site, which contains a large number of *Polygonum* seeds. Additionally, the high C/N ratios of peat sediments, which have a fibric or hemic appearance and substantial plant-derived contributions, are significantly higher than

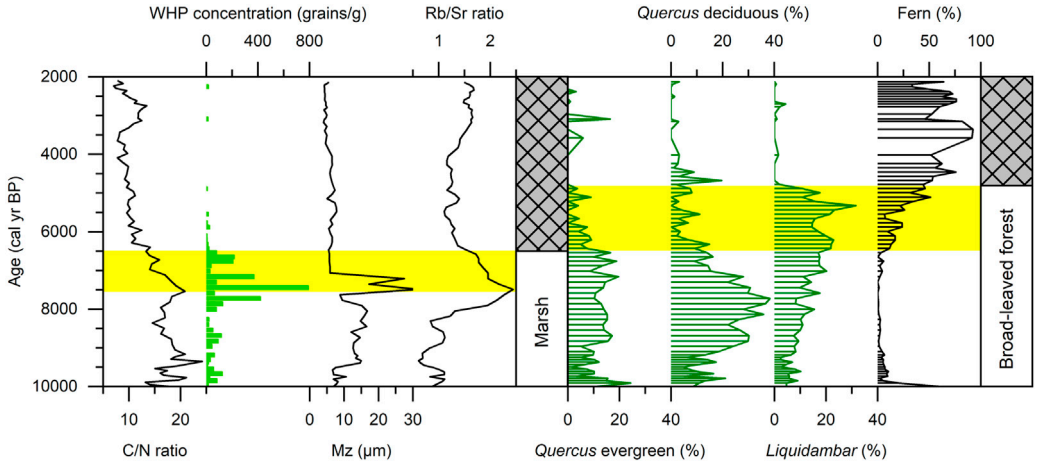

FIGURE 5
Comparison of palaeoenvironmental and palaeovegetation proxies in core LTD-12. The shaded yellow bars indicate the intervals that the marsh and forest are subjected to human disturbance.

those of mineral soils (Leifeld et al., 2020). Therefore, the high concentration of wetland herb pollen combined with the high level of C/N ratios between 10000 and 6500 cal yr BP indicates the persistence of the marshland landscape.

In this paper, we pay more attention to the process of the disappearance of marshland. Before the end of the marsh layer, Mz suddenly increased between 7500 and 7000 cal yr BP, with Rb/Sr ratio synchronously reaching a maximum (Figure 5). Although there are controversial explanations regarding grain-size indexes (Chen et al., 2021), the significant fluctuations in Mz indicate changes in the sedimentary environment. The Rb/Sr ratio has been widely used as a proxy for chemical weathering intensity (Yang et al., 2020), where a high Rb/Sr ratio indicates an enhancement of chemical weathering (Liu et al., 2014). This is because Sr typically substitutes for Ca in carbonate minerals and is more geochemically reactive than Rb (Liu et al., 2021). Complementary evidence from profile T5033 within the Luotuodun site corroborates the human–marsh interaction: The peat layer beneath the cultural layer (9th layers) is interspersed with pottery pieces, which began at 7212 ± 55 cal yr BP (2σ) (Supplementary Figure S1) (Nanjing Museum Archaeological Research Institute, 2003; Li et al., 2009; Li, 2011). Therefore, we attribute the changes in Mz and Rb/Sr ratio to anthropogenic disturbance in the marshland, which led to the degradation of marshlands and the intensification of soil erosion. By the time 6500 cal yr BP, the low-lying marsh was completely transformed, and the Neolithic community had built a massive settlement on the remains of the marshland.

5.2 Vegetation succession

Palynological evidence reveals that high forest cover was maintained in southern China during the mid-Holocene (Yi et al., 2003; Zhu et al., 2010; Yue et al., 2012; Li et al., 2013; Ma et al., 2016; Zhao et al., 2021); that was, sustained recovery since the Lateglacial, consistent with intensifying East Asian Summer Monsoon and warm climate. Although some recent studies based on non-pollen proxies indicate a drier mid-Holocene (e.g., Xie et al., 2013; Liu et al., 2019; Liu et al., 2021), these studies require complementary explanations for the possible decoupling of vegetation and precipitation changes.

In the Luotuodun area, the mixed broadleaf evergreen and deciduous forest, composed mainly of *Quercus* and *Liquidambar*, continued to exist between 10100 and 6500 cal yr BP (Zone 1 in the pollen assemblages, Figure 4). The decrease in *Pinus* and increase in *Quercus* mostly occurred between 9000–6500 cal yr BP, which is likely due to climatic factors as there is no evidence of Neolithic remains in the western Taihu Lake area during the early Holocene (Li, 2011). After 6500 cal yr BP, the pollen assemblages changed dramatically, reflecting an obvious shift in the regional vegetation landscape (Zone 2 in the pollen assemblages, Figure 4). This zone is characterized by declines in both *Quercus* evergreen and *Quercus* deciduous. However, this decline of the broad-leaved forest is not consistent with the relatively stable climate background by this time (Zhang et al., 2021). We conclude that changes in precipitation cannot explain the near-total disappearance of *Quercus*. Meanwhile, the fern that thrives in areas disturbed by forest clearance expanded sharply. We therefore contend such a big change in vegetation composition is caused by human deforestation, and further, date the onset of human deforestation to 6500 cal yr BP (Figure 5).

At 4800 cal yr BP, the broadleaf forest collapsed ecologically with the disappearance of *Liquidambar*. Pinus (especially *Pinus massoniana*) is a kind of secondary conifer species (Ma et al., 2020). For the period after 4800 cal yr BP, the long-term absolute dominance of *Pinus* indicates that a resemble modern landscape has formed.

5.3 Asynchronous destruction of marsh and forest

The inherent error and “old wood” problem of AMS ^{14}C dating would interfere with our determination of the absolute age at which events occurred and thus hinder us from understanding the sequencing of the anthropogenic transformation of marsh and forest based on different studies. However, multi-proxy analysis of a single core can subtly avoid this uncertainty. Our study provides

evidence of a pre-existing anthropogenic transformation of the marsh dating back to 7500 cal yr BP, which occurred 1000 years prior to the man-made destruction of the broadleaf forest (Figure 5).

There are simple explanations for the Neolithic ancients' preference for transforming marshlands. The importance of marshes on low-lying plains to Neolithic communities has been studied, as they provided valuable sources of food (Ma et al., 2020; Shao et al., 2021); the findings emphasize that marshlands, including lakeside and coastal swamps, would have been the ecological zone most suitable for the earliest rice cultivation (Zong et al., 2007). More importantly, the lush subtropical evergreen forests in the Lower Yangtze hindered settlement and movement in the Neolithic period (Zhao, 2016), because deforestation without iron tools was laborious.

In addition, we highlight some possible flaws in previous studies of past land use. As the marsh landscape is difficult to be reflected in the regional pollen signal, the footprint of marshland dynamics has been ignored. Therefore, the first beginning and intensity of the anthropogenic transformation of the terrestrial landscape may be greatly underestimated.

6 Conclusion

This study presents a detailed multi-proxy analysis of cores from the Luotuodun area, providing evidence for past land use. Our results show that the marsh was first disturbed by the Neolithic community at 7500 cal yr BP and subsequently destroyed at 6500 cal yr BP. Deforestation began at 6500 cal yr BP, resulting in the complete clearance of the original mixed evergreen and deciduous broadleaf forest by 4800 cal yr BP. Interestingly, prior to the confirmed deforestation, there was a priority for the transformation of marshes in low-lying areas. Our findings highlight a potential flaw in previous studies of past human land use, as the emergence and evolution of anthropogenic landscapes may have been greatly underestimated due to the lack of direct evidence of marshland changes.

Data availability statement

The raw data supporting the conclusion of this article will be made available by the authors, without undue reservation.

Author contributions

ZD: Conceptualization, formal analysis, writing, visualization. CM: Funding acquisition, methodology, project administration, supervision. LW: Investigation. YT: Investigation. KW: Investigation. LL: Supervision. DZ: Supervision. TS: Funding acquisition, supervision. CZ: Resources. All authors contributed to manuscript revision, read, and approved the submitted version.

Funding

This study was supported by Major project of National Social Science Fund of China (No. 20&ZD247), the National Natural Science Foundation of China (Nos. 41977389 and 42271173), the Frontiers Science Center for Critical Earth Material Cycling Fund (No. JBGS2102), and the Fundamental Research Funds for the Central Universities (No. 0209-14380097).

Conflict of interest

The authors declare that the research was conducted in the absence of any commercial or financial relationships that could be construed as a potential conflict of interest.

Publisher's note

All claims expressed in this article are solely those of the authors and do not necessarily represent those of their affiliated organizations, or those of the publisher, the editors and the reviewers. Any product that may be evaluated in this article, or claim that may be made by its manufacturer, is not guaranteed or endorsed by the publisher.

Supplementary material

The Supplementary Material for this article can be found online at: https://www.frontiersin.org/articles/10.3389/feart.2023.1143231/full#supplementary-material

References

Atahan, P., Itzstein-Davey, F., Taylor, D., Dodson, J., Qin, J., Zheng, H., et al. (2008). Holocene-aged sedimentary records of environmental changes and early agriculture in the lower Yangtze, China. *Quat. Sci. Rev.* 27, 556–570. doi:10.1016/j.quascirev.2007.11.003

Blaauw, M., and Christen, J. A. (2011). Flexible paleoclimate age-depth models using an autoregressive gamma process. *Bayesian Anal.* 6. doi:10.1214/11-ba618

Chen, H., Zhu, L., Wang, J., Ju, J., Ma, Q., and Xu, T. (2021). Paleoclimate changes over the past 13,000 years recorded by Chibuzhang Co sediments in the source region of the Yangtze River, China. *Palaeogeogr. Palaeoclimatol. Palaeoecol.* 573, 110433. doi:10.1016/j.palaeo.2021.110433

Ellis, E. C., Kaplan, J. O., Fuller, D. Q., Vavrus, S., Klein Goldewijk, K., and Verburg, P. H. (2013). Used planet: A global history. *Proc. Natl. Acad. Sci. U. S. A.* 110, 7978–7985. doi:10.1073/pnas.1217241110

Ellis, E. C., Gauthier, N., Klein Goldewijk, K., Bliege Bird, R., Boivin, N., Diaz, S., et al. (2021). People have shaped most of terrestrial nature for at least 12,000 years. *Proc. Natl. Acad. Sci. U. S. A.* 118, e2023483118. doi:10.1073/pnas.2023483118

Faegri, K., Kaland, P. E., and Krzywinski, K. (1989). *Textbook of pollen analysis*. John Wiley & Sons Ltd.

Foley, J. A., Defries, R., Asner, G. P., Barford, C., Bonan, G., Carpenter, S. R., et al. (2005). Global consequences of land use. *Science* 309, 570–574. doi:10.1126/science.1111772

Fuller, D. Q., and Stevens, C. J. (2019). Between domestication and civilization: The role of agriculture and arboriculture in the emergence of the first urban societies. *Veg. Hist. Archaeobot* 28, 263–282. doi:10.1007/s00334-019-00727-4

Fuller, D. Q., Qin, L., Zheng, Y., Zhao, Z., Chen, X., Hosoya, L. A., et al. (2009). The domestication process and domestication rate in rice: Spikelet bases from the lower Yangtze. *Science* 323, 1607–1610. doi:10.1126/science.1166605

Ge, Y., Zhang, K., and Yang, X. (2019). A 110-year pollen record of land use and land cover changes in an anthropogenic watershed landscape, eastern China: Understanding past human-environment interactions. *Sci. Total Environ.* 650, 2906–2918. doi:10.1016/j.scitotenv.2018.10.058

Grimm, E. C. (1987). CONISS - a FORTRAN-77 program for stratigraphically constrained cluster-analysis by the method of incremental sum of squares. *Comput. Geosciences* 13, 13–35. doi:10.1016/0098-3004(87)90022-7

Grimm, E. (1993). *TILIA v2. 0 (computer software)*. Springfield, II: Illinois State Museum, Research and Collections Center.

He, K., Lu, H., Sun, G., Wang, Y., Zheng, Y., Zheng, H., et al. (2022). Dynamic interaction between deforestation and rice cultivation during the holocene in the lower Yangtze river, China. *Front. Earth Sc-Switz* 10. doi:10.3389/feart.2022.849501

Leifeld, J., Klein, K., and Wust-Galley, C. (2020). Soil organic matter stoichiometry as indicator for peatland degradation. *Sci. Rep.* 10, 7634. doi:10.1038/s41598-020-64275-y

Li, L., Zhu, C., Lin, L., Zhao, Q., Shi, G., Zheng, C., et al. (2009). Evidence for marine transgression between 7500–5400BC at the Luotuodun site in yixing, jiangsu province. *J. Geogr. Sci.* 19, 671–680. doi:10.1007/s11442-009-0671-2

Li, J., Zheng, Z., Huang, K., Yang, S., Chase, B., Valsecchi, V., et al. (2013). Vegetation changes during the past 40,000 years in Central China from a long fossil record. *Quat. Int.* 310, 221–226. doi:10.1016/j.quaint.2012.01.009

Li, L. (2011). *Research on the environmental evolution and the missing reasons of the archeaological sites in Early Holocene in Taihu Lake area*. Doctor. Nanjing: Nanjing University.

Liu, J., Chen, J., Selvaraj, K., Xu, Q., Wang, Z., and Chen, F. (2014). Chemical weathering over the last 1200 years recorded in the sediments of gonghai lake, lvliang mountains, north China: A high-resolution proxy of past climate. *Boreas* 43, 914–923. doi:10.1111/bor.12072

Liu, B., Wang, N., Chen, M., Wu, X., Mo, D., Liu, J., et al. (2017). Earliest hydraulic enterprise in China, 5,100 years ago. *Proc. Natl. Acad. Sci. U. S. A.* 114, 13637–13642. doi:10.1073/pnas.1710516114

Liu, H., Gu, Y., Huang, X., Yu, Z., Xie, S., and Cheng, S. (2019). A 13,000-year peatland palaeohydrological response to the ENSO-related Asian monsoon precipitation changes in the middle Yangtze Valley. *Quat. Sci. Rev.* 212, 80–91. doi:10.1016/j.quascirev.2019.03.034

Liu, J. B., Shen, Z. W., Chen, W., Chen, J., Zhang, X., Chen, J. H., et al. (2021). Dipolar mode of precipitation changes between north China and the Yangtze River Valley existed over the entire Holocene: Evidence from the sediment record of Nanyi Lake. *Int. J. Climatol.* 41, 1667–1681. doi:10.1002/joc.6906

Liu, Y., Xiao, L., Cheng, Z., Liu, X., Dai, J., Zhao, X., et al. (2023). Anthropogenic impacts on vegetation and biodiversity of the lower Yangtze region during the mid-Holocene. *Quaternary Sci. Rev.* 299.

Lu, F. Z., Ma, C. M., Zhu, C., Lu, H. Y., Zhang, X. J., Huang, K. Y., et al. (2019). Variability of East Asian summer monsoon precipitation during the Holocene and possible forcing mechanisms. *Clim. Dynam* 52, 969–989. doi:10.1007/s00382-018-4175-6

Ma, T., Tarasov, P. E., Zheng, Z., Han, A., and Huang, K. (2016). Pollen- and charcoal-based evidence for climatic and human impact on vegetation in the northern edge of Wuyi Mountains, China, during the last 8200 years. *Holocene* 26, 1616–1626. doi:10.1177/0959683616641744

Ma, T., Rolett, B. V., Zheng, Z., and Zong, Y. (2020). Holocene coastal evolution preceded the expansion of paddy field rice farming. *Proc. Natl. Acad. Sci. U. S. A.* 117, 24138–24143. doi:10.1073/pnas.1919217117

Nanjing Museum Archaeological Research Institute (2003). Excavation on the neolithic Luotuodun site in yixing city, jiangsu. *Archaelogy* 7, 579–585. (In Chinese).

Nanjing Museum, Yixing Cultural Heritage Administration Committee (2009). An excavation report of Luotuodun site in Yixing. *Jiangsu. Southeast Cult.* 211, 26–44. (In Chinese).

Reimer, P. J., Austin, W. E. N., Bard, E., Bayliss, A., Blackwell, P. G., Bronk Ramsey, C., et al. (2020). The IntCal20 northern hemisphere radiocarbon age calibration curve (0–55 cal kBP). *Radiocarbon* 62, 725–757. doi:10.1017/rdc.2020.41

Shao, K., Zhang, J., He, K., Wang, C., and Lu, H. (2021). Impacts of the wetland environment on demographic development during the neolithic in the lower Yangtze region—based on peat and archaeological dates. *Front. Earth Sc-Switz* 9. doi:10.3389/feart.2021.635640

Su, Y., Guo, Q., Hu, T., Guan, H., Jin, S., An, S., et al. (2020). An updated vegetation map of China (1:1000000). *Sci. Bull.* 65, 1125–1136. doi:10.1016/j.scib.2020.04.004

Tang, L., Shu, J., Chen, J., and Wang, Z. (2019). Mid-to late Holocene vegetation change recorded at a Neolithic site in the Yangtze coastal plain, East China. *Quat. Int.* 519, 122–130. doi:10.1016/j.quaint.2018.12.031

Wang, F., Qian, N., Zhang, Y., and Yang, H. (1995). *Pollen flora of China*. Beijing: Science Press.

Xie, S., Evershed, R. P., Huang, X., Zhu, Z., Pancost, R. D., Meyers, P. A., et al. (2013). Concordant monsoon-driven postglacial hydrological changes in peat and stalagmite records and their impacts on prehistoric cultures in central China. *Geology* 41, 827–830. doi:10.1130/g34318.1

Yang, H., Zhao, Y., Cui, Q., Ren, W., and Li, Q. (2020). Paleoclimatic indication of X-ray fluorescence core-scanned Rb/Sr ratios: A case study in the zoige basin in the eastern Tibetan plateau. *Sci. China Earth Sci.* 64, 80–95. doi:10.1007/s11430-020-9667-7

Yi, S., Saito, Y., Zhao, Q., and Wang, P. (2003). Vegetation and climate changes in the Changjiang (Yangtze River) Delta, China, during the past 13,000 years inferred from pollen records. *Quat. Sci. Rev.* 22, 1501–1519. doi:10.1016/s0277-3791(03)00080-5

Yue, Y., Zheng, Z., Huang, K., Chevalier, M., Chase, B. M., Carré, M., et al. (2012). A continuous record of vegetation and climate change over the past 50,000years in the Fujian Province of eastern subtropical China. *Palaeogeogr. Palaeoclimatol. Palaeoecol.* 365-366, 115–123. doi:10.1016/j.palaeo.2012.09.018

Zhang, Z., Liu, J., Chen, J., Chen, S., Shen, Z., Chen, J., et al. (2021). Holocene climatic optimum in the East Asian monsoon region of China defined by climatic stability. *Earth-Science Rev.* 212, 103450. doi:10.1016/j.earscirev.2020.103450

Zhao, L., Ma, C., Wen, Z., Ye, W., Shang, G., and Tang, L. (2021). Vegetation dynamics and their response to Holocene climate change derived from multi-proxy records from Wangdongyang peat bog in southeast China. *Veg. Hist. Archaeobotany* 31, 247–260. doi:10.1007/s00334-021-00852-z

Zhao, D. (2016). Discussion on the relationship between the water change and cultural evolution around the Taihu Lake. *Cult. Relics South. China* 3, 201–207. (In Chinese).

Zhu, C., Ma, C. M., Yu, S. Y., Tang, L. Y., Zhang, W. Q., and Lu, X. F. (2010). A detailed pollen record of vegetation and climate changes in Central China during the past 16â*f*000 years. *Boreas* 39, 69–76. doi:10.1111/j.1502-3885.2009.00098.x

Zong, Y., Chen, Z., Innes, J. B., Chen, C., Wang, Z., and Wang, H. (2007). Fire and flood management of coastal swamp enabled first rice paddy cultivation in east China. *Nature* 449, 459–462. doi:10.1038/nature06135

frontiers | Frontiers in Earth Science

TYPE Original Research
PUBLISHED 06 July 2023
DOI 10.3389/feart.2023.1137528

Check for updates

OPEN ACCESS

EDITED BY
Harry F. Lee,
The Chinese University of Hong Kong, China

REVIEWED BY
Xianyong Cao,
Chinese Academy of Sciences (CAS), China
Xin Wang,
Wuhan University, China
Ray Liu,
British Museum, United Kingdom

*CORRESPONDENCE
Minmin Ma,
mamm@lzu.edu.cn
Guoke Chen,
chenguoke1980@sina.com

†These authors have contributed equally to this work

RECEIVED 04 January 2023
ACCEPTED 07 April 2023
PUBLISHED 06 July 2023

CITATION
Wei W, Ma M, Chen G, Dong J, Wu Z, Li H and Li X (2023), Human planting strategies and its relation to climate change during ~4,800–3,900 BP in the mid-lower Hulu River Valley, northwest China.
Front. Earth Sci. 11:1137528.
doi: 10.3389/feart.2023.1137528

COPYRIGHT
© 2023 Wei, Ma, Chen, Dong, Wu, Li and Li. This is an open-access article distributed under the terms of the Creative Commons Attribution License (CC BY). The use, distribution or reproduction in other forums is permitted, provided the original author(s) and the copyright owner(s) are credited and that the original publication in this journal is cited, in accordance with accepted academic practice. No use, distribution or reproduction is permitted which does not comply with these terms.

Human planting strategies and its relation to climate change during ~4,800–3,900 BP in the mid-lower Hulu River Valley, northwest China

Wenyu Wei[1], Minmin Ma[1*†], Guoke Chen[2*†], Jiajia Dong[1], Zekun Wu[1], Haiming Li[3,4] and Xiaobin Li[5]

[1]Ministry of Education Key Laboratory of Western China's Environmental Systems, College of Earth and Environmental Sciences, Lanzhou University, Lanzhou, China, [2]Gansu Provincial Institute of Cultural Relics and Archaeology Research, Lanzhou, China, [3]College of Humanities and Social Development, Nanjing Agricultural University, Nanjing, China, [4]Institution of Chinese Agricultural Civilization, Nanjing Agricultural University, Nanjing, China, [5]Zhuanglang County Museum, Pingliang, China

The response of agricultural societies to global climate events during the Neolithic (e.g., 4.2 ka event) is a scientific issue of general interest. In the mid-lower Hulu River Valley of northwest China, millet cultivation became the primary subsistence during the late Neolithic. Local paleoclimate studies have detected a notable decline in temperature and precipitation around 4,400 BP (Before Present), while the Qijia culture (4,200–3,600 BP) sites far outnumber those of the Lower Changshan culture (4,800–4,400 BP) in the area. Why the intensity of millet farming groups increased when climate was relatively cold and dry, however, has not been well understood. To explore the issue, we performed archaeobotanical analysis, grain size measurement, stable isotope analysis and radiocarbon dating in the excavated sites of the Zhongtianxingfucheng (ZTXFC) and Wangjiayangwan (WJYW), which were dated to between ~4,800–4,400 BP and ~4,200–3,900 BP, respectively. Our results demonstrate the overall declines in the proportion, grain sizes and carbon isotope values of millets from the WJYW site compared to ZTXFC. The nitrogen isotopes of millets from the two sites are similar [foxtail millet: 6.8‰ ± 1.9‰ (ZTXFC), 7.5‰ ± 1.5‰ (WJYW); broomcorn millet: 7.3‰ ± 2.0‰ (ZTXFC), 7.5‰ ± 1.2‰ (WJYW)]. These results suggest that the degree of field management during ~4,200–3,900 BP was lower than ~4,800–4,400 BP in the mid-lower Hulu River Valley. Instead of improving cultivation management or altering cropping patterns, Qijia millet farmers might have adopted a strategy of expanding cultivated lands to promote the social development under a relatively cold-dry climate.

KEYWORDS

archaeobotanical analysis, grain size, carbon and nitrogen isotope analysis, subsistence strategy, mid-lower Hulu River Valley, late Neolithic

1 Introduction

The response of human societies to global climate events during the Neolithic era, such as the 8.2 ka event, the 5.5 ka event and the 4.2 ka event, is a widely studied multidisciplinary issue (e.g., Flohr et al., 2016; Goldsmith et al., 2017; Wu et al., 2018; Park et al., 2019; Zhao, 2020). With the development and expansion of agriculture across Eurasia (Liu X et al., 2019; Dong et al., 2022a), global population significantly increased with the extensive expansion of farmer habitats during the late Neolithic (Styring et al., 2017; Dong et al., 2022b), which resulted in the rise of survival stress and social vulnerability to climate change (Kelly et al., 2012). Therefore, the impact of the 4.2 ka event on social evolution in the Old World has been intensively discussed in recent decades (Weiss, 2016; Ran and Chen, 2019; Manning et al., 2020). The 4.2 ka event has been proposed as an important trigger for the collapse of ancient civilizations in Mesopotamia (Cullen et al., 2000; Weiss, 2017) and India (Staubwasser et al., 2003). Additionally, the 4.2 ka event is suggested to have transformed the human settlement patterns in late Neolithic China (Xiao et al., 2019; He et al., 2022), resulting in the expansion and shrinkage of areas settled by millet farming groups and rice farming groups (He et al., 2022).

The responses of millet farming groups to the climatic deterioration event around 4,200 BP in different areas of north China were diverse. For example, settlement intensity of millet farming groups in east Inner Mongolia evidently declined (Xiao et al., 2019) and increased in the Yi-Luo River Valley and Gansu-Qinghai region (Liu and Feng, 2012; Liu L et al., 2019; He et al., 2022). In the mid-lower Hulu River Valley (MLHRV) of the western Loess Plateau, northwest China, intensive rain-fed agriculture was focused on millet cultivation since ~5,900 BP (Barton, 2009), and was the primary subsistence in the area during the late Neolithic period (Li et al., 2022a; Yang J et al., 2022; Yang Y et al., 2022). Paleoclimate studies from a lake in the nearby Liupan Mountains suggest that temperature and precipitation in the MLHRV declined around 4,400 BP and the overall climate trend was colder and dryer during ~4,400–3,600 BP than ~4,800–4,400 BP (Zhao et al., 2010; Chen et al., 2015). However, the third national archaeological survey in the MLHRV revealed that the site numbers of the Lower Changshan culture (4,800–4,400 BP) was much smaller than the Qijia culture (4,200–3,600 BP) (Figure 1; Li et al., 1993). This indicates that millet farming groups substantially expanded in the area under a relatively cold-dry climate. Previous studies have suggested that Neolithic groups might have successfully adapted to climate events in different ways, including the alteration of cropping patterns (Pokharia et al., 2017; Chen et al., 2020; Li R et al., 2020), the improvement of field management (Masi et al., 2014; Ren et al., 2021) and the enlargement of the cultivated land area (An et al., 2021). Nevertheless, differences in planting strategies between the Lower Changshan period and the Qijia period in the MLHRV remains unclear due to the absence of systematic archaeobotanical studies.

Recent archaeobotanical and stable isotope analysis of crops remains from investigated sites in the MLHRV provided a valuable dataset to facilitate understanding of cropping pattern variations and water and soil management for crops since ~6,000 BP (Li et al., 2022b). However, data from the excavated sites of the Lower Changshan and Qijia cultures are still scarce. Moreover, the measurement of millets grain sizes from archaeological sites in the MLHRV has not been reported, which is valuable to evaluate cropping strategies in prehistory (Motuzaite-Matuzeviciute et al., 2012; Bao et al., 2018). Recent excavations at the Zhongtianxingfucheng (ZTXFC) site of the Lower Changshan culture and the Wangjiayangwan (WJYW) site of the Qijia culture provide a rare opportunity to study strategies for millet farming and their relation to climate change during these two periods. In this paper, we report the results of radiocarbon dating, identification of plant remains, grain size measurement and carbon/nitrogen isotope analysis of charred millets grains from ZTXFC and WJYW sites. Results are then integrated with published archaeological and paleoclimate data to explore how millet farmers in the MLHRV responded to climate change during the Lower Changshan and Qijia periods.

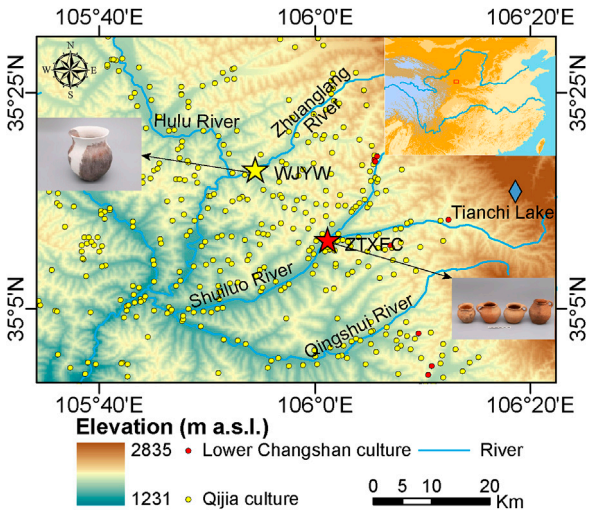

FIGURE 1
Distribution of the Lower Changshan and Qijia cultural sites in the mid-lower Hulu River Valley.

2 Study areas

The Lower Changshan culture is named after the discovery of the lower cultural remains at the Changshan site in Zhenyuan, Gansu (Hu, 1981). This has elements of the Yangshao culture and features of the Qijia culture, indicating a transitional stage from Yangshao culture to Qijia culture (Hu, 1991; Li et al., 1993). The Lower Changshan culture is mainly distributed in the Loess Plateau, such as Longdong area and southern Ningxia, and is dated to 4,800–4,400 BP in the Gansu (Li et al., 1993). The Lower Changshan cultural potteries includes clay potteries and coarse potteries, which are primarily orange and reddish brown (Hu, 1981). These potteries were mainly decorated with basket pattern and pile pattern (Li et al., 1993). The burial forms include vertical pit graves and earth-caved tombs (Li et al., 1993; Wei, 2021), and the skeletal position is mainly flexed and lying on the side (Wei, 2021).

The Qijia culture is widely distributed in the Gansu-Qinghai region and likely developed from the Lower Changshan culture through the Caiyuan type and was influenced by the Keshengzhuang culture (Wang, 2012). Qijia cultural potteries include clay red potteries, gray and red coarse potteries (Ye, 2014), decorated with cord-marking and vertical basket veins (Li et al., 1993; Underhill, 2013). The burial forms mainly include vertical pit graves, vertical and side chambers (Xie, 1986; Qian et al., 2014; Yang, 2017), and the skeletal position is mainly supine and extended and flexed and lying on the side (Chen, 2003; Underhill, 2013). The Qijia culture, dating to 4,600–3,500 BP, is mainly centered around 4,300–3,900 BP (Wang, 2012), and is dated between 4,200 and 3,600 BP in the mid-lower Hulu River Valley (Li et al., 2022b; Yang Y et al., 2022). Based on limited studies (Chen et al., 2020; Li et al., 2022b), the Lower Changshan and Qijia populations were mainly engaged in millet farming, supplemented by pig raising and hunting (Xie, 1975; The Institute of Archaeoloogy Chinese Academy of Social Sciences, 1999; Womack et al., 2021).

The Hulu River (34.72°–36.5°N, 105.5°–106.5°E) is located on the western Loess Plateau, with the Liupan Mountains to the east and the Qinling Mountains to the south (Han et al., 2020). The terrain gradually decreases from north to south and from east to west, and the vast majority of the basin is a loess hilly area with loose soil and sparse vegetation (Wang F et al., 2022). The study area is characterized by a temperate continental monsoon climate with relatively pronounced seasonal changes-hot and rainy in summer, rapidly cooling in autumn, and cold in winter (Han et al., 2020). According to the meteorological stations located on the mid-lower Hulu River (Jingning, Zhuanglang, and Qin'an), the mean annual temperature is 9.03°C and the mean annual precipitation is 444.3 mm (see http://data.cma.cn). The Hulu River is the largest tributary in the upper reaches of the Wei River. The basin is crisscrossed by ravines with a well-developed river composed of many tributaries, such as the Zhuanglang River, Shuiluo River, Qingshui River (Xin et al., 2016; Wang L et al., 2022).

The Zhongtianxingfucheng site (35.2°N, 106.0°E) is in the hilly and ravine region of the Loess Plateau, located on the terrace of the Shuiluo River in Zhuanglang county. In 2019, the Gansu Provincial Institute of Cultural Relics and Archaeology conducted rescue excavation of the ZTXFC site, with an excavated area of 2,100 m^2. The main part of the ZTXFC site is the Lower Changshan Period, and items including pottery, stone implements, bones, and teeth were unearthed. There are a wide variety of vessel classifications, the most common types are sand monaural pots excavated in ash pits, which could likely be early relics of the ZTXFC site from the Lower Changshan culture (Yang, 2012).

The Wangjiayangwan site (35.3°N, 105.9°E) is located in Zhuanglang county, situated on the terrace of the Zhuanglang River. In 2019, the Gansu Provincial Institute of Cultural Relics and Archaeology also conducted rescue excavation of the WJYW site, and the excavation area of WJYW is 3,100 m^2. The site includes two periods: the Qijia culture and the Qing Dynasty (1,644–1,912 AD). The later relics are located in the cultivated layer and come from the Qing Dynasty. Based on the distinctive convex shape with the white-grey floor as the building structure and the large double-ear pots unearthed in the house relics, it can be concluded that the early relics of the WJYW site are from the Qijia culture (Womack et al., 2017).

3 Materials and methods

To illuminate cropping patterns changes in the mid-lower Hulu River Valley during ~4,800–3,900 BP, we excavated two sites in 2019 within the study region shown in Figure 1. We used a targeted sampling strategy to sample the sediments in each layer of each unearthed relic unit. We sampled as far as possible to the middle of each layer to avoid inter-layer disturbance. Given the two sites were severely damaged, there were 84 samples collected from the WJYW site, all from house relics, and 18 samples were collected from the ZTXFC site and 16 samples of the samples were from ash pits and two of the samples were from house relics and kiln.

A total of 102 flotation soil samples were collected from two sites. The total amount of flotation soil collected from WJYW was 978.5 and 181 L from ZTXFC, with an average of 11.37 L per sample and a total of 1,159.5 L. The collected soil samples were all floated using the manual bucket flotation technique (Zhao, 2010). The floated objects with a specific gravity lighter than water, such as charcoal and charred plant seeds, floated upward. The objects were gathered with 0.2 mm aperture sieves, wrapped in gauze, and hung in a shady and cool area for desiccation. Then they were sorted through 0.35, 0.7, 1.2, and 4.0 mm mesh sieves. All seeds were selected using a ×40 stereo microscope (Zhao, 2010). The charred plant seeds were identified in the Environment Archaeology Laboratory, Lanzhou University.

One bone sample and three charred plant grain samples from the two sites were selected for accelerator mass spectrometry (AMS) radiocarbon dating (Table 1). One charred broomcorn millet seeds sample was measured at Beta Analytic in Miami, United States. The other samples were dated at the MOE Key Laboratory of Western China's Environmental Systems, Lanzhou University. The IntCal 20 calibration curve (Reimer et al., 2020) and the Libby half-life of 5,568 years were used in the calculation of all dates and the calibration was performed using OxCal v.4.4.4 (Ramsey, 2021). All ages are reported as 'cal. yr BP'.

To analyze the structure of past agricultural activities in the study area, the number of different plant species was recorded. However, different crop plants can vary considerably in weight and behave differently during harvesting, utilization, and carbonization (Yang et al., 2011). Therefore, simple ratios produced between species may not accurately correspond to the actual proportion of different species in use. To counteract this, we used a modified method of the Weight Ratio Function for different crops, proposed by Zhou et al. (2016) and Sheng et al. (2018). The Weight Ratio Function takes the average weight of 1,000 grains of the two main crops as conversion factors for estimating the actual yield percentage. This calculation is based on the results of the statistical analysis of the flotation samples (Eq. 1).

$$P(S) = \frac{N_s \times F_s}{N1 \times F1 + N2 \times F2} \quad (1)$$

Where N1 = number of foxtail millet grains, F1 = 2.6, N2 = number of broomcorn millet grains, F2 = 7.5, Ns = number of that certain crop, Fs = conversion factors of that certain crop, and P(S) = actual yield percentage of that certain crop.

The length, width, and thickness of the millet seeds were measured using a vernier caliper at the MOE Key Laboratory of Western China's Environmental Systems, Lanzhou University, Gansu Province, China. 462 mature and intact charred millets were selected for particle size

TABLE 1 Calibrated radiocarbon dates from ZTXFC and WJYW sites.

Site	Lab number	Sampling feature	Dated material	^{14}C age	Calibrated age (cal yr BP) 2 σ	Culture	Dating method	References
ZTXFC	LZU20315	Ash pit	Sheep bone	4,010 ± 30	4,567–4,414	Lower Changshan	AMS	Dong J et al. (2022)
ZTXFC	LZU20320	Tomb	Human bone	4,040 ± 30	4,612–4,418	Lower Changshan	AMS	Dong J et al. (2022)
ZTXFC	LZU20321	Tomb	Human bone	4,080 ± 20	4,795–4,446	Lower Changshan	AMS	This study
WJYW	Beta567015	House relic	Broomcorn millet	3,730 ± 30	4,221–3,981	Qijia	AMS	This study
WJYW	LZU20157	House relic	Pig bone	3,700 ± 20	4,144–3,976	Qijia	AMS	Dong J et al. (2022)
WJYW	LZU21266	House relic	Foxtail millet	3,650 ± 20	4,082–3,895	Qijia	AMS	This study
WJYW	LZU21249	House relic	Wheat	—	—	Modern	AMS	This study

measurement. The millets were placed in the sand tray in a suitable position. The longest, widest, and thickest parts of the millet seeds were measured under a stereoscopic microscope (Olympus SZX16), respectively, and recorded these data.

Forty-three randomly selected charred millet seeds were subjected to isotopic analysis. The charred millets were put into a test tube with 0.5 mol/L hydrochloric acid and then placed in a pot of water at 80°C for 30 min. Next the millets were repeatedly rinsed with pure water several times to neutral and then dried in an oven at 70°. Finally, the samples were ground into powder with a mortar and put into tinfoil bags. The $\delta^{13}C$ and $\delta^{15}N$ values of millet samples were measured with an automated carbon and nitrogen analyzer coupled with a Thermo Finnigan Flash DELTAplus XL mass spectrometer (Finnigan, Germany) at the MOE Key Laboratory of Western China's Environmental System at Lanzhou University. After ten samples, a standard (Graphite, $\delta^{13}C$: −16.0‰; Protein, $\delta^{15}N$: 5.94‰) was inserted into the sample list for calibration and stability monitoring. The analytical precision of the $\delta^{13}C$ and $\delta^{15}N$ values were ±0.2‰. All C and N isotopes were measured relative to Vienna Pee Dee Belemnite (V-PDB) and Ambient Inhalable Reservoir (AIR) standards, respectively.

In order to better use plant carbon isotope indicators to reflect ancient human management practices for agriculture, we used Farquhar et al. (1982) to air-correct $\delta^{13}C$ and obtain $\Delta^{13}C$ values (Eq. 2). Where $\delta^{13}C_{air}$ represents the $\delta^{13}C_{air}$ value in air at that time (Leuenberger et al., 1992; Francey et al., 1999; Ferrio et al., 2005), and $\delta^{13}C_{plant}$ represents the $\delta^{13}C$ value in plants.

$$\Delta^{13}C = \frac{\delta^{13}C_{air} - \delta^{13}C_{plant}}{1 + \delta^{13}C_{plant}} \quad (2)$$

4 Results

4.1 AMS radiocarbon dating

The calibrated ^{14}C ages are given with 2σ age ranges in Table 1; Figure 6D. Three bone samples were dated to between 4,795 and 4,414 cal yr BP, corresponding to the Lower Changshan period. One bone sample and two charred plant remain samples were dated to between 4,221 and 3,895 cal yr BP, corresponding to the Qijia period. One charred wheat was dated to be modern in the WJYW site, and it may have been redeposited from the upper sediments (Table 1).

4.2 Crop assemblages in different periods in the mid-lower Hulu River Valley during ~4,800–3,900 BP

A total of 8,258 charred crop seeds were identified from 102 flotation samples collected from two sites (Supplementary Table S1), including: 6,935 foxtail millet seeds (*Setaria italica*; Figure 2A), 558 broomcorn millet seeds (*Panicum miliaceum*; Figure 2B), 11 wheat seeds (*Triticum aestivum*; Figure 2C), and 16 barley seeds (*Hordeum vulgare*; Figure 2D). The remaining 738 seeds were composed of uncultivated species or weed remains (such as *Setaria viridis*, *Melilotus suaveolens*, *Atriplex patens*, *Salsolacollina pall*, *Avena fatua*, *Kochia scoparia*, *Digitaria sanguinalis*, *Carex tristachya*, *Rumex acetosa*, *Galium tricorne* and so on.) (Figure 2E–P). The wheat/barley are modern seeds from house relics in WJYW site, and they may have been redeposited from younger cultural layers. Therefore, we will not discuss it here, which has no influence on the final results and discussion.

Using the new additions to the archaeological record, linked both by agricultural practice and chronologically defined context, it is possible to chart agricultural development during ~4,800–3,900 BP in the MLHRV (Supplementary Table S1; Figure 6). 2,599 foxtail millet seeds (77.21% of weight) and 266 broomcorn millet seeds (22.79% of weight) were identified from 18 samples (181 L of soil in total) in the ZTXFC site. This indicates the predominance of a millet-based agriculture during the 4,800–4,400 BP. Between 4,200 and 3,900 BP, a mixed farming practice gradually emerged. 4,336 foxtail millet seeds (83.73% of weight), and 292 broomcorn millet seeds (16.27% of weight) were collected from 84 samples totaling 978.5 L of soil. 11 wheat and

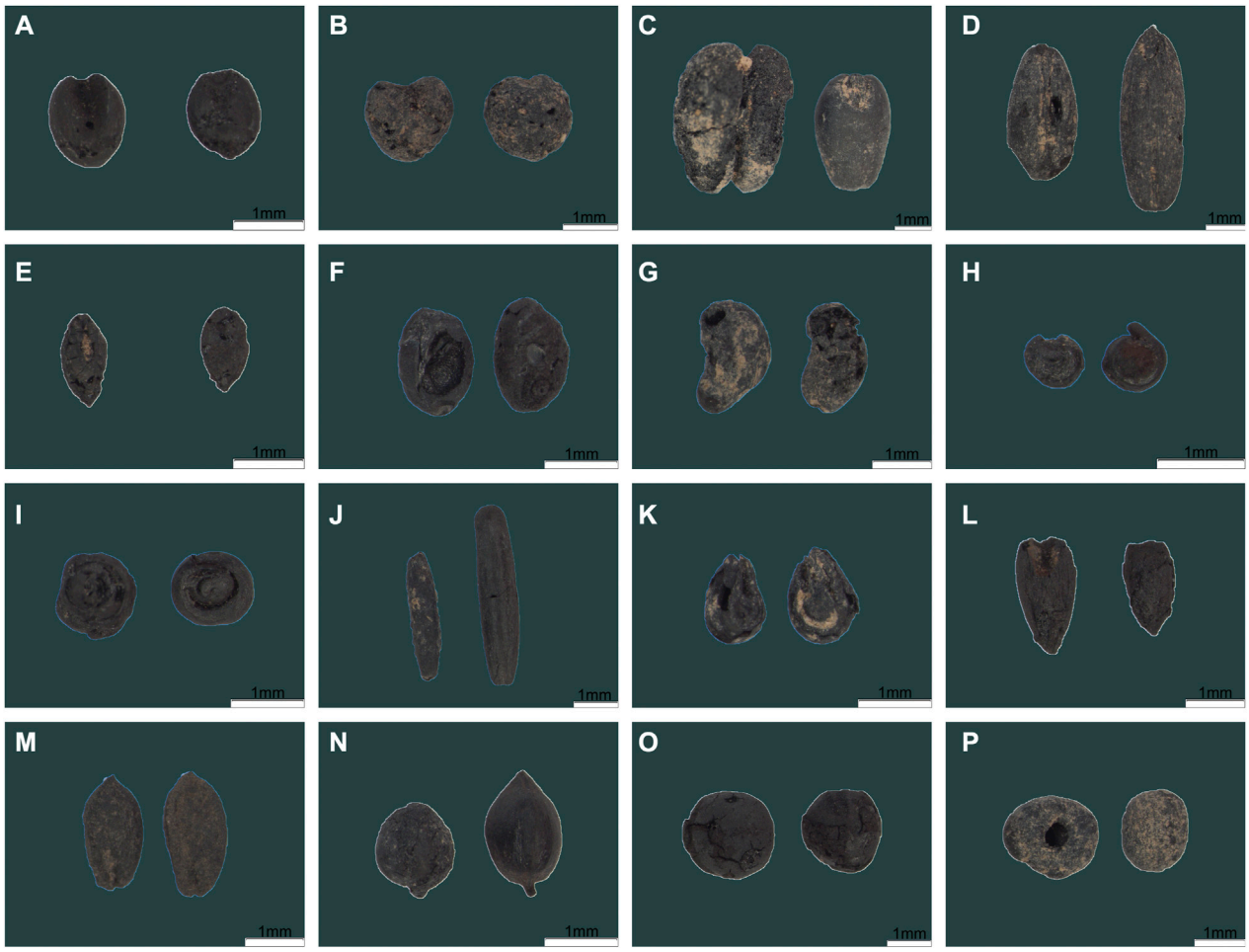

FIGURE 2
Charred plant seeds collected from ZTXFC and WJYW sites (scale bar: 1 mm): **(A)** *Setaria italica*, **(B)** *Panicum miliaceum*, **(C)** *Triticum aestivum*, **(D)** *Hordeum vulgare*, **(E)** *Setaria viridis*, **(F)** *Astragalus membranaceus*, **(G)** *Melilotus suaveolens*, **(H)** *Atriplex patens*, **(I)** *Salsolacollina pall*, **(J)** *Avena fatua*, **(K)** *Kochia scoparia*, **(L)** *Digitaria sanguinalis*, **(M)** *Carex tristachya*, **(N)** *Rumex acetosa*, **(O)** *Perilla frutescens*, **(P)** *Galium tricorne*.

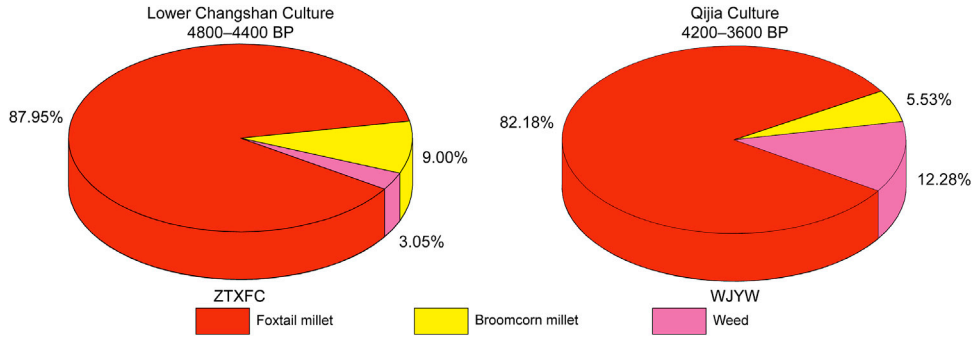

FIGURE 3
Results of archaeobotanical analysis from the ZTXFC and WJYW sites.

16 barley grains were identified from WJYW, which was probably due to a disturbed context given that similar issues were also encountered in previous studies (Table 1; e.g.; Dodson et al., 2013; Jia et al., 2013). It is worth noting that the dominant species (foxtail millet) continues to account for four-fifths of the total seeds in the assemblage (Figure 3).

TABLE 2 Statistical results regarding length, width, and thickness of single millet from ZTXFC and WJYW sites.

Site	Species	Type	Number	Mean (mm)	SD	Range (mm)
ZTXFC	Foxtail millet	Length	186	1.33	0.11	0.90–1.62
		Width	186	1.12	0.09	0.89–1.33
		Thickness	186	0.91	0.14	0.58–1.29
ZTXFC	Broomcorn millet	Length	63	1.61	0.13	1.38–1.96
		Width	63	1.53	0.13	1.32–1.89
		Thickness	63	1.32	0.15	1.03–1.80
WJYW	Foxtail millet	Length	140	1.36	0.18	0.95–1.99
		Width	140	1.12	0.14	0.74–1.77
		Thickness	140	0.84	0.18	0.50–1.55
WJYW	Broomcorn millet	Length	73	1.65	0.20	1.20–2.20
		Width	73	1.44	0.19	0.97–1.84
		Thickness	73	1.24	0.22	0.63–1.74

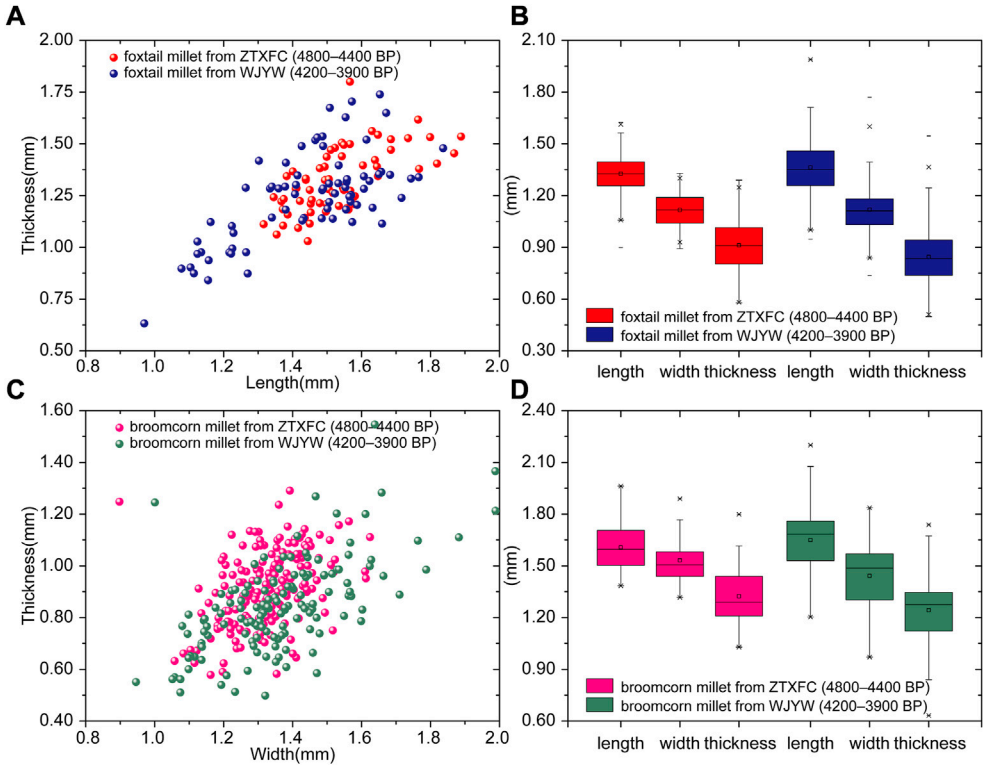

FIGURE 4
Scatter diagram and box plot detailing the length, width, and thickness of foxtail and broomcorn millets from ZTXFC and WJYW sites. **(A, B)** represent the result of foxtail millets; **(C, D)** represent the results of broomcorn millets.

4.3 Size of foxtail and broomcorn millet remains in the mid-lower Hulu River Valley during ~4,800–3,900 BP

A total of 326 foxtail millets and 136 broomcorn millets were measured and the mean values, ranges and standard deviations of length, width and thickness were calculated in this study (Table 2; Figure 4). The length, width, and thickness of the foxtail millets from ZTXFC site (4,800–4,400 BP) ranged from 0.90 to 1.62 mm (mean = 1.33 ± 0.11 mm), from 0.89 to 1.33 mm (mean = 1.12 ± 0.09 mm), and from 0.58 to 1.29 mm (mean = 0.91 ± 0.14 mm), respectively. For the broomcorn millets, the same measurements ranged from

TABLE 3 Summary results of $\delta^{13}C$ and $\delta^{15}N$ of millets from ZTXFC and WJYW sites.

Site	Species	Number	$\delta^{13}C$ (‰)			$\delta^{15}N$ (‰)		
			Mean	SD	Range	Mean	SD	Range
ZTXFC	Foxtail millet	11	−9.2	0.2	−9.6–−8.8	6.8	1.9	4.9–12.1
ZTXFC	Broomcorn millet	10	−9.7	0.3	−10.6–−9.3	7.3	2.0	5.0–13.0
WJYW	Foxtail millet	11	−9.5	0.3	−9.8–−8.8	7.5	1.5	5.7–11.5
WJYW	Broomcorn millet	11	−10.2	0.6	−11.7–−9.7	7.5	1.2	5.9–10.7

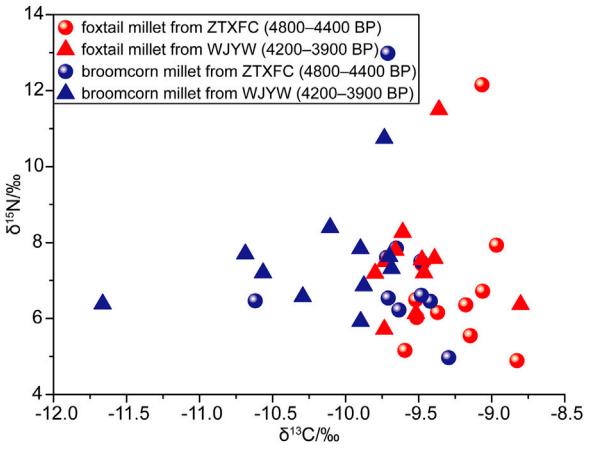

FIGURE 5
Scatter diagram of carbon and nitrogen isotope values for millets from ZTXFC and WJYW sites.

1.38 to 1.96 mm (mean = 1.61 ± 0.13 mm), from 1.32 to 1.89 mm (mean = 1.53 ± 0.13 mm), and from 1.03 to 1.80 mm (mean = 1.32 ± 0.15 mm), respectively. While the length, width, and thickness of the foxtail millets from WJYW site (4,200–3,900 BP) ranged from 0.95 to 1.99 mm (mean = 1.36 ± 0.18 mm), from 0.74 to 1.77 mm (mean = 1.12 ± 0.14 mm), and from 0.50 to 1.55 mm (mean = 0.84 ± 0.18 mm), respectively. The broomcorn millets ranged from 1.20 to 2.20 mm (mean = 1.65 ± 0.20 mm), from 0.97 to 1.84 mm (mean = 1.44 ± 0.19 mm), and from 0.63 to 1.74 mm (mean = 1.24 ± 0.22 mm), respectively. Statistical analysis of the grain size data of foxtail millets and broomcorn millets by SPSS showed that the length and thickness of the foxtail millets were statistically significant. For broomcorn millets width and thickness were statistically significant.

4.4 Carbon and nitrogen isotopes of foxtail and broomcorn millet in the mid-lower Hulu River Valley during ~4,800–3,900 BP

Stable isotopic analysis of the 22 foxtail millet samples and 21 broomcorn millet samples are presented in Table 3 and Figure 5. The broomcorn millet has a wider isotopic range than the foxtail millet in terms of $\delta^{13}C$ values, while the $\delta^{15}N$ values are opposite. During the Lower Changshan culture period (4,800–4,400 BP), the $\delta^{13}C$ and $\Delta^{13}C$ values of foxtail millet samples ranged from −9.6‰ to −8.8‰ (mean = −9.2‰ ± 0.2‰, n = 11) and 2.5‰–3.3‰ (mean = 3.0‰ ± 0.2‰). $\delta^{15}N$ ranged from 4.9‰ to 12.1‰ (mean = 6.8‰ ± 1.9‰, n = 11). The $\delta^{13}C$ and $\Delta^{13}C$ values of broomcorn millet samples ranged from −10.6‰ to −9.3‰ (mean = −9.7‰ ± 0.3‰, n = 10) and 3.0‰–4.4‰ (mean = 3.4‰ ± 0.3‰), respectively. $\delta^{15}N$ ranged from 5.0‰ to 13.0‰ (mean = 7.3‰ ± 2.0‰, n = 10). In the foxtail millet samples from the Qijia Culture period (4,200–3,900 BP), the $\delta^{13}C$, $\Delta^{13}C$, and $\delta^{15}N$ values ranged from −9.8‰ to −8.8‰ (mean = −9.5‰ ± 0.3‰, n = 11), from 2.4‰ to 3.4‰ (mean = 3.1‰ ± 0.3‰), and from 5.7‰ to 11.5‰ (mean = 7.5‰ ± 1.5‰, n = 11), respectively. The $\delta^{13}C$, $\Delta^{13}C$, and $\delta^{15}N$ values of broomcorn millet samples ranged from −11.7‰ to −9.7‰ (mean = −10.2‰ ± 0.6‰, n = 11), from 3.3‰ to 5.3‰ (mean = 3.8‰ ± 0.6‰), and from 5.9‰ to 10.7‰ (mean = 7.5‰ ± 1.2‰, n = 11), respectively.

5 Discussion

5.1 Human planting strategies in the mid-lower Hulu River Valley during ~4,800–3,900 BP

The results of archaeobotanical analysis from the ZTXFC and WJYW sites (Supplementary Table S1; Figure 3) show that foxtail millet was the dominant cultivated crop, and broomcorn millet acted as the auxiliary crop in the MLHRV during both ~4,800–4,400 BP and ~4,200–3,900 BP. Although the charred wheat was found in the sediment of the Xishanping site that dated was to 4,650 BP, the wheat was not directly dated (Li et al., 2007). Wheat remains excavated at the Gaozhuang site in Zhuanglang County were dated to 3,561–3,405 BP (Li, 2018), which is the earliest evidence for wheat appearing in the MLHRV. Though few charred grains of wheat and barley were identified from the WJYW site, the direct radiocarbon date of one charred wheat grain suggests that these West Asian domesticated crop remains were likely derived by disturbance from modern periods (Table 1). This phenomenon was also reported in archaeobotanical studies from other Neolithic sites of North China (Zhang et al., 2018). This indicates that humans may have not yet incorporated wheat and barley into their cropping patterns in the Hulu River Valley during this period. Nevertheless, the radiocarbon date of foxtail millet remains from the same flotation sample that yielded the wheat/barley (Table 1) reveals

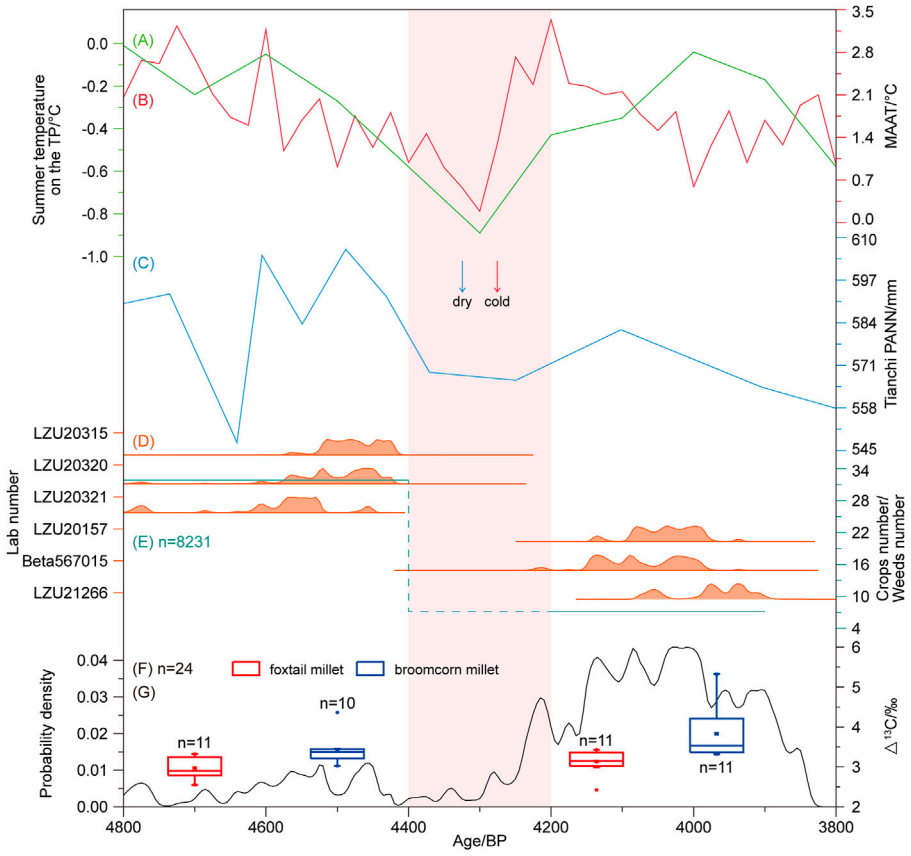

FIGURE 6
Human planting strategies and its relation to climate change during ~4,800–3,900 BP in the mid-lower Hulu River Valley, northwest China, compared with climate records, radiocarbon dates and $\Delta^{13}C$ values of millets. **(A)** Summer temperature reconstruction on the Tibetan Plateau (Zhang et al., 2022). **(B)** Mean annual air temperature (MAAT/°C) record from the Agassiz ice cap (Lecavalier et al., 2019). **(C)** Pollen-based annual precipitation (PANN/mm) reconstructed from Tianchi Lake in the past 6,000 years (Zhao et al., 2010; Chen et al., 2015). **(D)** Radiocarbon dates from the ZTXFC and WJYW sites. **(E)** Crop number/Weed number, n is the sum of crops number and weeds number from two sites. **(F)** Frequency during ~4,800–3,900 BP in the mid-lower Hulu River Valley. **(G)** $\Delta^{13}C$ value of foxtail and broomcorn millets from ZTXFC and WJYW. VPDB, Vienna Pee Dee Belemnite.

these remains of indigenous crop were utilized in Qijia period. In addition, other Qijia sites in the study area mainly grew foxtail and broomcorn millets, and only a very small amount of barleys were excavated from the Gaozhuang site (Li, 2018). Isotopic evidence also suggests that C_4 crops were mainly consumed in the western Loess Plateau during 5,300–4,000 BP (Dong J et al., 2022). The number and mass percent of foxtail millet remains in total plant remains in the ZTXFC and WJYW sites account for 87.95%/77.21% and 82.18%/83.73%, respectively. The same values for broomcorn millet at these two sites were 9.00%/22.79% and 5.53%/16.27%, respectively. This suggests that cropping patterns in the MLHRV were roughly similar during the Lower Changshan and Qijia periods. The significance of foxtail millet in plant subsistence strategy was slightly higher in the Qijia period than in the Lower Changshan period.

The increased weight of foxtail millet relative to broomcorn millet as a cropping strategy in the MLHRV during the Qijia period in comparison to the Banpo-Miaodigou period (~6,100–5,500 BP) and the late Yangshao period (~5,500–4,800 BP) were reported in previous archaeobotanical studies (Li et al., 2022b; Yang Y et al., 2022). Our results from the ZTXFC site are the first reported archaeobotanical data of the Lower Changshan culture. The proportion of weed remains in the plant remains at the ZTXFC site is only 3.05%, while the WJYW site reaches ~12.28%. To reduce sampling error (houses vs. ash pits), we compared the Lower Changshan data with all data derived from various Qijia residential contexts in the Western Loess Plateau. We found that the weed proportion of ash pits derived from other Qijia sites was 9%–16.8% (Yang, 2014; Li, 2018; Li et al., 2022b), which is closer to the Qijia result of this study (12.28%). It suggests that results from different residential contexts (houses vs. ash pits) may not be influenced in this case. These data likely indicate that human input to field management in the MLHRV during the Qijia period was less than in the Lower Changshan period (Figure 6E), though the cropping strategy were dominated by foxtail millet with broomcorn millet as an auxiliary during both periods.

Carbon and nitrogen isotopes of crop remains unearthed from archaeological sites were used to study ancient human management behaviors of cultivated land, for example, irrigation and fertilization (Wang et al., 2018; Li et al., 2022b; Dong Y et al., 2022; Liu et al.,

2022). The $\delta^{13}C$ value of foxtail and broomcorn millet remains from the ZTXFC and WJYW sites (Table 3; Figure 5) show that the $\delta^{13}C$ values of millets from the WJYW site are more negative than in the ZTXFC site. The $\delta^{15}N$ values of millets from the WJYW site overlap with and are slightly higher than in the ZTXFC site. The mean $\delta^{13}C$ and $\delta^{15}N$ values of foxtail millet remains are different from the broomcorn millet remains, which may be related to the physiological differences between the two species (An et al., 2015).

The $\delta^{13}C$ values of plants might have been affected by varying atmospheric $\delta^{13}C$ values during different periods of the Holocene (Cleveland, 1979; Leuenberger et al., 1992; Francey et al., 1999; Indermühle et al., 1999; Ferrio et al., 2005). Therefore, we air-corrected the carbon isotope values for all samples to obtain $\Delta^{13}C$ values (Eq. (2); Farquhar et al., 1982). The $\Delta^{13}C$ values of crops can be affected by the physiological properties of plants themselves and by external environmental factors (O'leary, 1981; O'leary, 1988; Farquhar et al., 1982; 1989; Farquhar and Richards, 1984; Wallace et al., 2013). Physiological properties of plants include photosynthesis pathway, plant species, and different parts of the same plant species (O'Leary, 1981; 1988; Farquhar et al., 1989; Hattersley and Watson, 1992; An et al., 2015). However, since foxtail and broomcorn millet are gramineous C_4 plants, their $\Delta^{13}C$ values from the ZTXFC and WJYW sites were mainly affected by environmental conditions rather than physiological difference.

Previous analysis of carbon isotopes of millet remains from the archaeological sites in the nearby Qin'an and Lixian counties suggest temperature differences are not the main factor affecting the $\delta^{13}C$ values of millets (Ji, 2007). Therefore, water availability for the growth of millet crops in the study area is closely related to water conditions that may be affected by changes in precipitation or human irrigation behavior. Considering the long-run tradition of rain-fed farming for foxtail and broomcorn millet, even in modern North China, it is unlikely that human irrigated these drought-resistant millets during the late Neolithic. Moreover, the mean $\Delta^{13}C$ values of millet remains from the WJYW and ZTXFC sites are lower than the mean $\Delta^{13}C$ values of *S. viridis* samples grown under modern natural precipitation, indicating that artificial irrigation management was not applied during ~4,800–3,900 BP (An et al., 2015; Li, 2018). Modern experiments on the Loess Plateau and elsewhere indicate that the $\Delta^{13}C$ values of C_4 grasses are negatively correlated with rainfall (Wang et al., 2005; Li, 2018; Sanborn et al., 2021; Dong Y et al., 2022). The $\Delta^{13}C$ values of millet remains at the WJYW site higher than those at the ZTXFC site (Figure 6G), suggesting that water availability of millet crops in the WJYW was likely lower than ZTXFC site. The pollen percentage data from the Tianchi Lake sediment indicated that precipitation was lower during ~4,200–3,800 BP than ~4,800–4,400 BP (Figure 6C; Zhao et al., 2010; Chen et al., 2015). Due to the Tianchi Lake is 30 km away from these two sites, the precipitation reconstruction data derived from the Lake is a suitable and reliable record for human actives in the MLHRV. This is a further demonstration of the relatively low water availability in the Qijia period compared with Lower Changshan period, suggesting that the $\Delta^{13}C$ values of millet remains from the ZTXFC and WJYW sites were primarily affected by the decreased precipitation (Figure 6C), instead of other factors, such as fertilization behavior.

The ranges of $\delta^{15}N$ values for foxtail and broomcorn millet remains in the WJYW and ZTXFC sites are quite wide (Figure 5). However, no statistically significant differences of $\delta^{15}N$ values for foxtail and broomcorn millet remains from these two sites are detected by the statistical analysis of variance (ANOVA, foxtail millet: $p = 0.349$; broomcorn millet: $p = 0.808$). This indicates the soil fertility characteristics for millet crop growth in the WJYW and ZTXFC sites were similar. The $\delta^{15}N$ values for all samples were higher than the estimated moderate fertilization level (3.5‰, Li et al., 2022b), and significantly higher than the local vegetation baseline (1.9‰, Barton, 2009) and fertilization level from the Dadiwan site in the Yangshao period (6,500–4,800 BP, Yang et al., 2022). This suggested humans probably added organic fertilizers (animal manure, sewage, food waste, and so on) to the cultivated lands in the MLHRV during ~4,800–4,400 BP and ~4,200–3,900 BP, as were reported at Neolithic sites in Eurasia (Bol et al., 2005; Bogaard et al., 2007; Aguilera et al., 2008; Bogaard et al., 2013; Araus et al., 2014). However, the relationship between the $\delta^{15}N$ values of crop remains and fertilization behaviors in the area still needs to be further examined by detailed and modern simulation experiments.

The measurement of crop remains grain size provides a perspective for studying human cultivating behavior of the major crops (Willcox, 2004; Motuzaite-Matuzeviciute et al., 2012; Bao et al., 2018). According to grain size data analysis from numerous sites in North China, foxtail and broomcorn millet grain sizes generally increased from the Neolithic to historical periods (Bao et al., 2018). The same diachronic change was also detected in the western Loess Plateau (Li, 2018), suggesting humans continuously performed breeding selection on these two indigenous crops in North China. However, we observe the opposite trend for millets grain size variation in the MLHRV from ~4,800–4,400 BP to ~4,200–3,900 BP which was based on the measurements of millets grain sizes at the ZTXFC and WJYW sites (Table 2; Figure 4). The difference of length and thickness of foxtail millet remians are statistically significant. The same notable divergence in broomcorn millet remains is reflected by the width and thickness. Therefore, the change of foxtail and broomcorn millet grain sizes from the Lower Changshan to Qijia culture can be evaluated by those parameters. The results show that grain sizes for both millet crops at the WJYW site were overall smaller than the ZTXFC site (Figure 4), suggesting human might have not engaged in artificial breeding of millet crops during the Qijia period. This is consistent with other investigated Qijia sites in the study region (Supplementary Table S2). Compared with the grain size of millets from the ZTXFC site (Lower Changshan culture), grain size of millets from all contexts of Qijia sites in this region were overall smaller (Supplementary Table S2).

Crop grain sizes may be influenced by multiple factors, such as domestication and hereditary properties (Li et al., 2011; Fuller et al., 2014), maturity (Motuzaite-Matuzeviciute et al., 2012) and the environmental conditions of crop growth (Araus et al., 1999; Willcox, 2004). Immaturity may be an important influencing factor for the smaller grain size of millets (Motuzaite-Matuzeviciute et al., 2012), which was mainly examined by the morphology of millets grains. According to the evaluative criteria proposed by Song et al. (2012), all measured millet remains from the WJYW and ZTXFC sites were mature millets, as the length-width ratio of foxtail and broomcorn millet remains are basically same at these two sites (Table 2). The primary factor affecting grain size of millet remains at the ZTXFC and WJYW sites may be the

environmental conditions of millets growth, such as water stress and soil fertility (Araus et al., 1999; Willcox, 2004). As was mentioned above, the soil fertility for millets growth at the ZTXFC and WJYW sites were basically similar, while water availability for millets growth was lower at WJYW than ZTXFC. This further demonstrated that the decreased precipitation in the MLHRV was responsible for the reduction in the grain sizes of millet crops during the Qijia period in comparison to the Lower Changshan period.

5.2 How millet farming groups responded to climate change in the mid-lower Hulu River Valley during ~4,800–3,900 BP

Climate changes, especially rapid and extreme climate events, are proposed as an important factor for cultural evolution and the transformation of subsistence strategies in different corners of Eurasia during the Neolithic periods (Staubwasser et al., 2003; Wu and Liu, 2004; Weiss, 2017; Park et al., 2019; Ran and Chen, 2019; Zhang H et al., 2021), including northwest China (Dong et al., 2012; Zhou et al., 2016; Cao and Dong, 2020; Ren et al., 2021). While social resilience to climate change gradually increased with innovations and the dispersal of agricultural techniques across Eurasia, Neolithic groups could adopt different strategies to cope with climate change (Yang et al., 2019; Yang et al., 2020; Dong et al., 2021; Tao et al., 2022). In the Apulia region of southern Italy, humans altered cropping patterns as an adaptation response to the rapid dry-humid fluctuations during ~8,500–5,700 BP (Fiorentino et al., 2013). At the Jinchankou site in Qinghai, human increased field management during ~4,100–3,700 BP to cope with climate (Ren et al., 2021). In North China, the areas utilized for millet cultivation extensively expanded, facilitating the growth in population during and after the 4.2 ka climate event (He et al., 2022).

In the MLHRV, a climate event around 5,500 BP triggered the transition of the primary cultivated crop from broomcorn millet to the relatively high-yielding foxtail millet (Yang Y et al., 2022). This might have contributed to the development of millet-pig intensive agriculture in the area (Yang J et al., 2022). Recent studies of lake sediments in the Liupan Mountains, the closest high-resolution paleoclimate archives to the MLHRV, and temperature reconstruction from the Tibetan Plateau and Agassiz ice cap, reveal a rapid decline in temperature and precipitation at ~4,400 BP (Figures 6A–C; Zhao et al., 2010; Chen et al., 2015; Lecavalier et al., 2019; Zhang et al., 2022). This generally corresponds with paleoclimate records in surrounding areas (Tan et al., 2020; Zhang C et al., 2021). The lowest temperature and precipitation of 4,800–3,800 BP in the MLHRV occurred between ~4,400 and 4,200 BP, corresponding to the gap between the Lower Changshan and Qijia periods in the area (Figure 6). This suggests that the cold-dry climate during these two centuries probably led to the collapse of the Lower Changshan society in the MLHRV. This heavily relied on the production of frost-sensitive millet crops which was susceptible to climate change, especially substantial drops of temperature.

Climate turned warmer and wetter to some extent in the MLHRV around 4,200 BP, and Qijia groups settled widely in the area during the subsequent centuries (Figure 1). The number of Qijia sites in the MLHRV reached 381, which was much more than the Lower Changshan sites (8), while climate was colder and dryer during 4,200–3,800 BP than 4,800–4,400 BP. Our results of archaeobotanical analysis, grain size measurement, and stable isotope analysis at the ZTXFC and WJYW sites reveal that the cropping patterns remained consistent, while the level of farmland management was regressive from the Lower Changshan to Qijia periods. There is no evidence to suggest that humans strengthened the behavior of irrigation, fertilization or breeding during the Qijia period in comparison to the Lower Changshan period. Furthermore, the decline of precipitation during the Qijia period compared with Lower Changshan period resulted in the increase of water stress for millet growth and then the reduction of millet grains. However, both the intensity and space of human settlements in the MLHRV during the Qijia period were significantly larger than the Lower Changshan period (Figures 1, 6F). After excluding the extreme values, the ranges of $\delta^{15}N$ values for foxtail millet and broomcorn millet remains during the Qijia period are significantly wider (ANOVA, foxtail millet: $p = 0.003$, broomcorn millet: $p = 0.002$) than the Lower Changshan period in the Western Loess Plateau (Supplementary Table S3; Yang, 2021; Li et al., 2022b). This indicated that Qijia populations cultivated millet in farmlands with different fertility conditions and expanded their farmlands. This suggests that Qijia groups may have adopted a strategy of expanding farmlands to promote social development, although climate was relatively cold and dry compared with Lower Changshan and Yangshao periods. This strategy of agricultural extensification was also witnessed in contemporaneous Yellow River Valleys (He et al., 2022). Additionally, massive emigration of millet farming groups occurred in some areas of North China, such as eastern Inner Mongolia, probably due to the spatial differences in social resilience and the amplitude of climate change influencing the growth of millet crops. Qijia population may have adopted new crops, domesticated animals, and metallurgy to cope with climate change in the later period. For instance, humans incorporated wheat and barley farming, animal herding, metallurgy, and luxury (e.g., jade) into their economic system in the Hexi Corridor (Chen, 2017; Yang et al., 2019; Cao, 2022; Ren et al., 2022) and western Loess Plateau during the Qijia period (Li, 2018; Ren et al., 2021; Cao, 2022; Wang L et al., 2022; Zhang, 2022). The diversified economic strategy enhanced Qijia social resilience to cope with climate change.

6 Conclusion

Through archaeobotanical analysis, radiocarbon dating, grain size measurement, and stable isotope studies at the ZTXFC and WJYW sites, we reveal the characteristics of planting strategies in the MLHRV during the Lower Changshan and Qijia periods. The proportions of foxtail millet and broomcorn millet in plant remains account for 87.95%/9.00% and 82.18%/5.53%, while those of weeds are 3.05% and 12.28% in the ZTXFC and WJYW sites, respectively. This suggests that rain-fed agriculture served as the dominant plant utilization strategy, while human input to field management declined from ~4,800–4,400 BP to ~4,200–3,900 BP in the MLHRV. Measurements and stable isotope analysis results of carbonized millet grains demonstrates that the grain size of millets and water availability during the Qijia period was lower than in the Lower Changshan period, which was likely affected by the decline of

temperature and precipitation. This pattern of planting strategies is supported from previous archaeobotanical studies in the MLHRV. These indicate that millet farming groups in the area might have neither altered cropping patterns nor improved their farmland management. Instead, they enlarged their cultivated lands to support the rapid growth of local populations during the Qijia period, when climate was relatively cold and dry in comparison to the Lower Changshan period. Our work provides a valuable case study to understand the pattern of human-environment interaction at a local scale in millet farming areas during the late Neolithic.

Data availability statement

The original contributions presented in the study are included in the article/Supplementary Material, further inquiries can be directed to the corresponding authors.

Author contributions

The study was designed by WW and MM. GC, JD, and ZW conducted field works and sample collection. WW and HL completed experiments and data correction. WW and MM analyzed data and designed the figures. WW, MM, GC, JD, ZW, HL, and XL wrote the manuscript. All authors discussed the results and commented on the manuscript.

Funding

This work was supported by the Second Tibetan Plateau Scientifific Expedition and Research Program (STEP) (Grant No. 2019QZKK0601), the National Key R&D Program of China (Grant No. 2018YFA0606402), the Fundamental Research Funds for the Central Universities (Grant No. lzujbky-2021-77), Natural Science Foundation of Jiangsu Province, China (Grant No. BK20221027), the Open Foundation of MOE Key Laboratory of Western China's Environmental System, Lanzhou University and the Fundamental Research Funds for the Central Universities (Grant No. lzujbky-2021-kb01), the National Natural Science Foundation of China (Grant Nos. 41871076).

Conflict of interest

The authors declare that the research was conducted in the absence of any commercial or financial relationships that could be construed as a potential conflict of interest.

Publisher's note

All claims expressed in this article are solely those of the authors and do not necessarily represent those of their affiliated organizations, or those of the publisher, the editors and the reviewers. Any product that may be evaluated in this article, or claim that may be made by its manufacturer, is not guaranteed or endorsed by the publisher.

Supplementary material

The Supplementary Material for this article can be found online at: https://www.frontiersin.org/articles/10.3389/feart.2023.1137528/full#supplementary-material

References

Aguilera, M., Araus, J. L., Voltas, J., Rodríguez-Ariza, M. O., Molina, F., Rovira, N., et al. (2008). Stable carbon and nitrogen isotopes and quality traits of fossil cereal grains provide clues on sustainability at the beginnings of Mediterranean agriculture. *Rapid Commun. Mass Spectrom.* 22, 1653–1663. doi:10.1002/rcm.3501

An, C., Dong, W., Li, H., Zhang, P., Zhao, Y., Zhao, X., et al. (2015). Variability of the stable carbon isotope ratio in modern and archaeological millets: Evidence from northern China. *J. Archaeol. Sci.* 53, 316–322. doi:10.1016/j.jas.2014.11.001

An, J., Kirleis, W., and Jin, G. (2021). Understanding the collapse of the longshan culture (4400–3800 BP) and the 4.2 ka event in the haidai region of China – from an agricultural perspective. *Environ. Archaeol.*, 1–15. doi:10.1080/14614103.2021.2003583

Araus, J. L., Febrero, A., Catala, M., Molist, M., Voltas, J., and Romagosa, I. (1999). Crop water availability in early agriculture: Evidence from carbon isotope discrimination of seeds from a tenth millennium BP site on the euphrates. *Glob. Change Biol.* 5, 201–212. doi:10.1046/j.1365-2486.1999.00213.x

Araus, J. L., Ferrio, J. P., Voltas, J., Aguilera, M., and Buxó, R. (2014). Agronomic conditions and crop evolution in ancient Near East agriculture. *Nat. Commun.* 5, 3953. doi:10.1038/ncomms4953

Bao, Y., Zhou, X., Liu, H., Hu, S., Zhao, K., Atahan, P., et al. (2018). Evolution of prehistoric dryland agriculture in the arid and semi-arid transition zone in northern China. *PLoS One* 13, e0198750. doi:10.1371/journal.pone.0198750

Barton, L. W. (2009). *Early food production in China's western Loess Plateau*. [Davis (USA)]: University of California.

Bogaard, A., Fraser, R., Heaton, T. H. E., Wallace, M., Vaiglova, P., Charles, M., et al. (2013). Crop manuring and intensive land management by Europe's first farmers. *Proc. Natl. Acad. Sci. U. S. A.* 110, 12589–12594. doi:10.1073/pnas.1305918110

Bogaard, A., Heaton, T. H. E., Poulton, P., and Merbach, I. (2007). The impact of manuring on nitrogen isotope ratios in cereals: Archaeological implications for reconstruction of diet and crop management practices. *J. Archaeol. Sci.* 34, 335–343. doi:10.1016/j.jas.2006.04.009

Bol, R., Eriksen, J., Smith, P., Garnett, M. H., Coleman, K., and Christensen, B. T. (2005). The natural abundance of 13C, 15N, 34S and 14C in archived (1923–2000) plant and soil samples from the Askov long-term experiments on animal manure and mineral fertilizer. *Rapid Commun. Mass Spectrom.* 19, 3216–3226. doi:10.1002/rcm.2156

Cao, F. (2022). Characteristics and processes of jade-using during the prehistoric period in the Gan-Qing area (in Chinese with English Abstract). *Sichuan Cult. Relics* 221, 43–59.

Cao, H., and Dong, G. (2020). Social development and living environment changes in the Northeast Tibetan Plateau and contiguous regions during the late prehistoric period. *Reg. Sustain.* 1, 59–67. doi:10.1016/j.regsus.2020.09.001

Chen, F., Xu, Q., Chen, J., Birks, H. J. B., Liu, J., Zhang, S., et al. (2015). East Asian summer monsoon precipitation variability since the last deglaciation. *Sci. Rep.* 5, 11186. doi:10.1038/srep11186

Chen, G. (2017). Metallurgical community of xichengyi-qijia culture: Early metal-making specialists in the hexi corridor and related issues (in Chinese with English abstract). *Archaeol. Cult. Relics* 05, 37–44.

Chen, H. (2003). Analysis on the posture of the human bones seen in the pre-historic graves in Gansu and Qinghai (in Chinese with English abstract). *J. Anc. Civilizations* 2, 138–153.

Chen, T., Qiu, M., Liu, R., Li, H., Hou, H., Howarth, P., et al. (2020). Human responses to climate change in the late prehistoric Western Loess Plateau, northwest China. *Radiocarbon* 62, 1193–1207. doi:10.1017/RDC.2020.32

Cleveland, W. S. (1979). Robust locally weighted regression and smoothing scatterplots. *J. Am. Stat. Assoc.* 74, 829–836. doi:10.1080/01621459.1979.10481038

Cullen, H. M., deMenocal, P. B., Hemming, S., Hemming, G., Brown, F. H., Guilderson, T., et al. (2000). Climate change and the collapse of the Akkadian empire: Evidence from the deep sea. *Geology* 28, 379–382. doi:10.1130/0091-7613(2000)028<0379:ccatco>2.3.co;2

Dodson, J. R., Li, X., Zhou, X., Zhao, K., Sun, N., and Atahan, P. (2013). Origin and spread of wheat in China. *Quat. Sci. Rev.* 72, 108–111. doi:10.1016/j.quascirev.2013.04.021

Dong, G., Du, L., and Wei, W. (2021). The impact of early trans-Eurasian exchange on animal utilization in northern China during 5000–2500 BP. *Holocene* 31, 294–301. doi:10.1177/0959683620941169

Dong, G., Du, L., Yang, L., Lu, M., Qiu, M., Li, H., et al. (2022a). Dispersal of crop-livestock and geographical-temporal variation of subsistence along the Steppe and Silk Roads across Eurasia in prehistory. *Sci. China Earth Sci.* 65, 1187–1210. doi:10.1007/s11430-021-9929-x

Dong, G., Jia, X., An, C., Chen, F., Zhao, Y., Tao, S., et al. (2012). Mid-Holocene climate change and its effect on prehistoric cultural evolution in eastern Qinghai Province, China. *Quat. Res.* 77, 23–30. doi:10.1016/j.yqres.2011.10.004

Dong, G., Lu, Y., Zhang, S., Huang, X., and Ma, M. (2022b). Spatiotemporal variation in human settlements and their interaction with living environments in Neolithic and Bronze Age China. *Prog. Phys. Geogr.* 46, 949–967. doi:10.1177/03091333221087992

Dong, J., Wang, S., Chen, G., Wei, W., Du, L., Xu, Y., et al. (2022). Stable isotopic evidence for human and animal diets from the late neolithic to the ming dynasty in the middle-lower reaches of the Hulu River Valley, NW China. *Front. Ecol. Evol.* 10, 905371. doi:10.3389/fevo.2022.905371

Dong Y, Y., Bi, X., Wu, R., Belfield, E. J., Harberd, N. P., Christensen, B. T., et al. (2022). The potential of stable carbon and nitrogen isotope analysis of foxtail and broomcorn millets for investigating ancient farming systems. *Front. Plant Sci.* 13, 1. doi:10.3389/fpls.2022.1018312

Farquhar, G. D., Ehleringer, J. R., and Hubick, K. T. (1989). Carbon isotope discrimination and photosynthesis. *Annu. Rev. Plant Physiol. Plant Mol. Biol.* 40, 503–537. doi:10.1146/annurev.pp.40.060189.002443

Farquhar, G. D., and Richards, R. A. (1984). Isotopic composition of plant carbon correlates with water-use efficiency of wheat genotypes. *Funct. Plant Biol.* 11, 539–552. doi:10.1071/pp9840539

Farquhar, G., O'Leary, M., and Berry, J. (1982). On the relationship between carbon isotope discrimination and the intercellular carbon dioxide concentration in leaves. *Funct. Plant Biol.* 9, 121. doi:10.1071/pp9820121

Ferrio, J. P., Araus, J. L., Buxó, R., Voltas, J., and Bort, J. (2005). Water management practices and climate in ancient agriculture: Inferences from the stable isotope composition of archaeobotanical remains. *Veg. Hist. Archaeobot.* 14, 510–517. doi:10.1007/s00334-005-0062-2

Fiorentino, G., Caldara, M., De Santis, V., D'Oronzo, C., Muntoni, I. M., Simone, O., et al. (2013). Climate changes and human–environment interactions in the Apulia region of southeastern Italy during the Neolithic period. *Holocene* 23, 1297–1316. doi:10.1177/0959683613486942

Flohr, P., Fleitmann, D., Matthews, R., Matthews, W., and Black, S. (2016). Evidence of resilience to past climate change in Southwest Asia: Early farming communities and the 9.2 and 8.2 ka events. *Quat. Sci. Rev.* 136, 23–39. doi:10.1016/j.quascirev.2015.06.022

Francey, R. J., Allison, C. E., Etheridge, D. M., Trudinger, C. M., Enting, I. G., Leuenberger, M., et al. (1999). A 1000-year high precision record of delta13C in atmospheric CO2. *Tellus B* 51, 170–193. doi:10.1034/j.1600-0889.1999.t01-1-00005.x

Fuller, D. Q., Denham, T., Arroyo-Kalin, M., Lucas, L., Stevens, C. J., Qin, L., et al. (2014). Convergent evolution and parallelism in plant domestication revealed by an expanding archaeological record. *Proc. Natl. Acad. Sci. U. S. A.* 111, 6147–6152. doi:10.1073/pnas.1308937110

Goldsmith, Y., Broecker, W. S., Xu, H., Polissar, P. J., deMenocal, P. B., Porat, N., et al. (2017). Northward extent of East Asian monsoon covaries with intensity on orbital and millennial timescales. *Proc. Natl. Acad. Sci. U. S. A.* 114, 1817–1821. doi:10.1073/pnas.1616708114

Han, H., Hou, J., Huang, M., Li, Z., Xu, K., Zhang, D., et al. (2020). Impact of soil and water conservation measures and precipitation on streamflow in the middle and lower reaches of the Hulu River Basin, China. *Catena* 195, 104792. doi:10.1016/j.catena.2020.104792

Hattersley, P. W., and Watson, L. (1992). "Diversification of photosynthesis," in *Grass evolution and domestication*. Editor G. P. Chapman (Cambridge: Cambridge University Press), 38–116.

He, K., Lu, H., Jin, G., Wang, C., Zhang, H., Zhang, J., et al. (2022). Antipodal pattern of millet and rice demography in response to 4.2 ka climate event in China. *Quat. Sci. Rev.* 295, 107786. doi:10.1016/j.quascirev.2022.107786

Hu, Q. (1991). Answer to "A brief analysis of the lower changshan remains in zhenyuan Longdong" (in Chinese). *Archaeology* 03, 238–244.

Hu, Q. (1981). Brief report on excavation of changshan site in zhenyuan county, Longdong (in Chinese). *Archaeology* 03, 201–210.

Indermühle, A., Stocker, T. F., Joos, F., Fischer, H., Smith, H. J., Wahlen, M., et al. (1999). Holocene carbon-cycle dynamics based on CO2 trapped in ice at Taylor Dome, Antarctica. *Nature* 398, 121–126. doi:10.1038/18158

Ji, D. (2007). *Environmental archaeological perspective: Dispersal of anatomically modern human and origin of agriculture in northern China-A case study in Gansu and Ningxia*. [Lanzhou (China)]: Lanzhou University.

Jia, X., Dong, G., Li, H., Brunson, K., Chen, F., Ma, M., et al. (2013). The development of agriculture and its impact on cultural expansion during the late Neolithic in the Western Loess Plateau, China. *Holocene* 23, 85–92. doi:10.1177/0959683612450203

Kelly, R. L., Surovell, T. A., Shuman, B. N., and Smith, G. M. (2012). A continuous climatic impact on Holocene human population in the Rocky Mountains. *Proc. Natl. Acad. Sci. U. S. A.* 110, 443–447. doi:10.1073/pnas.1201341110

Lecavalier, B., Fisher, D. A., Milne, G. A., Vinther, B. M., Tarasov, L., Huybrechts, P., et al. (2019). Data from: Oxygen isotope ratio and reconstructed temperature record from the Agassiz ice cap, Greenland. *PANGAEA. (2019).* doi:10.1594/PANGAEA.904113

Leuenberger, M., Siegenthaler, U., and Langway, C. (1992). Carbon isotope composition of atmospheric CO^2 during the last ice age from an Antarctic ice core. *Nature* 357, 488–490. doi:10.1038/357488a0

Li, F., Li, S., and Shui, T. (1993). Ancient culture and ancient environment of Hulu River basin (in Chinese). *Archaeology* 9, 822–842.

Li, H. (2018). *Ancient strategies of crop use on the western Chinese Loess Plateau from Neolithic to historical periods*. [Lanzhou (China)]: Lanzhou University.

Li, H., Cui, Y., James, N., Ritchey, M., Liu, F., Zhang, J., et al. (2022a). Spatiotemporal variation of agricultural patterns in different geomorphologic and climatic environments in the eastern Loess Plateau, north-central China during the late Neolithic and Bronze Ages. *Sci. China Earth Sci.* 65, 934–948. doi:10.1007/s11430-021-9879-x

Li, H., Sun, Y., Yang, Y., Cui, Y., Ren, L., Li, H., et al. (2022b). Water and soil management strategies and the introduction of wheat and barley to northern China: An isotopic analysis of cultivation on the Loess Plateau. *Antiquity* 96, 1478–1494. doi:10.15184/aqy.2022.138

Li, R., Lv, F., Yang, L., Liu, F., Liu, R., and Dong, G. (2020). Spatial–Temporal variation of cropping patterns in relation to climate change in neolithic China. *Atmosphere* 11, 677. doi:10.3390/atmos11070677

Li, X. Q., Zhou, X. Y., Zhou, J., Dodson, J., Zhang, H. B., and Shang, X. (2007). The earliest agricultural diversification of China recorded by biological indicators at Xishanping site, Gansu (in Chinese). *Sci. China Earth Sci.* 37, 934–940.

Li, Y., Fan, C., Xing, Y., Jiang, Y., Luo, L., Sun, L., et al. (2011). Natural variation in GS5 plays an important role in regulating grain size and yield in rice. *Nat. Genet.* 43, 1266–1269. doi:10.1038/ng.977

Liu, B., Lu, Y., Yang, Y., Wei, W., and Chen, G. (2022). Evaluating water fertilizer coupling on the variations in millet chaff size during the late seventh century in northwest China: Morphological and carbon and nitrogen isotopic evidence from the chashancun cemetery. *Sustainability* 14, 3581. doi:10.3390/su14063581

Liu, F., and Feng, Z. (2012). A dramatic climatic transition at ~4000 cal. yr BP and its cultural responses in Chinese cultural domains. *Holocene* 22, 1181–1197. doi:10.1177/0959683612441839

Liu, L., Chen, X., Wright, H., Xu, H., Li, Y., Chen, G., et al. (2019). Rise and fall of complex societies in the Yiluo region, North China: The spatial and temporal changes. *Quat. Int.* 521, 4–15. doi:10.1016/j.quaint.2019.05.025

Liu, X., Jones, P. J., Motuzaite Matuzeviciute, G., Hunt, H. V., Lister, D. L., An, T., et al. (2019). From ecological opportunism to multi-cropping: Mapping food globalisation in prehistory. *Quat. Sci. Rev.* 206, 21–28. doi:10.1016/j.quascirev.2018.12.017

Manning, S. W., Lorentzen, B., Welton, L., Batiuk, S., and Harrison, T. P. (2020). Beyond megadrought and collapse in the Northern Levant: The chronology of Tell Tayinat and two historical inflection episodes, around 4.2ka BP, and following 3.2ka BP. *PLoS One* 15, e0240799. doi:10.1371/journal.pone.0240799

Masi, A., Sadori, L., Balossi Restelli, F., Baneschi, I., and Zanchetta, G. (2014). Stable carbon isotope analysis as a crop management indicator at arslantepe (malatya, Turkey) during the late chalcolithic and early bronze age. *Veg. Hist. Archaeobot.* 23, 751–760. doi:10.1007/s00334-013-0421-3

Motuzaite-Matuzeviciute, G., Hunt, H. V., and Jones, M. K. (2012). Experimental approaches to understanding variation in grain size in Panicum miliaceum (broomcorn millet) and its relevance for interpreting archaeobotanical assemblages. *Veg. Hist. Archaeobot.* 21, 69–77. doi:10.1007/s00334-011-0322-2

O'Leary, M. H. (1981). Carbon isotope fractionation in plants. *Phytochemistry* 20, 553–567. doi:10.1016/0031-9422(81)85134-5

O'Leary, M. H. (1988). Carbon isotopes in photosynthesis. *BioScience* 38, 328–336. doi:10.2307/1310735

Park, J., Park, J., Yi, S., Cheul Kim, J., Lee, E., and Choi, J. (2019). Abrupt Holocene climate shifts in coastal East Asia, including the 8.2 ka, 4.2 ka, and 2.8 ka BP events, and societal responses on the Korean peninsula. *Sci. Rep.* 9, 10806. doi:10.1038/s41598-019-47264-8

Pokharia, A. K., Agnihotri, R., Sharma, S., Bajpai, S., Nath, J., Kumaran, R. N., et al. (2017). Altered cropping pattern and cultural continuation with declined prosperity following abrupt and extreme arid event at ~4,200 yrs BP: Evidence from an Indus archaeological site Khirsara, Gujarat, Western India. *PLoS One* 12, e0185684. doi:10.1371/journal.pone.0185684

Qian, Y., Wang, Y., Mao, R., and Xie, Y. (2014). Excavation report of Qijia culture tomb in mogou cemetery excavation brief of Qijia culture tombs in mogou cemetery, lintan, Gansu province in 2009 (in Chinese). *Wenwu Cult. Relics* 697, 4–23.

Ramsey, B. C. (2021). OxCal. version. Available at: https://c14.arch.ox.ac.uk/oxcal.html (Accessed, 2021).

Ran, M., and Chen, L. (2019). The 4.2 ka BP climatic event and its cultural responses. *Quat. Int.* 521, 158–167. doi:10.1016/j.quaint.2019.05.030

Reimer, P. J., Austin, W. E. N., Bard, E., Bayliss, A., Blackwell, P. G., Bronk Ramsey, C., et al. (2020). The IntCal20 northern hemisphere radiocarbon age calibration curve (0–55 cal kBP). *Radiocarbon* 62, 725–757. doi:10.1017/rdc.2020.41

Ren, L., Yang, Y., Qiu, M., Brunson, K., Chen, G., and Dong, G. (2022). Direct dating of the earliest domesticated cattle and caprines in northwestern China reveals the history of pastoralism in the Gansu-Qinghai region. *J. Archaeol. Sci.* 144, 105627. doi:10.1016/j.jas.2022.105627

Ren, L., Yang, Y., Wang, Q., Zhang, S., Chen, T., Cui, Y., et al. (2021). The transformation of cropping patterns from late neolithic to early iron age (5900–2100 BP) in the gansu–qinghai region of northwest China. *Holocene* 31, 183–193. doi:10.1177/0959683620941137

Sanborn, L. H., Reid, R. E., Bradley, A. S., and Liu, X. (2021). The effect of water availability on the carbon and nitrogen isotope composition of a C4 plant (pearl millet, Pennisetum glaucum). *J. Archaeol. Sci. Rep.* 38, 103047. doi:10.1016/j.jasrep.2021.103047

Sheng, P., Shang, X., Sun, Z., Yang, L., Guo, X., and Jones, M. K. (2018). North-south patterning of millet agriculture on the Loess Plateau: Late Neolithic adaptations to water stress, NW China. *Holocene* 28, 1554–1563. doi:10.1177/0959683618782610

Song, J., Zhao, Z., and Fuller, D. Q. (2012). The archaeobotanical significance of immature millet grains: An experimental case study of Chinese millet crop processing. *Veg. Hist. Archaeobot.* 22, 141–152. doi:10.1007/s00334-012-0366-y

Staubwasser, M., Sirocko, F., Grootes, P. M., and Segl, M. (2003). Climate change at the 4.2 ka BP termination of the Indus valley civilization and Holocene south Asian monsoon variability. *Geophys. Res. Lett.* 30, 1. doi:10.1029/2002gl016822

Styring, A. K., Charles, M., Fantone, F., Hald, M. M., McMahon, A., Meadow, R. H., et al. (2017). Isotope evidence for agricultural extensification reveals how the world's first cities were fed. *Nat. Plants* 3, 17076–17111. doi:10.1038/nplants.2017.76

Tan, L., Li, Y., Wang, X., Cai, Y., Lin, F., Cheng, H., et al. (2020). Holocene monsoon change and abrupt events on the western Chinese Loess Plateau as revealed by accurately dated stalagmites. *Geophys. Res. Lett.* 47. doi:10.1029/2020gl090273

Tao, D., Zhang, R., Xu, J., Wu, Q., Wei, Q., Gu, W., et al. (2022). Agricultural extensification or intensification: Nitrogen isotopic investigation into late Yangshao agricultural strategies in the middle Yellow River area. *J. Archaeol. Sci. Rep.* 44, 103534. doi:10.1016/j.jasrep.2022.103534

The Institute of Archaeoloogy Chinese Academy of Social Sciences (1999). *Shizhaocun and xishanping* (in Chinese). Beijing: Encyclopedia of China Publishing House.

Underhill, A. (2013). *A companion to Chinese archaeology*. New Jersey: Wiley-Blackwell.

Wallace, M., Jones, G., Charles, M., Fraser, R., Halstead, P., Heaton, T. H. E., et al. (2013). Stable carbon isotope analysis as a direct means of inferring crop water status and water management practices. *World Archaeol.* 45, 388–409. doi:10.1080/00438243.2013.821671

Wang, F., He, J., Han, F., Zhao, Q., and Zhang, H. (2022). Quantitative allocation of soil and water conservation measures in Xihulu River basin of Liupan Mountain in loess hilly and gully region (in Chinese). *Gansu Agric.* 4, 58–63. doi:10.15979/j.cnki.cn62-1104/f.2022.04.019

Wang, G., Han, J., Zhou, L., Xiong, X., Tan, M., Wu, Z., et al. (2005). Study on the stable carbon isotopic composition of C4 plants in loess region of northern China (in Chinese). *Sci. China Earth Sci.* 12, 1174–1179.

Wang, H. (2012). Sequence and pattern of archaeology culture in Neolithic-Bronze Age in Gansu-Qinghai province (in Chinese). *Collect. Stud. Archaeol.* 9, 210–243.

Wang, L., Mei, J., Chen, K., Mao, R., Qian, Y., Wang, H., et al. (2022). Budget-constraint admissible output consensus tracking for intermittent-interaction singular multiagent networks. *Archaeology* 658, 71–80. doi:10.1016/j.isatra.2021.10.021

Wang, X., Fuller, B. T., Zhang, P., Hu, S., Hu, Y., and Shang, X. (2018). Millet manuring as a driving force for the Late Neolithic agricultural expansion of north China. *Sci. Rep.* 8, 5552. doi:10.1038/s41598-018-23315-4

Wei, J. (2021). *Research on the tombs of changshan lower culture*. [Lanzhou (China)]: Northwest Normal University.

Weiss, H. (2016). Global megadrought, societal collapse and resilience at 4.2-3.9 ka BP across the Mediterranean and west Asia. *Past. Glob. Change Mag.* 24, 62–63. doi:10.22498/pages.24.2.62

Weiss, H. (2017). *Megadrought and collapse: From early agriculture to Angkor*. Oxford: University Press.

Willcox, G. (2004). Measuring grain size and identifying near eastern cereal domestication: Evidence from the euphrates valley. *J. Archaeol. Sci.* 31, 145–150. doi:10.1016/j.jas.2003.07.003

Womack, A., Flad, R., Zhou, J., Brunson, K., Toro, F. H., Su, X., et al. (2021). The majiayao to Qijia transition: Exploring the intersection of technological and social continuity and change. *Asian Archaeol.* 4, 95–120. doi:10.1007/s41826-021-00041-x

Womack, A., Jaffe, Y., Zhou, J., Hung, L., Wang, H., Li, S., et al. (2017). Mapping qijiaping: New work on the type-site of the Qijia culture (2300–1500 B.C.) in Gansu province, China. *J. Field Archaeol.* 42, 488–502. doi:10.1080/00934690.2017.1384669

Wu, W., and Liu, T. (2004). Possible role of the "Holocene event 3" on the collapse of neolithic cultures around the central plain of China. *Quat. Int.* 117, 153–166. doi:10.1016/s1040-6182(03)00125-3

Wu, W., Zheng, H., Hou, M., and Ge, Q. (2018). The 5.5 cal ka BP climate event, population growth, circumscription and the emergence of the earliest complex societies in China. *Sci. China Earth Sci.* 61, 134–148. doi:10.1007/s11430-017-9157-1

Xiao, J., Zhang, S., Fan, J., Wen, R., Xu, Q., Inouchi, Y., et al. (2019). The 4.2 ka event and its resulting cultural interruption in the Daihai Lake basin at the East Asian summer monsoon margin. *Quat. Int.* 527, 87–93. doi:10.1016/j.quaint.2018.06.025

Xie, D. (1986). A brief discussion on the tombs of Qijia culture (in Chinese). *Archaeology* 2, 147–161.

Xie, D. (1975). Qijia cultural cemetery of qinweijia in yongjing county, Gansu (in Chinese). *Acta Archaeol. Sin.* 2, 57–96.

Xin, H., Dai, C., Cao, W., and Yang, B., and Yellow River water conservancy commission tianshui hydrological and water resources survey bureau. (2016). analysis of hydrological characteristics in Hulu River basin (in Chinese). *Water Resour. Hydropower Northeast* 34, 32. doi:10.14124/j.cnki.dbslsd22-1097.2016.05.014

Yang, H. (2017). *Study on the tombs of Qijia culture in Hexi area*. [Lanzhou (China)]: Northwest Minzu University.

Yang, J. (2012). *The studies of prehistoric culture in Longdong area*. [Zhengzhou (China)]: Zhengzhou University.

Yang, J., Zhang, D., Yang, X., Wang, W., Perry, L., Fuller, D. Q., et al. (2022). Sustainable intensification of millet–pig agriculture in Neolithic North China. *Nat. Sustain.* 5, 780–786. doi:10.1038/s41893-022-00905-9

Yang, L., Shi, Z., Zhang, S., and Lee, H. F. (2020). Climate change, geopolitics, and human settlements in the hexi corridor over the last 5,000 years. *ACTA Geol. SIN-ENGL* 94, 612–623. doi:10.1111/1755-6724.14529

Yang, L. (2021). *Strategies of crop use on the southern Chinese Loess Plateau from late neolithic to bronze age*. [Lanzhou (China)]: Lanzhou University.

Yang, Q., Li, X., Liu, W., Zhou, X., Zhao, K., and Sun, N. (2011). Carbon isotope fractionation during low temperature carbonization of foxtail and common millets. *Org. Geochem.* 42, 713–719. doi:10.1016/j.orggeochem.2011.06.012

Yang, Y., Ren, L., Dong, G., Cui, Y., Liu, R., Chen, G., et al. (2019). Economic change in the prehistoric Hexi corridor (4800–2200 bp), north-west China. *Archaeometry* 61, 957–976. doi:10.1111/arcm.12464

Yang, Y. (2014). *The analysis of charred plant seeds at Jinchankou site and lijiaping site during Qijia Culture Period in the hehuang region*. Lanzhou, China: Lanzhou University.

Yang, Y., Wang, J., Li, G., Dong, J., Cao, H., Ma, M., et al. (2022). Shift in subsistence crop dominance from broomcorn millet to foxtail millet around 5500 BP in the Western Loess Plateau. *Front. Plant Sci.* 13, 939340. doi:10.3389/fpls.2022.939340

Ye, S. (2014). A comprehensive study of pottery in Qijia culture (in Chinese). *Young Society* (01), 342.

Zhang, C., Zhao, C., Yu, S.-Y., Yang, X., Cheng, J., Zhang, X., et al. (2022). Seasonal imprint of Holocene temperature reconstruction on the Tibetan Plateau. *Earth-Sci. Rev.* 226, 103927. doi:10.1016/j.earscirev.2022.103927

Zhang, C., Zhao, C., Zhou, A., Zhang, H., Liu, W., Feng, X., et al. (2021). Quantification of temperature and precipitation changes in northern China during the "5000-year" Chinese History. *Quat. Sci. Rev.* 255, 106819. doi:10.1016/j.quascirev.2021.106819

Zhang, H., Cheng, H., Sinha, A., Spötl, C., Cai, Y., Liu, B., et al. (2021). Collapse of the Liangzhu and other Neolithic cultures in the lower Yangtze region in response to climate change. *Sci. Adv.* 7, eabi9275. doi:10.1126/sciadv.abi9275

Zhang, J., Chen, Z., Lan, W., Yang, Y., Luo, W., Yao, L., et al. (2018). The new progresses of the paleoethnobotanical studies of the jiahu site in wuyang, henan (in Chinese with English abstract). *Archaeology* 4, 100–110.

Zhang, S. (2022). *Times new roman arrangement and research of jade unearthed from Qijia culture*. [Dalian (China)]: Liaoning Normal University.

Zhao, C. (2020). The climate fluctuation of the 8.2 ka BP cooling event and the transition into neolithic lifeways in North China. *Quaternary* 3, 23. doi:10.3390/quat3030023

Zhao, Y., Chen, F., Zhou, A., Yu, Z., and Zhang, K. (2010). Vegetation history, climate change and human activities over the last 6200 years on the Liupan Mountains in the southwestern Loess Plateau in central China. *Palaeogeogr. Palaeoclimatol. Palaeoecol.* 293, 197–205. doi:10.1016/j.palaeo.2010.05.020

Zhao, Z. (2010). *Paleoethnobotany: Theories, methods and practice* (in Chinese). Beijing: Science Press.

Zhou, X., Li, X., John, D., and Zhao, K. (2016). Rapid agricultural transformation in the prehistoric Hexi corridor, China. *Quat. Int.* 426, 33–41. doi:10.1016/j.quaint.2016.04.021

Frontiers in Earth Science

Investigates the processes operating within the major spheres of our planet

Advances our understanding across the earth sciences, providing a theoretical background for better use of our planet's resources and equipping us to face major environmental challenges.

Discover the latest Research Topics

See more →

Frontiers

Avenue du Tribunal-Fédéral 34
1005 Lausanne, Switzerland
frontiersin.org

Contact us

+41 (0)21 510 17 00
frontiersin.org/about/contact